The Miocene Carbonates in Time and Space On- and Offshore SW Palawan, Philippines

Dissertation
zur Erlangung des Doktorgrades
der Mathematisch-Naturwissenschaftlichen Fakultät
der Christian-Albrechts-Universität zu Kiel

vorgelegt von
Stefan K. Rehm
geboren in Hamburg

Kiel 2003

TOTAL FINA ELF

This investigation was possible due to the cooperation of GEOMAR, Research Center for Marine Geosciences, Kiel/ Germany, CEREGE, Centre Européen de Recherche et d'Enseignement de Géosciences de l'Environnement, Aix-en-Provence/ France and TOTALFINAELF Oil Company, Paris/ France.

Hiermit erkläre ich an Eides statt, dass die vorliegende Abhandlung, abgesehen der Beratungen durch meine akademischen Lehrer, nach Inhalt und Form meine eigene Arbeit darstellt. Ferner habe ich weder diese noch eine ähnliche Arbeit an einer anderen Abteilung oder Hochschule im Rahmen eines Prüfungsverfahrens vorgelegt.

Stefan K. Rehm

Promoter/ Referent: _____

Copromoter/ Koreferent: _____

Day of Disputation/ Tag der mündlichen Prüfung: _____

Approved for print/ zum Druck genehmigt: _____

The Dean/ Der Dekan

Acknowledgements

I would like to express my gratitude and debt to Professor Dr. Wolf-Christian Dullo (Kiel) and Dr. Gilbert F. Camoin (Aix-en-Provence) for the opportunity to prepare this dissertation under their supervision. Additionally, I thank Prof. Dr. Wolf-Christian Dullo for his company during the first field trip and his guiding during the time at Geomar. I would like to extend my thanks to Dr. Gilbert F. Camoin, especially for the short but very efficient and inspiring meetings in Noumea and Aix-en-Provence.

It is of great importance for me to thank Dr. Dietrich Horn (Essen) for his support regarding the interpretation of the offshore subsurface data set. This work benefited substantially from his experience and council.

Dr. Philippe Lapointe (Paris) is thanked for the initiation of this project and his support to realize the field trips and a number of additional trips as well as for pushing the project.

In particular, I thank Dr. Robert Boichard (Pau) for the most constructive fieldwork including guidance, fruitful discussions and private lessons on various geological themes.

Special and personal thanks goes to Dr. V. Joseph Foronda (Manila), who was the crucial person concerning all contacts and logistics in the Philippines. Without his support, not even a part of this investigation would have been realistic.

For very helpful contributions I would like to thank: Dr. Willem Renema (Leiden) for providing the larger foraminiferal biostratigraphy and Dr. Roger Anglada (Marseille) for his dating of planktonic foraminifera. Dr. Dorothee Spiegler (Kiel) assisted with her check of the biostratigraphic reports of the 3 wells and Dr. Juan C. Braga (Granada) for his help regarding the determination of the red algae.

I am also grateful to Dr. Ken Johnson (Los Angeles), Dr. Nancy F. Budd (Iowa City) and Dr. Brain R. Rosen (London) for valuable comments on the coral assemblage.

Dr. John J. G. Reijmer (Kiel) I thank for answering carbonate sedimentological questions immediately. Dr. Florian Böhm (Kiel) and Prof. Dr. Anton Eisenhauer (Kiel) are acknowledged for helpful discussions and comments regarding the Sr isotope stratigraphy.

Special thanks goes to Dr. Griselda J. Garcia-Bausa (Manila) and Dr. Ismael U. Ocampo (Manila) from the Department of Energy (DOE), who enabled the extension of the study to the offshore area by providing the considerable offshore data set.

My friends Andres Rüggeberg and Henrike Schünemann I would like to thank for sharing the time of my PhD including the discussion of all matters coming up while struggling for a PhD as well as for the last days and nights to help me bringing this document to the final print-out version.

Further thanks go to Martin Ziegler who assisted me with laboratory work and Jun & Vincent for their guiding and assistance every day in the jungle.

With many thanks for your love and support I would like to express how helpful it was to know, that you, mum, dad and Thomas, Cornelia, Markus and Susanne accompany me all the time. Danke.

Of course, the warmest 'thank you' I have spared till last: Danke Steffi, für all Deine Liebe, Unterstützung, Geduld und Hartnäckigkeit das Leben mit einem Geologen teilen zu wollen, sowie das ermöglichen von Familie und Promotion. Danke für das Sorgen um unseren Sohn Lasse Nepomuk. Lasse, danke für jedes einzelne Lächeln und die ruhigen Nächte.

The project was founded by the Deutsche Forschungsgemeinschaft project DU129/ 27 "Karbopore", the Ministère de la Recherche (France) and TOTALFINAELF (France).

Abstract

Cenozoic shallow-water carbonates developed most extensively in SE Asia influenced by external parameters such as sea level fluctuation, tectonic, terrestrial runoff, volcanic influx and oceanic swells. The view to isolate the imprints of controlling mechanisms in an area providing several different geological settings leads to the investigation of recently discovered outcrops of Miocene age in the Southwest of Palawan Island (Philippines), supplemented by a considerable subsurface survey of coeval deposits in the related offshore area. The high potential of the hydrocarbon provinces around the southern South China Sea with multitude reservoirs in Cenozoic carbonates was an additional argument to look for promising outcrops for a detailed study of the evolution of Miocene carbonate in the vicinities onshore.

Onshore SW Palawan in the area of Quezon, carbonate outcrops of late Early Miocene to Middle Miocene age (N7 - N14/ N15) represent lateral extended ("platform-/ ramp-like") carbonates and reefal build-ups in a tectonically stable frame. The succession throughout these carbonates documents the evolution from the establishment of carbonate deposition followed by a lagoonal setting to a ramp-like setting to finally the creation of isolated build-ups after the demise of the lateral extended carbonates. This evolution is associated with a general increase of the relative sea level, which is clearly indicated in the change of the carbonate composition and biota, especially the larger foraminiferal assemblage. The late Early Miocene carbonates overlie conformably shales. Massive grainstones prevail at the base. Gravel in the lower part of these carbonates indicates the occurrence of a shoreline in the vicinity (initial stage). Packstones, wackestones and (coral-)floatstones with Alveolinoidae and Soritidae (lagoonal setting) and foraminiferal grainstone with Amphisteginidae, Nummulitidae and Lepidocyclinidae (upper slope deposits) comprise the overlying units. Upsection, finer packstones and later fine, monotonous mud- to wackestone with planktonic foraminifera and variable content of shales, indicate an increasing water depth and quieter environment (deeper slope/ basin). The direct contact between the uppermost layers of the lateral extended carbonates and the overlying carbonate build-ups could only be expected at one site (Albion Head), whereas the second isolated build-up developed on an intercalation of deep marine shales (Devel Peak). Variable depositional conditions as a consequence of sea level fluctuations can be observed through facies changes along the reef profile of Devel Peak.

Offshore SW Palawan, the reinterpretation of an extensive seismic survey and 3 wells (Penascosa-1, Santiago A-1X, Anepahan A-1X) yields a depositional model for the

development of the sedimentary sequences from Early Miocene to recent time. According to this model, an Early Miocene carbonate platform (N5) overlies unconformably Cretaceous (?) to Lower Tertiary clastics. Whereas the broad carbonate platform drowned, which is illustrated by a time gap of three nannoplankton zones to the overlying clastics in well Penascosa-1, isolated reefal structures of various sizes continued to grow probably on structural highs. The well Santiago A-1X drilled a marginal pinnacle of a large build-up (Great Atoll Reef) whereas the well Anepahan A-1X tested an isolated pinnacle structure. Both wells report a continuous sedimentation during the Middle Miocene (N9) between the top of the carbonates and the overlying siliciclastic sediments. Therefore, the increase of terrestrial influx, resulting in basinwards prograding clastic sequences, buried most of the reefal carbonates in Middle Miocene time. In general, the backstepping of the carbonate depositions from E towards the W coincides with the progradation of the clastic sequences in the same direction.

Mainly the detailed stratigraphy as well as the dimensions of the carbonates on- and offshore combined with sedimentological criteria lead to the over-all-model that the carbonates of the onshore study area correlates with the stage of build-up development offshore. Thereby, the evolution of the carbonates in SW Palawan highlights the dominance of sea level changes as triggering mechanism additionally influenced by terrestrial runoff. However, the onshore study provides new insights in the development and facies distribution within Cenozoic build-ups, which are often the target of hydrocarbon prospects.

The following document presents the data of the microfacies analysis including thin section analysis, cathodoluminescence- and stable oxygen and carbon isotope analysis interrelated to a detailed biostratigraphy and single $^{87}Sr/^{86}Sr$ measurements in order to unravel the history of the carbonates in time and space. Finally, the generated over-all-model is compared to other Cenozoic carbonates of the Philippines, the offshore area of the South China Sea and world-wide to prove their global implication.

Kurzfassung

Ausgedehnte känozoische Flachwasser-Karbonate entwickelten sich in Südost Asien unter dem Einfluss von externen Parametern wie Meeresspiegelschwankungen, Tektonik, terrestrischem und vulkanischem Eintrag sowie ozeanischen Strömungen. In Hinblick auf die Unterscheidung von Kontrollfaktoren in einer Region, die mehrere geologische Rahmenbedingungen aufweist, führte zu der Untersuchung der neu entdeckter miozäner Geländeufschlüsse im Südwesten der philippinischen Insel Palawan ('onshore'). Diese Untersuchung wurden ergänzt durch umfangreiche Untergrundsuntersuchungen von zeitgleichen Ablagerungen im angrenzenden Seegebiet ('offshore'). Das hohe Potential der Kohlenwasserstoff-Provinzen in der südlichen Süd-China-See mit einer Vielzahl von Vorkommen in känozoischen Karbonaten war ein weitere Grund für die Suche nach vielversprechenden Geländeaufschlüssen in der Umgebung, um die Entwicklung der Miozänen Karbonate detailliert zu untersuchen.

Im Gebiet um Quezon in Südwest Palawan stellen die späten Untermiozänen bis Mittelmiozänen (N7 - N14/ N15) karbonatischen Geländeaufschlüsse lateral ausgedehnte (plattform-/ rampen-ähnliche) Karbonate und riffartige Körper in einer tektonisch stabilen Umgebung dar. Die Abfolge der Karbonate dokumentiert ihre Entwicklung von der Etablierung der Karbonatablagerungen über lagunäre Bedingungen, zu einer rampen-ähnlichen Anordnung und letztendlich dem Aufbau isolierter riffartiger Körper nach dem Untergang der lateral ausgedehnten Karbonate. Diese Entwicklung ist verbunden mit einem generellen Anstieg des relativen Meeresspiegels, was deutlich wiedergegeben ist durch die Veränderungen der Karbonatzusammensetzung und der Biota, insbesondere der Großforaminiferen-vergesellschaftung. Die späten Untermiozänen Karbonate überlagern konkordant Tone. Massive Grainstones herrschen an der Basis vor. Gerölle in dem unteren Teil dieser Karbonate deutet das Existieren einer nahegelegene Küstenlinie an (Initiales Stadium). Packstones, Wackestones und (Korallen-)Floatstones mit Alveolinidae und Soritidae (lagunäre Ablagerungen) sowie Foraminiferen-Grainstones mit Amphisteginidae, Nummulitidae and Lepidocyclinidae (obere Hangablagerungen) umfassen die überlagernde Einheit. In der Fortsetzung spiegeln feine Packstones und später feine, monotone Mud- bis Wackestones mit planktonischen Foraminiferen und variablen Gehalten an Tonen zunehmende Wassertiefe und ruhigeres Milieu wider (tieferer Hang/ Becken). Der direkte Kontakt zwischen den lateral ausgedehnten Karbonaten und den riffartigen Körpern kann nur an einer Lokation angenommen werden (Albion Head), während sich der zweite riffartige Körper auf einer Einschaltung von tief-marinen Tonen entwickelt hat (Devel Peak). Variable Sedimentationsbedingungen als Ergebnis von Meeresspiegel-

schwankungen können anhand von Faziesveränderungen im Riff-Profil von Devel Peak gesehen werden.

Die Neuinterpretation der umfangreichen seismischen Untersuchungen und 3 Bohrungen (Penascosa-1, Santiago A-1X, Anepahan A-1X) im Seegebiet vor Südwest Palawan ('offshore') liefern ein Sedimentationsmodell für die Entwicklung der Sedimentationsabfolge vom Untermiozän bis heute. Entsprechend diesem Modell, überlagert eine untermiozäne Karbonatplattform diskordant Kreide (?) bis untertertiäre Klastika. Während die ausgedehnte Karbonatplattform ertrinkt, was durch eine Schichtlücke zu den überlagernden Klastika von 3 Nannoplankton-Zonen in der Bohrung Penascosa-1 angezeigt wird, wachsen isolierte Riff-Strukturen unterschiedlicher Größe vermutlich auf Anhöhen weiter. Die Bohrung Santiago A-1X erreichte ein randliches Nadelriff des Großen Atoll Riffes, während die Bohrung Anepahan A-1X eine isolierte Nadelriff-Struktur erbohrte. Beide Bohrungen ergeben eine durchgehende Sedimentation im Mittelmiozän (N9) zwischen dem Top der Karbonate und den überlagernden Klastika. Somit begrub ein erhöhter Eintrag von terrestrischen Materials, der beckenwerts progradierende Abfolgen bildete, die meisten riffartigen Karbonate im Mittelmiozän. Generell stimmt das Zurückziehen der Karbonate von Ost nach West mit dem Progradieren der klastischen Abfolge in die selbe Richtung überein.

Hauptsächlich die detaillierte Stratigraphie sowie die Dimension der Karbonate 'onshore' und 'offshore', kombiniert mit sedimentologischen Kriterien, führt zu dem Gesamtmodell, daß die karbonatischen Geländeaufschlüsse mit dem Stadium der Riffentwicklung im 'offshore' Bereich korrelieren. Dabei hebt die Entwicklung der Karbonate in SW Palawan die Dominanz von Meeresspiegelschwankungen als Steuerungsfaktor, zusätzlich beeinflußt durch terrestrischen Eintrag, hervor. Die Geländeuntersuchen liefern in diesem Zusammenhang neue Einblicke in die Entwicklung und Fazieverteilung innerhalb der känozoischen Strukturen, die häufig Kohlenwasserstoff-Reserven erwarten lassen.

Das vorliegende Dokument präsentiert die Daten der Mikrofazieanalyse, die Dünnschliff-Auswertung, Kathodolumineszens- und Stabile Sauerstoff- und Kohlenstoff Isotopen-Untersuchungen einschließt, verknüpft mit einer detaillierten Biostratigraphie und einzelnen $^{87}Sr/^{86}Sr$ Messungen im Hinblick auf die Entschlüsselung der Geschichte der Karbonate in Zeit und Raum. Letztendlich wird das erstellte Gesamtmodel mit andern känozoischen Karbonaten im Bereich der Philippinen, der Süd-China-See und weltweit verglichen, um globale Folgerungen zu prüfen.

Résumé

Le dévelopement extensif des plates-formes carbonatées cénozoïques dans le Sud-Est asiatique a été contrôlé par les fluctuations du niveau marin, les mouvements tectoniques, les flux terrigènes et volcaniques et les paramètres océanographiques. Dans le but d'établir l'importance de ces différents contrôles dans une région caractérisée par des contextes géologiques différents, ce travail est basé sur l'étude de nouveaux affleurements miocènes au Sud-Ouest de Palawan (Philippines) et de données de subsurface obtenues sur des dépôts d'âge comparable reconnus au large de Palawan. Le grand potentiel de la province pétrolière de Mer de Chine Méridionale et la présence de nombreux réservoirs dans les dépôts carbonatés de plates-formes cénozoïques constituaient des raisons supplémentaires pour conduire une étude détaillée de l'évolution des carbonates miocènes de plates-formes de Palawan.

Au Sud-Ouest de Palawan, dans la région ed Quezon, les dépôts carbonatés de plates-formes d'âge Miocène inférieur à moyen (N7 - N14/ N15) correspondent à des plates-formes étendues (plates-formes, rampes) et à des édifices récifaux développés dans un régime tectonique stable. La succession étudiée permet de retracer l'évolution des systèmes carbonatés depuis leur installation jusqu'au développement tardif d'édifices isolés, en passant par l'établissement d'environnements lagonaires puis de rampes carbonatées. Cette évolution est contrôlée par une montée relative du niveau marin également reflétée par l'évolution des assemblages biologiques et plus particulièrement des associations de grands foraminifères.

Les carbonates du Miocènes inférieur reposent sur des dépôts argileux. Des grainstones massifs caractérisent la base de la série carbonatée ; par ailleurs, l'abondance de particules grossières indique la proximité d'une ligne de rivage (stade initial). Des packstones, des wackestones et des floatstones à Coraux renfermant un assemblage de grands Foraminifères benthiques à Amphisteginidae, Nummulitidae et Lepidocyclinidae (dépôts de pente supérieure) forment l'unité suivante. Dans la partie supérieure de la série, des packtones fins et des wackestones et mudstones argileux à Foraminifères planctoniques caractérisent un environnement de dépôt plus profond et plus calme (dépôts de pente et de bassin). Le contact direct entre les couches supérieures et les édifices carbonatés sus-jacents n'a pu être observé que dans un seul site (Albion Head), alors que le deuxième édifice carbonaté ne s'est développé qu'après l'intercalation de dépôts argileux profonds (Devel Peak). Des variations concernant les conditions de dépôt sont observées dans le secteur de Devel Peak et reflètent l'influence de fluctuations du niveau marin.

Au large de Palawan, la réinterprétation de lignes sismiques et de trois forages (Penascosa-1, Santiago A-1X, Anepahan A-1X) a permis d'établir un modèle de dépôt pour les séries datées du Miocène à l'Actuel. Une plate-forme carbonatée du Miocènes inférieur (N5) s'est établie sur des dépôts térrigènes du Crétacé (?) et du Cénozoïque inférieur. Lors de l'ennoyage de la plate-forme, marqué par l'absence de trois zones de nannoplancton dans les dépôts terrigènes sus-jacents du forage Penascosa-1, des structures récifales isolées de tailles variables ont continué à se devélopper sur des hauts-fonds.

Le forage Santiago A-1X a permis de documenter un pinacle appartenant à un édifice important (Great Atoll Reef) alors que le forage Anepahan A-1X concerne un pinacle isolé. Dans ces deux forages la sédimentation est continue au cours du Miocène moyen (N9), entre le sommet de la série carbonatée et les dépôts terrigènes sus-jacents. Les dépôts terrigènes ont recouvert la plupart des plates-formes carbonatées au cours du Miocène moyen. Le *backstepping* des plates-formes carbonatées de l'Est vers l'Ouest coïncide avec la progradation des séries terrigènes dans la même direction.

Les données stratigraphiques couplées avec les résultats de l'étude sédimentologique on permis de déterminer que l'évolution des plates-formes carbonatées du Sud-Ouest de Palawan a été principalement gouvernée par les fluctuations du niveau marin. L'étude détaillée des édifices carbonatés miocènes a permis d'apporter des données nouvelles sur la distribution des faciès et le développement de ces édifices.

Le présent travail comprend une étude détaillée de microfaciès, des données de cathodoluminescence et des résultats d'analyses isotopiques (isotopes stables du carbone et de l'oxygène) qui ont été couplés à une étude biostratigraphique et des mesures de rapports isotopiques du strontium ($^{87}Sr/^{86}Sr$) permettant ainsi de reconstituer l'évolution des plates-formes carbonatées dans l'espace et dans le temps. Enfin, le modèle ainsi reconstitué est comparé à celui concernant d'autres plates-formes carbonatées des Philippines, de Mer de Chine méridionale et d'autres régions afin de les replacer dans un cadre général d'évolution des plates-formes carbonatées au cours du Miocène.

Content

1. Introduction

1.1 State of the Art

Globally, the Cenozoic time period provides the most extensive occurrence of shallow water carbonate depositions between 30° S and 50° N. The majority of these carbonates are found in three main areas: (1) the western Atlantic province including Middle America, Caribbean and the eastern coast of North America (New Jersey shelf), (2) the Tethyan province including the Mediterranean and Middle East as well as (3) the Indo-Pacific province including SE Asia and the western Pacific. The studies along the passive margin of the western Atlantic province are concentrated dominantly on the, since Late Cenozoic isolated, carbonate platform of the Great Bahama Bank (e.g. SCHLAGER & GINSBURG, 1981; DROXLER & SCHLAGER, 1985; SCHLAGER et al., 1994; EBERLI et al., 1997a) as well as the New Jersey shelf (e.g. GREENLEE et al., 1988; MOUNTAIN et al., 1994; AUSTIN et al., 1998). Observations within the Bahama Banks in the late eighties leads to greatest interest in the sedimentation processes on the margins of carbonate platforms and shelves. Margin progradation was shown to be an important process of platform evolution (EBERLI & GINSBURG, 1987, 1988, 1989). The architecture and margin progradation processes are closely related to reef development, which marks again major changes in lithology, biotas, and depositional processes in the shallow water area behind (GINSBURG, 2001). However, very soon the circumstances and mechanisms, which triggered the episodic evolution of the margins become of interest and hence, beside the climate, the sea level changes, relative and in a global scale (eustasy), are in the focus of a number of studies of shallow-water carbonates and sequence stratigraphy (e.g. HAQ et al., 1987, 1988; ABREU & ANDERSON, 1998; EBERLI et al., 1996; PEKAR & MILLER, 1996; MILLER et al., 1998, PEKAR et al., 2002).

Shallow water carbonate systems are of fundamental interest in unravelling sea level history, because they are extreme sensitive to climatic and environmental changes (CAMOIN, 2001), wheras the region between the paleo-shoreline and the paleo-inner to middle shelf seems to be most promising (MILLER et al., 1998). The end members of sea level rise/ fall are the exposure or the phenomenon of drowning, i.e. in sense of SCHAGER (1981) the demise of carbonate production as result of an increasing sea level. The drowning were described from several different carbonate platforms as well as isolated reef structures (e.g. SCHLAGER, 1981, 1989, 1998; ALBERT & DROXLER, 1991; ERLICH et al., 1990; ERLICH et al., 1991; SAGER et al., 1993; BETZLER et al., 1995; ISERN et al., 1996). The existence of a correlation between

sequence boundaries and glacioeustatic sea level changes were shown in the Cenozoic section of the New Jersey Transect on- and offshore (MILLER et al., 1998; PEKAR et al., 2002) as well as by remarkably similar architectures of margins with widely contrasting tectonic and sedimentary histories world-wide (BARTEK et al., 1991). This emphasises that eustasy is a fundamental control on the stratigraphic record, even if it is clear that the climate and tectonic are responsible for, just as sea level changes as, temporal and local fluctuation in sediment supply, sediment types, and oceanic current regimes. Consequently, these mechanisms controlling the sedimentary process create together a significant sedimentary succession, which might have again, socially-relevance in sense of the distribution of natural resources (e.g. potable water, hydrocarbon, metallic ores). Therefore, to isolate the imprint of each of these effects and to obtain the knowledge of their changes through time would provide a powerful tool to characterise sedimentary systems, which would be among others of major interest for the new target of carbonate reservoirs of hydrocarbon. Furthermore, although the subsurface exploration techniques combined with sequence stratigraphy already provide an impressive picture of the underground, to decipher subsurface geology, onshore equivalents are necessary to prove fundamental assumption, which have to be made.

However, to attain this challenging goal, a detailed carbonate facies analysis in time and space of additional records, eventually in different geodynamic setting, are necessary. Within the SE Asia region the Cenozoic carbonate development is associated with the greatest diversity in tectonic settings and depositional systems (WILSON, 2002) and offers, therefore, the excellent place to study shallow water carbonates development in the world. Furthermore, the equatorial carbonates of SE Asia have significant economic potential due to their major target of hydrocarbon exploration since 30 yr. (EPTING, 1980; FULTHORPE & SCHLANGER, 1989; DOWNEY, 1990; WILSON & BOSENCE, 1997), which might offer the direct transfer of results to potential reservoirs in the region. The definition of the Philippine archipelago as objective of this investigation ground on the primary idea to study Oligo-Miocene carbonate development in different tectonic setting and depositional conditions. As result of the plate tectonic evolution in SE Asia (HALL, 1996), several different setting are concentrated within the territory of the Philippines relatively close together. Most of the Philippines are related to the mobile belt with tectonic activities and volcanism in the E, whereas Palawan in the W and the Sulu Sea in the S grounds on a stable microcontinental fragment. Furthermore, within the Philippine archipelago eleven large basins with significant terrestrial influence developed

during the Cenozoic time, beside carbonates, this are formed in an open ocean on structural highs. Despite these promising circumstances the complicated situation in the field (e.g. tower karst results to 100s m high vertical cliffs, dense vegetation or tangly jungle makes outcrops inaccessible), no promising and accessible outcrops in the Visayan Basin or Central Luzon Basin as well as the political situation in the years 2000 and 2001 lead to the concentration on the Palawan, western Philippines. This island seems to be very promising, due to the existence of on- and offshore carbonates (plus offshore surveys including seismic and wells), the proximity to the new hydrocarbon production area in NW Palawan as well as the opportunity of new discoveries.

With the exception of the geological description of the archipelago by CORBY et al. (1951) and the extensive work on geodynamics, stratigraphy and general sedimentary formations in the Visayan by the Philippine-German Technical Co-operation Project "Visayan Sea Basin Study" (PORTH & V. DANIELS, 1989) as well as internal study of the oil industries, the Miocene carbonates of the Philippines have received little attention up to now. In the western Philippines previous investigations were also rare and the existing publications were either very general (PARK & PETERSON, 1979) or focus on biostratigraphic targets by using spot samples only (HASHIMOTO & MATSUMARU, 1982; WOLFART et al., 1986). Anyhow, still some links on a geological map 1 : 2,500,000 (FERNANDEZ, 1981) refer to the presence of carbonates in N- as well as in S-Palawan. Although little information is available, outcrops of Miocene carbonates, so far not reported in literature, were discovered in SW-Palawan during two field campaigns in 2000 and 2001.

The newly discovered carbonate outcrops around Quezon, close to the south-western coast, were investigated to unravel the Miocene carboante development and to evaluate the mechanisms controlling the deposition of there sediments. The questions included (i) what were the paleoenvironment characteristics of the study area, (ii) how was the evolution of the carbonate area on- and offshore in time and space, (iii) is there any correlation possible between on- and offshore sequences, (iv) what were the mechanisms triggering the development of the carbonates and their build ups as well as (v) how were the diagenetic responds concerning the development and preservation of the porosity? However, due to the available, often poorly preserved, sample material and a predominate burial diagenesis, the conclusive appraisal of the development and preservation of porosity in the carbonate rocks as responds of primary facies patterns and external influence needs some additional studies.

This thesis comprises three parts . A general part at the beginning includes the "Introduction" and "Materials and Methods". The following chapters presens the results. Since the study focused on two study areas - the onshore and offshore area - this is split into an onshore and an offshore chapter ("Principle Data Base: Onshore", " Principle Data Base: Offshore"). The last part provides the interpretation of the findings, "The Development of the Miocene Carbonates On- and Offshore SW Palawan". The thesis ends with a comparison with other sites on the Philippines, in the offshore area of the South China Sea, and Miocene outcrops found world-wide ("Miocene Carbonates from SW Palawan in a Global Frame").

This study has been supported significantly by the Department of Energy (DOE), Manila with the kind provision of an extensive seismic- and well data set of the south-western offshore area of Palawan.

1.2 Geological Setting

1.2.1 Regional Geodynamics

The SE-Asia region is an area with a complex subduction-collision history imposed by the actions and reactions generated by the Pacific, Eurasian and Indo-Australian plate motions as well as by several microplates (HALL & WILSON, 2000). Following the model of TAPPONNIER et al. (1982), the creation of the present-day plate tectonic framework of the SE Asia region starts with the separation of India from Antarctica and Australia at about 105 Ma ago. The later collision of India with Eurasia between 44 and 38 Ma results in the drift of the Indochina to the SE and later China to the ESE, whereas they are separated from each other by the left-lateral, strike-slip Red River Fault (Fig. 1). These motions might have triggered the renewed N-S extension in the South China continental margins, which results in the spreading of the present-day South China Sea in the Late Eocene to Oligocene (rifting phase). However, RU & PIGOTT (1986) postulate an episodic rifting already during the Late Cretaceous, beside late Eocene and late early Miocene activities. In general, this N-S extension in the South China Sea is confirmed by marine magnetic anomaly lineations correlated by TAYLOR & HAYES (1980, 1983). During the Early Miocene the seafloor spreading of the South China Sea shifts to NW-SE direction (LEE & LAWVER, 1994). The collision of the North Palawan microcontinental block with the clockwise rotated West Philippine Block (HALL, 1995) ceased the spreading (drifting phase) of the South China Sea around the Middle Miocene: end

of the Early Miocene/ 17 Ma (HOLLOWAY, 1982; TAYLOR & HAYES, 1983; DALY et al., 1991; LEE & LAWVER, 1994) or in the Middle Miocene/ magnetic Anomaly A5/ 8.7-19.2 (GALLAGHER, 1987), biozone N14/ 11.5 Ma (WILLIAMS, 1992). However, uplift in South and Central Palawan are demonstrated in the Middle Miocene at 14.7 Ma (KUDRASS et al., 1986), suggesting that subduction did not terminate until that time. Whereas DALY et al. (1991) assume that the migration of the Philippine arc ended in the collision with north Palawan in the late Miocene (10 Ma) associated with an uplift in the outer Sulu Sea, postulated GALLAGHER (1987) and LONGLEY (1997) a collision within the magnetic Anomaly A3, respectively 5 Ma. Anyhow, there seems to be no doubt that no active tectonics exists along the NW Borneo/ Palawan area since 5 Ma ago.

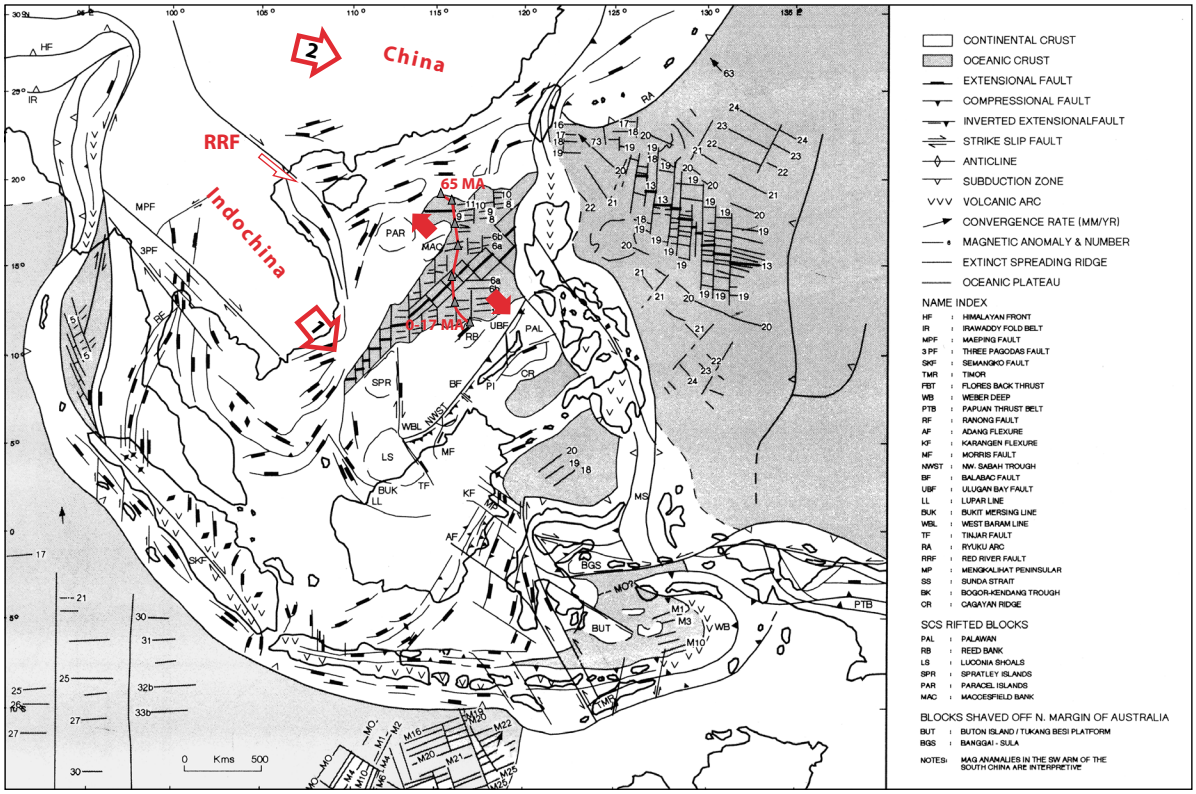

Fig. 1: Map of SE Asia tectonic elements after LONGLEY (1997) supplemented with general tectonic movements after TAPPONNIER et al. (1982) and a dated flowline of LEE & LAWVER (1994).

The microcontinents on the Mesozoic South China continental margin between Taiwan and Hainan Island, like the North Palawan Block or the Reed Bank, initially rifted away from South China margins since the late Cretaceous (HOLLOWAY, 1982) before they started travelling thousands of kilometers to the SE. In contrast, the ophiolite-dominated southern part of Palawan is interpreted as the accretionary wedge of an suggested fossil subduction

zone running from N-Borneo in NE direction to the northern Philippines (HAMILTON, 1979; HOLLOWAY, 1982; HINZ et al., 1983). However, during Early Miocene time a small S-Palawan landmass with a passive margin might be located close to the Reed Bank in the South China Sea (CLENNELL, 1996), which is most probably partly integrated in the southern part of Palawan today. An active subduction on the eastern side of the South China Sea still exists in the Manila Trench between Taiwan and Mindoro (LEE & LAWVER, 1994), but generally, passive continental margins in the NW and SE dominate the small oceanic basin today.

1.2.2 Philippines

In south-eastern Asia the Republic of the Philippines consists of an archipelago of more than 7000 Islands on a territory of approximately 300.000 km^2 between latitude 21°25' N and 4°23' N and longitude 116° E and 127° E. It is surrounded by the Philippine Sea (E), the South China Sea (W) and the Celebes Sea (S). Geologically, the Philippine archipelago is trapped between the oblique convergent boundary of the Philippine Sea Plate and the eastern margin of the Eurasian plate (e. g. DALY, 1991; LEE & LAVWER, 1994; HALL, 1996, 1997, 1998, 2002). In between, the major sinistral strike-slip Philippine Fault tending from the NNW - SSE, which is inferred to have only been active since the Mio-Pliocene (AURELIO et al., 1991). In general, the Philippine archipelago can be divided into the major province of the mobile belt, extending from Luzon in the N to Mindanao in the S, and a relative stable area on a continental fragment including Palawan in the W and the Sulu Sea in the S (RANGIN et al., 1989). The basement of the archipelago is made up of thick sediments of Permo-Carboniferous age, probably deposited in a geosynclinal environment, which later converted to folded mountain belts (CAROZZI et al., 1976). Mountain building, which extended up to the Jurassic times, was apparently accompanied by wide metamorphism and intrusion of granitoid rocks. These igneous and metamorphic rocks underlie approximately 30% of the present landmass of the Philippines (CAROZZI et al., 1976). Additionally, Late Paleozoic, i.e. Permian and locally very restricted Carboniferous, as well as Triassic limestones and schists, are exposed in northern and central Palawan Island (MITCHELL et al., 1985; KIESSLING & FLÜGEL, 2000). The majority of the Philippines is composed of ophiolites and volcanic arc rocks as well as sediments of at least Jurassic, Cretaceous, Tertiary and Quaternary age (CAROZZI et al., 1976; HOLLOWAY, 1982; MITCHELL et al., 1986; WILSON, 2002). During

Tertiary times widely spread volcanism occurred in the eastern Philippines, which disturbed the sedimentary successions found in seven well-defined basins. As oldest Tertiary sediments, carbonate and siliciclastic deposits were described from the Eocene of Ilocos Norte/ NW Luzon (SMITH, 1907), E Zambales/ Central Luzon (GARRISON et al., 1979), Mindoro (TEVES, 1956; SAREWITZ & KARIG, 1986), Central Cebu (PORTH et al., 1989), W Bohol (CORBY et al., 1951; TEVES, 1956), Cauayan area/ SW Negros (PORTH et al., 1989), Davao and northern Mindanao (CORBY, 1951; MITCHELL et al., 1986). However, the most extensive sedimentation of carbonates in the Philippines took place between the Oligo-Miocene time. Thereby, the carbonates developed in 3 main tectonic settings throughout the South China Sea and the Philippines. These were passive continental margins, convergent plate boundaries, and obliquely convergent plate boundaries (FULTHORPE & SCHLANGER, 1989). Examples of plate boundary related settings in the Philippines are the fore-arc basins (Illoio Basin/ Panay, Agusan-Davao Basin/ Mindanao and Cotabato Basin/ W Mindanao) and the back-arc basins (Visayan Basin/ Cebu). Additionally, carbonates occur on intraoceanic volcanic arcs (WILSON, 2002) as well as on rifting microcontinental blocks, such as for example in the area of the Dangerous Grounds, the Reed Bank or NW Palawan (HINZ & SCHLÜTER, 1985; SCHLÜTER et al., 1996).

1.2.3 Miocene Carbonates

Major Miocene carbonate provinces are known around the world, such as in the Caribbean the Great- and Little Bahama Bank (cf. SCHLAGER & GINSBURG, 1981; CAREW & MYLROIE, 1997; MELIM & MASAFERRO, 1997; EBERLI et al., 1997b; GINSBURG, 2001), the New Jersey continental shelf (cf. MILLER et al., 1998), in the Mediterranean region (cf. POMAR, 1991, 2001a/b; POMAR & WARD, 1995; ROBERTSON, 1998), the Red Sea (cf. BOSWORTH & MCCLAY, 2001; BUCHBINDER, 1996), the Maldives in the Indian Ocean (cf. AUBERT & DROXLER, 1992, 1996; BELOPOLSKY, 2000) and in eastern Australia with the Great Barrier Reef (cf. DAVIES & EDGEWOOD, 1994) and the Marion-/ Queensland Plateau (cf. DAVIES et al., 1989; MCKENZIE & DAVIES, 1993; BETZLER et al., 1993; BETZLER, 1997; ISERN et al., 2001). Therefore, the carbonates of the Caribbean (21° - 27°30' N), New Jersey continental shelf (38°30' - 40°N), the Mediterranean region (31° - 42° N), the Red Sea (10° - 30° N) and the carbonates on the eastern coast of Australia (10° - 30° S) are subtropical to temperate carbonates. The Maldives (8° - 0° N) are an example of equatorial carbonates. The high

frequency of carbonate reefs within the latitudes of 27° S to 48° N around the world during the Oligo-Miocene time compared to 25° S and 32° N for Holocene reefs (JORDAN, 1990; KIESSLING, 2001) provides further evidence of apparently very suitable conditions for shallow-water carbonates during a globally relative high sea level (HAQ et al., 1987, 1988) and warm temperatures during the Late Oligocene Warming and the Mid-Miocene climate optimum (ZACHOS et al., 2001). Cool water carbonates in higher latitudes and/ or deep-waters were described (JAMES & BONE, 1991), but are, as so far known, of minor significance.

The SE Asia region hosted the most extensive Cenozoic equatorial (latitude ~10° N/ S) carbonate production in the world, whereas a most prolific modern carbonate production in their clear shallow-waters with almost half the world's coral reefs and the greatest diversity of corals are the analogous to the ancient carbonate deposits (SALM & HALIM, 1984; TOMASCIK et al., 1997; WILSON, 2002). Referring the concept that modern zooxanthellate corals are closely related to the sea-surface temperature, their occurrence in ancient deposits is commonly thought to indicate paleoclimate, especially the temperature component of the climate (FRAKES et al., 1992; JOHNSON et al., 1996). However, beside the temperature, the development of the carbonates in SE Asia was affected by a huge variety of factors, such as terrestrial runoff, tectonics, volcanisms, eustasy and oceanography. Therefore, the carbonate sedimentation occurs in the full range of tectonic settings with diverse depositional settings (WILSON, 2002). Extensive carbonates were best-developed on shelves with limited clastic input or on isolated bathymetric highs.

Most of the studied outcrops and offshore platforms of the Cenozoic carbonates are found throughout Indonesia (Sumatra, NW off- and E onshore Borneo, Sulawesi/ Moluccas/ Nusa Tenggara), New Guinea and the Philippines (Visayan Basin, SE Luzon, offshore NW and W Palawan). However, the distribution of the carbonate in Cenozoic time and space shows, with respect to the plate tectonic reconstruction of HALL (1996) (Fig. 2), that Sumatra, Java, Borneo and Sulawesi are grouped in the W around the Equator, New Guinea were in the E at about 10° - 15° S and the Philippines were split of in the central Philippines (Visayan Basin) in the SE, the main island Luzon further N and Palawan somewhere within the South China Sea. Consequently, the age and range of the carbonate deposits documents remarkable differences. Based on the compilation of WILSON (2002) of several different publications, it is indicated that in the W (Sumatra) the carbonate development was almost restricted to the Early Miocene (DE SMET, 1992), whereas the carbonates in the backarc setting of E Java developed with some interceptions between Late Eocene to Late Miocene time (BRANSDEN &

MATTHEWS, 1992; CUCCI & CLARK, 1993). Further eastwards in E Borneo carbonates are deposited all throughout the Oligocene and Miocene, before the E Sulawesi ophiolite provide a continuous stratigraphic succession covering additionally the Eocene (WILSON & MOSS, 1999).

Within the outlines of the present-day Philippine archipelago, the main and best-described Cenozoic carbonate province is the Visayan Basin (cf. MÜLLER & V. DANIELS, 1981; PORTH & V. DANIELS, 1989; FORONDA, 1994; CAROZZI, 1995). There, the shallow-water carbonates developed during the Early Oligocene, Late Oligocene to Early Miocene, Early Miocene to Middle Miocene and Late Miocene time, whereas hiatuses or non-marine clastics separate the periods of carbonate development from each other. The most complete and thickest sedimentary section was found on Cebu Island, which was apparently the center of the Visayan Basin during most of the younger Tertiary time. However, Cenozoic carbonates occur also on Bohol, Camotes, Leyte, Masbate, Panay, and Negros (Fig. 3). The oldest Cenozoic carbonates indicate Eocene age and mentioned as local occurrences from Mindanao, Southeast Luzon and Marinduque (SMITH, 1907; CORBY et al., 1951; GARRISON et al., 1979; MITCHELL et al., 1986; DAVID et al., 1997). The three small and local Eocene carbonate exposures on Negros, Cebu and Bohol (CORBY et al., 1951) are still questionable. Other scattered outcrops of smaller dimensions were discovered on Luzon with an Oligocene to lower Miocene age, and on Mindanao of Late Miocene to Pliocene age (CORBY et al., 1951).

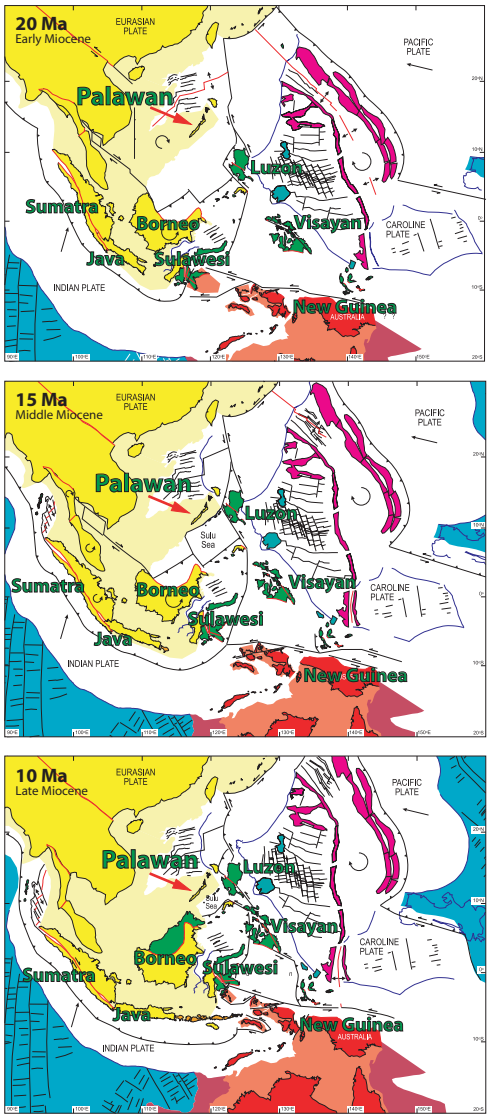

Fig. 2: Plate tectonic reconstruction of the area around the South China Sea during 20 Ma, 15 Ma and 10 Ma before present to illustrate the position of Sumatra, Java, Borneo, Sulawesi, New Guinea and the Philippines during the Miocene carbonate development (after HALL, 1996).

Beside the Visayan Basin, extensive carbonates develop offshore NW Palawan and within the South China Sea (Dangerous Ground, Reed Bank). The Nido Limestone known from offshore

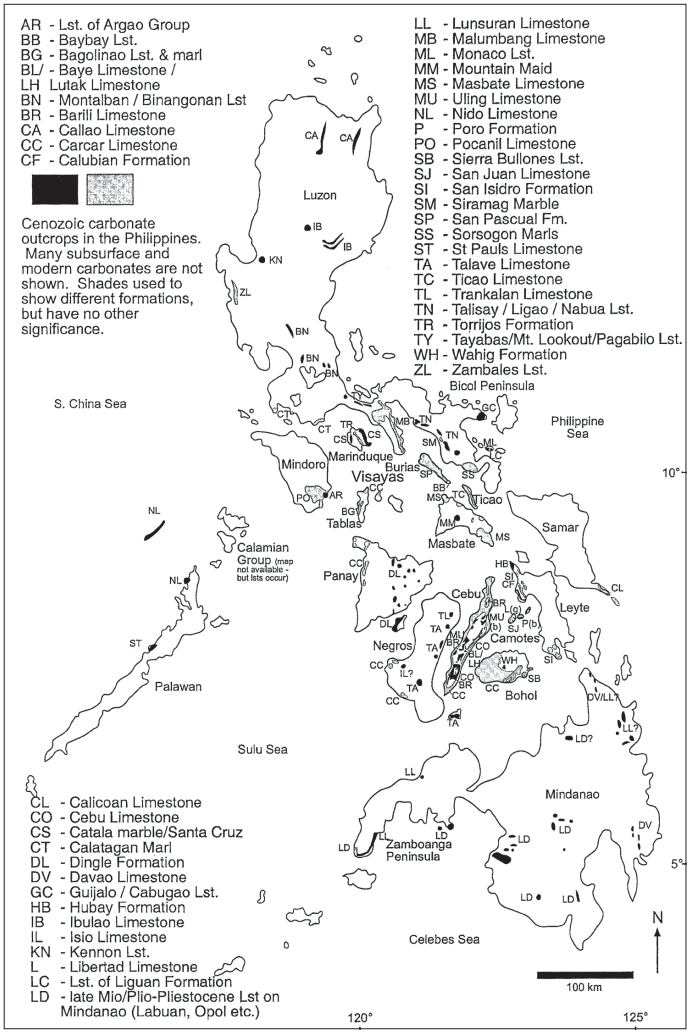

Fig. 3: Distribution of Cenozoic carbonates in and around the Philippine archipelago (from WILSON, 2002).

NW Palawan is made up of the platform carbonate, which was already established in the Early Oligocene time, and some overlying reefal build-ups ranging from the Late Oligocene to the end of the Early Miocene (LONGMAN, 1985; GRÖTSCH & MERCADIER, 1999). Around Sabang at the western coast of N-Palawan in the "St. Paul Subterranean River National Park", the significant carbonate cliffs are interpreted as an onshore equivalent of the Nido Limestone (WIEDICKE, 1987). S-Palawan is mostly interpreted as ophiolite bearing accretionary wedge and hence no carbonates are expected. Anyhow, REYES (1971) refers to several limestones outcrops in S-Palawan, whereas the Ransang Formation with extensive massive limestones in the Barrio Ransang might be the largest occurrence. But nevertheless, no description or detailed study exists so far so that they are actually unknown.

The here studied Miocene carbonates onshore SW Palawan in the area around Quezon and offshore SW Palawan were not presented before as well. Furthermore, with the exception of

two sites in the onshore study area mentioned by PARK & PETERSON (1979) all outcrops are new discovery.

1.3 Study area

1.3.1 Onshore

The onshore study area of this project is located in SW-Palawan about 140 km S of Puerto Princesa on the western coast of Palawan around the small town Quezon (Fig. 4). The most important road for the study was a more than 50-km long, but blind, gravel road, which runs along the coast from Quezon to the North. Some small side roads exist in the area, often it is impossible to pass them with a car and they end frequently after a few km. A net of small trails opens up parts of the study areas by walking. Two major rivers, Iwahig River and Tumarabong River, are crossing the study area and drain the interior East of Quezon. The rivers discharge into the South China Sea North of Quezon. Swampland with mangroves characterises most of the coastline. Small agriculturally used areas and coconut trees line the road to the north, whereas dense tropical forest or tall grassland covers the interior part of the study area. Primary jungle still exists only on the peninsula Albion Head in the West.

The field campaign was mainly concentrated on a carbonate area including the so-called ”limestone jungle”. The elongation of the carbonate area averages about 16 km from Devel Peak in the NE towards the Malanut Range in the SW. The maximum extension goes up to 5 km. The area is bordered in the NW by the sea and to the E and the S by poorly exposed siliciclastics and volcanic deposits.
The investigation of the carbonates based on the study of 8 different sites (Fig. B: location-maps): Taglupa Profile/ Foundation Area, Salty Creek Section - Maasin Profile, Tumarabong River Section/ Slope Profile, Theo's Place, Quezon Section/ Quezon Town, Albion Head and Devel Peak. Besides, some siliciclastic deposits were studied on the two small islands Nakoda Island and Tamlangon Island close to the mainland of Palawan.
Only the reefal build-ups Albion Head and Devel Peak are already known by the oil industry (PARK & PETERSON, 1979). Since the early eighties the existence of Miocene carbonates around Quezon was published by HASHIMOTO & MATSUMARU (1982) with the dating of larger foraminifera in some spot samples from the area. Details descriptions of the carbonates or notes about any other of these outcrops do not exist until now.

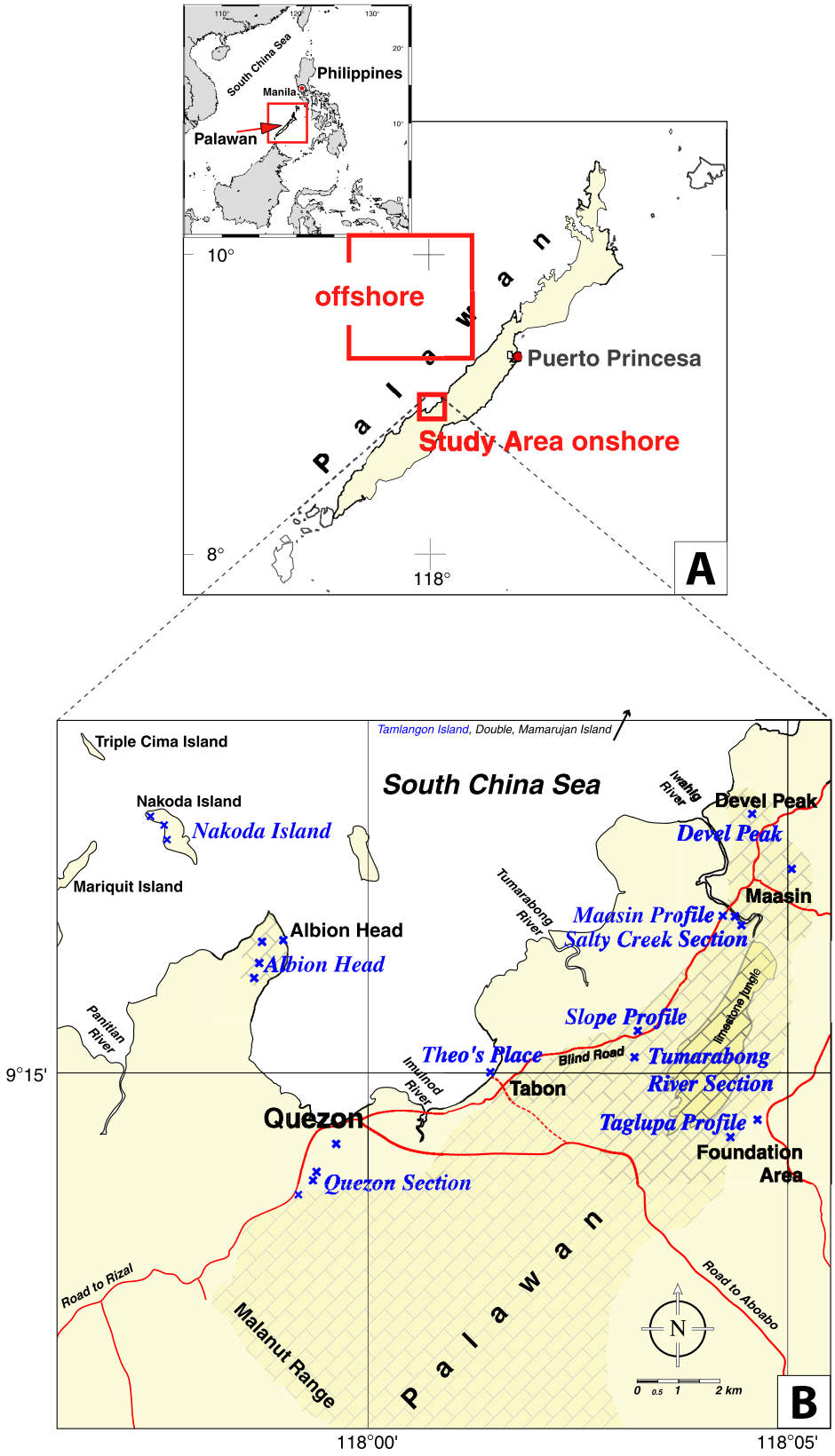

Fig. 4: Map of the Palawan Island in the W of the Philippines indicating the on- and offshore study areas (A); onshore study area around Quezon on the SW coast of Palawan mention the outcorps and names of the studied sites as well as the extension of the carbonate area around Quezon with the standard limestone signature (B).

The **Taglupa Profile** (N 09°14.354', E 118°04.275') was discovered in the E of the study area coming from a road connecting Maasin in the N with the main road between Quezon and Aboabo on the E coast (cf. Fig. 4B: location-maps). The profile was recorded on the northwestern cliff side of a NE-SW orientated ridge at an elevation of ~ 80 m above present sea level. Isolated samples (N 09°14.420', E 118°04.393') of the surrounding area (Foundation Area) were added to the samples of the profile.

The **Salty Creek Section -Maasin Profile** follows the Iwahig River in a sub-parallel direction in the northeastern part of the study area. At the Maasin School and close to the bridge crossing the Iwahig River a side road of about 1-km length branches off to the SE from the northwards running road. This side road passes in the Northeast a part of the strip made up of carbonates. Along this side road, 6 profiles, with an elevation between 5 - 35 m above present sea level, form together the Salty Creek Section:

Salty Creek 1	N 09°16.451', E 118°04.531'
Salty Creek 2	N 09°16.527', E 118°04.442'
Salty Creek 3	N 09°16.629', E 118°04.477'
Salty Creek 4	N 09°16.616', E 118°04.411' -> N 09°16.753', E 118°04.378'
Salty Creek 5	N 09°16.769', E 118°04.352'
Maasin Profile	N 09°16.825', E 118°04.332'

The Salty Creek 1 and Salty Creek 5 are small outcrops created by road-cuts. Salty Creek 2 and Salty Creek 3 were examined at profiles of 5 to 15 m high vertical walls whereas Salty Creek 4 covers outcrops of beds inside the side road itself. The Maasin Profile was studied in the talus of the main road, close to the Maasin School.

The **Tumarabong River Section** was studied at a ~ 20 m high and 150 m long cliff on the NW riverside about 1 km upstream from the Tumarabong River bridge, close to the Tumarabong waterfalls. The section was reached by a trail on the western riverside. The cliff tops a NE aligned ridge, about 40-m above the level of the river. The Tumarabong River Section is based on a 20 m high vertical profile crossing the sequence of the cliff (N 09°15.178', E 118°03.175').

The **Slope Profile** is placed about 400 m WSW of the Tumarabong River Bridge, N beside the main road. A few metres wide valley cuts in N-S direction a small some 100-m elongated

ridge. The NE side of the small valley provides a 28 m long and 12 m high cross section through the carbonate sequence (N 09°15.549', E 118°03.081'; ~ 5 m above present sea level).

Theo's Place is the so-called outcrop of carbonate beds inside the sea at the Tabon Village Resort, Tabon/ Quezon (N 09°14.786', E 118°01.247'; 0 m above present sea level). The study and sampling of the beds were only possible during low tide. The 50 m long and NW orientated section stretches from the beach into the sea, north of the small sea-bridge leading to the artificial island with the restaurant of the resort.

The **Quezon Sections** were reached by leaving Quezon on the road towards the SW. Several small hills or ridges with an elevation of about 60-m above present sea level line up in a distance of approximately 200-m E of the road. On their western and southern flanks layers of carbonates are cropping out and were discovered because of the recently burned grassland. Three separate profiles across the sequences add up to 45 m in thickness:

Quezon Section I	N 09°13.266', E 117°59.141'
Quezon Section II	N 09°13.331', E 117°59.346'
Quezon Section III	N 09°13.517', E 117°59.343'

In Quezon town some single samples were collected at the end of a small road east of the high school of Quezon (N 09°13.571', E 117°59.934'; ~20 m above present sea level).

The peninsula of **Albion Head** defines the western side of the Malanut Bay outside of Quezon. The peninsula is made up of a carbonate formation called ”Tabon Cave Complex”, which is separated from the mainland by mangroves. The complex with a high point (N 09°16.229’, E 117°58.833’) of 203 m above present sea level holds more than 100 caves; of which some have a huge size. Steep flanks and vertical walls, as well as narrow and deep valleys inside the complex determine the morphology. One profile was examined on the S side of Albion Head. These Tarung Profile starts at the Tarung Cave (N 09°15.971', E 117°58.725', 1 m above present sea level) and goes up to an anticline about 100 m above present sea level. Additional sampling was made close to the high point and in the interior part of the carbonate complex. Some loose siliciclastic rocks were also collected SW off the Tabon Cave Complex at Sultan Hill (N 09°16.056', E 117°58.424'; ~10 m above present sea level).

Devel Peak is a small, 168 m high mountain in the N of the study area close to the south-western coast of Palawan (N 09°18.059', E 118°04.633'). It forms the separated north-western part of a 2.5 km long ridge of carbonate rocks leading inland in south-eastern direction from the Treacherous Bay; the south-eastern part of this ridge is called "Eastern Ridge". The morphology of Devel Peak is characterised by a relatively steep south-western hillside and a steep to vertical flank on the north-eastern side. The mount is forested, but not by primary jungle. Around the base of Devel Peak trails pass from the main road in north-western direction to the beach. Additional, a few trails climb up the hill on the NE side, but none approaches the top of the hill. Nevertheless, the complete sequence of Devel Peak from the basis (N 09°18.125', E 118°04.746'; 2 m above present sea level) to the top was studied on the southern side of Devel Peak.

Beside the sites on the island of Palawan, outcrops on the small islands Tamlangon Island in the N, Double Island, Mamarujan Island, Nakoda Island, Triple Cima Island and Mariquit Island in the S were visited. However, the study of the siliciclastic deposits was concentrated on the western sides of **Nakoda Island** (N 09°17.955', E 117°57.425') off Albion Head and **Tamlangon Island** (N 09°21.683', E 118°03.246') N off Devel Peak.

1.3.2 Offshore

The shelf to the W of the islands of Palawan and Busuanga is part of the hydrocarbon province of the South China Sea. Consequently, the oil industry acquired seismic data and a high number of wells were drilled in order to explore the oil and gas reserves. The data set used for the evaluation of the offshore area to the NW off the onshore study area was released by the Department of Energy, Manila. It covers an area from latitudes 9°20' N to 10°05' N and longitudes 117°35' E to 118°10' E. The wells are 40 km (Santiago A-1X) and 75 km (Anepahan A-1X, Penascosa-1) N of Quezon and 45 to 50 km off the western coast of Palawan (Fig. 5). The data set includes information of three wells and some 1,222-line kilometres of reflection seismic.

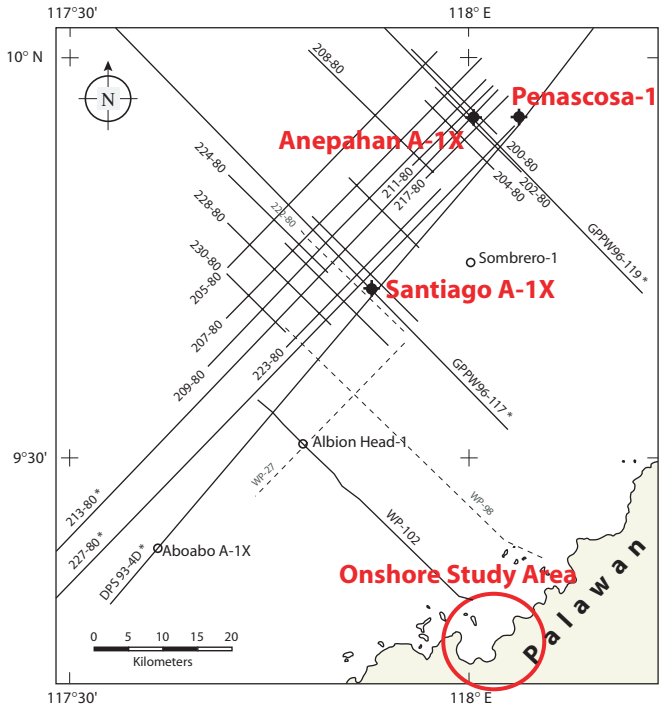

Fig. 5: Location map of the seismic survey provided by the Department of Energy (DOE), Manila. The locations of the wells drilled offshore SW Palawan are indicated, regional lines are annotated with a star.

1.3.2.1 Seismic Survey

The four vintages of the available seismic data NW Palawan were acquired between 1974 and 1996. They add up to 1,222 km (Tab. 1). The majority of the coverage used for the interpretations was shot in 1980.

Survey	Year	Lines	Line kilometre	
			NW-SE	SW-NE
Line 102	1974	1	41.0	
WP 80-Survey	1980	10	170.8	
		8		416.2
DPS 93-4 Line	1993	1		290.0
GPPW 96-Survey	1996	2	304.0	
Sum			515.8	706.2
Total line kilometres				**1,222.0**

Tab. 1: List of seismic line kilometres, provided by the Department of Energy, Manila.

The seismic lines were generally shot perpendicular and parallel to the present-day W coastline of Palawan in NW-SE and SW-NE directions (Fig. 5). N of Quezon the seismic

survey stays about 35 km away the coastline. The conversion of the different scaled seismic lines results in an unique horizontal scale of 1.0 km equalling 0.86 cm for the displays of 1 sec TWT per 5 cm.

1.3.2.2 Wells

Close to the study area in SW Palawan, 6 offshore exploration wells were drilled. The available data set is from the three wells Penascosa-1, Santiago A-1X and Anepahan A-1X (Fig. 6) and includes beside a number of reports the composite logs and biostratigraphy logs of all three wells. Furthermore, the data of some additional borehole surveys (e.g. gamma-ray log, density log etc.) were mainly accessible form Santiago A-1X for this study.

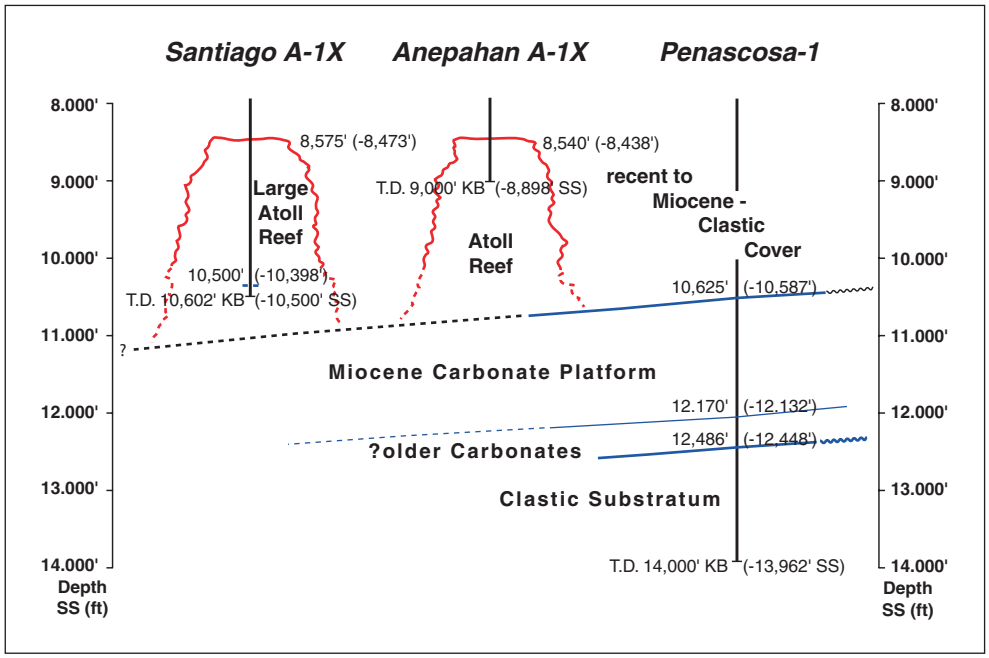

Fig. 6: Simplified sketch of the three studied wells offshore SW Palawan giving the depth in ft KB and ft sub-sea (SS) of the contacts of carbonates to siliciclastics as well as the total depth of the wells.

Penascosa-1

N 09°55'22", E 118°03'49", 77 km N of Quezon

The well was spudded by Champlin Philippines Inc. on June 19, 1975 and completed at a total depth of 14,000 ft. KB (-4,255.6 m Sub Sea) on November 20, 1975. The water depth at the drilling location is 116 ft. (-35.4 m), while the Kelly Bushing (KB) as benchmark for the depth is located 38 ft. above mean sea level.

The Lower Miocene platform carbonates were recovered below a thick section of Pleistocene to Middle Miocene clastics at a depth of 10,625 ft. KB (-3226.9 m Sub Sea) (Fig. 6). The base of the carbonates was reached at 12,486 ft. KB (-3794.2 m Sub Sea). The well was abandoned in Upper to Lower Cretaceous clastics at its total depth.

Santiago A-1X

N 09°42'45.86", E 117°52'25.38", 55 km NNW of Quezon

The well was spudded by Phillips Petroleum Company Philippines on May 7, 1980 and completed at a total depth of 10,602 ft. KB (-3200. 4m Sub Sea) on July, 17, 1980. The water depth at the drilling location is 1,283 ft (-391.1 m), while the KB is 102 ft. above mean sea level.

Below a siliciclastic sequence, the well discovered at a depth of 8,575 ft. KB (-2582.6 m Sub Sea) a Miocene carbonate pinnacle on the SE flank of the Great Atoll Reef. The Great Atoll Reef developed on the Miocene platform carbonates, which was reached (questionably) in the well at a depth of 10,500 ft KB (-3169.3 m Sub Sea). The total thickness of the reef section of the Santiago pinnacle is 1,925 ft. (586.7 m). The underlying platform carbonates are reported on the Composite Log of the well just to be touched at 10500 ft. KB shortly above the total depth of the well of 10,602 ft. KB.

Anepahan A-1X

N 09°55'36.46", E 118°00'6.87", 77 km N of Quezon

The well was spudded by Phillips Petroleum Company Philippines on November 27, 1981 and completed at a total depth of 9,000 ft. KB (-2712.1 m Sub Sea) on January 26, 1982. The water depth at the drilling location is 1,453 ft. (- 411.8 m), while the KB is 102 ft. above mean sea level.

The well was drilled on an isolated pinnacle reef structure, which continued its growth on the underlying carbonate platform. The contact between the overlying siliciclastics and the carbonates is penetrated at a depth of 8,540 ft. KB (-2571.9 m Sub Sea). Down to the total depth, the drilled reef section of the well adds up to 460 ft., (140.2 m).

2. Material and Methods

2.1 Logistics

The Philippine Carbonate Study is a co-operation project of GEOMAR, Research Center for Marine Geosciences, Kiel/ Germany, CEREGE, Centre Européen de Recherche et d'Enseignement de Géosciences de l´Environnement, Aix-en-Provence/ France and TOTALFINAELF Oil Company, Paris/ France. Dipl.-Geol. Stefan K. Rehm has carried out all together three trips to the Philippines on behalf of the Philippine Carbonate Study between 1999 and 2001. In the first year, a three-week management trip for logistic arrangements and the selection of the study area was made. From 20th of February to 15th of May 2000 the first and from 03rd of March to 22nd of April 2001 the second field campaign to the Philippines took place.

The journeys to the Philippines were without any remarkable complications. The political situation on Palawan seemed to be relatively stable during the two field campaigns in the year 2000 and 2001. The risk of kidnapping seemed not to exist, in contrast to the situation on Mindanao, where the political situation prevented the visit of the Miocene carbonate area around Cagayan de Oro in the year 2000. The roads on Palawan demand a 4x4 car, electricity breaks down frequently, international calls are complicated and internet access was only provided in the main town Puerto Princesa.

All outcrops were accessible from the car in a walking-time not longer than half an hour or by boat (Albion Head). Nevertheless, sometimes tangly jungle had to be passed and steep to vertical walls made it complicated or impossible to approach the top of the sequences. In some cases, climbing equipment was used.

During the first field campaign 2000 logistic support was provided by Supply Oilfield Services, Inc., Manila (SOS). During the second field campaign 2001 all logistic arrangements like permits (e.g. working permit for the area of Albion Head), field assistance, car and boat hire as well as the shipment of samples were arranged independently based on the contacts and experiences made in the years before.
The Tabon Village Resort in Tabon Village/ Quezon was the base camp during both the field campaigns.

2.2 Field work

The study of the Miocene carbonates in SW Palawan ground on a classical fieldwork during 2 field campaigns in the years 2000 and 2001. Before these campaigns, the study area had to be defines. This was done after the first visit on the Philippines in the year 1999 with many different discussions at the University of the Philippines (Manila), the Mines and Geosciences Bureau (Manila and Cebu City) and the Department of Energy (Manila). Different sites were visited on Luzon, Cebu as well as on Palawan. Due to the political situation, it was refrained from the visit on Mindanao in the area around Cagayan de Oro. The accessibility of the Miocene outcrops, the number of different paleoenvironments (platform vs. reef), the option to get an extended offshore survey nearby and the logistic situation were the main factors for the selection of the study area around Quezon. The study of aerial photographs and the daily expeditions in the field result in the discovery of the different new outcrops, beside the already known carbonates of Albion Head and Devel Peak. The sampling was made in order to collect representative sample material of the different lithofacies across an assumed stratigraphic section. The mainly hand-size samples were taken orientated, while an arrow indicates the upstrata direction. Each sampling point was marked in the field with a red (2000) or blue (2001) point. Perpendicular to the basis of the beds each outcrop was measured so that finally the total thickness of the sedimentary sequence could be calculated by adding the measured thicknesses. Gaps were measured horizontal in order to estimate the thickness of the strata by using the trigonometric function of horizontal distances and the angle of dipping. The orientation and the dip of the bedding were measured with a "Freiberger Gefüge Kompaß". Location were defined by using a Garmin Etrex GPS instrument.

2.3 Facies Analysis

The facies analysis refers to the principle that the collection of sediment-petrographical, paleontological and textural features, macroscopic and microscopic, reflects the paelaeoenvironmental conditions at the time of the development of the rocks (FLÜGEL, 1978). The macroscopic descriptions combine field observations regarding the lithology and observations made at the cut rock samples. The microscopic proceeding is based on 613 30 μmm thick thin section of a size of 3 x 4.5 cm. 19 thin sections of lager size supplement the batch. The description of a thin section follows a working sheet. The sheet summarise the composition of the skeletal grain and non-biogenic components, the texture, structure and the

grain size of the rocks as well as diagenetic features. The assemblage of the skeletal grains differentiate larger foraminifera, divided into 9 families, small benthic and planktonic foraminifera, red and green algae, branching corals, head corals, bryozoans, echinoderms, bivalves/ oysters and gastropods, brachiopods, ostracods as well as serpulids. The portion of each component was estimated semi-quantitative based on the comparison charts for frequency estimation of FLÜGEL (1978, p. 155-165). The existence of a component was recorded with 1, wherase 5, 10, 25, 50, 75 and 100 document the content of a component at the whole thin section. The textural and structural as well as the diagenetic features and cements were classified as missing or poor (0), rare or moderate (1), a few or well (2) and abundant or excellent (3). The relationship of the 3 different grain sizes micrite, arenite and rudite adds up to 100%. Additionally, the ratio between micritic and sparitic matrix, components and matrix as well as bioclasts and biomorpha are indicated with 1:9, 5:5 or 9:1. Finally, the carbonate rocks were classified after DUNHAM (1962) with modifications of EMBRY & KLOVAN (1972) (in FLÜGEL, 1978, p. 301).
The documentation in kind of photographs was made with the digital camera "AixioCam" of Zeiss as well as an Olympus camera.

2.4 Total Carbon Analysis

The number of 441 samples was prepared for the total carbon analysis with the CARLO ERBA Elemental Analyst Model NA 1500 CN. Therefore, a representative piece of about 15 g was cut of the field sample. It was cleaned with dest. H_2O, dried with pressure air and by a temperature of 60°C and finally ground with an agate ball mill to a homogeneous powder. Afterwards, between 3,5 to 6,5 mg of each sample were tared and filled into a small tin container.
The instrument analytical method of the total carbon (TC) is based on the complete and instantaneous oxidation of the carbon in the sample by „flash combustion" at 1050°C. A constant flow of Helium (carrier gas) carries the combustion products (N_2, NO_x, CO_2, H_2O, SO_2 and SO_3) through a reduction furnace into the chromatographic column, where the gases are separated and detected with a thermal conductivity detector (TCD). The TCD provides an output signal proportional to the concentration of the individual components of the mixture. The raw data are a number of counts.

The calibration for each set of samples (n = 50) grounds on 6 standard measurements (Acetanilid: N = 10,36%, C = 71,09 %) and 3 blanks. Each of the measured standard material should have a different weight between 0,2 mg and 1,5 mg in order to calculate the gradient of the linear distribution. This is necessary for the statistical analysis of the data and later the calculation of the $CaCO_3$ content in the sample. To solve the equation, which yields finally the TC content of a sample, the detected counts were corrected by the subtraction of the average value of the 3 blank measurements. These corrected counts were divided by the value of the linear gradient of the 6 standard measurements, which results in the amount of μg C. The output of the division of μg C and the weight of the analysed sample material in mg, again divided by 10, provides the TC of the sample in percentage. With the assumption that no or minimal organic carbon is included in the sample material, the multiplication of %TC with 8,333 results in the weight percentage of $CaCO_3$ of the whole rock.
With respect to the lithology and the preservation of the carbonate samples, only the first set of 20 samples run as duplicate measurements. In this study, the content of $CaCO_3$ used as indicator for the non-carbonate (siliciclastic) proportion in the samples. The exact quantification of the TC is of less interest, rather than general trends should supplement the study of the development of the carbonate sequences.

Operating Parameter for TC/N analyses

- Oxidation furnace temperature 1050°C
- Reduction furnace temperature 650°C
- GC column oven and detector block temperature 75°C
- Filament temperature 190°C
- Helium carrier gas flow rate (main) 80 ml/ min
- Helium carrier gas flow rate (reference) 40 ml/ min
- Oxygen flow rate 25 ml/ min
- Total analytical time 240 sec.

Reactor packing for TC/N

- Combustion reactor: Chromium Oxide/Silvered cobaltous cobaltic oxide
- Reduction reactor: copper

2.5 Structural Analysis

The structural analysis of the sedimentary deposits around Quezon grounds on the measurements of the orientation and the dip of sedimentary surfaces at 24 spots as well as on aerial photographs in a scale of 1:25.000. The few field observations of structural elements are a result of the strong karstification of the carbonates and the mostly dense cover of vegetation. The litho- and biostratigraphy and facies correlations supplement the evaluation.
The orientation and the dip of planar surfaces were measured with a "Freiberger Gefüge Kompaß". The data of the different sites are separately presented as pole-points in the low-hemisphere, equal-area projection (“Schmidt’sches Netz”) (SCHMIDT, 1925). All collected data are checked regarding their quality with respect to the general context of each measurement and if the single measurement is representative for the site. This procedure results in a selection of 270 measurements, each of it representative for its spot. With the differentiation of the collection spots, a statistical analysis of these data (Gaussian distribution) was made.
All calculations and illustrations regarding the data analysis were generated by using the TectonicVB (PPC) 1.4a program.

In the context of field observations like vertical or steep cliffs or facies discontinuations, lineaments were mapped on a set of 14 aerial photographs (1:25.000). It results in a net of lineaments, which were then grouped by their azimuth and eventually their types of displacements. Based on this interpretation, different fault systems were distinguished and the necessary stress regimes were deduced from their relationship to each other. Sometimes, only the identification of the relationship between a lineament and a special stress regime allowed the characterisation of the types of displacements.

2.6 $^{87}Sr/^{86}Sr$ & X-ray Diffractometry

Four samples found in the carbonate area around Quezon have been prepared for the $^{87}Sr/^{86}Sr$ analysis. The sample materials (0,0148 g and 0,0144 g) of the two samples B-33 and SP-96 from Devel Peak were drilled from two different fragments of an oyster shell. The bivalve of sample L1-13B from Devel Peak was cleaned from surrounding carbonate sediment and a coating of weathered material before 0,2959 g of the shell was broken off. A piece (0,2513 g)

of the macroscopically well-preserved bivalve (T-d1), which was associated at the Tumarabong River Section with a speleothem crust, was only cleaned superficially.
To qualify the present-day carbonate modification of the primary aragonitic mineralogy of the bivalve from the Tumarabong River Section (T-d1) the X-ray diffractometry (XRD) technique has been used.

$^{87}Sr/^{86}Sr$

The sample material for the $^{87}Sr/^{86}Sr$-analysis was mechanically cleaned and washed with double-distilled water. Representative splits were selected and twice dissolved with 0.46 N HCl. Based on leaching experiments (Eisenhauer, pers. comm.), this acidity was chosen to assure complete reaction of the carbonate phase at a negligible level of Sr contribution from potentially incorporated detrital silicates. From aliquots (20 to 50 μl) of the double-centrifuged solutions (2-ml) Sr was chromatographically extracted and purified in two subsequent runs on standard Dowex cation exchange resin (2.5 N HCl calibrated chemistry). Sr-isotope composition was measured with Re-double filament technique on a Finnigan MAT 262 RPQ+ in static mode. 100 to 200 ratios were collected for each measurement, which resulted in a within-run precision of better than 0.000010 (2 SE) of the $^{87}Sr/^{86}Sr$ value for most of the samples. During the whole procedure Sr blank was determined to a maximum value of 500 pg. However, sample sizes are sufficiently large (approx. 1 μg of Sr) that blank corrections are negligible. External reproducibility was monitored by measurements of the standard NIST 987. The measured values (0.71025 +/-7) agree with the certified value of 0.71034 +/-26.

Two measurements of the standard NBS 987, one analysis of the standard before, the second after the sample analysis, were within the laboratory variance. Therefore, no further correction of the data is required (Tab. 2).

Sample	Measurement	Standard Deviation
NBS 987; #1	0,710256	3e-006
NBS 987; #2	0,710246	4e-006

Tab. 2: Measurements of the $^{87}Sr/^{86}Sr$ NBS 987 standard. #1 was measured before, #2 after the analysis of the sample material.

For comparison with the MCARTHUR et al. (2001) database for strontium isotope stratigraphy (SIS), the presented data are corrected for interlaboratory bias to a NIST 987 value of 0.710248 (MCARTHUR et al., 2001). For the chronostratigraphic correlation (mean SIS-ages in Ma) an external precision of 0.000030 (2 standard deviations) is applied on our data set. This value is the long-term reproducibility of repeated measurements of the NIST 987 standard. In combination with the statistical error of the MCARTHUR et al. (2001) data base, the presented maximum SIS-age range could be deduced for each sample analysis.

X-ray Diffractometry

The sample preparation for the XRD-analysis starts with the careful drilling of the sample material (T-d1). In order to receive a homogeneous powder of the sample, it was ground by hand in an agate mortar for four minutes. The procedure of grinding are required to provide an optimal peak intensity for the XRD-analysis (MILLIMAN, 1974). Each sample was pressed afterwards into an aluminium sample holder. A Phillips PW 1700 X-ray diffractometer with a Cobalt K-alpha tube was used at 40 kV and 35 mA. The sample was scanned with a scanning speed of 0.01° per second from 20° to 40° (°2Θ). The generated X-ray diffraction file was prepared to analyse the presence of aragonite and calcite. The program MacDiff 4.2.5 was used to determine the amount of calcite and aragonite within the sample by the measurement of the peak area (MILLIMAN, 1974; PETSCHICK, 1996).

2.7 Stable Oxygen and Carbon Isotopes

The stable oxygen and carbon isotope signatures were analysed for 92 isotopic samples from 68 carbonates of the onshore study area in SW-Palawan. The number of 58 rock samples provides 35 spots of sparite cement, 26 spots of undefined sparite and 12 spots of micrite, which were big enough to drill with a 0.5 mm dental driller by low revolutions per minute under a microscope between 8,4 μg (which could be critical) to 151.9 μg of the characteristic carbonate. Before the drilling process the spots were mechanically and with high pressure air cleaned. After the drilling the small bore hole were controlled in order to check, if no surrounding material contaminated the isotopic sample. For the analysis of the 19 bulk samples between 566.1 - 113.6 μg of the homogeneous carbonate sample powder, which were already prepared for the total carbon content analysis (cf. chapter 2.4), were used.

The analytic proceeding run on a Finnigan MAT 251 mass spectrometer installed at the Leibniz Laboratory for Radiometric Dating and Stable Isotope Research, Kiel/ Germany. The instrument is online coupled to the Carbo-Kiel device (Internationally: Kiel Device I) for automated CO_2 preparation from carbonate samples for isotope analysis. The digestion of the carbonate samples was triggered by adding 100% ortho-phosphoric acid at 73°C in a vacuum. The weight of the sample material may range between 10 μg to about 600 μg.
External accuracy (on the δ scale) is ±0.05‰ for carbon and ±0.08‰ for oxygen isotopes. The results are calibrated by using the Carbonate Isotope Standard NBS 20 of the National Institute of Standards and Technology (Gaithersburg, Maryland) and reported on the Pee Dee belemnite (PDB) scale. The reproducibility was checked by replicate analysis of internal reference materials with $\delta^{18}O$ = -4,85‰ PDB and $\delta^{18}O$ = +2,45‰ as well as the NBS 19 stable isotope reference material ($\delta^{18}O$ = -2,20‰ PDB).

2.8 Cathodoluminescence Technique

At the "Centre Scientifique et Technique" (CST) of TOTALFINAELF, St. Rémy lès Chevreuse the cold cathodoluminescence facility on an Olympus BH-2 microscope with x2.5, x5, x10, x20 lenses and a Photonic Science camera system of TOTALFINAELF were used to create 82 cathodoluminescence images. Additionally, to each cathodoluminescence image the associated images of normal and polarised light has been made. With respect to the occurrence of different cements, the detailed study was limited to eight uncovered carbonate thin sections from Devel Peak, Tumarabong River Section and Theo's Place.

Analytic parameters:

Microscope:	Olympus BH-2
Video camera:	Photonic Science
Regular board	Citl CCL 8200Mk4
Lenses/ Magnification:	IC x5 MD Plan 5
	IC x10 MD Plan 10
	IC x20 MS Plan 20
	(x2.5, Plan-Neofluar, Zeiss)
Gun Type:	cold cathode gun
Gun Energy:	16.8 kV
Gun Current:	~ 441 μA
Ambient Gas:	residual gas
Vacuum:	18.7 – 22.4 mbar

Integrated Time:	2.00 – 3.00
Wait(s).	0
ALC:	on
Gain:	12 – 18 dB
Shutt.	1/100
Thin section thickness:	~ 30 μm
Thin section surface:	smooth polished

2.9 Proceeding of Offshore Data

Seismic

The seismic surveys ground on different acoustical impedances of different sequences. Consequently, the character of each sequence (respectively lithology, pore fluid) results in different intervals velocities, whereas the seismic lines are the documentation of the record. The details of the acquisition, processing and original display parameters of the seismic survey are shown on Table 3.

		Line 102	WP80-Survey	Line DPS 93-4	GPPW 96-Survey
Acquisition Parameter					
Date of Acquisition		June 1974	July 1980	January 1993	July/ August 1996
Company		GSI	Western	Digicon	Geco-Parakla
Energy Source					
Source		Airgun	Airgun	Airgun array	Airgun
Gun Depth	[m]	7.6	5.5	6.0	7.0
Volume	[in2]	1,200		4,590	
Pressure	[p.s.i.]	N.A.	N.A.	1,900	2,000
Shot Point Intervals	[m]		33.33		
Receiver Arrangements					
Streamer Depth	[m]	9.75	12.0	8.0	7.0 - 8.0
Streamer Length	[m]	2,400	3,451	3,575	5,400
Geophone (Groups)		48	96	96	96
Instrumentation					
Record Length	[s]	6	6	7	8
Sample Rate	[ms]	4.0	2.0	2.0	2.0
Recording Filter					
Low Cut	[Hz / db]	8 / 18	N.A.	3 / 6	3 / 18
Hig Cut	[Hz / db]	62 / 72	N.A.	160 / 72	180 / 70

Continuation next page

Processing Parameter	Common Depth Point Stack	FK Migration	F-X Migration using smoothed stacking velocity	Space Frequency Migration
Display Parameter				
Vertical Scale [in/s]	3.75	3.76	-	-
[cm/s]	9.53	9.53	5	5
Horizontal Scale	1 : 15,748	1 : 31,348	1 : 50,000	2 : 50,000
	50 SP = 5 km	150 SP = 5 km	200 SP = 5 km	200 SP = 5 km
Polarity		Black = negative	Black = negative	Trough = negative
Datum Plane	Sea Level	Sea Level	Sea Level	Sea Level

Tab. 3: Acquisition, processing and original display parameters of the seismic survey made available by the Department of Energy, (DOE) Manila offshore W Palawan.

The seismic lines of the four different surveys were displayed at various scales. Therefore, the vertical scales of 1 sec two-way-travel-time (TWT) was converted to 5 cm. The horizontal scales of the WP 80-survey, which comprise the main coverage of the studied area, were squeezed to 50 % of their original length and the scales of the DPS 93-4 and the two lines of the GPPW 96-survey were adjusted accordingly. The resulting horizontal scale for all surveys was 1.0 km equalling 0.86 cm for the displays of 1-sec. TWT per 5 cm.

With the exception of the WP 80-survey, a detailed location map was provided for the available lines by the Department of Energy (DOE), Manila. The run of the WP 80-survey was, therefore, constructed based on the shot point locations of the various line intersections. Slight inaccuracies might occur, but are considered to be of minor importance and do not affect the general interpretation.

Correlation between Well Sections and Seismic Horizons

The connection between the lithological/ stratigraphical sections drilled by the three key wells and the seismic lines bases on the time/ depth relations. It was derived from the velocity information, which are given on the composite logs of the three wells as follows:

Penascosa-1: Integrated Travel Times – ITT
Santiago A-1X: Corrected Check Shot Times
Anepahan A-1X: Corrected Check Shot Times

The Integrated Travel Times of Penascosa-1 were taken from the sonic logs recorded between 560 and 13,860 ft. (KB), added and adjusted to the mean sea level. The Check Shot Times of

Santiago A-1X and Anepahan A-1X bases on the integration of the well velocity surveys and the sonic logs, which were corrected to the mean sea level. Finally, a time/ depth curves of each well were constructed (Fig. 7), whereas the time is given as two-way-travel-times in sec. and the depth in metres. The interval velocities of Penascosa-1 and the wells Santiago A-1X and Anepahan A-1X are different throughout the overburden clastic section down to the top of the Miocene carbonates. The higher interval velocities at the Penascosa-1 location are caused by shelf edge carbonates and coarser grained clastics, while the lower interval velocities in the wells Santiago A-1X and Anepahan A-1X are caused by fine grained turbiditic clastics deposited off the shelf into the deeper water environment.

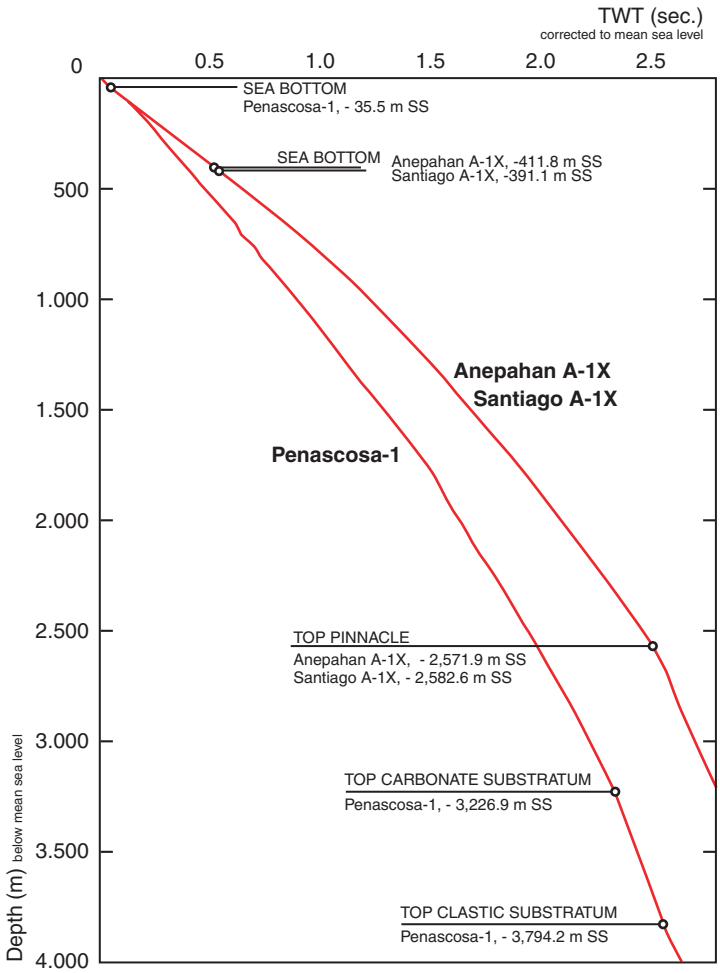

Fig. 7: Time/ depth correlation indicates velocities within the three wells constructed from the Integrated Travel Times (Penascosa-1) and the Corrected Check Shot Times (Santiago A-1X, Anepahan A-1X).

The conversion of the seismic reflection times into sub-sea depths in the present-day deeper water area off the shelf of Palawan around the sites of Santiago A-1X and Anepahan A-1X

grounds as well on the time/ depth relation. On the shelf around the site of Penascosa-1 the Interval Transit Travel Times were used to calculate for the entire section the interval velocities of individual sequences. The resulting curve was directly correlated with the two seismic lines DPS 93-4 and WP 227-80 shot in the immediate vicinity of the well location (Fig. 8). The tie between seismic reflections and interval velocities is obvious and the quality of the correlation has to be considered as reliable.

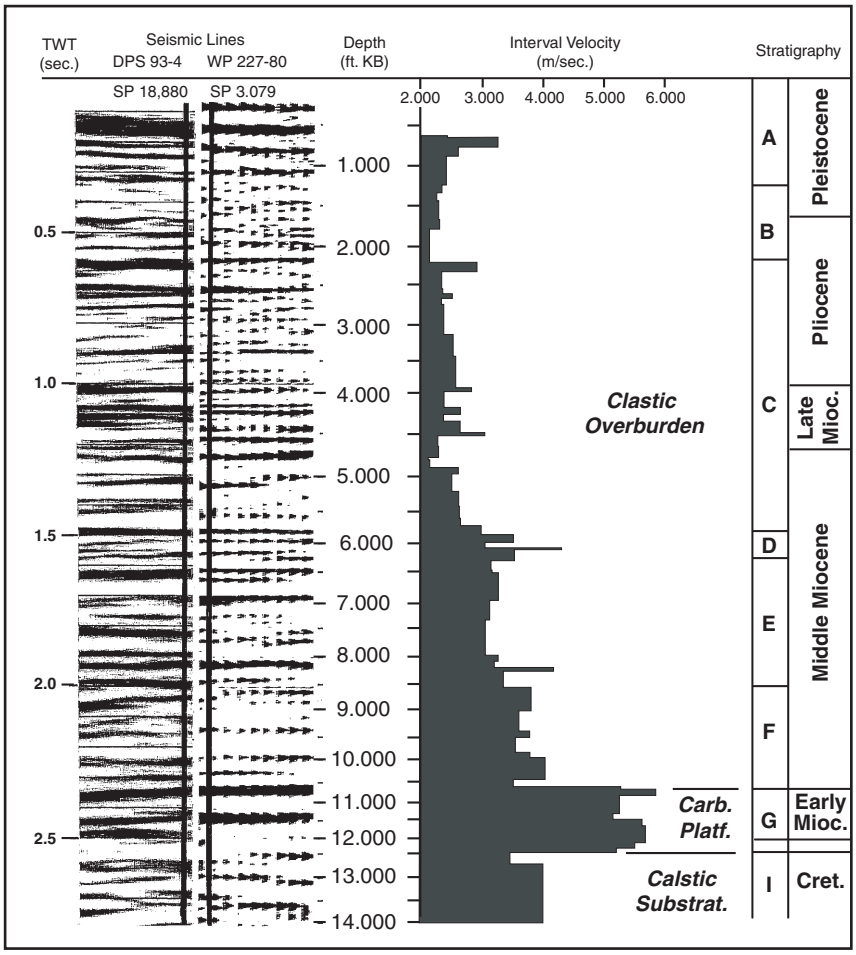

Fig. 8: Conversion of Two Way Travel Time in seconds (s TWT) to ft below KB by using the Internal Velocity time in m/ sec. supplemented by the correlation to the simplified stratigraphy.

3. Principle Database: Onshore

3.1 Facies Analysis

Introduction

The results of the facies analysis present the field observations connected with the study of more than 550 thin sections. A detailed study of the larger foraminifera association and a focus on the development of the corals at Devel Peak, as well as the estimation of the terrestrial content in the carbonates supplements the database.

The collages of different sites allow the examination of the development of the shallow water carbonates in time and space. The tectonic survey indicates no significant displacements influenced the sedimentary succession recorded in the study area (cf. chapter 3.4 Tectonic). Therefore, based on the field observations and the constant dipping of the strata to the NW, we are coming up with the following lithostratigraphic succession: The Taglupa Profile in the Foundation Area documents the lowermost carbonate deposits. The Salty Creek Section up to the Maasin Profile provides the outcrops of the overlying carbonates deposits. The Tumarabong River Section, the Slope Profile and the Iwahig River Profile are additional section within the carbonate succession, which supplements information regarding the lateral extension throughout the study area of the development. The outcrop located at Theo's Place and the Quezon Section are interpreted as the uppermost deposits in the succession of the lateral extended carbonates around Quezon, further upstrata from Maasin Profile. The build-ups of Devel Peak and Albion Head were formed after the carbonates discovered S and E of Quezon.

3.1.1 Foundation Area and Taglupa Profile

The area on the eastern side of the limestone jungle and therefore in the SE of the study area are called Foundation Area (cf. Fig. 4). The deposits in this area are made up of thin-bedded red-brownish weathered shales, silts or fine sands. Neither on the macroscopic nor on the microscopic scale, marine components are observed, whereas a very fine content of plant debris suggests a terrestrial origin of the siliciclastic deposits. The deposits are dipping with an average of 16° to eastern directions.

The Taglupa Profile is one spot in the Foundation Area providing a carbonate sequence of 15 m in total thickness (Fig. 9), which was studied along the base level of a 30-m high cliff. This

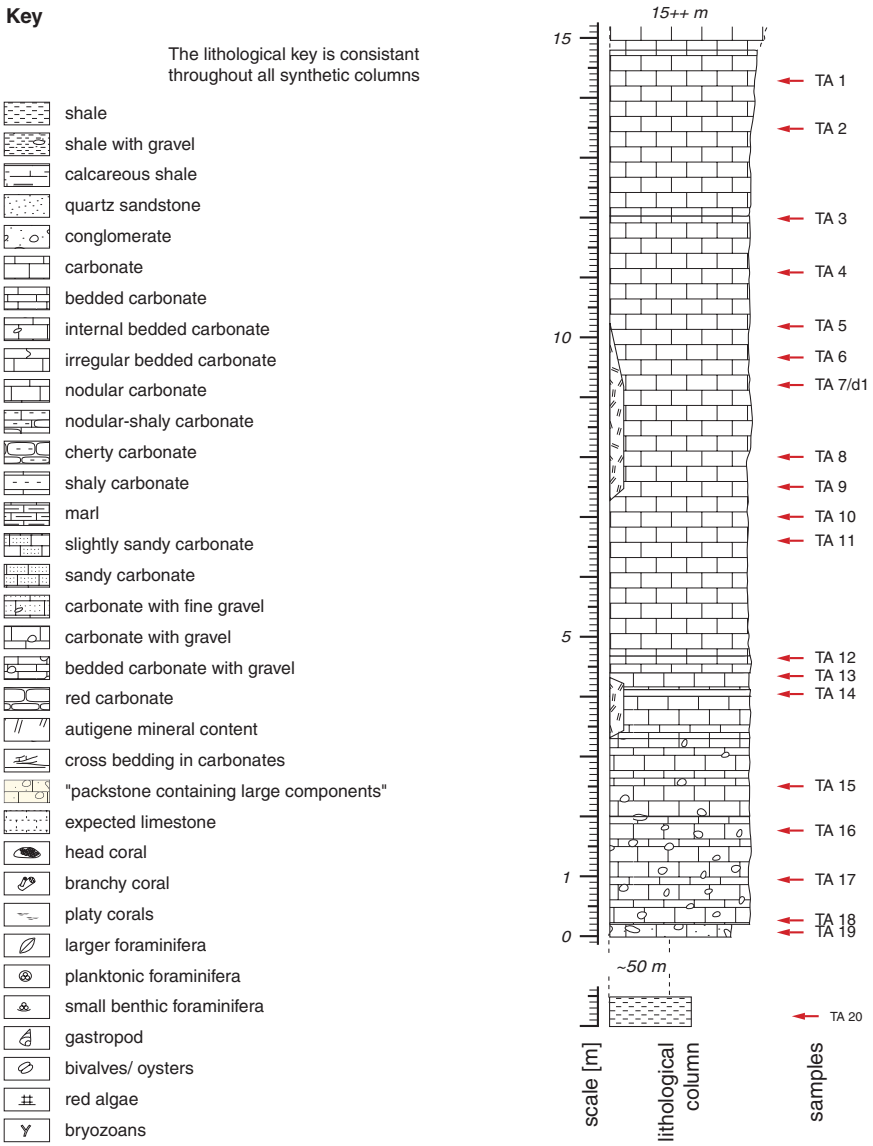

Fig. 9: Synthetic column of Taglupa Profile with sample positions as well as the key for all following columns.

cliff overlies, on top of a NE-SW elongated geomorphological ridge, the siliciclastic deposits of the Foundation Area. The underlying shales are cropping out 50 m below the base level of the cliff at the NW flank of the ridge, so that their contact is not accessible in the field. Even if the dip of the carbonates with an average of 17° seems to correspond with the underlying shales, the orientation of the carbonates with an azimuth around 234° (in contrast to an average of 97° for the shales) indicates obviously an angular discontinuity between the siliciclastic and the overlying carbonates.

The massive, white weathered carbonates of the cliff show some recent karst holes, which are in general of cm to dm size, but can also reach a few meters in size. The holes are partly filled

with speleothems. The lowermost 2-m of the sequence are rudstones, whereas the overlying carbonates classified as grain- to packstones. At the basis of the section skeletal grains and intra-/ extraclasts occur at equal proportions (Fig. 10). All gravels of igneous rocks, sandstones and carbonates (wackestones and rudstones) are rounded to well-rounded. The millimeter-sized quartz grains are sub-rounded to rounded. The gravel and quartz content as well as a fine debris of terrestrial plants decreases upwards, so that gravels were not observed higher than 3 m above the base level. The skeletal grains are dominated by molluscs (bivalves, oysters) and bryozoans, beside red algae (*Aethesolithon*, *Jania*) and some echinoderm fragments. Brachiopods are generally rare. Some corals observed in the lowermost strata before they become rare upsection. The larger foraminifera content increases upwards. The first observed Nummulitidae 1 m above the base level follow their consequent increase up to a level 7 m above the basis. Within the overlying 3-m Nummulitidae disappear nearly completely. Therefore, Amphisteginidae appear in the upper part of the section together with Acervulinidae. Some single specimens of Alveolinidae are found in the grain- to packstones whereas Soritidae occur only in two upper samples close to the top. Planktonic foraminifera, small benthic foraminifera and ostracods are not discovered throughout the whole sequence. Some peloids occur in the upper part of the sequence.
The quality of the sorting increases already inside the rudstone levels, which corresponds to moderately pronounced internal bedding. Finally, it comes up to a moderate sorting in the grain- to packstones. The occurrence of sutured or concave/convex contacts of the components decreases, even if the compaction increases slightly (broken components, stylolites). The brownish colour of most of the carbonates in the upper part of the section suggests an impregnation by iron-rich fluids. Partly, biogenic fragments are phosphatized. The internal structure of some oyster fragments is still preserved. In contrast, many of the skeletal grains were exposed to strong solution, recrystallisation or, especially in the uppermost 3 m of the section, to the conversion into microsparite like the red algae. Additionally, some early destructive mechanisms like the boring activity of organisms are observed. Geopetal structures are common.

The total carbon content (TCC) record of the sample collected in the Foundation Area and at the Taglupa Profile illustrates a rapid increase of the TCC (Fig. 11). The calculated content of $CaCO_3$ in the basic shales, siltstones and fine sandstones show a range between 1 to 5% of $CaCO_3$. The lowermost carbonates collected within the first 2 m of the Taglupa Profile (up to

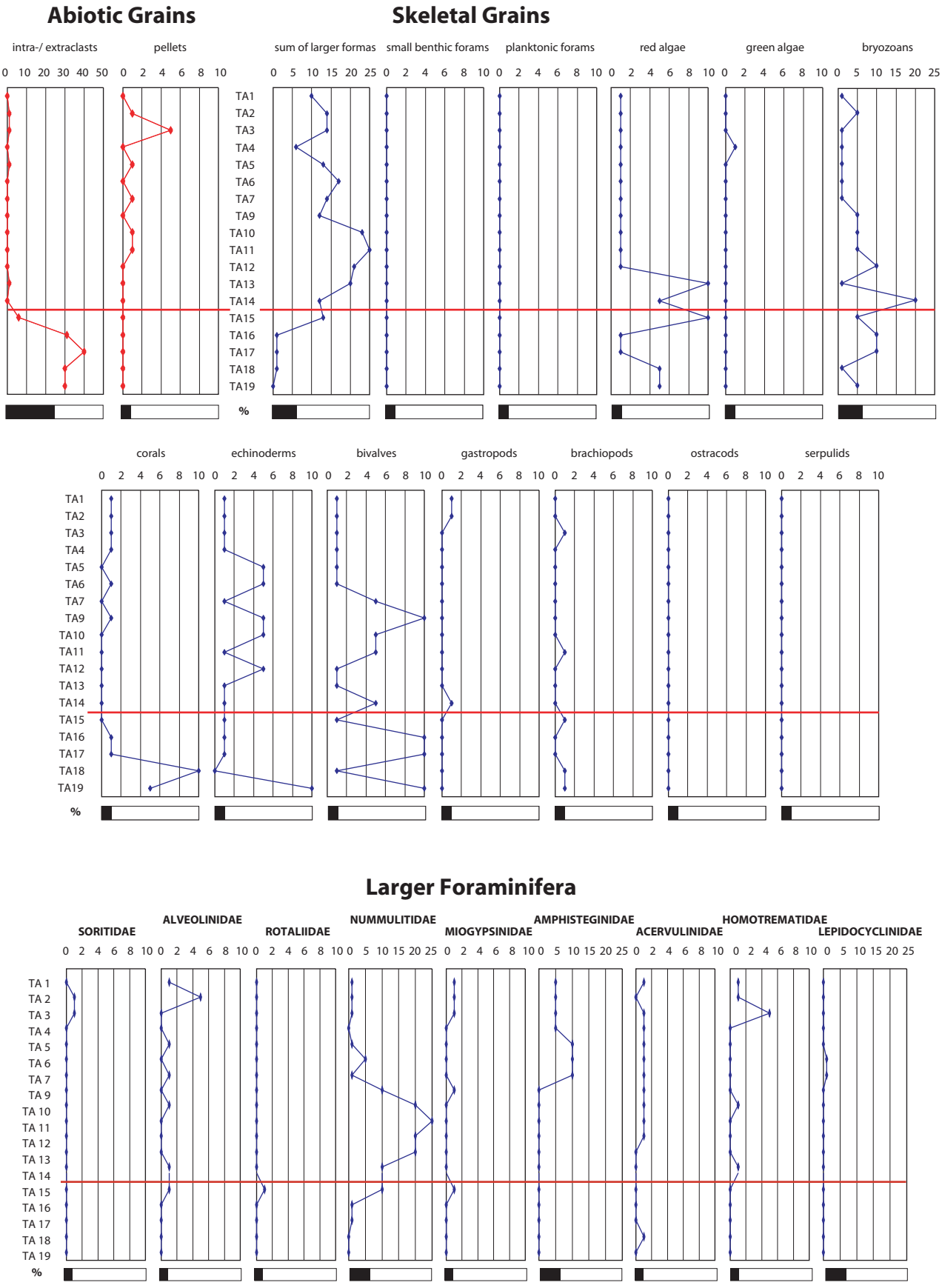

Fig. 10: Semi-quantitative frequency estimation of common skeletal grains, intra-/ extraclasts, pellets and larger foraminiferal assemblage in the samples of the Taglupa Profile reflecting their development upstrata throughout time.

sample 16) yield a $CaCO_3$ content of less than 85%, which is related to the siliciclastic content. Form sample TA15 upstrata the $CaCO_3$ content is always higher than 94% and without major variances throughout the profile.

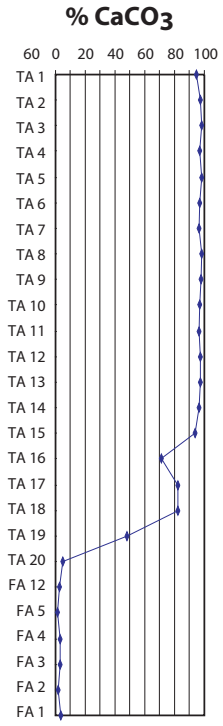

Fig. 11: Calculated $CaCO_3$ content in the samples from the Foundation Area and of the Taglupa profile upstrata.

Excerpt: The lowermost sediments in the study area are represented by the shales, silt- or fine sandstones of the Foundation Area, which are overlain with an angular discontinuity by the rudstones and later pack- to grainstones of the Taglupa Profile. A high content of terrestrial gravel and quartz as well as fine plant debris within the first meters of the carbonate section decreases rapidly upwards. Larger foraminifera become dominant in the assemblage of the skeletal grains, whereas the different biogenic components show a high variance concerning their portion. Therefore, the sedimentary record documents the establishment of carbonate deposits in a marine environment close to a landmass without a pronounced open marine influence.

3.1.2 Salty Creek Section - Maasin Profile/ Iwahig River

The succession of the Salty Creek Section up to the Maasin Profile was studied at the 6 separate outcrops Salty Creek 1 to 5 and the Maasin Profile. The total thickness of the sequence adds up to 215 m. Based on the different characters of the sedimentary record and facies changes, the succession was divided into 3 sequence A, B and C (Fig. 12). Sequence A, 57 m thick, is based on the outcrops of Salty Creek 1 and the lower part of Salty Creek 2. It is characterised by the alternation of massive carbonates and marine shales. A significant packstone layer with larger components marks the contact between sequences A and B. Above this contact, well-bedded pack- to grainstones represent Sequence B in the upper part of the Salty Creek 2, 3 and 4. Together they add up to a 73-m thick succession. The deposits of the last sequence (Sequence C), about 85-m thick, are characterised by fine carbonates with a low fossil content and some intercalations of thin-bedded shales. These deposits were found in the outcrops of Salty Creek 5 and the Maasin Profile, although these outcrops provide only

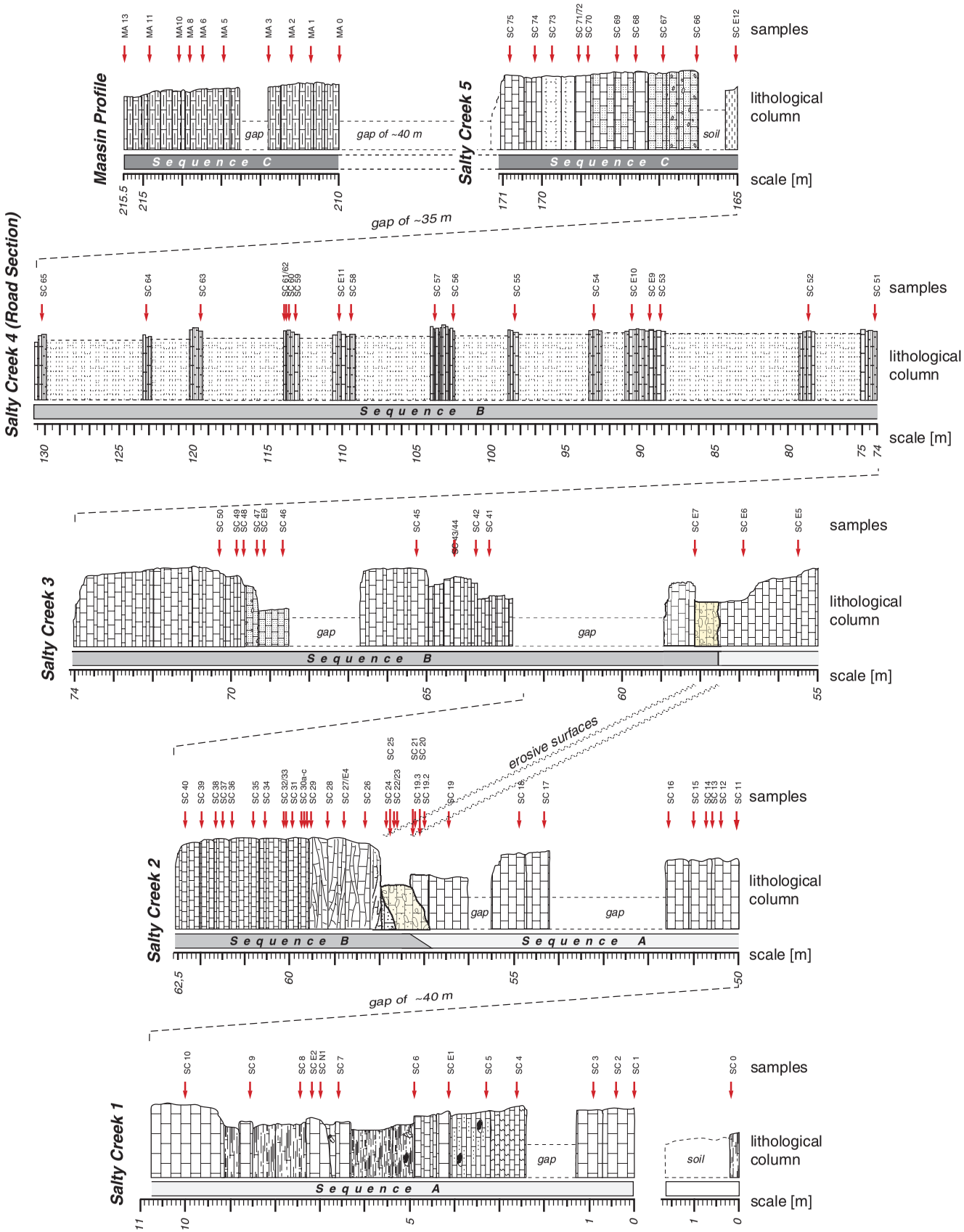

Fig. 12: Synthetic column throughout the whole Salty Creek Section - Maasin Profile with sample positions and estimated thickness of gaps. Three sequences of carbonate development are illustrated; the significant horizon of the "packstone containing larger components" is coloured.

10 m of the sequence. However, additional samples were collected parallel to the upper part of the succession at the eastern side of the Iwahig River nearby and supplement the information concerning the upper part of the Salty Creek Section - Maasin Profile.
The composition of the skeletal grains and the larger foraminiferal assemblage illustrates as well the lithological development (Fig. 13.1-3).

Sequence A

The lowermost outcrop of the Salty Creek Section was found in a small creek SE in the vicinity of the profile Salty Creek 1. A 40-cm thick outcrop of the cm-thick bedded claystones to siltstones is superposed by 1.45 m of soil. A little terrestrial plant debris is observed in the siliciclastic deposits, whereas microfossils seem to be absent.
About 20 m above the creek, the first massive carbonate layers marks the basis of the Sequence A in the Salty Creek 1 profile (Fig. 14). A road cuts through the most southern SW-NE striking ridge and produces the 25.5-m long S-N stretching profile on top of it. The layers dip to the NNW with 9-18° and come up to a thickness of 10.7 m of the succession. The exposure of shaley lithologies within the section to tropical weathering resulted in some young soil horizons and therefore potential gaps in the lithological column. Beside marine shales, up to several dm thick massive floatstones to wackestones dominate the carbonates of the Salty Creek 1 profile. The transitions to packstones observed locally and the thickness of some individual carbonate layers varies laterally. Nodular bedding occurs in a 70-cm thick layer 2.5 m above the basis of Salty Creek 1. Some carbonate beds show slight compaction features like the deformation of biogenic bored holes or a few broken skeletal grains. However, the often biomorph preserved components are mostly not in contact and refer to no compaction features. The grain sizes, composition and sorting of the carbonates vary strongly. Fragile forms of molluscs, massive as well as branching *Porites* of 10 mm in diameter are common in all carbonates. Furthermore, coralline red algae (*Aethesolithon problematicum, Sporolithon* sp., *Hydrolithon, Mesophyllum* sp., *Jania*) and small benthic foraminifera (Miliolids) occur in different amounts. Some rare fragments of dasyclads are found associated with the significant occurrence of Soritidae and Alveolinidae at the basis and at the top of the Salty Creek 1 profile (sample SC2, SC3, SC9, SC10). Bryozoans, echinoderms are very rare, whereas planktonic foraminifera and brachiopods were no observed. A single pyrite mineral in the carbonates was found in the upper part of the profile (SC10). The intercalations of internal mm-thin bedded marine shales are 30 to 140 cm thick and contain a variable content

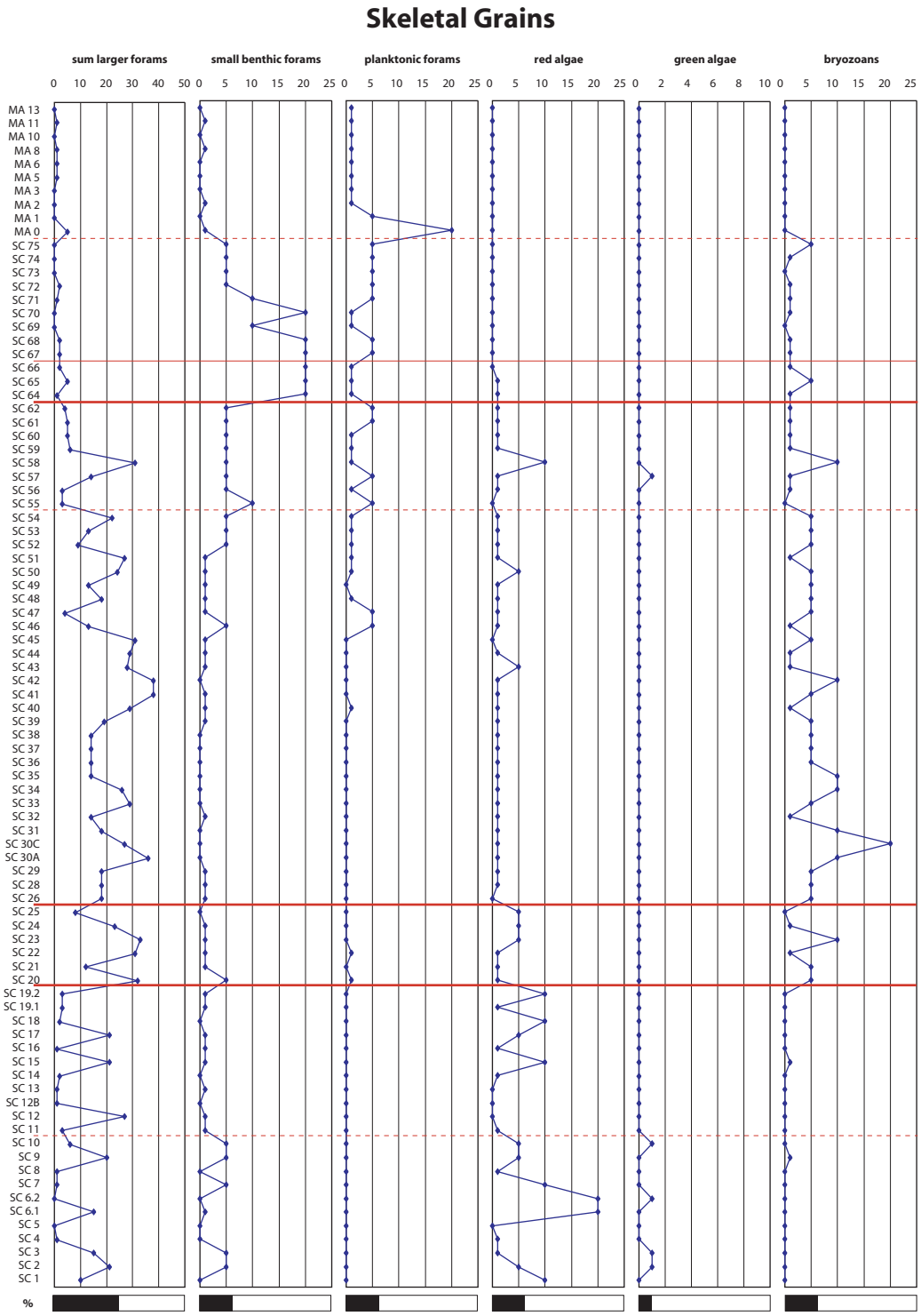

Fig. 13.1: Semi-quantitative frequency estimation of common skeletal grains (part 1) in the thin sections of the Salty Creek Section - Maasin Profile reflecting their development upstrata throughout time.

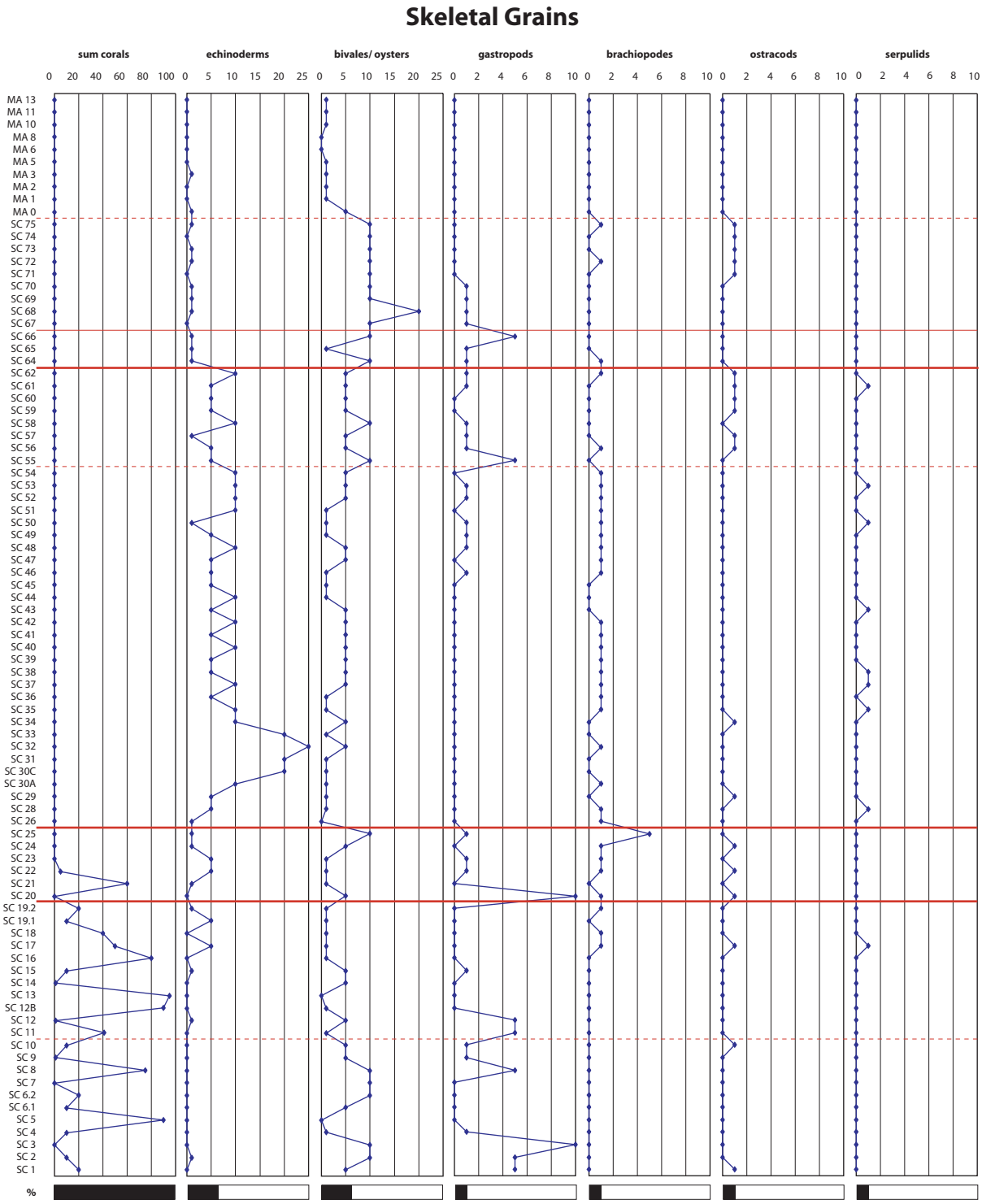

Fig. 13.2: Semi-quantitative frequency estimation of common skeletal grains (part 2) in the thin sections of the Salty Creek Section - Maasin Profile reflecting their development upstrata throughout time.

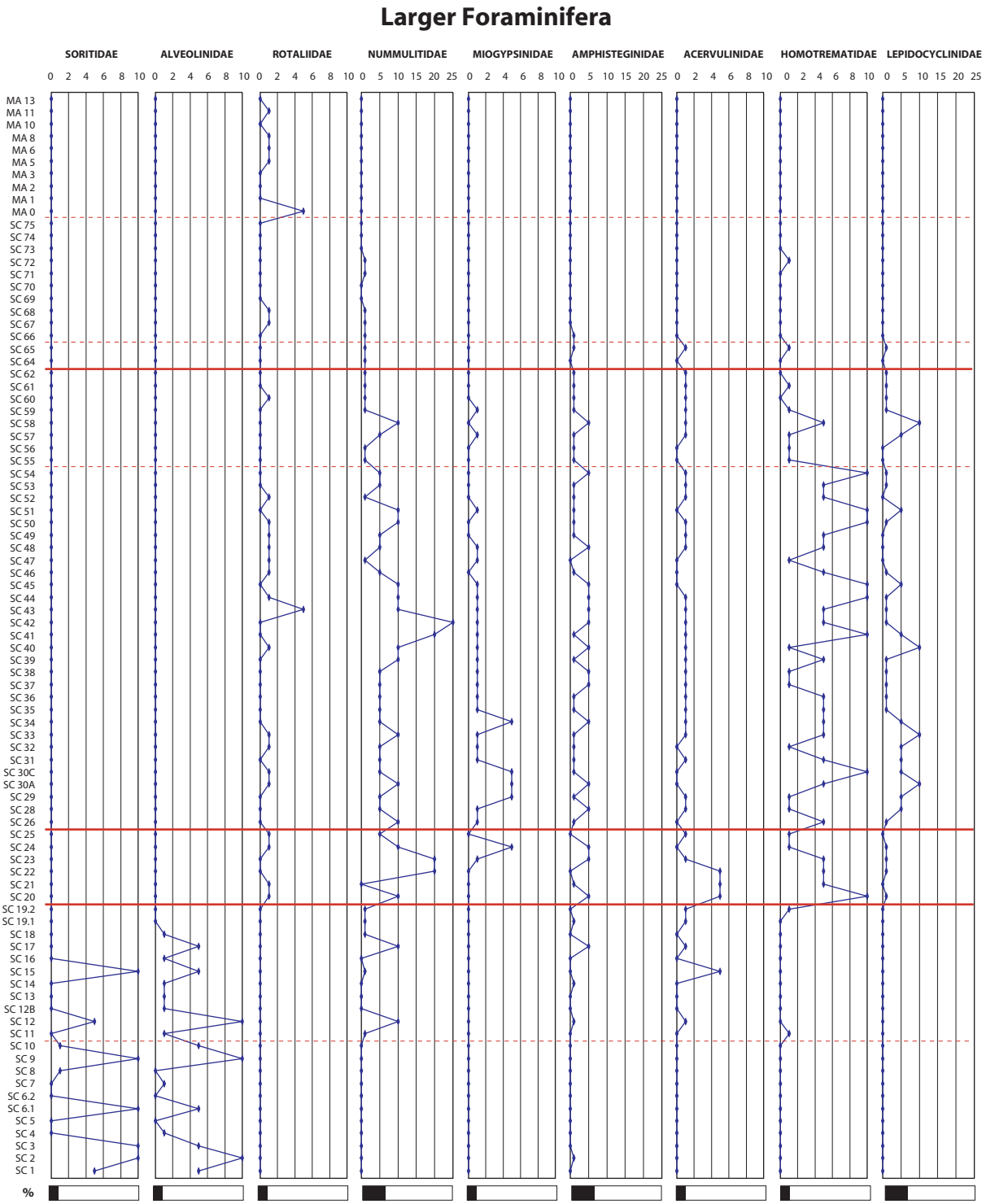

Fig. 13.3: Semi-quantitative frequency estimation of larger foraminiferal assemblage in the samples of the Salty Creek Section - Maasin Profile reflecting their development upstrata throughout time.

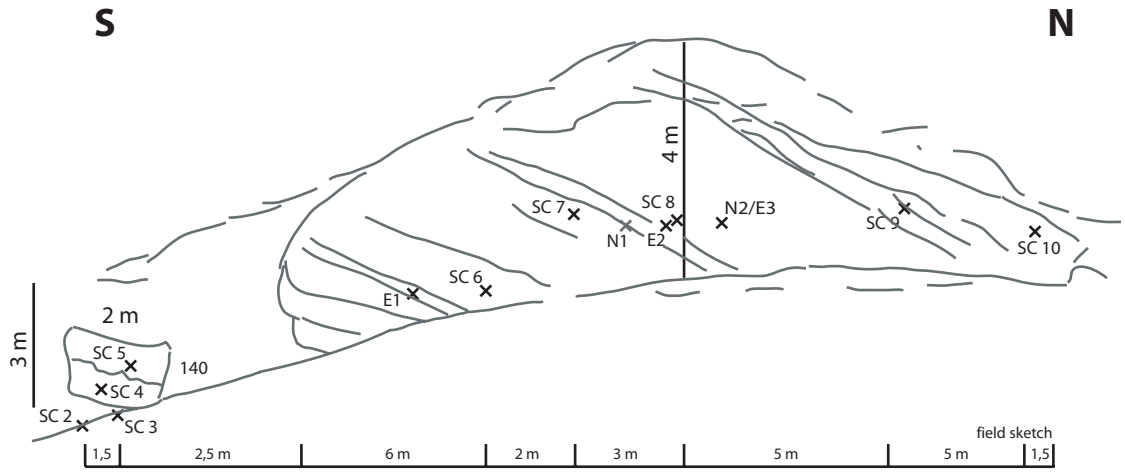

Fig. 14: Field sketch of the outcrop of Salty Creek 1 profile.

of skeletal grains of well preserved small bivalves and gastropods as well as fragments of coral branches of 2-5 mm in diameter. Especially at the contact between carbonate banks and shales, massive corals are sometimes present. The poritid corals are often bored and provide geopetal features.

The continuation of the Sequence A crops out at the lower part (up to 7 m above the basis) of Salty Creek 2, which is about 130 m NE of Salty Creek 1. The best estimation of the gap between the outcrops is 40 m. The floatstones or wackestones in the lower part of the Salty Creek 2 shows no major change regarding the composition compared to the carbonates at Salty Creek 1. Hence, a consistent sedimentary record is expected for the whole Sequence A from the Salty Creek 1 up to the lower part of Salty Creek 2, even if the intercalation of shales decreases throughout the sequence. Three 40-60 cm thick layers dip with an average of 20° to the NW and form a small 160-cm high wall at the basis of Salty Creek 2 (cf. Fig. 12). The contact between the lowermost layer and the middle layer is irregular. Superficially, the carbonates show a net of small furrows and holes produced by karstification. Massive coral heads, up to the size of a few dm in diameter, stick out of the wall. Additionally, the skeletal grains are composed of poritid corals, red algae (*Neogoniolithon* sp., *Lithoporella*) and larger foraminifera as well as of molluscs and some echinoderms. Whereas echinoderms increasing since the Salty Creek 1 profile, the content of molluscs and small benthic foraminifera decrease. The sorting of the components varies strongly and correlates to different portions of matrix. Bioturbation is only observed in the wackestones. The massive corals are often bored and some show indication of cyanobacterial activities. Some holes are partly filled with carbonate mud or peloids so that geopetal structures have been created. The samples SC17 to

SC19 collected in the uppermost layers of the lower part of Salty Creek 2 are characterised by a secondary microsparitic matrix, but the primary features of the floatstones are still noticeable and confirm that no major change affected the lithology.

Contact between Sequence A and Sequence B

A significant layer of 50 cm to 80 cm in thickness steps back 1.5 m from the cliff front and caps the lower part of the Salty Creek 2 profile with an erosive basis. The layer shows no karstification features. It is made up of packstones with a variable amount of carbonate mud and larger components. The small skeletal grains of the packstones are dominated by larger foraminifera (Nummulitidae, Amphisteginidae, Acervulinidae, Homotrematidae) bryozoans, echinoderms as well as small shells of bivalves and gastropods. Additionally, some rare planktonic foraminifera (*Orbulina*) occur beside up to 5% of sub-angular quartz grains. The packstones are internally bedded and the small components are orientated. As larger components are included rounded to well-rounded volcanic and some sandstone gravels of 0.5 to 8 cm in size, marine par-autochthonous carbonate boulders up to a size of 12 cm and small gravels of a restricted carbonate environment. Furthermore, biomorph-preserved marine fossils like bivalves up to 4 cm, gastropods up to 6 cm, coronas of echinoderms and massive coral heads with a diameter of 15 cm supplement the larger components of this layer. The larger components are not sorted and show no orientation or changes regarding the grain size. This significant horizon is easily traceable to the Salty Creek 3 profile, which is about 170 m NE of Salty Creek 2. The components there are slightly smaller than those at Salty Creek 2, but the general character and the erosive contacts at the base and at the top are equivalent.

Sequence B

Above the packstones containing larger components, the Sequence B starts in the upper part of the Salty Creek 2 profile with significantly bedded packstones or grainstones dipping about 18° to the NW. Small karst holes and fine furrows following the bedding are common and vary slightly in their character in relation to small changes in the composition of the packstones. In a 1.3-m thick sequence at the basis of the upper part of the profile, internal sedimentary structures are preserved (Fig. 15). These three layers show truncations, planar-inclined sets, fore- and onsets. However, the cm to dm thick beds of the upper sequence of the Salty Creek 2 profile are horizontal or sub-horizontal and sometimes wedge-shaped. Irregular bed surfaces may refer to small hiatuses. About 2 mm long larger foraminifera

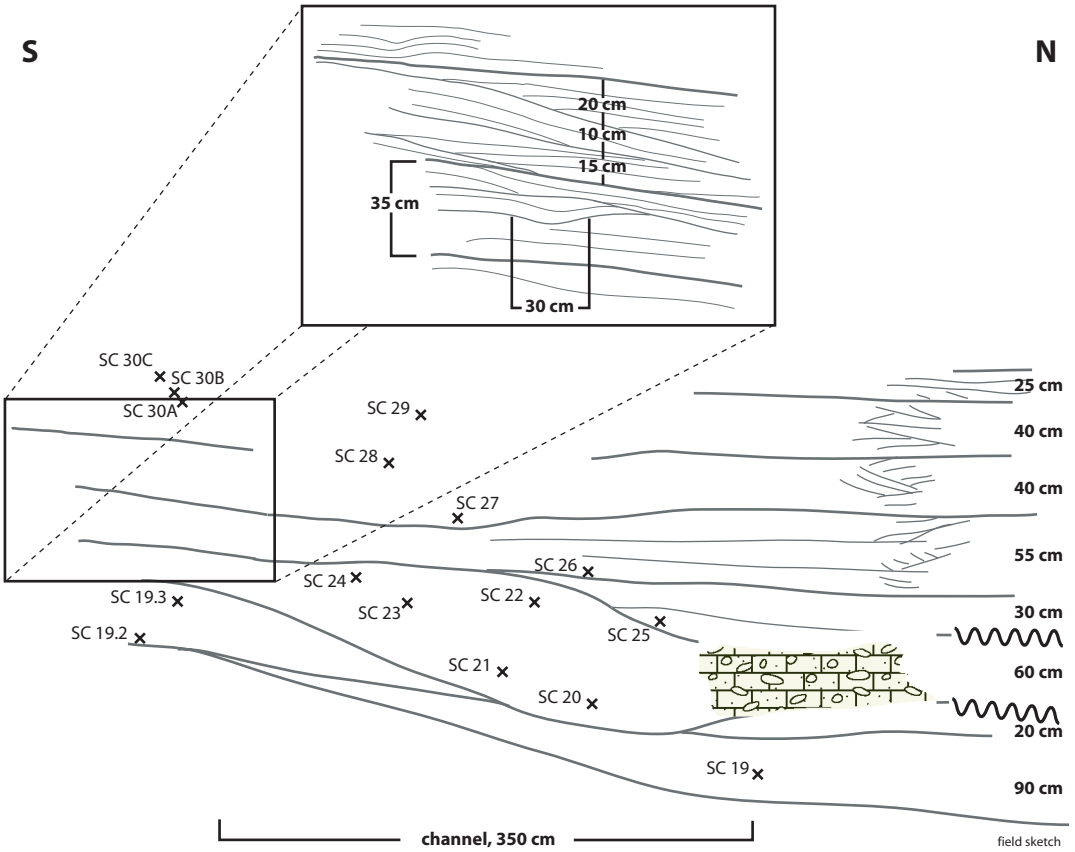

Fig. 15: Field sketch of the middle part of Salty Creek 2 profile showing the significant horizon made up of the packstones containing larger components as well as the cross-bedding of the carbonate beds above.

(Nummulitidae, Lepidocyclinidae, Amphisteginidae, Homotrematidae, Miogypsinidae), bryozoans and echinoderms dominate the skeletal grains of the packstones. Corals are absent and red algae are less frequent in the packstones than in the underlying floatstones. The occurrence of a few small benthic foraminifera (Miliolids) is patchy. Gastropods vanish. Some small fragments of brachiopod spines and a few serpulids occur. Peloids were not observed. The portion of quartz grains fluctuates strongly between the different beds from 0 to 10% of the total grains. Terrestrial plant fragments are locally included as fine scattered debris in the well-sorted and often internally bedded carbonates. All components are grain-supported and consequently point and tangential contacts are common. Some concave-convex and sutured contacts indicate a moderate compaction of some horizons.

The character of the 1 m thick layer overlying the significant packstone layer in Salty Creek 3 (cf. Fig. 12) is very similar to the deposits seen at Salty Creek 2. Therefore, after a gap of about 4 m, the continuation of the sequence is found in a 4-m thick outcrop in Salty Creek 3.

This outcrop displays no major changes in sedimentary conditions towards the top. A few small benthic foraminifera (Miliolids) occur continuously as well as some endichnia with a diameter of 1.5 cm. An intercalation of a 0.8-m thick quartz-sand rich carbonate ($CaCO_3$ ~70%) follows 1.8 m further upwards in the sequence. Bioturbation, relicts of terrestrial plant debris and cm-sized rounded sandstone gravels are significant features of this described in the underlying layers. The transition to the overlying carbonates is gradual. Quartz, homogenous gravel of 1 cm size and endichnia with a diameter of 1 cm still exist 50 cm above the quartz-rich carbonate. Within this part of the sequence, sedimentary structures like tangential-concave sets are observed as well, while the layers further topwards are again dm-thick and horizontal to sub-horizontal bedded. The field observations do not indicate significant changes within the sequence. However, the sedimentary record yields first evidences for a gradual change in the depositional environment above the quartz-rich carbonate horizon. The general composition of the packstones is similar to the underlying packstones, but, additionally, planktonic foraminifera and small fragments of gastropods occur. Miogypsinidae are limited in number and, in general, the larger foraminifera are not as abundant as below.

The continuation of the Sequence B is recorded inside the side the road, 75 m towards the W from the Salty Creek 3 profile. This Salty Creek 4 profile covers a horizontal distance of 200 m towards the NNW (cf. Fig. 12). The profile with a total thickness of 56.5 m is based on the recurrent escape of sets of cm-thick bedded packstones. They are dipping towards the NW with an average of 18°. The composition of the packstones confirms the trend of a gradual change above the quartz-rich layer. Additional skeletal grains are ostracods, which are usually associated with very fine packstones. The content of micrite is increasing and the grains become very fine, which results in. many small unidentified components. The packstones are well sorted even if single cm-sized bioclasts (bivalves, crinoids, echinoids) or gravel are found as well as an accumulation of echinoderm fragments. Orientation of the skeletal grains and internal bedding is less frequent in Salty Creek 4. One single glauconite mineral is recorded from the sample SC 54. The sample SC 55 provides species of the planktonic foraminifera *Globigerina* and *Globigerinoides*, sample SC 57 *Orbulina universa*. Red algae (*Mesophyllum* sp., *Jania, Corallina*) were identified in the sample SC 58. Biogenic activity in the deposition area is represented by the existence of a few endochnias. Small discontinuities probably occur along the sequence due to the observation of some irregular surfaces of beds.

Sequence C

The Salty Creek 4 profile ends in the NNW in front of a shallow but 120-m wide depression. On the northern side of the depression the road cuts through a moderately pronounced SW-NE stretching ridge and creates the Salty Creek 5 profile with the uppermost carbonate beds of the Salty Creek Section (cf. Fig. 12). The related thickness of gap between Salty Creek 4 and Salty Creek 5 are calculated with about 35 m. The carbonates at Salty Creek 5 alternate with shales and some layers are covered by soil. The solid carbonate layers show rare karstification features and dip with 18° towards the NW. Internal bedding is unusual in these massive carbonates. The carbonates are classified as very fine packstones up to wackestones, but the composition changes significantly. Larger foraminifera disappear above sample SC 66 with the exception of a few Nummulitidae that stay behind until SC 72. Small benthic and planktonic foraminifera (*Orbulina* sp., *O. universa*, *Globorotalia periphoacuta*) as well as thin shells of bivalves are abundant in the micritic matrix with a relatively high content of pellets. In addition, some fragments of bryozoans, echinoderms and ostracods occur. The quartz content is low while shale becomes more important.

About 100 m northwards from the Salty Creek 5 profile, the side road intersects the main road, which leads along the western coast to the N. About 75 m in SW direction on the main road, close to the Maasin School, a the small profile of the Maasin Profile was recovered in the road and at its eastern talus (cf. Fig. 12). The total thickness of the Maasin Profile adds up to only 5.5 m, while the gap to the Salty Creek 5 are estimated with about 40 m. The massive carbonate beds are between 20 cm and 40 cm thick and dip to the NW with 13° to 23°. With the exception of some common planktonic foraminifera (*Orbulina*, *Praeorbulina*) and a few thin shells of bivalves, skeletal grains are absent. On the thin section scale, the proportion of the components was sometimes estimated to more than 10%, but nevertheless, the carbonates of the layers have to be classified as massive mudstones containing a relatively high content of shale and local accumulations of skeletal grains.

Along the Iwahig River Profile the facies of 8 samples collected 100 m up- and downstream from the Iwahig River Bridge coincide with the facies along the Salty Creek Section and at the Maasin Profile. The lithostratigraphic lower samples IR1 to IR3 show a similar composition as the samples SC59 to SC66. However, the samples from the Iwahig River Profile contain less fragments of larger foraminifera and, in contrast to the Salty Creek Section, they document no increase of benthic foraminifera upwards. The upper samples taken along the river are classified as mud- to wackestones, similar to the carbonates forming

the Maasin Profile. In conclusion, the additional transect along the Iwahig River Profile supports the development of the carbonates documented in the upper part of the Salty Creek Section and the Maasin Profile.

Total Carbon Content

The data set of the total carbon content (TCC) from the Salty Creek Section - Maasin Profile documents less obvious the division of the succession into 3 sequences than seen in the field and thin sections (Fig. 16). Nevertheless, the different content of TCC illustrates well the observed lithological changes.

Sample SC0 is classified as shale and yields only 1% $CaCO_3$. The samples SC1 to SC10 are collected at the Salty Creek 1 profile, which is characterised by the alternation of shales and carbonates. Even if only carbonates are shown in the diagram (Fig. 16), the TCC record exhibits a high variability. Higher contents of shale reduce the $CaCO_3$ content to less than 80% (SC4), whereas in contrast the shales in the Salty Creek 1 profile show up to 33% $CaCO_3$. The close relationship between the carbonates and the shales is obvious. Upstrata the sequence of the lower part of the Salty Creek Section 2 (SC11 - SC19) has in average a $CaCO_3$ content of more than 97%, which represents the purest carbonate throughout the Salty Creek Section. However, a slight decreasing trend are indicated and lead to the samples SC20 to SC24 above, which were collected within the significant packstone layer with larger components. The lithological change is reflected by a decrease of 15% of the $CaCO_3$ content from one to the other layer and the increasing variance of the $CaCO_3$ content. The characteristic of high variance and low TCC are also found in the overlying layers

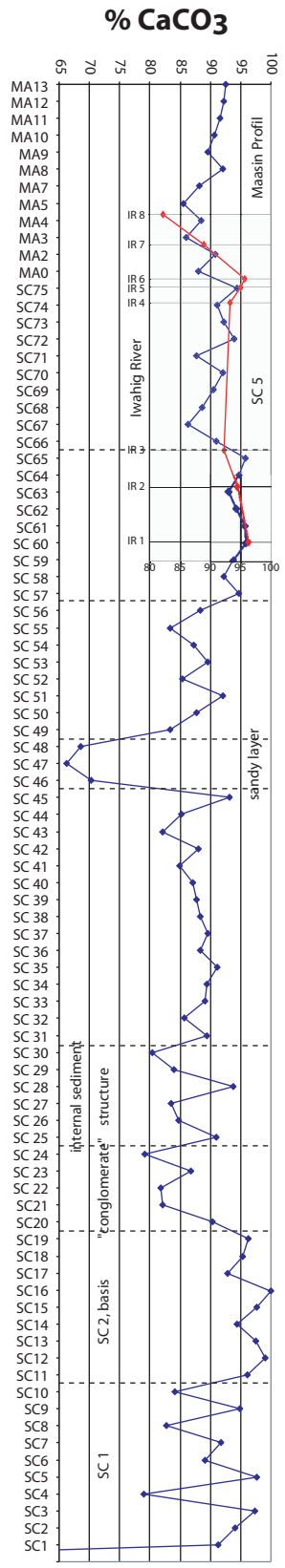

Fig. 16: Calculated CaCO3 content upstrata of the samples from the Salty Creek Section - Maasin Profile and the Iwahig River Profile.

(up to sample SC30). In contrast, the 8-m well-bedded pack- to grainstones sequence above are made up of 85-90% $CaCO_3$, whereas an decreasing trend exists towards the quartz-sand rich layer. This layer is represented by the samples SC46, SC47 and SC48, which show the most significant change in the TCC record. The $CaCO_3$ content decreases rapidly at the basis contact to 70, 66 and 69% respectively. Even if the change of the $CaCO_3$ content above the quartz-rich layer is not as abrupt as at the basis, 60 cm above the intercalation the $CaCO_3$ content and SC65 document a relative high $CaCO_3$ content (94%) with low variance. The samples above with a mean $CaCO_3$ content of 90% represent the Salty Creek 5 profile and the Maasin Profile. No clear trend could be identified. The $CaCO_3$ content decreases to 86% (sample MA5) followed by an increase up to 92% in the uppermost sample (MA13) of the Salty Creek Section - Maasin Profile.

The samples from the parallel running Iwahig River Profile and the samples from the upper part or the Salty Creek Section - Maasin Profile were correlated based on the microfacies study, before they were added into the diagram of the Salty Creek Section - Maasin Profile. This connection results in a close relationship between both TCC records. Both, the calculated $CaCO_3$ content and the changes correspond.

Excerpt: The Salty Creek Section up to the Maasin Profile includes 3 sequences named A, B and C. Throughout the lowermost Sequence A marine shales alternate with float- to wackestones containing corals and a larger foraminiferal assemblage of Soritidae and Alveolinidae beside well preserved molluscs. The deposits demonstrate low water energy conditions in an area with water depth between a few meters up to a few 10^{th} of meters. A significant and lateral traceable horizon of an internal bedded packstone, which includes up to several cm-sized component of terrestrial and marine origin marks the transition between sequences A and B. Sequence B is characterised by well-bedded larger foraminiferal packstones. The changed larger foraminifera content is made up of Nummulitidae, Lepidocyclinidae, Amphisteginidae, Homotrematidae, and Miogypsinidae and refer to moderate, but higher water energy conditions than below, in a shallow water environment. The grain size throughout the sequence decreases upsection, whereas small benthic foraminifera and planktonic foraminifera increase. Finally, massive and fine carbonates with only few small skeletal grains occur within the uppermost Sequence C, beside some marine shale intercalations. A deepening of depositional environment is therefore indicated.

3.1.3 Tumarabong River Section/ Slope Profile

The Tumarabong River Section is located close to the Tumarabong River waterfalls, 3-km linear distance to the SW from the Salty Creek Section. The outcrop supports the succession recorded in the Salty Creek Section. The carbonate section of the Tumarabong River Section is divided into two major sequences of 10 m and 11 m in thickness, which are equivalent to Sequence A and B described in the Salty Creek Section (Fig. 17). The inclination of the layers at the Tumarabong River Section averages 18° towards the NW, which corresponds to the measurements from Salty Creek Section and provides therefore, further evidence for the correlation of both sections.

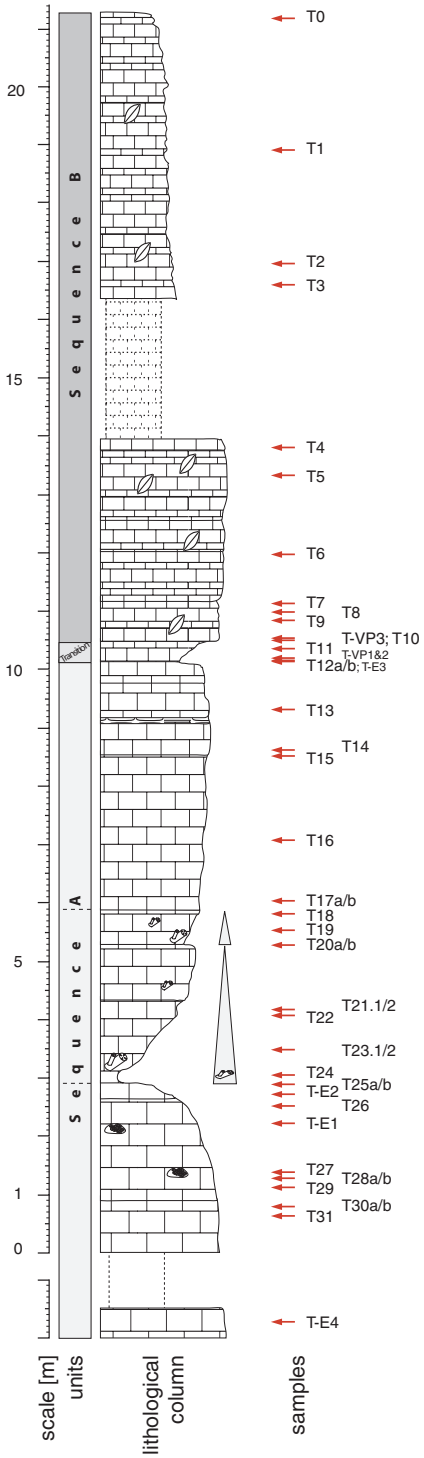

Sequence A

The 10-m thick lower Sequence A of the Tumarabong River Section is characterised in the field by massive white altered carbonates. Even if bedding is not significant, some carbonate layers between a few dm and up to 3 m in thickness can be distinguished. The relief of the slightly karstified float- to wackestones is smooth. It exhibits only a few cm- to dm-sized karst holes. However, the uppermost 1-m thick layer of the Sequence A also displays the white weathered surface, but a freshly broken rock is slightly brownish coloured and karst holes are abundant. The

Fig. 17: Synthetic column throughout the Tumarabong River Section showing sample positions. Two sequences of carbonate development are documented; an accumulation of coral branches exists in the lower part and a thin but significant horizon marks the transition between both sequences.

primary float- to wackestones are characterised today by neomorphic spars and microspars. Recent to sub-recent speleothems occur in some of the karst holes. Soil features like alveolar structures are commonly associated with modern plant fragments. The micritic matrix of the float- to wackestones includes a low to moderate shale content. Poritidae corals are the biggest and the most common biota in Sequence A (Fig. 18.1). They protrude as isolated massive coral heads of dm size from the wall close to the base and form a 3-m thick accumulation of southwards orientated branching corals 2.9 m above the base, which shows a decrease of their sizes and amount upwards. A slight increase in sizes and amount in the upper part of the accumulation layer occur, before finally coral branches are very rare upstrata. The skeletal grains beside the corals are abundant larger foraminifera, gastropods, bivalves, red algae and echinoderms. Small-benthic foraminifera (Miliolids) and some ostracods are less common. Serpulids are very rare and brachiopods are restricted to the horizon characterised by the coral accumulation. The larger foraminifera belong to Alveolinidae (*Flosculinella* sp.) and Soritidae (Fig. 18.2). Furthermore, encrusting forms (Acervulinidae) are preserved in the carbonates. Alveolinidae are the dominant forms within this assemblage. Sizes up to 6 mm were measured for *Flosculinella* sp., but the length of 2 mm is common. Soritidae typically have an average of 2 to 4 mm in length, but may reach 6 mm as well. The sections of encrusting forms of foraminifera reach a length of more than 1 cm in thin sections. Peloids are only observed in the Sequence A.

Contact between Sequence A and Sequence B

The contact between the Sequence A and B consists of a transition horizon of 40 cm in thickness. The massive wackestones are characterised by a mixture of components referring to the underlying as well as to the overlying layers. The contrast of the massive carbonates below and the well-bedded carbonates above is obvious in the field. Moreover, a small cavity and an overhang up to 5 m formed by the overlying bedded carbonates run along the cliff of the Tumarabong River Section.

The wackestones contain some single large components. Most of the skeletal grains are similar to those of the Sequence A (corals, larger foraminifera, molluscs, red algae and echinoderms). However, this horizon exhibits additionally a high amount of bryozoans fragments, different species of larger foraminifera (mainly belonging to Amphisteginidae, Lepidocyclinidae and Nummulitidae) as well as very small and fragile benthic and planktonic foraminifera. Besides, plane and thin shells of ostracods and some very rare fragments of

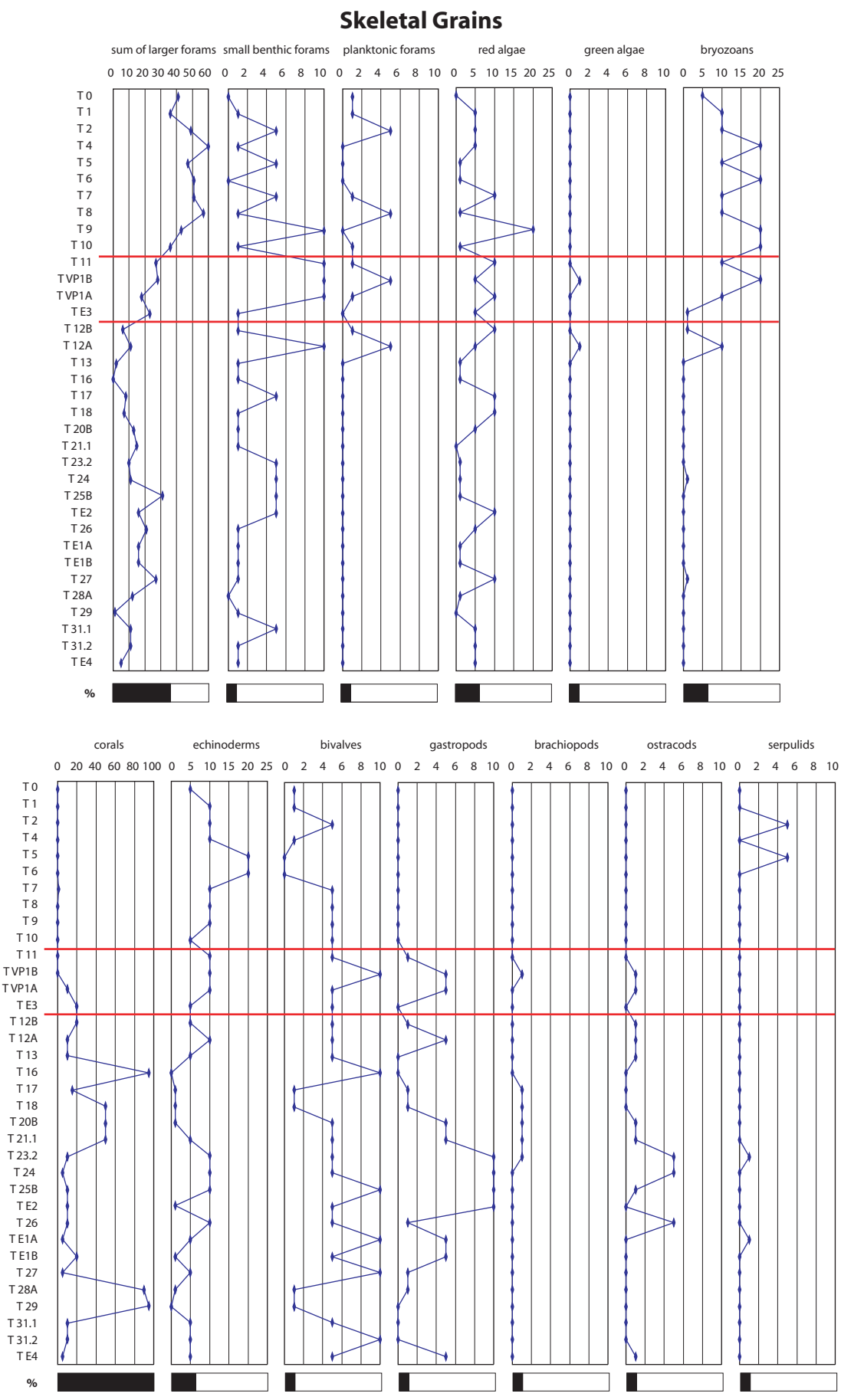

Fig. 18.1: Semi-quantitative frequency estimation of common skeletal grains in the thin sections of the Tumarabong River Section reflecting their development upstrata throughout time.

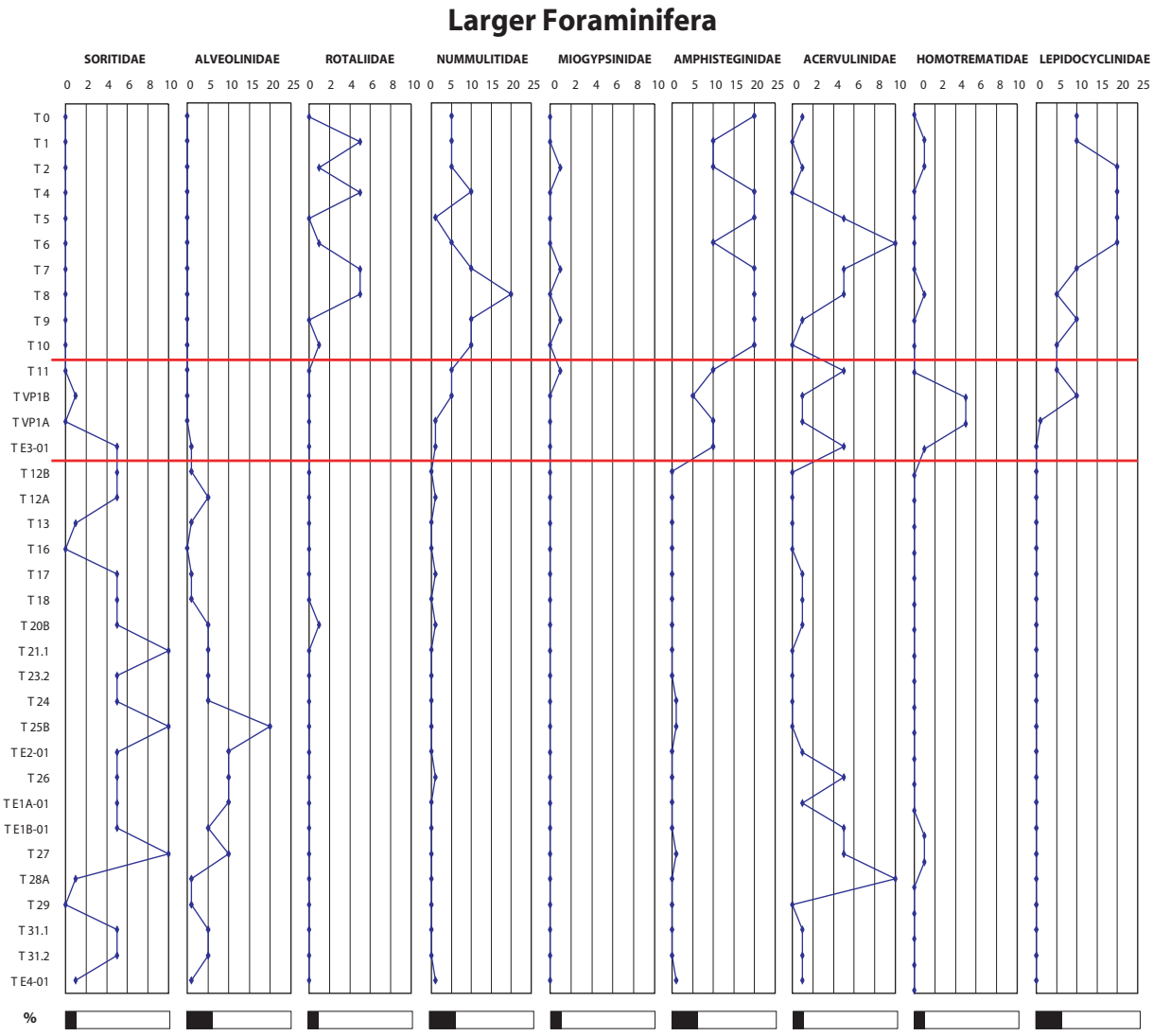

Fig. 18.2: Semi-quantitative frequency estimation of larger foraminiferal assemblage in the samples of the Tumarabong River Section reflecting their development upstrata throughout time.

dasyclads occur. Especially the small benthic foraminifera and bryozoans show a significant increase, whereas planktonic foraminifera are documented for the first time in the succession. Bioturbation does not effect the pristine skeletal grains. The matrix of the wackestones is dark-grey and dense, which is related to a significant content of shale. Even if stylolites are observed, the components do not show any compaction features. Some coral fragments are phosphatised. Intraclasts of a few mm in size are rounded or broken and apparently belong to two different depositional environments. The clasts and sand-sized quartz grains are common in the deposits, whereas a few pyrite minerals are scattered. A cm-thick accumulation of large fossils, including a biomorph 3-cm big corona of an echinoid and well-preserved shells of molluscs, are found on top of the transitional sequence.

Sequence B

In contrast to the Sequence A, the Sequence B is composed of grey, bedded and well-sorted packstones. The feather-edged rock surface in the outcrop refers to a strong karstification of the 11-m thick upper carbonate succession of the Tumarabong River Section. The thickness of the beds increases from dm-scale to m-scale within the first 4 m of the Sequence B (cf. Fig. 17). Internal bedding and the orientation of the grains are common in the packstones. Some single sand-sized quartz grains occur towards the top. A few cm-sized intraclasts, which are reworked from the underlying layers, large bivalves and occasional phosphate in the chambers of larger foraminifera, are restricted to the lowermost 1.50 m of the Sequence B. The composition of these packstones is relatively homogenous, whereas the sorting improves upwards. Slight changes concerning the micrite content and the composition of the biogenic assemblage are observed locally. Larger foraminifera present the majority of the components. Amphisteginidae (size, 1 – 1.5 mm), Lepidocyclinidae (size, 2 – 3 mm up to 4 mm) and Nummulitidae (size, 2 – 3 mm) dominate the larger foraminiferal assemblage. Additional skeletal grains include frequent fragments of bryozoans and echinoderms. Bivalves, red algae and small benthic foraminifera are relatively common, but theirs abundance decreases upwards. The planktonic foraminifera (*Globigerina*, *Orbulina*) are preserved in various amounts throughout the sequence. The complete lack of corals in the Sequence B is, with respect to their abundance in the Sequence A, most remarkable. Gastropods, brachiopods, ostracods and green algae were also not observed.

Slope Profile

Upstrata and about 300 N of the Tumarabong River Section the so-called "Slope Profile" was discovered close to the road. The N-S orientated 28-m long and 12-m high cross section provides an outcrop of well-bedded pack- to grainstones showing a number of different sedimentary sets (Fig. 19). Thereby, the outcrop corresponds still to the deposits of the Sequence B.

Very slight variations regarding the composition and size of the skeletal grains as well as the content of micrite occur within and between the layers, each 5 to 25 cm thick. The variations result most commonly in the internal bedding of the carbonates. The lowermost sample (S1) is a very fine micritic packstone with abundant planktonic foraminifera and thin shells. The sample S2 is a moderate sorted packstone containing larger foraminifera (Lepidocyclinidae, Amphisteginidae and some Nummulitidae), bryozoans and bivalves beside some planktonic

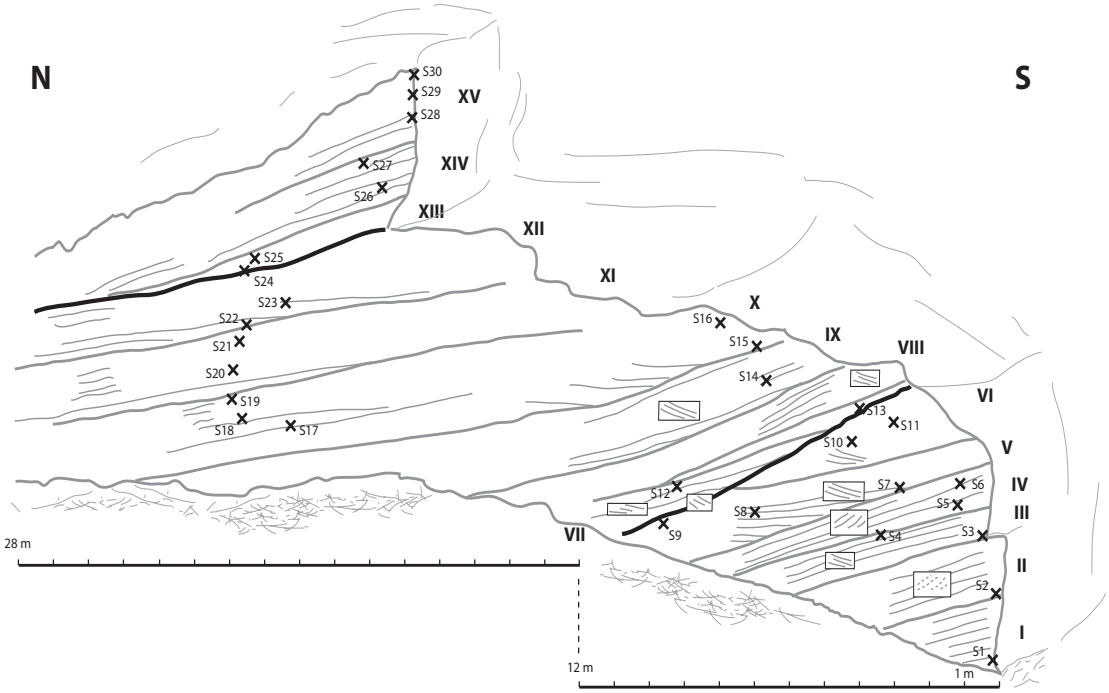

Fig. 19: Field sketch of the Slope Profile presenting the cross section through an elongated carbonate-sand body with their sedimentary structures.

foraminifera. Further upstrata the content of the larger components decreases up to sample S5, which has the same composition as S1, before the amount of the larger components increases again up to sample S8. The samples S9 to S11 are pack- to grainstones with a high number of Amphisteginidae. Besides, some echinoderms, bryozoans, bivalves, red algae and encrusting foraminifera occur. Only a few planktonic foraminifera are included in these samples. Above, larger components disappear in the packstones, until the sample S14 documents similar features as seen in S1. The composition of these very fine packstones with planktonic foraminifera shows no major changes up to sample S24, which is the lowermost sample of the upper sequence made up of very fine packstones with a significant high content of micrite and less planktonic foraminifera.

These slightly different compositions of the packstones coincide to significant sedimentary structures. Based on the erosive contacts at the basis and at the top, 15 sets of beds are defined within the cross-section. Furthermore, 2 major erosive contacts between Set VI and Set VII as well as between Set XII and Set XIII are observed. The sets of the lower unit of sets (Set I - Set VI) and the middle unit of sets (Set VII - Set XII) are characterised by onlaps or downlaps. Within the small outcrop, the shape of the layers in the upper unit of sets (Set XIII - Set XV) indicates only horizontal or sub-horizontal bedding. Changes in the depositional

environment, which result in a shift from a set characterised by onlaps to a set characterised by downlaps, are restricted to the lower unit of sets. In general, onlaps to the S are usual while only Set II and Set IV indicate downlaps to northern directions. The changes regarding the character of the sets correspond to changes in the packstone composition, i.e. larger components (larger foraminifera, bryozoans, bivalves) are only frequent in the lower unit. They disappear in the lowermost part of the middle unit of sets, before the sedimentary record upstrata displays a unique fine sediment composition. Above the erosive contact between the middle and the upper unit of sets, the content of micrite increases while the content of fine skeletal grains is reduced.

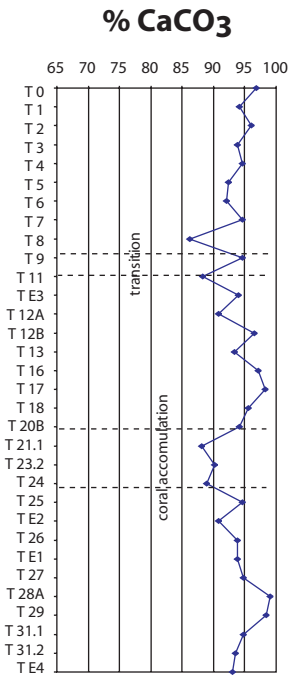

Fig. 20: Calculated $CaCO_3$ content in the samples from the Tumarabong River Section upstrata.

Total Carbon Content

The analysed Total Carbon Content (TCC) of the samples from the Tumarabong River Section range between 86 to 99% (Fig. 20). The data, which show a reduced content of $CaCO_3$ (less than 90%), are measured in sample T24, T23.2 and T21.1 as well as T11. All of these samples are from the horizon of coral accumulation or the transition horizon (T11). The underlying samples indicate already a general decreasing trend toward these samples. The lowest content of $CaCO_3$ (86%) in sample T8 demonstrates that thin shaley carbonates are intercalated into the Sequence B made up of bedded pack- to grainstones.

Two additional samples from the Slope Profile yield 94 and 95% TCC, which fits into the range, measured for the samples from the Sequence B.

Excerpt: The skeletal grains of the massive float- to wackestone of the Sequence A of the Tumarabong River Section are dominated by massive and branching corals beside molluscs and a larger foraminiferal assemblage made up of Soritidae and Alveolinidae. The larger foraminiferal assemblage and the branching corals (max. diameter 20 mm) suggest generally low water energy conditions in a shallow water environment. Above a 40-cm thick transition horizon representing components of both, Sequence A and B, well-bedded pack- to

grainstones with a changed larger foraminiferal assemblage of Amphisteginidae, Lepidocyclinidae and Nummulitidae are deposited. Similar to the Sequence B of the Salty Creek Section, the shallow water deposits refer to moderate, but higher water energy conditions than in the sequence below. The Tumarabong River Section demonstrates the same evolution as seen in the transition from the Sequence A to B in Salty Creek Section. The discovery of the Slope Profile, which is characterised by sedimentary sets made up of pack- to grainstones, provides a cross section through a shoal body and supplements therefore the carbonate development observed in the Sequence B of the Salty Creek Section.

3.1.4 Theo's Place - Quezon Section

The site called Theo's Place is located on the property of the Tabon Village Resort. The linear distance between the resort at the beach of Tabon and the Maasin Profile in the ENE direction adds up to 6.2 km. The north-westwards dipping of the layers suggest that the Theo's Place section is the continuation of the Maasin Profile. This is supported by the homogeneous lithological characters throughout the area and the unchanged lithology at Theo's Place. With the assumption of a constant orientation of the layers, the estimated total thickness between Theo's Place and Maasin Profile is estimated up to about 300 m. The 50-m long section at Theo's Place is located -0.50 m blow present sea level and is therefore only accessible during low tide. Several layers crop out and represent the carbonate sequence of a total thickness of a 17.5 m (Fig. 21). Eight samples were collected. All of them are very fine-grained carbonates. Following the high content of shale and therefore the reduced carbonate content (82 - 86% of $CaCO_3$; Fig. 22), they have to be classified as marls. The fossil content is restricted to small planktonic foraminifera (*Orbulina*) and some nannoplankton (*Sphenolithus abies*,

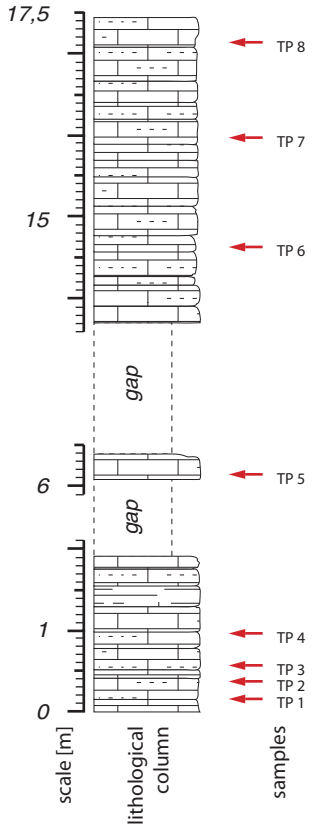

Fig. 21: Synthetic column of the succession of Theo's Place with indication of sample positions.

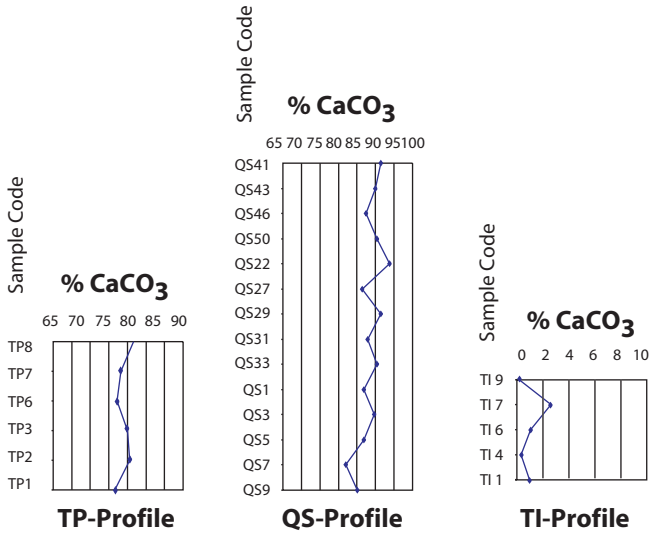

Fig. 22: Calculated $CaCO_3$ content in the samples from Theo's Place, the Quezon Section as well as the Tamlangon Island upstrata (Tamlangon Island: cf. chapter 3.1.7).

Helicosphaera carteri, *Reticulofenestra pseudoumbilica* (C. Müller, pers. comm.). The small fossils are accumulated in small pockets. One single pyrite mineral of 4 mm in size exists in sample TP 7.2.

The 3 separated profiles of the Quezon Section are located SW of Quezon, about 200 m E from the main road to Rizal (cf. Fig. 4, p.12). Each single profile comprises a number of small outcrops found on the western flanks of different hills. The hills are some ten metres high. A small creek valley, which produces an estimated 3 km long N-S running lineation in the aerial photograph (cf. chapter 3.4, Fig. 45), separates the Quezon Section I from the two other sites (Quezon Section II & Quezon Section III) . Nevertheless, the characteristics of the deposits and the dip and azimuth of the layers at the 3 single sites (Quezon Section I 076/18, Quezon Section II 101/21, Quezon Section III 099/19) do not document any change across the creek valley. These fine-grained muddy carbonates that include a certain amount of shale, are classified as mudstones or as marls (82 - 94% of $CaCO_3$; Fig. 22). These rocks form massive layers of 10 to 120 cm in thickness, which show no internal structures in the field. Nodular bedding is only observed in the middle part of the Quezon Section II profile. On the thin section scale, faint internal bedding is given by slight variations in the shale content. The fossil content of the carbonates or marls is poor and restricted to planktonic foraminifera, mainly *Globigerina*, *Globigerinopsis*, *Orbulina* and *Praeorbulina*, as well as very rare thin shells of bivalves and small benthic foraminifera. The general size of the fossils ranges between 0.1 to 0.5 mm. Skeletal grains of 1 mm in size are rare. Red-brown altered mineral grains of less than 1 mm in size are observed. Their amount varies, but does not reach a content of more than 1%.

The lithological characteristics and the facies of the sediments cropping out at Theo's Place, at the Quezon Section as well as at the Maasin Profile are similar. Additional samples collected between these three sites support the lateral extension of the facies.

Excerpt: The bedded mudstones to marls recovered from Theo's Place and the Quezon Section contain a low portion of small skeletal grains (planktonic foraminifera, thin shells) and refer to the same depositional environment with low water energy conditions in deeper water as deduced from the deposits at the Maasin Profile. Theo's Place and the Quezon Section provide outcrops of carbonates deposited above the Maasin Profile in the carbonate succession.

3.1.5 Devel Peak

A Miocene build-up forms the hill of Devel Peak 13 km NE of Quezon. The reefal carbonate sequence of 215 m overlies siliciclastic deposits. The sequence was studied from the basis to the top on the southern side and adds up to 225 m (Fig. 23). Changes in the depositional environment during the development of Devel Peak are documented by facies changes throughout the section. The observation of significant horizons, characterised by a high content of terrestrial material or masses of corals, leads therefore to the division of the succession into 7 sequences. The lowermost Sequence I (10.4 m thick) made up of siliciclastic deposits. A carbonate level with high content of terrestrial material marks the base of the carbonate Sequence II (41 m thick) as well as of Sequence III (40 m thick). Levels with masses of corals define the base of the overlying sequences IV to VII. The thickness of these carbonate sequences is 45 m, 19 m, 36 m and 26 m respectively.

Sequence I

The Sequence I begins with thin-bedded shales. Within the first 90-cm of the shales, gravels of sandstone, igneous rocks and carbonates occur. The sizes of the gravels reach up to 2 cm in the lowermost 30-cm thick layer, whereas above the gravel is not bigger than 1 cm. Skeletal grains are missing in the shales. Fine calcareous sandstones with sub-rounded grains overly the shale. Within the sandstone section, a shift from massive layers to dm thick and internal-bedded layers exists. Some rare and reworked small benthic and larger foraminifera (Amphisteginidae, Soritidae) as well as red algae fragments occur in the uppermost sandstone layers. A slight trend of an increasing amount of skeletal grains is observed. The orientations of the siliciclastic deposits were measured with 296/20.

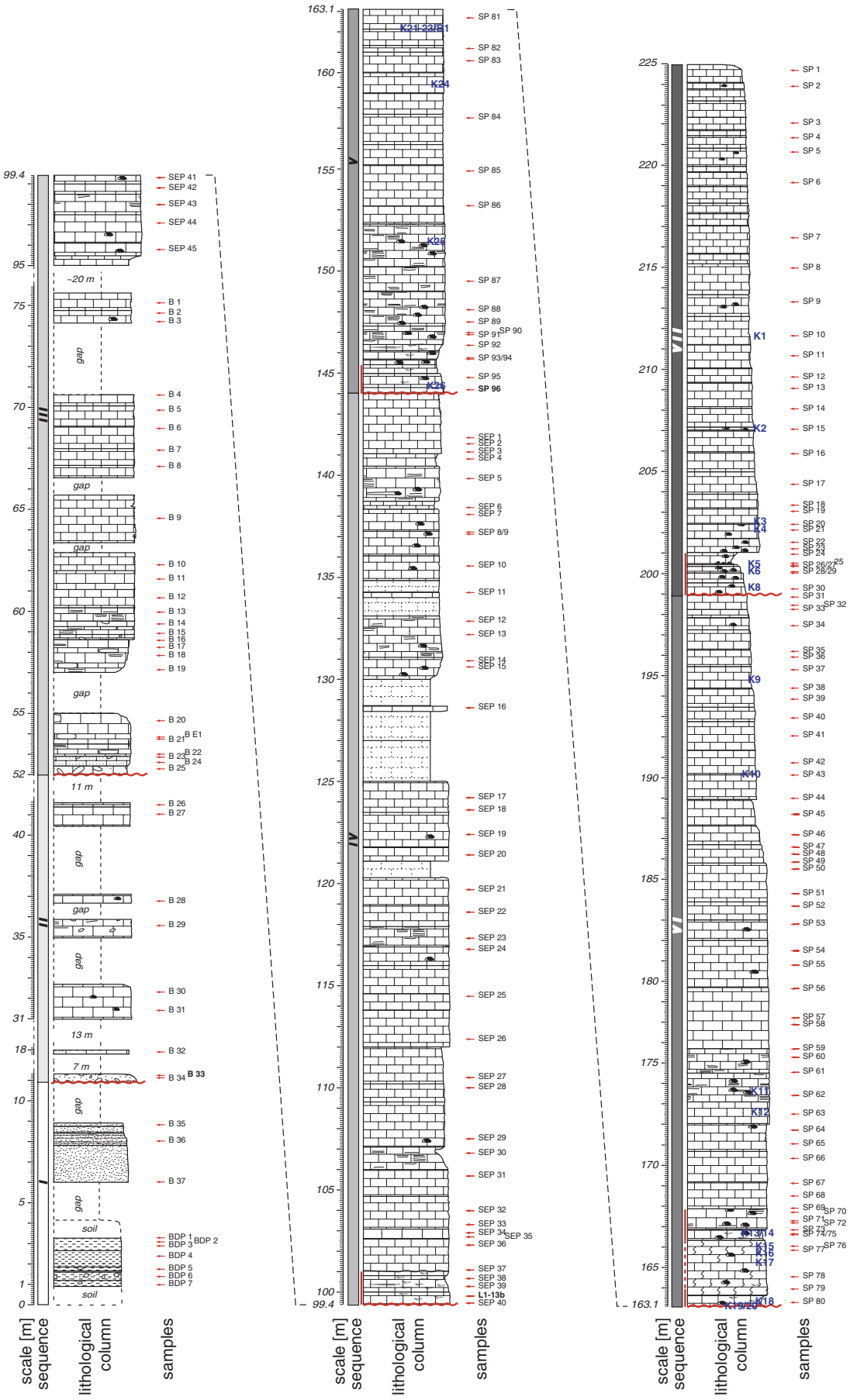

Fig. 23: Synthetic column throughout the Devel Peak build-up with sample positions; K-samples are extra coral samples. Seven sequences of build-up development are illustrated; the significant horizon of masses of corals are indicated by coral head- and platy coral symbole.

Sequence II

The orientation of the conformably overlying rudstones to floatstones and packstones of the Sequence II averages 280/19. The record of this carbonate sequence is only based on some outcrops, each some decimeter or a few meters thick. The carbonates are massive, nodular or internal bedded. The micrite content is always quite high. A 30-cm thick carbonate conglomerate marks the base of the Sequence II and is classified as moderately sorted rudstone. It contains abundant quartz grains and up to 3-cm large and rounded gravels of the same composition as in the shales of Sequence I. Furthermore, larger foraminifera (Nummulitidae and Amphisteginidae), red algae, echinoderms and bryozoans are frequent (Fig. 24.1-3). Some gastropods, a few several-cm large oyster shells and abundant small benthic foraminifera are additional biota. Corals are very rare in the lowermost sample of Sequence II, but increases constantly in the floatstones upstrata. In contrast, the content of gravel decreases upwards. These general trends are documented even if the depositions were subject of a relative high variability regarding the grain size, sorting and the assemblage of the skeletal grains. The uppermost sample of the Sequence II (B26) is a dense and fine packstone made up of fragments of molluscs, small benthic and planktonic foraminifera as well as echinoderms. Larger foraminifera are rare (Rotaliidae, Nummulitidae). All the carbonates of Sequence II indicate an evolution from a terrestrial influence to the accumulation of fragments of reef dwellers and finally to a well-sorted fine packstone containing small benthic and planktonic foraminifera.

Sequence III

Similar to the level recorded at 10.5 m, poorly sorted carbonates with a content of quartz-sand and gravels (up to 1 cm) occur at 52 m above the base level of Devel Peak. This high content of siliciclastic component in the carbonates defines the basis of Sequence III, whereas gravels and quartz disappear almost completely within the lowermost 3 m of the sequence and only carbonates with more than 95% $CaCO_3$ were deposited above. Despite some variances regarding the micrite content and the grain size of the skeletal grains, mainly the massive carbonates are classified as packstones. They contain dominantly red algae, larger foraminifera and molluscs, beside abundant small benthic foraminifera. The high amount of planktonic foraminifera, some gastropods and a few green algae are restricted to the first 7 m of Sequence III, which coincide with only a few larger components in the carbonates. Above, an increase of larger foraminifera, red algae and brachiopods are documented. Some corals

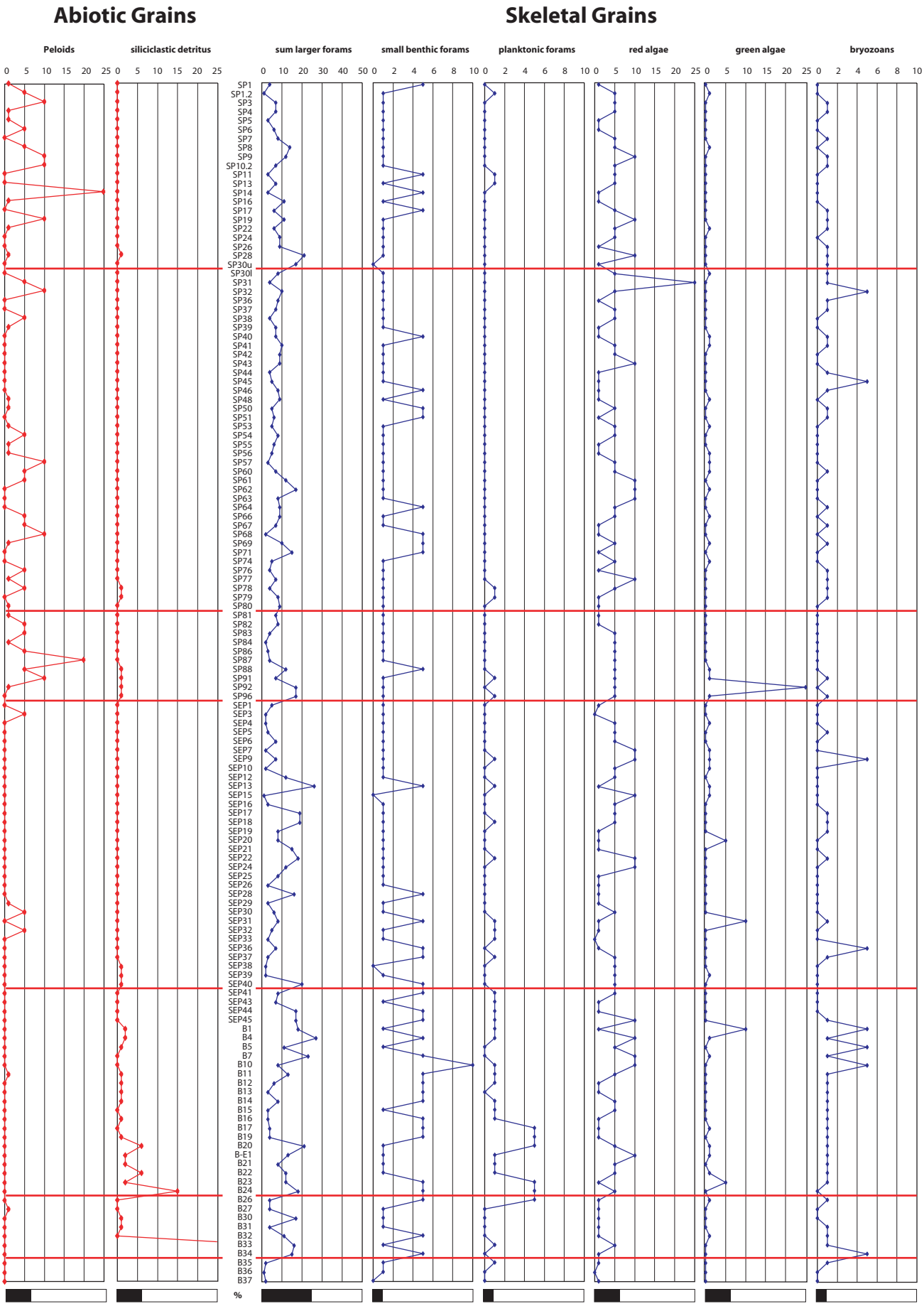

Fig. 24.1: Semi-quantitative frequency estimation of abiotic components and common skeletal grains (part 1) in the thin sections of Devel Peak build-up reflecting their development upstrata throughout time.

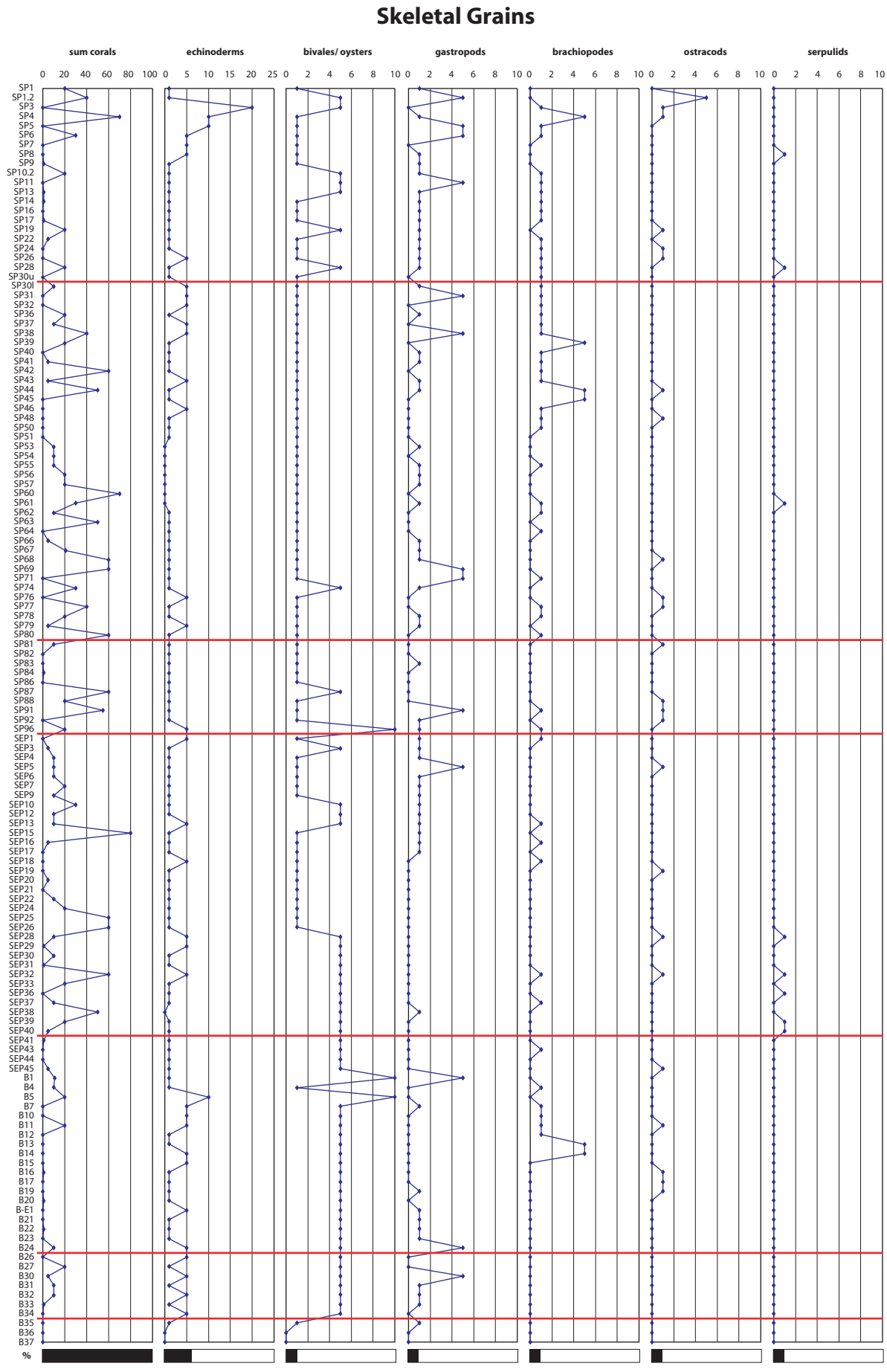

Fig. 24.2: Semi-quantitative frequency estimation of common skeletal grains (part 2) in the thin sections of Devel Peak build-up reflecting their development upstrata throughout time.

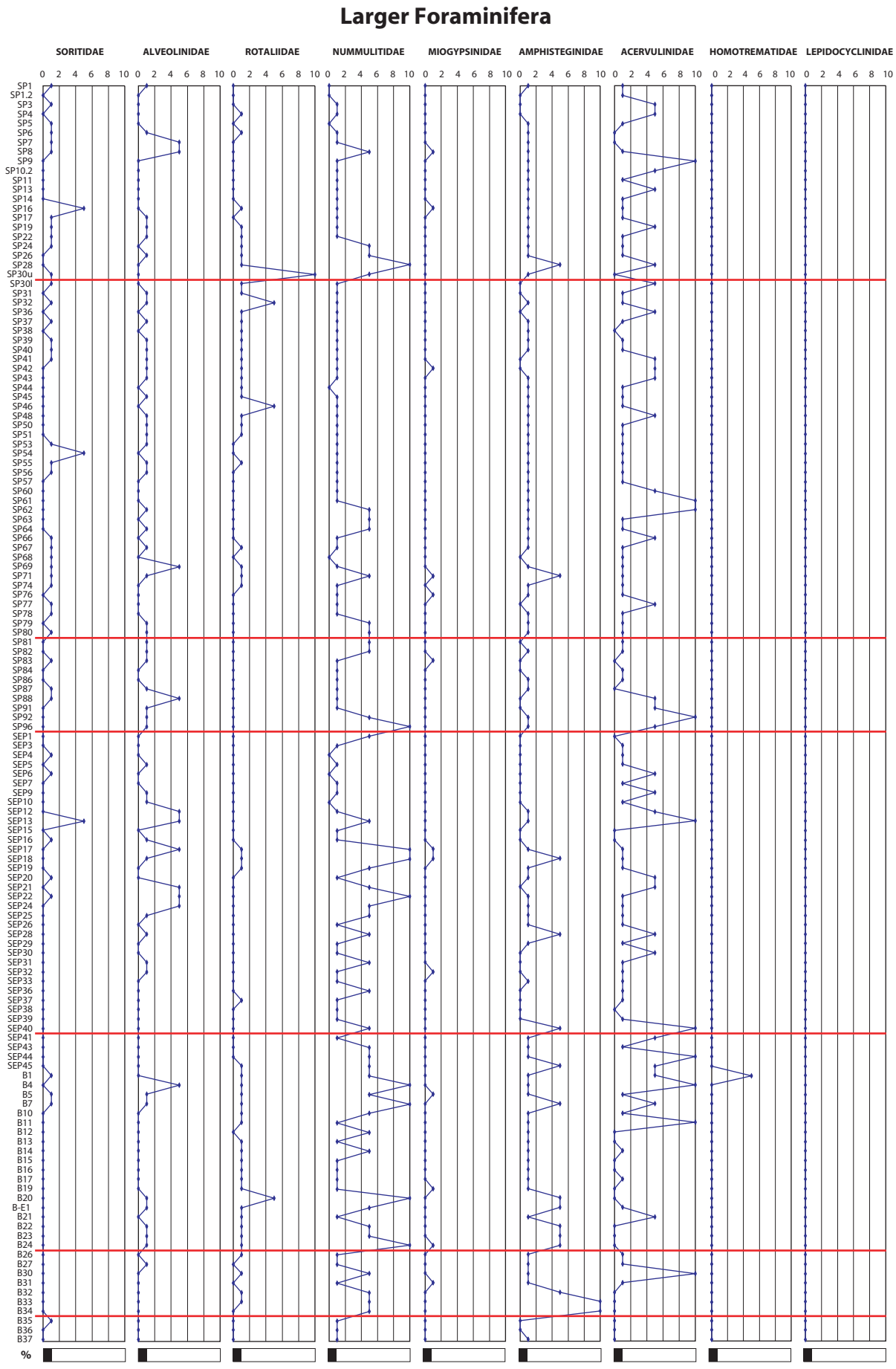

Fig. 24.3: Semi-quantitative frequency estimation of the larger foraminiferal assemblage in the thin sections of Devel Peak build-up reflecting their development upstrata throughout time.

occur in the upper part of the sequence. However, close to the top the amount of all larger components, with the exception of bivalves, is reduced.

Sequence IV to Sequence VII

Sequences IV to VII are characterised by massive carbonates that are usually strongly karstified. Some layers show internal bedding. The abundance of corals is the most significant feature of the sequences. Thereby, significant levels with masses of corals were observed in the field and used to define the base of each sequence. However, the division of this upper carbonate succession is only slightly documented in the thin sections, because changes in the composition are small and are not directly related to the coral levels so that the composition of the carbonates in between the corals is the same as below and above. The appearance of a siliciclastic content is the only observed correspondence reflected in the thin sections. Most of the carbonates throughout the succession are packstones, whereas the content of micrite varies and some larger coralline red algae and/ or corals might be included. In general, corals, larger foraminifera and red algae dominate the assemblage of skeletal grains, whereas encrusting foraminifera (Acervulinidae) frequently cover coralline red algae and corals. Different amounts of molluscs, some green algae and echinoderms are also included. Planktonic foraminifera disappear in the upper third of the carbonate succession. Within Sequence IV, small benthic foraminifera are less abundant, whereas in contrast gastropods occur more frequently above SEP17. Peloids are common from Sequence V upwards, i.e. in the uppermost 84-m of the build-up. Throughout sequences V to VII, the overall quantity of larger foraminifera documents a very slight decrease. The carbonates of the Sequence VII provide again a higher content of molluscs and an increase of the echinoderms observed in the last 10 m of the carbonate sequence of Devel Peak.

Coral Levels

The lithologies of the horizons dominated by masses of corals are classified as coral-boundstones or as coral-rudstones. They are often associated with encrusting foraminifera or red algae. Within the Devel Peak section, four of these significant horizons are recorded 100 m, 144 m, 163 m and 199 m above the base level. The thickness of the level is usually a few meters, but varies laterally.

Up to 1-cm thick platy *Porites* characterise the 2 - 3 m thick coral level 100 m above the basis of Devel Peak. The corals are in situ and form a narrow frame of corals, which results in

coral-boundstones. The sediment between the corals is very fine and contains a high portion of shale. In contrast, the coral level 144-m above the basis of Devel Peak is the only coral level, which is characterised by a coral accumulation. Even if the corals are not in place, referring to their preservation they are par-autochthone. The thickness of the dominant platy *Porites* decreases within the 2.3-m thick level from 8 cm at the basis to 3 cm at the top. The coral-rudstones contain high amounts of molluscs, red and green algae as well as planktonic foraminifera. The matrix includes shales and some quartz. The coral level 163-m is dominated by dm-sized massive coral heads; large heads (e.g. 60 x 30 x 50 cm) were recovered close to the top. Often these corals are encrusted by larger foraminifera and/ or red algae. Besides, at the basis of this level a single spot with westward-orientated branching corals with a diameter of 2 -3 cm was found. Additional observations at the NE flank of Devel Peak suggest that the basis-contact of this coral level is characterised by a low angle unconformity. Within the uppermost coral level at 199-m again many of massive corals occur, some of them up to

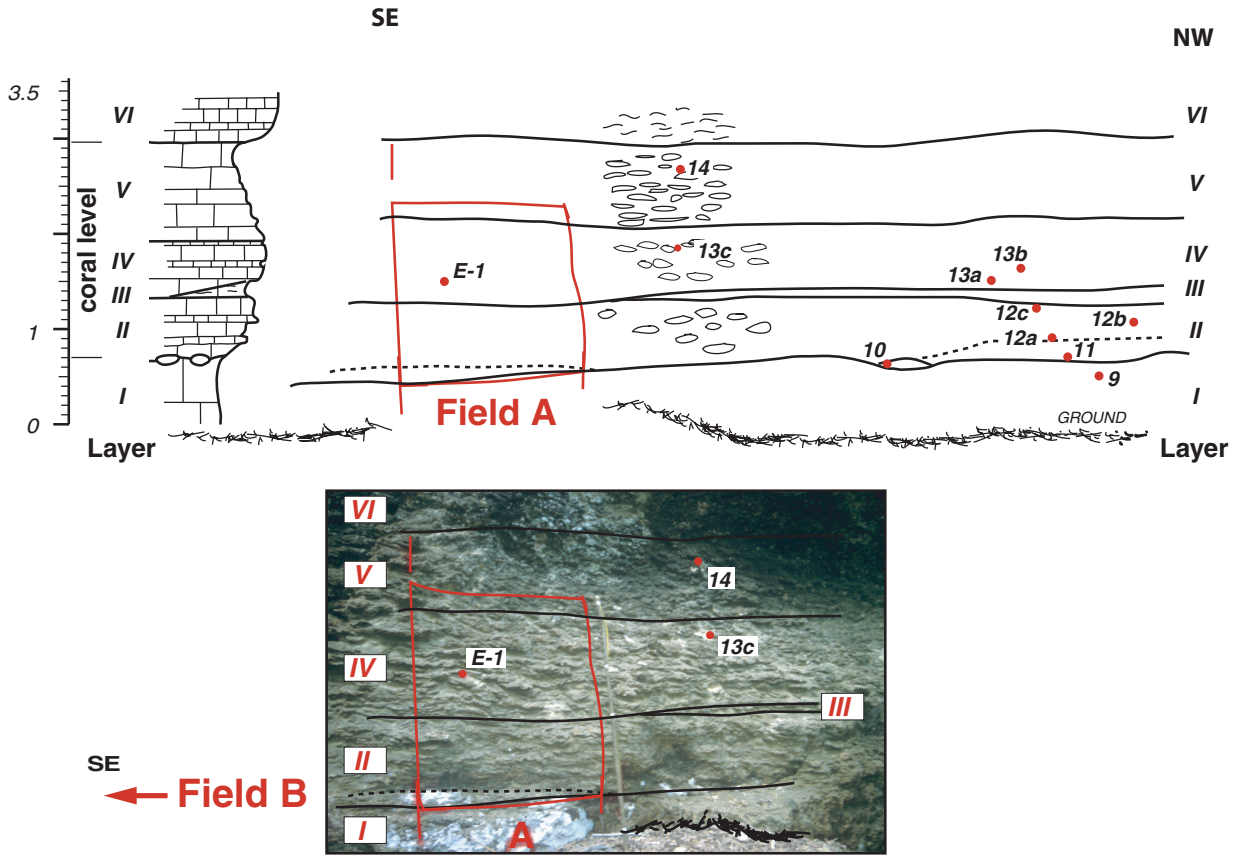

Fig. 25: Field sketch with lithological column and field photograph of the coral level 100-m above the base of Devel Peak containing masses of platy corals. Field A marks the square, where 180 points were counted for a statistical analysis; the second field (Field B) is 3.30 m south-eastwards.

several dm in size. Orientated branching corals with 1 - 2 cm in diameter and lengths of 10 - 15 cm are accumulated between the massive corals, which are in place.

Shape Evolution of Platy *Porites*

Due to the observation that platy *Porites* in the coral horizon 100-m above the base of Devel Peak show different shapes from flat, bowl-shaped, cup-shaped up to massive forms, an investigation follows the question, if within this level any vertical trend regarding their shape exists.

Therefore, the distribution of the different shape types (flat, bowl, cup, massive) and the inverse orientation of specimens was studied within the 2.5 m thick coral level on the NE flank of Devel Peak (Fig. 25). For the statistical analysis 180 points were counted at each of

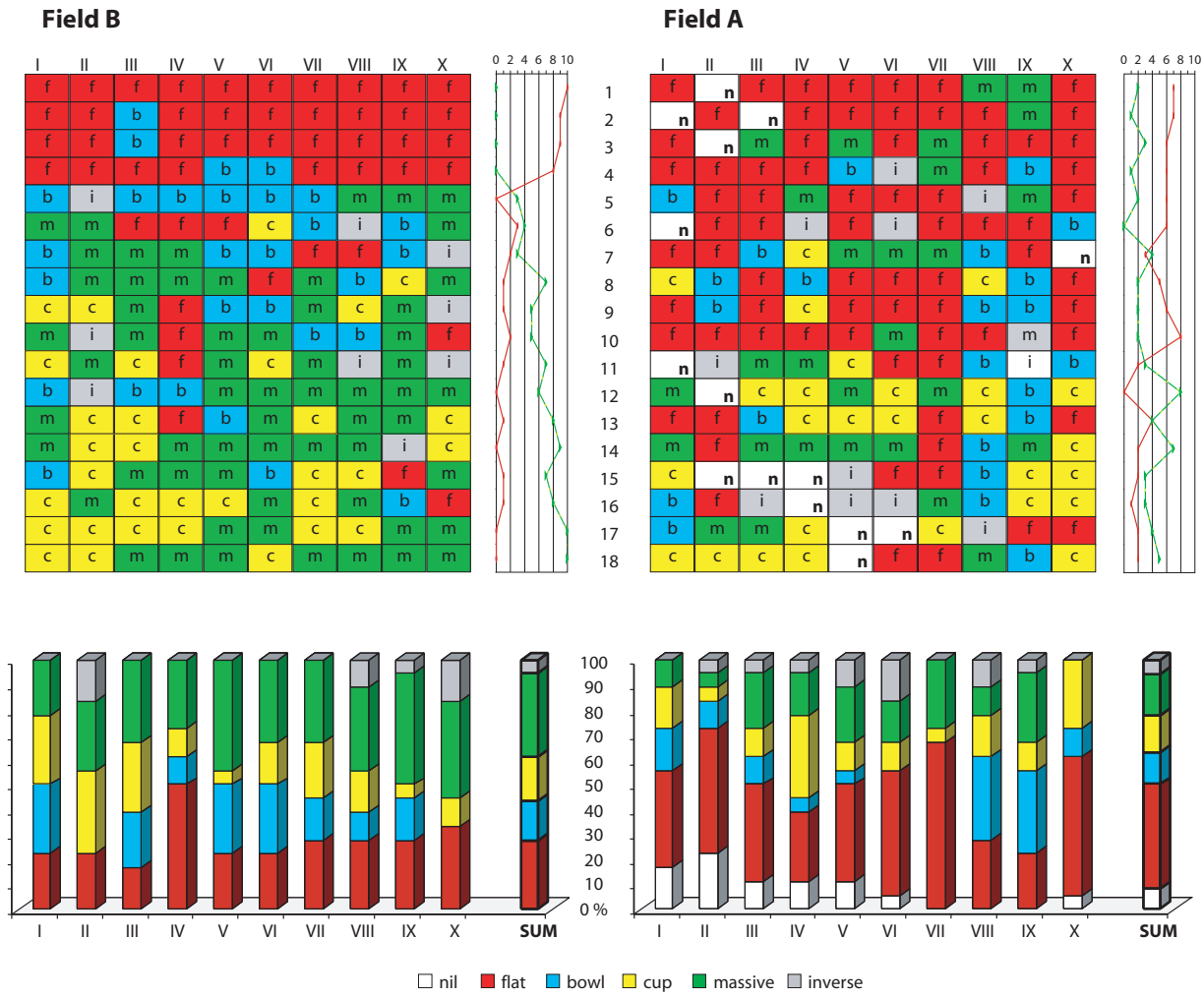

Fig. 26: Distribution of different shape types of platy Porites at two fields (A & B) of 1.5 m^2 in size based each on the point counting of 180 points; red = flat, blue = bowl, yellow = cup, green = massive, grey = inverse, white = nil; upper graphs: distribution in the field; lower graphs: rates of each shape type within a lines and their total sum.

two 1.5 m^2 large grids applied on the coral level (Fig. 26). The points on the grid have a fixed distance of 10 cm along 10 vertical lines and 18 horizontal lines. The distance between the Field A in the NW and the Field B is 3.30 m. At each point of the grid the shape of the coral was defined. In case no coral was encountered, it was noted with nil.

In both fields a trend from massive and cup shaped corals at the base to flat shaped corals at the top are reported. The trend is clearly documented in Field B with rare and scattered flat corals in the lower part and separated by a sharp contact the dominance of flat form 140 cm above the base. This development exists as well in Field A, but less significant. In Field A the shift is documented 80-cm above the basis, 40 cm lower than in Field B. However, the different level of the shift result from a slightly different positioning of the fields.

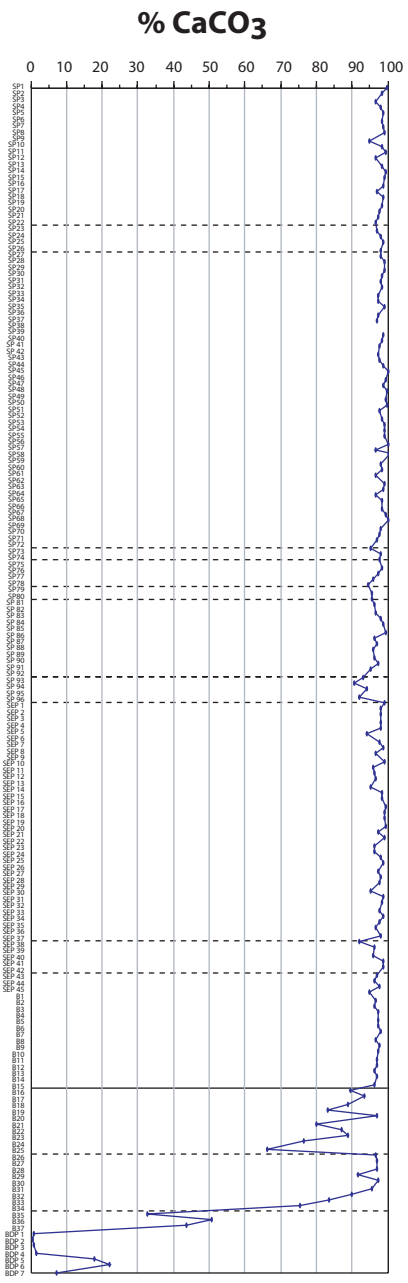

Fig. 27: Calculated $CaCO_3$ content of 184 samples upstrata Devel Peak section.

Total Carbon Content

The total carbon content (TCC) analysis, made of 184 samples throughout the whole sequence of Devel Peak, documents a 60-m thick initial stage of carbonate deposition overlain by a sequence of pure carbonates, which show only slight variations regarding the TCC (Fig. 27).

Following the TCC analysis, the initial stage of carbonate deposition at Devel Peak is characterised by 2 steps. The first step represents the transition from siliciclastic deposits with low $CaCO_3$ content (Sequence I) to carbonate deposits with more than 97% $CaCO_3$ (Sequence II). The relative high contents of $CaCO_3$ of the samples BDP7 to BDP5 is related to some cm-sized carbonate gravels. The beginning of the second step corresponds with the base of Sequence III and therefore

with the content of gravels and quartz in the carbonates. The abrupt decrease of the $CaCO_3$ content to only 66% follows directly the increase of the $CaCO_3$ content up to a content of more than 95% $CaCO_3$. The initial stage of carbonate deposition documented by the TCC ends within the Sequence III.

Throughout the overlying carbonate succession of 165 m, the mean content of $CaCO_3$ calculated for 155 samples is 98%. The very slight variations are related to small portions of shale, whereas only a few samples yield a $CaCO_3$ content of less than 95%. These samples corresponds to the horizons characterises by masses of corals at 100 m, 144 m and 163 m. Towards the top of all coral horizons the same feature of a decreasing $CaCO_3$ content are observed. Whereas this observation is significant and more rapid in the lower coral horizon, upwards the succession it is less pronounced.

Excerpt: The succession of Devel Peak demonstrates the establishment of a reefal build-up above a siliciclastic base. Within the siliciclastic deposits the transition from quiet and deep marine conditions to a shallow water environment with terrestrial influence are indicated. The overlying initial stage of carbonate deposition is characterised by rudstones to floatstones and packstones. Beside the carbonate conglomerate at the basis of the initial carbonates, a second level with gravel and quartz interrupted temporally the carbonate development, which was deposited in a shallow water environment with increasing distance to a terrestrial influence. Above this initial stage of the carbonate succession, packstones, containing an assemblage of corals, larger foraminifera and red algae as well as some molluscs and echinoderms, are dominate. Four significant levels with masses of corals occur and reflect changes in the paleoenvironment. With the exception of a shale content in the matrix of the coral levels a terrestrial influence are not documented. The carbonates are deposited under full marine and moderate water energy conditions of a shallow water environment suitable for the corals.

3.1.6 Albion Head

In the SW of the study area, the peninsula of Albion Head is made of a Miocene build-up (Fig. 28). Due to the protection of that area by the National Museum (Manila) and the morphology with vertical walls, narrow and deep valleys as well as more than 100 caves, the study of a continuous profile was restricted to the southern side of the complex. There, the

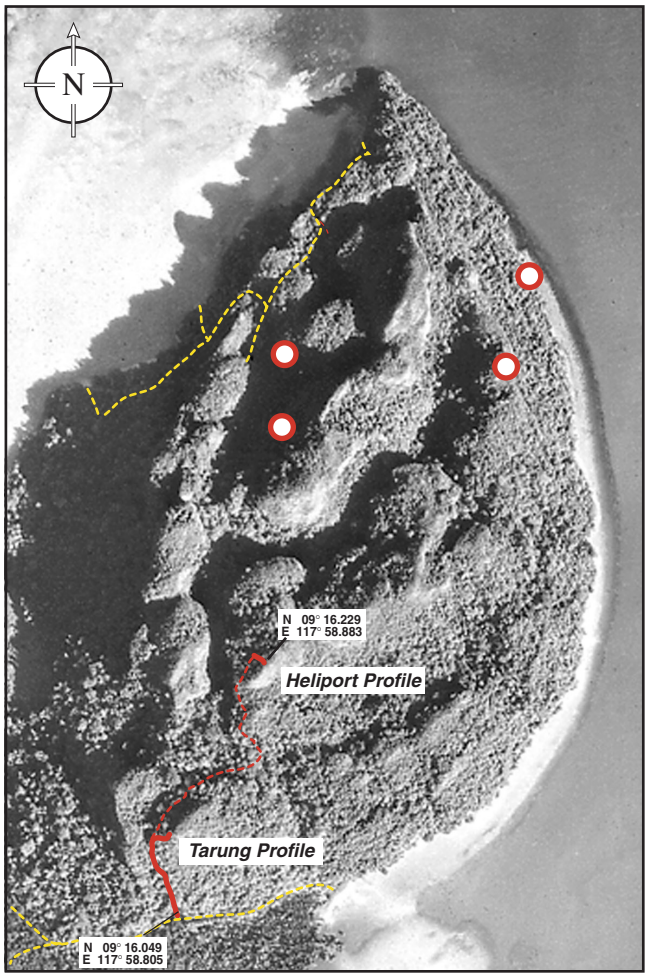

Fig. 28: Aerial photography of the peninsula of Albion Head indicating pathways (yellow), Tarung- and Heliport Profile (red) as well as four localities of spot samples.

Tarung Profile covers a 101-m thick carbonate sequence, which starts at sea level. Additionally, 9 samples were collected throughout a 19-m thick section reaching the highest point of Albion Head and isolated samples from the inner part and the NE side of Albion Head are supplemented as well.

No siliciclastic intercalations are observed within the strongly karstified carbonate complex of Albion Head. Massive carbonate deposits with some dm-bedded parts dominate the sequence of the Tarung Profile (Fig. 29). Internal bedding or the preservation of sedimentary structures is rare in the carbonates. One significant facies change exists throughout the Tarung Profile. The lower part of the sequence up to 30.5 m is made up of packstones. Larger foraminifera (Nummulitidae, Amphisteginidae) are the main skeletal grains, beside red algae, echinoderms, bryozoans and bivalves (Fig. 30.1-2). Corals are very rare in these carbonates. In contrast, above, corals (planar or branching *Porites*) are the major components whereas the amount of larger foraminifera and red algae are significantly reduced. Echinoderms, bivalves as well as bryozoans show also a slight decrease further topwards. However, planktonic foraminifera and a portion of shale in the matrix are restricted to the samples above TAR35A. The carbonates are classified as boundstones, floatstones or rudstones. Some samples are classified as packstones. Furthermore, the facies of the carbonates of the upper part of the Tarung Profile follows a weakly documented cyclicity. Four peak in coral abundance coincide with the lack of larger foraminifera. The cycles start with packstones (TAR37), followed by

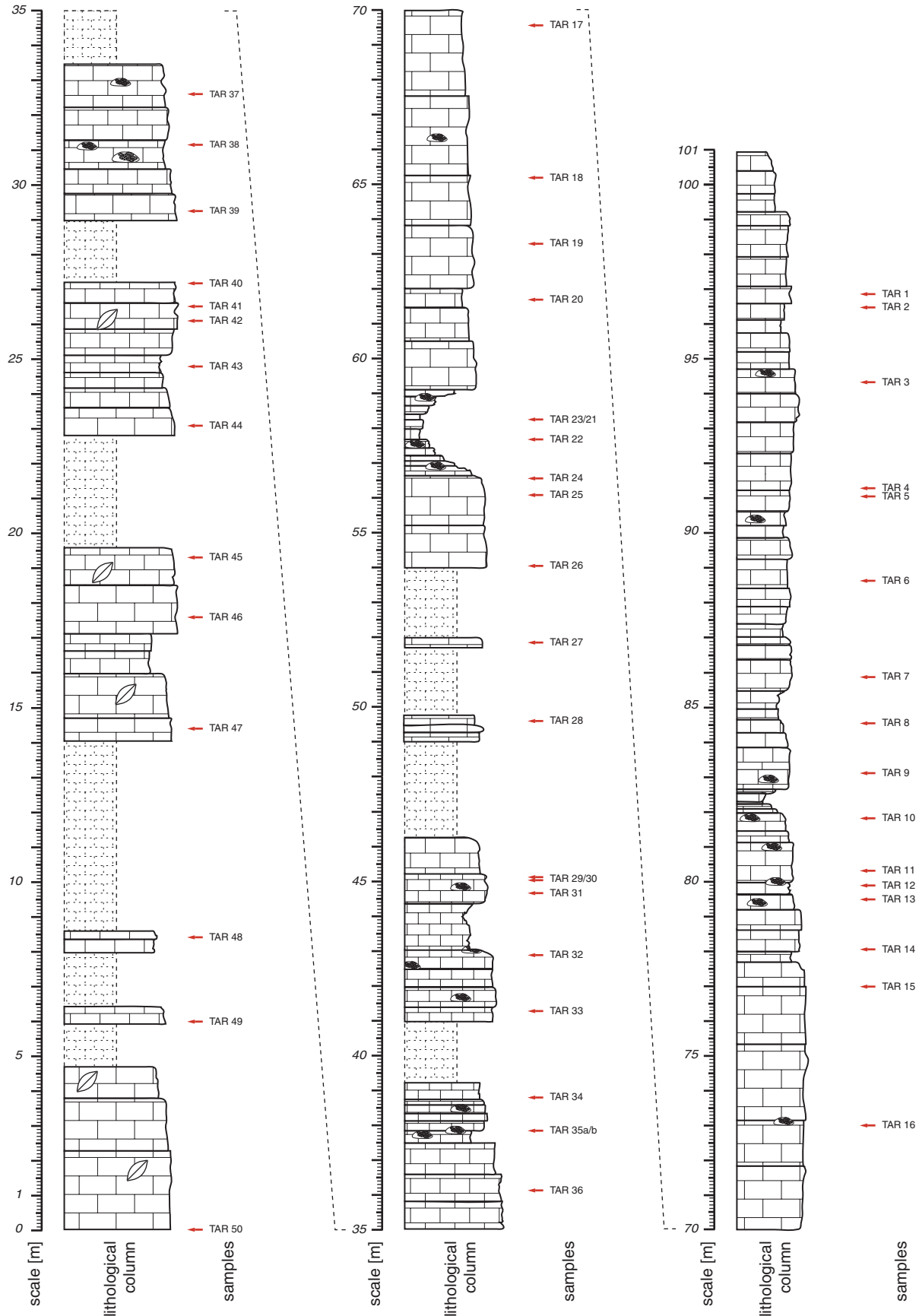

Fig. 29: Synthetic column throughout the Tarung Profile at the southern side of Albion Head; sample positions are indicated.

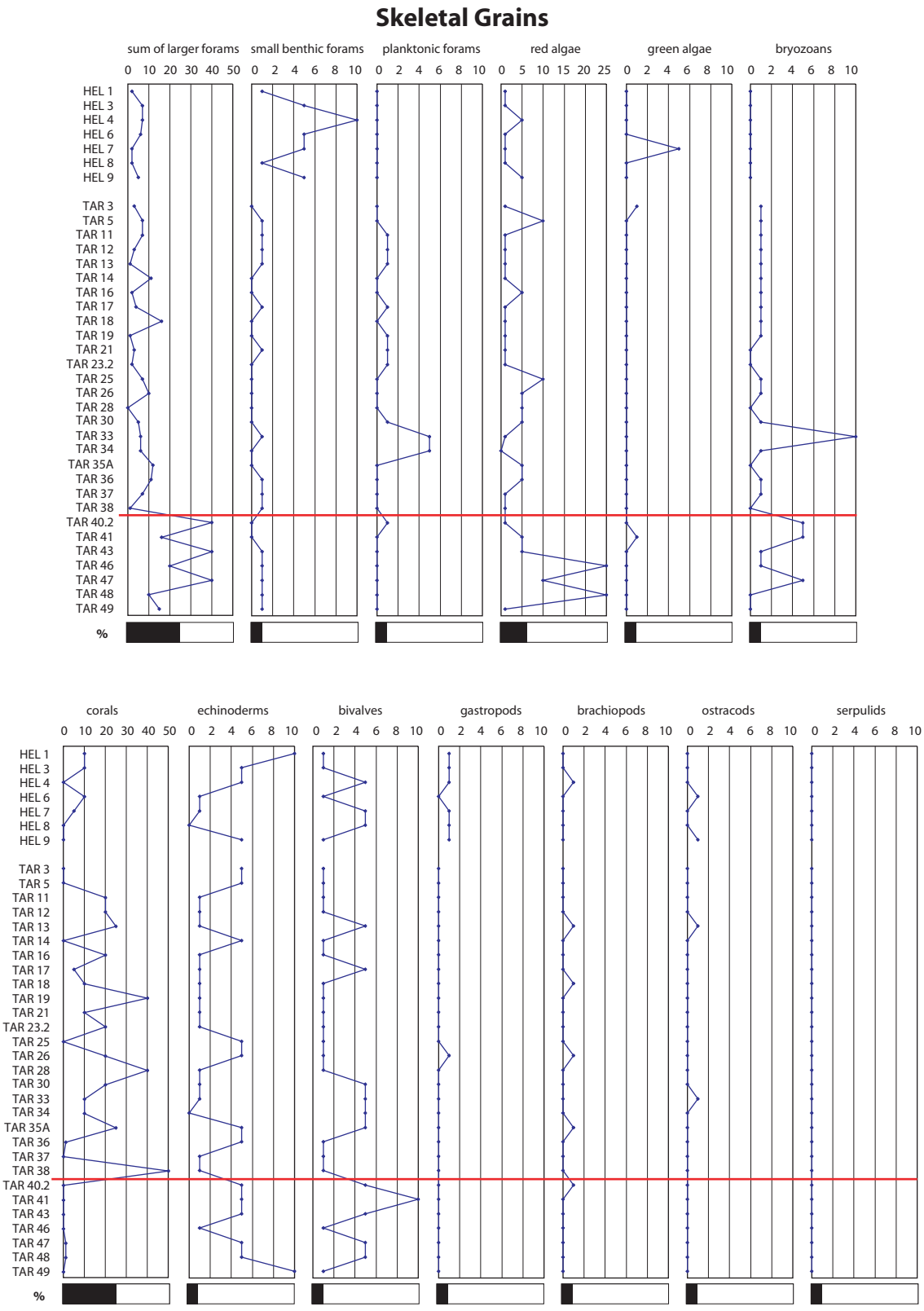

Fig. 30.1: Semi-quantitative frequency estimation of common skeletal grains in the thin sections of the Tarung Profile and Heliport Profile (Albion Head) reflecting their evolution upstrata throughout time.

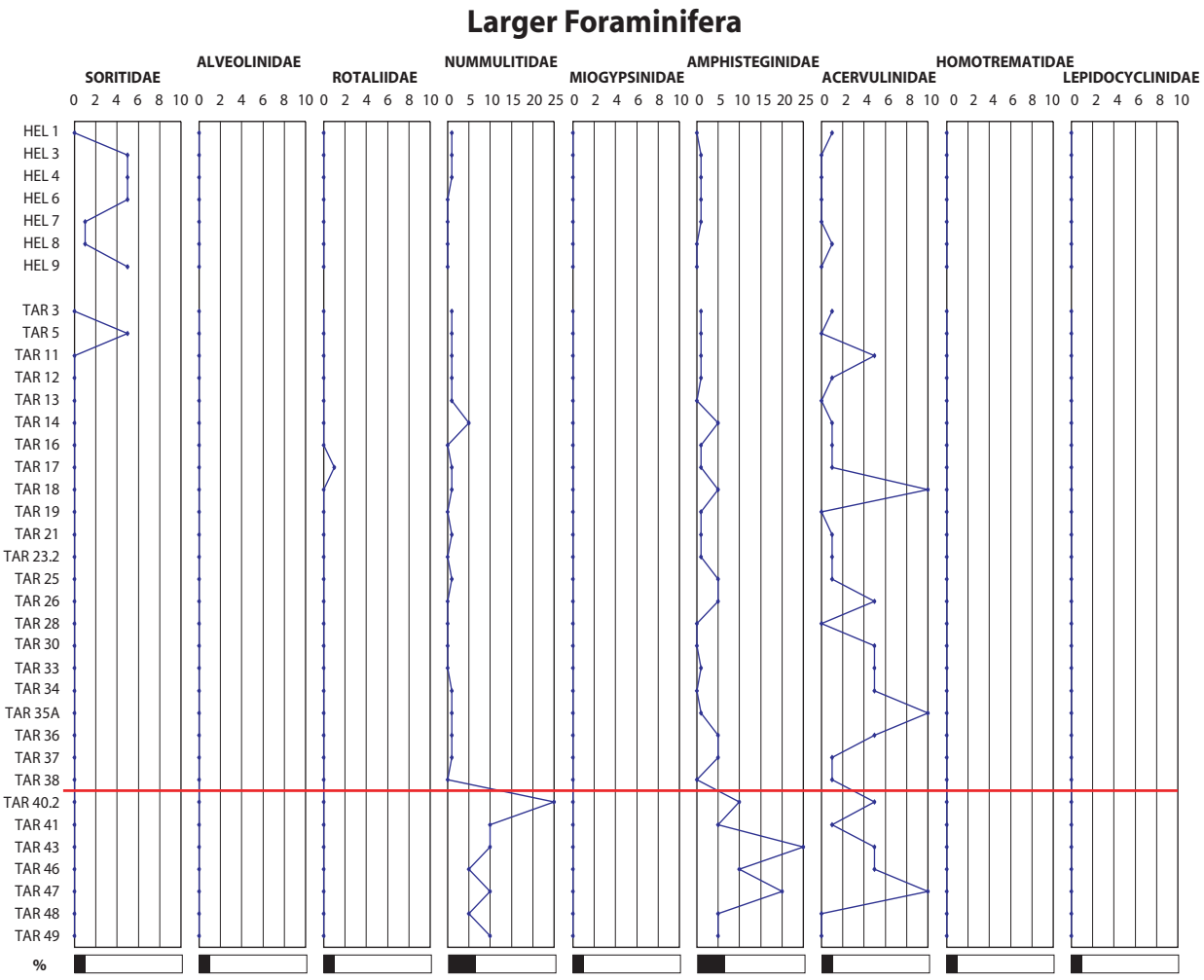

Fig. 30.2: Semi-quantitative frequency estimation of the larger foraminiferal assemblage in the thin sections of the Tarung Profile and Heliport Profile (Albion Head) reflecting their evolution upstrata throughout time.

boundstones (TAR35A) and ends with a coral accumulation in floatstones or rudstones (TAR28, TAR26).

The light coloured and massive carbonates found close to the highest point of Albion Head (Heliport Profile) represent a different facies compared to the Tarung Profile. Small benthic foraminifera, bivalves and gastropods dominate the skeletal grains of the wacke- to packstones throughout the uppermost 19-m of the carbonate sequence of Albion Head (Fig. 31). The amount of larger foraminifera is not very significant. However, most of the specimens of larger foraminifera are related to Soritidae and only a very few Nummulitidae or Amphisteginidae occur (Fig. 30.2). Some massive corals are scattered in the carbonates. Some of them are weathered and cropping out at the highest point of Albion Head. Planktonic foraminifera and bryozoans are missing.

The carbonates of the inner part of Albion Head are always massive. Bedding or other sedimentary structures were not observed. The composition of the skeletal grains of 5 samples collected in the inner part of Albion Head is characterised by larger foraminifera (Nummulitidae, Amphisteginidae, Soritidae), red algae and small benthic foraminifera. Bivalves and echinoderms provide additionally some fragments. Due to a high content of carbonate mud, the carbonates are pack- to wackestones. Nevertheless, corals as larger components are abundant.

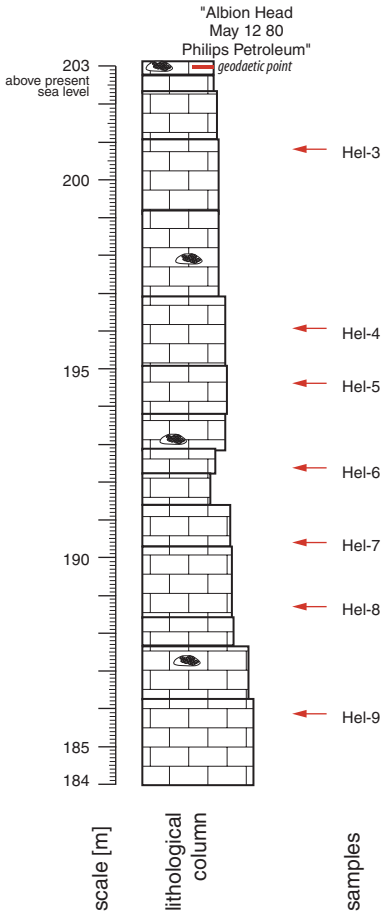

Fig. 31 Synthetic column of the top section (Heliport Profile) of Albion Head; sample positions are indicated.

Along the eastern side of Albion Head, about 80 m above present sea level four smaller build-ups rim the inner part of the carbonate complex. At one single location, these massive packstones provide some sedimentary structures, which indicate fore-sets dipping up to 64° to the eastern directions.
Below these build-ups, at the NE shoreline of Albion Head carbonate layers between some dm up to 1-m in thickness dip with 18° to 25° seawards to eastern directions. The contact between the layers is irregular. Thin beds of reefal debris (cm-sized bivalves, crinoids, corals) are intercalated into the sequence of predominate massive grain- to rudstone layers.

Southwest off the carbonate complex of Albion Head a selection of loose rocks is mainly made up of well-sorted, laminated sand- to siltstones. One larger block (1 x 1.5 m) of a poorly sorted breccia is characterised by broken rock fragments of different origin and sizes bedded without any contacts in a dense matrix of dark-grey mud.

Total Carbon Content

The total carbon content (TCC) record yields in general a $CaCO_3$ content of more than 95% (Fig. 32). Throughout the Tarung Profile, one single sample (TAR33) yields a $CaCO_3$ content

of only 87%. It marks the beginning of a middle part of the profile, which shows a higher variance in the record between 92 to 100% $CaCO_3$, whereas the samples below and above documents a mean $CaCO_3$ content of 98%.

The analysed samples from the internal area and the north-western side as well as the Heliport Profile do not indicate any significant changes or trends regarding the $CaCO_3$ content. Their mean $CaCO_3$ content is calculated with 98%.

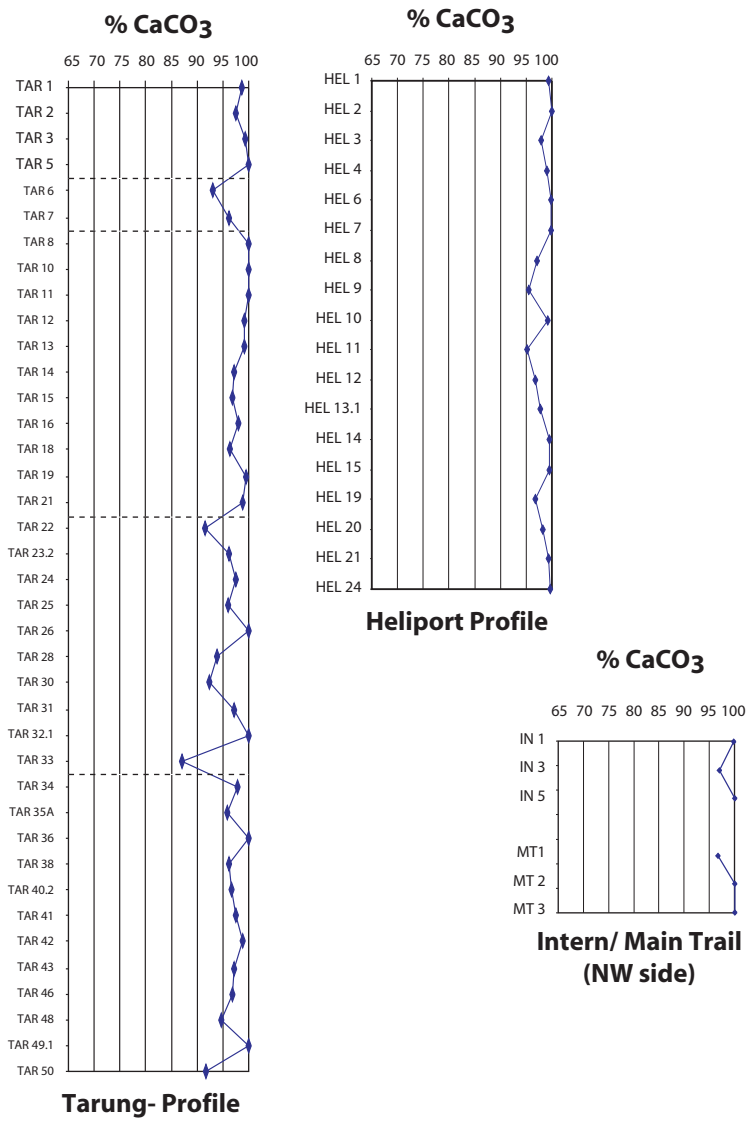

Fig. 32: Calculated $CaCO_3$ content upstrata of the samples from the Tarung- and Heliport Profile as well as spot samples from the NW side (MT) and inner part (IN) of the build-up of Albion Head.

Excerpt: The outcrops at the southern and the north-eastern side of Albion Head refer to deposits of the lower flanks of a build-up. A larger foraminiferal packstone forms the lower third of the Tarung Profile in the S and fore-sets with reefal debris in the NE dipping with 18° to 25° seawards to eastern directions. Within the Tarung Profile the change to a coral dominated succession further upwards exist and links to reefal deposits. Samples from the inner part of the carbonate complex dominated by carbonate mud. The pack- to wackestones is massive and contains small benthic foraminifera, molluscs, larger foraminifera and red algae. They were deposited in quiet and shallow water so that the carbonate complex of Albion Head documents probably a small atoll structure.

Southwest of the carbonate complex loose laminated sand- to siltstones and a block of a siliciclastic breccia are observed.

3.1.7 Offshore Islands

In the area around Quezon, several small islands are located a few km off the coast. On Tamlangon Island, Double Island and Mamarujan Island in the N and on Nakoda Island, Triple Cima Island and Mariquit Island off Albion Head siliciclastic deposits are cropping out.

The layers on the islands off Albion Head (Nakoda Island, Mariquit Island, Triple Cima Island) are dipping to southern directions. Consequently, the m- to dm-scaled massive beds in the north represent the lithostratigraphic base of the succession, while the layers with a thickness between 5 to 50 cm in the S of Nakoda Island are related to the lithostratigraphic top. The longest continuous exposure occurs on Nakoda Island. Over a thickness of estimated 200 m, mostly coarse grained sandstones are cropping out. The lower part of the sandstones is characterised by coarse- to very coarse-grained sandstones, which are made of sometimes cm-sized feldspar (plagioclase and alkali feldspar) and quartz. Moreover, a significant abundance of glauconites occur in all samples. Some rare coaly plant remains up to 5 cm in size are additionally observed in the field. These sandstones show no gradation and macroscopic and microscopic poor sorting. Further upwards the sandstones are still coarse grained before the medium grained and moderately sorted sandstones close to the top of the sequence contain intercalations of clay-silt layers. These uppermost deposits are dominated by quartz.

The S dipping sandstones, which occur on the northern islands (Tamlangon Island, Double Island, Mamarujan Island), are bedded in dm-scale and made of pure quartz grains. The grain size of the different sandstone layers, studied along a 14-m thick sequence on Tamlangon Island, ranges between very coarse- and fine-grained. Macroscopicly, the sorting seems to be quite good, but on a microscopic scale, the coarser varieties are less sorted than the finer varieties. The higher level of sorting correlates with a better rounding of the single grains up to a sub-rounded shape. Gradation is restricted to some slight internal changes in the coarser sandstones.

In conclusion, the siliciclastic deposits found on the islands off the study area are related to one single sequence, which documents a trend of fining-upward. It corresponds to the observations and interpretation of PARK & PETERSON (1979).

3.2 Diagenesis

The diagenesis of the carbonate deposits encompasses compaction, cementation, dissolution and microbial micritization as well as changes in the mineralogy (aragonite/ high-Mg calcite converts completely to calcite/ low-Mg calcite) and their isotopic signature. Dolomitization has not been observed in the onshore samples. The carbonates seem to be only recently affected by some meteoric influence and the depth of the metamorphic window was never reached.

3.2.1 Thin Section Study

This chapter presents the diagenetic features of the onshore carbonates observed during the study of the thin sections. Furthermore, due to the fact that porosity (and permeability) affects, but also reacts to most of the diagenetic processes their amount, distribution and character are added, whereas the classification of the porosity types follows the schema of CHOQUETTE & PRAY (1970). The Taglupa Profile and Salty Creek Section - Maasin Profile are used to demonstrate changes throughout the lateral extended carbonates, whereas the profile of Devel Peak are used for the build-up carbonates.

The most significant diagenetic processes documented in the samples are cementation, dissolution and neomorphism. Compaction is on the macroscopic as well as on the thin section scale low to moderate and has no major effect on the deposits. Microbial micritization is only a local effect, mainly observed on massive coral heads in the lower part of the Salty Creek Section.

Lateral Extended Carbonates

The content of sparite in a thin section is illustrated by the ration of micrite-content vs. sparite-content in a thin section (Fig. 33.1). However, the sparite content displays not necessarily only the content of the cements, because sparite is as well a product of neomorphic processes. Therefore, the second column shows the ratio of cement-related sparite vs. neomorphic sparite and illustrates where the content of sparite refers only too cementation (100%) and where (in the lower part of the Salty Creek Section) additionally neomorphic processes have to be expected. The neomorphic processes correspond to the floatstones, where the aragonitic corals and a few molluscs were completely converted to neomorphic

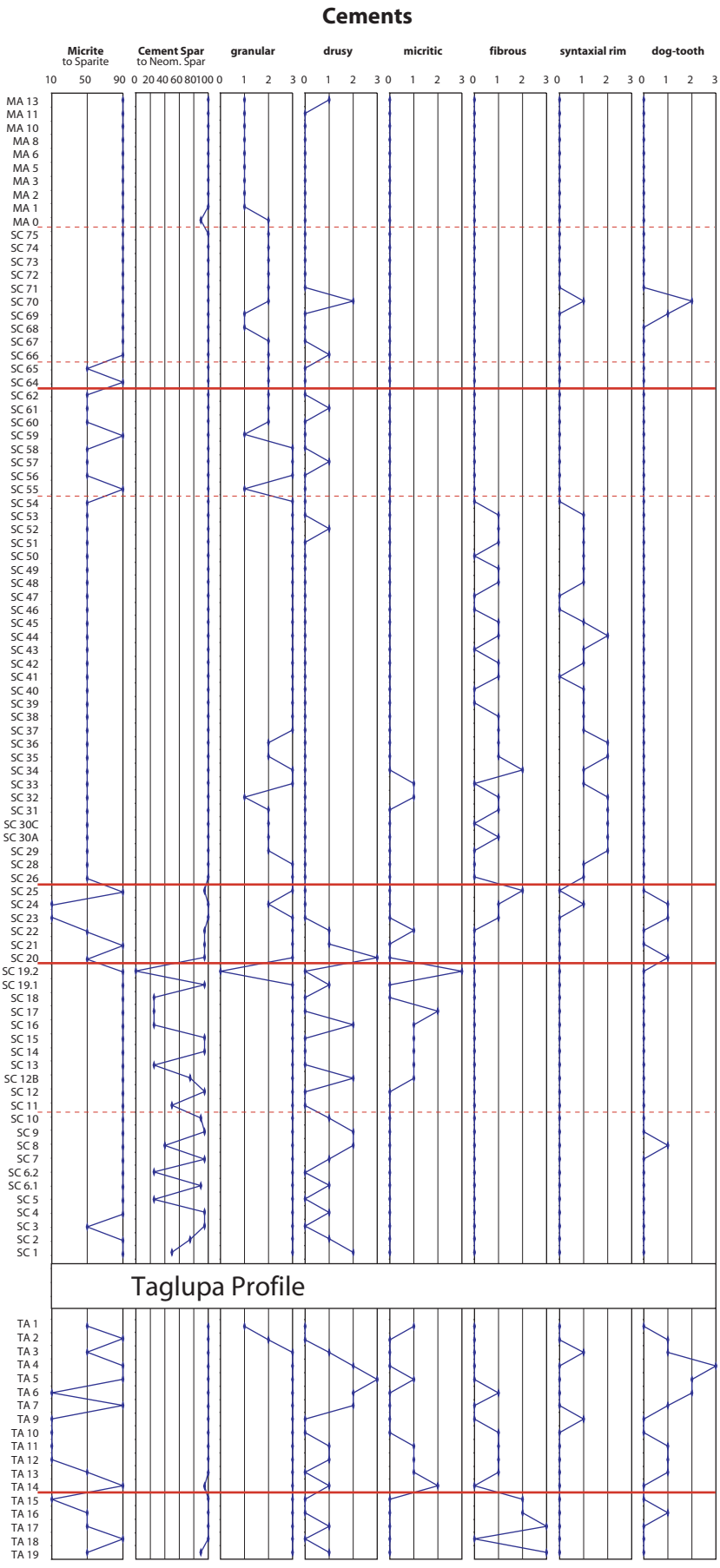

Fig. 33.1: Estimation of relative frequency of matrix- (micrite vs. sparite), sparite- (cement vs. neomorphic spar) and cement types throughout the samples of the Taglupa Profile and the Salty Creek Section - Maasin Profile.

spars. Furthermore, some neomorphic spars contain relicts of the micritic matrix or skeletal grains and cut into the matrix.

Anyhow, 6 different cement types have been observed: granular-, drusy-, micritic-, fibrous-, syntaxial- and dog-tooth cement. Radiaxial fibrous-, meniscus- or dripstone cements were not found. All cements are presently calcitic, even if a primary aragonitic mineralogy have to be assumed especially for the fibrous cements. Additionally to the lack of aragonite, dolomite or other cements were also not detected in the carbonates onshore.

Within a single thin section, up to 4 different cement types were identified, whereas more than 2 cement generations are rare. Most commonly is a micritic-, fibrous- or dog-tooth early cement overgrown by later granular or drusy cement. Only once, in a recrystallised coral head in the lower part of the Salty Creek Section an example of bladed-prismatic calcite has been observed as early cement. The size if the fibrous cements is less than 0.1 mm, whereas single crystals of the dog-tooth cement could reach 0.25 mm. The granular cement crystals range between 0.1 - 0.25 mm and the larger drusy crystals between 0.5 up to 2 mm. Most of the granular and drusy cements are clean. The prevailing granular cement occurs throughout the whole section, even if it is less abundant in the uppermost fine samples of the Maasin Profile (Fig. 33.1). Drusy and also a few dog-tooth cements exist preferably in the lower part of the section (Taglupa Profile, Salty Creek 1, lower part of Salty Creek 2 profile). The fibrous cement is observed in the lower part of the Taglupa Profile as well as in the carbonate sands of the Salty Creek Section. Whereas this cement type is often associated with the larger foraminifera, syntaxial cement is closely related to echinoderms. Therefore, syntaxial cement is common in the lower part of the carbonate sands together with the abundant echinoderms. Both cement types (fibrous, syntaxial) disappear together with a significant decrease of larger foraminifera and bryozoans as well as the increase of small benthic-, planktonic foraminifera and molluscs in the upper part of the Stage 2 of Salty Creek Section (cf. Fig. 12, p.36).

The precipitation of cements in open pores took place when the pore-fluids are supersaturated with respect to the cement phase. In this context the diagenetic process of dissolution is important to create additional porosity and the high concentration of Ca^{++} and CO_3^{--} to develop calcitic or aragonitic cements. Within the onshore carbonates, ancient dissolution produced as fabric selective dissolution of components (mainly corals and molluscs) moldic porosity. No fabric selective dissolution created some pressure solution (stylolites, sutured component surfaces) and a few channels as well as the common vugs and cavities observed in the field. In

general, the vugs and cavities are frequently still open and suggest being a product of recent karstification.
Whereas aggressive water is the main factor for dissolution, compaction triggered the pressure solution. Beside the later generated stylolites, concave-convex- and/or sutured component contacts as result of pressure solution, a few thin sections show additionally deformation and broken components. Anyhow, the low to moderate compaction in general is best documented by the component contacts. No or point contacts between the components, referring to low compaction, are associated with the carbonates with a high content of micritic matrix (mud-, wacke- and floatstones) in the lower and uppermost part of the section (Fig. compaction). Within the carbonate sand deposits (pack- and grainstones) of the middle part of the section all components are in contact and point- as well as tangential contacts prevail. Here, some concave-convex- and sutured component contacts are observed, which are related to a moderate compaction and not (like in the lowermost samples of the Taglupa Profile) to a different petrography of the components (carbonates against siliciclastic gravel).

The illustrated total porosity (Fig. 33.2) is estimated for each thin section by adding the open porosity and the porosity filled with cements. Within the lateral extended carbonates once 40% of total porosity was observed, but the mean value ranges between 5 and 25%. The general decreasing trend of the total porosity upwards corresponds to finer sediments so that consequently the mud- to wackestones of the Maasin Profile show the lowest total porosity with maximal 5%. The relative high total porosity in the micritic-dominated sediment of the lower part of the section is a result of molds and some channels. The floatstones contain abundant molluscs and corals whereas the matrix is often shaley.
The open porosity is low in the lower and the uppermost part of the section. The carbonates of the Taglupa Profile and the Maasin Profile have mainly no open pores, whereas at Salty Creek 1 profile 1% porosity was found. Higher amounts of open porosity (1 to 10%) contain the lateral extended carbonates, which correlates to the carbonate sand deposits of the upper Salty Creek 2 profile, Salty Creek 3, 4 and 5 profile. However, the increase of the porosity in the middle part of the section is only partly related to the abundant interparticle porosity, which occur besides in the pack - and rudstones of the Taglupa Profile (Fig. 33.3). The main reason seems to be the observed high amounts of vug porosity in the carbonate sands, which is related to recent dissolution.

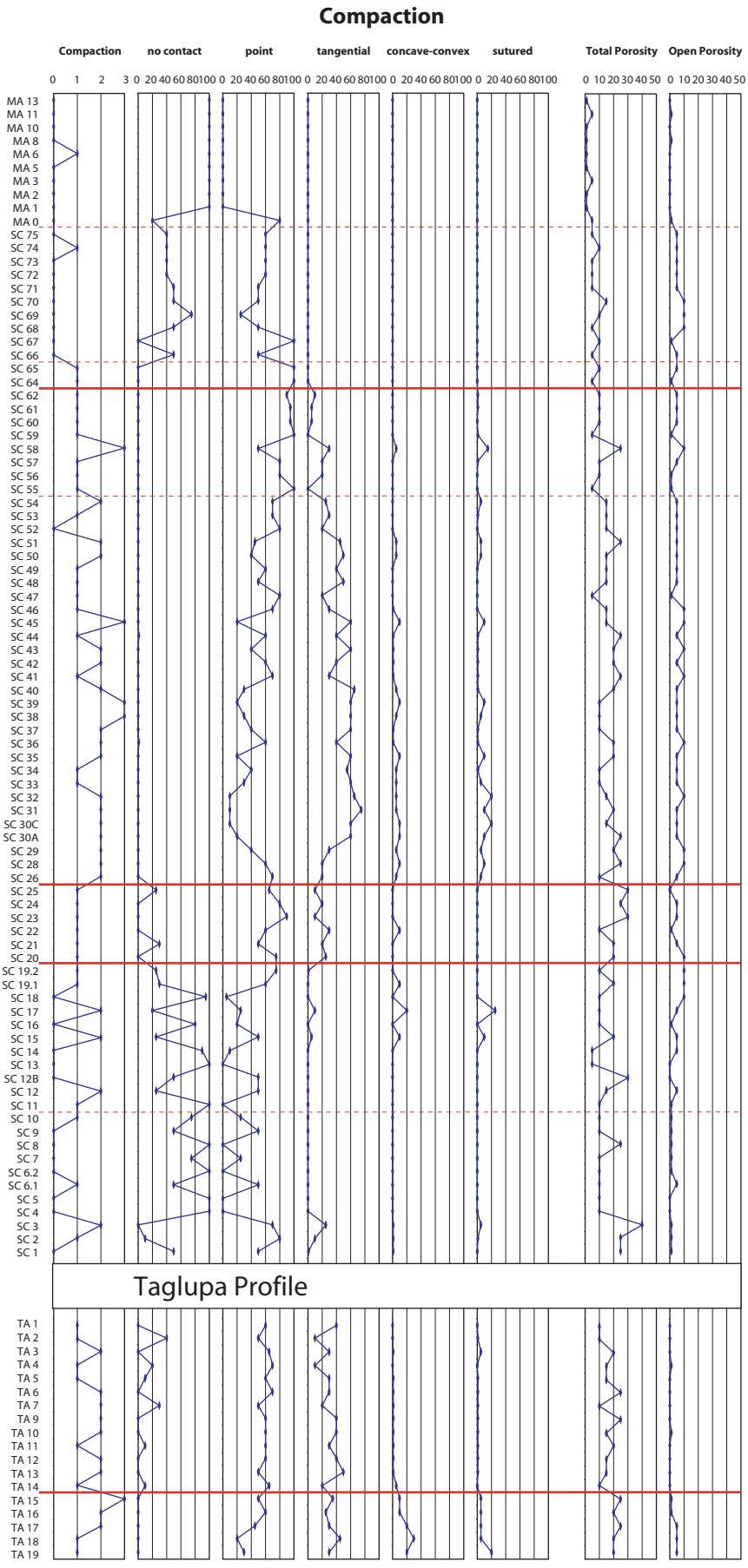

Fig. 33.2: Semi-quantitative frequency estimation of component contact types, total- and open porosity throughout the samples of the Taglupa Profile and the Salty Creek Section - Maasin Profile.

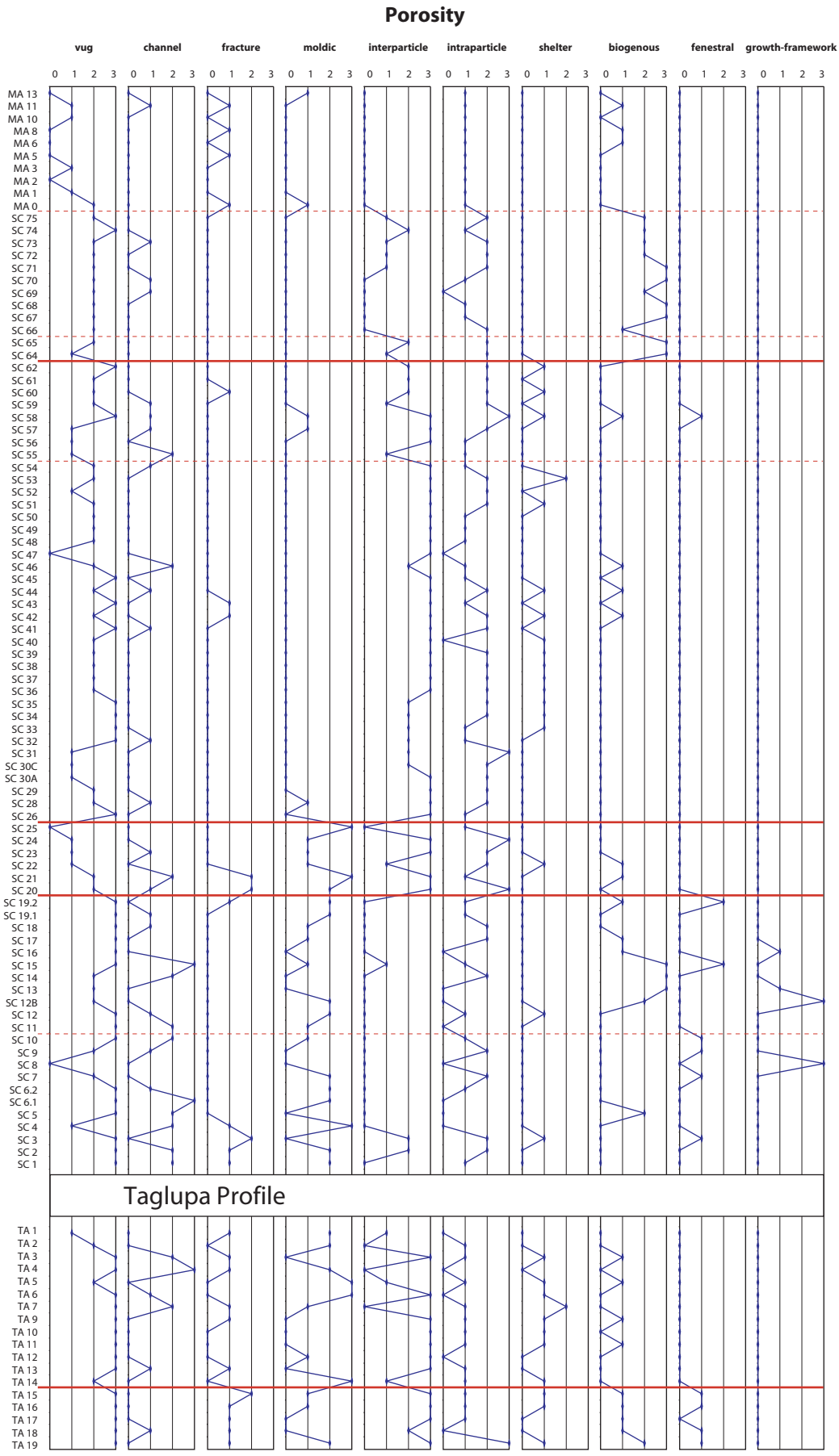

Fig. 33.3: Estimation of relative frequency of porosity types throughout the samples of the Taglupa Profile and the Salty Creek Section - Maasin Profile.

The lack of strong compaction leads, one hand to the preservation of some primary porosity, mostly as interparticle-, intraparticle-, and shelter porosity, on the other hand to only small and rare additional fracture porosity (Fig. 33.3). Consequently, the fracture porosity is of low significance for the total porosity. The same applies for some small fenestral porosity (produced by encrusting red algae and/or larger foraminifera) and the growth-framework porosity of the patchy head corals, which are both, restricted to the lower part of the Salty Creek Section. The biogenous porosity might result in significant porosity, but in the studied samples, the created porosity was often filled again with sediment, before the diagenetic processes affected the carbonates. Hence, the biogenous porosity is more a proxy of biogenic activity than indicating significant porosity.
Finally, beside the primary porosity, dissolution processes created almost all of the additional porosity (moldic-, channel-, vug porosity) in the lateral extended carbonates. Intercrystalline porosity was never observed.

Build-up Carbonates

Similar as in the lateral extended carbonates, all cements observed in the build-up of Devel Peak as well as at Albion Head are calcitic and dominated by sparite. Due to the fact that the primary aragonitic corals and molluscs occur throughout the whole succession, in most of the samples a variable portion of neomorphic sparite occur (Fig. 34.1). The amount of neomorphic sparite correlates with the amount of corals and molluscs in a sample. Consequently, with respect to an increase of corals in the upper part of the succession, also the amount of neomorphic spars as well as drusy cements increases slightly. Anyhow, a number of samples throughout the succession contain additional patches of neomorphic spar. Nevertheless, granular cement type prevails in the build-ups similar to the lateral extended carbonates. The most significant different regarding the cement types is that beside granular-, drusy- and some micritic cement no other cement type occurs significantly. Fibrous-, syntaxial-, dog-tooth cement were observed in a very few samples throughout the succession, whereas meniscus- and dripstone cement were never found. Furthermore, with the exception that drusy- and micritic cements are slightly more abundant in the upper part of the succession, the amount of the different cements shows no significant relation to the different lithologies or the different development stages of the build-up of Devel Peak.
During the diagenetic process, an older dissolution process affected the carbonates and produced the moldic porosity. This is completely closed today. Later dissolution seems to be

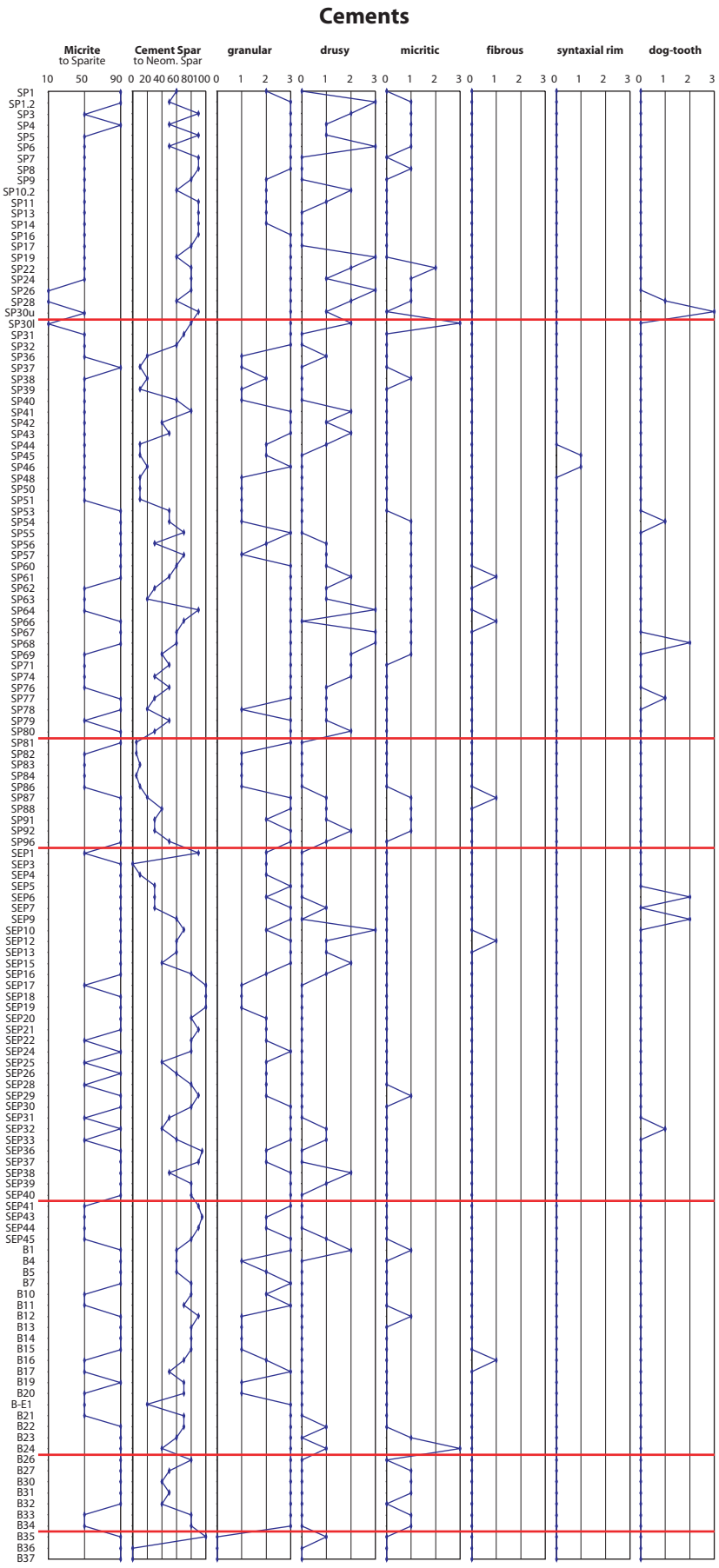

Fig. 34.1: Estimation of relative frequency of matrix- (micrite vs. sparite), sparite- (cement vs. neomorphic spar) and cement types throughout the samples of the Devel Peak build-up.

restricted to the recent or sub-recent strong karstification processes, which created channels and numbers of vugs in the thin sections as well as several huge cavities, specially observed at Albion Head. Pressure solution is rare and very low. Only some broken components refer to a moderate compaction of some samples (mainly in the uppermost part of the succession) before they were completely lithified. Therefore, the different component contacts (prevailing point- and tangential contacts) do not provide any useful indications of compaction rather than reflecting the primary texture of the carbonates (Fig. 34.2).

The total porosity estimated in the thin sections seems to be lower than in the lateral extended carbonates (Fig. 34.2). With the exception of some samples from the upper part of the succession, the ranges of 5 to 15% total porosity covers most of the samples. Even if compaction did not reduce the primary porosity, the amount of the interparticle-, intraparticle- and shelter porosity is (especially in the lower part of the succession) relative low, because of the high content of micrite throughout the build-up carbonates (Fig. 34.3). Therefore, only the moldic porosity represents a significant amount of older porosity, because fracture- as well as fenestral porosity is always very small. The vug and channel porosity leads to most of the total and almost all of the open porosity. Growth-framework porosity was neither in the field nor in the thin sections observed, like intercrystalline porosity.

Excerpt: The record of the diagenetic processes in the onshore carbonates is restricted to the precipitation of some small early cements (fibrous, dog-tooth, micrite), which are observed in the lateral extended carbonates, and the widely spread later cement generation made up of the dominate granular- and some drusy cements. Furthermore, pressure solution and broken components refers to a low to moderate compaction, whereas mainly moldic porosity indicate ancient dissolution processes. Neomorphism affects mainly corals and some molluscs, but produced also some patchy spots of neomorphic spars. In general, obvious relationships between the composition and development of the carbonates and the diagenetic features are only indicated in the lateral extended carbonates.
The estimation of the total porosity is strongly affected by the recent overprint of the ongoing karstification process. Almost all of the open porosity is recent.

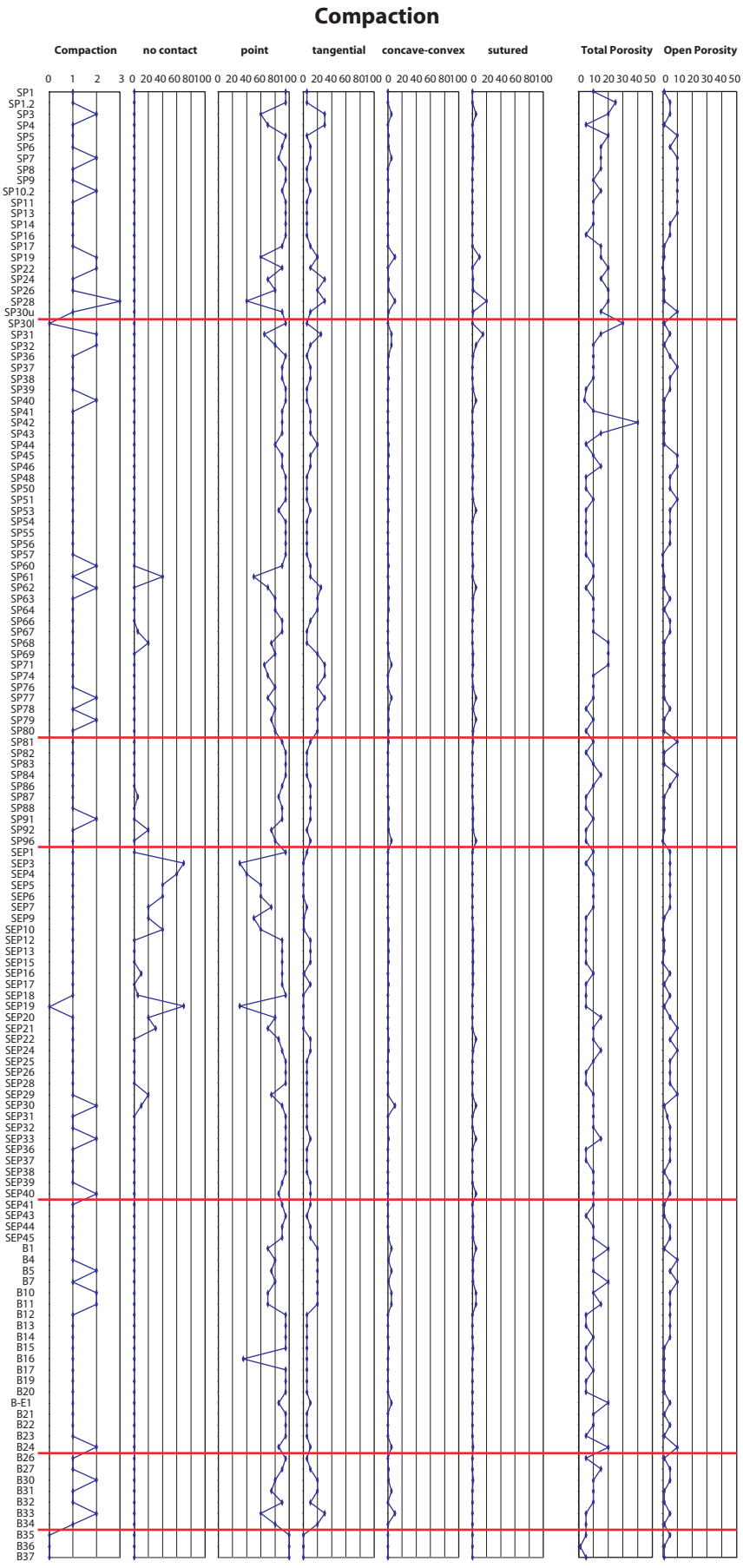

Fig. 34.2: Semi-quantitative frequency estimation of component contact types, total- and open porosity throughout the samples of the Devel Peak build-up.

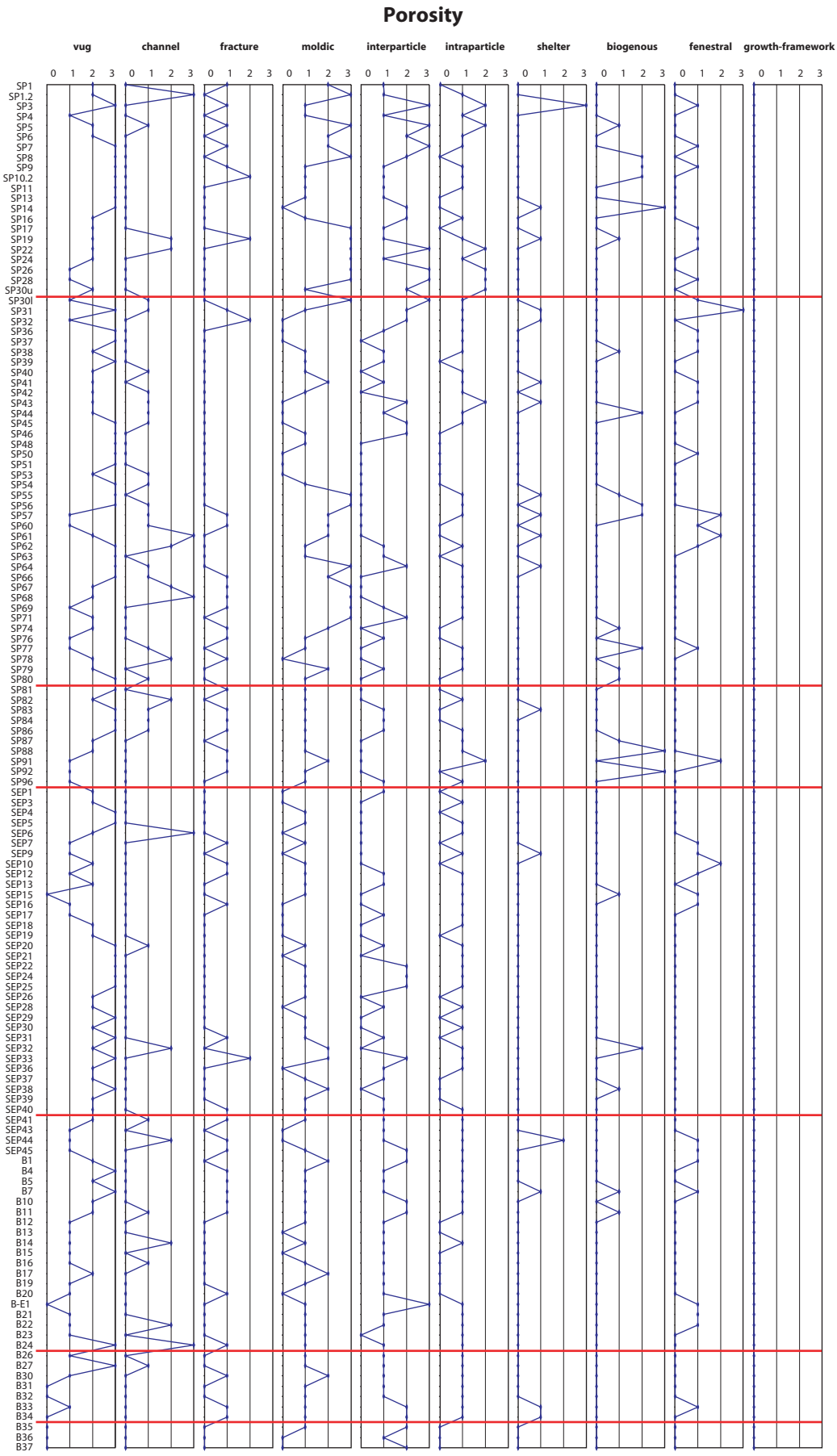

Fig. 34.3: Estimation of relative frequency of porosity types throughout the samples of the Devel Peak build-up.

3.2.2 Cathodoluminescence analysis

Due to the fact that many of the onshore samples are diageneticly strongly influenced and it is well known that the cathodoluminescence often reverals outlines and internal structures of fossils or cements which are invisible in planar or polaried light microscopy, several thin sections from the Tumarabong River Section and Devel Peak as well as some scattered samples were studied with a cold cathode microscopic equipment. Furthermore, as result of changes of crystal field parameters the cathodoluminescence color allow the distinction of the orange calcite vs. the green aragonite (HENDERSON & IMBUSCH, 1989; YANG et al., 1995). Fluctuations in the chemisty of the pore fluids but also changes in the rate of crystal growth are additionally reflected in the zonation of carbonate crystals (TEN HAVE & HEIJNEN, 1985). However, even if the role of Mn^{2+} as the most important activator element and Fe^{2+} as the inhibitor in calcites and dolomites is widely accepted, the correlation of the cathodoluminescence intensity and the Mn concentration is still controversial discussed (HABERMANN et al., 2000). Nevertheless, in many limestones, there is a similar pattern of luminescent zones in calcitic spar cements: the spar commonly shows a non-luminescent - bright - dull (or final dull yellow) zonation with increasing burial (e.g. FANK et al., 1982; GROVER & READ, 1983; FRYKMAN, 1986; DOROBEK, 1997)

The results of the cathodoluminescence study of thin sections from SW-Palawan provide, unfortunately, only very little feature, which are usefull for the evaluation of the diagenetic history. The most significant observation is that despite the high frequence of primary aragonitic components (e.g. corals, molluscs) today not one single indication of aragonite has been observed. Most of the samples show no or very slight luminescence effects with a dark orange cathodoluminescence color. Anyhow, within the larger foraminiferal packstones of the Tumarabong River Section some components, like the larger foraminifera, display a slight dissolution process, followed by a thin fibrous and bright luminescenet cement rim around the component before a non-luminescent granular sparit closed the open pores (Fig. 35). The same development is documented in the planktonic foraminifera (*Orbulina*) found further upsection in a mudstone.

In a sample from the lower part of Devel Peak the best of some examples containing a small cavity with some internal sediment but also large (up to 1.5 mm in size) sparite crystals was recovered. The sparite cement did not fill the pore space so that still open porosity exists. On the left side of the pore, the development of the cement was studied in detail. Therefore, a

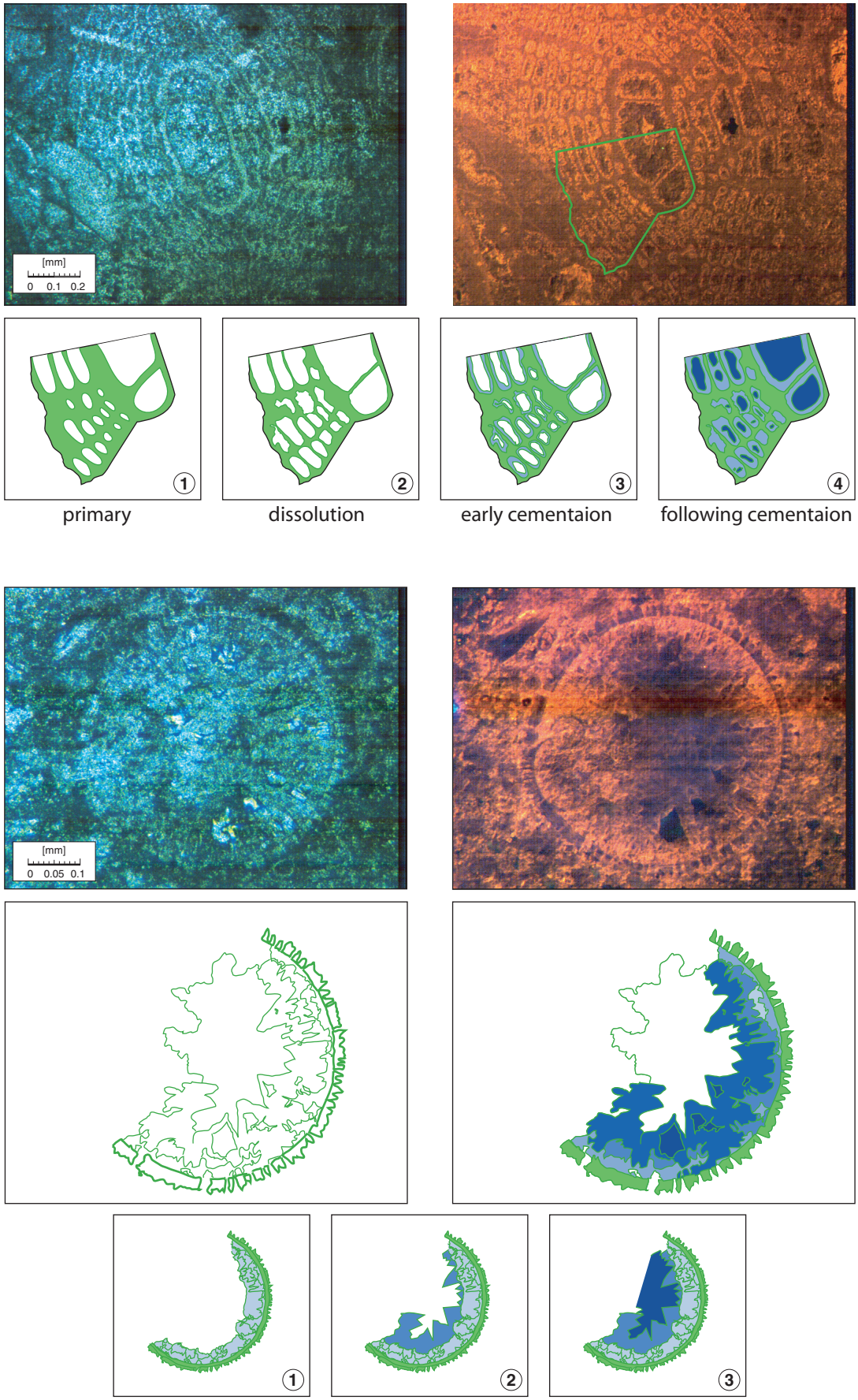

Fig. 35: Normal light microscope images and cathodoluminescence images of a larger foraminifera (*Lepidocyclina* (*Eulepidina*) *planata*) and a planktonic foraminifera (*Orbulina*) with the interpretation of cement generations from early (light blue) to later (dark blue) stages below.

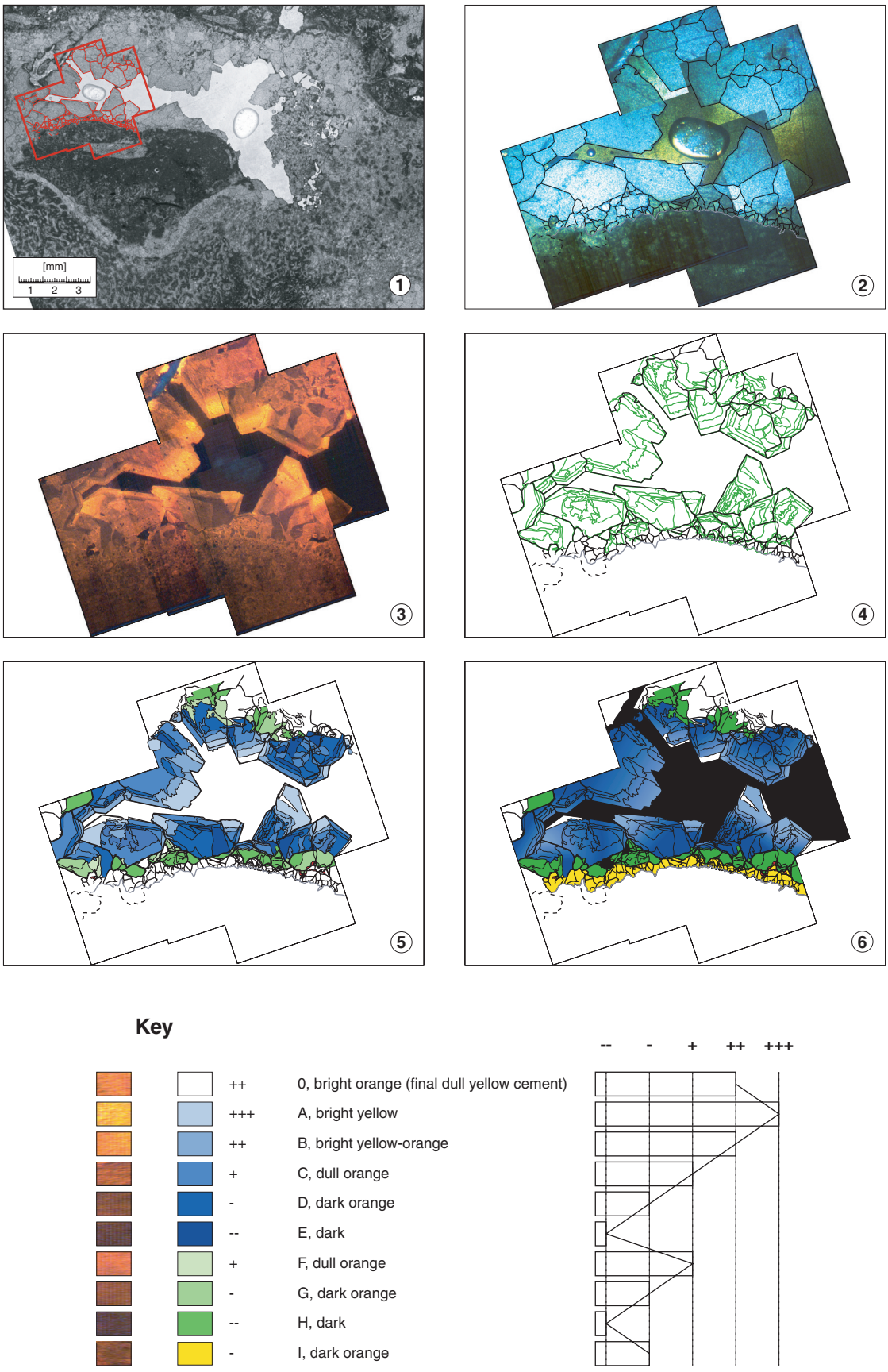

Fig. 36: Normal light microscope thin section images with outline of focus (1); polarization light (2) and cathodoluminescence (3) image mosaic of focus area with large sparite crystals prograding into an open pore; photohraph 4 shows the outlines of the different luminescence zones in the crystals seen in the cathodoluminescence image, photohraph 5 the detailed and photohraph 6 the simplified interpretation. The key indicates upwards the chronology of the different colours of the luminescence zones.

mosaic of 5 cathodoluminescence images was created (Fig. 36), which should cover all possible stages of cement precipitation. Whereas the outlines of the single crystals could be identified already in the planar or polarised light of the microscope, the cathodoluminescence image yield additionally the confirmation that the first smaller granular cement and larger crystals on top of it document two separate cement generations. The lower cement generation shows almost no variance in their dark orange to non-luminescent colour. In contrast, the clear granular to drusy cements above passes twice from dark orange cathodoluminescence colour into dull orange colour, whereas in the big sparite crystals additionally a final bright coloured stage is visible. Furthermore, the later cements indicate in parts a moderately pronounced zonation.

3.2.3 Stable Oxygen and Carbon Isotope Record

During the precipitation or later modification of carbonates, a characteristic stable isotope signature ($\delta^{13}C$ and $\delta^{18}O$) were impressed into the carbonates in consideration of the isotopic signature of the involved fluid and the temperature. Consequently, the stable isotope signature of a carbonate provides an indication of the prevailing conditions during their precipitation.
In order to ensure the assignment of the measured data set to different settings and eventually different time periods, four carbonate categories were distinguished: (1) sparitic cement, (2) undefined sparite, which includes the sparite of recrystallised skeletal grains (e.g. corals, molluscs), larger sparitic spots or undefined sparite, (3) micrite and (4) bulk sample, which were taken from a homogeneous powder of the whole carbonate sample. With the exception of the bulk samples, all the selected rocks offer one or more spots of the remained carbonate categories, which is big enough to drill the small amount of sample material without any contamination of the surrounding carbonates. Thereby, the selected samples are spread over the whole area of lateral extended carbonates and the build-up of Devel Peak.

The data set of 93 isotopic ratios of $\delta^{13}C$ and $\delta^{18}O$ are presented in the 6 scatter diagrams of Fig. 37. The two uppermost graphs A & B show all data points sorted first by sites (A) and secondly by the four carbonate categories: cements, undefined sparite, micrite and bulk samples (B). The 4 graphs C - F below show each carbonate category separately. Here, the data points are sorted again by sites.

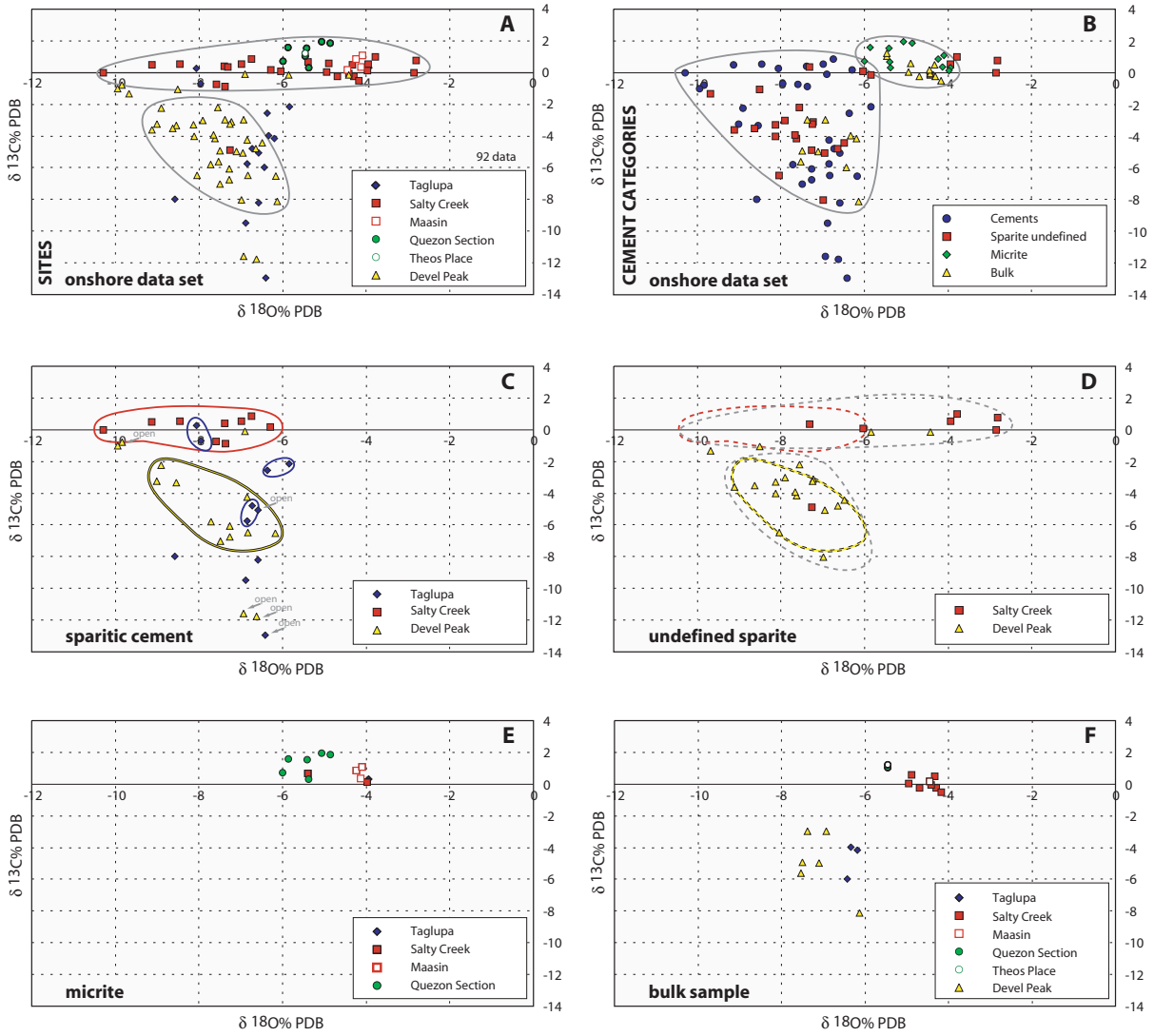

Fig. 37: Six scatter diagrams of 92 stable oxygen and carbon isotope data from samples of the onshore study area; All data divided by sites (A) and by the four cement categories Cements, Sparite undefined, Micrite and Bulk (B) are shown in the two uppermost graphs; diagram C - F presents each, the data of one cement categorie divided by sites.

The first scatter diagram A (Fig. 37) documents that (with the exception of only 1 data point) all of the 36 isotopic rations of the Salty Creek Section, Maasin Profile, Theo's Place and Quezon Section plot within the small range of $\delta^{13}C$ values of +2 to -1‰ $\delta^{13}C$. However, the range of $\delta^{18}O$ from -3 to 10.5‰ $\delta^{18}O$ is very wide. In contrast to the samples of the lateral extended carbonates, the isotopic ratios of Devel Peak plot mainly, but with several exemptions, between -2 to -8‰ $\delta^{13}C$ and -6 to -9‰ $\delta^{18}O$. Finally, the Taglupa Profile at the base of the onshore carbonates succession has an outstanding position regarding the isotopic signatures, because the distribution of these samples is hardly unique, even if some samples fit into the ranges of the lateral extended and build-up carbonates. However, it has to be

emphasised that these carbonates at the base of the carbonate succession contain beside different terrestrial gravels also partly a relative high portion of plant debris.

The second scatter diagram B (Fig. 37) shows the same complete data set as diagram A, but sorted by the four categories. Again, two significant concentrations, but with different outlines than before, are deduced from the diagram. All data points of the micrite and bulk sample categories are concentrated in the relative small area between +2 to -1‰ $\delta^{13}C$ and -4 to -6‰ $\delta^{18}O$. The isotopic ration of the cements and undefined sparite ranges between +1 to -10‰ $\delta^{13}C$ and -6 to -10.5‰ $\delta^{18}O$. Two groups of 4 and 3 data points, which belong to the cements and undefined sparite, show an offset. One group (4 data points) is characterised by slightly positive $\delta^{13}C$ (0 to +1‰ $\delta^{13}C$) and low $\delta^{18}O$ (-2.57 to -4‰ $\delta^{18}O$) values, the other by very negative $\delta^{13}C$ values (-11.5‰ to -13‰ $\delta^{13}C$). As illustrated in the scatter diagram of the cements (Fig. 37C) the three data points with very negative $\delta^{13}C$ are collected from samples of Devel Peak and the Taglupa Profile. The probably significant similarity of them is that the sampled cements hemed still open pores. Additionally, the sample (-5.08‰ $\delta^{13}C$/ -6.58‰ $\delta^{18}O$) collected at the Taglupa Profile provides a link, that some depletion of the $\delta^{13}C$ might be related to the open pores. This sample should actually corresponds with the samples -2.13‰ $\delta^{13}C$/ -5.84‰ $\delta^{18}O$ and -2.57‰ $\delta^{13}C$/ -6.36‰ $\delta^{18}O$, because all three samples were taken from the microscopically same rim cement around skeletal grains in one rock sample (TA1). In general, the isotopic ratios of the cements represent two different signatures: All cements of the Salty Creek Section are characterises by an isotopic ration between +1 to -1‰ $\delta^{13}C$ and -6 to -10.5‰ $\delta^{18}O$. These cements are related to fabric selective (primary) porosity like interparticle-, intraparticle- or shelter porosity and only two samples are related to a fracture. Another cements are found at Devel Peak. It ranges predominately between -2 to -8‰ $\delta^{13}C$ and -6 to -9‰ $\delta^{18}O$, whereas the cements found in fabric and not fabric selective porosity show close coherence with recrystallised corals. The three samples of Devel Peak plotting into the field of the cements of Salty Creek Section were drilled from a shelter-, an intraparticle porosity and a fracture. However, the isotopic signatures of both cements do not reflect any trend of isotopic changes, which correlates with the stratigraphy of the related sites.

The isotopic ratios measured in the undefined sparite samples (Fig. 37D) correspond nicely with the two different isotopic signatures of the cements. The both additional samples of the Salty Creek Section with isotopic rations of +0.36‰ $\delta^{13}C$/ -7.31‰ $\delta^{18}O$ and +0.10‰ $\delta^{13}C$/ -

6.04‰ $\delta^{18}O$ correlates perfectly with the clearly defined sparite cements of Salty Creek Section. The data points of the Salty Creek Section in the range +1 to 0‰ $\delta^{13}C$ and -2.8 to -4‰ $\delta^{18}O$ show with more positive $\delta^{18}O$ values an offset to the Salty Creek Section cements. These samples are, in contrast, related to recrystallised coral. With the exception of one single sample (-4.79‰ $\delta^{13}C$/ 6.64‰ $\delta^{18}O$), made up of the sparite found in a mold of a mollusc, all samples of Devel Peak are also related to recrystallised corals. Almost all of these samples plot in the same field as the cements of Devel Peak.

The scatter diagram of the micrite (Fig. 37E) document a narrow range (+2 - 0‰ $\delta^{13}C$/ -4 - -6‰ $\delta^{18}O$) for the micrite found throughout the lateral extended carbonates, from the base (Taglupa Profile) to the top (Quezon Section) of the succession.

The plot of the bulk carbonate samples reflects (Fig. 37F) the isotopic ratios of the micrite of the lateral extended carbonates or of the cements/ neomorphic spars of Devel Peak. In conclusion, the bulk samples confirm the detailed studies of carbonates.

3.3 Stratigraphy

The stratigraphy of the sedimentary sequences of the study area onshore and the offshore survey results from biostratigraphic data based on larger foraminifera, planktonic foraminifera and nannoplankton, besides some lithostratigraphic field observations. For the collection of these data thin sections and some smear-slides of the field samples were studied. The biostratigraphic data of the three wells offshore based on ditch cutting samples, sidewall cores and thin section studies reported from Robertson Research, Singapore (TIDEY et al., 1975; TROELSTRA, 1981; HUGHES & VAROL, 1982). Referring to the "Look-Up Table version 3:10/99" (MCARTHUR et al., 2001) the measurements of the $^{87}Sr/^{86}Sr$ ration of two oyster shell and one aragonitic bivalve supplements the stratigraphic data by a numerical age for Devel Peak. The numerical age given by the $^{87}Sr/^{86}Sr$ ratio of a sub-recent bivalve from the Tumarabong River Section dates a late flooding event during the development of the onshore study area.

3.3.1 Larger foraminifera

Larger foraminifera are abundant and well known from SE Asia and the Philippines. Their biostratigraphic potential for the whole Indopacific region has been the subject of many

papers. Therefore, the "East Indian Letter Classification" of the Tertiary based on larger foraminifera was introduced by VAN DER VLERK & UMBGROVEN (1927). Cenozoic larger foraminifera from SE Asia were studied intensively over the last 30 years in many investigations with biostratigraphic perspectives (e.g. HANZAWA & HASHIMOTO, 1970; HASHIMOTO et al., 1977; MÜLLER & VON DANIELS, 1981; HASHIMOTO & MATSUMARU, 1982; HASHIMOTO & MATSUMARU, 1984; COSICO et al., 1989; RENEMA & TROELSTRA 2001).

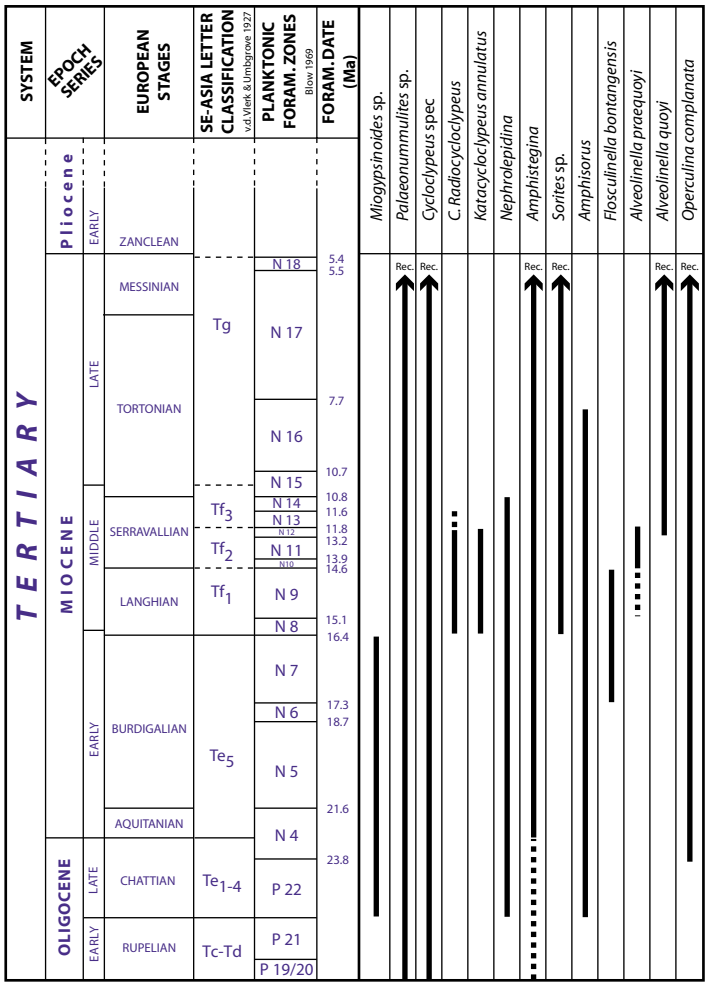

Fig. 38: Range of larger foraminifera with biostratigraphic significance for the study area in SW-Palawan. Chronostratigraphy after MÜLLER et al. (1989) with modifications of W. Renema/ Leiden (pers. comm. 2002).

The samples from the study area in SW Palawan contain several foraminifera taxa, which are useful for dating. Figure 38 summarises the distribution of major larger foraminifera with respect to the biostratigraphic zonation of VAN DER VLERK & UMBGROVEN (1927) and BLOW (1969). The biostratigraphy based on larger foraminifera was provided by W. Renema/

Leiden. Even if many different individuals of larger foraminifera were recovered from the samples, the study turns out that the moderate or sometimes very poor preservation of the foraminifera limits additionally the number of the well-orientated sections. Hence, the classification of many of them on the species level is quite difficult. A high resolution of the dating is therefore impossible. The determination up to the genus level has been done without major problems and allows an assignation of a Middle Miocene age for these carbonates (Fig. 39).

Taglupa Profile

Only the sample TA2 contains sufficient sections of larger foraminifera, which allow their determination and estimation of the age.

Miogypsinidae Vaughan, 1928
Miogypsinoides Yabe & Hanzawa, 1928
Miogypsinoides sp.

Alveolinidae Ehrenberg, 1839
Flosculinella bontangensis Rutten, 1913

Nummulitidae de Blainville, 1825
Palaeonummulites (Schubert 1908)
Palaeonummulites sp.

Miogypsinoides (N7 and older) and *Flosculinella bontangensis* (N7 and younger) co-occur only in the uppermost Te_5 (cf. Fig. range of LF), equivalent to latest Burdigalian. Even if the genus *Flosculinella* did occur earlier than Te_5, the individuals in sample TA2 are all spindle shaped, which indicates that they may correspond to *F. bontangensis*. *Flosculinella* differs from *Borelis* in having two layers of chambers in each whorl, a line of large basal chambers and a line of small top chambers. The age is estimated as N7 (late Early Miocene).

Salty Creek

The carbonates of the Salty Creek Section contain plenty of different individuals, but often as fragments. The determination of those is often difficult.

Throughout the whole Salty Creek Section significant specimens belonging to the Lepidocyclinidae family are found and classified as *Nephrolepidina*. However, even if *Nephrolepidina* are very different compared to the genera *Eulepidina*, the microspheric generation can not separate them up to now. The classification in that case is based on the associated larger foraminiferal assemblage, because both genera have different stratigraphic ranges: *Nephrolepidina* Te_{1-4} - Tf_3 (Late Oligocene - Middle Miocene), *Eulepidina* Tc - Te_5

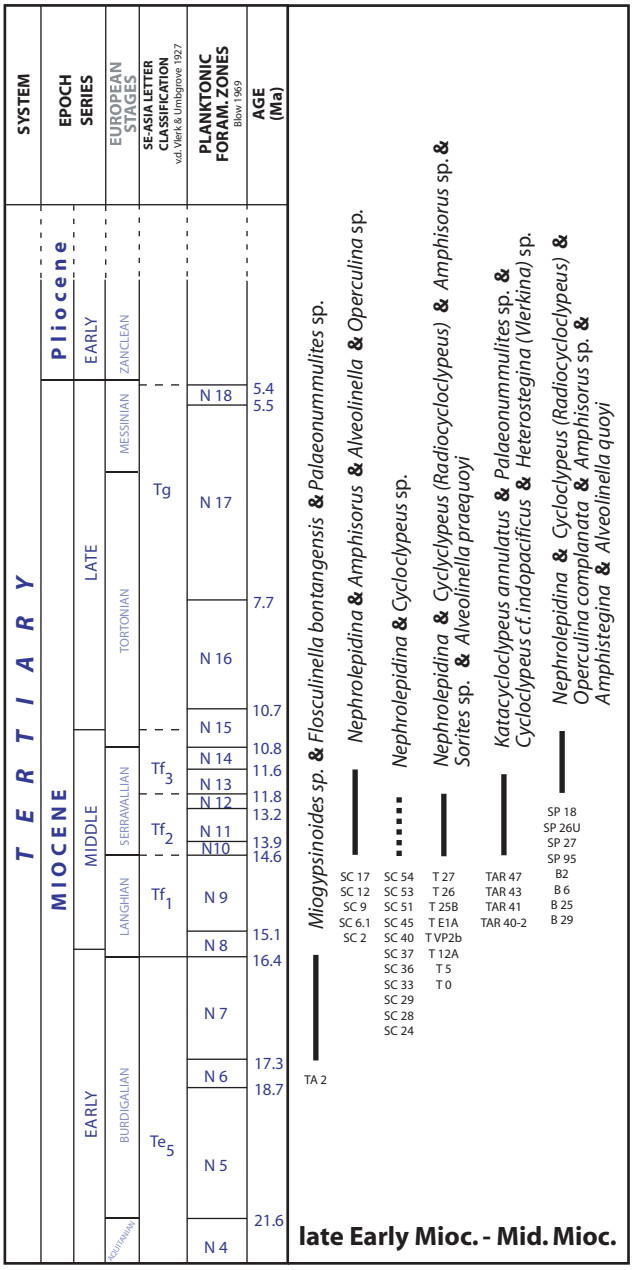

Fig. 39: Age-diagnostic larger foraminiferal assemblages discovered from onshore samples of Taglupa Profile, Salty Creek Section, Tumarabong River Section, Albion Head and Devel Peak.

(Early Oligocene - Early Miocene). Furthermore, it has to be emphasised that both, *Eulepidina* and *Nephrolepidina* were not used as subgenera of *Lepidocyclina* like some authors do. Since *Lepidocyclina* is restricted to the Caribbean and the Americas consequently it would be not correct (Renema, pers. comm.).

The examples of *Operculina* in the thin sections are unidentified on species level (*Operculina* sp). It is not sure whether this is the same *Operculina* described in MÜLLER et al. (1989a).

MÜLLER et al. (1989a) used the species as different from *O. complanata* in the biostratigraphy, but without giving clear specifications of the individual to verify the species.

Lower part

Lepidocyclinidae Scheffen, 1932
Nephrolepidina (Douvillé 1911)

Soritidae Ehrenberg, 1839
Amphisorus (Ehrenberg 1839)

Alveolinidae Ehrenberg, 1839
Alveolinella (Douvillé 1906)

Nummulitidae de Blainville,1825
Operculina (d'Orbigny 1826)
Operculina sp.

Nephrolepidina indicates an age of Late Oligocene to Middle Miocene, Te_{1-4} to Tf_3 (P22 - N14). The sections of *Alveolinella* are not perfectly orientated most probable the individuals should be assigned to the species *Alveolinella quoyi*, which is restricted to Tf_3 and younger (N12 - rec.). *Operculina* sp. occurs from T_0 to recent and could not be used in that case as diagnostic for Middle Miocene age. Nevertheless, the assemblage suggests an age around Tf_2 to early Tf_3 (Middle Miocene).

Upper part

Lepidocyclinidae Scheffen, 1932
Nephrolepidina (Douvillé 1911)

Nummulitidae de Blainville, 1825
Cycloclypeus (Carpenter 1856)
Cycloclypeus sp.

Cycloclypeus occurs (Late Oligocene to recent time; P22 - rec.) in addition to the *Nephrolepidina* (P22 - N14). Some fragments of *Flosculinella* or primitive *Alveolinella*, which is not always easy to distinguish, might indicate an age of N7 and younger for *Flosculinella* or Tf_2 (N10/ N11) and younger for *Alveolinella*. Considering, that *Austrotrillina* is expected in this facies type and that *Austrotrillina* is abundant throughout its range elsewhere in SE Asia, their absence may suggest an age of Middle Miocene (Tf_2). However, it seems not reasonable to give a more definite age assignment than based on presence *Nephrolepidina* and *Cycloclypeus*, i.e. Late Oligocene to late Middle Miocene (P22 - N14).

Tumarabong River Section

Lepidocyclinidae Scheffen, 1932
Nephrolepidina (Douvillé 1911)

Nummulitidae de Blainville, 1825
Cycloclypeus (Radiocycloclypeus) (Tan 1932)

Soritidae Ehrenberg, 1839
Amphisorus (Ehrenberg 1839)
Amphisorus sp.

Soritidae Ehrenberg, 1839
Sorites (Ehrenberg 1839)
Sorites sp.

Alveolinidae Ehrenberg, 1839
Alveolinella praequoyi (Wonders and Adams 1991)

Cycloclypeus (Radiocycloclypeus) is restricted to the upper part of the Tumarabong River profile, whereas *Nephrolepidina* is dominant in this part of the sequence. The species of *Nephrolepidina* provides with their range of occurrence from Te_{1-4} - Tf_3 a less exact age than *C. (Radiocycloclypeus)*, which occurs only in the time range Tf_1 - Tf_2. Without the occurrence of *Australotrillina howchini, Alveolinella praequoyi* is actually restricted to Tf_2 (N10/ N11), which would provide a well-defined age, because of the assured determination based on some excellent sections. This assemblage of larger foraminifera implies that the profile has an age of Middle Miocene (Tf_2).

Devel Peak

The samples of Devel Peak show over the whole profile almost the same assemblage of larger foraminifera.

Lepidocyclinidae Scheffen, 1932
Nephrolepidina (Douvillé 1911)

Nummulitidae de Blainville, 1825
Cycloclypeus (Radiocycloclypeus) (Tan, 1932)

Nummulitidae de Blainville, 1825
Operculina complanata (Defrance, 1822)

Soritidae Ehrenberg, 1839
Amphisorus (Ehrenberg 1839)
Amphisorus sp.

Amphisteginidae Cushman, 1927
Amphistegina (d'Orbigny 1826)

Alveolinidae Ehrenberg, 1839
Alveolinella quoyi (d'Orbigny 1826)

The co-occurrence of *Alveolinella quoyi* and *Cycloclypeus* (*Radiocycloclypeus)* results in an age of Tf_3/ Late Serravallian. *Nephrolepidina* has its last occurrence date by definition at the Tf_2/ Tf_3 boundary so that this confirms the age of late Middle Miocene. *Operculina complanata* is a widespread species, with a first occurrence in Te_{1-4} (Late Oligocene) or earlier and provide no diagnostic dating like *Amphisorus* sp. and *Amphistegina* as well.

Albion Head

Nummulitidae de Blainville, 1825
Palaeonummulites (Schubert 1908)
Palaeonummulites sp.

Nummulitidae de Blainville, 1825
Cycloclypeus (Carpenter 1856)
Cycloclypeus sp.

Nummulitidae de Blainville, 1825
Cycloclypeus (Carpenter 1856)
Cycloclypeus cf *indopacificus*

Nummulitidae de Blainville, 1825
Cycloclypeus (Carpenter 1856)
Katacycloclypeus annulatus (Martin 1880)

Amphisteginidae Cushman, 1927
Amphistegina sp. (d'Orbigny 1826)

Nummulitidae de Blainville, 1825
Cycloclypeus (Carpenter 1856)
Heterostegina (*Vlerkina*) sp.

The occurrence of *Katacycloclypeus annulatus* attributes in Indonesia to an age of middle Miocene (Tf_1 - Tf_2). It is accompanied by *Palaeonummulites* sp. and *Cycloclypeus* cf. *indopacificus*, which range from Tf_2 to Tg. In addition, *Heterostegina* (*Vlerkina*) sp. implies Tf_2 so that the larger foraminiferal assemblage indicates most likely an age of Middle Miocene (Serravallian).

In conclusion, the age given by the larger foraminiferal assemblage from the onshore study area around Quezon is mainly dated, beside some Early Miocene, as Middle Miocene (pers. comm. Renema). In detail, the Taglupa Profile is made of the oldest carbonates with an age of late Te_5 (N7, late Early Miocene), whereas the deposits of the Salty Creek Section - Maasin Profile, Tumarabong River Section, Quezon Section and Theo's Place attributed to N8 - N9

(lower Middle Miocene). Albion Head and Devel Peak range from zone Tf_2 to Tf_3 and are therefore of (upper) Middle Miocene age.
The larger foraminifera biostratigraphy confirms the lithostratigraphic field observations, but could not give more precision regarding assumed or observed discontinuities. Their resolution is not high enough.

3.3.2 Planktonic Foraminifera & Nannoplankton

BLOW (1969) provided a detailed subdivision of Cenocoic times with his definition of Neogene Zones (N. zones) based on planktonic foraminifera. With the assistance of R. Anglada (pers. comm.) some age diagnostic taxa of planktonic foraminifera were found in a selection of thin sections. Eight thin sections are from the Salty Creek Section and Maasin Profile. Three samples along the riverside of the Iwahig River were added to supplement the upper part of the Salty Creek Section. Based on the lithostratigraphic field observation four samples from Quezon and the Quezon Section were selected in order to date the youngest layers of the onshore study. As confirmation and reference for the correlation two samples of the core of the well Santiago A-1X were studied.
Additional to the thin sections and planktonic foraminifera study, smear slides have been made of 6 rock samples in order to find some nannoplankton. Only two samples (TP7 & SC E10) provide a very poor assemblage of age diagnostic nannoplankton, which was identified by C. Müller.

The determination of the planktonic foraminifera from the onshore samples provided with the zones N8 to N10 an age of late Early Miocene to Middle Miocene (Fig. 40).
In the lower part of Salty Creek Section, 3 thin sections (SC20, SC46, SC52) yield couples of *Orbulina* together with no significant sections of planktonic foraminifera. An age between latest Late Miocene and early Middle Miocene seems to be most probable for these samples. The species of *Globigerina* and *Globigerinoides* in sample SC55 do not provide enough details for an exact age, but lithostratigraphically upwards (SC57) the first occurrence of *Orbulina universa* (N9 - N23) indicates the early Middle Miocene. Some very small forms of planktonic foraminifera together with *Orbulina* link to the Middle Miocene age (SC67). Not only *Orbulina universa* associated with species of *Globorotalia peripheroacuta* (N9 - N10) in sample SC71 confirms this age, but also the nannoplankton found in sample SC-E10. Large

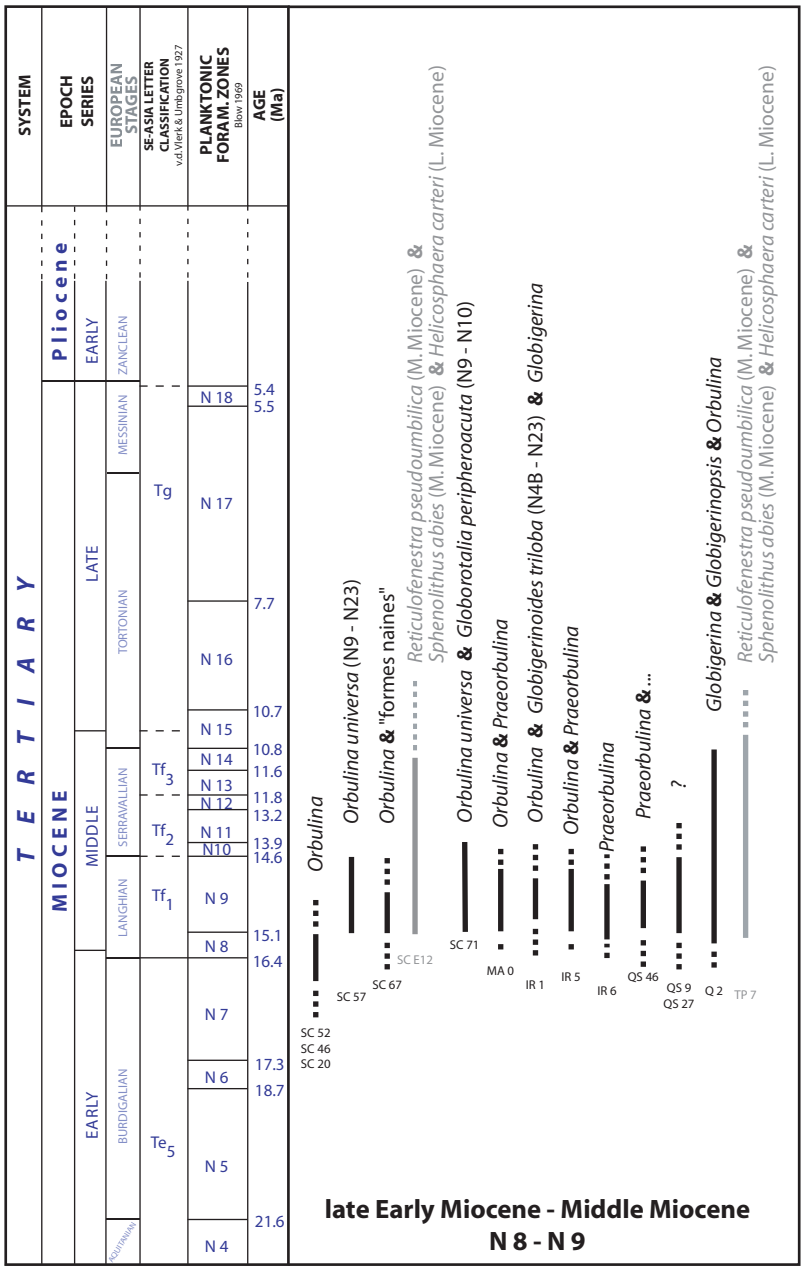

Fig. 40: Age-diagnostic planktonic foraminiferal assemblages and nannoplankton discovered from onshore samples of Salty Creek Section, Maasin Profile, Iwahig River Profile, Theo's Place and Quezon Section.

individuals of *Reticulofenestra pseudoumbilica* (M. Miocene) and a few *Sphenolithus abies* (M. Miocene) are recovered, beside questionable *Helicosphaera carteri* (L. Miocene). The lithostratigraphic continuation with the thin section MA0 from the Maasin Profile contains *Orbulina* and *Praeorbulina* indicating Middle Miocene age again.

The locations of the 3 samples collected along the Iwahig River (IR1, IR5, IR6) correspond with the uppermost part of the Salty Creek Section and the Maasin Profile. Their planktonic

content with *Orbulina*, *Praeorbulina*, *Globigerinoides triloba* (N4B - N23) and *Globigernina* results in Middle Miocene age and correlates therefore perfectly with the dating from the upper part of the Salty Creek Section.
In the S of the study area the mudstones (Q2, QS9, QS27, QS46) include species of *Globigerina*, *Globigerinopsis*, *Orbulina* and *Preaorbulina*. Hence, the sediments are dated as Middle Miocene, maybe late Middle Miocene age. One sample from the profile at Theo's Place (TP7) yields the same assemblage of nannoplankton as sample SC-E10, but *Sphenolithus abies* is most common besides *Helicosphaera carteri* and *Reticulofenestra pseudoumbilica*. This results in the interpretation of a Middle Miocene or maybe Late Miocene age for the sample. It seems to be most probable that the uppermost layers of the study area are found at Theo's Place with an age of late Middle Miocene to early Late Miocene.

3.3.3 $^{87}Sr/^{86}Sr$

The measurement of the $^{87}Sr/^{86}Sr$ ratio was implemented in order to get a numerical age for the deposits of the onshore study area by using the "Look-Up Table version 3:10/99" (MCARTHUR et al., 2001). However, only three promising samples for this analysis exist (B33, L1-13B and SP96), which are all from Devel Peak.
Each of the samples B-33 and SP-96 provides two different well-preserved cm-sized shell fragment of an oyster. The fragments show their primary internal structure in the thin section, which allows the assumption that no neomorphic processes have affected the oysters since their death. With respect to the aim to date the time of sedimentation and not a later diagenetic event, the preservation of the primary shell calcite is vital. The sample L1-13B from Devel Peak is a 4 x 4,5 cm large marine bivalve belonging to the Chlamys Group (Pectinidae). The bivalve was collected within the carbonate sequence of Devel Peak and both valves were still connected in the outcrop. This suggests an autochthonous deposition or a very limited transportation. In contrast to most of the bivalves, the Pectinidae use calcite as carbonate modification in the whole ostracum (ZIEGLER, 1983). This circumstance and the observation of the primary internal structures of the shells manifests the necessary prerequisite of a primary mineralogy and that no significant diagenetic process like recrystallisation took place.

Sample	Measurement	Internal Error
B-33	0,708923	3e-006
L1-13B	0,708913	3e-006
SP-96	0,708985	3e-006

Tab. 4: $^{87}Sr/^{86}Sr$ measurements of samples from Devel Peak.

The analysis of the three samples from Devel Peak resulted in values between 0,708913 and 0,708985 (Tab. 4).

The calculation of the numerical age from the $^{87}Sr/^{86}Sr$ ratio of the samples (Tab. 5) is based on the "Look-Up Table version 3:10/99" (MCARTHUR et al., 2001). The most critical factor concerning the calculation of a numerical age by using the $^{87}Sr/^{86}Sr$ ratios is the necessary assumption that the measured $^{87}Sr/^{86}Sr$ ratios represent the primary $^{87}Sr/^{86}Sr$ signal of the open marine ocean at the time of the carbonate precipitation. Hence, a significant influence of rivers during the development of the carbonates, diagenetic processes associated with an exchange of fluids (open system) and finally the contamination of the samples with terrigenious material of the continental crust have to be excluded. Otherwise, the $^{87}Sr/^{86}Sr$ ratio would be enriched in ^{87}Sr, because the continental crust has higher $^{87}Sr/^{86}Sr$ values than marine waters, which also receive Sr with low $^{87}Sr/^{86}Sr$ ratios from the mid-ocean ridges. Consequently, continental weathering and erosion results in a much higher value of the $^{87}Sr/^{86}Sr$ ratio in river waters than in marine waters (MCARTHUR, 1994). Due to the fact that the values of $^{87}Sr/^{86}Sr$ increases continuously since the Eocene (MCARTHUR, 1994) a modification of the primary $^{87}Sr/^{86}Sr$ ratio by any of these mechanisms would result in a calculated numerical age which is too young.

Site	Sample	years in MA					m from base level
		Min	-	Date	+	Max	
Devel Peak	SP-96	5,50	0,51	6,01	1,04	7,05	145.9
	L1-13B	6,95	2,05	9,00	1,49	10,49	99.6
	B-33	6,61	1,93	8,54	1,61	10,15	11.2

Tab. 5: Calculated numerical age of the samples based on the "Look-Up Table version 3:10/99" (MCARTHUR et al., 2001).

The samples collected at Devel Peak show an age of 6 to 9 Ma (Fig. 41), which indicates Late Miocene age. The lowermost sample B-33 of the carbonate sequence of Devel Peak results in a numerical age of 8,54 (+1,61/-1,93) Ma. About 90 m above B-33, the $^{87}Sr/^{86}Sr$ value of the sample L1-13B suggests 9,00 (+1,49/-2,05) Ma in age. The sample SP-96 is located

additional 50 m higher than L1-13B in the sequence and yields an age of 6,01 (+1,61/-1,93) Ma.

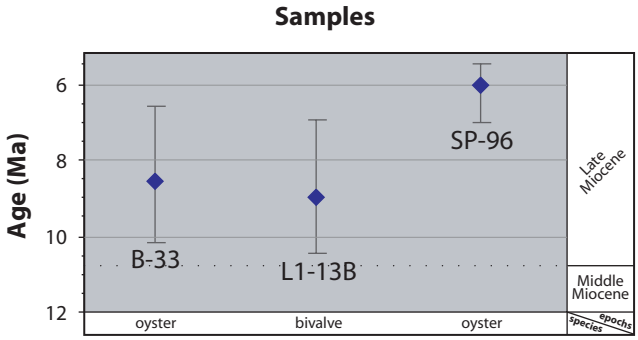

Fig. 41: Numerical age data of Devel Peak (B-33, L1-13B, SP-96) with standard deviation error bars (= 95% confidence intervals).

With respect to the external reproducibility of +/-3e-5, the $^{87}Sr/^{86}Sr$ analysis confirms a continuously younger age throughout the sequence of Devel Peak. The Late Miocene age (N16 - N17) agrees also with the field observations indicating that the Devel Peak build-up was formed after the demise of the lateral extended carbonate during the Middle Miocene age (N8 - N10). However, the calculated numerical age of Devel Peak is most probably too young. The sample B-33 contains cm-sized sandstone gravel whereas samples L1-13B (total $CaCO_3$ = 90,56%) and SP-96 (total $CaCO_3$ = 92,21%) include a significant shale content in their matrix. The contamination of the small amounts of sample material with matrix would result in higher values of the $^{87}Sr/^{86}Sr$ ratios leading to a younger estimated age. The observation that the calculated numerical age of B-33 is slightly younger than that of L1-13B, even if the sample L1-13B was collected 89-m upstrata from B-33 in the undisturbed stratigraphic section, supports the possibility of a contamination. Accordingly, an age of late Middle Miocene seems to be more reasonable for the build-up of Devel Peak.

Dating of Secondary Carbonate Precipitation

At the Tumarabong River Section some crusts of speleothems are precipitated on the ledge below the cavity, which exists 3 m above the base level of the section (cf. Fig. 17, p. 48). Furthermore, an 80-cm in diameter and 1.5 m high stalagmite-like body with vertical grooves produced by weathering is placed below the studied profile of the Tumarabong River Section. These carbonates have no direct relation to the Miocene carbonate sequence of the section.

Nevertheless, due to the fact that well-preserved shells of marine bivalves were cemented within the secondary carbonate precipitation, the dating of the precipitation by $^{87}Sr/^{86}Sr$ might provide an indication, concerning the time when the related karst system functioned.

One sample (T-d1) of a 7 x 8-cm large shell of a marine bivalve belonging to *Meretrix* sp. (Veneridae) from the Tumarabong River Section was analysed. The shell is pristine and shows no macroscopic features of fossilisation. Additionally, also the internal structures within the outer and the inner layers are visible in a thin section. However, as the primary mineralogy of these Veneridae shells should be aragonite (CARTER, 1990) the present-day mineralogy was checked with X-ray diffractometry analysis.
The diffractogram (Fig. 42) shows the 3 most prominent calcite peaks (2ø: 1: 26.5793/ 2: 33.8018/ 3: 36.0587), but no indication of aragonite (2ø: 1: 24.3589/ 2: 25.7523/ 3: 30.2007). The analysis yields obviously a purely calcitic mineralogy of the shell from Tumarabong River Section.

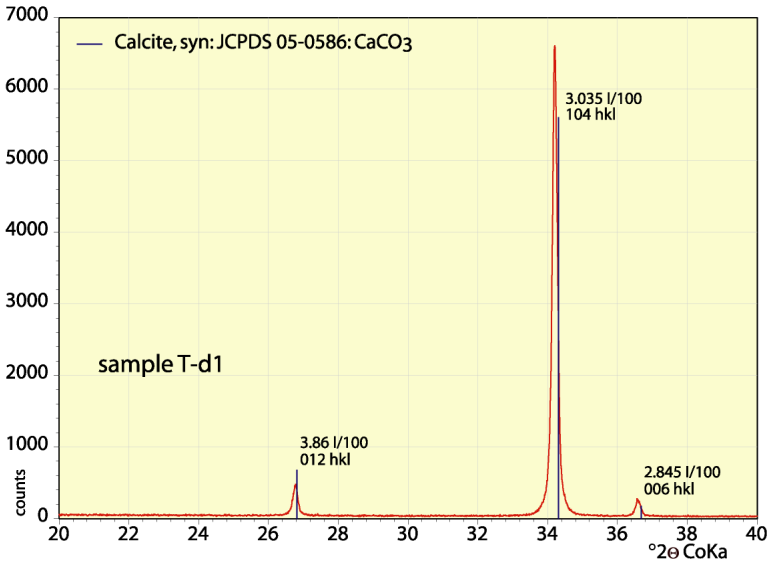

Fig. 42: Diffractogram of the sample T-d1 created with the MacDiff program yields the three most significant peaks of calcite.

The XRD analysis indicates therefore a complete neomorphic conversion of the carbonate mineralogy, which contradicts the macroscopic and microscopic observations of a pristine shell. The character of the present-day mineralogy of the shell is the weakest point of the dating.

The 87Sr/86Sr analysis of the bivalve yields a 87Sr/86Sr ratio of 0,709161(+/-3e-6). Following the "Look-Up Table version 3:10/99" (McArthur et al., 2001) an age of 460 (+680/ -500) ky are indicated, which refers to the Pleistocene (Tab. 6).

Site	Sample	years in MA					m from base level
		Min	-	Date	+	Max	
Tumarabong RS	T-d1	recent	0,50	0,46	0,72	1,18	2.9

Tab. 6: Calculated numerical age of the sample T-d1 based on the "Look-Up Table version 3:10/99" (MCARTHUR et al., 2001).

Consequently, the bivalve sample from the Tumarabong River Section (T-d1) shows a clear offset to the other three samples (Fig. 43), which is consistent with the field observations. Nevertheless, with respect to a primary aragonitic shell mineralogy and the inconsistent result from the XRD analysis, the age might document the time of a diagenetic event, which has not to be necessarily time-equivalent with the time of the flooding of the karst system and the precipitation of the speleothems.

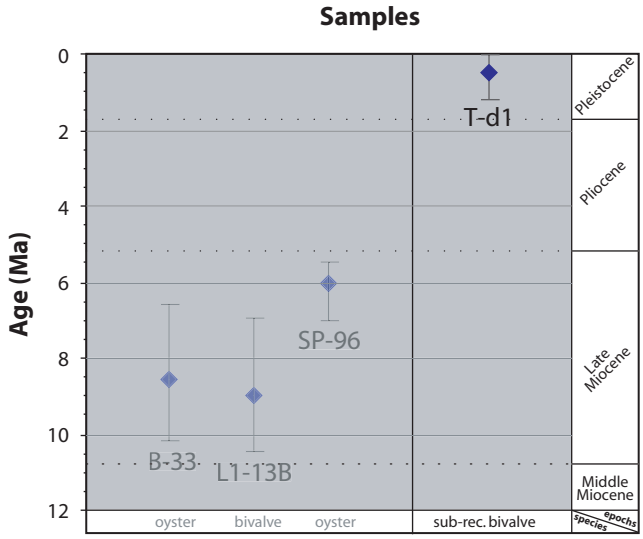

Fig. 43: Numerical age data of Tumarabong River Section (T-d1) with standard deviation error bars (= 95% confidence intervals).

3.3.4 Stratigraphy of the Onshore Deposits

The stratigraphic data of larger foraminifera, planktonic foraminifera and nannoplankton as well as the calculated numerical age provided by the $^{87}Sr/^{86}Sr$ analysis, supported by the

lithostratigraphic and tectonic observations, results in an age of mainly Middle Miocene for the carbonate deposits around Quezon.

The tectonic (cf. chapter 3.3) do not disturb any of the studied sections and the small displacements between different sites are possible to unravel. Therefore, the lithostratigraphy provides the frame for the dating, i.e. the Taglupa Profile represent the lowermost carbonates, followed by the Salty Creek Section and Maasin Profile, whereas the carbonates at Theo's Place illustrates the youngest lateral extended carbonates in the study area. The reefal structures of Albion Head and Devel Peak were formed after the development of the lateral extended carbonates S and E of Quezon.

Due to the available material, the biostratigraphy of the larger foraminifera is less detailed than the biostratigraphy of the planktonic foraminifera (Fig. 44). Nevertheless, the identified assemblages of both, larger foraminifera and planktonic foraminifera, yield a time range from late Early Miocene to Middle Miocene. The larger foraminifera indicate a slightly younger age (Tf_2 = N10-N12) than the planktonic foraminifera (Tf_1 = N8-N9). But finally, a late Early Miocene age seems to be most probable for the Taglupa Profile, whereas the sections from the base of the Salty Creek Section up to Theo's Place indicate a lower Middle Miocene age. The dating of the reefal structures of Devel Peak and Albion Head is only based on the larger foraminifera. The assemblages provide an age of Middle Miocene (Tf_2 to Tf_3), which suggest their development after the demise of the lateral extended carbonates. This result corresponds to the field observations and the lithostratigraphy. In contrast, the calculated numerical age based on the $^{87}Sr/^{86}Sr$ analysis of the three samples from Devel Peak contradict to this dating in that case that the absolute age attribute to N16 to N17 (Late Miocene), which is younger than expected. Nevertheless, with respect to the possibility of a contamination of the sample with terrestrial material (cf. chapter 3.2.3), the provided age might be too young. A slight correction would result in a Middle Miocene age, which corresponds to the biostratigraphy. Finally, the biostratigraphic data suggest that between the demise of the lateral extended carbonates and the development of the reefal structure of Albion Head seems to be no time gap, whereas Devel Peak might be formed one or two planktonic foraminifera zones later.

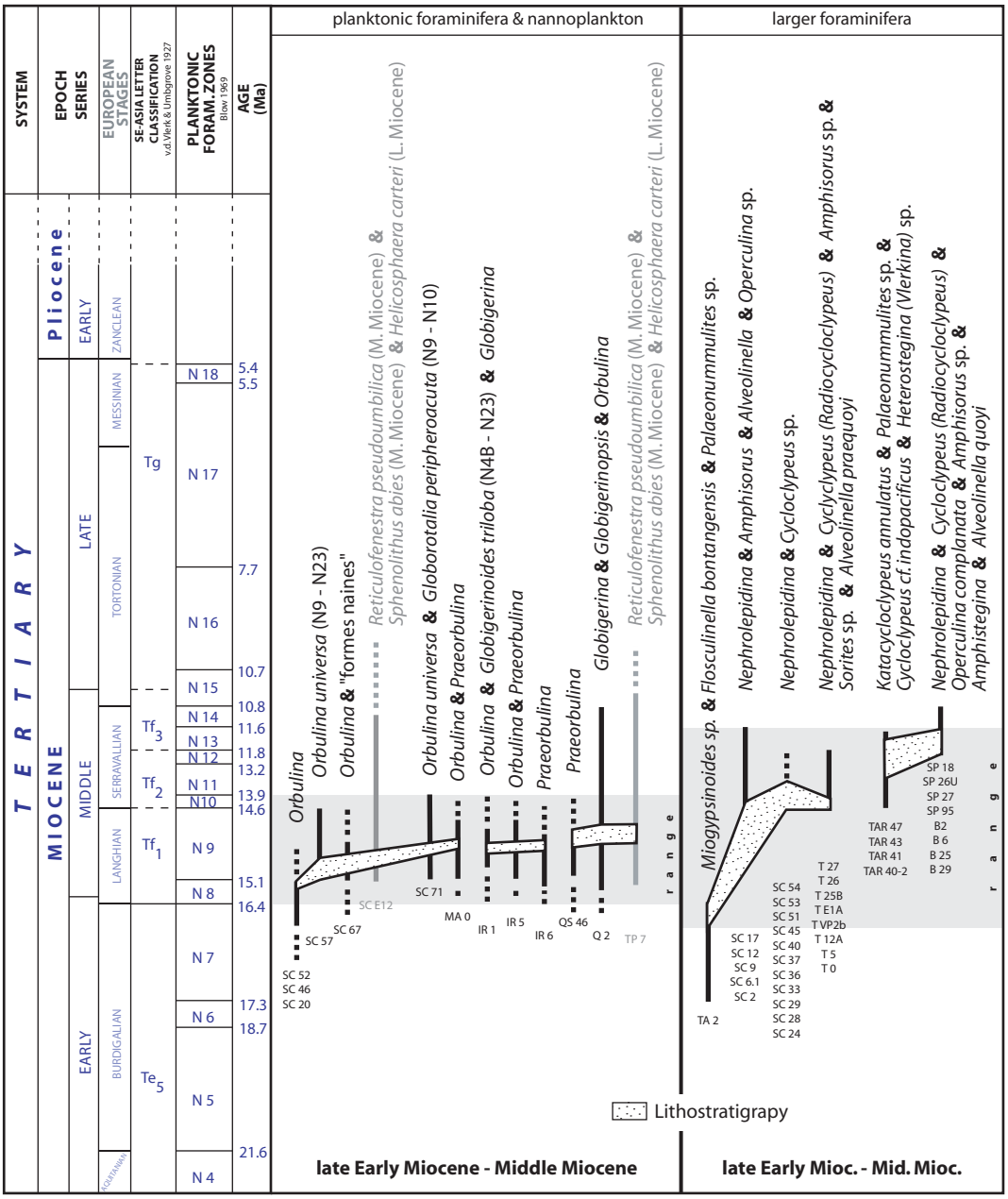

Fig. 44: Biostratigraphy of the onshore carbonates based on larger foraminifera (W. Renema/ Leiden), planktonic foraminifera (R. Anglada/ Marseille) and nannoplankton correlated with the lithostratigraphic observations in the field.

3.4 Structural analysis

The structural analysis was made in order to show that tectonic displacements, vertical or horizontal, do not affect the general lithostratigraphic sequences of the study area.

In general, the Miocene limestones of the Quezon area are relatively undeformed. Therefore, the study of the structural setting of the deposits around Quezon indicates a low to moderate tectonic stress, which was related to 3 different stress regimes (Fig. 45): The first event was

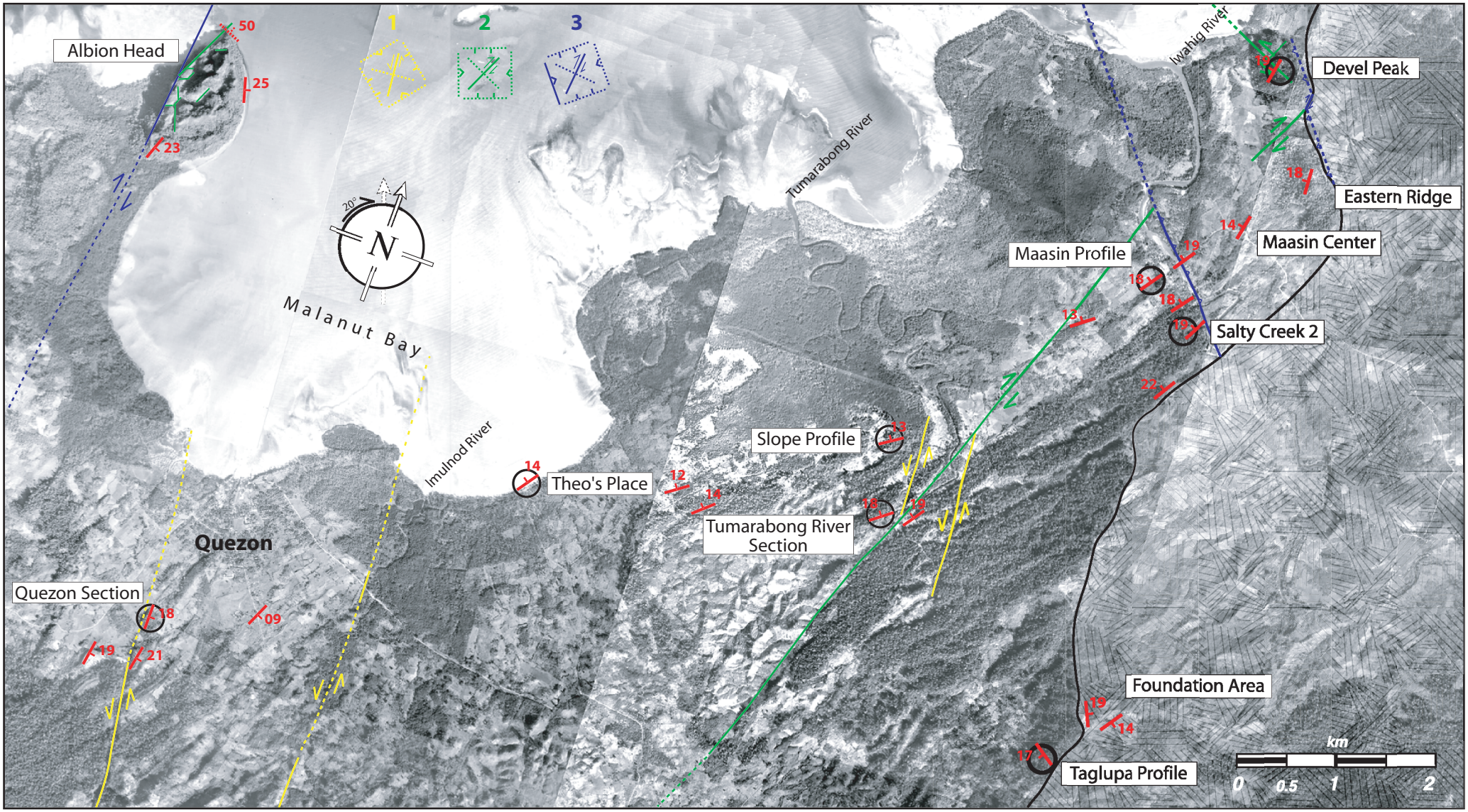

Fig. 45: Aerial photography from the study area around Quezon, SW Palawan, including tectonic lineaments and faults related to 3 tectonic stress regims. Sites and bedding of strata are indicated.

an early NE-SW orientated extension (yellow). The second stress regime was characterised by WSW-ENE compression (green), whereas the third tectonic event was recognised as a NE-SW compression (blue). The consistent orientation and dip of the carbonate layers in different parts of the study area documents the existence of a NNE-SSW stretching synclinal structure. The carbonate sequence overlies the sub-horizontal to slightly E dipping older shales with a low-angle unconformity. Folding has not been observed at any place of the study area.

With respect to the sedimentary origin, the dip of the studied carbonate and siliciclastic sediments shows a low variance within a range of 09° to 26°. The average dip is of 17°. A few sedimentary surfaces with a higher or lower angle of dipping occur, but they are generally linked to local sedimentary bodies and therefore they are not representative for the whole study area.

The orientation of the layers is different between the sites in the East, West and North. The shales, which are cropping out in the Foundation Area in the SE of the study area, are dipping slightly to the east (Fig. 46), while the direct overlying carbonates at the Taglupa Profile are dipping to southern directions. This setting refers to an angle discontinuity between the siliciclastic sub-stratum and the Miocene carbonate sequence.

The carbonates found in the E at Devel Peak, at the Eastern Ridge and at Maasin Center are dipping to the W (Fig. 46). Eight measurements from the Eastern Ridge show no consistent direction of the dip. This confirms the field observation that single blocks on the lower flanks are recently tilted. Data closer to the top of the Eastern Ridge correspond to the data from Devel Peak and dip to the W.

Further to the W in the study area between the Iwahig River and Quezon, the most significant direction of the dip in the study area are documented in the Salty Creek Section - Maasin Profile, at the Tumarabong River Section, and at Theo's Place as well as in the carbonates along the blind road to the N. All the layers are dipping to the NW, whereas the variation of the orientation is with a ranges from 298° to 326° very slight (Fig. 46). Three data points collected at the Slope Profile dip to the S, but following the field observations these measurements are related to internal sedimentary structures and do not represent the general orientation.

In contrast, the layers of the W part of the study area are dipping to the E (az. 76°-114°). Even if the measurements collected at the Quezon Section dip slightly steeper compared to the measurement taken S of Quezon, both sites represent a uniform azimuth to the E for the dip

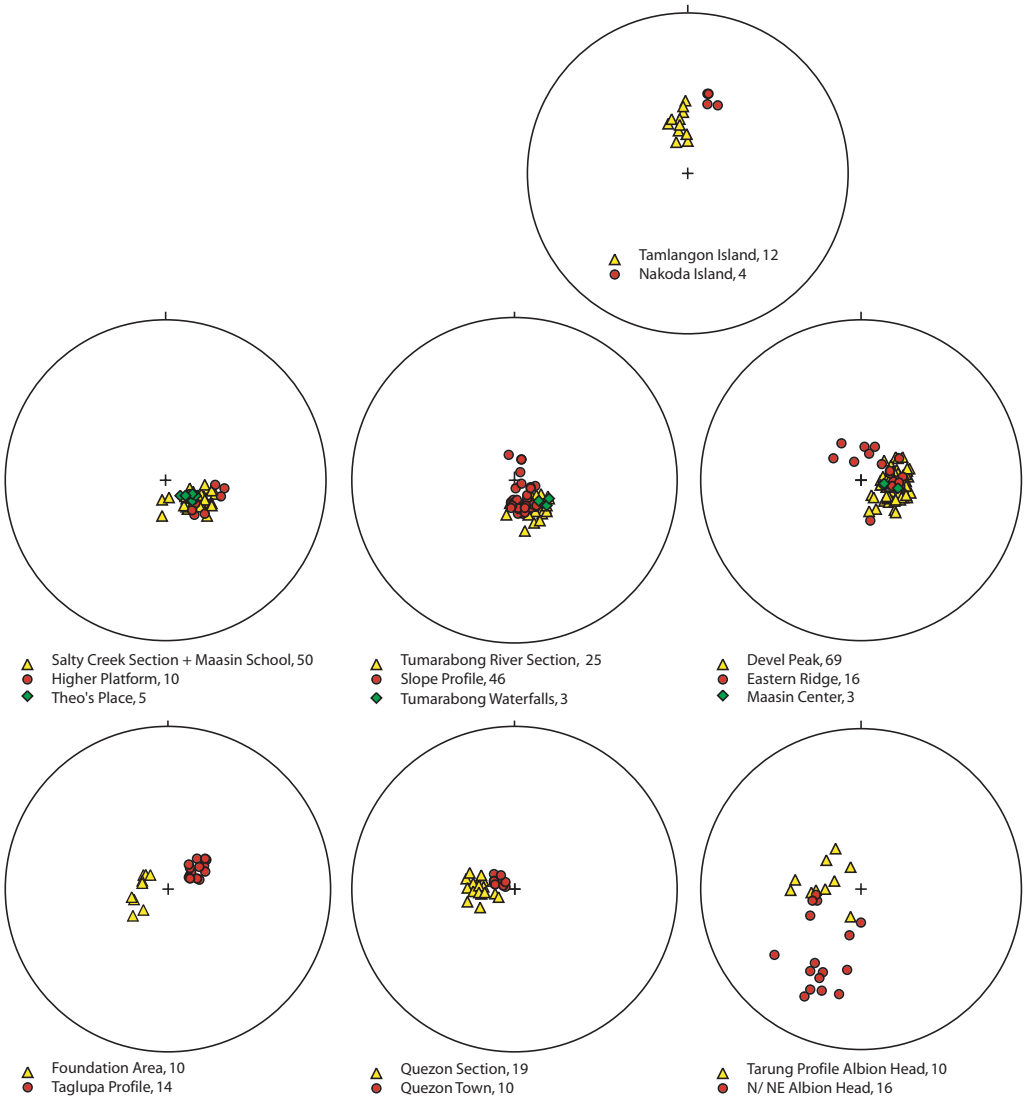

Fig. 46: Pole diagrams presenting 312 data of strike and dip of the depositional strata collected in the onshore study area and sorted by sites.

(Fig. 46). The bedding measured on the southern side of Albion Head (Tarung Profile) correspond generally with an eastward dipping, but with a slightly more southern orientation the data shows less consistency (Fig. 46). Along the eastern shoreline of Albion Head, the beds are usually dipping eastwards as well. However, the orientation and dip of the layers is often modify, if fore reef deposits were development; this results in the measured orientations to the NE with a dip between 42°-64°.

Additional to the observations onshore Palawan some structural data were collected on two small Islands close to the coastline (Fig. 46). The thickly bedded coarse grained sandstone layers on Nakoda Island, N off Albion Head, and the fine grained dm-bedded layers of Tamlangon Island, N off Devel Peak, strike E-W and dip with 29° to the S.

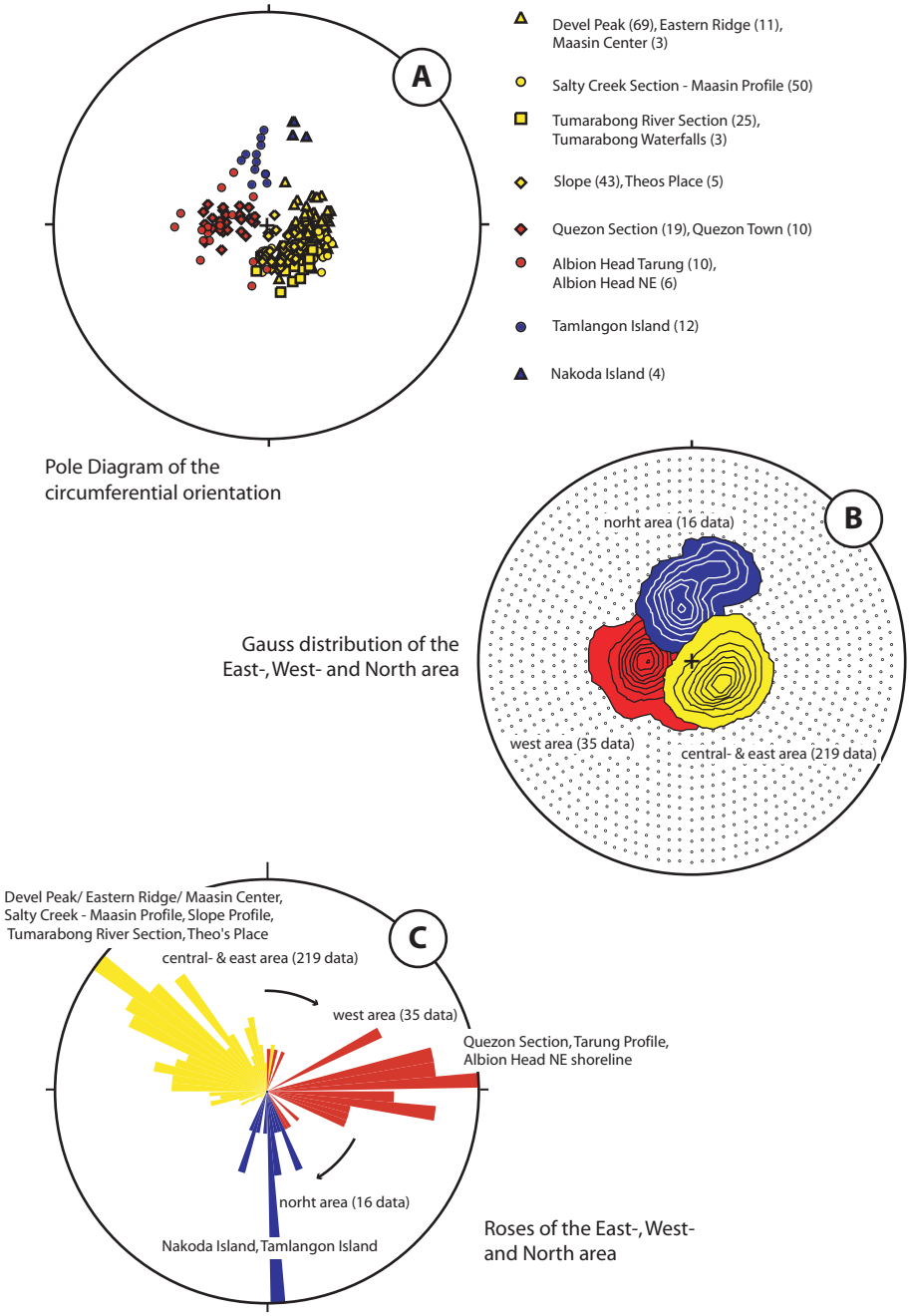

Fig. 47: Pole Diagram (A) of 312 strike-dip data of the onshore study area sorted by sites reflecting the orientation at the sites (East, West, North) as well as Gauss Distribution Diagram (B) and Rose Diagram (C) of the 312 data from the East-, West- and North area. All showing circumferential oriantation of the strata.

The Gauss distribution of all 270 representative measurements of the east and central part of the study area, the western part and the northern islands offshore are calculated and documents 3 areas of concentration (Fig. 47). These overall picture demonstrates a shift from

the E to the W and finally to the N of a circumferential direction of dipping around Quezon. It refers to the existence of a synclinal structure, whereas the NNE-SSW running axis follows the Imulnod River into the Malanut Bay.

The aerial photographs show most remarkable the NE-SW orientated lineaments (Fig. 45). These represent the prevailing dipping of the carbonate layers to the NW or E and not tectonic features. Lineaments caused by tectonic movements strike in four prevalent directions: 175°, 025°, 005°, and 140°. They are related to three tectonic events. The first event was an early NE-SW orientated extension, followed by a WSW-ENE compression and finally a NE-SW compression.

The types of most of the lineaments are verified on the base of their relationship to each other, and through the biostratigraphy, facies correlation, field observations and their relation in a stress field. Only the dextral shearing in the W with the direction of 025° and some sinistral transversal displacement (az. 175°) up to an estimated displacement of 250 m is identifiable in the aerial photographs itself.

The first stress regime (yellow) results in the study area in only 4 sinistral transversal displacement. The 2 displacements of about 250-m in the limestone jungle are well documented. In contrast, the lineament between Theo's Place and Quezon is weakly recorded on the photograph. However, the shift of the direction of dipping with an angle of more than 20° over the shore distance, the biostratigraphic data and a small outcrop close to the road showing chaotic bedding confirms its existence and the sinistral displacement. The affiliation of this fault to the first tectonic event based on the correlation to other N-S orientated lineaments in the study area.

The most significant features in the field are cliffs, like in the vicinity of the Tumarabong River Section, at Devel Peak and at Albion Head, which were often triggered by fracturing. With the exception of the N-S orientated cliffs of the sinistral shearing of the first NE-SW extensional event around Tumarabong River, most of the cliffs are a result of the second stress regime with WSW-ENE compression (green). The NE-SW cliffs close to the Tumarabong River document the several km long dextral transversal fault of the second tectonic event, which limits presently the limestone jungle in the W. The WSW-ENE compression produced also the large cliffs on the NE side of Devel Peak as well as a few observed south-eastward dipping normal fault. The sinistral transversal displacements in NW-SE direction at Devel Peak and the dextral transversal displacements in NE-SW direction

between Devel Peak and the Eastern Ridge supports the interpretation that the second tectonic event affected Devel Peak. Furthermore, most of the cliffs at Albion Head are coincident with the second tectonic event. Consequently, the WSW-ENE orientated cliffs indicate thrust faults, while NNW-SSE trending cliffs indicate normal faults.

The third stress regime (blue) creates the most significant tectonic displacement at the Malanut Range, SW of the study area. The several km long and a few hundred meters high carbonate cliff restricted the occurrence of carbonates to the SW with a thrust fault. Additionally, the N-S orientated dextral shearing in this stress field triggered the development of the large cliff at the NW side of Albion Head. Beside the field observation of cliffs, the facies discontinuity with a displacement of estimated 100 m between the Maasin Profile and the eastern side of the Iwahig River was important for the identification of the lineation, which follows a part of the river bed of the Iwahig River (az. 140°). This lineation runs parallel to the carbonate cliff of the Malanut Range as well as parallel to the contact between the carbonates and the shales NE of Devel Peak. Therefore, two thrust faults are also assumed to be the reason for the discontinuities in the E of the study area, even if the direction of the dip of the fault surfaces could not be proved. However, a SW direction of the dip of the fault NE of Devel Peak seems to be reasonable due to the present morphology.

Excerpt: The first tectonic event was an early NE-SW orientated extension. It produced four sinistral transversal faults in the area of the lateral extended carbonates. WSW-ENE compression characterised the second tectonic event. It produced a several km long dextral transversal fault, which limits presently the limestone jungle in the W. Furthermore, the carbonate build-ups of Albion Head and Devel Peak were fractured during the second tectonic event, which probably availed the development of the present-day tower karst morphology at Albion Head. The third and last tectonic event recognised in the study area combines the lineament directions 005° and 140° azimuth in one single event of NE-SW compression with almost N-S dextral shearing. This event defined the carbonate area around Quezon at the Malanut Range and at Devel Peak. Therefore, this confirms the observation that the carbonates in the NE and E (Devel Peak, Eastern Ridge) appear faulted against shales and basalts of presumed Cretaceous age (PARK & PETERSON, 1979).

Even if some vertical and horizontal displacements have been identified as well as a synclinal structure, the tectonic has no significant effect on the Miocene carbonate deposits regarding

there present-day setting around Quezon. With respect to the tectonic, undisturbed sequences through the lateral extended carbonates and the reefal structures exist, which allow the study of the carbonates in time and space in the area.

4. Principle Database: Offshore

4.1 Seismic Survey

4.1.1 Lithostratigraphic Sequences

The definition of major lithostratigraphic sequences in the reflection seismic data is based on the correlation of the seismic data and the well data. Hence, two of the most significant reflections, which exist in the seismic lines, are possible to allocate with the contact between the Miocene carbonates and the under- and overlying siliciclastics (Fig. 48). The significant reflection at the top of the carbonates results from the contact between the overlying siliciclastics that are characterised by low interval velocities (about 3500 m/sec) into the tight and dense carbonates (interval velocities 4000 - 4675 m/sec reefal structures; 5150 - 5800 m/sec carbonate platform). The base of the carbonates is characterised again by a velocity inversion, but in that case from the high acoustical impedance into the acoustically less

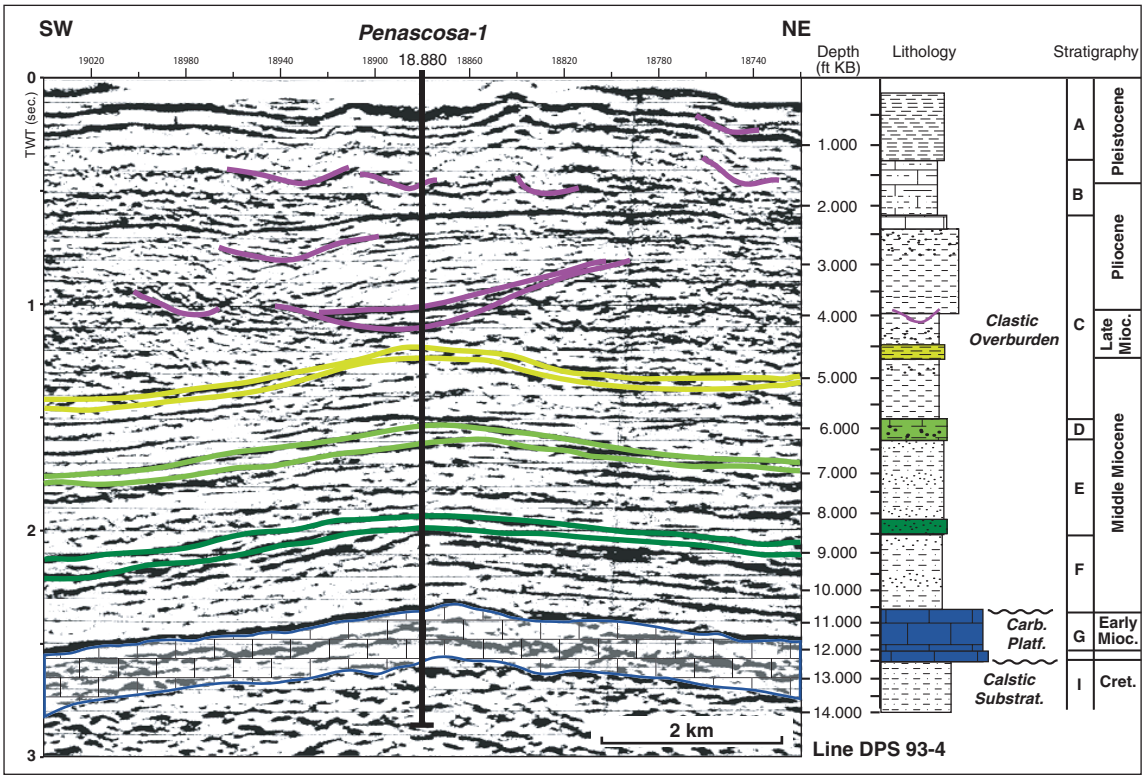

Fig. 48: The correlation between seismic record and well data are documented by a part of the seismic profile DPS 93-4 in seconds TWT and ft below KB including the Penascosa-1 well location. The Miocene carbonate platform (blue) reflection, significant reflections of the overlying prograding clastic sequences (green colours) and erosive channel (purple) correlated to a lithological column, which illustrates the general lithologies recovered in the well using standard signaturs. A simplified stratigraphy is indicated at the right.

impedant underlying clastics. The estimated average interval velocity of the clastic substratum is 4015 m/sec.

Most of the Miocene carbonates represent a Miocene platform, which are recognisable in the seismic data widely spread. In some areas the carbonate deposition continued and created atoll structures or pinnacle-type reefs, which are on top of the platform carbonates (Fig. 49). The internal impedance contrast between the platform and the reefal carbonates is generally not significant enough to cause a reliable reflection. Therefore, the identification of the top of the platform carbonates in these parts is less certain or impossible. Nevertheless, the position of the contact between platform and reef are estimated by building up an assumed thickness from the base of the carbonate section. In cases that no seismic reflection of the carbonate base is identifiable, the part of the sequence related to the platform carbonates could only be guessed.

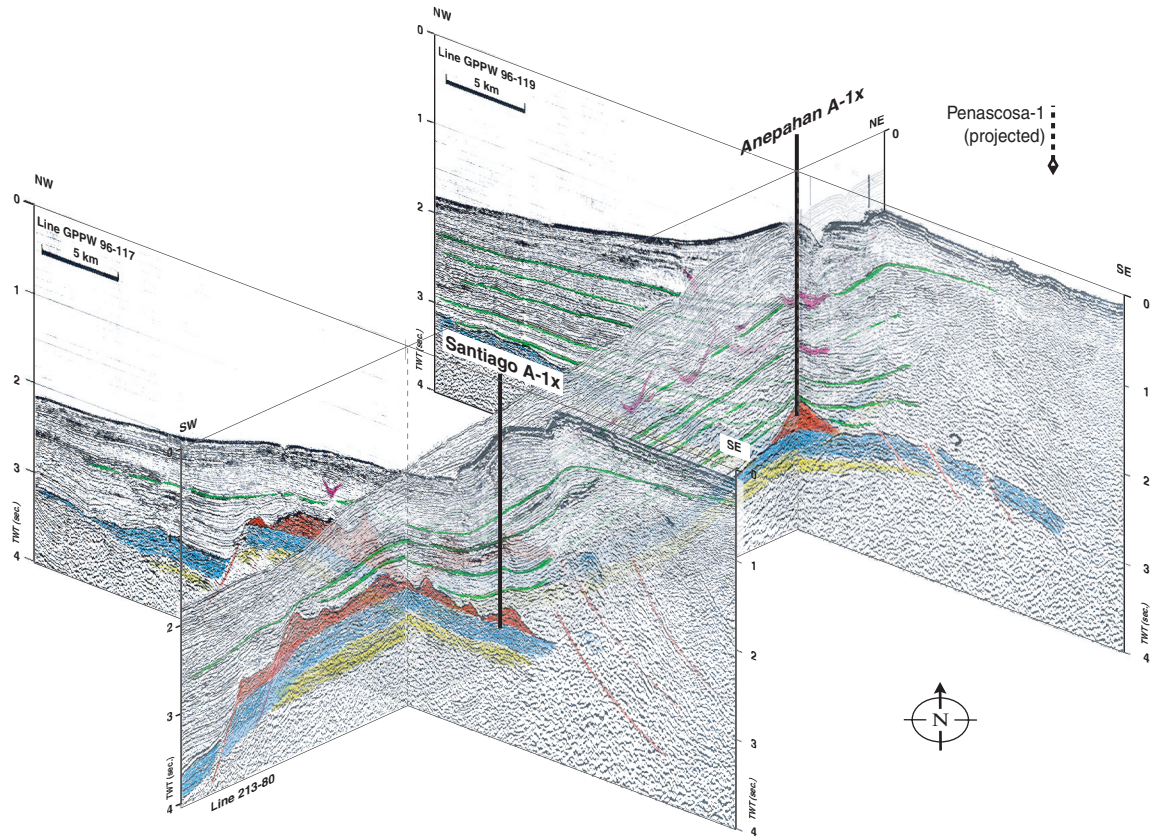

Fig. 49: Simple 3-D diagram made of SW-NE running line 213-80 and NW-SE running lines GPPW 96-117 and 96-119 recorded in seconds TWT, which shows the position of the 3 wells in the offshore study area penetrating the Miocene carbonate platform (blue) or the build-ups (red) above the Cretaceous substratum (yellow); green are prograding clastic sequences.

Within the overburden sediments of Miocene to Pleistocene age, different impedances of the intervals result in continuous seismic reflections. These illustrate in general a well-bedded sequence as well as the progradation of the sediments westwards (Fig. 49).

4.1.2 Great Atoll Reef

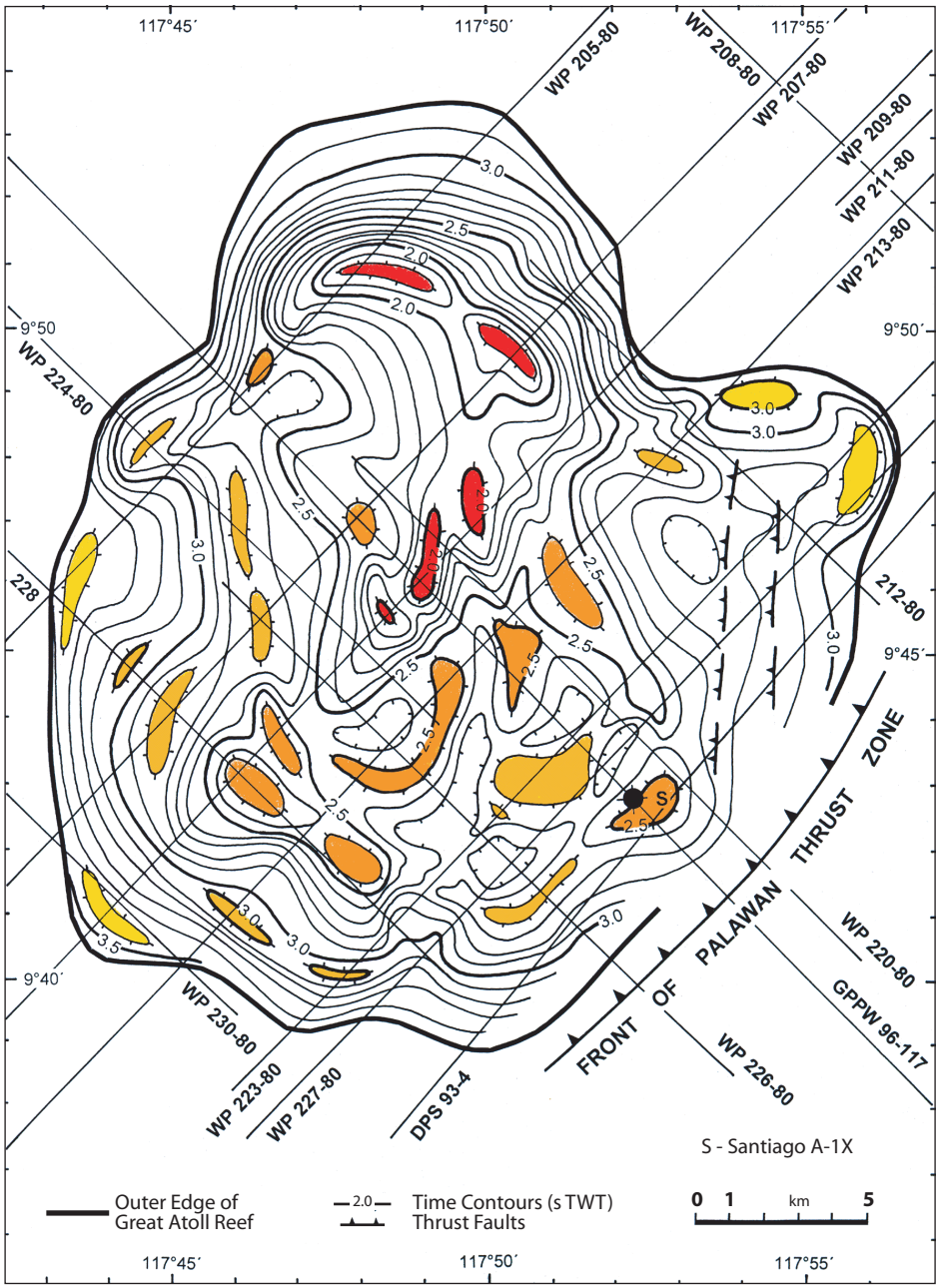

Fig. 50: Generalised map of structure contour lines of the Great Atoll Reef in seconds TWT below sea level and Front of Palawan Thrust Zone. Red indicates highest/ youngest peaks, dark to light orange lower pinnacles within the Great Atoll Reef structure.

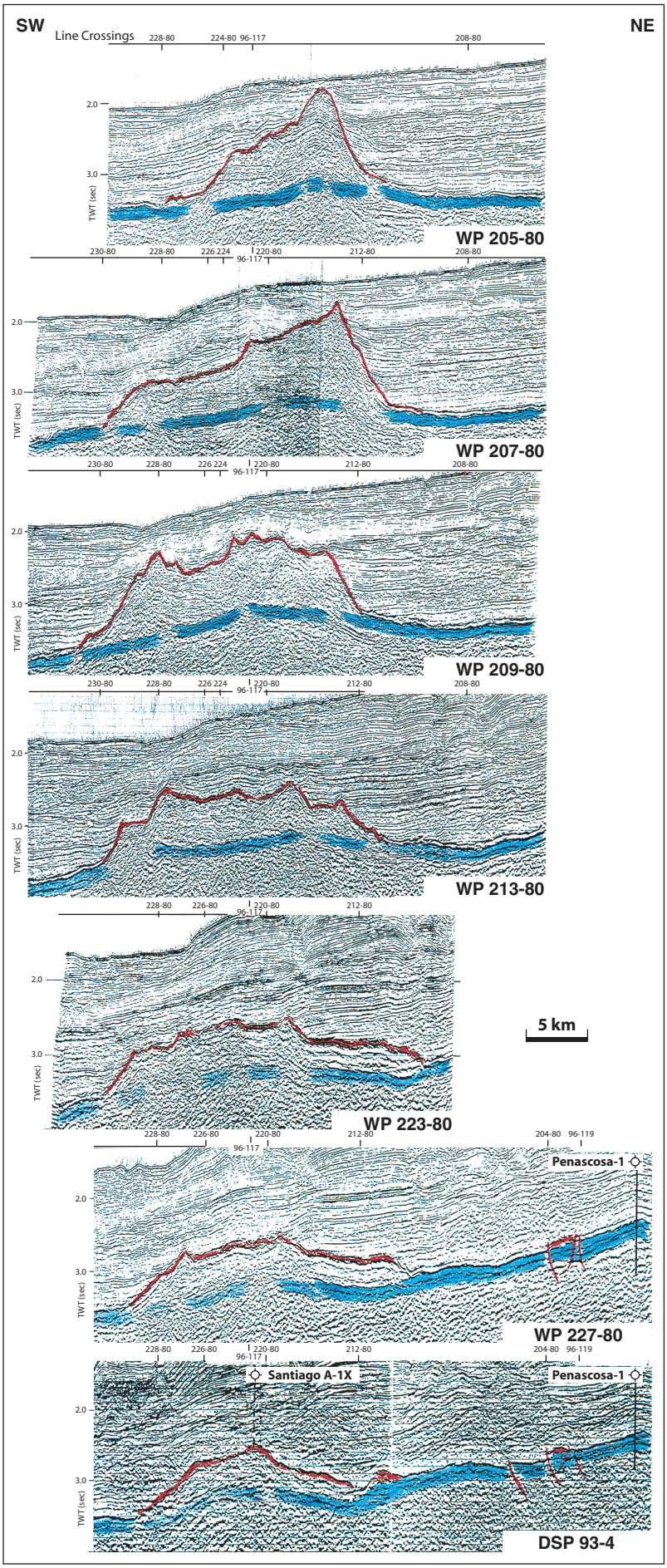

Fig. 51: Seismic profiles running from SW to NE showing the outline of the Great Atoll Reef (red). It overlies the Miocene Carbonate Platform (blue) and were finally burden by clastics. The top of the Miocene Carbonate Platform are taken from well Penascosa-1 through line DPS 93-4 and WP 227-80. Thrust faults affecting the platform carbonates are indicated. The distances between the parallel lines 205-80, 207-80, 209-80, 213-80, 223-80 and 227-80 are 4.7, 2.5, 2.5, 3.5 and 1.2 km. Line DSP 93-4 runs 0.3 (NE end at Penascosa-1) to 3.2 (SW end) km further south-eastwards from line 227-80.

The mapping of the Great Atoll Reef bases on a set of 7 NW-SE and 7 SW-NE striking profiles (Fig. 50). The Great Atoll Reef describes an almost round (slightly N-S elongated) carbonate area with a size of 27 by 23 km and at the highest peak approximately 2,400 m in thickness, which is surrounded by deep-water siliciclastics. Despite a generalised map of the structure, 29 single peaks of different sizes and shape are mapped. An elongated shape of the outlines of the patchy reef bodies dominates, whereas most of them running parallel to the outline of the Great Atoll Reef. Hence, the structure is called "atoll" even no extinct, subsiding volcano was involved in the development, like at "true oceanic atoll". The seismic SW-NE profiles of the Great Atoll Reef document that the highest peak exists in the North (Fig. 51: WP 205-80). A steep slope faces to northern directions, whereas the southern flank goes down more gently. Further to the SE the structure becomes relatively flat and internal reefal bodies are less significant.

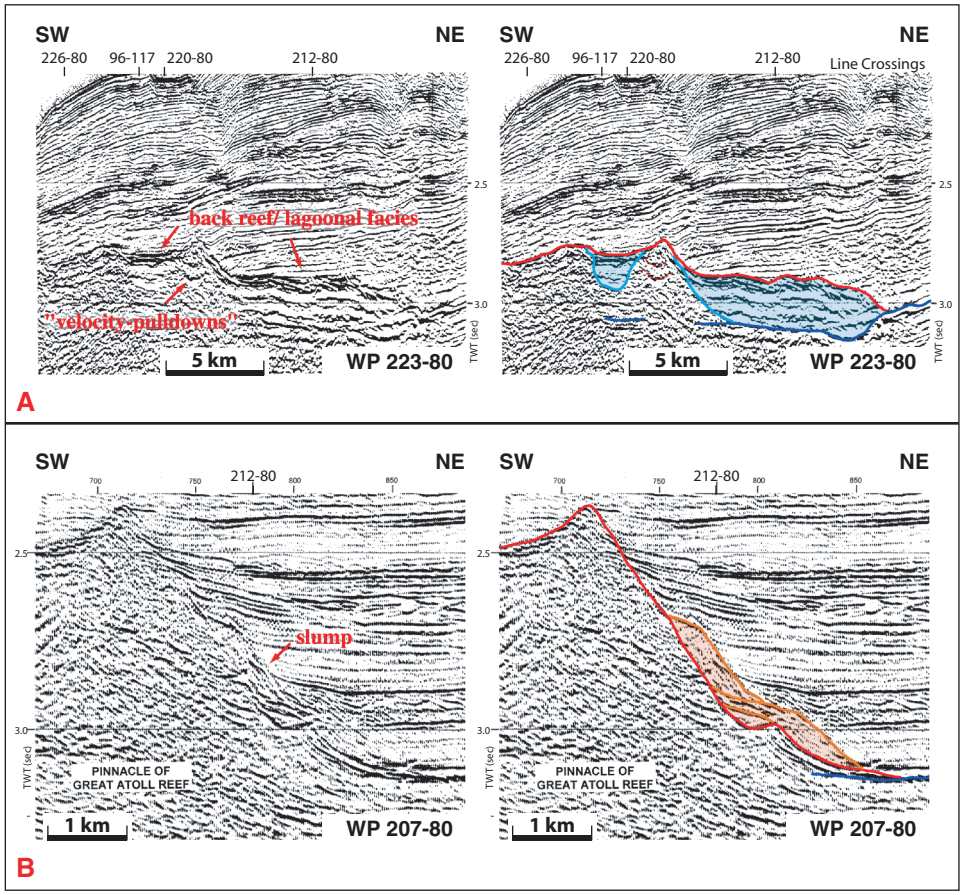

Fig. 52: Seismic profiles running from SW to NE: A well-bedded back reef/ lagoonal facies (light blue) are related to the internal part and the eastern side of the Great Atoll Reef; "velocity pulldown" features are indicated. B slumps at the northern slop of the Great Atoll Reef (orange).

The initial growth if the build-up was probably triggered by a pre-existing fault-related topography, although the structural setting of the substratum is seismically obscured by the build-up. Some weakly pronounced N-S trending faults are only indicated at the E flank of the Great Atoll Reef. They seem to control both the outline and internal facies of the build-up. The reef growth occurred during multiple phases throughout the late Early Miocene to the Pliocene. However, the development of the pinnacle reef bodies within the structure were probable a result of oceanic currents and/ or wind activities, rather than a rejuvenation of earlier tectonics or the westward thrusting of the indicated front of the Palawan Thrust Zone.

Facies Identification

The seismic record of the carbonates of the Great Atoll Reef is of different characters. Therefore, attempts were made to define the facies and growth history of the Great Atoll Reef by means of seismic sequence stratigraphy based on the following assumptions:

- The generally unstratified facies at the wells Santiago A-1X and Anepahan A-1X shows a poor reflectivity without continuous reflections (noisy areas). With respect to the surrounding lithologies, the interval velocity seems to be slightly lower due higher porosities. It causes "velocity-pulldowns" below the cores of the pinnacle-reefs (Fig. 52A: WP 223-80).
- Continuous reflections are related to the well-bedded back-reef/ lagoonal facies due to a better stratification in a protected and eventually slightly deeper environment in the internal part and of the eastern side on the Great Atoll Reef (Fig. 52A: WP 223-80).
- Sets of internally chaotic bodies at the outer seaward edges of the build-ups refer to slumps and reef debris from the reef top and the slops (Fig. 52B: WP 207-80).

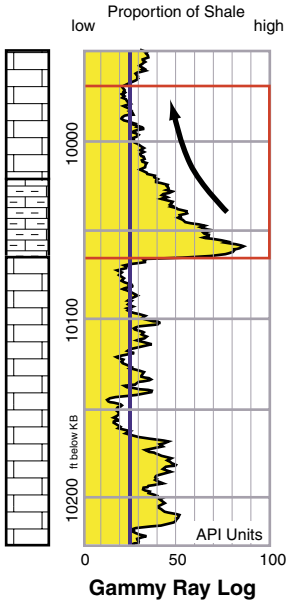

Fig. 53: Part of the Gamma Ray Log of the well Santiago A-1X between 9,550' and 10,225' KB showing the abrupt increase of shale content in the carbonates.

Furthermore, within the Great Atoll Reef body, a number of continuous reflections can be identified, which are either caused by emersions of the reef and subaerial erosions or by an increased influx of fine-grained terrigeneous clastics in suspension.

Evidence for the latter case is indicated in the Santiago A-1X well section at a depth of 10,068' KB, where an abrupt influx of clay took place, followed by a gradual upward decrease until the normal limestone lithology was reached again at a depth of 9,985' KB (Fig. 53).

4.1.3 Anepahan A-1X

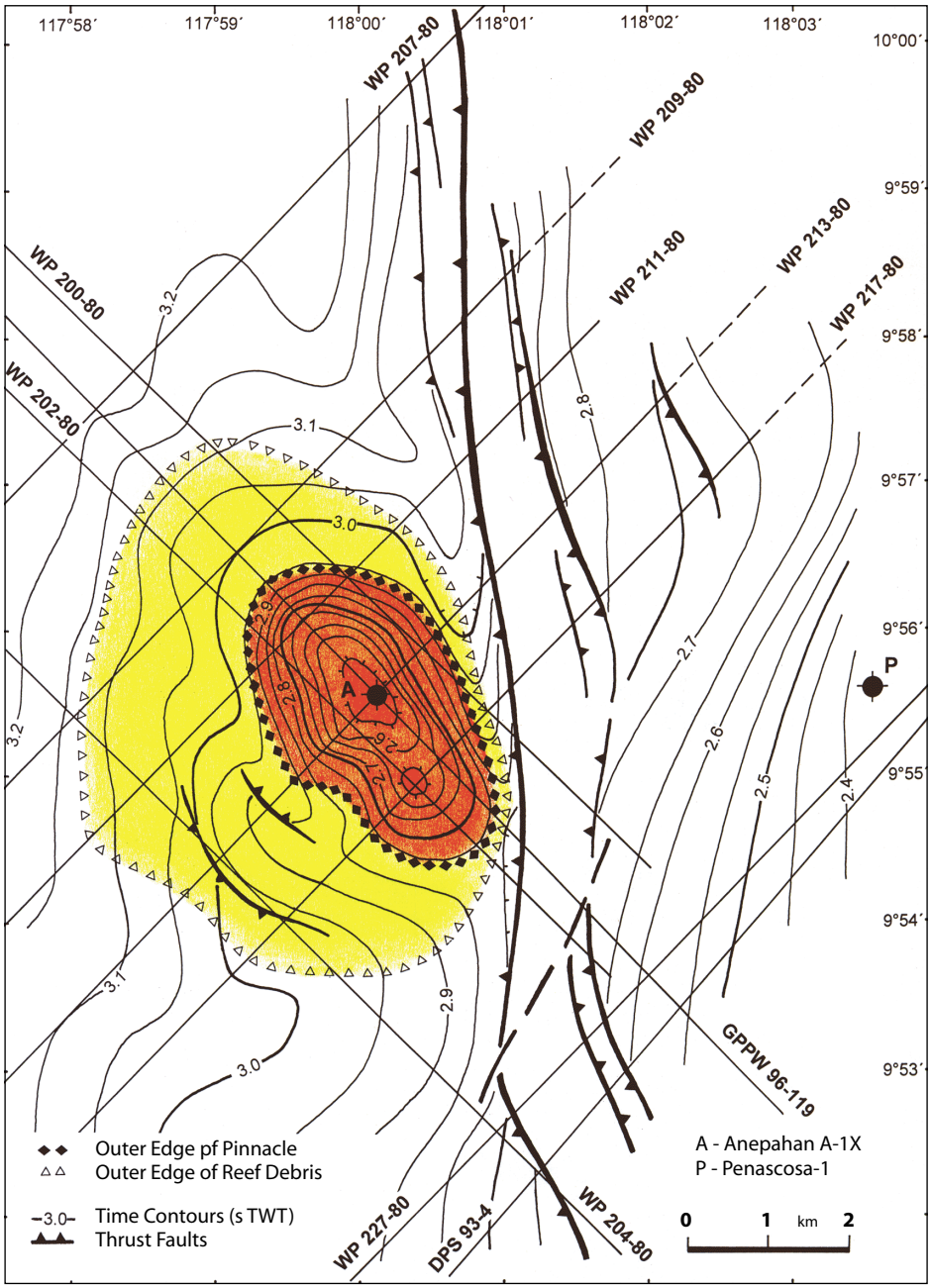

Fig. 54: Generalised map shows structure contour lines of Top Anepahan A-1X Pinnacle Reef, respectively Top Miocene Carbonate Platform in seconds TWT below sea level and thrust faults affecting Miocene Carbonate Platform. Red indicates outer edge of pinnacle reef, yellow surrounding reef debris.

The mapping of the Anepahan A-1X structure and the structural pattern near by grounds on 11 seismic lines (4 running NW - SE, 7 running SW - NE). The outlines of the outer edge of the pinnacle and the surrounding reef debris were plotted on a map of velocity-related (s TWT) time contour lines of the top of the Miocene platform carbonates, respectively the top of the Anepahan A-1X pinnacle reef (Fig. 54). The exceptionally steep gradient of the time contours of the Miocene carbonate platform W of the well Penascosa-1 is caused (1) by the decrease of the interval velocity of the overburden section reflecting a facies change from high velocity shelf carbonates and sandstones in the well Penascosa-1 to low velocity deep-water turbiditic shales in the well Anepahan A1-X, and (2) by the increase of the water depth westwards. Actually, the platform carbonates are almost sub-horizontal, whereas the well Penascosa-1 encountered the top of the platform carbonates at 2.340 s TWT (-3,226.9 m SS) and the well Anepahan A-1X the top of the pinnacle reef at 2.515 s TWT (-2,571.9 M SS). Anyhow, based on the seismic survey the tested pinnacle reef body with a best-estimated height of about 900 m and a dimension of approximately 2.5 to 4.2 km are surrounded by reef debris. The asymmetric fan of reef debris reaches on the western side of the pinnacle an extension of 2.5 km, whereas in contrast no or very small amounts of reef debris exist on the eastern side. The elongated pinnacle is NW - SE orientated. As seen most significant in line WP 211-80 and line WP 217-80, the morphology of the pinnacle is characterised by a very steep north-eastern side and a less steep slope to the SW (Fig. 55). Two high-points form the structure (WP 202-80), whereas the more extended body is in the NW (Fig. 56).

The N-S trending thrust fault pattern observed in the available seismic surveys in between the Anepahan A-1X pinnacle reef and the well Penascosa-1 refers to a old system of thrust faults, which is related to the rifting of the South China Sea during the Late Eocene to Oligocene. The strike-slip movements rejuvenated this old system after the deposition of the early Miocene platform carbonates and affect them. Below the reef debris SW of the Anepahan A-1X structure, a weakly pronounced structural high occur (WP 204-80), which is defined by NW - SE running thrust faults. However, since the reef body seismically obscures the structural setting in the platform carbonates below, the possible existence of additional faults must be further on subject of speculations.

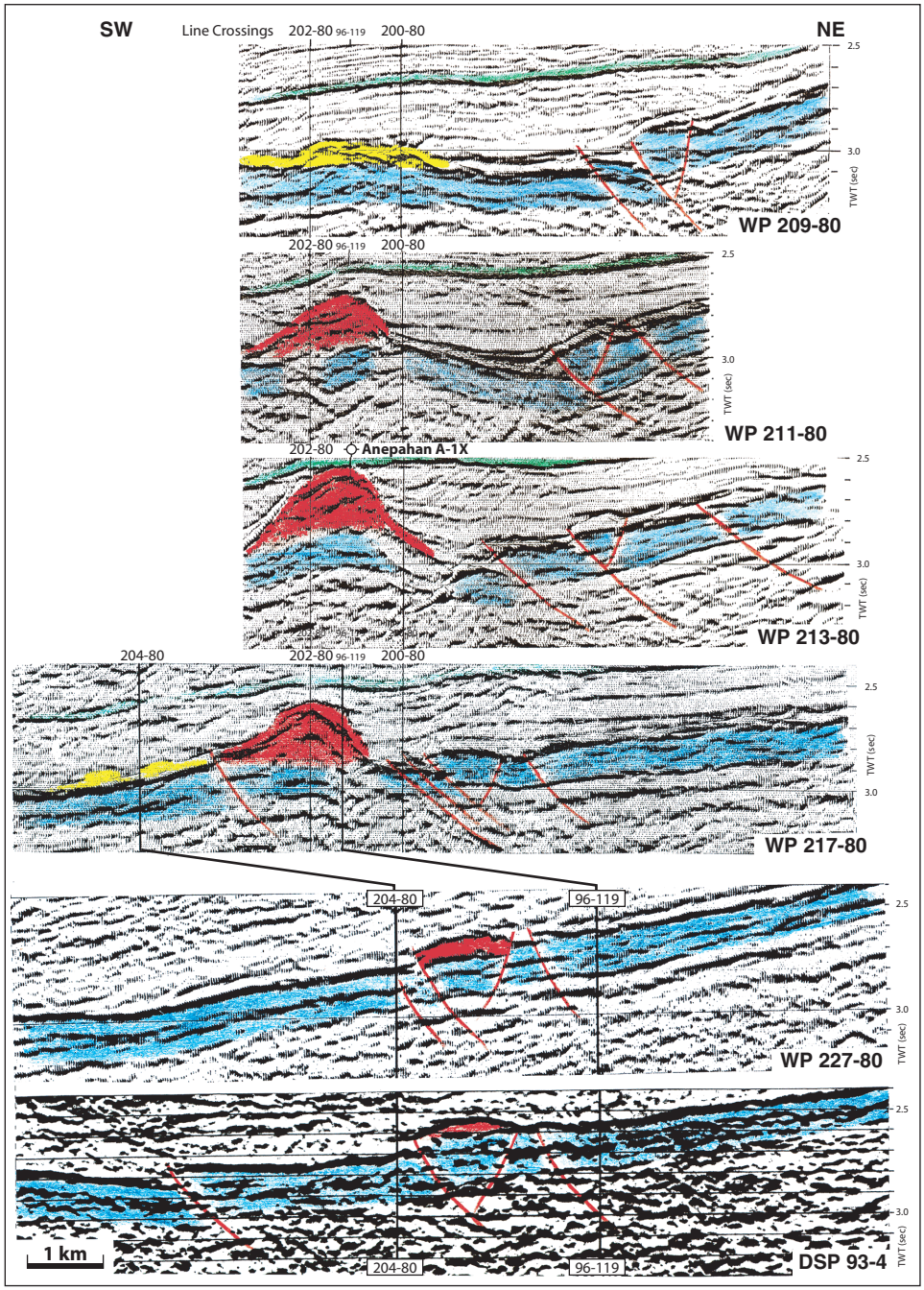

Fig. 55: Seismic profiles running from SW to NE showing Anepahan A-1X Pinnacle Reef (red) and their related reefal debris (yellow), overlying the Miocene Carbonate Platform (blue). Overburden clastics are green coloured. The top of the Miocene Carbonate Platform are taken from well Penascosa-1 through line DPS 93-4 and WP 227-80. Thrust faults affecting the platform carbonates are indicated. The distances between line 209-80 and 217-80 are 1.1 - 1.3 km. Line 227-80 runs parallel in 3.7 km distance to the SE, line DSP 93-4 460 (NE end) to 840 (SW end) m further south-eastwards from line 227-80.

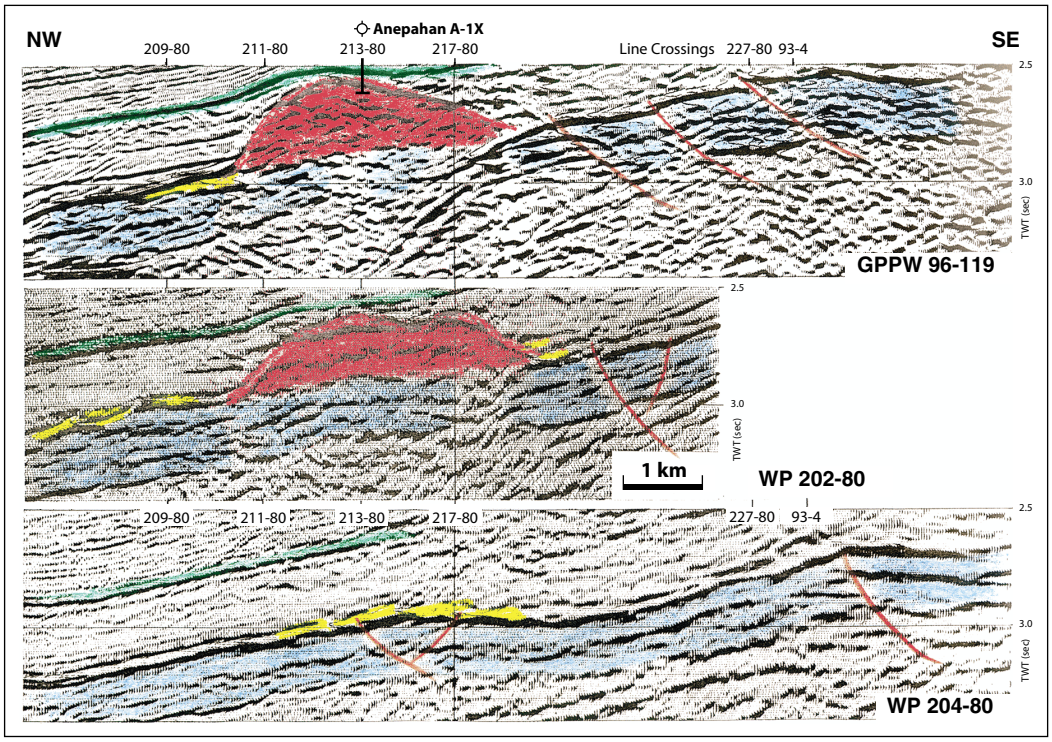

Fig. 56: Seismic profiles running from NW to SE showing Anepahan A-1X Pinnacle Reef (red) and their related reefal debris (yellow), overlying the Miocene Carbonate Platform (blue). Overburden clastics are green coloured. Thrust faults affecting the platform carbonates are indicated. The distance between line 96-119 and 202-80 is 0.4 km, between 202-80 and 204-80 in the SW 2.4 km.

4.1.4 Erosive Channels

On the present-day seafloor as well as within the clastic succession overlying the Miocene carbonates exist numerous of erosive channels offshore Palawan. The recent channels start at the shelf break in water depth of about 200 m and die in the deeper water between 1,000 m and 1,100 m (Fig. 57). They are between 10 and 15 km long and 1 to 2.5 km wide. The maximal erosion up to 200 m occurs in the areas where the slope of the continental shelf shows the steepest gradient, i.e. in the upper and central part of the channel (Fig. 58: Line WP 213-80.

Since the early Pliocene time, most of the channels remained fairly at the same position during the deposition of the upper 900 - 1,150 m of sediment. This indicates that the general tectonic setting and therefore also the drainage pattern off the island of Palawan are quite stable over a long period of time. Nevertheless, the prograding shelf filled some older channels and shifted the center of erosion seawards.

The sites of Penascosa-1 and Anepahan A-1X are placed close to an active erosive channel on the present seafloor. In both wells, the base of the stable channels was drilled in a depth of

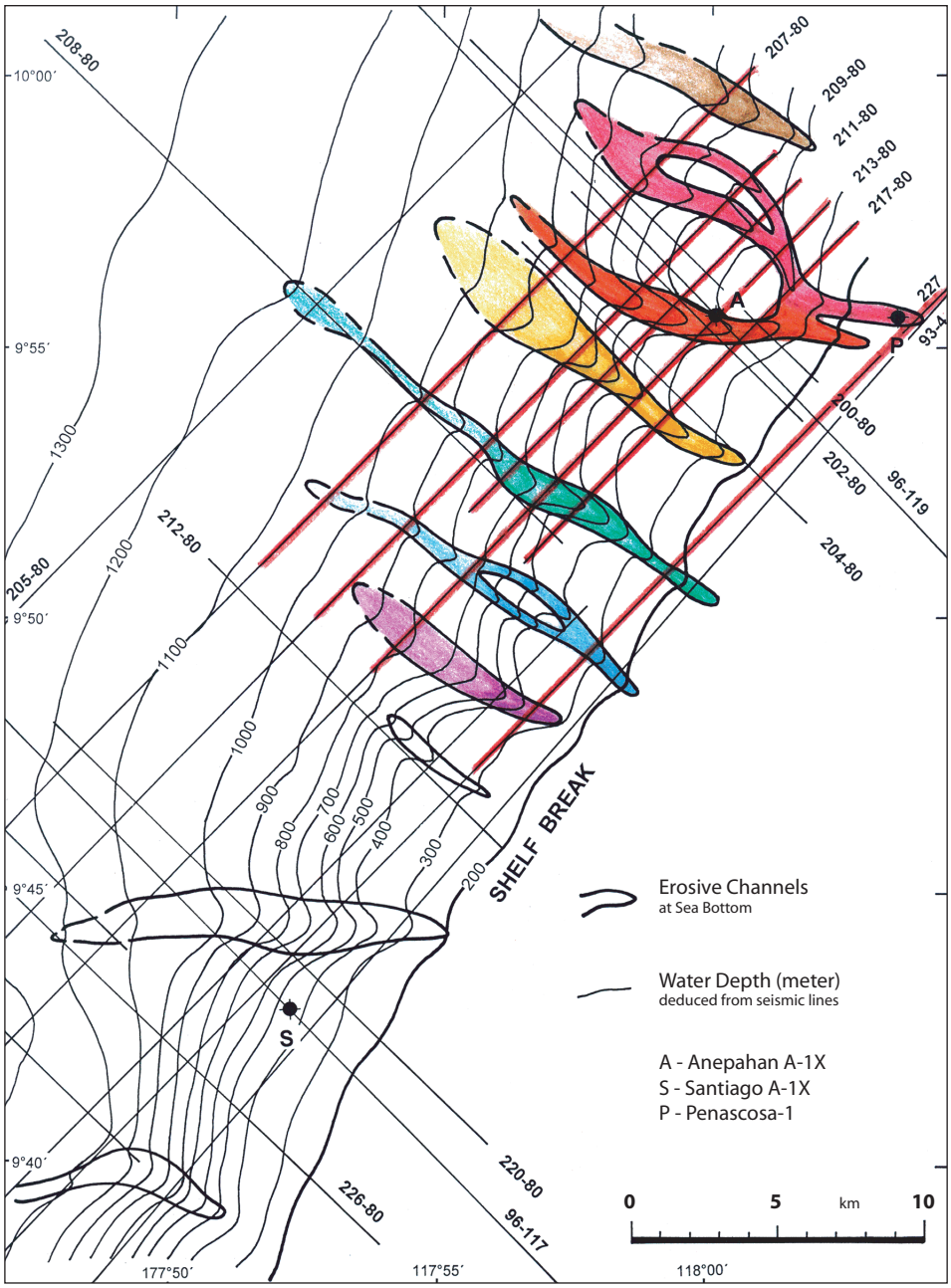

Fig. 57: Lateral distribution and outlines of recent erosive channels at the seafloor along the shelf break of SW Palawan. Contour lines of the seafloor topography are interpolated from the water depth indications on the seismic lines of the WP 80-survey (water depth values every 20 shot points, i.e. 0.67 km) and the GPPW 96-survey (water depth values every 50 shot points, i.e. 1.25 km).

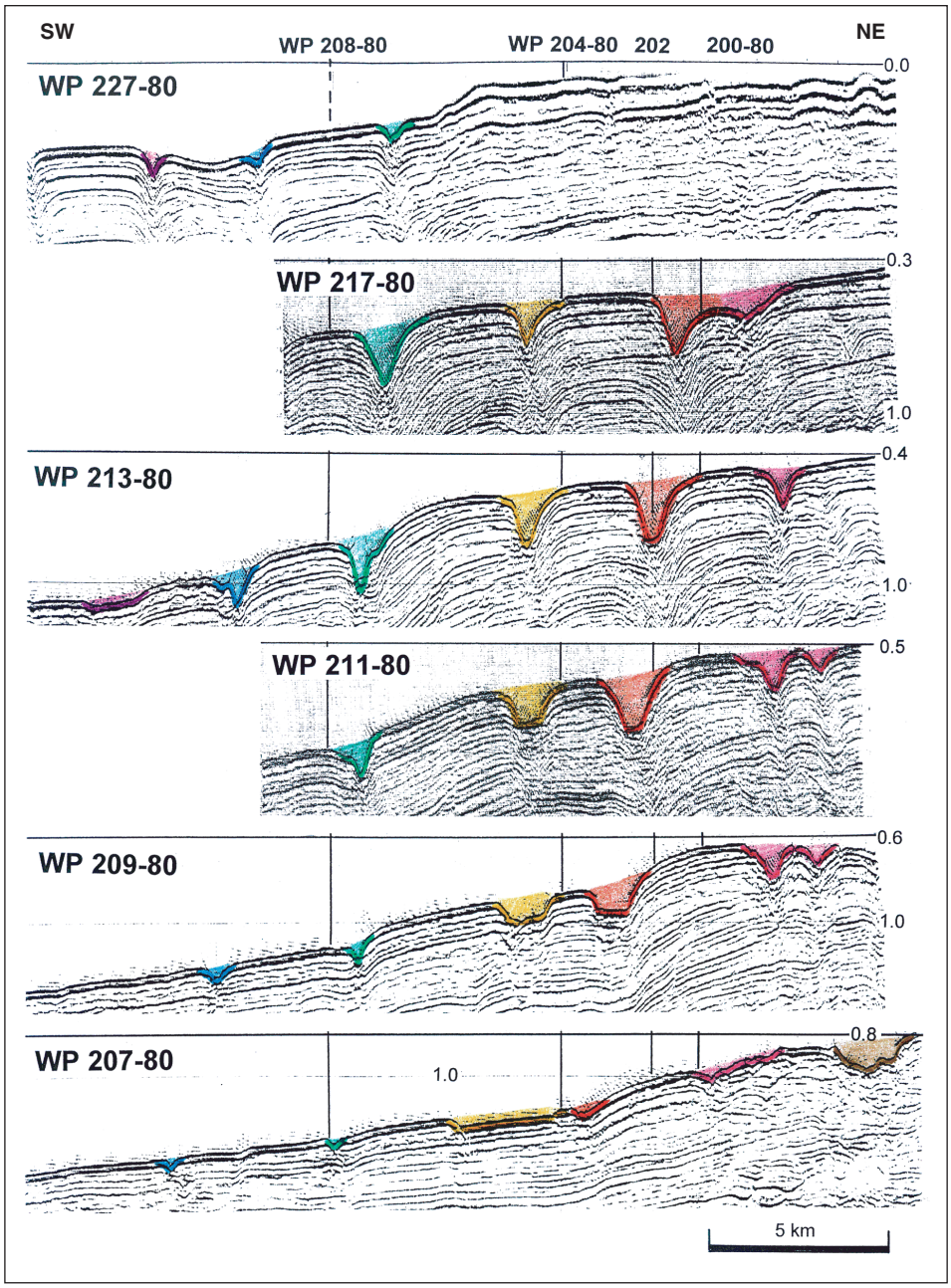

Fig. 58: Seismic profiles of the seafloor running parallel to the shelf break of SW Palawan and showing incisions of recent channels into the ground. Some of the channels reflect stable positions over long time peroids. Line WP 227-80 is the closest line to the shelf in a water depth of 200 m, whereas WP 207-80 are located out in the basin in a water depth between 1,000 and 1,100 m.

3,723 ft KB (Penascosa-1) and 4,125 ft KB (Anepahan A-1X). The observed channel base in the respective seismic line tied into the well data correlated with lithological and stratigraphical changes. An abrupt change from an acoustically less impedant channel filling to more compacted shales of the undisturbed underlying section is reflected in the composite log of Anepahan A-1X (Fig. 59). Furthermore, the biostratigraphic data confirm the discordance between the Late Miocene and Pliocene age (cf. chapter 4.3.3). The structural setting of the Lower Miocene carbonates has apparently not controlled the location of the channels so that channels even occur on top of the Anepahan pinnacle reef.

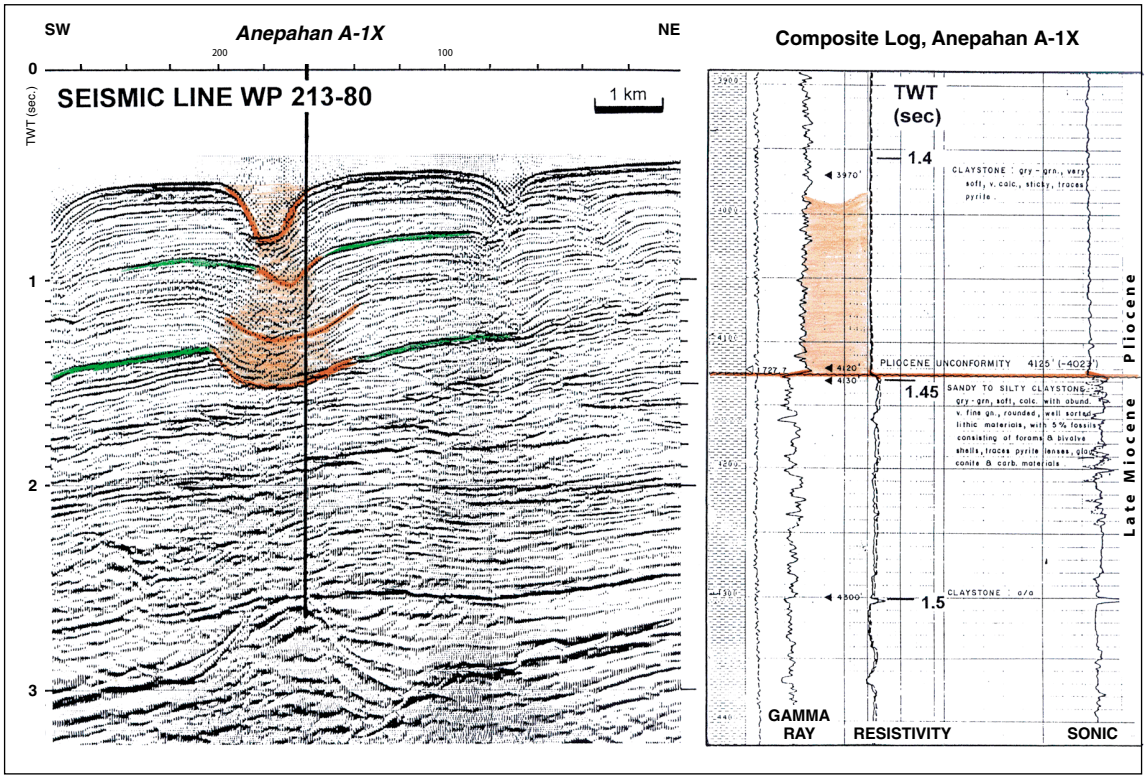

Fig. 59: Part of the seismic profile WP 213-80 showing the incision of a recent channels into the present seafloor (red) in the vicinity of the well Anepahan A-1X. Beside the seismic profile, the Gamma Ray -, Resistivity- and Sonic Log document the related base of the channel in a depth of 4,125' KB. The channel has a almost stable position since the Pliocene time.

4.2 Well Sections

4.2.1 Offshore Succession

The offshore succession are generated from the three wells Penascosa-1, Santiago A-1X and Anepahan A-1X.

The oldest sediments known from the study area offshore Palawan are the clastic substratum below the Miocene carbonates. They are most probably of Early Cretaceous age and were therefore deposited before the beginning of the rifting in the South China Sea during Late Eocene to Oligocene (TAYLOR & HAYES, 1980, 1983). The well Penascosa-1 encountered between 12,553' KB and the total depth of 14,000' KB these shales, which are interbedded with sandstones and siltstones below 13,220' KB (Fig. 60). The hard and dense shales are dark grey to black, slightly calcareous to non-calcareous, with silty bands, calcite and pyrite vein fills and possible slickensides. The organic carbon content is generally fairly low, the kerogene of coaly to woody nature. The interbedded sandstones are light grey, fair to poorly sorted, with a silt to clay matrix, in parts dolomitic or cemented by silica. The environment of deposition is interpreted as deep-water bathyal (TIDEY et al., 1975).

A basal conglomerate composed of cherts in a quartz-sand matrix overlain unconformably the shales of the substratum with a sharp contact at 12,565' KB in the well Penascosa-1. The porosities are according to log interpretations in the range of 13 - 14%. The interpretation results in an inner sublitoral environment for the deposition during the early syn-rift phase prior to the opening of the South China Sea (TIDEY et al., 1975). There is good evidence in seismic data that this section thickens in half-grabens further seawards of the study area offshore Palawan. A transition zones made of dolomitic shales which grade into the dolomites of the overlying platform carbonates follows topwards between 12,486' - 12,510' KB. The platform carbonates are present over the entire study area offshore Palawan according to seismic data and extends north-eastwards beyond the Nido oilfield and to the NW as far as the Malampaya gas and oil pool. The platform carbonates were penetrated in the Penascosa-1 well from 10,625' - 12,485' KB. The composite log of the Santiago A-1X well reports also the platform carbonates between 10,500' KB and the total depth of 10,602' KB. Since no lithological changes occur at this depth, there are certain doubts about this interpretation. In addition, the seismic correlation also suggests a greater depth of the platform carbonates. The platform carbonates itself are composed of massive, fine crystalline, dense dolomites in the lower part of the Penascosa-1 section at 12,170' - 12,552' KB with intercalated by dolomitic limestones between 12,303' - 12,460' KB. Above fossiliferous limestones with foraminifera, shell fragments, echinoid spines, abundant corals with some large coralline red algae fragments are deposited. The porosity is poor to almost not visible, even if fossil vugs occur occasionally. Dark grey shaley stylolites are common. The paleoenvironment was a protected shelf with shallow to very shallow water depth (TIDEY et al., 1975).

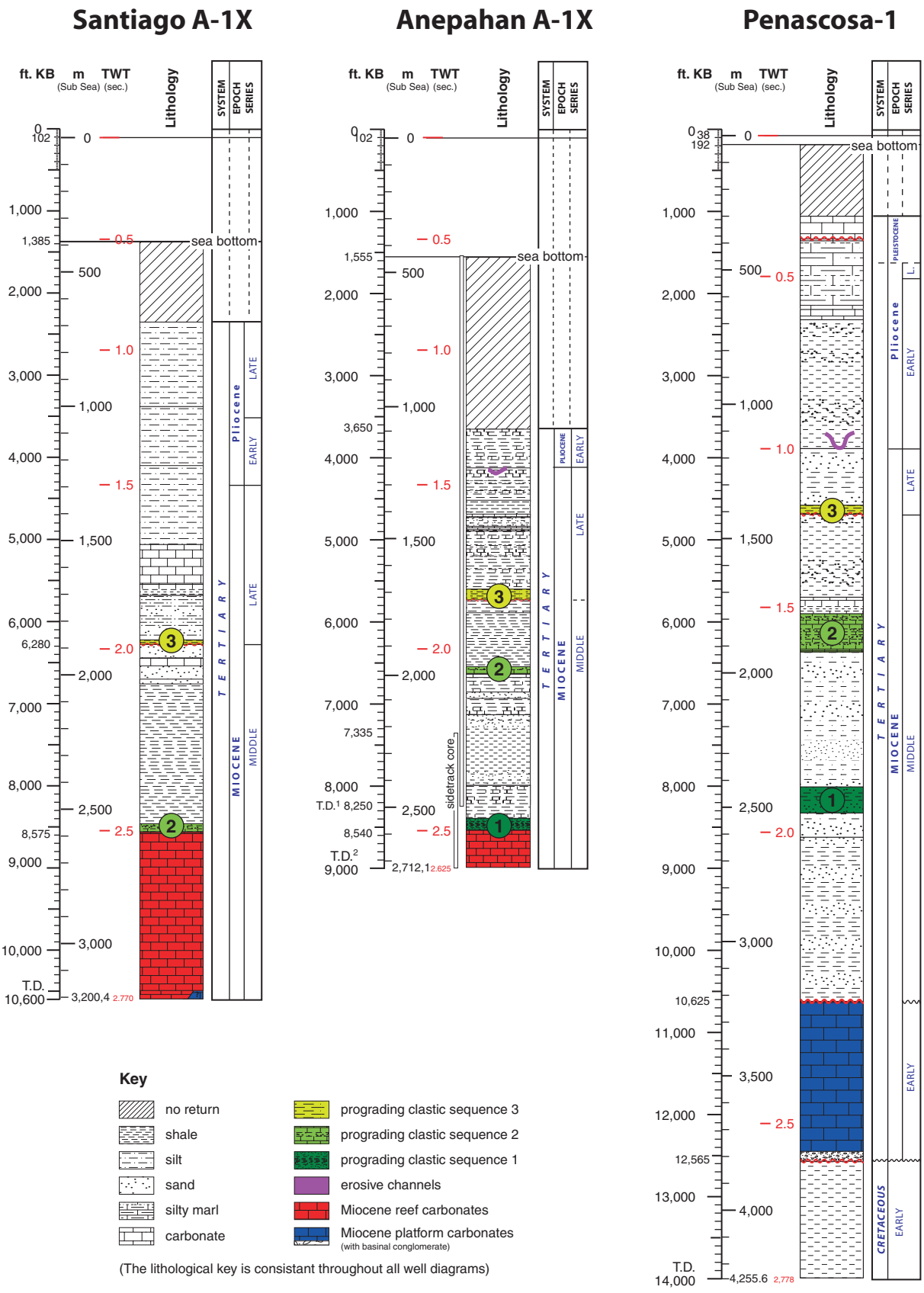

Fig. 60: Well sections in ft below KB, meters and seconds Two-Way-Traveltime (s TWT) of the 3 studied wells Santiago A-1X, Anepahan A-1X and Penascosa-1 illustrating the general lithologies and ages.

The lithologies of the reefal carbonates drilled in the well Santiago A-1X and Anepahan A-1X are characterised generally as biomicrite including abundant fossil fragments. Nevertheless, the limestones of the structures are made of course of many different varieties regarding the composition, but detailed lithological descriptions are missing.

The recovered sediments of the overburden clastic sequence are in all three wells prevalent fine siliciclastic materials, mainly shales. Some of the shale or silts are partly calcareous. Furthermore, throughout the sequence of Santiago A-1X some intercalations of carbonate layers occur, whereas in the sequences of Anepahan A-1X and Penascosa-1 the intercalation of carbonate layers is less prominent. However, about 1,100 ft of a limestone sequence caps the section of Penascosa-1.However.

4.2.2 Facies Analysis of Core Samples

Within the sections of the three studied offshore wells Penascosa 1, Santiago A-1X and Anepahan A-1X some short parts of the drilled carbonate sequence were cored. The 2 core sections of Penascosa 1 at 10,673 -10,698 ft below KB (KB = 38 ft above sea level) and 12,738' - 12,769' below KB were fully recovery, but not available for this study. Therefore, the following thin section study are restricted to some samples from two available cores recovered in the wells Santiago A-1X and Anepahan A-1X.

Santiago A-1X

The carbonates of the Santiago A-1X well were cored at a depth of 8.655' below KB (KB = 102' above sea level), 80' below the contact with the overlying siliciclastic deposits. The recovery of the 44' long core was 36' (82%). The depth for the core given by the driller is corrected based on the logging depth, which results in a subtraction of 18'. The Department of Energy (DOE, Manila) provided 15 rock samples of the core (Tab. 7).

The recovered limestones are described as light grey to light tan and often very hard calcarenites or biomicrites. Based on the thin section study the lower part of the core (8.699' - 8.682') is classified as poorly sorted floatstones including some intraclasts. Upcore, the carbonates grade into larger foraminifera floatstones with a high content of planktonic foraminifera and then to a planktonic foraminifera wackestone from 8.664' upwards. Additionally, some bedded dark larger foraminiferal packstone occur locally between 8.674,2' and 8.679' in the middle part of the core.

Samples	Driller Depth below KB	Log Depth below KB
SA 1/1b	8.682,0	8.664,0
SA 2	8.684,0	8.666,0
SA 2b	8.684,2	8.666,2
SA 3	8.688,0	8.670,0
SA 4	8.691,0	8.673,0
SA 3b	8.692,2	8.674,2
SA 5	8.694,0	8.676,0
SA 6/4b	8.697,0	8.679,0
SA 7	8.700,0	8.682,0
SA 8	8.702,0	8.684,0
SA 9	8.705,0	8.687,0
SA 10	8.708,0	8.690,0
SA 11	8.711,0	8.693,0
SA 12	8.714,0	8.696,0
SA 13	8.717,0	8.699,0

Tab. 7: Depth in ft below KB of the 17 samples of the core from Santiago A-1X given by the driller and corrected with respect to the logs.

The matrix of the carbonates is constantly micrite, but the assemblage and the relation of the skeletal grains to each other vary. The texture of the carbonates changes significantly in the uppermost part of the core from predominately point and tangential contacts to no contacts in sample SA1. Larger foraminifera, some up to 5 mm in size (Nummulitidae), are always abundant and belonging mainly to Nummulitidae, Amphisteginidae, Acervulinidae, Homotrematidae and Lepidocyclinidae (Fig. 61). However, only one single representative of Soritidae was found, very few Alveolinidae were restricted to two lower samples, and a few Miogypsinidae were discovered from two samples in the upper part of the core. Nevertheless, the portion of all larger foraminifera accounts for 10 to 23% of total biota. The sum of larger foraminifera does not indicate any preferred level of higher larger foraminifera amounts. Their distribution is randomly. Beside the larger foraminifera, red algae are frequent and show a clear increase in the middle part (SA 5 to SA 7) of the core section. Echinoderms and corals occur over the whole section, but with different amounts. Green algae are recovered

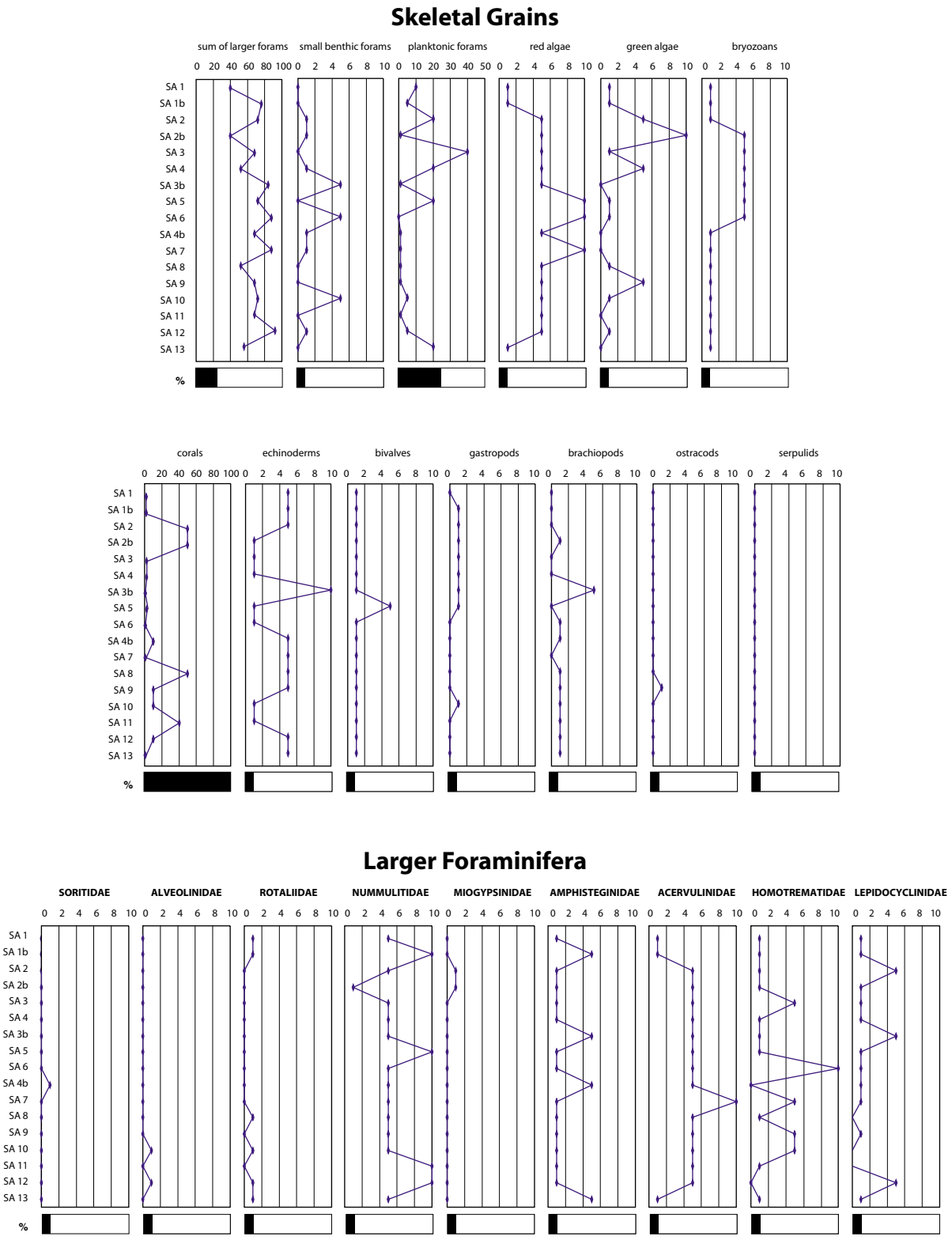

Fig. 61: Semi-quantitative frequency estimation of skeletal grains and larger foraminiferal assemblage of the core samples of the well Santiago A-1X

especially in the upper part, like the planktonic foraminifera. Even if green algae and planktonic foraminifera occur together, their respective amounts are negative correlated. Small benthic foraminifera decrease upcore.

Anepahan A-1X

In a depth of 8.556' below KB (KB = 102 ft above sea level) and 16 ft below the top of the carbonates a core of 44' was recovered in the well Anepahan A-1X. The depth given by the driller is corrected based on the logging depth, which results in a subtraction of 7'. The Department of Energy (DOE, Manila) provided 10 rock samples of the core (Tab. 8).

Samples	Driller Depth below KB	Log Depth below KB
AN 1	8.563,0	8.556,0
AN 2	8.565,0	8.558,0
AN 3	8.568,0	8.561,0
AN 4	8.571,0	8.564,0
AN 5	8.575,0	8.568,0
AN 6	8.579,0	8.572,0
AN 7	8.585,0	8.578,0
AN 8	8.590,0	8.583,0
AN 9	8.595,0	8.588,0
AN 10	8.605,0	8.598,0

Tab. 8: Depth in ft below KB of the 10 samples of the core from Anepahan A-1X given by the driller and corrected with respect to the logs.

The macroscopic core description given in the graphic core logs provides only the differentiation between biomicrite and biocalcarenite alternating twice. The massive white and tight biomicrite between 8.556' to 8.564' and 8.574' to 8.589' contains foraminifera, coral fragment, algae and bivalves, which are totally replaced by sparite.

The thin section study of 10 samples provides some more detailed information about the texture of the carbonates, even if a strong secondary diagenetic imprint destroys some features of the wacke- to floatstones and partly grainstones. Larger foraminifera are frequent. Their assemblage is made of specimens of Soritidae, Alveolinidae, Miogypsinidae, Amphisteginidae, Acervulinidae and Lepidocyclinidae (Fig. 62). Homotrematidae and

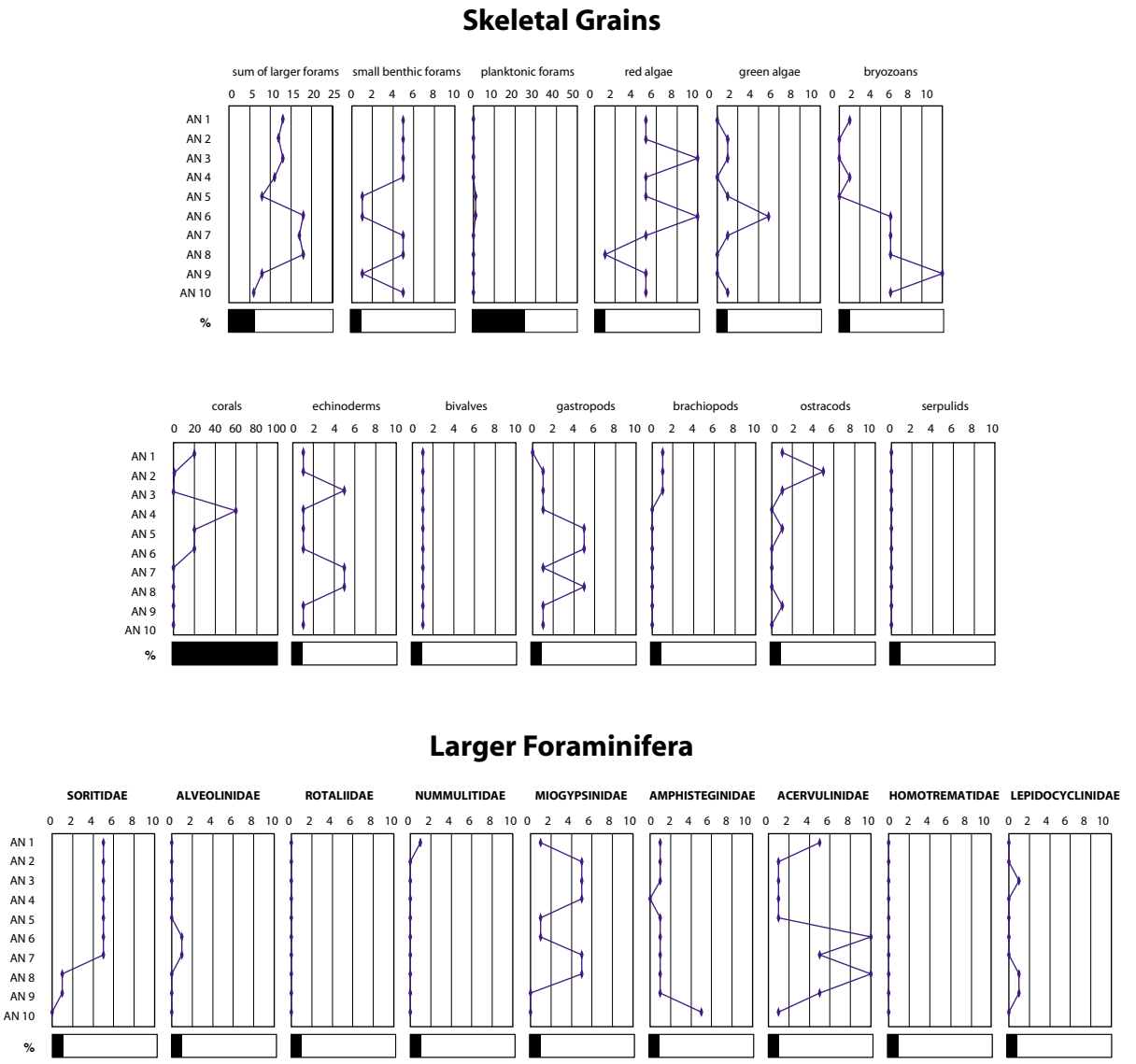

Fig. 62: Semi-quantitative frequency estimation of skeletal grains and larger foraminiferal assemblage of the core samples of the well Anepahan A-1X.

Rotaliidae are missing, while one single species of Nummulitidae was discovered in the uppermost sample. Soritidae increase from the lowermost samples with no specimen to a constant amount of 5%. Also quite common are Acervulinidae and Miogypsinidae. In general, the portion of all larger foraminifera in the biota ranges from 5 to 20%, whereas only the samples AN8 - AN6 document a higher amount of more than 15%. In general, the amounts are lower than in the well Santiago A-1X. Beside the larger foraminifera, red algae and small benthic foraminifera (Miliolidae) are quite common in all samples. In contrast, planktonic foraminifera are restricted to sample AN 5 and AN 6, which correlates with a lower amount of small benthic foraminifera. Fragments of green algae are found in 6 samples and are abundant

in sample AN6 together with the first massive corals. Bryozoans show a clear decrease upcore, whereas ostracods increase. Gastropods and brachiopods vanish in the upper part of the core.

4.2.3 Diagenesis Offshore

Santiago A-1X

The available reports of the well Santiago A-1X do not provide any details about the Miocene reefal limestones penetrated by the well between 8,575' and the T.D. of 10,625'. Therefore, the information about the diagenesis and porosity are limited to a internal document of Phillips Petroleum Ltd, Philippines (1980) with a general core description, the study of the provided rock samples as well as the Bulk Density Log.

Within the core section, all cements as well as the neomorphic spar of mainly corals are granular or drusy (Fig. 63). Based on the thin section study, only one cement generation could be identified. Broken and/or deformed skeletal grains as well as concave-convex- and sutured component contacts document the moderate compaction. Stylolites are common in the upper part of the core and decreases downcore. Besides, the compaction produced some additional fracture porosity, interparticle- and intraparticle porosity in the larger foraminiferal packstones were preserved. The dissolution results in moldic porosity, which is more abundant in the upper part of the core. This correlates with higher amounts of corals and green algae. A partly relative strong secondary dissolution created a high amount of vug- and channel porosity. The total porosity with an estimated range from 5 to 20% includes both, fabric selective and no fabric selective porosity, closed and still open porosity. However, the open porosity, which is in the middle part of the core quite high, grounds predominantly on the vug- and channel porosity in the packstones. The estimation open porosity of 10 - 20% corresponds well with the measured porosity values of 16,5 & 17,2% determined by Phillips Petroleum Ltd, Philippines. Anyhow, throughout the core the open porosity is generally poor to fair (0,2 - 4,1%, Phillips Petroleum Ltd, Philippines).

The Bulk Density Log of the well Santiago A-1X provide the only available information regarding the porosity throughout the whole Miocene carbonate succession between 8,575 - 10,625'. The log reflects strong variability of the porosity within these carbonates, even if a

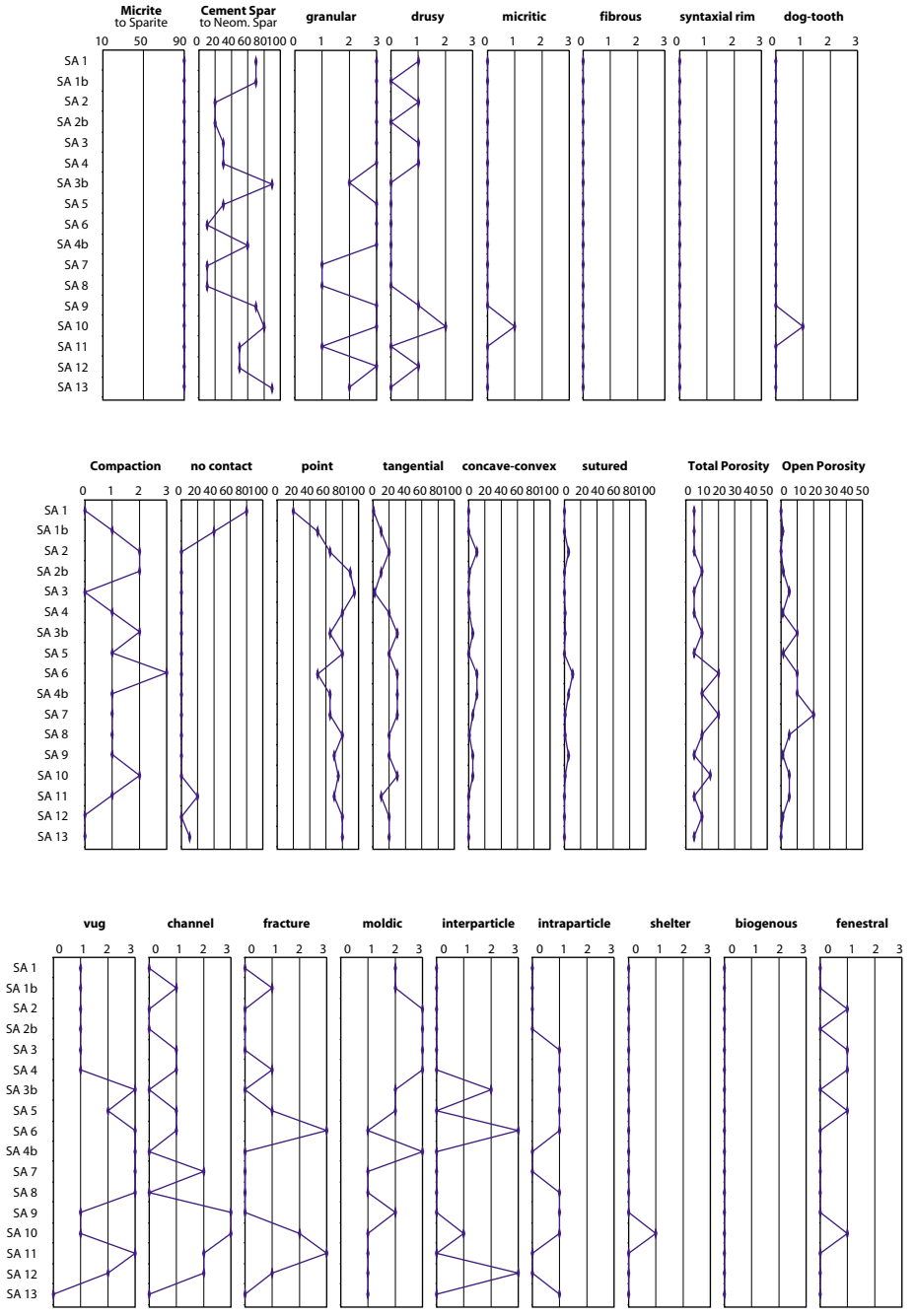

Fig. 63: Estimation of relative frequency of matrix- (micrite vs. sparite), sparite- (cement vs. neomorphic spar), cement- and porosity types as well as semi-quantitative frequency estimation of contact types, total- and open porosity within the core samples of the well Santiago A-1X.

continuous trend to lower porosity from the base up to 8,950' is significant. Above (8,950' - 8,575'), the porosity varies drastically and no trend is identified.

The sequence between 9,330' to 10,230' are used to illustrate two different settings, which lead to well-cemented parts in the carbonate sequence (Fig. 64). Both setting are closely linked to the content of shale in the carbonates, which is deduced form the Gamma-Ray Log.

One of the settings is related to an abrupt and significant increase of the shale content in the carbonates. Thereby, the shaley carbonate (10,065') caps a here 40 ft thick (10,065' - 10,105') well-cemented carbonate sequence, which is characterised by a high bulk density record of more than 2.55 g/cm^3 and moderate shale content. Secondly, in parts of very pure carbonates the porosity is also very low, as well documented between 9,613' and 9,581'. However, the details of the facies are missing, but the pure carbonates might refer to a high content of frame-builders (e.g. corals) so that the content of aragonite was probably high.

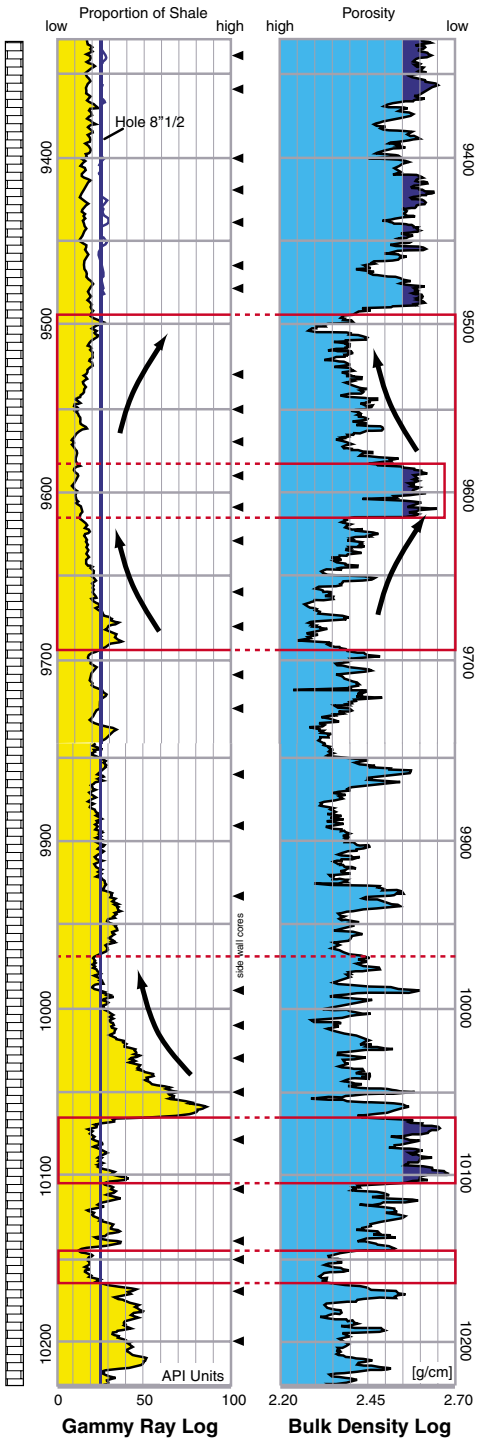

Fig. 64: Gamma Ray- (GRL) and Bulk Density Log (BDL) between 9,330' - 10,230' KB from the composite log of the well Santiago A-1X. Remarkable sequences of low or high shale content are indicated in the GRL, strong cementation of the carbonates in the BDL. Arrows refer to the changes upcore/ in time.

Anepahan A-1X

The available database of the well Anepahan A-1X does not allow an evaluation of the Anepahan carbonate build-up regarding their diagenetic history and the development of porosity. The observations are local and provide therefore only a probably small window of the history. Nevertheless, the 10 rock samples of the core document the most extensive and complex diagenetic story seen in the samples from the Philippines. The study were supplemented by unpublished documents of Phillips Petroleum Ltd, Philippines (1982), which present a generalised core description and the short description of 5 carbonate sidewall cores within the carbonate succession. Well logs were not available.

Throughout the samples of the core of Anepahan A-1X, the different diagenesis feature changes upcore with respect to the facies of the

carbonates and furthermore, each single thin section shows with several cement generations different stages of the diagenetic process.

The recovered wacke- to floatstones and pack- to grainstones exhibit a micritic and/or sparitic matrix (Fig. 65). Most of the sparite content in the samples is related to cement filling open porosity. Nevertheless, neomorphism produced a few spots of neomorphic spars (e.g. AN2) and affected the corals. Hence, the portion of neomorphic spar correlates to the occurrence of corals in the samples AN4, 5 and 6 between 8,571' and 8,581'. Anyhow, calcitic cements prevail over the whole core section, even if granular dolomite occur with different amount in the micritic matrix (AN1) or along fractures and channels (AN6 & 10). Nevertheless, in almost all samples light granular cements is abundant, whereas both, the topwards increasing drusy cement (crystals up to 2 mm) and the topwards decreasing subaeric speleothems prevail in different samples. Early fibrous- and/or radiaxial fibrous cement coated skeletal grains,

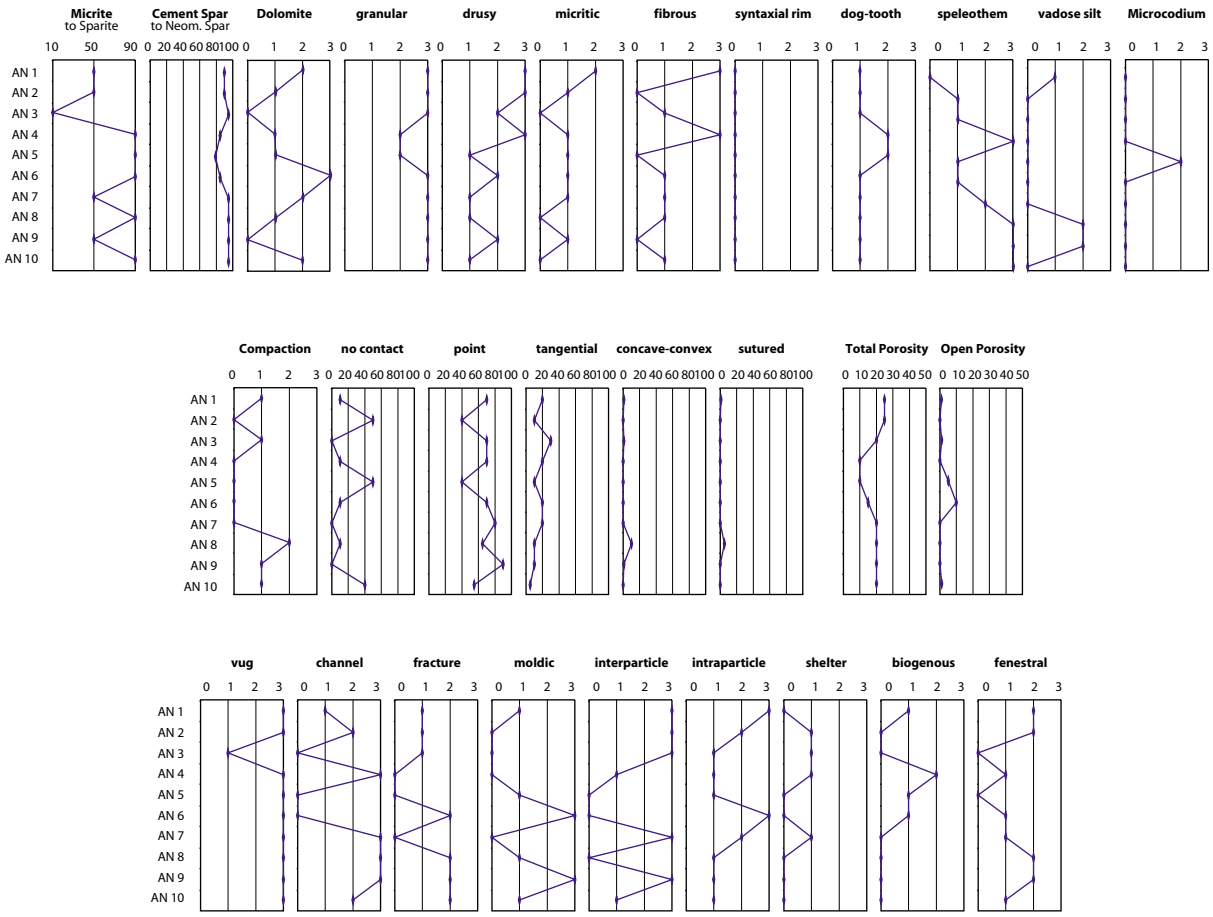

Fig. 65: Estimation of relation of matrix- (micrite vs. sparite), sparite- (cement vs. neomorphic spar), cement- and porosity types as well as semi-quantitative frequency estimation of contact types, total- and open porosity within the core samples of the well Anepahan A-1X.

whereas their development is of different quality. Predominantly these cement types were observed in the upper part of the core section. Dog-tooth cement is often related to the drusy cement and exists with no major significance in all samples. Vadose silt was found in two samples between 8,589' - 8,596' as well as in sample AN1. The sample AN5 contains a high amount of Microcodium (AN5), which bloom with no respect to any fabric in the carbonate. Syntaxial-, fenestral- and growth-framework cements are missing in the samples.

Beside the changes of the different cement types throughout the core section, a chronology of the diagenetic processes is recorded in these carbonates (Fig. 66). The earliest process affecting some skeletal grains (possibly before their deposition) is the encrusting of a component by larger foraminifera or red algae. Even if this is no diagenetic process, it provides the preservation of the outlines of a gastropod (AN6), which allow the reconstruction of the diagenetic processes. The first diagenetic process, also observed in the gastropod, is the destructive bioerosion by boring, followed by a dissolution. Other components (like aragonitic corals) are exposed to an early neomorphic process. These very early effects accompanied the precipitation of the first cements, mainly fibrous-, radiaxial rim- and/ or granular cements, before again some sediment were accumulated in existing holes. After this first stage of diagenesis, which is closely related to the depositional environment, strong meteoric dissolution created a high amount of vugs and channels, before the subaeric carbonate precipitation produced speleothems and Microcodium as well as some vadose silt. A slight motions in the parts of the carbonates results in the fracturing of some speleothems. Due to the fact that the dolomite cuts into speleothems indicate their later development. Partly fibrous- and dog-

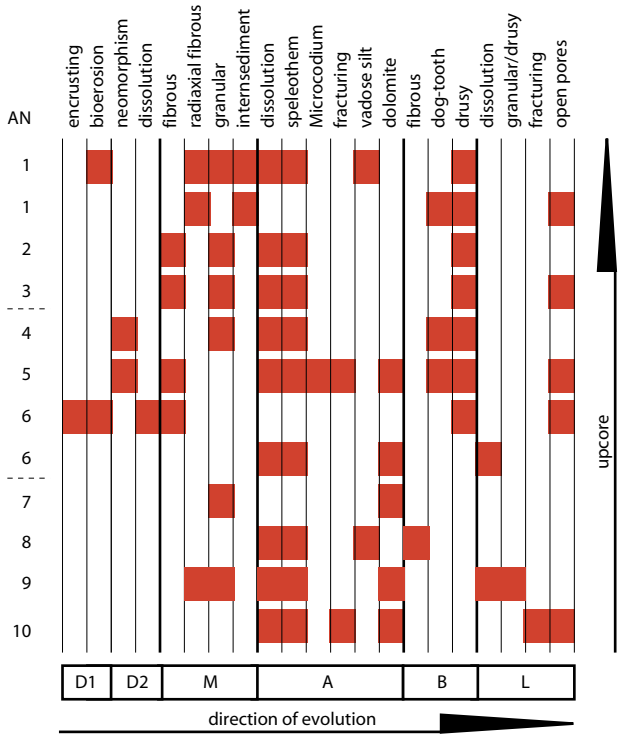

Fig. 66: Evolution of different cement types throughout the 10 rock samples of the core of the well Anepahan A-1X. Upwards the 12 thin sections of the samples are plotted in their stratigraphic order, whereas each observed cement type is plotted on the x-axis in the relative chronology of evolution. The letters indicate the general diagenetic periods: D = during deposition, M = early marine, A = subaerial, B = burial, L = late.

tooth cement is observed on the speleothems, before drusy cements, sometimes with micritic relicts, closed almost all open porosity. Finally, within the last stage (channel-) dissolution occurred, followed by the refilling of the porosity with granular or drusy cements. Not only because of some very late fracturing, a low amount of unconnected open pores still exists.

Likewise, the component contacts indicate no major compaction so that concave-convex- or sutured contacts were observed only once and sometimes the number of no component contacts is quite high (50%). Nevertheless, fractures as well as stylolites reflect some slight compaction. The fracture porosity supplements the estimate total porosity of 10 - 25%. However, the microcrystalline to crystalline fractures, some up to 0.5 mm in width, occur beside unconnected vugs up to 2 mm in the biocalcarenite (8,564' - 8,574' & 8,585 - 8,596'). This porosity is typically filled with dark grey blocky dolomite, granular sparite or speleothems. The horizontal permeability averages 0.05 - 0.10 Md and the total fluid porosity was calculated by Phillips Petroleum Ltd, Philippines with 2.0 - 3.7%. The abundant fauna of molluscs, algae and foraminifera (40-60%) of the pack- to grainstones is replaced by sparite. Nevertheless, these carbonates contain abundant but closed primary interparticle- and intraparticle- porosity. Between 8,574’ - 8,581’ and 8,596 - 8,605’ granular or slightly drusy sparit fills the molds, vugs, fractures and pore spaces at stylolites. Anyhow, some of these pores (mainly vugs, channels and fractures) are not completely closed, which leaves open pores up to a few mm in size. The horizontal permeability of the biocalcarenite averages 0.05 - 0.13 Md and the total fluid porosity were calculated with 1.4 - 7.0% by Phillips Petroleum Ltd, Philippines.
Only 3 of the 5 described carbonate sidewall cores were taken below the core section. The descriptions yield for two of the three cores (8,770’ & 8,920’) very good interparticle porosity supplemented by some vugs and fractures. The sidewall core in between (8,820’) is characterised by micrite so that some stylolites occur and only poor visual porosity is indicated.

Finally, even if the diagenetic story discovered from the 10 rock samples of the core seems to demonstrate a complete diagenetic story, the transfer to the whole Miocene carbonate succession of the Anepahan build-up seems to be, with respect to the proportions, not reasonable. The core section represents only 44 ft of the 460-ft thick penetrated carbonate succession at the top of the pinnacle, which is best estimated about 3,000 ft high.

4.3.1 Biostratigraphy Penascosa-1

Robertson Research (Singapore) was assigned to prepare the micropaleontology and stratigraphy of the well Penascosa-1. Cutting samples collected at 10-foot intervals were composited to 20-foot intervals and processed to recover their foraminiferal assemblages over the interval from 1,040' - 14,000' (ft below KB). In addition to 600 cutting samples, 49 sidewall cores and several samples from the two conventional cores were processed for foraminifera. The results are summarised in the Oilfield Report No. 351 (TIDEY et al., 1975). Together with D. Spiegler/ Kiel the data were checked and some present updates regarding the occurrence of taxa related to the Neogene Zones after BLOW (1969) were interlaced (Fig. 67).

The following 26 age diagnostic planktonic foraminifera taxa were reported:

Biorbulina bilobata (N9 - N23)
Globigerina druryi
Globigerina nepenthes (N14 - N19)
Globigerinatella sicanus (N7 - N9)
Globigerinoides immaturus (N5 - N23),
Globigerinoides subquadratus (N5 - N14)
Globigerinoides triloba (N4B - N23),
Globigernina binaiensis (P22 - N5)
Globoquadrina altispira altispira (N4B -N19)
Globoquadrina dehiscens dehiscens (N4B - N18)
Globorotalia acostaensis (N14 - N23)
Globorotalia continuosa (N6 - N14)
Globorotalia fohsi lobata (N11 - N12)
Globorotalia merotumida (N17 - N19)
Globorotalia multicamerata (N18 - N20)
Globorotalia peripheroacuta (N9 - N10)
Globorotalia peripheroronda (N6 - N10)
Globorotalia plesiotumida (N17 - N19)
Globorotalia tosaensis (N21 - N22).
Globorotalia truncatulionides (N22 - N23)
Globorotalia tumida (N18 - N23)
Globorotalia venezuelana (P18 - N19)
Orbilina universa (N9 - N23),
Orbulina suturalis (N8 - N23)
Pulleniatina obliquiloculata (N21 - N23)
Sphaeroidinellopsis subdehiscens subdehiscens

The samples in the interval from 1,040' to 1,320' contain five planktonic foraminifera taxa: *Orbilina universa* (N9 - N23), *Globigerinoides triloba* (N4B - N23), *Globigerinoides immaturus* (N5 - N23), *Globorotalia tumida* (N18 - N23) and *Pulleniatina obliquiloculata* (N21 - N23). These taxa have their last occurrence in N23 and indicate, therefore, a Pleistocene age (N22 to N23) for this interval. The transition from the uppermost interval to the interval from 1.320' to 1.820' seems to be characterised by a longer hiatus. The age at 1.320' is assigned to be lower N22, which is based on the occurrence of *Globorotalia truncatulionides* (N22 - N23) and *Globorotalia tosaensis* (N21 - N22). The report of

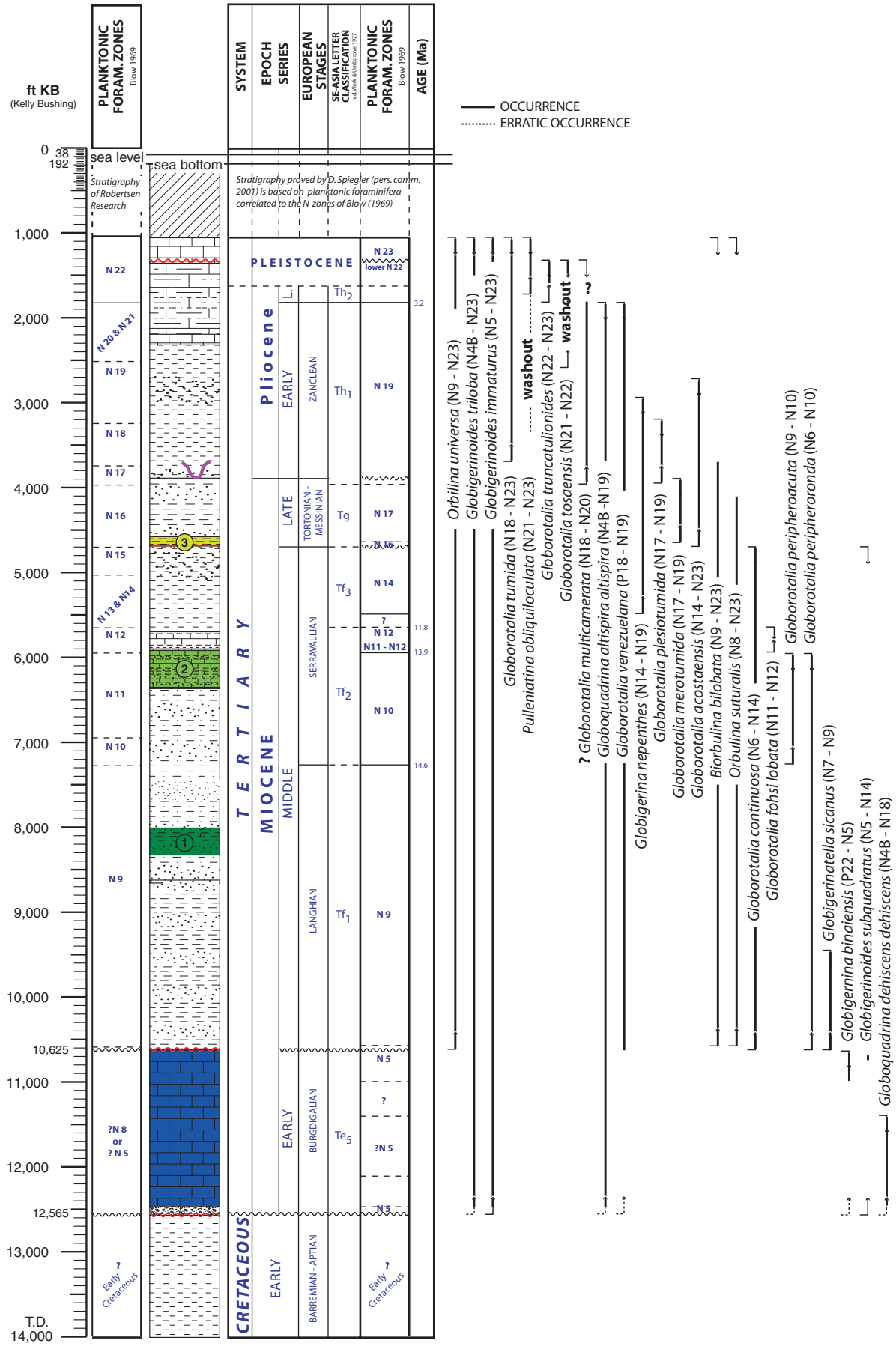

Fig. 67: Biostratigraphy of the well Penascosa-1 based on planktonic foraminifera: left hand side reported biostratigraphy (TIDEY et al., 1975), right hand side new biostratigraphy indicating range of occurrence within the well section.

Globorotalia multicamerata (N18 - N20) might be due to a wrong determination, because their appearance together with *Globorotalia truncatulionides* and *Globorotalia tosaensis* is unusual. Otherwise, it suggests to be reworked material. The last occurrence of *Globoquadrina altispira altispira* (N4B -N19) and *Globorotalia venezuelana* (P18 - N19) yield an age of N19 at the depth of 1.820'. The recovery of *Globigerina nepenthes* (N14 - N19) at a depth of 2.920' and *Globorotalia merotumida* (N17 - N19) at a depth of 3.910' show the extensive thickness of N19 over 2.090'. The first occurrence of *Globorotalia plesiotumida* (N17 - N19) at 3.970' marks the top of N17. The time interval of N18 could not be proved in the well section. The first occurrence of *Globorotalia acostaensis* (N14 - N23) and the last occurrence of *Globorotalia continuosa* (N6 - N14) indicates the contact between N14 and N16 at a depth of 4,700'. Like N18, also the zone N15 is not recorded in the well and N13 can not be separated from N14, because neither *Globigerina druryi* nor *Sphaeroidinellopsis subdehiscens subdehiscens* were identified. The next clear diagnostic age of N12 is provided downhole by the last recovery of *Globorotalia fohsi lobata* (N11 - N12) from a depth of 5,650'. The first occurrence of these species at a depth of 5,950' also confirm the contact to N10, which is additionally proven by the last occurrence of *Globorotalia peripheroacuta* (N9 - N10) and *Globorotalia peripheroronda* (N6 - N10). The uppermost level of N9 bases on the first occurrence of *Globorotalia peripheroacuta* (7,280'). The assemblage of planktonic foraminifera (*Orbulina suturalis* (N8 - N23), *Biorbulina bilobata* (N9 - N23), *Orbulina universa* (N9 - N23), *Globorotalia peripheroronda* (N6 - N10) and *Globigerinatella sicanus* (N7 - N9)) from a sidewall core taken at 10,590' endorses the basis of N9. The lack of zonal markers downhole to the top of the carbonate sequence (10,625') may be due to the presence of a condensed sequence or more probably to an unconformity to the overlying siliciclastics. The interval from 10,625' to 11,000' provides quite limited age diagnostic species, but the occurrence of *Globigerina binaiensis* (P22 - N5) and *Globigerinoides subquadratus* (N5 - N14) points at an age of N5 in a depth of 10,690'. Between 11.000' and 11,400', no fossils are recovered so that the upper part of the carbonates is poorly dated. The identification of *Nummulites* sp. in some thin section from the interval 11,400' to 12,120' would suggest an age not younger than lower Oligocene. However, the specimens are poorly preserved and obscured by recrystallisation, as well as the confusion with taxa belonging to Amphisteginidae easily possible. Hence, most probable the determinations are wrong, which contradicts an age not younger than lower Oligocene. Furthermore, below this interval an assemblage of planktonic foraminifera including *Globigerinoides immaturus* (N5 - N23),

Globigerinoides triloba (N4B - N23), *Globoquadrina altispira altispira* (N4B -N19) and *Globoquadrina dehiscens dehiscens* (N4B - N18) was found at a depth of 12,490' to 12,565', which suggests an age of N5 as most probable. At 12,565' the carbonate sequence of the well Penascosa-1 overlies with an unconformity grey shale of Early Cretaceous age. Palynomorpha and calcareous nannoplankton prove this age.

4.3.2 Biostratigraphy Santiago A-1X

Robertson Research (Singapore) conducted the paleontological study 1981 using 310 ditch cutting samples and 83 sidewall cores of the well Santiago A-1X. It results in the Report No. 944 (TROELSTRA, 1981), which includes a Biostratigraphic Data Summery Log. With D. Spiegler/ Kiel the data were checked and some present updates regarding the occurrence of taxa are included (Fig. 68).

The following 10 age diagnostic planktonic foraminifera taxa and 6 larger foraminifera taxa were reported.

Amphistegina sp.,
Cycloclypeus sp.
Flosculinella bontangensis (N7 - N9)
Globigerina druryi
Globigerinoides extremus (N16 - N21).
Globorotalia margaritae (N19 - N20)
Globorotalia menardii dextral (N18 - N21)
Globorotalia menardii sinistral top of N17
Globorotalia peripheroacuta (N9 - N10)
Globorotalia peripheroronda (N6 - N10)
Globorotalia scitula (N9 - rec.)
Globorotalia tumida (first occurrence N18)
Miliolids
Miogypsina sp.
Operculina sp.,
sinistral *Neogloboquadrina acostaensis* (N16 - rec.)

The uppermost dated well section in a depth of 2,400' - 3,510' (ft below KB) of the well Santiago A-1X has been assigned to the age of Late Pliocene (Neogene Zone N21, BLOW 1969) based on the presence of *Globigerinoides extremus* (N16 - N21). The highest occurrence of *Globorotalia margaritae* (N19 - N20) is used as a marker for the lower boundary of the Late Pliocene (N21), while their reemergence indicates the basis of the Early Pliocene section in a depth of 4,380'. This level of the Miocene/ Pliocene boundary closely coincides with a distinct downhole decrease in abundance of *Globorotalia tumida* (first occurrence N18), a species whose first evolutionary appearance is often used to mark the

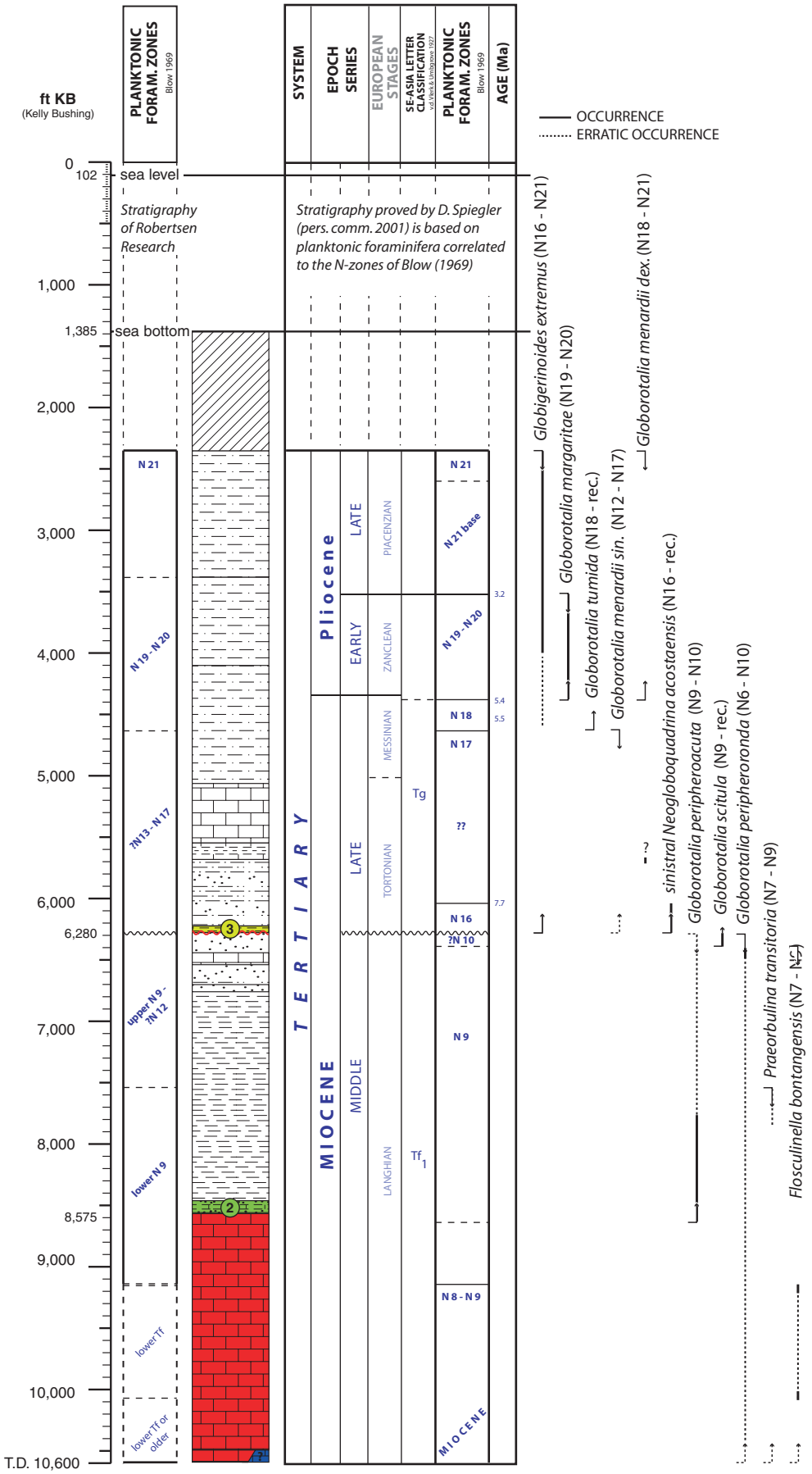

Fig. 68: Biostratigraphy of the well Santiago A-1X based on planktonic foraminifera: left hand side reported biostratigraphy (TROELSTRA, 1981), right hand side new biostratigraphy indicating range of occurrence within the well section.

Miocene/ Pliocene boundary. In a depth of 4,640', the last occurrence of *Globorotalia menardii sinistral* indicates the top of N17. One single taxa of *Globorotalia menardii dextral* (N18 - N21) is recovered from 5,700' and would contradict the expected age of N17 in that depth. The appearance of the consistent *sinistral Neogloboquadrina acostaensis* (N16 - rec.) confirms an age of N16 between 6,040' to 6,280'. The basis of N16 (6,280') is characterised by an unconformity, because this level contains sporadic species referable to *Globorotalia peripheroacuta* (N9 - N10) as well as *Globorotalia scitula* (N9 - rec.). Closely downhole it is followed by rare specimens of *Globorotalia peripheroronda* (N6 - N10) at 6,490' and *Globigerina druryi* (6,520'). Although these forms, together with other species with an extinction level in the Middle Miocene, only occur consistently below 7,600', their presence at 6,280' indicates that at least a Middle Miocene age (N10 top) has been penetrated at this depth. At the top of the carbonate sequence, starting at 8,572' in depth and continuing further downhole, the occurrence of benthic foraminifera decreases rapidly. Nevertheless, the first specimens of *Globorotalia peripheroacuta* were recovered from a depth of 8,640' and provide a biostratigraphic link for middle N9. In the limestone sequence of the well (8,572' - 10,600') a very few specimens of larger foraminifera determinate as *Operculina* sp., *Amphistegina* sp., *Cycloclypeus* sp. and miliolids represent the poor foraminiferal presents. *Flosculinella bontangensis* (N7 - N9) are found in two thin sections (9,140' & 10,080') of the sequence and suggest Middle to Early Miocene age. Even if no age-indicative species were found for this interval, Early to Middle Miocene seems to be most probable. The carbonate sequence below 10,080' contains the same biota as found in the directly overlying limestone sequence. However, the biogenic assemblage is relatively poor and no age-diagnostic species were recovered, except for questionable specimens of *Miogypsina* sp. (10,260') and *Globigerinoides* sp. (10,510'). This would suggest that the age of the lowermost 520 ft of the Santiago A-1X well sequence are not older than Miocene.

In addition, the two offshore samples S3 and S5 were taken from the core of the well Santiago A-1X in a depth of 8.670,0' and 8.676,0' (ft below KB) to identify age diagnostic planktonic foraminifera. The assemblage of the taxa *Praeorbulina*, *Globoquadrina* ex gr. *dehiscens* (N5 – N18) and *Globigerinoides* suggests an age of Middle Miocene for the sample S5. The sample S3 seems to be slightly younger, which is based on the identification of the taxa *Orbulina*, *Globoquadrina*, *Globigerina* and *Globigerinoides*. Nevertheless, a Middle Miocene age is clearly indicated.

This result confirms the age given by the biostratigraphic report of Robertson Research No. 944 (TROELSTRA, 1981).

4.3.3 Biostratigraphy Anepahan A-1X

The biostratigraphy of the well Anepahan A-1X made by Robertson Research (Singapore) grounds on the analysis of 206 ditch cuttings, 58 sidewall core samples and 4 thin sections. The ditch cuttings were collected at intervals of 30 ft over the entire well section from 3,650' to 8,250' T.D. (ft below KB) and the side-track section 7,335' to 9,000' T.D.. The sidewall core samples are covering the interval from 3,650' - 7,320' and 7,400' - 9,000'. The results are summarised in the Report No. 1106 (HUGHES & VAROL, 1982), which includes a micropaleontological analysis chart and a biostratigraphic data summary log. In order to update some of the data of the planktonic foraminifera these documents were also checked by D. Spiegler/ Kiel. This check shows co-occurrence of several planktonic foraminifera taxa, which obviously could not exist together due to their range of appearance (Spiegler pers. comm.). This discrepancies results in the assumption of wrong determinations or the dating of material, which have been broken down during the drilling operation; intensive caving was emphasised in the report. Nevertheless, the last occurrences of some planktonic foraminifera taxa were used to provide some biostratigraphic indications (Fig. 69). The given time lines indicate always the youngest possible age of the level.

The following 10 age diagnostic planktonic foraminifera taxa were reported.

Globigerina nepenthes (N14 - N19)
Globigerinoides altiaperturus (N5 - N13)
Globigerinoides obliquus obliquus (N8 - N19)
Globigerinoides triloba (N4B - N23)
Globoquadrina altispira altispira (N4B -N19)
Globoquadrina altispira globosa (N5 -N16)
Globorotalia obesa (N5 - N15)
Globorotalia peripheroronda (N6 - N10).
Globorotalia siakensis (= *G. mayeri*) N3 - N14
Praeorbulina glomerosa circularis (N8 - N9)

The interval between 3,650' and 3,970' is dated as N19 based on the last occurrence of *Globigerinoides obliquus obliquus* (N8 - N19), *Globigerina nepenthes* (N14 - N19) and *Globoquadrina altispira altispira* (N4B -N19). The last occurrence of *Globoquadrina altispira globosa* (N5 -N16) at a depth of 4,120' indicates an age of N16, while 10' below *Globorotalia obesa* (N5 - N15) displays the age of N15. Although, this dating is questionable,

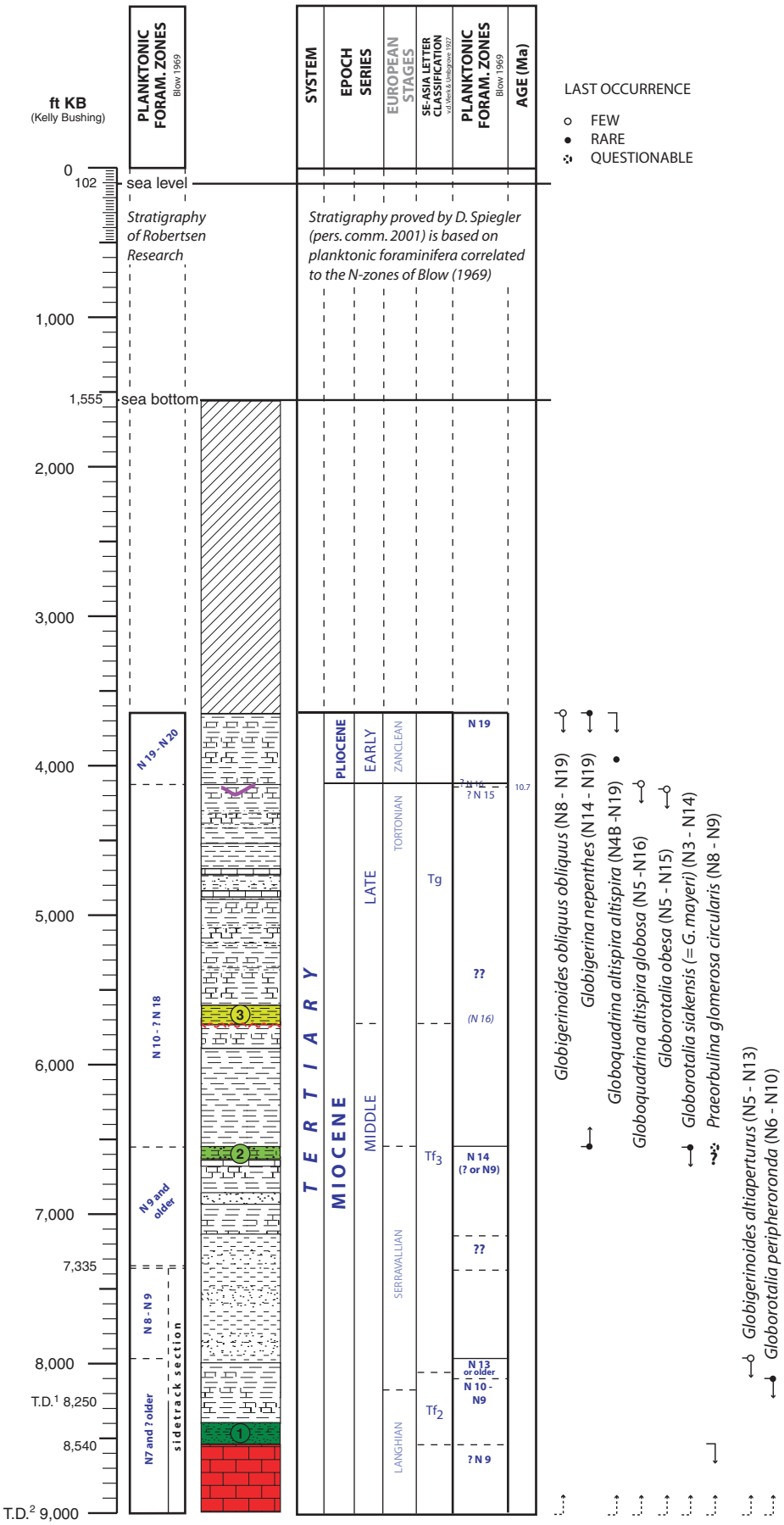

Fig. 69: Biostratigraphy of the well Anepahan A-1X based on planktonic foraminifera: left hand side reported biostratigraphy (HUGHES & VAROL, 1982), right hand side new biostratigraphy indicating range of occurrence within the well section with limited value due to questionalbe determinations.

because at the depth of 4,125' the base of a large channel have been localised so that these few examples of *Globoquadrina altispira globosa* and *Globorotalia obesa* refers most probable to reworked material. Down to the depth of 6,540', the assemblage of planktonic foraminifera did not provide any age. Nevertheless, based on seismic correlation to the well Penascosa-1 the sediments above 5,750' are possibly of an age of N16. The next age diagnostic taxa were recovered from a depth of 6,540'. *Globorotalia siakensis* (= *G. mayeri*) appears from N3 - N14 and suggests an age of N14. The first occurrence of *Globigerina nepenthes* (N14 - N19) at the same depth supports this dating. Rare individuals of *Praeorbulina glomerosa circularis* (N8 - N9) seem to contradict this interpretation and an unquestionable dating seems to be not reasonable. In the interval from 7,140' and 7,400', no planktonic foraminifera are found except *Globigerinoides triloba* (N4B - N23), which is useless for the dating in that case. The sample from a depth of 7,984' contains as uppermost sample in the well section a few species of *Globigerinoides altiaperturus* (N5 - N13) and indicates therefore that this level is not older than N13. Below that (8.100') an age of N10 is marked by rare numbers of *Globorotalia peripheroronda* (N6 - N10).

The samples of the side-track section from 7,335' to 9,000' T.D. did not provide any additional evidence for a well-defined dating. The carbonate sequence starting at a depth of 8,540' down to the total depth of 9,000' contains a very poor fauna and the evaluated date of Early Miocene (HUGHES & VAROL, 1982) at the T.D. could not be proved. Finally, the sequence below 6.540' seems to be not younger than N14, whereas an age of N9 could be also possible. In general, Middle Miocene, maybe the uppermost Early Miocene was penetrated by the well Anepahan A-1X.

4.4 Depositional History Offshore SW Palawan

Marine platform carbonates overly shale/ sandstone intercalations of Cretaceous age. The fairly uniform lithology of the platform carbonates is prevailed by limestones, whereas some dolomite intercalations are restricted to the basal part of the section. The clay content is quite low. Variations are modest a few cycles with a ´fining-upward´ sequence under- and overlain by shale-rich carbonates were deposited at the Penascosa-1 location. Due to the seismic survey, the platform carbonates are present over most of the studied offshore area. Deposition of these carbonates ceased at the end of nannoplankton zone N5 according to biostratigraphic analyses of samples of the Pensacosa-1 well. The contact between the carbonates and the

overlying clastics is sharp in this well. Above a transition zone of some 15-m with increasing fine-siliciclastic content, grey silty shales with rich assemblages of planktonic foraminifera (N9, Middle Miocene) were deposited.

The carbonate deposition continued in selected parts of the offshore area. Isolated pinnacle-type reef bodies developed like the Anepahan structure, an approximately 2.5 by 4.2 km pinnacle with a best estimated height of about 900 m as well as the Great Atoll Reef, a 17.5 by 25 km reef complex, which might reach an estimated height of minimum 2,400 m. These build-ups overly directly the Miocene platform carbonates. Whereas most of the pinnacles are buried in the Middle Miocene from siliciclastics, some pinnacles (like on the Great Atoll Reef) grown up to the Pliocene time. Contrary to the uniform platform carbonates, the lithology and consequently the growth history of the pinnacle reefs are rather complex as derived from electrical logs of the Santiago A-1X well. In particular, the shale content of the carbonates varies significantly from generally high proportions in the lower third of the reef complex and a decrease in its middle and upper parts. Some of the shale-rich layers indicate cyclic sedimentation with an abrupt influx of clay and a steady upward decrease. The presence of some back reef facies and slumps related the Great Atoll Reef could be inferred from seismic data. These deposits occur in depressions between the various pinnacle-type culminations of the reef complex or respectively along their flanks.

The overburden clastics prograding basinwards so that various drowning sequences can be identified. The clastic cover, upwards successively younger up to a Pliocene age, has been dated not older than N9 (Middle Miocene) so that a time gap of three N-zones exists at the site of Penascosa-1 and probably no or only a little gap between the reef complexes and the overlying clastics. The clastic cover, which encases the pinnacle-type reefs, is dominantly composed of deep water shales with intercalations of both, carbonates and sandstones and even conglomerates. Mainly above a significant Late Miocene - Pliocene discontinuity numerous erosional channels occur. These channels show often a stable position until recent time so that they are still active on the present-day seafloor.

5. The Development of Miocene Carbonates on- and offshore SW Palawan

The evaluation of the carbonates in both study areas, on- and offshore SW Palawan, have to be done with respect to their different dimensions. Whereas the onshore area between Devel Peak and Malanut Range cover an area, which is 16 km long and up to about 5 km wide, the offshore area covers a region of about 40 by 80 km. Furthermore, the altitude of the build-ups Albion Head and Devel Peak reaches 203 and 168 m above mean sea surface, whereas the Anepahan pinnacle structure offshore is approximately 900 m high and covers an area on the underlying platform of 2 by 5 km. Even bigger is the huge reef complex of the Great Atoll Reef offshore with a base of 17.5 by 25 km and an estimated maximal thickness of probably more than 2,400 m.

Consequently, the onshore study area do not provide an example, which is big enough to use the concepts of a carbonate platform or carbonate ramp with dimensions of several 10s or 100s km^2 in terms of READ (1985). Nevertheless, the different facies zones documented in the carbonate succession agree with the patterns known from carbonate platform and carbonate ramp models. Hence, the different settings are here described as "platform-like" and "ramp-like" settings.

5.1 Onshore SW Palawan

Miocene carbonates were studied in the area of Quezon (onshore SW Palawan). With the exception of Albion Head and Devel Peak, which were mentioned by PARK & PETERSON (1979), this synthesis bases on the study of new discovered outcrops. Due to little or no vertical or horizontal tectonic displacements and no folding in the study area, the different sections offer the opportunity to study the development of the carbonates in time and space. The general carbonate succession documents the evolution from the carbonate accumulation with a strong terrestrial influence to full marine conditions on an outer carbonate slope followed by the later growth of some build-ups. Biostratigraphic data of larger foraminifera and planktonic foraminifera as well as nannoplankton were used to determine the Miocene age and to confirm the lithostratigraphy of the general succession.

5.1.1 Distribution in Time and Space

The Miocene carbonate along the coast around Quezon occur in the geological setting of S-Palawan, which is dominated by strongly deformed ophiolites, amphibolites and greenschist rocks. Sandstones, shales and limestones are mixed into this setting of a melange zone related to an accreted terrane formed by an assumed fossil subduction zone off SW Palawan (PORTH, 1984; HOLLOWAY, 1982; HASHIMOTO, 1981; HAMILTON, 1979). In contrast, HINZ & SCHLÜTER (1985) conclude that the area of central and S-Palawan is a part of the Dangerous Grounds/ Reed Bank - North Palawan - Calamian microcontinent and the ophiolite-bearing wedge was overthrusted onto the southern margin due to the relative north-eastward movement of the Cagayan Ridge in the Sulu Sea. However, the observed structural elements within the Quezon carbonate area do not reflect any strong deformation: Regional tectonic displacements, horizontal or vertical as well as folds are not observed at any place within the carbonate area. Only some local displacements of not more than a few 100-m have been identified. Three transversal faults between the Salty Creek Section - Maasin Profile in the E and the Tumarabong River Section/ Slope Profile in the W explain the well-proved correlation between Salty Creek Section and the Tumarabong River Section/ Slope Profile. All other tectonic movements (vertical or horizontal) within the carbonate area have no relevance for the carbonate successions in the study area. The fracturing of the Devel Peak and Albion Head build-ups might trigger the development of the present-day tower karst morphology with the vertical cliff, but do not indicate any significant displacements within the carbonate successions. The widely consistent orientations of the sedimentary strata document a NNE-SSW stretching and shallow synclinal structure. The depositional successions of the Taglupa Profile up to Theo's Place as well as of Devel Peak are related to the slightly (12 - 22°) NW dipping SE-flank of the synclinal structure, whereas the strata of Quezon Section and Albion Head on the NW-flank dip eastwards (09-25°).

The carbonate area around Quezon, with low tectonic stress, is limited to the SW with a prominent SSE-NNW running cliff of the Malanut Range. The sharp contact and a vertical offset of some 100-m suggest that a large scaled, maybe regional thrust fault had to be accountable for it. An equivalent contact W of Devel Peak might occur, but younger volcano-clastics cover this area. This observation might allow the assumption that the carbonate area around Quezon represents an overthrusted Miocene carbonate nappe. Although, whether the genesis is a product of the fossil subduction zone (HAMILTON, 1979 and others) or of the

north-eastward movement of the Cagayan Ridge (HINZ & SCHLÜTER, 1985) last subject of speculations.

With respect to the tectonic analysis and the biostratigraphy, it turns out that the lithostratigraphic observations made in the field has been confirmed and provide a useful frame for the study. The biostratigraphic dating of the carbonates discovered at the Taglupa Profile, the Salty Creek Section - Maasin Profile, the Tumarabong River Section and at Theo's Place - Quezon Section results in a late Early Miocene to Middle Miocene age (N7 - N9) (Fig. 70). The joint occurrence of *Miogypsinoides* (N7 and older) and *Flosculinella bontangensis* (N7 and younger) since the lower part of the Taglupa Profile indicate a late Early Miocene age, which is the oldest age given to the carbonates in Quezon area. The relative short time, which probably exist between the deposition of the sediments at the Taglupa Profile and the lowermost deposits of Salty Creek Section could not be defined by biostratigraphy, due to their limited resolution. The gap in the section does not refer coercively to a significant hiatus in the depositional succession, rather than the outcrop situation in the jungle. The planktonic foraminiferal assemblage (*Praeorbulina*, *Orbulina*, *Globigerina*, *Globorotalia peripheroacuta*) as well as some nannoplankton (*Reticulofenestra pseudoumbilica*, *Sphenolithus abies*, *Helicosphaera carteri*) identified throughout the Salty Creek Section, Maasin Profile and the Iwahig River Profile, indicate an age of Middle Miocene (N8 - N9). The larger foraminiferal assemblage (*Cycloclypeus (Radiocycloclypeus)*, *Nephrolepidina*, *Alveolinella praequoyi*) of these sections as well as from the Tumarabong River Section are assigned to be also Middle Miocene in age. However, the data of larger foraminifera indicate often a slightly younger age (Tf_2 = N9 - N10) than the planktonic foraminifera and nannoplankton. But nevertheless, an age of N9 is most probable for both sections, which confirms the lithostratigraphic correlation between the Tumarabong River

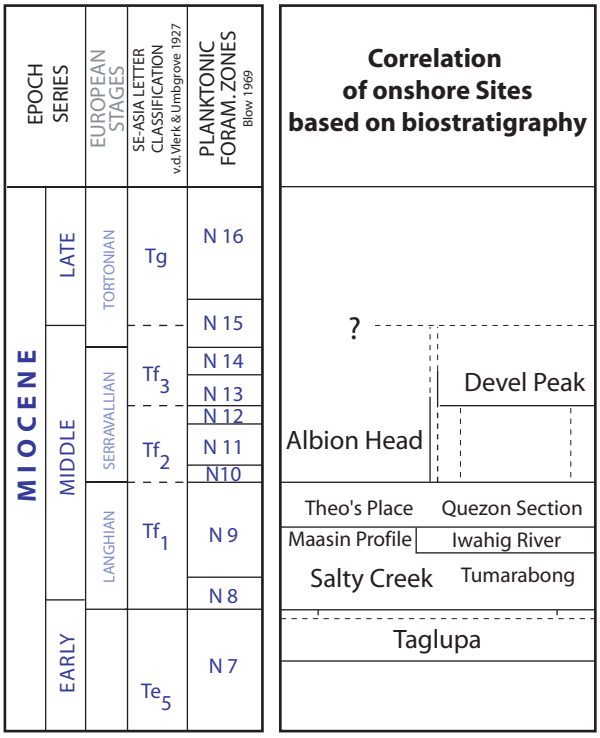

Fig. 70: Biostratigraphic correlation of the onshore sites.

Section and the Salty Creek Section (cf. chapter 3.1.3). The mudstones discovered at Theo's Place and the Quezon Section provide a poor assemblage of skeletal grains. Anyhow, *Orbulina*, *Praeorbulina*, *Globigerina* and *Globigerinopsis* were found in the Quezon Section, which refers to Middle Miocene age (N9). The poor nannoplankton assemblage of Theo's Place is dominated by *Sphenolithus abies* and indicates in general an age of Middle Miocene. The continuous lithostratigraphic succession, confirmed by several spot samples in between the Maasin Profile and Theo's Place, leads to the conclusion that the sequences of the Quezon Section and Theo's Place were deposited together during the upper Middle Miocene (upper N9), i.e. later than the section found at the Maasin Profile.

The stratigraphic position of the two carbonate build-ups Albion Head and Devel Peak in the carbonate succession is slightly different. The build-up of Albion Head is separated in the field by mangroves from the lateral extended carbonates discovered S and E of Quezon. Anyhow, the location of Albion Head further to the NW than all previous carbonates (Taglupa Profile to Quezon Section/ Theo's Place) suggests a lithostratigraphic position above these lateral extended carbonates. A larger foraminiferal assemblage (*Katacycloclypeus annulatus*, *Palaeonummulites* sp., *Cycloclypeus* cf. *indopacificus*, *Heterostegina* (*Vlerkina*) sp.) was recovered from samples collected in the lower part of the Tarung Profile in the S of Albion Head. It indicates an age of Middle Miocene (Tf_2). This confirms the lithostratigraphic interpretation that the development of reefal carbonates took place after the sedimentation of the strata at Quezon Section and Theo's Place. No gap exists between the uppermost fine carbonates (N9) and the build-up of Albion Head (Tf_2 = N10-N12). Following the observation made in the carbonates discovered between Taglupa Profile and Quezon Section/ Theo's Place, the biostratigraphic data of the larger foraminifera comes up with a slightly younger age than indicated by the planktonic foraminifera and nannoplankton. Hence, the age of the deposits of Albion Head might be pushed further down in age and therefore, come closer to the underlying lateral extended carbonates. Moreover, the samples were collected close to the base of Albion Head so that they are consequently related to some early carbonate deposits. But even the foraminiferal packstones represent some fore- or back-reef deposits, which suggest that some slightly older carbonates might exist. All this arguments confirm the carbonate deposits of Albion Head document most probably a local, but continuously carbonate deposition in the area, without a gap in the carbonate succession.

The biostratigraphic data of the Devel Peak build-up are based on a larger foraminiferal assemblage (*Nephrolepidina*, *Cycloclypeus* (*Radiocycloclypeus*), *Operculina complanata*,

Amphisorus sp., *Amphistegina*, *Alveolinella quoyi*), which provides an Middle Miocene age, close to the Tf_2/ Tf_3 boundary, for the whole sequence. Three samples of two oysters and a pectinidae were dated using $^{87}Sr/^{86}Sr$ ratios, which results in Late Miocene age (N16/ N17). However, with respect to the probable contamination of the sample with some terrestrial material of the matrix, an age corrected to late Middle Miocene seems to be more reasonable, in agreement with the biostratigraphic data. In contrast to Albion Head, a time gap of 1 or 2 planktonic foraminiferal zones has to be assumed between the lateral extended carbonates and Devel Peak. An additional argument for the existence of this gap provides the observed siliciclastic deposits below the carbonates of Devel Peak, which are related to quiet and probably deeper water conditions.

As a conclusion, based on lithostratigraphy and biostratigraphy, clearly one carbonate episode results in the establishment of the lateral extended carbonates during the late Early Miocene and their evolution throughout the Middle Miocene (N9) as well as the development of the Albion Head build-up. The development of the Devel Peak build-up shows a close relationship to Albion Head, even if siliciclastics underlie the build-up and the biostratigraphy provide a slightly younger age than indicated for the base of Albion Head. Nevertheless, due to the same lithostratigraphic position and setting in the field around Quezon, Devel Peak seems to be part of the carbonate episode during the Middle Miocene. Consequently, the carbonates around Quezon represent one single period of carbonate deposition.

5.1.2 Evolution of Carbonate System during the Miocene

Most of the Miocene carbonates around Quezon are related to the successive development of a platform-like followed by a ramp-like setting (Taglupa Profile, Salty Creek Section - Maasin Profile/ Iwahig River Profile, Tumarabong River Section, Theo's Place, Quezon Section). In contrast, Albion Head and Devel Peak outcrops correspond to two carbonate build-ups. The demonstration of the evolution of the depositional environment of the lateral extended carbonates is here based on the Taglupa Profile and the Salty Creek Section - Maasin Profile. The study of the build-ups is mainly based on the continuous profile from Devel Peak, but data from Albion Head supplement the evaluation of the build-ups.

5.1.2.1 Carbonates in Platform-like/ Ramp-like Setting

The lowermost carbonate deposits at the Taglupa Profile overly with a low angle the undated shales, cropping out in the Foundation Area. Therefore, the carbonates represent the initial development stage of the Miocene carbonates found onshore. Bivalves, bryozoans, red algae and Nummulitidae are forming the pioneer community of the biota (Fig. 71.1-2). A significant high content (up to 40%) of rounded gravels of igneous rock, sandstones and carbonates in the rudstones at the base of the section suggests the existence of a shoreline with relatively high water energy conditions in the vicinity. The decrease of the gravel content upwards reflects the retreat of the shoreline related to a transgressive event. The coeval increase in the carbonate content is especially recorded by the great development of the larger foraminiferal assemblages. The dominance of the larger foraminifera (Nummulitidae, Amphisteginidae, Alveolinidae and some Soritidae) and the sedimentological criteria (e.g. grain size mainly of the sand fraction) suggest a deposition in a shallow water environment characterised by moderately high water energy.

The upper samples from the Taglupa Profile already links to quiet depositional conditions due to an increase of the carbonate mud content and peloids. Moreover, some phosphatized grains refer to poorly ventilated parts in the paleoenvironment. Upwards (Salty Creek 1 profile) the deposition of fine sediments (marine shales alternate with float- to wackestones) and the occurrence of small fragile molluscs and branching corals confirm the existence of general low water energy conditions. The local poor sorting of the deposits and high content of the gravel-sized skeletal fragments in the carbonate mud (floatstones) demonstrate that no major currents and therefore transportation exist and thus support this interpretation. However, the great variability in composition, the occurrence of branching corals beside head corals, Soritidae (*Amphisorus*), Alveolinidae (*Alveolinella*), some rare fragments of dasyclads and red algae (*Sporolithon*, *Hydrolithon*, *Mesophyllum*) lead to a heterogeneous paleoenvironment with both shallow (near the wave base) and deeper (up to 35 m) water areas corresponding to the subtidal of an inner shelf (RENEMA & TROELSTRA, 2001; GEEL, 2000; RASSER & PILLER, 1997; BOSENCE, 1991). Furthermore, the depositional record suggests a small-scaled relief in the depositional area with lateral changes in thickness of some carbonate layers, whereas carbonates and shale deposits co-exist. The shallow water areas probably occur as patches, characterised by corals or by sandy bottom with seaweeds and higher water energy, which seem to be the preferable environment for Soritidae and Alveolinidae (CHAPRONIERE, 1975; WIEDICKE, 1987; RENEMA & TROELSTRA, 2001). This setting recorded in the depositional

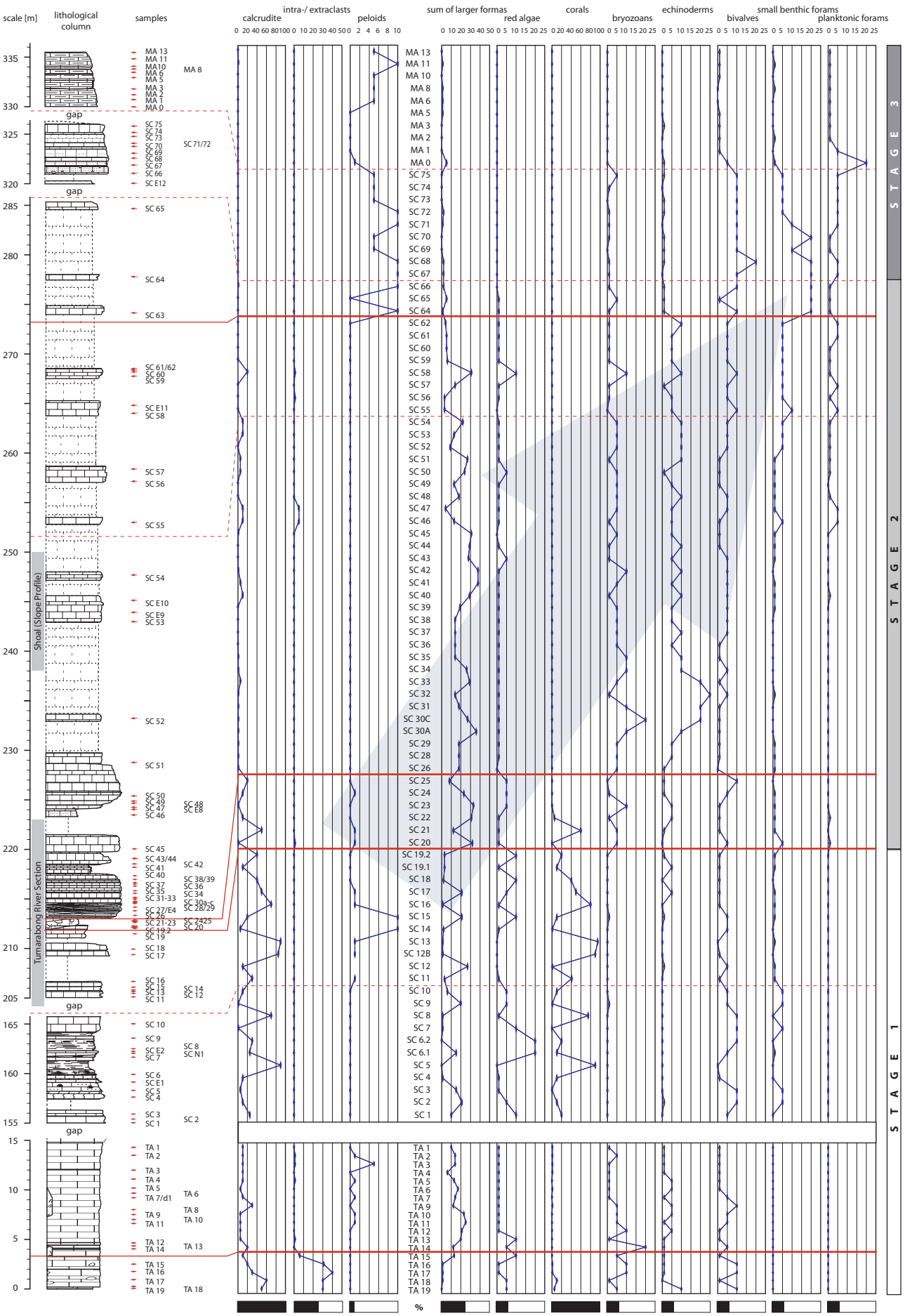

Fig. 71.1: Semi-quantitative frequency estimation of grain size, abiotic components and selected skeletal grains throughout the lateral extended carbonates onshore using the Salty Creek Section - Maasin Profile and the succession of Theo's Place.

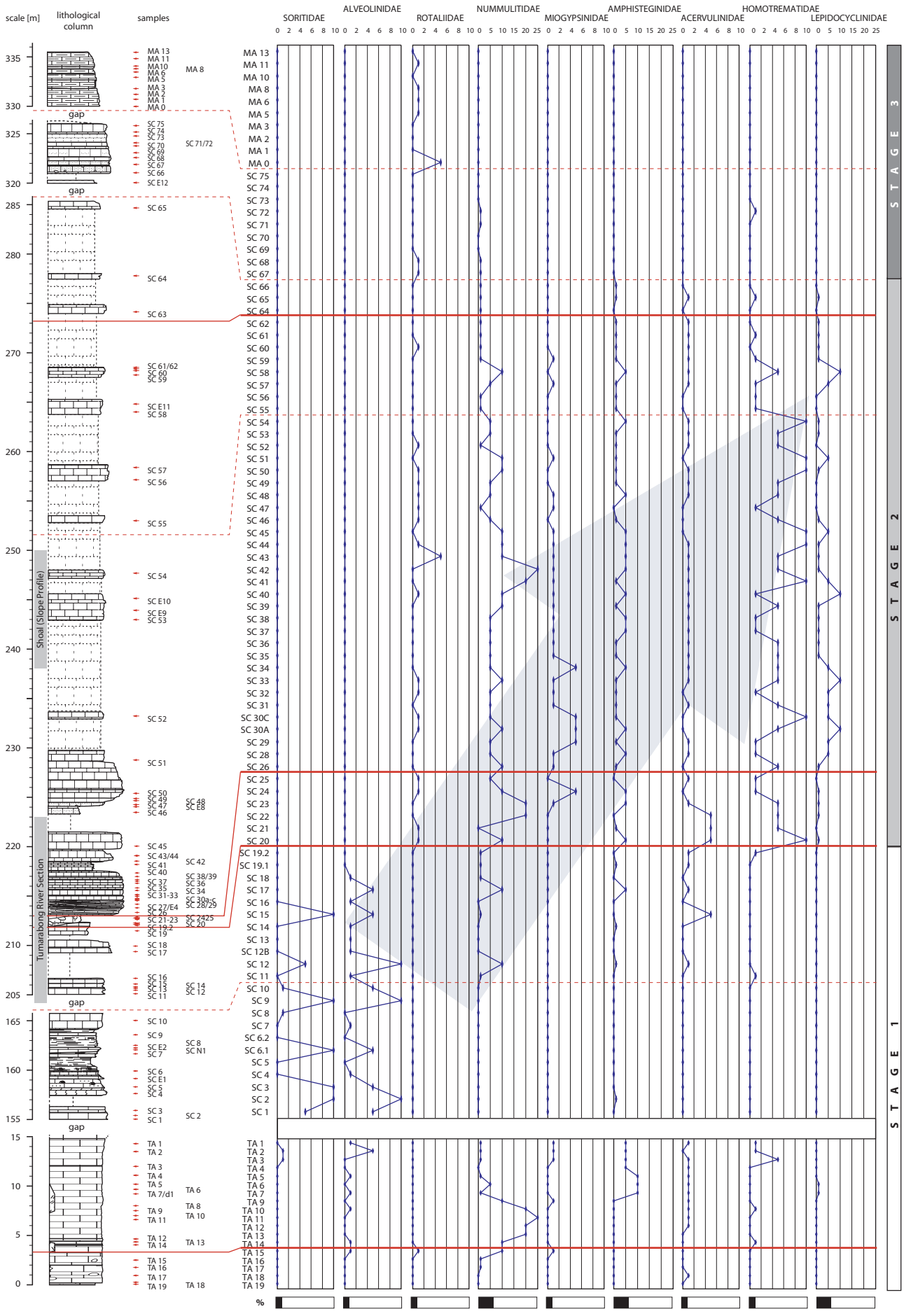

Fig. 71.2: Semi-quantitative frequency estimation of larger foraminiferal assemblage throughout the lateral extended carbonates onshore beside the Salty Creek Section - Maasin Profile and the succession of Theo's Place

succession from the upper part of the Taglupa Profile and the Salty Creek 1 profile indicates to a protected paleoenvironment such as in a lagoon (HALLOCK & GLENN, 1986). Obviously, the area of general calm environmental conditions with some poorly ventilated parts needed a barrier against higher water energy coming from the open ocean. But, based on the field observations, the type of barrier could not be defined; however, shoals seem to be more probable than large reef barriers, because reefs should be preserved somewhere.

With an up to 3.0-m thick accumulation of branching corals, the sedimentary record of the lower part of the Tumarabong River Section provides an example of a coral patch in the lagoonal setting (directly below Salty Creek 2 profile). The fining-upward trend together with a decrease of the amount of the southward orientated coral branches leads to the first documented event of temporary higher water energy conditions (e.g. storm) entering the protected environment from the open ocean in the north. However, the lack of a significant erosive base and the less diverse biota results in the assumption that the waves were strong enough to destroy the fragile corals but to weak to accumulate material throughout the whole area.

The establishment of marine conditions with an increasing portion of carbonate deposits continues upwards, reflected by pure carbonates (averages >97%) with large massive Porites (lower part of the Salty Creek 2 profile). The strong influence of a landmass changed through time to a full marine and carbonate dominated paleoenvironment. Whereas the decreasing number of Soritidae and Alveolinidae and some peloids still link to shallow water/ moderate water energy conditions like on an inner shelf, the increasing content of Nummulitidae and Amphisteginidae associated with the slightly increase of echinoderms suggests foraminiferal shoals or reefal area with higher water energy conditions nearby (CARROZI et al., 1976). The massive coral heads and reduced number of branching forms as well as fewer molluscs and small benthic foraminifera refer also to higher water energy conditions, probably related to a more open marine environment. Even if the different quality of sorting of the carbonates documents variations in the water energy regimes, the mostly high content of carbonate mud and the occurrence of some fragments of the fragile red algae (*Neogoniolithon, Lithoporella*), suggest still low water energy conditions in a water depth of about 20 to 35-m (RASSER & PILLER, 1997).

Upwards, another depositional setting than a lagoonal are necessary to explain the genesis of a widespread significant horizon (Salty Creek 2, 3 and slightly modified at the Tumarabong River Section). This horizon marks the base of the well-sorted packstone sequence above.

Even if the base contact of the horizon is erosive, the depositional change is not abrupt. This observation and the co-existence of well-rounded gravel (1 - 8 cm) and quartz grains beside large pristine marine skeletal component and planktonic foraminifera scattered in the "matrix" of well-bedded packstones contradict the possibility that this horizon is made up of river-transported material, beach-, storm- or tsunami deposits as well as deposits generated by seismic activity (seismite). The larger foraminiferal assemblage (Nummulitidae, Amphisteginidae, Miogypsinidae, Homotrematidae, Lepidocyclinidae) and the composition of the skeletal grains with echinoderms, molluscs, some planktonic foraminifera and again bryozoans together with the disappearance of corals throughout this horizon represent carbonate sand deposits from the upper part of a open-marine slope with moderate to higher water energy conditions (GEEL, 2000; KIDWELL & HOLLAND, 1991; HALLOCK & GLENN, 1986; CARROZI et al., 1976; CHAPRONIERE, 1975). However, the high number of single gravels without any orientation and different sizes in these packstones yields the important link for the interpretation, that this horizon represents the shift from a platform-like to a ramp-like setting. Because, the transport of gravels across a deeper lagoonal environment to an outer slope would be impossible, whereas the gravitate movement of single well-rounded gravels from a shoreline in the vicinity down a low-angle slope seems to be the only plausible mechanism, which would create well-bedded packstones with scattered gravels up to 8 cm in a tropic area. The shift in the setting might be most probable the result of the filling of the lagoonal area. The channels, which cut into this significant horizon, as well as internal sediment structures (internal erosive surfaces, truncations, onlaps, fore-sets) in the direct overlying layers, suggest a tidal influence in the shallow water environment (a few meters/ deeper tidal) and demonstrates furthermore a low stand of the relative sea level. The terrestrial content (quartz grains and rare small gravels) in the lower part of the consistent deposition of internal bedded packstones decreases upsection, which indicates that after the temporary regressive event the general transgressive trend continuos with the aggradation of packstones on the open slope.

Upwards (Salty Creek 3 profile), again a short sea level drop and therefore a regressive cycle pushes the shoreline closer to the depositional environment (high content of quartz, small gravel, plant debris). However, above the intercalation of the quartz-rich layer, the well-bedded foraminiferal packstones (*Cycloclypeus*, *Amphistegina*, *Heterostegina*, *Operculina*, *Nephrolepidina*) with bryozoans, echinoderms and the lack of corals refer again clearly to the deposits of an outer slope (HALLOCK & GLENN, 1986; CHAPRONIERE, 1975). The orientation

of the larger foraminifera as well as the occurrence of *Orbulina* in the lower part of the packstone sequence suggest a position still in the upper part of the slope with moderate water energy conditions (HALLOCK & GLENN, 1986; MÜLLER et al., 1989a). Furthermore, the discovery of a pack- to grainstone shoal body, above the Tumarabong River Section and in the stratigraphic level of the lower packstone sequence in the Salty Creek Section, yields additional evidence for the shallower water area of a the upper slope. The different sets of the shoal are separated by erosive surfaces. The internal beds showing predominantly onlaps to southern directions and thus support the transgressive trend southwards. Only two sets of beds prograde northwards and contain larger components. Beside their indication of a temporary stop of the transgressive trend or a slight regression, they provide the indication that the shallow water environment has to be expected somewhere in the S and consequently the basin in the N.

The packstones further upsection reflect (based on the limit outcrops) the gradual deepening of the depositional environment in time with the decrease of larger foraminifera, a finer grain sizes as well as some planktonic foraminifera and the increasing micrite content. Hence, the deeper position on the slope is a result of a relative sea level rise on a transgressive system track. An assemblage of red algae (*Mesophyllum* sp., *Jania, Corallina*) was discovered in the upper part of the packstone sequence, which is typical for a water depth between 20 to 100 m (BOSENCE, 1991) or around 40 m (GHOSH, 2002). However, the red algae are not insitu and occur as fragments so that their transportation has to be expected. Nevertheless, with respect to the composition of the carbonates and the occurrence of very rare glauconite grains deeper water (eventually between 40 and 100 m or deeper) in an open marine environment with moderate sedimentation rates is assumed.

The gradual deepening seen in the packstones continues upwards and leads to massive mudstones or marls containing only some planktonic and a few small benthic foraminifera, as well as thin shells of bivalves and peloids (Maasin Profile, Theo's Place, Quezon Section). These deposits of the uppermost part of the lateral extended carbonate succession indicate low water energy conditions in a deeper basin. Furthermore, due to the fact that the larger foraminifera house symbiotic algae, light is the most important factor for their occurrence. Therefore, the lack of larger foraminifera in almost all layers of the mudstones indicates both, a deep water environment below the euphotic zone (in general >200 m water depth) and a great distance to shallower water areas.

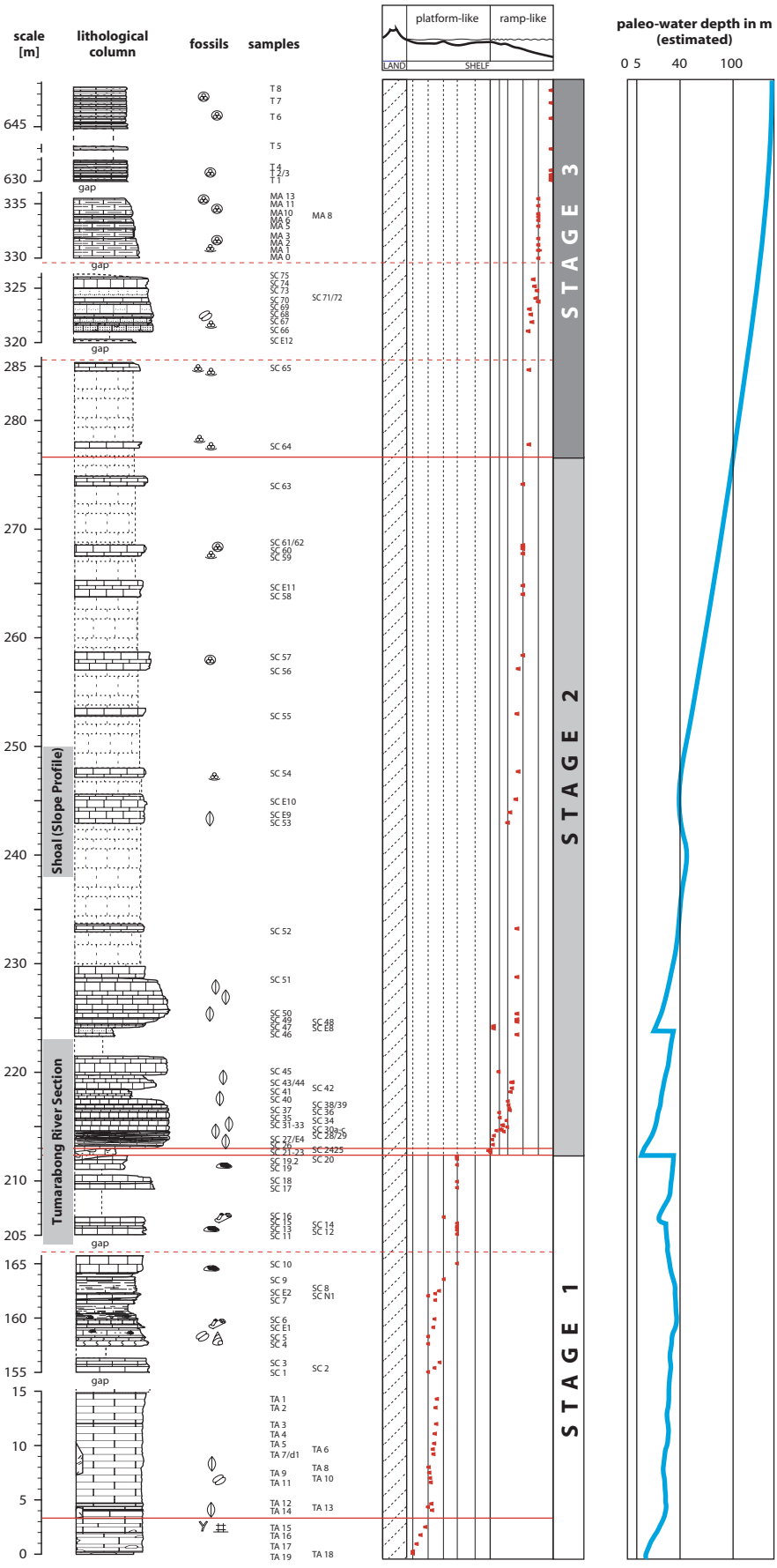

Fig. 72: Synthetic column throughout the lateral extended carbonates onshore using the Salty Creek Section - Maasin Profile and succession of Theo's Place. Indicated are the dominant content of skeletal grains, paleoenvironmental position of each sample and the changes of the relative sea level.

Excerpt: Finally, the transect through the lateral extended carbonates discovered onshore in SW Palawan illustrate 3 stages (1, 2, and 3) of carbonate development in time (Fig. 72). The lowermost Stage 1 found at the Taglupa Profile, the Salty Creek 1 and the lower part of the Salty Creek 2 profile, shows the establishment of carbonate deposits with a shoreline in the vicinity followed by a protected paleoenvironment of a lagoonal setting. This development is generally related to a transgressive system track, whereas a water depth of not more than 40 m is assumed. Above, a relative sea level low stand follows, before the platform-like setting converted to a ramp-like setting (Salty Creek 2 & 3, Tumarabong River Section) so that this succession with a trend of deepening upsection is attributed to Stage 2 of the carbonate development. The shift from a platform- to a ramp-like model as result of the filling of the lagoonal area corresponds to a short regressive cycle and relative sea level low stand, whereas upwards the sea level rises again during the transgressive system track. Due to the composition of the carbonates, a water depth of less than 100 m is suggests for Stage 2. The last stage (Stage 3) includes the carbonate deposits of the deeper slope and a basin with very fine deposits in a deep-water environment. The deposits demonstrate the highest relative sea level in the study area.

In conclusion, the evolution from a platform-like to a ramp-like setting followed by an increasing deepening on the slope occurs between the latest Early Miocene and the middle Miocene in a time range of approximately 2 m.y.. Therefore, the changes of the carbonate facies throughout the area around Quezon represent the development of a carbonate area in time and not one time slice of a paleoenvironment with their different facies zone somewhere within the Middle Miocene.

5.1.2.2 Build-ups

Both build-ups onshore, Devel Peak and Albion Head were formed after the demise of the lateral extended carbonates in the study area. However, even if the contact to the underlying deposits at Albion Head is not accessible in the field, the biostratigraphy indicates that this build-up follows directly the carbonate accumulation on a deeper slope. In contrast, Devel Peak shows a gap of 1 to 2 N-zones (BLOW, 1969) to the underlying deeper water carbonates and intercalated siliciclastic deposits.

Albion Head

Even if the outcrop situation is limited at Albion Head, the study of the geometry of the carbonate complex results in a small atoll-like structure or a part of it (Fig. 73).

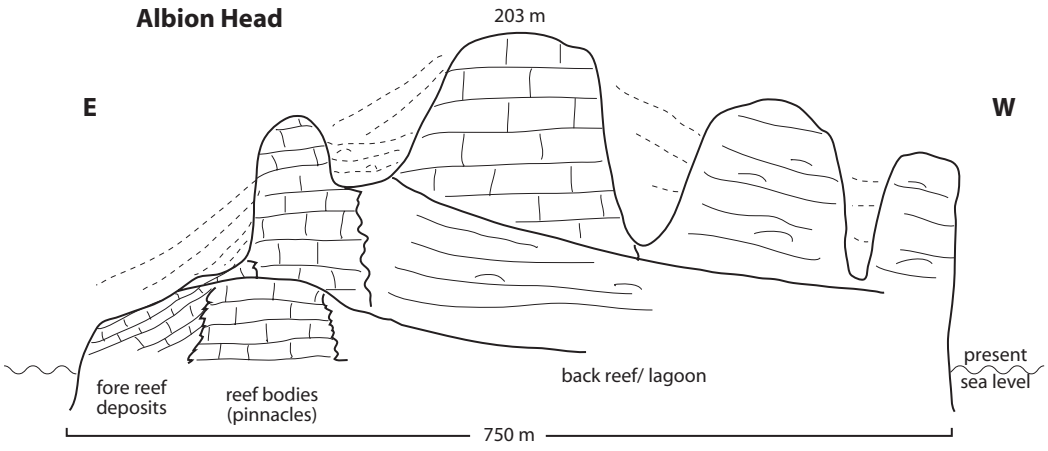

Fig. 73: Idealised cross section through the carbonate complex of Albion Head showing fore reef area in the E, a backstepping rim of reefal structures and back reef/ lagoonal area westwards; incitions of deep valleys related to tower karst.

The outcrops at the base of the build-up present lithologies and sedimentary structures referring to reef-slope deposits. They are made up of bedded packstones with larger foraminifera, red algae, echinoderms, bryozoans and bivalves (base Taglupa Profile in the SW) or grain- to rudstone with cm-sized bivalves, echinoderms and some corals (NE shoreline). These bedded deposits dip always down-slope with measured angle between 23° and 36°.

Further upwards, the present-day morphology suggests a belt of smaller reefal pinnacles. Spot samples and the upper part of the Taglupa Profile show a significant increase of platy, branching and massive corals together with common reef dwellers (e.g. echinoderms, molluscs, red algae, bryozoans) in the floatstones, rudstones or boundstones. These carbonates are interpreted as a reef-front or the associated reef body. Furthermore, a very weakly pronounced cyclicity is observed within the upper part of the Tarung Profile. Four cycles are characterised by a higher abundance of corals coincided with the lack of larger foraminifera at the base of each cycle, followed by a packstones sequence upwards. Each cycle suggests a relative sea level rise.

In contrast to the small build-ups, quiet water conditions of a protected paleoenvironment are reflected by the massive wacke- to packstones with mainly small benthic foraminifera, bivalves and gastropods and scattered corals in the inner part of carbonate complex. The lack of planktonic foraminifera supports the interpretation of a protected environment in a lagoonal setting.

Devel Peak

The carbonate build-up of Devel Peak (with the continuation in the Eastern Ridge) starts to grow later than Albion Head and on siliciclastics. The sedimentary record of the underlying siliciclastics reflect the transition from a deeper and quiet water environment to shallow water/ high-energy conditions close to a shoreline (shales - fine sandstones - conglomerate with marine skeletal grains and 3-cm large and rounded gravels). This relative sea level fall created suitable conditions for the establishment of the carbonates recorded above.

In general, the carbonates were studied on the southern and south-eastern side of Devel Peak. Throughout the succession, the decrease of planktonic foraminifera followed by an increase of peloids (Fig. 74) as well as a change from a Nummulitidae/ Amphisteginidae-dominated larger foraminiferal assemblage to a Soritidae/ Alveolinidae-dominated assemblage illustrate the change of the depositional conditions: an influence of both, a shoreline and the open ocean at the base of the succession changed to full marine conditions in a relative protected environment. This evolution coincided with a general transgressive trend, which shows 6 cycles of relative sea level changes (Fig. 75). Significant layers, which contain twice terrestrial material (gravels, quartz grains) and four times masses of corals associated with a content of shale, mark the levels of relative sea level low-stand.

Due to the significant decrease of gravel and quartz grains upwards to the 52-m level in the Devel Peak succession, the lowermost carbonates document the retreat of a shoreline and consequently a relative sea level rise (Cycle 1). The composition of the packstones or sometimes rudstones to floatstones with different amounts of larger foraminifera, red algae, bivalves, echinoderms, bryozoans and small benthic foraminifera as well as some planktonic foraminifera indicate some variations of the conditions (water energy, water depth) during their accumulation in the general shallow water paleoenvironment. The repetition of a carbonate containing again terrestrial material (gravel and quartz grains) displays the progradation of the shoreline basinwards as a result of relative sea level fall. However, due to smaller gravels and a lower siliciclastic content as in the carbonate conglomerate at the base

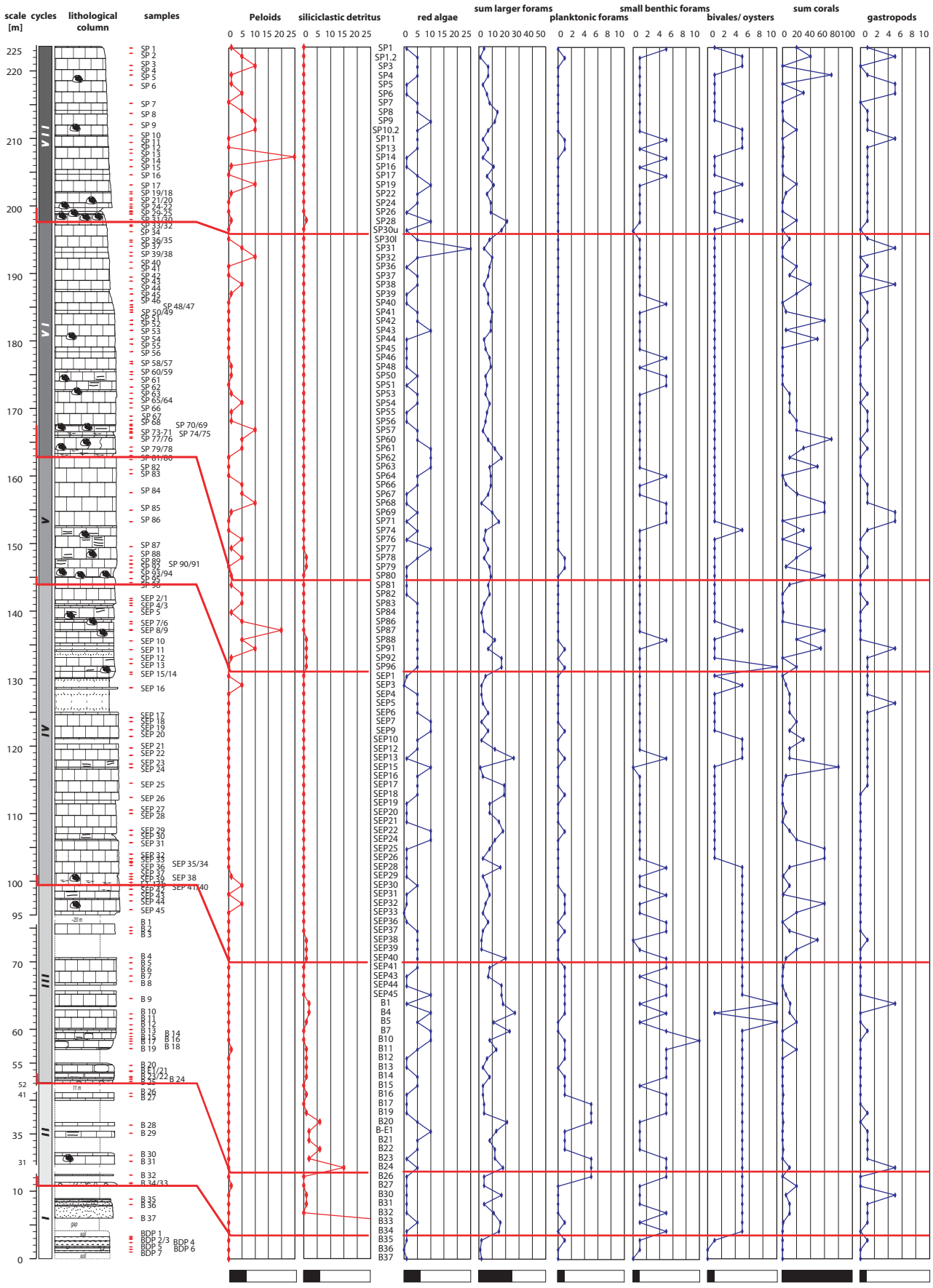

Fig. 74: Semi-quantitative frequency estimation of abiotic components and selected skeletal grains throughout the build-up of Devel Peak.

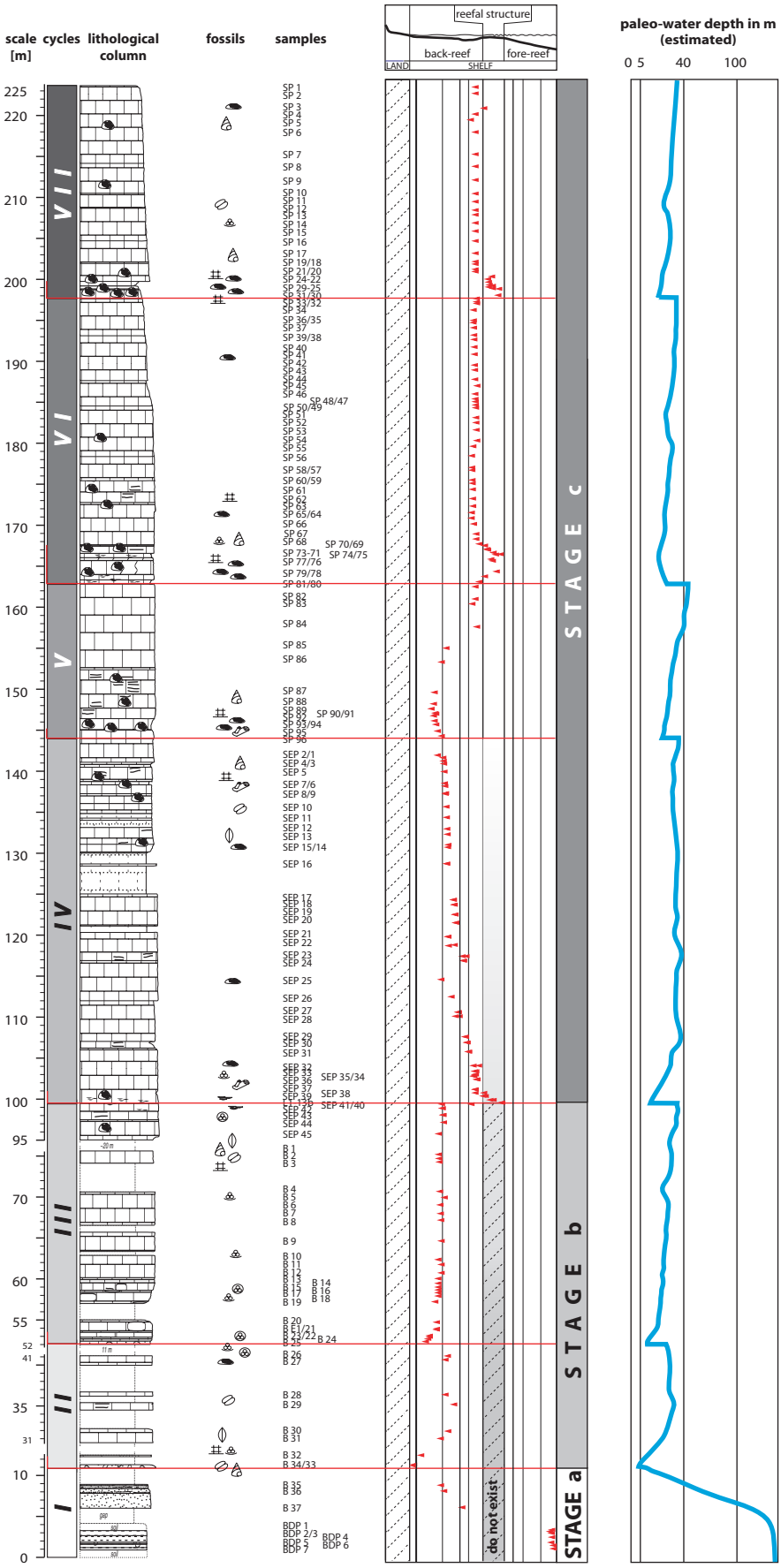

Fig. 75: Synthetic column throughout the build-up of Devel Peak with indicated dominant content of skeletal grains, paleoenvironmental position of each sample and the changes of the relative sea level through time.

of Devel Peak, the shoreline was probably still relative far away. Therefore, the relative sea level fall ceasing Cycle 1 is interpreted as relative small compared to the first one.

The significant decrease of the siliciclastic content and establishment of pure carbonates (more than 95% $CaCO_3$) together with the occurrence of corals further upwards provide evidences for full marine conditions. The transgressive trend continuous (Cycle 2), whereas moderate to low water energy conditions in a shallow-water environment prevail, demonstrated by the dominance of massive packstones with red algae, larger foraminifera, molluscs and abundant small benthic foraminifera. The deepening process is supported by the occurrence of a few green algae in the lower part of this sequence (typically shallow water components) and the higher content of micrite and finer grained carbonates of a deeper paleoenvironment upwards. The open marine influence in the lower part of the sequence is clearly shown in high amounts of planktonic foraminifera, which reduces upwards.

The first significant layer with masses of corals in the succession (100-m level) marks the top of the depositional record of Cycle 2. A narrow framework of Poritidae (coral-boundstone) forms the 2 to 3-m thick coral level. The often by red algae and/or larger foraminifera encrusted corals yield clear evidence for a relative sea level drop followed immediately by a sea level rise again. Beside the fact that masses of corals overly fine-grained packstones with only some corals, the sharp contact at the base and a significant portion of shales display an abrupt sea level drop. Furthermore, the shape of *Porites* confirms this interpretation, because massive and cup-shaped forms are dominant in the lower part of the coral level. The platy forms reach a thickness up to 8 cm so that all features refer to higher water energy conditions in shallow water during a relative sea level low-stand. Upwards, almost only flat and more fragile (max. 3-cm thick) platy *Porites* occur, which are related to a lower water energy regime and a declined insolation in a deeper water. This following sea level rise corresponds to Cycle 3 and is supported also by a decrease of corals and a lack of shale content (or any other components referring to an influence of a landmass) in the overlying massive packstones. Beside a still variable number of corals, the composition of molluscs changes from a bivalves-dominate to a gastropod-dominate assemblage. Together with the rare occurrence of planktonic foraminifera and some peloids in a few samples, it displays conditions that are more restricted.

Anyhow, the composition of the packstones (corals, larger foraminifera, red algae, molluscs, some echinoderms, encrusting foraminifera, a few green algae) shows in general no major variance throughout the upper part of the Devel Peak succession, except the appearance of

abundant peloids and a very slight decrease of larger foraminifera. These carbonates suggest a back-reef setting in a mainly slightly deeper and moderate to quiet water energy regime for their accumulation. However, additional 3 significant coral layers report short sea level low-stands and lead to the differentiation of Cycles 4, 5 and 6. The coral level 144-m above the basis of Devel Peak (end of Cycle 3) documents a slightly lower sea level by a coral accumulation (coral-rudstone) containing high amounts of molluscs, red and green algae as well as some planktonic foraminifera. The skeletal grains seems to be par-autochthone or from the surrounding area nearby so that the deposits are probably generated by higher wave energy. The entering of these waves seemed to be possible, because of a period of relative sea level low-stand. Furthermore, a content of shale and some quartz grains provide additional evidence for sea level change and a regressive event. Additional coral levels (163 and 199 m in the succession), which are intercalated into the packstone sequence, represent a relative sea level drop with the establishment of masses of several dm-large coral heads (insitu). An erosive base at the 163-m level suggests also the exposure of the carbonates to high water energy in very shallow water. However, the associated regressions documented in these levels are less obvious, because the reduced $CaCO_3$ content caused by a small portion of shales is only weakly distinct.

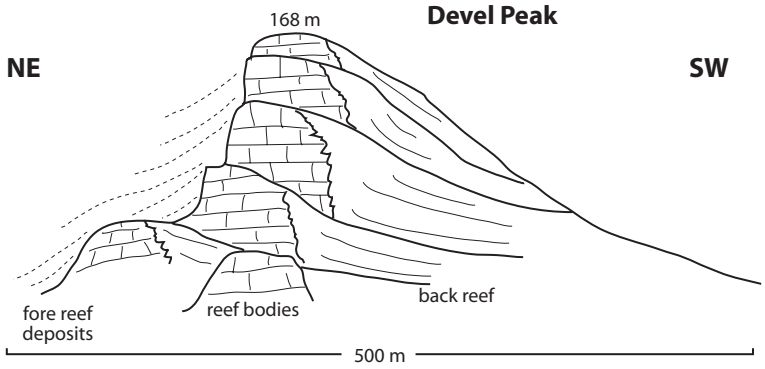

Fig. 76: Idealised cross section through the build-up of Devel Peak showing the backstepping to south-western directions.

The results of the detailed study of the continuous profile at Devel Peak added by the field observations yield a model of the geometry of Devel Peak (Fig. 76). The counterpart of the prominent and vertical cliff on the NE side of Devel Peak is the accessible steep flank at the SW side. The existence of smaller reef bodies on the northern and eastern flanks results in the

assumption that the present-day morphology reflects some features of the primary morphology.

The cliff shows four ledges each associated with a step backward of the cliff front. The ledges correspond to the four significant levels with masses of corals and mark each the beginning of a cycle of sea level changes. Therefore, the geometry of the build-up suggests the south-westwards retreating of the reefal structures, which seems to be triggered by relative sea level changes. Each sea level drop allowed the corals to grow and to create a reef-like stadium. However, these reefal stadiums are relative short, because the masses of corals were not able to catch-up the following sea level rise. Moreover, the morphology leads to the assumption that a reefal front was exposed to the NE, whereas the lithologies recovered along the profile in the SE and S indicate the slightly deeper water of a more protected back-reef setting. Nevertheless, with respect to the field observations and the size of Devel Peak, the build-up show no clear lateral zonation, rather than give an example of a deeper, but still shallow-water, carbonate accumulation. This relative small structural provides excellent condition for the corals during relative sea level low-stands so that those reef-like stadiums were developed.

Siliciclastics

A selection of loose siliciclastic rocks SW of Albion Head and well-bedded sandstones N and NW of the study area are probably related to a Bouma-Sequence, a product of turbidity currents (BOUMA et al., 1986). This provides evidence for the existence of a deep-water environment. However, due to the missing of a new age-control their stratigraphic position is still unverified. REYES (1971) described depositions in the area around Quezon made up of deeper water siliciclastic with an age - based on foraminifera and nannoplankton - between late Early to Late Miocene. In contrast, PARK & PETERSON (1979) interpreted the sequences found on the small islands as sub-stratum of the carbonates. The tubidite trench filling should be accumulated (based on some arenaceous foraminifera and flora) during the Paleocene to Eocene time.

Consequently, following REYES (1971) and therefore a development of these siliciclastics during the Miocene, the deposits represent the deep-water environment in between carbonate build-ups; similar to the situation observed in the offshore study area. Otherwise, i.e. following the dating as Paleocene or Eocene deposits (PARK & PETERSON, 1979) the present-day position of the deep-water deposits must be explained with tectonic movements younger than Miocene time.

Excerpt: As last products of the Middle Miocene carbonate event, which generated all carbonates around Quezon, Albion Head and Devel Peak are formed. Whereas at Albion Head a continuous carbonate deposition is expected, throughout the section of Devel Peak a siliciclastic substratum (Stage a), an initial carbonate stadium (Stage b) and the carbonate accumulation with reef-like stadiums under full marine conditions (Stage c) are represented (cf. Fig. 75). With the exception of the siliciclastic substratum of Devel Peak, the deposits suggest only small relative sea level changes, probably in a range of a few meters. A deepening of the paleoenvironment upwards could not be deduced from the sedimentary record. Nevertheless, a general trend of sea level rise associated with a transgression is expected, because sediments are continuously accumulated without filling up the accommodation space. The slight sea level drops are the remarkable events in the record so that the related deposits mark seven cycles of sea level changes. Additionally, the section of Devel Peak demonstrates upwards the development of a lagoonal setting as result of the development of a barrier. Both structures (Albion Head & Devel Peak) are placed on the northern margin of the carbonate area, eventually surrounded by siliciclastic deposits of deep-water environment.

5.1.3 Diagenetic History Onshore

The diagenetic features observed in the thin sections of the lateral extended and build-up carbonates of SW-Palawan onshore are dominated by cementation and neomorphic processes as well as moderate compaction, which refers to an early burial diagenesis impact. Nevertheless, the diagenetic history starts already in the depositional environment, because locally microbial micritization (mainly affecting corals) represent a destructive diagenesis by cyanobacteria. A slightly pronounced dissolution follows, before some early micritic or fibrous fringes cement rims indicate the first step of lithification under still marine conditions (cf. cathodoluminescence). The thin cement fringes predominately occur in the carbonate sands of the lateral extended carbonates and are missing at Devel Peak. It leads to the assumption that these cements were precipitated, because of early fluid circulation in the relatively porous carbonates. Bladed-prismatic calcite as an additional early cement is interpreted as a product of meteoric to brackish water influence (BATHURST, 1975; CHOQUETTE & JAMES, 1987). However, this cement was observed only once, so that a fresh water influence seems to be without major significance in general for the lateral extended

carbonate rather than a phenomenon, which has to be expected in a shallow-water environment relatively close to a shoreline. The characteristic clear, granular to drusy calcite cements of the burial diagenesis of shallow marine/ peritidal limestones (CHOQUETTE & JAMES, 1987) occur dominantly in almost all of the carbonates as filling of primary as well as of secondary porosity (moldic-, fracture, channel porosity). The cathodoluminescence analysis supports the two different cement generations of the slightly pronounced early marine cement and the dominant burial cements. Furthermore, the observed transition from non-luminescent to bright cathodoluminescence colour in drusy cements corresponds to the succession (non-luminescent - bright - dull (or final dull yellow)), which is described from many limestones and interpreted as a product of increasingly reducing nature of the pore-fluids during the burial (e.g. FANK et al., 1982; GROVER & READ, 1983; FRYKMAN, 1986; DOROBEK, 1997). The missing of the last stage (dull luminescence) is probably only related to moderate burial of the onshore carbonates or the incomplete cementation due to a time of limed or missing supersaturated fluids (still open porosity exists). Besides the granular and drusy cements, some syntaxial cements are associated with echinoderm fragments and occur in the coarse carbonates. Their appearance is also typical for the burial calcite precipitation like the patches of neomorphic spars in the floatstones. Furthermore, the neomorphic processes, but also recrystallisation, transformed all primary metastable carbonates (aragonite, high-Mg-calcite) of corals, molluscs, green- and coralline red algae as well as cements into calcite/ low-Mg-calcite. This lack of aragonite has been confirmed by the cathodoluminescence analysis of the thin sections, which did not indicate any green cathodoluminescence colours anywhere. Therefore, due to the additional lack of dolomite throughout the onshore carbonates, calcite is the only present carbonate phase onshore.

The observed compaction features (orientation of elongated bioclasts, concave-convex component contacts, fracturing of skeletal grains, ductile deformation) illustrate the first stages of the increasing mechanical compaction of the unlithified sediments during the increasing overburden stresses by further deposits (TUCKER & WRIGHT, 1990, p. 358). These features were found predominantly in the carbonate sand deposits, whereas the broken grains might refer to a depth of several hundred meters (SCHLANGER, 1964; SALLER, 1984). The sutured component contacts in the carbonate sands as well as the small stylolites (thin section scale) as product of chemical compaction suggesting some additional compaction. However, the carbonates document in general only a relative low to moderate compaction, because still primary porosity (inter-/ intraparticle porosity) exists and not all skeletal grains are broken.

These could be a result of a effectively lower compaction or of early consolidation of the sediments by some granular cements of the earliest burial diagenesis. If the relative limited compaction in the coarse carbonates could be also explained by the existence of an overpressure in their pores due to shales and shaley mudstones to marls at the base and top, which might acted as seals, must be subject of speculation.

The carbonates never reach the stage of the late burial diagenesis, which would transfer calcite to dolomite. The last diagenetic process is the most efficient present subaerial dissolution (karstification) of the carbonates triggered by the high humidity and strong biological activities characterising the tropical weathering, which results in the jagged to sharply pointed peaks and vertical fluted walls (LONGMAN & BROWNLEE, 1980). The present day morphology at Albion Head suggests being an example of tower karst morphology (PURDY & WALTHAM, 1999).

In general, the porosity, ancient and recent, is mostly related to coarse carbonates. These carbonates provide primary porosity, on the strength of the low to moderate compaction, but predominately the recent karstification corroded the coarse carbonates. Consequently, they have the highest open porosity today.

The oxygen isotope signature of shallow-marine cements and sediments depends largely on the seawater/ fluid $\delta^{18}O$ composition and the temperature (CRAIG & GORDON, 1965). The $\delta^{18}O$ range is typical -0.5 to +3‰ in modern marine environments (TUCKER & WRIGHT, 1990). At 16.5°C a calcite is balanced regarding the $\delta^{18}O$ with the SMOW (standard mean ocean water), i.e. the value is 0‰ $\delta^{18}O$ and increasing temperature leads to lighter $\delta^{18}O$ values (JOACHIMSKI, 1991). As illustrated in the Fig. 77, many organisms do precipitate carbonate with $\delta^{18}O$ values suggesting isotopic equilibrium with the water in which they were living (molluscs, planktonic foraminifera, brachiopods). Others, like corals or red algae, deviate from the predicted isotopic equilibrium value to lighter values. In contrast to the

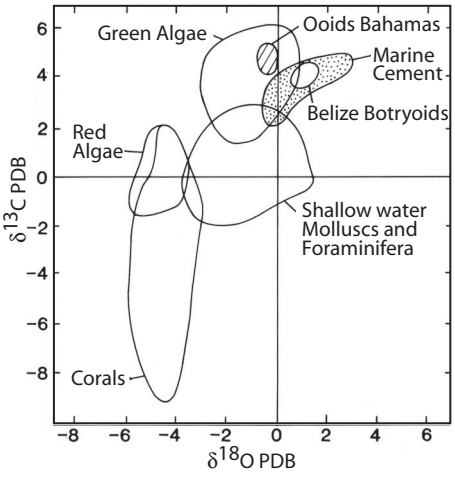

Fig. 77: Stable isotope signature of Recent skeletal grains, ooids and marine cements. After various sources including LAND & GOREAU (1979), MILLIMAN (1974), JAMES & GINSBURG (1979), and ANDERSON & ARTHUR (1983); in TUCKER & WRIGHT (1990, p. 324).

relative narrow range of the $\delta^{18}O$, the $\delta^{13}C$ values show a wide variance. Recent inorganic carbonates have typically a value between +2 and +5‰ $\delta^{13}C$, whereas especially corals incorporate values from +2 to -9‰ $\delta^{13}C$ (cf. Fig. 77). An almost similar range (+2‰ and -10‰ $\delta^{13}C$) for fossil carbonates is supposed by JOACHIMSKI (1991). Anyhow, $\delta^{13}C$ could be easily changed by some content of organic carbon (-9 to -33‰ $\delta^{13}C$ (DEINES, 1980)), river discharge (-6 to -9‰ $\delta^{13}C$ (ANDERSON & ARTHUR, 1983)) or photosynthesis. Additionally, during the burial diagenesis the stable isotope signature of $\delta^{13}C$ and $\delta^{18}O$ changes toward lighter ratios. Whereas $\delta^{13}C$ declines only slightly, $\delta^{18}O$ drops sharply (DICKSON & COLEMAN, 1980; CHOQUETTE & JAMES, 1987).

The 92 data of the onshore carbonates illustrate most significantly these typical burial diagenesis pathway with 3 stages up to -10.5‰ $\delta^{18}O$, whereas each stage is lighter in $\delta^{18}O$ values than the previous one (Fig. 78).

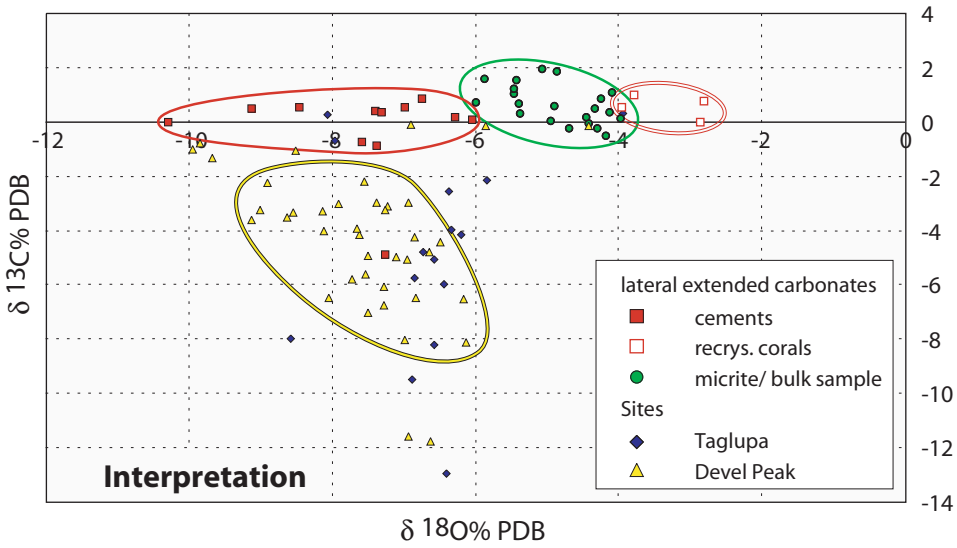

Fig. 78: Scatter diagram of 92 stable isotope data of oxygen and carbon grouped by sites (Taglupa Profile, lateral extenden carbonates, Devel Peak) and additionally in the lateral extended carbonates by carbonate categories. Interpretation leads to 4 concentrations, all referring to the dominante process of burial diagenesis.

In general, the variance of the $\delta^{13}C$ of all samples of the lateral extended carbonates is very low. Anyhow, the identification of a very slight decrease of $\delta^{13}C$ values towards lighter $\delta^{18}O$ corresponds to the concept of CHOQUETTE & JAMES (1987). In contrast, the development from the $\delta^{18}O$ of the recrystallised corals (-2.8 to -4‰ $\delta^{18}O$) to the $\delta^{18}O$ of cements (up to -10.5‰ $\delta^{18}O$) reflects most significantly the temperature-related fractionation between water and

carbonate during an increasing burial (CRAIG & GORDON, 1965). This observed development corresponds to the depositional chronology of the carbonates. The $\delta^{18}O$ values of the 4 isotope samples of 3 recrystallised corals from the lateral extended carbonates correspond to the $\delta^{18}O$ values of recent corals (cf. Fig. 77). An early neomorphic process seems to preserve their primary isotopic signature, which was controlled by the vital effect of the corals. Anyhow, even inside one coral the increasing trend to burial diagenesis is documented. The calcite sample from a recrystallised part of a coral septum indicates the first diagenetic process (-2.81 ‰ $\delta^{18}O$), whereas the cement in between the corallites is already lighter (-3.78‰ $\delta^{18}O$) and refers therefore to a later stage of the diagenesis. Within the range of -4 to -6‰ $\delta^{18}O$, all micrite and bulk samples are concentrated. Even with respect to the $\delta^{18}O$ seawater curve of BILLUPS & SCHRAG (2002), the value of the $\delta^{18}O$ of the tropical Miocene ocean is unknown and the equation of CRAIG & GORDON (1965) could not be solved exactly. Nevertheless, it seems that no major difference exists between the $\delta^{18}O$ values of the Middle Miocene and the present. Therefore, the best estimations result in temperatures of more than 35°C for the fluids, which affect the micritic carbonates. Even if we are dealing with tropical carbonates, this temperature is fairly to high for a tropical biocoenosis. (Recently, the water temperature ranges in the region of the South China Sea between 26 and 30°C during the year (LEVITUS & BOYER, 1994).) Therefore, these micrite and bulk samples document a first slight burial diagenetic overprint and not the primary isotopic signature of the seawater. Finally, the stable isotope record of the granular cements of the lateral extended carbonates displays a clear enrichment of the ^{16}O-isotope (-6 to -10.5‰ $\delta^{18}O$) as a result of higher temperatures and depleted fluids in the burial conditions.

The distribution of the data points of Devel Peak shows a clear offset to the lateral expended carbonates due to lighter $\delta^{13}C$ values. However, the $\delta^{18}O$ records correlate perfectly. The fact, that most of the samples were taken from recrystallised corals, the existence of high amounts of corals in the build-up combined with an autochemical cementation (CHOQUETTE & JAMES, 1987) might result in the preservation of the light $\delta^{13}C$ signature, which is characteristic for recent corals (cf. Fig. 77). Hence, the offset between the lateral extended carbonates and the build-up is interpreted as only one final stage of burial diagenesis, where the primary isotopic signature of each carbonate leads to the offset, rather than two different cements generation.

In contrast to all other samples, the isotopic ratios of the Taglupa Profile do not provide any significant concentration. However, most of the samples plot within a narrow range of $\delta^{18}O$

(-5.84 - 6.89‰ $\delta^{18}O$), which corresponds again perfectly with the final stage of burial diagenesis. Taking into account, that the carbonates of the Taglupa Profile are the initial carbonate deposits, overlying shales below the onshore carbonate succession and indicate a shoreline in the vicinity, the partly high content of organic matter is probably responsible for the very light $\delta^{13}C$ values.

Beside the thin section study and the cathodoluminescence analysis, the study of the stable oxygen and carbon isotope signatures of the four carbonate categories provides additional evidence, for the interpretation that after a slightly pronounced marine diagenesis a burial diagenesis dominates the diagenetic history of the onshore carbonates, before recently strong subaerial alteration affects the Miocene carbonates onshore.

5.2 Offshore SW Palawan

The offshore data set, kindly provided by the Department of Energy (DOE), Manila, allows the generation of a detailed depositional model relatively close to the onshore study area around Quezon in SW Palawan from the Miocene to recent time. The reinterpretation of the data set leads to some new insights and a model valid beyond the outlines of the about 55-km^2 large offshore study area.

5.2.1 Offshore Setting

The opening of the present-day South China Sea during Late Eocene to Oligocene is preceded a rifting on the proto-China continental margin from Late Cretaceous to the Late Eocene time (TAYLOR & HAYES, 1980; HOLLOWAY 1982). This early rifting and contemporaneous crustal extension of the seafloor results in the formation of a complex system of NE-SW striking half-graben structures separated by structural highs (Fig. 79), like observed in the area of the Dangerous Grounds, a region with numerous shallow and exposed reefs located between the Reed Bank off S-Palawan and Natuna Island N of Kalimantan (HOLLOWAY, 1982; HINZ & SCHLÜTER, 1985; FULTHORPE & SCHLANGER, 1989). The half-grabens were filled with thick sections of lacustrine clastics until the rifting ceased at late Eocene time (KATZ & KELLY, 1987). At the same time, the horst and graben topography was almost levelled and deltaic to marginal marine clastics were deposited (HINZ & SCHLÜTER, 1985).

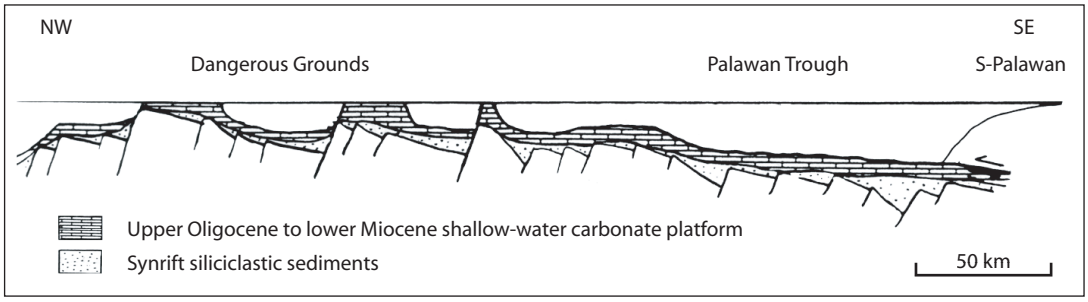

Fig. 79: Hypothetical cross section during early Miocene from S-Palawan to the Dangerous Grounds showing normal faulting in the area of Dangerous Grounds and thrusting of continental fragments beneath S-Palawan, after FULTHORPE & SCHLANGER (1989)

This pattern characterises the basement below the Miocene to recent sedimentary sequences of carbonates and siliciclastics within the South China Sea. However, within the study area these basement structures are only observed NW of the Great Atoll Reef so that it seems to have minor importance for the study area, like structural features in general. More important is the position of the study area close to a landmass not only today but also in the Miocene. The terrestrial influx affected the build-ups during their development, before they were buried below them. Thereby, the margin of the landmass was passive so that the proposed subduction zone (HAMILTON, 1979 and others) had to be located further to the SE.

With respect to different interval velocities throughout the depositional successions, the pretended morphology of the wide spread early Miocene platform is originally horizontal to sub-horizontal, even if some small structural highs might have promoted the continuation of carbonate deposition in local areas (Great Atoll Reef, Anepahan A-1X pinnacle reef). Furthermore, the biostratigraphic correlation of the significant prograding clastic sequences 1 to 3, observed in the seismic survey of the overburden clastics, is coherent in the 3 wells; however, it has to be taken into account that the biostratigraphy of the well Anepahan A-1X is dubiously.

5.2.2 Facies Distribution during the Miocene Offshore

The study of the offshore data set results in different depositional environments during the Miocene. Changes occur laterally as well as vertically.

An extended carbonate production on a platform exists during the Early Miocene in the SE South China Sea (HINZ & SCHLÜTER, 1985; KUDRASS et al., 1986; FULTHORPE & SCHLANGER, 1989; ERLICH et al., 1993) such as documented within the whole study area.

Facies changes within the carbonate platform could not be established based on the available data set. However, HINZ & SCHLÜTER (1985) expect carbonate deposits of both, higher water energy conditions of carbonate platforms and banks developed on topographic highs and low energy conditions of basinal carbonates and shales created in the deeper surrounding areas. Based on dreged samples, KUDRASS et al. (1986) could divide lagoonal-, reefoid-, very shallow marine-, shallow open marine and deep (~50 m) open marine settings, whereas the shallow open marine environment dominates and therefore the results are typical for a carbonate platform (SCHLAGER, 1981; READ, 1982). Additionally, the interpretation of these carbonates as platform carbonates is based also on their lateral dimension of several 100 km^2. However, their geometry (carbonate platform or carbonate ramp) could not be defined.
The Early Miocene carbonate platform is overlain by local Middle Miocene carbonate build-ups of different sizes (Great Atoll Reef, Anepahan A-1X Pinnacle Reef) and types. Within the heterogeneous structure of the Great Atoll Reef, a number of different facies types is expected. Even if only one peripheral pinnacle was tested (Santiago A-1X) within the Great Atoll Reef and, therefore, the composition of most facies types are subject of speculations, the seismic record indicates clearly different zones (noisy zones vs. well-stratified zones or parts showing internal sedimentary structures). Moreover, GRÖTSCH & MERCADIER (1999) were able to distinguish 8 facies types within the assimilable build-up of Malampaya and Camago, which supports the idea of a complex carbonate body. In contrast, the Anepahan A-1X pinnacle reef might show, with respect to the smaller size, less pronounced facies zonation. However, at that site significant lobes of reef debris are identified, which might be controlled by wind action from the NE, affecting the reef top and transporting the material predominantly south-westwards.
Whereas the carbonate build-ups represent shallow water conditions or may be in lagoonal settings of the Great Atoll Reef water depth of some 10s of meters, shales and turbidite deposits in between indicate quiet conditions in a deep-water environment.

The vertical facies changes could only be attained from the 3 wells. However, due to the fact that no core samples were available for the well Penascosa-1 and the lithostratigraphic description is very simplified, a more detailed vertical evaluation of the facies throughout the platform carbonates was not possible. Following TIDEY et al. (1975), the facies changed throughout the platform from an early sublittoral to a protected shallow-water environment later on. Anyhow, the rock samples plus the core description and borehole measurements of

the well Santiago A-1X allow the interpretation that within the Great Atoll Reef facies variations occurred, probably very close together in time and space. All deposits document a carbonate-dominated shallow-water paleoenvironment. Different amounts of shale in the carbonates are probably related to pulses of the prograding siliciclastics from time to time (cf. chapter 5.2.4). The core section refers to moderate water energy conditions due to the relative high amounts of micrite in the float-, wacke- and packstones. Nevertheless, beside the characteristic assemblage of skeletal grains (corals, larger foraminifera, red- & green algae, echinoderms) of a back-reef setting, some high amounts of planktonic foraminifera indicate (sometimes strong) open marine influence, especially in the upper part of the core section. In general, the core supports the interpretation of an isolated heterogeneous atoll structure with reefal and lagoonal settings. The carbonates penetrated in the well Anepahan A-1X are only represented in the data set by the 10 rock samples so that the evaluation of the facies, respectively the paleoenvironment, is limited. These samples reflect shallow-water conditions with almost similar conditions as shown in the well Santiago A-1X. However, the lower content of corals, very rare planktonic foraminifera and Nummulitidae, but relative high numbers of gastropods and some ostracods results in the interpretation of a more restricted and quiet-water paleoenvironment at Anepahan A-1X than at Santiago A-1X. Nevertheless, due to the fact of the limited information, the indicated paleoenvironment must be not consequently the same throughout the whole build-up succession. Hence, no major differences are expected between both reefal sites, even if Anepahan A-1X is a pinnacle reef body with less coexisting facies zone than the atoll structure of Santiago A-1X contains.

5.2.3 Diagenetic History Offshore

Based on the limited data regarding the facies and diagenetic features of the Miocene carbonates offshore, drilled in the wells Santiago A-1X and Anepahan A-1X, the diagenetic interpretation could probably not provide the all-embracing diagenetic history. Nevertheless, some features seem to be significant enough to assume their general validity.

Santiago A-1X

Within the samples from the well Santiago A-1X, only one cement generation of granular and drusy cements and neomorphic spars similar in their morphology, sizes and characters to the onshore cements are observed. These sparites suggest that only a burial diagenetic process

affected the carbonates significantly, whereas moderate compaction is illustrated by broken or deformed components. The reported stylolites in the core seem to demonstrate a close relationship to different lithologies (decreasing amount downcore), but the generalised core description does not provide enough detail to unravel the relationships. Most significant are non-fabric selective open pores in the packstones (vugs, channels) referring to some leaching by aggressive waters without later cement precipitation. However, dissolution by meteroric waters is probably the only process, which is likely to create this porosity (CHOQUETTE & PRAY, 1970). Hence, the carbonates have to be in contact with the meteoric-phreatic zone or were subaerial exposed during in the later diagenetic history. The still open porosity are interpreted as a result of a very late dissolution process or that no permeability exists, which would allow the necessary fluid circulation for the cement precipitation. Furthermore, it has to be emphasised that, like as observed in the onshore carbonates, the (open) porosity is associated to coarse carbonates. The characteristic heterogeneous composition and the existence of primary porosity and permeability, which allows the circulation of a not-supersaturated fluid, seems to be an important factor to trigger the development of porosity in the carbonates. In contrast, the tailback of fluids below a seal and therefore the enrichment of solved carbonate in the fluid (= supersaturated fluids) results in the opposite effect: the cementation. This is nicely demonstrated by the Bulk-Density and Gamma-Ray Log in the lower part of the penetrated Miocene carbonate succession in the well Santiago A-1X. There, a well-cemented carbonate is capped by a carbonate with very high shale content, which acts as seal. The explanation of the strong cementation in parts of very poor carbonates (shale content very low) is more difficult, because detailed descriptions of the carbonates were not available. Nevertheless, the pure carbonates in a reefal build-up like the drilled Santiago A-1X pinnacle reef body, are probably related to very high amounts of frame-builders, which predominately create aragonitic skeletons (e.g. corals). This metastabile carbonate modification could be easily solved and results therefore in both, a high porosity and the supersaturated fluid to create cements.

Anepahan A-1X

The short core section close to the top of the Anepahan A-1X pinnacle structure documents in contrast to all other carbonates on- and offshore a well-documented diagenetic history. Whereas the burial diagenesis dominates all carbonates from the other sites, the 10 rock samples from Anepahan A-1X provide additionally and here as most significant features clear

indications of their subaerial exposure. Anyhow, the early diagenetic processes (bioerosion, early marine fibrous cements, neomorphism, dissolution) as well as the features of a burial diagenesis (granular and drusy cements, fractures, pressure solution) exist, like in the other carbonates on- and offshore.

The interpretation of a subaerial exposure is based on abundant speleothems, vadose silt and *Microcodium*. Even if *Microcodium* is still a microproblematicum and the genesis of the subspherical mosaic of calcite prisms is subject of discussions (inorganic precipitation (ROSSI & CANAVERAS, 1999) or calcified root cells (ALONSO-ZARZA et al., 1998)), there raise no doubts about the subaerial conditions during their development. Beside the unique features of subaerial exposure inside the Anepahan A-1X core, the occurrence of small granular dolomite is also restricted to these samples. Due to the fact, that this single occurrence of dolomite is associated with a subaerial exposure, the mixing-zone dolomitization model, this stems from the work of HANSHAW et al. (1971), appears to be the most reasonable model. However, the lack of geochemical analysis and cathodoluminescence makes it difficult to apply confidently for a model and therefore, the final evaluation of the dolomite genesis, but also the speleothems, is complicated.

5.2.4 Depositional Model Offshore

The integration of 1,222 line-km of seismic survey and data of 3 wells offshore SW Palawan yields a depositional model for the development of the sedimentary succession from Miocene to recent time. Parts of the seismic record of line WP 213-80, GPPW 96-119 and DPS 93-4 are used to illustrate this evolution (Fig. 80):

- Early to Middle Miocene platform carbonates (dark blue) overlie unconformably Cretaceous clastics;
- isolated build-ups (red) of various sizes occur on top of the platform;
- carbonates covered by Middle Miocene to recent clastics (green to orange) that display basinwards prograding sequences and erosional channels.

Only within the well Penascosa-1, the substratum of the Miocene carbonates has been penetrated. Some discovered siliciclastic sediments refer to a deep-water environment with deltaic influence indicated by coaly plant debris (TIDEY et al., 1975; HINZ & SCHLÜTER,

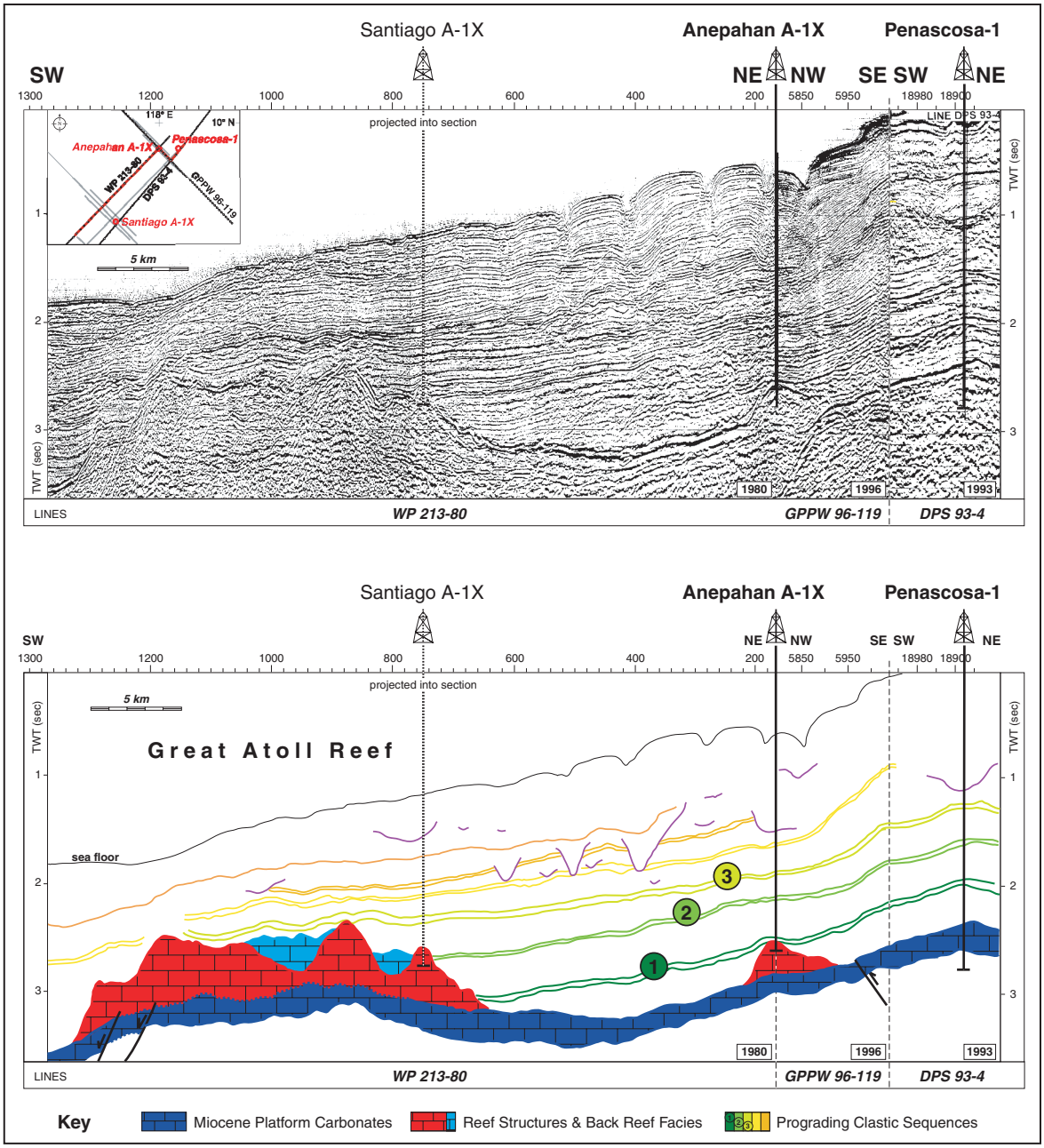

Fig. 80: Synthetic seismic profile made up of parts of the lines WP 213-80, GPPW 96-119 and DPS 93-4 to demonstrate the general depositional model offshore SW Palawan. Above the drowned Miocene carbonate platform (blue), isolated carbonate build-ups of various sizes and with different facies zones developed (red/ light blue) before a basinwards prograding clastic sequence buried all carbonates between Middel Miocene (N9) and recent time.

1985). Most probably, the deposits are of Early Cretaceous age. Consequently, they were accumulated before the beginning of the rifting in the South China Sea during the Late Eocene to Oligocene (TAYLOR & HAYES, 1980, 1983) and before the long period of eustatic sea level high-stand (> 200 m above present sea level) from the Upper Cretaceous until the Lower Oligocene (HAQ et al., 1987, 1988). Above a hiatus from the Upper Cretaceous to the

Oligocene, a basal conglomerate, composed of cherts in a quartz-sand matrix, displays an inner sublittoral environment in a vicinity to the shoreline. The reworked material is dated at the site of Penascosa-1 with an age of Early Miocene (N5) just as the 567 m thick carbonate platform sequence above. The general rise of sea level from 30 to 15 Ma (early Oligocene to Middle Miocene) together with the early to middle Miocene climatic warming (SAVIN et al. 1985; MORLEY, 1998) results in favorable conditions for the development of tropical carbonates from New Zealand to Japan (FULTHROPE & SCHLANGER, 1989). Between NW Borneo and NW Palawan in the South China Sea the size and distribution of the carbonates were mainly structurally controlled and often related to continental blocks (CLENNELL, 1996; DOROBEK, 1997; GRÖTSCH & MERCADIER, 1999, WILSON et al., 2000). The carbonate deposits reflect both, higher water energy conditions of carbonate platforms and banks developed on topographic highs and low energy conditions of basinal carbonates and shales created in the deeper surrounding areas. With respect to the globally relative low sea levels associated with the minimum degree of coastal onlap at the boundary between TB1 & 2 (HAQ et al., 1988), the basinal conglomerate in the well Penascosa-1 was correlated to an age of 20.5 Ma, whereas the offshore platform carbonates are developed during the transgressive event of the following shore term cycle (20.5 - 18.5 Ma).

Within the well Penascosa-1 a hiatus of 3 planktonic foraminiferal zones (BLOW, 1969) exists between the top of the platform carbonates and the overburden clastics, which indicates the drowning of the platform without siliciclastic influx as important factor of the termination. DOROBEK (1997) postulated that the rapid subsidence leading to the abrupt drowning of the carbonate platform over large parts along the south-eastern side of the South China Sea is a result of the combination of post-rift thermal subsidence and flexural subsidence of continental crust. Even if the extended carbonate deposition ceased in Early Miocene times and deeper-water environment with shales and depositions from turbidity currents occurred, in small areas suitable conditions for the growth of isolated reefs (Anepahan A-1X pinnacle reef) or atoll-like structures (Great Atoll Reef) maintained. In these areas, the carbonate deposition could most probably continue without any gap. Although, the well Santiago A-1X should reportedly penetrate Middle Miocene (N9 - N8) platform carbonates between 10,500' and 10,602' KB, the dating itself, seismic correlation and no lithological change results in the interpretation that this well did not reach the Early Miocene carbonate platform. Therefore, the well data does not contradict the idea of continuous carbonate deposition at the sites of the build-ups. The basement morphology was probably the prime controlling factor for the

development of the Miocene build-ups during the sea level rise. Further tectonic control by rejuvenated wrench tectonics, as proposed for the Nido build-ups in NW Palawan (GRÖTSCH & MERCADIER, 1999), seems to have no significant effect for both sites, Santiago A-1X and Anepahan A-1X. However, the available data set does not allow the detailed evaluation of the relation between the tectonic and the build-ups, because the carbonates obscure the seismic reflections below.

The growth of the isolated reef bodies took place in multiple phases as evidenced by the Santiago A-1X well section. Pulses of basinwards prograding clastics from the landmass of S Palawan cause the variations of shale within the reef section. These are most probably related to the relative sea level changes mention in the eustatic sea level curve (HAQ et al., 1988), which produced cyclic phases of drowning and emergence of the reefal complexes. An exposure of a build-up is documented in the core close to the top of the Anepahan A-1X, which contains subaerial cements and *Microcodium*. Anyhow, the death of the various reefal structures took place at different times, whereas the growth of the Anepahan A-1X pinnacle was stopped first with their subaerial exposure followed by the overburden with the clastic sequence 1. The Great Atoll Reef, however, continued growing until the Pleistocene (cf. Line WP 205-80, Fig. 51, p.118), even if later the basinwards prograding siliciclastic sediments cover the pinnacles one by one. Nevertheless, also the overburden clastics are affected by sea level changes so that the discontinuity at the base of the prograding clastic sequence 3, which were found in all 3 wells, correlates to the significant eustatic sea level low stand at the Miocene-Pliocene boundary between TB3.3 and 3.4 (HAQ et al., 1988). Moreover, this discontinuity is equal to one of the regional unconformities observed by TAMESIS et al. (1973), RILLERA, (1983) and HINZ & SCHLÜTER (1985).

Furthermore, several erosive channels occur within the overburden clastics. Some of them remained fairly at the same position through the Pleistocene to recent time, which reflects a quiet stable tectonic setting and drainage pattern off the island of Palawan for a long time period.

The generated deposition model from early Miocene to recent times illustrates with an unconformity to the Cretaceous deposits below, the establishment of an Early Miocene carbonate platform during a short period of sea level low stand, followed by their drowning also in the Early Miocene. Some isolated reef structures still developed continuously, before finally all carbonates were overburden by a clastic cover. The siliciclastic sequences range in

age from the Middle Miocene to the Present. These sequences are prograding westwards and demonstrate the backstepping of the carbonates in the same direction. The general tectonic setting was stable since Pliocene, since the proposed collision of the Philippine Arc with the Palawan Block around 5 Ma (GALLAGHER, 1987; LONGLEY, 1997).
Finally, it has to be emphasised that in sense of SCHLAGER (1981) only the carbonate platform drowned, whereas the growth of the reefal structures was terminated by terrigeneous influx.

5.3 How do On- and Offshore Areas come together?

To establish a model, how the onshore and the offshore study area, both of Miocene age, are linked, requires first of all the consideration of the dimensions, a detailed stratigraphy as well as the depositional record found in both areas. The correlation with carbonates described in N-Palawan on- and offshore and the interpretation of sea level changes might lead to the generation of an over-all-model, how on- and offshore study area developed together in Miocene time.

5.3.1 Dimension, Stratigraphy and Depositional Record

Offshore, the several 100-km^2 large carbonate platform is overlain in the study area by 2 local reefal build-ups. One, the Great Atoll Reef, grounds on a 27 by 23-km large base and their highest peak is approximately 2,400 m in height. The other build-up, the pinnacle reef of Anepahan A-1X has a basinal extension of 2.5 by 4.5 km and is about 900 m in height. In contrast, the dimensions onshore are much smaller. The whole carbonate study area covers an area of 16 by 5 km. The larger build-up, Albion Head, is a 1.5 km long, up to 1.0 km wide and 203 m high carbonate complex, whereas Devel Peak as north-western part of a 2.5-km long NW-SE ridge, reaches only an altitude of 168 m rising on a base of 800 by 500 m. All in all the carbonate depositions onshore add up from the Taglupa Profile to the top of the youngest deposits at Devel Peak to the best-estimated total thickness of 900 to 1000 m. With respect to this enormous difference in dimensions between on- and offshore platforms and build-ups, (the Great Atoll Reef is larger than the whole onshore study area), the idea was born that the onshore study area is not a small part of an extensive carbonate platform or carbonate ramp in sense of thick shallow-water sequence with several 100-km^2 in lateral extension (AHR, 1973; READ, 1982), rather than might represent an additional atoll-like

structure comparable to the Great Atoll Reef. Beside the corresponding dimensions lateral and horizontal, all features of the depositional record found in the carbonates onshore could be expected in a heterogeneous depositional environment of an atoll: the establishment of the carbonates, lagoonal and ramp-like setting, deeper water areas with very fine sediment deposition and reefal structures. Furthermore, the fossil assemblages of the drilled reefs offshore and the reefal structures onshore are resembled and show for example the same characteristics regarding the larger foraminiferal associations. The existence of the land mass of S-Palawan in the vicinity, like proposed by CLENNELL (1996), would explain the siliciclastic content (gravel, quartz, plant debris) included in the basinal carbonates onshore (Taglupa Profile) as well as in some slope deposits (Salty Creek Section). The detailed stratigraphy supports the idea that the Great Atoll Reef and the onshore study area are time equivalent. The platform carbonates are dated as Early Miocene (N5), whereas the reefal structures offshore show an age of lower Middle Miocene (N8 - N9) and this correlates perfectly to the age (N7 - N9) of the lateral extended carbonates onshore (Fig. 81). An equivalent to the Middle Miocene age of the build-up carbonates of Albion Head and Devel Peak were not discovered in any of the 3 studied wells offshore. But taking into account that the well Santiago A-1X drilled a peripheral pinnacle of the Great Atoll Reef and the highest pinnacle in the structure are dated (based on the seismic survey) as Pliocene in age, the build-ups onshore corresponds as well with the depositional succession offshore. Furthermore, continuous reef growth throughout the Quaternary until today is known from the Reed Bank as well as from numerous shoals of the Dangerous Grounds (KUDRASS et al, 1986).

5.3.2 Correlation to N-Palawan

The time-related correlation of the carbonates of SW-Palawan to the carbonates of N- and NW-Palawan (i.e. N/ NE of the proposed Ulugan Bay Fault (HAMILTON, 1979), which separated N- and S-Palawan along a N-S running line from the Honda Bay on the E coast to the Ulugan Bay on the W coast) is not possible. The onshore platform carbonates of the St. Pauls Complex (WIEDICKE, 1987) as well as the reefal carbonates of the Nido Limestone in the Malampaya and Camago carbonate build-up offshore NW-Palawan (GRÖTSCH & MERCADIER, 1999) drowned at the end of the Early Miocene time (Fig. 81). In contrast, the carbonates in SW-Palawan developed later, between the middle Early Miocene to Middle Miocene.

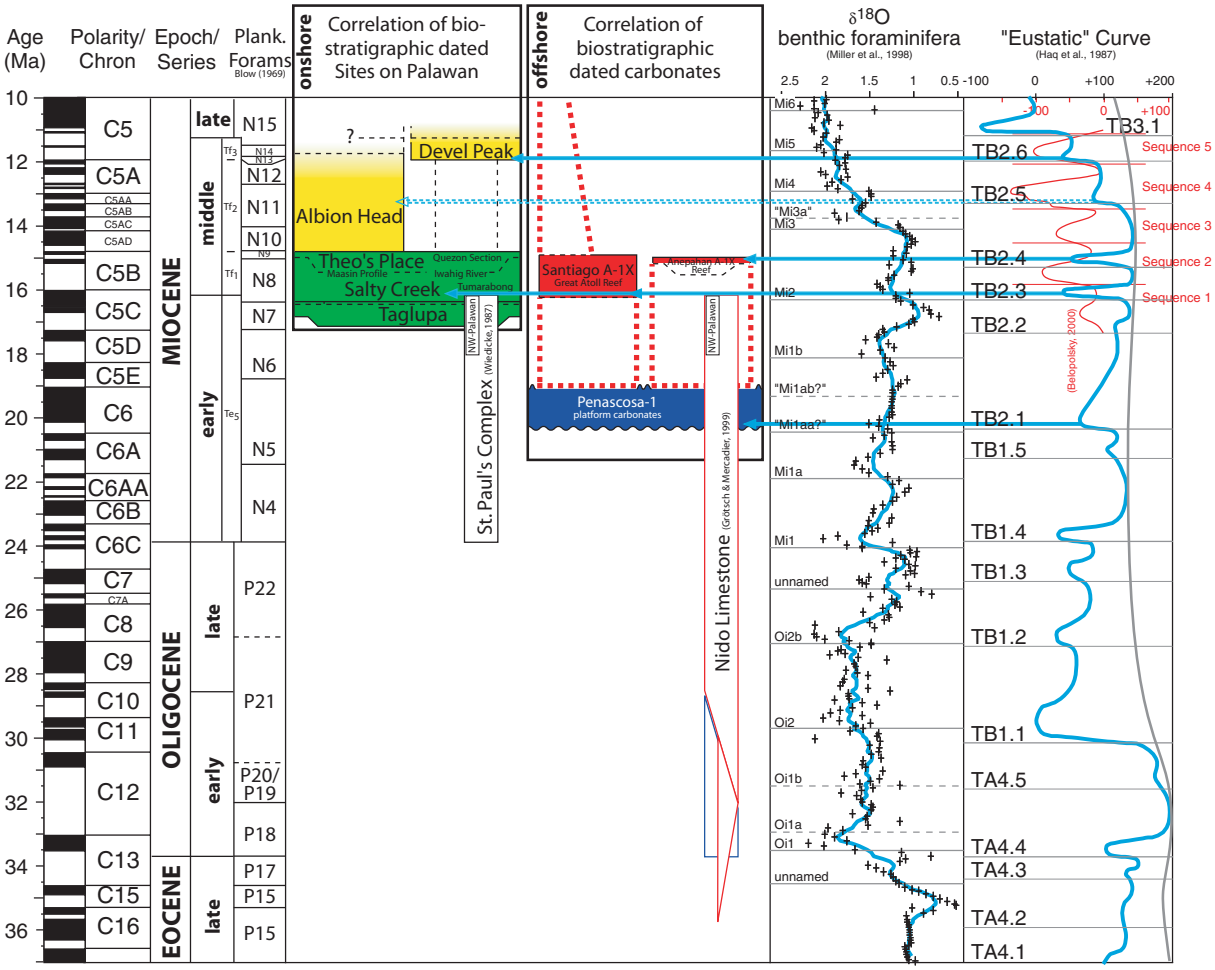

Fig. 81: Time-related on- and offshore sites correlated to published on- and offshore carbonate sites of N-Palawan as well as a $\delta^{18}O$ benthic foraminifera record from the Atlantic (MILLER et al., 1998) together with the Eustatic Curves of HAQ (1987). Low Stand Wedges of Early to Middle Miocene time documented in the depositional record of the study areas. are indicated.

5.3.3 Sea Level Changes

The development of shallow-water carbonate deposits is sensitive to changes in the environmental conditions such as relative sea level changes, wind or current, nutrient content, and water temperature, because they are composed predominantly of biogenic remains. However, the relative sea level is responsible for both, the accommodation space and the sediment supply. Here, the depositional record of the on- and offshore study areas shows that changes in the fossil assemblage, composition and texture of the sediments are closely related to relative sea level changes.

In order to check, if any relationship between the regional relative sea level changes and global sea level changes exists, the well-dated on- and offshore carbonates from SW-Palawan were combined, via the stratigraphy, with the "Eustatic Curve" of HAQ et al. (1987) and a

curve based on a $\delta^{18}O$ record of benthic foraminifera presented by MILLER et al. (1998) (Fig. 81). Thereby, both curves provide a reconstruction of the history of the global sea level. HAQ et al. (1987, 1988) applied the concept of sequence stratigraphy (VAIL et al., 1977) to a global array of proprietary Exxon Production Research data from the Malay-, South Sumatra- and NW Borneo Basins plus other basins not within SE-Asia comprising seismic profiles, wells and outcrops. MILLER et al. (1988) used a deep-sea $\delta^{18}O$ record (>2,000 m) made up of a stacked composition of *Cibicidoides* spp. from several DSDP sites in the Atlantic and Pacific Ocean obtained far from continental margins, which has been smoothed to remove all periods longer than ~1 m.y.. The latter concept based on the fact, that ice preferentially sequesters light oxygen isotopes and therefore the fluctuations of the ice volume cause changes in global seawater $\delta^{18}O$ ($\delta^{18}O_W$). Whereas global $\delta^{18}O_W$ changes are recorded by the benthic and planktonic foraminifera along with variations in seawater temperature and local isotopic composition, deep-water $\delta^{18}O$ records provide a proxy for ice volume and glacioeustatic sea level changes. The correlation of the $\delta^{18}O$ record with shelf-slope sequences, onshore sequences, the Bahamian reflections (EBERLI et al., 1997a) and the inferred eustatic record of HAQ et al. (1987) supports their value (MILLER et al., 1998).

The more recent global deep-sea oxygen isotope record of ZACHOS et al. (2001) includes data of more than 40 DSDP and ODP site and covers the whole Tertiary time. However, even this curve documents in general the same pattern as the curve of MILLER et al. (1998), it is unconsidered here, because it provides less details in the Miocene time, due to a longer time period, which was covered.

The combination of the studied successions from SW-Palawan with the curves indicating eustatic sea level changes yields especially to the "Haq-curve" remarkable analogies between time periods of low stand wedges (sea level low stand) and the observed depositional record in SW-Palawan. Four of the five major sea level drops during the middle Early Miocene to Middle Miocene are documented in the studied successions. Only one sea level low stand has not been observed, but this is most probably related to the limited accessibility of outcrops at Albion Head, rather than to the missing.

The offshore carbonate platform is dated as N5 and a conglomerate at the base of the platform overlies older deposits with a hiatus. This lithology documents the reworking and erosion of the underlying succession, which is most likely related to a relative sea level low stand. With respect to the age, the wide lateral extension and the depositional record, the correlation to the sea level low stand of Tejas B2.1 (TB2.1) of HAQ et al. (1987) seems to be obvious.

The next two sea level low stands indicated by the "Haq-curve" upwards are very significant, because of their short periodicity and high amplitude. Whereas the first sea level drop corresponds to the boundary of the Early to Middle Miocene (N8), the second one is dated as N9. The first sea level low stand of TB2.3 took place while the lower part of Salty Creek Section was deposited. Hence, the widespread significant horizon with large components in a well-bedded packstone matrix, which marks (associated with a relative sea level low stand) the change from a lagoonal to a ramp-like setting in the succession of the lateral extended carbonates onshore, corresponds perfectly to the global sea level low stand proposed by the "Haq-curve". Therefore, these deposits are interpreted as their product. Offshore, this first pronounced sea level low stand might be penetrated only in the well Santiago A-1X. The rapid increase of shales in the carbonates at 10,060 ft KB to a very high content, which was only reached once, might be related to this sea level drop. However, due to the available data set, this interpretation is still subject of speculation.

With respect to the age of the deposits, the second pronounced sea level low stand (TB2.4) is well reported in the uppermost Miocene carbonates of the well section of Anepahan A-1X. There, features of a subaerial exposure are preserved (speleothems, vadose silt, *Microcodium*), which illustrated a sea level low stand without any doubt. Furthermore, in case the first occurrence of dolomite in the time-equivalent carbonates of the well Santiago A-1X are interpreted as an influence of fresh-water, it would support a subaerial exposure of parts of the Great Atoll Reef nearby. The sea level drop at TB2.4 is not documented onshore. The resolution of the dating of the onshore deposits is not detailed enough to decide wether the sea level drop took place in between the deposition of the fine carbonates/ marls of Theo's Place and the development of Albion Head or between the Maasin Profile and Theo's Place. In both cases, there must exist an indication in the onshore study area, but with respect to the outcrop situation in the field, the discovery of any feature of a sea level low stand or a subaerial exposure during Miocene seems to be impossible. However, since the Maasin Profile very calm conditions of deep water exists and makes it hard to imagine that a subaerial exposure occur at any place of the onshore study area. Moreover, it seems to be possible that the deep-water conditions at that time predicted a major impact in the onshore area.

Further on in time, the next low stand wedge indicated by the "Haq-curve" is neither in the offshore nor in the onshore succession clearly observed. Whereas offshore a slight indication exists in the well Penascosa-1 with a 200-ft thick carbonate sequence deposited around 13 Ma in the shale-dominated clastic succession, onshore the missing continuous profile at Albion

Head inhibit the discovery of an evidence eventually.

The last sea level low stand within the Middle Miocene is proposed to be at the boundary of N12 to N13. The carbonates close to the base of Devel Peak are dated as Tf_2/ Tf_3 (= N12/ N13), whereas Devel Peak is formed on a siliciclastic sequence, which documents a regressive event (shales - fine sandstone - conglomerate). The correlation of the onshore observations and the sea level low stand proposed by the "Haq-curve" seems to be reasonable. Offshore, no indications could be identified.

The $\delta^{18}O$ curve of MILLER at al. (1998) reflects changes in the Antarctic ice volume and therefore global sea level changes. It correlates widely with the "Haq-curve". Anyhow, the sea level drop around 13 Ma ago is not reported in Miller's curve, whereas the "Haq-curve" as well as the depositional record offshore SW-Palawan provide clear evidences for a sea level low stand. The low stand wedge of TB2.5 of the "Haq-curve" corresponds neither with the Miocene $\delta^{18}O$ maxima 3, 3a nor 4 (Mi3, "Mi3a", Mi4) of MILLER et al. (1998). However, this event was not observed in the studied successions so that it could not be proved. Despite the offset between the TB2.6 (Haq) and the Mi5 (Miller) sequence boundary, both might be reflected in the depositional record of SW-Palawan. The clear connection between the sea level low stand promoted by HAQ et al. (1987) and the initial carbonate deposition at Devel Peak was already shown. Taking into account that the amplitudes of the $\delta^{18}O$ changes seems to be very small during this time period (MILLER et al., 1998), the coral horizons within the carbonate succession of Devel Peak, which document small (a few meters) sea level changes, are related to the small sea level changes reflected by the $\delta^{18}O$ record.

Besides, a relative sea level curve of the Maldives (Indian Ocean) are reconstructed from prograding sequences based on seismic cross sections (BELOPOLSKY, 2000). However, due to the limited data set and missing time-controls in the study of the Maldives, agreements, at the moment neither to the published records (HAQ et al., 1987; MILLER et al. 1998) nor the depositional record of SW-Palawan, are hardly to draw. (Note: new ODP proposal No 514 of A. Droxler and A. Belopolsky is submitted)

Finally, the perfect correlation of significant depositional horizons in the on- and offshore successions of SW-Palawan exists to the low stand wedges/ sea level low stands of HAQ et al. (1987, 1988). Even if the "Haq-curve" as a benchmark became under severe criticism by MIALL (1992), the application of the curve to the basins of SE-Asia received some qualified support with the statement of HUTCHISON (1986) that the excellent correlation of the eustatic

sea levels with transgressions and regressions in SE-Asia may be an artefact of over-dependence upon SE-Asia basins during the compilation of eustatic curves. Consequently, the observation here leads to the interpretation that the relative sea level changes in the study area are closely related to "global" sea level changes. Nevertheless, the eustatic sea level curve of HAQ et al. (1987) indicates a relative sea level high stand during the Middle Miocene, which shift to a general regressive trend in the late Middle Miocene. Therefore, the trend of deepening demonstrated in the onshore study area as well as the continuous development of the build-ups in the late Middle Miocene refers to some subsidence in the area. Tectonic related movements seem to have no significance, because major faults or fault systems were not observed in the vicinity.

Despite this remarkable relationship between sea level and the carbonate accumulation on- and offshore, the elongation of the Devel Peak - Eastern Ridge structure and the Anepahan A-1X structure in NW - SE direction as well as their comparable morphology with a steep or vertical north-eastern side and a less steep slope to the SW, provide evidence that these build-ups were faced, in general, to the same oceanographic conditions, i.e. ocean currents and prevailing wind direction. The part of a build-up, which is exposed to strongest currents and wave action, has the highest potential of reef growth. Consequently, the observation that all build-ups (Santiago A-1X, Anepahan A-1X and Devel Peak) host their highest peaks toward the NW, suggest the strongest current and/ or wave action from the NW. The steep flanks to the NE at Devel Peak and Anepahan A-1X might be a result of a higher contour-current resulting in a by-pass or erosive margin (SCHLAGER & GINSBURG, 1981). A stronger contour-current could be developed as a result of decreasing water depth eastwards to a landmass, which had forced the NW current to southern directions. The assumption of a dominating NE paleo-wind direction grounds on the south-westwards progradational lobes of reef debris, deposited at the Anepahan A-1X pinnacle reef. These lobes were caused by offbank transportation from the build-up top and upper slope in proximal basinal areas.
Furthermore, due to the different time of development of Devel Peak and Anepahan A-1X, it leads to the assumption that the general oceanographic conditions were stable over several m.y., maybe as result of the S Palawan landmass always in the vicinity.

5.3.4 Over-all-Model

During the middle Early Miocene to the Middle Miocene, sea level fluctuations seem to be the most important control factor the evolution of the shallow water carbonates and the progradation of siliciclastic sequences from the landmass in the vicinity in SW-Palawan. Therefore, the evolution of the on- and offshore study area is illustrated with respect to relative sea level changes in 10 sketches throughout middle Early Miocene to Middle Miocene time (Fig. 82). The synthetic and idealised cross sections run from the study area, which crops out today onshore (right, "onshore study area"), to the offshore area (left), whereas all indicated sites actually are not in line. The model is based on the generated depositional models of both areas as well as detailed observations.

Sketch A: The first cross section illustrates the establishment of the wide spread Miocene carbonate platform (blue) during the drifting phase of the South China Sea upon a basement characterised by a complex system of NE-SW striking horst and half-grabens. The related normal faults of an extensional regime developed in pre-Middle Oligocene time (HINZ & SCHLÜTER, 1985; FULTHORPE & SCHLANGER, 1989). In the well Penascosa-1 the platform carbonates are dated as N5 (middle Early Miocene) and the basinal conglomerate correlates perfectly with the sea level low stand of TB2.1 (HAQ et al. 1987). Nevertheless, seismic data correlated to the Sampaguita well on the Reed Bank (DU BOIS, 1981) indicate the existence of the platform since the Upper Oligocene further off in the South China Sea (HOLLOWAY, 1982; HINZ & SCHLÜTER, 1985), which suggests a prograding of the platform eastwards. Onshore, no time-equivalent depositions are cropping out in the study area so that the existence of platform carbonate somewhere in the bedrock is hypothetical (open blue boxes).

Sketch B: A long continuous transgressive cycle characterised the upper Early Miocene time. The carbonate platform offshore still drowned in the Early Miocene (N5). Probably on top of structural highs, lateral restricted carbonate deposition continued and formed build-ups(red). A still extensional regime results in some normal faults on the outer side of the Great Atoll Reef equivalent as observed by GRÖTSCH & MERCARDIER (1999) in the Block 38,

Fig. 82: Ten hypothetic sketches running from the present-day onshore study area (right) to the offshore study area (left) in the time from middle Early Miocene to Middle Miocene. Sea level change as major mechanism triggers the development of the carbonate areas and resulting a early carbonate platform, which drowned, whereas spatial build-up survive until clastic buried them at different times. The present-day onshore study area was closer to a landmass than the offshore area. ==>

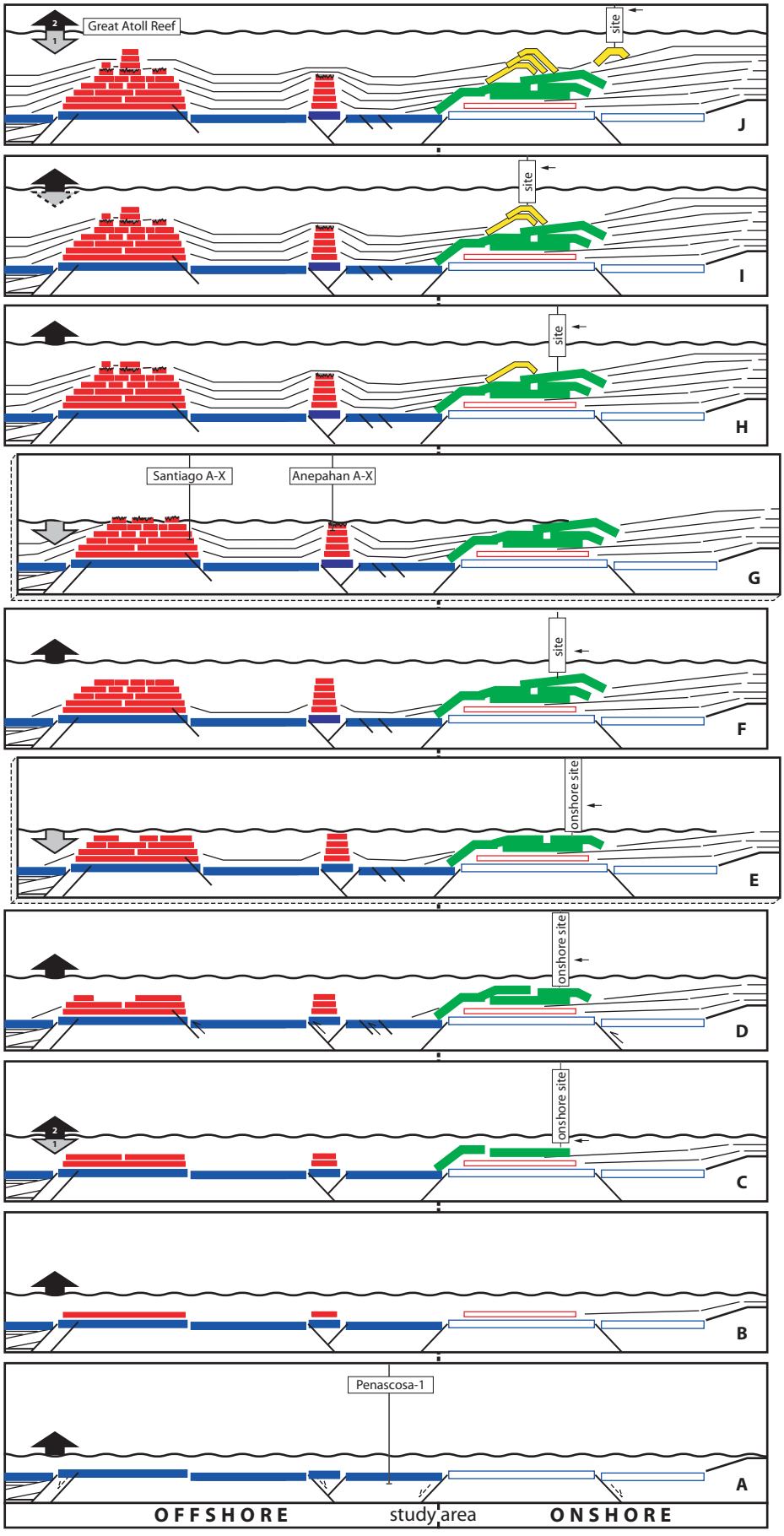

N13-N14 (11.5-12 Ma)
TB2.6 (LSW-TR)
+ Devel Peak (build-up)

N10-N12 (12-14.5 Ma)
TB2.4- TB2.6 (HS-HS)
+ Albion Head (build-up)

N9/N10 (14.8 Ma)
TB2.4 (HS)
+ Theo' Place/ Quezon Section (deeper slope)

N9 (15 Ma)
TB2.4 (LSW)
+ regression Anepahan A-1X exposure offshore

N8 (15.5 Ma)
TB2.3 - 2.4 (TR-HS)
+ Upper Part Salty Creek Section (slope carbonates)

N8 (16 Ma)
TB2.3 (LSW)
+ Transition Lower to Upper Part Salty Creek Section (carbonate+gravel)

N7/N8 (16.5 Ma)
TB2.2/2.3 (HS)
+ Lower Part Salty Creek Section (lagoonal carbonates)

N7 (17 Ma)
TB2.2 (LSW-TR)
+ Taglupa Profile (initial carbonates)

N6 (18 Ma)
TB2.1 (HS)
+ Riff/ Atoll

N5 (20.5 -19 Ma)
TB2.1 (LSW,TR)
Offshore Platform during drift phase

off NW-Palawan. No well drilled these reefal carbonates of late Early Miocene (N6). Onshore, no time-equivalent depositions to these carbonates offshore are cropping out in the study area as well so that the continuation of the carbonate deposition somewhere in the bedrock is hypothetical (open red box). The progradation of siliciclastics from a landmass in the vicinity (thin black) is most probable, but even if shales underlie younger carbonates in the onshore study area, an age-control is missing so that this assumption is not yet proven.

Sketch C: As result of a small sea level fall, followed by a transgressive cycle in the late Early Miocene (N7), the carbonate production was able to catch-up again sea level in some areas (NEUMANN & MACINTYRE, 1985). Therefore, in the present-day onshore area, the lateral extended carbonates (green) established above shales in the vicinity of a shoreline (Taglupa Profile). Offshore the build-ups keep-up with sea level.

Sketch D: With increasing sea level to a high stand level, a lagoonal setting was established in the onshore study area at the boundary of N7 to N8. The carbonates keep-up with the rising sea level during the late early Miocene, whereas in contrast the carbonates of N-Palawan drowned at the end of the Early Miocene (WIEDICKE, 1986; GRÖTSCH & MERCARDIER, 1999). Even if some transpressional movement during the Middle Miocene (like demonstrated in the carbonates offshore NW Palawan, GRÖTSCH & MERCARDIER, 1999) affected the platform carbonates and results in some small-scaled thrusting in the study area offshore, here the survival of the build-ups seems to be independent. In general, the build-ups continue to grow.

Sketch E: This sketch represents the dramatic global sea level drop at the Early-/ Middle Miocene boundary (TB2.3, HAQ et al. 1987). Within the onshore study area it results in a change of the paleoenvironmental conditions from a protected, quiet-water lagoonal environment with about 40 m water depth to an open ramp-like setting, represented by well-bedded foraminiferal sand generated in a few meters of water depth. Before a sharp erosive contact marks the sea level low stand in the field, the increase of carbonate deposits above the deeper lagoonal sediments displays already a sea level fall. Additionally, the sea level fall results in a levelling of some carbonate bodies protecting the earlier lagoon. An associated regression is documented impressively by scattered, cm- to dm-large igneous and sedimentary rocks in the well-bedded carbonate sands level above the erosive contact. Furthermore, the

shift of the shoreline basinwards increases the amount of suspension transported into the ocean. Therefore, even if the sea level low stand probably did not result in a subaerial exposure of the carbonate build-ups offshore, a higher shale content in the well Santiago A-1X might be related to this event.

Sketch F: The rapid sea level rise during TB2.3 (HAQ et al., 1987) up to the same high-stand sea level as before, is documented onshore by the slope sediments, which indicate a deepening upwards. Based on the available data offshore, the development of the carbonate build-ups is subject of speculation. However, with respect to the carbonate further upward in the well section, they were not drowned. But, if not the second sea level drop with again an amplitude of several 10s of meters (HAQ et al., 1987) stopped the tendency of deepening, most of the carbonates on- and offshore were probably drowned.

Sketch G: The pinnacle of Anepahan A-1X was subaerialy exposed during the sea level low stand of TB2.4 (HAQ et al., 1987). The coeval carbonates of Santiago A-1X show no exposure features. But they contain some dolomite, which might be related to a mixed-water zone and therefore indicate some exposure within the carbonate complex of the Great Atoll Reef. In the onshore study area, no evidences of this sea level drop were discovered. The deep water setting in the area during N9 might predict the subaerial exposure. Indications of more shallow water conditions probably occur, but were not observed, because of missing outcrops. Nevertheless, a significant regression is expected, which results in the increasing export of fine material in the offshore basin.

Sketch H: The following, also very rapid sea level rise allows the reinstallation of the deep water setting documented in the sedimentary record of Theo's Place and the Quezon section. If shallow-water carbonates already existed at the beginning of N10, they are limited regarding their extension (undiscovered base of Albion Head). Offshore, the pinnacle reef of Anepahan A-1X was overburden with prograding siliciclastic deposits, like some part of the Great Atoll Reef as well. Anyhow, within the Great Atoll Reef some local reefs continued to grow.

Sketch I: Neither in the offshore, nor in the onshore study area the sea level drop 13 Ma ago is recorded, due to missing sections. Nevertheless, the slight transgression afterwards

allows Albion Head as well as local pinnacles within the Great Atoll Reef to continue their development. The south-westward backstepping of Albion Head, illustrated by the morphology of the carbonate complex, is probably related to the sea level still stand and filling of the accommodation space.

Sketch J: Finally, the significant sea level drop at the Tf_2/ Tf_3 boundary (HAQ et al., 1987) created conditions for the development of an additional build-up in the onshore study area above an intercalation of fine siliciclastic deposits (Devel Peak). The backstepping of the reef bodies or reef fronts south-eastwards continued. Additional, several smaller sea level changes have been observed at Devel Peak. Offshore the number of growing pinnacles within the Great Atoll Reef decreases, but some still grow.
The boundary between Middle and Late Miocene with one of the largest sea level drops within the Cenozoic era, is only observed as erosive surface below N16 in the overburden siliciclastics of all 3 wells offshore. If a subaerial exposure was the reason for the demise of the carbonate build-ups in the onshore area seems to be possible, but remains (eventually always) a subject of speculation.

Referring to this evolution model, the siliciclastic deposits of turbidites discovered on the small islands along the coast of Quezon area and as loose rock samples SW of Albion Head are interpreted as time-equivalent to the carbonates of the onshore study area, even if the age was not proved recently. However, the depositional model offshore demonstrates the coexistence of carbonate accumulation and deep-water deposits nearby and supports the interpretation. As consequence it has to be emphasised that the whole carbonate area discovered onshore was restricted during the Miocene time in western and northern direction by a deeper basin, whereas a landmass to the east limited their extension toward this direction. This leads to the conclusion that the deposits discovered onshore represent an equivalent structure like the Great Atoll Reef, even if the influence by a landmass was probably higher. Thereby, the onshore area provides evidences that these kind of isolated carbonate structures comprise several different facies areas with lagoonal- and ramp-like setting as well as reefs, like postulated for the Malampaya and Camago build-up in the NW of Palawan (GRÖTSCH & MERCADIER, 1999).

6. Miocene Carbonates from SW Palawan in a Global Frame

The Cenozoic equatorial carbonates of SE Asia, and therefore also the carbonates of the Philippines, are quite different to their (sub)tropical and temperate counterparts in a number of important ways (WILSON, 2002). In contrast to most of the Cenozoic carbonate deposition provinces world-wide, the carbonate sedimentation in SE Asia takes place in a number of different tectonic and depositional settings. Hence, it will be important to evaluate the relevance of the observations from the study areas on- and offshore SW Palawan in the context of the Geology of the Philippines, the surrounding offshore region as well as the world-wide occurrence of Miocene carbonate deposits.

6.1 Characteristic of the SW Palawan Carbonates

The carbonates discovered in the study areas on- and offshore SW Palawan (SW Palawan Carbonates) document carbonate precipitation under tropical warm- and shallow-water conditions from the Early Miocene (N5) to the Late Middle Miocene (N14), locally up to the Pliocene (highest Peak of Great Atoll Reef). The carbonates were deposited in protected (locally maybe also restricted) and open marine environments with prevailing low to moderate water energy conditions and shallow water depth, but also in deeper parts of the slope and within a basin. Carbonates form lateral extended ("two-dimensional") deposits and local build-ups with varying dimensions (1 km^2 to a few 10s km^2). Siliciclastic deposits within the carbonate succession were found in both, the shallow water environment as coastal gravel onshore or as higher shale content in the offshore carbonates. Besides, turbidite deposits and deep-sea shales refer to a deeper basin. During the Middle Miocene carbonates and siliciclastics were deposited simultaneously, whereas the late Middle Miocene progradation of the terrestrial influx basinwards terminated carbonate precipitation in most of the isolated carbonate areas. In contrast, the preceding Early Miocene carbonate platform offshore, which occurs throughout the entire South China Sea, drowned already in the Early Miocene (N5).

Neither changes in the regional tectonic setting nor other major tectonics such as faulting or folding affected the SW Palawan Carbonates on- and offshore. Nevertheless, the continuation of the carbonate production in spatially limited areas leads to the assumption that their survival was only possible on some structural highs of the underlying platform. Most probably, subsidence resulted in a continuous deepening during the development of the lateral extended and reefal carbonates. Thereby, not only the development of Albion Head and Devel

Peak during a general regressive trend, but also their backstepping indicates significant subsidence during their time of deposition.

The SW Palawan Carbonates developed on a continental shelf/ continental fragment in the vicinity to the shoreline (Santiago A-1X and Anepahan A-1X) or directly adjacent (onshore area). Strong terrestrial runoff is documented in some levels of the carbonate succession. The studied on- and offshore carbonate area of SW Palawan rifted together with the S-Palawan landmass (CLENNELL, 1996) as one continental block south-eastwards, whereas the isolated carbonate build-ups themselves report no separate motion. Volcanism did not affect the SW Palawan Carbonates. Furthermore, the large-scale oceanographic regime within the open ocean of the South China Sea suggests being generally stable throughout the Cenozoic time in that region. Relative sea level changes as result of eustatic variances of the sea level and subsidence seem to be the most powerful mechanism for controlling carbonate precipitation. It controls the development of the Miocene SW Palawan Carbonates by transgression and regression, which results (1) directly in shallowing- or deepening upwards and thereby the "build-up", "build-out", "build-in" and exposure/ drowning of the carbonates (EPTING, 1980) or (2) indirectly in fluctuations regarding the terrestrial influx.

6.2 SW Palawan Carbonates and the Philippines

Visayan Basin

Within the outlines of the archipelago of the Philippines the most significant Cenozoic carbonates occur in the central part and are, therefore, related to the Visayan Basin. In contrast to the well-established open marine conditions in the South China Sea or the Philippine Sea, the Visayan Basin is as "intercontinental" basin relatively small, restricted and young. The Neogene marine sedimentation in the Visayan Basin occurred around islands, on adjacent shelves and in intervening basinal areas (MÜLLER et al., 1989a; CARROZI, 1995). It was strongly influenced by multiple tectonic phases (RANGIN et al., 1989). Due to the position of the Visayan Basin in the mobile belt of the Philippines with complex tectonic and several emerged landmasses, the carbonates are often associated with siliciclastics and volcanic material. Furthermore, the sedimentary successions are characterised by rapid lateral and vertical facies changes, related to tectonics, eustasy and variation in clastic input (MÜLLER et al., 1989b).

With the exception of three small, local and questionable Eocene limestone exposures, the lowermost proved marine deposits within the Visayan Basin are siltstones with some remnants of bioclastic limestones of the Lutak Hill Limestone Formation on Cebu (JURGAN & DOMINGO, 1989), which are dated as Middle Oligocene (NP23/ 24). This coincides with the time of the establishment of the basin (MÜLLER et al., 1989b).

Overlying the thin transgressive clastics are upper Oligocene to lower Miocene bioclastic carbonates deposited in a shallow-water carbonate platform environment with localised patch reefs and isolated low-relief build-ups that interfinger with mixed carbonate-clastic shelves. Many of these shallow-water carbonates pass laterally into time-equivalent resedimented slope deposits or deeper water lithologies of the outer neritic to bathyal environment. These Oligo-Miocene limestones were discovered on Negros (Trankalan Limestone), Cebu (Cebu Limestone), Leyte (Kantaring Limestone), Masbata (Mountain Maid Limestone), Burias (San Pascual Formation) and Panay (Dingle Formation) (CORBY et al., 1951; PORTH et al., 1989). On the eastern Islands of the Visayan Basin (Leyte, Masbate and Burias), these carbonates are additionally associated with volcanoclastics. Beside the lateral variation of facies, FORONDA (1994) provides the best example of an evolution of carbonate development within the Visayan Basin on the base of the late Oligocene to early Miocene Cebu- and Malubog Formation of Cebu. These deposits represent the sedimentary filling of the central part of the early Visayan Basin with a lower coal member, the Cebu Limestone and the overlying mudstones, siltstones and sandstones of the Malubong Formation (FORONDA, 1994). The whole succession throughout the late Oligocene to early Miocene time represents the transgressive evolution from the eustatic sea level lowstand at 30 Ma to a relative high stand at 22 Ma (HAQ et al., 1988; FORONDA, 1994). The first short-term transgressive cycle is documented by a coal facies. The overlying carbonates of the Cebu Limestone show a continuous transgression with wacke- to packstones deposited in a lagoonal setting. They are succeeded by foraminifera pack- to grainstones or rudstones, which are interpretated as sediment accumulations of shallow shoals occurring in a sublittoral environment affected by currents of different strength (JURGAN & DOMINGO, 1989; FORONDA, 1994). Above hemipelagic deposits (lime mud) on a deeper slope are documented, before finally the carbonates are burdened by fine siliciclastics in a deep-water environment (FORONDA, 1994). The combination of rising sea level and rapid subsidence led to the deepening of the depositional environment and finally the demise of the carbonates (FORONDA, 1994). Even if

the conformably overlying mudrocks exist, a significant terrestrial influx does not seem to be the mechanism, which triggered the demise of the carbonates.

After the demise of the late Oligocene to early Miocene carbonates, extensive shallow-water to slope carbonates (latest Early Miocene to the Middle Miocene) developed, which coincide with significant volcanism. These time equivalent deposits to the SW Palawan Carbonates on Cebu, bearing the Uling Limestone. It is made up of hard, dense biocalcarenites and biomicrites, developed in shallow-marine environment mainly as coral-shoal, back-reef or lagoonal facies (JURGAN, 1980). Outcrops of a fore-reef facies and small reef bodies are limited onshore. Offshore in the N Tañon Strait, the Tubaran-1X well drilled a time equivalent build-up (unpubl. Data DOE). Platform and reefal carbonates of the Uling Limestone reach up to the late Middle Miocene (N14), before the area was probably exposed. In many areas of the Visayan Basin parts of the Middle Miocene deposits are missing due to tectonic uplift and erosion (MÜLLER et al., 1989a; RANGIN et al., 1989). The latest Middle Miocene time was a period of little carbonate sedimentation due to considerable influx of siliciclastics and volcanic material or non-deposition related to exposure.
The carbonate deposition in the Visayan Basin during the uppermost Miocene to the Pliocene is related to the initiation of block faulting during the Late Miocene, forming basinal grabens and structural highs associated with a general shallowing in the region (MÜLLER et al., 1989b). Shallow-water carbonates or build-ups are passing laterally into slope or deeper water marls.

In general, three significant carbonate periods are documented in the Visayan Basin during Cenozoic time. The carbonate development is characterised by the relative small basins with its narrow shelves, terrestrial influx and volcanism. Whereas these factors limit the extension of carbonate production, tectonic activity in the Visayan Basin resulted in both, the triggering of the carbonate establishment (Late Miocene) as well as their demise (early Miocene drowning, late Middle Miocene exposure).
Compared to the SW Palawan Carbonates the carbonate development in the Visayan Basin was affected by a number of additional factors, which do not exist (volcanism, tectonic, smaller/ limited basin) or have minor impact (terrestrial runoff) during the carbonate development in SW Palawan. However, even if some of the external factors are for the Visayan Basin and the SW Palawan Carbonates different, the general characteristics of their

development are similar in the onshore study area in SW Palawan and in the Visayan Basin. The time equivalent Uling Limestone discovered on Cebu shows similarly the establishment of carbonate production, followed by a platform setting, which ends up in a reefal stage. But, due to a lack of detailed studies of the Uling Limestone, this correlation is very lean. The depositional model for the Miocene carbonate development of the Visayan Basin (CAROZZI, 1976, 1995) suggests reefs as wave-resistant, constructional barrier and atoll systems along the edge of the narrow shelves associated with tidal channels and lower energy back-reef areas. This model does not apply completely to the Palawan study area. Because in contrast, the SW Palawan Carbonates developed, presumably as spatial limited area, on a carbonate platform in a vicinity or adjacent to a shoreline, but not directly attached to it.

The detailed study of the late Oligocene to early Miocene deposits on Cebu (FORONDA, 1994) provide a good database for comparison with our study, despite some differences regarding the time of development and some depositional characters (e.g. Cebu: coal member at the base, higher terrestrial influence, more extended). In both areas, the general evolution from a lagoonal to a deeper slope environment with finally a deep marine cover is documented by equivalent carbonate deposits. Most significant is the existence of foraminifera sands in both areas, which follows on top the lagoonal setting. Furthermore, some internal variances related to eustatic sea level changes and the overall deepening throughout the succession are observed in both areas. However, a reefal stadium, like in SW Palawan (Albion Head, Devel Peak), close to the demise of the platform carbonates was not emphasised in the Visayan Basin. This might lead to the conclusion that the sea level rise and a stronger subsidence drowned the carbonates in the Visayan Basin, whereas the SW Palawan Carbonates were buried by siliciclastics (offshore area).

Despite several different influences the carbonate development and their overall depositional record predominately seems to be dependent on the relative (or eustatic) sea level. In that context, the SW Palawan Carbonates provide an interesting data set, which is linked directly to the highest amplitude of sea level fluctuations, due to the lack of tectonic influence.

Beside the Visayan Basin only the offshore area of NW Palawan was subject of more detailed studies of Cenozoic carbonates (cf. chapter 6.3), whereas the existence of additional outcrops was mentioned, but not investigated in detail. Therefore, efficient correlations are not possible.

6.3 SW Palawan Carbonates and the Offshore Carbonates

The SW Palawan Carbonates were studied in an area closely related to the hydrocarbon-bearing province of SE Asia, which spans around the southern coasts of the South China Sea from N Palawan to Borneo/ Sarawak, the Malay Peninsula, Thailand and Vietnam. Additional discoveries were made in Sumatra, Java, E Borneo and Sulawesi. All together, the total hydrocarbon reserves of SE Asia are estimated between 31 to 35 billion barrels of oil (bbls) and between 207 to 281 trillion standard cubic feet (Tscf) of gas (SHAW, 1990; NATION, 1994; LONGLEY, 1997). Cenozoic carbonates are the major target within several of these hydrocarbon provinces. The SW Palawan Carbonates are situated close to the new hydrocarbon productive field from an Early Miocene build-up in NW Palawan. It may offer, therefore, a useful example that can be compared to the carbonate provinces of the eastern South China Sea, the Lucian Province and the new discoveries from Vietnam.

6.3.1 Eastern South China Sea

Close to the study area in SW Palawan, the lower Miocene carbonate build-ups of the NW Palawan offshore area trap estimated 3.3 Tscf of gas underlain by an oil leg of 120 million barrels of gas and condensate (MOZETIC et al., 2000). This setting allows the first and until now, the only significant commercial oil-production in the Philippines. During the eighties small oil and gas discoveries from fractured lower Miocene carbonate build-ups in approximately 6,800 ft depth (~2,070 mSS) within the Nido B field were developed, beside small and less significant Miocene sandstone oil fields in the region (LONGMAN & BROWNLEE, 1980; DOWNEY, 1990). In October 2001 the commissioning of the production from the first large-scaled deep water gas field (water depth ~820 mSS, top of reservoir at about 2,700 mSS) proceeded in the Philippines. The reservoir rocks are shallow water carbonates of the Oligo-Miocene Malampaya-Camago build-up (Nido Limestones) within the Block SC 38 NW off Palawan (MOZETIC, et al., 2000; GRÖTSCH & MERCADIER, 1999; Shell Philippines Exploration B.V. press releases, autumn 2001). However, several build-ups of the region were drilled and found to be non-commercial or even dry. This might not only be related to porosity and/ or permeability problems within the carbonates, but also could result from possible leakages in the overburden clastics (DOWNEY, 1999).

At the eastern margin of the South China Sea, the NW - SE extensional basin associated with block faulting formed a rugged sea floor topography overlain by broad late Early Oligocene Nido platform carbonates (HINZ & SCHLÜTER, 1985; FULTHORPE & SCHLANGER, 1989; GRÖTSCH & MERCADIER, 1999). The distribution and orientation of the highs and lows dictated still the position of the carbonate build-ups during the Late Oligocene to Early Miocene, whereas the build-ups are often bounded by Eocene normal faults (LONGMAN, 1985; GRÖTSCH & MERCADIER, 1999). This primary early tectonic control was succeeded by a Middle Miocene rejuvenation and tectonic inversion of the normal faults by transpressional movements. This resulted eventually in some thrust faults and affected the oceanward margin of the build-ups and the overburden clastics (GRÖTSCH & MERCADIER, 1999). Furthermore, GRÖTSCH & MERCADIER (1999) show for the Malampaya-Camago build-up that the aggradational and backstepping build-up development was mainly a result of a rapid sea level rise. This is illustrated on the landward margin by an abrupt disappearance of *Halimeda* sp., concomitant with the income of reefal bioclasts (corals, sponges). This was interpreted as a major backstepping of the landward margin associated with a change of the depositional environment from a shallow-water platform interior to slope facies (GRÖTSCH & MERCADIER, 1999). Despite the general transgressive trend, sea-level fluctuations still may have caused temporary exposures. However, beside the sea level control of the growth history of the build-up, the distribution of a number of different facies zones (reef-, back-reef-, lagoonal-, shoals-, slopes facies) and the topographic outline of the build-up are strongly related to ocean currents and swells as well as prevailing wind directions. Therefore, the major reef framework and the steep flank (by-passing or erosive margin, SCHLAGER & GINSBURG, 1981) on the western and oceanward facing side refers to the influence of currents and swells. Lobes of reef debris in south- to south-western direction indicated a prevailing wind direction from the NE (GRÖTSCH & MERCADIER, 1999). The carbonate deposition ends in the Early Miocene. Thereby, both, a high terrestrial influx, and a preceding drowning before the deposition of the deep-water clastic cover seems to be possible. Based on the descriptions there is no significant argument of drowning in sense of SCHLAGER (1981, 1989). Because no clear time gap or a hardground, which separates shallow-water carbonates from overlying deep-marine deposits, seem to exist, such as described in many examples (e.g HINE & STEINMETZ, 1984; SALLER et al., 1993; ERLICH et al., 1990).

Neither the underlying platform carbonates (Early Oligocene) nor the build-up stage (Late Oligocene to Early Miocene) were affected by volcanism or significant terrestrial influx, even if deep-water clastics surround the spatial carbonate build-ups already in the Miocene.

Throughout wide parts of the eastern South China Sea, the Nido Limestones typify the key stratigraphic sequence. The base usually marks the late Early/ Middle Oligocene boundary and the top upper Late Oligocene to Early Miocene boundary (e.g. KUDRASS et al., 1986; SCHLÜTER et al., 1996; GRÖTSCH & MERCADIER, 1999). So the offshore NW Palawan carbonates developed exactly during the first larger transgressive cycle of HAQ et al. (1987, 1988) from 30 to 21 MA, i.e. they were established during the sea-level lowstand after one of the most significant sea-level drops during the Cenozoic. In contrast, the carbonate development on local topographic highs in the area of the Reed Bank (N) and the Dangerous Grounds (S), located further westwards offshore in the South China Sea, continued their growth up to the Middle Miocene or locally even to the present (SCHLÜTER et al., 1996). This suggests that tectonics and different rates of subsidence in block-faulted areas are able to overrule the strong influence of sea-level changes. Because in the open marine setting of these isolated carbonate plateaus on old continental fragments from the China main continent around 140 and 190 sea miles off Palawan no other influence (e.g. terrestrial runoff, volcanism) has affected the carbonate production. The development of the carbonates represents an interaction between tectonics, subsidence and sea-level fluctuations only.

The late Early Oligocene to Early Miocene carbonates of the Nido Limestones in NW Palawan as well as the Reed Bank and the Dangerous Grounds do not represent time-equivalents to the Early Miocene to Late Miocene SW Palawan. However, both the Nido Limestones and the SW Palawan Carbonates established themselves after a substantial sea-level drop: the Nido Limestones at 30 Ma, the SW Palawan Carbonates at 20.5 Ma. Furthermore, after the demise of the platform carbonates in the Reed Bank and Dangerous Grounds areas the platform development probably shifted with the sea level drop to the previously deeper part of the Palawan Trough, where the platform development survived for a shore time period until 19 Ma. Likewise in offshore regions of the South China Sea again spatial limited carbonate build-ups on structural highs catch-up with sea level rise and continued to develop until the Middle Miocene, Late Miocene or locally the Pliocene time

(Great Atoll Reef). Even if subsidence affected the carbonate development of the SW Palawan Carbonates as well, tectonic activities had no impact.

As additional feature, the outline of the topography of the build-ups in the NW Palawan offshore area, interpreted as a link to prevailing ocean currents or wind directions (GRÖTSCH & MERCADIER, 1999), would suggest that in the study area in SW Palawan a prevailing NE wind existed. The strongest oceanic current probably hit the build-ups from northern directions, which might be related to a contour-current along the N-S elongate shelf of the S Palawan landmass.

6.3.2 The Luconia Province, Offshore NW Borneo

The Luconia Province, offshore Sarawak (Malaysia) on Borneo, is with 240 km^2 one of the largest SE-Asian carbonate provinces with more than 200 platforms and build-ups. The carbonates were formed on top of a block-faulted continental fragment ("Lucionia Shoals", CLENNELL, 1996) mainly during the Early- to Middle Miocene, whereas some pinnacle might reach the Late Miocene (EPTING, 1980; NOAD, 2001). Today more than 40 build-ups have been tested, and contain an estimated 40 Tscf of gas reserves (VAHRENKAMP, 1998; NOAD, 2001). In the vicinity toward the NW, the Middle- to Upper Miocene build-up of the Natuna Platform exists in an almost similar setting as the Luconia Province on the same continental fragment (MAY & EYLES, 1985; RUDOLPH & LEHMANN, 1989; DUNN et al., 1996). The Agip well AL-1X encountered within the studied build-up 1,600 m of porous, gas productive carbonates of the Terumbu Formation as well (RUDOLPH & LEHMANN, 1989).

Both, Luconia Province and the Natuna Platform are closely related to a shelf area of a landmass (EPTING, 1980; VAHRENKAMP et al., 2000; MAY & EYLES, 1985). However, a probably more narrow shelf area related to the Luconia Province resulted in a content of terrestrial material (clay) up to 10% in some carbonate levels and, additionally, the demise in the Upper Miocene was possibly also associated with an increase in clastic input into the region (EPTING, 1980). In contrast, the Natuna Platform carbonates contain usually less than 1% detrital clay, so that higher amounts are local and rare. This observation reflects the dominance of a carbonate shelf nearby. Within the Luconia Province carbonates were deposited from the late Early Miocene to the early Late Miocene (~18 to ~10 Ma) (VAHRENKAMP, 1998; NOAD, 2001). The studied Terumba Carbonates in the Natuna Platform indicates for the early period up to a hiatus an age from 16.5 Ma to 9.8 Ma (Lower Terumba

Carbonates) before the carbonate deposition ends at 5.4 Ma (Upper, reefal Terumba Carbonates) (MAY & EYLES, 1985). In general, the characteristics of the depositional patterns in both areas are almost similar. Thereby, the eustatic sea level changes and local tectonics mainly control the development of the carbonates. EPTING (1980) identified, beside repeated subaerial exposures observed in many build-ups, 4 different depositional environments including protected-, reefal-, shallow open-marine- and deeper open-marine settings, which lead to the definition of sequences reflecting "build-up", "build-out", "build-in" and submerged stadiums as responds to sea level fluctuations. As well, a close relationship between sea level and depositional record are presented from the Terumbu Carbonates, which leads to 9 depositional sequences (RUDOPH & LEHMANN, 1989; DUNN et al., 1996). Anyhow, oceanic currents and prevailing paleo-wind directions additionally modify the deposits and result at the Natuna Platform in a significant by-pass platform margin at the seaward side and a depositional margin on the opposite side (SCHLAGER & GINSBURG, 1981; MAY & EYLES, 1985; VAHRENKAMP, 2000).

The carbonate development NW offshore Borneo represents a time-equivalent carbonate development to the study area of SW Palawan. Moreover, the setting in the vicinity of a landmass agrees well. The main difference seems to be the strong tectonic activity in the area offshore Borneo, which did not exist in SW Palawan. With the exception of the Anepahan A-1X pinnacle reef structure no exposure was observed in SW Palawan, whereas in contrast repeated exposures were reported for build-ups of the Luconia Provinces as well as the hiatus in the carbonate succession of the Terumba Carbonates. This observation leads to the assumption that the SW Palawan Carbonates are deposited in a slightly deeper paleoenvironment or if the amplitude of the sea level fluctuations was smaller is subject of speculation.

6.3.3 Offshore Vietnam

The outstanding position of the offshore area of Vietnam refers to a variety of carbonate accumulation types: Platforms, characterised by broad areas of essentially flat carbonates, small build-ups, typically 1-2 km across, large build-ups, typically 5-10 km across, pelagic carbonates, developed on structural highs and less common high pinnacle reef structures

overlying a block-faulted basement (MAYALL et al., 1997). These carbonates developed from Middle Miocene to Lower Pliocene (MATTHEWS et al., 1997).

The comparison of the carbonates offshore Vietnam to the SW Palawan Carbonates documents, similar to the other carbonate provinces around the South China Sea, in general the same mechanisms controlling the depositional environments such as sea level fluctuations, terrestrial influx, tectonic, subsidence, as well as oceanic currents and prevailing paleo-wind directions. These results in almost similar rock types, where foraminiferal packstones of the shallow-water platform- and slope areas, framestones related to reefal structures and wacke- or mudstones representing deeper quiet-water environment of a lagoonal setting or basin are reported. The main difference is the common observation of subaerial exposure in the carbonates from the offshore area of Vietnam (MAYALL et al., 1997), which is a rare feature in the SW Palawan Carbonates. It is also remarkable that the small build-ups (1-2 km across) are described as 'rooted in the underling platform facies without any prominent structural control' (MAYALL et al., 1997, p. 117). This example of the lack of usual tectonic influence during the establishment of the build-up supports the observations made in the SW Palawan Carbonates, where tectonic influence is also missing. OLSON & DOROBEK (2000) highlight the style and significance of structural inversion, which corresponds also across the South China Sea to the observation of GRÖTSCH & MERCADIER (1999) made in the offshore carbonates of NW Palawan; equivalents were not observed in SW Palawan.

In conclusion, around the South China Sea the tropical shallow-water carbonates occur mainly in the time window of Late Oligocene to Middle/ Late Miocene, whereas some local build-ups might grow until the present. The carbonate production is primary controlled by the relative sea level fluctuation. However, it is the sum of the eustatic sea level changes, subsidence and tectonic. During the Cenozoic time both the eustatic sea level curve (HAQ et al., 1988) documents substantial changes (HAQ et al., 1987) and the South China Sea was a highly tectonic active area. Most of the carbonates were affected by a pre-sedimentary, block-fault related, rugged topography as well as locally syn-sedimentary by the rejuvenation and inversion of old normal fault systems during a transpressive regime, which affected the flanks of some build-ups. In contrast to the preceding mechanisms sea level, subsidence and tectonic, which act constructive as well as destructive on the carbonate production, the terrestrial influx as the fourth important controlling factor obstructs the carbonate

development. All additional primary mechanisms associated with the creation of the Oligo-Miocene carbonates such as water energy and circulation, light, nutrients or biological activities resulted in spatial differences, but had no existential influence on the development of the Cenozoic carbonates in the South China Sea region.
Most of the authors describe the demise of the carbonate development in the South China Sea as a drowning event, often only based on the observation that carbonates are overlain by deep-water clastics. Neither a time gap between the clastics nor the indication that the "drowned" carbonates are shallow-water deposits nor the existence of a hardground or condensed sequence are provided to support this interpretation. Therefore, it seems to be possible that the demise of several carbonates is strongly pushed by an increasing terrestrial runoff. However, in sense of SCHLAGER (1981) drowning of carbonate platforms or reefs were defined as an event where relative sea level outpaces carbonate accumulation, which excludes termination of carbonate growth by terrestrial influx. Nevertheless, the existence of well-studied drowning sequences within the South China Sea are provided by ERLICH et al. (1990) from the Pearl River Mouth Basin, off China. Several wells including core sections and seismic surveys provide good evidence that a rapid facies change at the top of the Liuhua Platform, a condensed sequence, spanning up to 3.3 m.y. as well as overlying glauconitic, shaly limestone-silts represent the drowning of this platform.

Within this setting of the South China Sea, the SW Palawan Carbonates have an outstanding position. The general features of the depositional record of the SW Palawan Carbonates correspond without exceptions to the observations described around the South China Sea. However, the mechanisms, which triggered significantly their development are reduced to the eustatic sea level fluctuations and a continuous subsidence. Tectonics, like in all other areas, have no or only very low impact on the carbonate development. This provides (a) the opportunity to study eustatic sea level changes and (b) might allow the link between the major Cenozoic carbonate provinces world-wide, all characterised by passive continental margins with low tectonic activities, and the SE Asia region.

6.4 SW Palawan Carbonates: Their Implication World-wide

The Bahama Banks are the classic example of an isolated platform system. Their development started at the Cretaceous/ early Tertiary time with their fragmentation followed by the

coalescence of the smaller banks from Middle Eocene to Middle Miocene to one large platform (MELIM & MASSAFERRO, 1997; EBERLI & GINSBURG, 1989; MASAFERRO & EBERLI, 1994). However, the investigations concentrate mainly on the geometrical platform evolution from Miocene to recent time as respond to sea-level changes rather than on detailed studies of their development throughout the Miocene. Furthermore, the sizes of the Bahama Banks and the general different setting (tectonic, geographical position, no terrestrial influx) are different in nature than the SW Palawan Carbonates. Nevertheless, the relationship of sea-level fluctuations and carbonate development or models of resulting geometries provide useful coherences for the interpretation of the SW Palawan Carbonates (cf. chapter 5).

The best-studied examples of Miocene carbonates outside the Indo-Pacific are known from the Mediterranean region. Especially POMAR (e.g. 1991, 2001a/b) with his investigations of the Balearic Islands provides a number of detailed carbonate sedimentological observations with respect to sea-level changes and their implication for sequence stratigraphy. Mallorca Island as central objective of the studies has a basin-range configuration that resulted from extensional faulting during the Late Miocene to Early Pleistocene (POMAR & WARD, 1995). The NE-trending thrust sheets characterise horst blocks of the Alpine foldbelt forming the mountain range of the island. These are a product of NW thrusting during Early- to Middle Miocene (RAMOS-GUERRERO et al., 1989). The Upper Miocene to Pleistocene platform deposits of the Alcudia -, Santanyí - and Llucmajor Platform are attached to the highlands and onlap to the folded Mesozoic to Middle Miocene rocks. The so-called "Reef Complex" is one of the three Upper Miocene units, which documents a part of a reef-rimmed carbonate shelf that generally prograded westwards across the Llucmajor Platform (POMAR, 1991, 1993). Within the Reef Complex four main lithofacies were distinguished: lagoon/ back reef-, reef core-, reef slope/ fore reef- and open shelf/ shallow basin facies, whereas the carbonate development was not affected by a significant terrestrial runoff. Some beach deposits and foreshore deposits are restricted to the inner lagoon (POMAR, 1991). Sea-level changes model the geometry of the platform deposits. The reef front shows aggradation during sea-level rise and basinwards progradation during sea-level high- and lowstands. As could be expected erosional surfaces including exposures occurred during sea-level fall (POMAR, 1991).

In terms of biogenic responds and therefore different lithofacies as well as changes in the geometry, sea-level fluctuations are defined as the main controlling factor of the carbonate development in the area of the Balearic Islands. This applies also for the SW Palawan Carbonates. However, beside the slight time offset (Mallorca = Upper Miocene, SW Palawan

Carbonates = Middle Miocene), the general setting is quite different and illustrates especially one significant difference between equatorial and temperate carbonates. Even if the Llucmajor Platform is attached to a mountain range (high relief = primary high potential of erosion), the terrestrial influx is low due to the temperate climate resulting in less erosion. In contrast, the SW Palawan Carbonates are positioned in an equatorial-humid climate and thus in some levels are strongly affected by terrestrial runoff. Consequently, carbonates like those in the Visayan Basin (e.g. FORONDA, 1994), which developed as attached platforms in the equatorial region, are usually characterised by a carbonate-siliciclastic mixed system. This leads to an important aspect of the SE Asian carbonates, which are often affected by terrestrial influx: the demise of these carbonates is not only defined by a relative sea level rise. Often increasing terrestrial influx buried the carbonates. Finally, this mostly fine siliciclastic cover could act as seal on top of potential carbonate reservoir rocks and is, hence, one of the reasons of the successful hydrocarbon exploration in SE Asia.

7. Conclusion

The study of several newly discovered outcrops around Quezon in the SW of Palawan Island (Philippines) supplemented by a subsurface survey in the adjacent offshore area allows the reconstruction of the history of Early to Middle Miocene carbonate deposits. The investigation is the first example of Middle Miocene carbonates W of Palawan interpreted in time and space.

The investigation mainly designed as onshore study, focuses on a SW-NE elongated carbonate area of about 16 km by maximal 5 km. Most of the outcrops are placed on the eastern flank of a shallow and NNE-SSW stretching synclinal structure. No relevant tectonic displacements neither vertical nor horizontal disturb the sedimentary succession and folding does not exist. Therefore, the area offers the possibility to study an almost complete undisturbed Miocene carbonate profile.

The stratigraphic control of the succesion relies on larger foraminifera and planktonic foraminifera as well as some nannoplankton. As a result the lowermost strata from the Taglupa Profile is attributed to the late Early Miocene (N7), because of the joint occurrence of *Miogypsinoides* and *Flosculinella bontangensis*. The overlying and (according to the resolution of the biostratigraphic scales) almost complete succession of lateral extended carbonates corresponds to the Middle Miocene age. The uppermost lateral extended carbonates found at Theo's Place represent a stratigraphic level of N9 indicated by *Orbulina*, *Praeorbulina*, *Globigerina* and *Globigerinopsis*. The lowermost part of the Albion Head build-up has been dated as N10 to N12 and documents that the carbonate sedimentation continous locally after the demise of the lateral extended carbonates. In contrast, the carbonates at Devel Peak build-up were deposited during N13. Anyhow, due to the missing age control of the upper strata of Albion Head, the correlation between the both reefal structures is still unclear. However, the whole carbonate succession onshore with the best-estimated total thickness of 900 to 1,000 m is interpreted as being formed during one single period of carbonate deposition.

With the exception of the reefal structures Albion Head and Devel Peak, all outcrops are related to the 650-m thick succession of lateral extended carbonates (in contrast to build-up carbonates). The composition of the carbonates documents a general trend of deepening in time throughout the succesion: Massive grainstones including gravels of a shoreline in the

vicinity mark the establishment of the carbonate deposits during a relative sea level low stand at the base of the succession. Packstones, wackestones and (coral-)floatstones are related to a lagoonal setting during a transgressive system track. After a significant regression, the foraminifera grainstones or packstones are deposited on an upper slope. Finer packstones and later on fine, monotonous mud- to wackestone with variable content of shales show quiet water conditions of deeper water on the lower slope or within the basin due to ongoing flooding. Furthermore, the foraminiferal assemblages reflect additionally the deepening with a shift from a dominance of Alveolinoidae and Soritidae to Amphisteginidae, Nummulitidae and Lepidocyclinidae. The uppermost strata of the deep-water areas contain, instead of larger foraminifera, only planktonic foraminifera.
Whereas the deepening of the paleoenvironment led to a demise of the lateral extended carbonates, the reefal carbonates track the sea level rise. At Albion Head carbonates were continuously accumulated. In contrast, the reefal build-up of Devel Peak was established after a regressive event above an intercalation of deep-water siliciclastics.

The onshore succession shows significantly the trend of deepening, whereas the termination of these carbonates could not be defined. Neither a characteristic drowning sequences (cf. ERLICH et al., 1990) nor a cover of terrestrial material are preserved onshore.

Offshore, biostratigraphic data indicate that widely spread and well defined platform carbonates were established between Early Oligocene time further offshore in the South China Sea (KUDRASS et al., 1986) and Early Miocene time (N5) as documented in the well Penascosa-1. This well demonstrates significantly the drowning of the Miocene carbonate platform in the Early Miocene (N5) by a hiatus of 3 nannoplankton zones between the carbonates and the overlying later deep-water clastics. Coevally the carbonate accumulation continued in spatial limited areas of structural highs and resulted in isolated build-ups. The dimensions of their base vary from 10 to 600 km^2 and their height varies from 900 m (Anepahan A-1X) to 2,400 m (Great Atoll Reef). In contrast to the drowned underlying carbonate platform, the build-ups were buried by clastic, mostly in the Middle Miocene.

The detailed biostratigraphic data on- and offshore results in the connection of both study areas and the general depositional model, which includes (1) the development and later drowning of a preceding Oligo-Miocene carbonate platform, (2) the subsequent growth of

isolated build-ups until the middle Miocene or some single pinnacles until the Pliocene and (3) the basinward progradation of clastics covering the build-up carbonates during the Middle Miocene and persisting until recent time.
Whereas offshore the complet succession is documented by seismics and wells, onshore the shallow to deeper water carbonates developed between late Early to Middle Miocene time. Accordingly, the whole onshore area is interpreted as an additional large, isolated build-up such as the Great Atoll Reef structure. The coeval depositional history and the almost similar dimensions support the interpretation.

Besides the depositional history, the diagenetic impact on the deposits is dominated by a moderately pronounced burial diagenesis. Early diagenetic processes affecting the SW Palawan Carbonates are minimal in the depositional environment. Subaerial exposure is only observed locally in the offshore well Anepahan A-1X indicated by speleothems, vadose silt, *Microcodium* and the occurrence of dolomite. However, the leaching and the resulting in non-fabric selective open porosity in the well Santiago A-1X refers also to some meteoric or mixed water influence close to the sea surface. It suggests that exposure is a more common feature in build-up structures than observed in the available data base. The grain size and the terrestrial content suggest to be the responsible factors for the development of the porosity in the studied carbonates.

<u>In summary, this detailed study of the Miocene carbonates from SW Palawan provides:</u>

- a detailed carbonate sedimentological study based on a number of so far unknown outcrops in SW Palawan;
- a detailed biostratigraphic study on- and offshore SW Palawan resulting in an on-/ offshore correlation;
- the first onshore equivalent to offshore build-ups W off Palawan and therewith insights of the facies development of the isolated build-ups;
- the reconstruction of regional sea-level fluctuation and their correlation to the eustatic curve (HAQ et al., 1987);
- an example of non- or low tectonic influenced carbonate development in SE Asia;
- the definition of the termination of the carbonate depositions (drowning vs. overburden terrestrial influx);
- a depositional model from Oligocene to recent time for the Palawan trough.

With the exception of environmental parameters such as light, nutrients, temperature, salinity, local oceanic currents and the substratum, carbonate platforms and reefal growth commonly track relative sea level fluctuations. This leads to the conclusion, that carbonates show a so far similar pattern of depositional environments and therefore resulting rock types. However, whereas tectonic and subsidence as further possible influences are directly connected to changes of the relative sea level, the significant effects of terrestrial influx proposed to be the key to the own peculiarity of each carbonate deposition center. It results in different primary facies and because of that varying potential of preservation or corrosion throughout time. As final conclusion, the terrestrial content in carbonates has substantial relevance for the successful exploration of economical resources such as drinking water or hydrocarbon from carbonate reservoirs, especially in the equatorial region of SE Asia with high terrestrial runoff.

8. References

Abreu, V.S. and Anderson, J.B. (1998): Glacial eustasy during the Cenozoic: sequence stratigraphic implication. - AAPG Bull., 82(7): 1385-1400.

Ahr, W.M. (1973): The carbonate ramp: an alternative to the shelf model. - Transactions of the Gulf Coast Association of Geological Societies, 23: 221-225.

Albert, O. and Droxler, A.W. (1991): Growth, partial drowning and recovery of the Maldives shallow carbonate system, established in the early Eocene on the volcanic trail of the Reunion hot spot (equatorial Indian Ocean). - Geological Society of America, Annual Meeting, 1991, Abstracts with Programs, 22: 67.

Alonso-Zarza, A.M., Esther Sanz, M., Calvo, J.P., and Estevez, P. (1998): Calcified root cells in Miocene pedogenic carbonates of the Madrid Basin; evidence for the origin of Microcodium b. - Sedimentary Geology, 116(1-2): 81-97.

Anderson, T.F. and Arthur, M.A. (1983): Stable isotopes of oxygen and carbon and their application to sedimentologic and paleoenvironmental problems. In: M.A. Arthur, T.F. Anderson, I.R. Kaplan, J. Veizer, and L.S. Land (eds.), Stable isotopes in sedimentary geology. SEPM Short Course, 10. Society of Sedimentary Geology, Tulsa, 1-151 pp.

Aubert, O. and Droxler, A.W. (1992): General Cenozoic evolution of the Maldives carbonate system (equatorial Indian Ocean). - Bull. Centre Rech. Explor.-Prod. Elf-Aquitaine, 15(1): 113-136.

Aubert, O. and Droxler, A.W. (1996): Seismic stratigraphy and depositional signatures of the Maldives carbonate system (Indian Ocea). - Marine Petrol. Geol., 13(5): 503-536.

Aurelio, M.A., Barrier, E., Rangin, C., and Müller, C. (1991): The Philippne Fault in the late Cenozoic tectonic evolution of the Bondoc - Masbate - N. Leyte area, central Philippines. - Journal of SE Asian Earth Sciences, 6: 221-238.

Austin Jr., J.A., Christie-Blick, N., Malone, M.J., and et al. (1998): Proc. ODP, Init. Repts., 174A: College Station, TX (Ocean Drilling Program).

Bartek, L.R., Vail, P.R., Anderson, J.B., Emmet, P.A., and Wu, S. (1991): Effect of Cenozoic ice sheet fluctuations in Antarctica on the stratigraphic signature of the Neogene. - J. Geophys. Res., 96(B4): 6753-6778.

Bathurst, R.G.C. (1975): Carbonate sediments and their diagenesis. - Developments in sedimentology, 12. Elsevier Scientific Publishing Co., Amsterdam, 658 pp.

Belopolsky, A.V. (2000): Tectonic and eustatic controls on the evolution of the Maldive carbonate platform. - PhD Thesis, Rice University, Houston, 267 pp.

Betzler, C. (1997): Ecological controls on geometries of carbonate platforms: Miocene/ Pliocene shallow-water microfaunas and carbonate biofacies from Queensland Plateau (NE Australia). - Facies, 37: 147-166.

Betzler, C., Brachert, T.C., and Kroon, D. (1995): Role of climate in partial drowning of the Queensland Plateau carbonate platform (northeastern Australia). - Mar. Geol., 123(1-2): 11-32.

Betzler, C., Kroon, D., Gartner, S., and Wei, W. (1993): Eocene to Miocene chrono-

stratigraphy of the Queensland Plateau: Control of the climate and sea level on platform evolution. In: J.A. McKenzie, P.J. Davies, A. Palmer-Julson, and et al. (eds.), Proc. ODP, Sci. Results, 133: College Station, TX (Ocean Drilling Program), 281-289 pp.

Billups, K. and Schrag, D.P. (2002): Paleotemperatures and ice volume of the past 27 Myr revisited with paired Mg/Ca and $^{18}O/^{16}O$ measurements on benthic foraminifera. - Paleoceanography, 17(1): 1-11.

Blow, W.H. (1969): Late Middle Eocene to Recent planktonic foraminiferal biostratigraphy. - 1st Internat. Conf. on Planktonic Microfossils, Geneva, Switzerland, 1969: 199-422.

Bosence, D.W.J. (1991): Coraline Algae: mineralization, taxonomy, and palaeoecology. In: R. Riding (ed.), Calcareous algae and stromatolites. Springer-Verlag, Berlin - Heidelberg - New York - London, 98-113 pp.

Bosworth, W. and McClay, K. (2001): Structural and stratigraphic evolution of the Gulf of Suez Rift, Egypt; a synthesis. - Memoires du Museum National d'Histoire Naturelle, 186: 567-606.

Bouma, A.H., Normark, W.R., and Barnes, N.E. (1986): Submarine fans and related turbidite systems. - Springer-Verlag, New York, 351 pp.

Bransden, P.J.E. and Matthews, S.J. (1992): Structural and stratigraphic evolution of the East Java Sea, Indonesia. - Indonesian Petroleum Association, Proceedings 21st Annual Convention: 417-453.

Buchbinder, B. (1996): Miocene carbonates of the eastern Mediterranean, the Red Sea and the Mesopotamian Basin; geodynamic and eustatic controls. - Concepts in Sedimentology and Paleontology, 5: 89-96.

Camoin, G.F. (2001): Paleoceanology of reefs and carbonate platforms: Miocene to modern. - Palaeogeogr. Palaeoclimatol. Palaeoecol., 175: 1-6.

Carew, J.L. and Mylroie, J.E. (1997): Geology of the Bahamas. In: H.L. Vacher and T.M. Quinn (eds.), Geology and hydrogeology of carbonate islands, Elsevier Scientific Publishing Co., Amsterdam, 91-139 pp.

Carozzi, A.V. (1995): Depositional models and reservoir properties of Miocene reefs, Visayan Islands, Phillippines. - Journal of Petroleum Geology, 18(1): 29-48.

Carozzi, A.V., Reyes, M.V., and Ocampo, V.P. (1976): Microfacies and microfossils of the Miocene reef carbonates of the Philippines. - Special Publication Philippine Oil Development Company, 1: 1-79.

Carter, J.G. (1990): Skeletal biomineralisation: paterns, processes and evolutionary trends. - 1. Van Nostrand Peinhold, New York, 832 pp.

Chaproniere, G.C.H. (1975): Palaeoecology of Oligo-Miocene larger foraminiferida, Australia. - Alcheringa, 1: 37-58.

Choquette, P.W. and James, N.P. (1987): Diagenesis #12. Diagenesis in Limestones - 3. The deep burial environment. - Geoscienes Canada, 14(1): 3-35.

Choquette, P.W. and Pray, L.C. (1970): Geologic nomenclature and classification of porosity in sedimentary carbonates. - AAPG Bull., 54(2): 207-250.

Clennell, M.B. (1996): Far-field and gravity tectonics in Miocene basins of Sabah, Malaysia.

In: R. Hall and D.J. Blundell (eds.), Tectonic evolution of Southeast Asia. Geolological Society Special Publication, London, 106, 307-320 pp.

Corby, G.W. and et al. (1951): Geology and oil possibilities of the Philippines. - Techn. Bull. Dept. Agr. and Natur. Res., 21: 367.

Cosico, R., Gramann, F., and Porth, H. (1989): Larger foraminifera from the Visayan Basin and adjacent areas of the Philippines (Eocene through Miocene). In: H. Porth and C.H. von Daniels (eds.), On the geology and hydrocarbon prospects of the Visayan Basin, Philippines, 70. BGR, Hannover, 147-205 pp.

Craig, H. and Gordon, L.I. (1965): Isotopic oceanography-deuterium and oxygen 18 variations in the ocean and the marine atmosphere, Symposium on marine geochemistry, 3. Occasional Publication - University of Rhode Island, Rhode Island, 277-374 pp.

Cucci, M.A. and Clark, M.H. (1993): Sequence stratigraphy of Miocene carbonate buildups, Java Sea. In: R.G. Loucks and J.F. Sarg (eds.), Carbonate sequence stratigraphy, recent developments and applications. Memoir, 57. American Association of Petroleum Geologists, Tulsa, 291-303 pp.

Daly, M.C., Cooper, M.A., Wilson, I., Smith, D.G., and Hooper, B.G.D. (1991): Cenozoic plate tectonics and basin evolution in Indonesia. - Marine Petrol. Geol., 8: 2-21.

David Jr., S., Stephan, J.-F., Delteilb, J., Müller, C., Butterlind, J., Bellone, H., and Billedoa, E. (1997): Geology and tectonic history of Southeastern Luzon, Philippines. - J Asian Earth Sci., 15(4-5): 435-452.

Davies, P. and Edgewood, D. (1994): Evolution of the Great Barrier Reef. - Australian Geologist, 92: 21-24.

Davies, P.J., Symonds, P.A., Feary, D.A., and Pigram, C.J. (1989): The evolution of the carbonate platforms of northeast Australia. In: P.D. Crevello, J.L. Wilson, J.F. Sarg, and J.F. Read (eds.), Controls on Carbonate Platform and Basin Development, 44. Spec. Publ. - Society of Economic Paleontologists and Mineralogists, 233-258 pp.

de Smet, M.E.M. (1992): A guide of the stratigraphy of Sumatra, Part 2: Tertiary. Research in SE Asia Internal Report, London University, London.

Deines, P. (1980): The isotopic composition of reduced organic carbon. In: P. Fritz and J.C. Fontes (eds.), Handbook of environmental isotope geochemistry. The terrestrial environment, A, 1. Elsevier Scientific Publishing Co., Amsterdam, 329-406 pp.

Dickson, J.A.D. and Coleman, M.L. (1980): Changes in carbon and oxygen isotope composition during limestone diagenesis. - Sedimentology, 27: 107-118.

Dorobek, S.L. (1997): Miocene carbonate platforms of the South China Sea region; tectonic controls on platform inception and termination. - American Association of Petroleum Geologists and Society of Economic Paleontologists and Mineralogists, Annual Meeting 1997, Abstracts & Program, 6: 29.

Downey, M.W. (1990): Criteria for successful exploration for Miocene reef production in the Philippines. - AAPG Bull., 74(6): 971.

Droxler, A.W. and Schlager, W. (1985): Glacial versus interglacial sedimentation rates and turbidite frequency in the Bahamas. - Geology, 13(11): 799-802.

Du Bois, E.P. (1981): Review of principal hydrocarbon bearing basins of the South China Sea area. - Energy, 6(11): 1113-1140.

Dunham, R.J. (1962): Classification of carbonate rocks according to depositional texture. In: W.E. Ham (ed.), Classification of carbonate rocks, 1. Mem. Am. Ass. Petrol. Geol., Tulsa, 108-121 pp.

Dunn, P.A., Kozar, M.G., and Budiyono, J. (1996): Application of geoscience technology in a geologic study of the Natuna gas field, Natuna Sea, offshore Indonesia. - Proceeding of the 25th Annual Convention of the Indonesian Petroleum Association, 1996, 25: 117-130.

Eberli, G.P. and Ginsburg, R.N. (1987): Segmentation and coalescence of Cenozoic carbonate platforms, northwestern Great Bahama Bank. - Geology, 15(1): 75-79.

Eberli, G.P. and Ginsburg, R.N. (1988): Aggrading and prograding infill of buried Cenozoic seaways, northwestern Great Bahama Bank. In: A.W. Bally (ed.), Atlas of seismic stratigraphy, v. 2. AAPG Studies in Geology, 27. American Association of Petroleum Geologists, Tulsa, 97-103 pp.

Eberli, G.P. and Ginsburg, R.N. (1989): Cenozoic progradation of northwestern Great Bahama Bank, a record of lateral platform growth and sea-level fluctuations. In: P.D. Crevello, J.J. Wilson, J.F. Sarg, and J.F. Read (eds.), Controls on carbonate platform and basin development. Special Publication, 44. SEPM Society for Sedimentary Geology, Tulsa, 339-351 pp.

Eberli, G.P., Swart, P.K., and Malone, M. (1996): The record of Neogene sea-level changes on the slopes of western Great Bahama Bank; results from ODP Leg 166. - Geological Society of America, 28th annual meeting, Denver, 1996, 28: 43.

Eberli, G.P., Swart, P.K., Malone, M.J., and et al. (1997a): Proc. ODP, Init. Repts., 166: College Station, TX (Ocean Drilling Program).

Eberli, G.P., Swart, P.K., McNeill, D.F., Kenter, J.A.M., Anselmetti, F.S., Melim, L.A., and Ginsburg, R.N. (1997b): A synopsis of the Bahamas Drilling Project: results from two deep core borings drilled on the Great Bahama Bank. In: Eberli, G.P., Swart, P.K., Malone, M.J., and et al. (eds.), Proc. ODP, Init. Repts., 166: College Station, TX (Ocean Drilling Program), 23-42 pp.

Embry, A.F. and Klovan, E.J. (1972): Absolute water depth limits of Late Devonian paleoecological zones. - Geol. Rundsch., 61(2): 672-686.

Epting, M. (1980): Sedimentology of Miocene carbonate Buildups, Central Luconia, offshore Sarawak. - Bull. Geol. Soc. Malaysia, 12: 17-30.

Erlich, R.N., Barrett, S.F., and Bai Ju, G. (1991): Drowning events on carbonate platforms; a key to hydrocarbon entrapment? - Proceedings of Offshore Technology Conference, 1: 101-112.

Erlich, R.N., Barrett, S.F., and Ju, G.B. (1990): Seismic and geologic characteristics of drowning events on carbonate platforms. - AAPG Bull., 74(10): 1523-1537.

Erlich, R.N., Longo Jr., A.P., and Hyare, S. (1993): Response of carbonate platform margins to drowning; evidence of environmental collapse. In: R.G. Loucks and J.F. Sarg (eds.), Carbonate sequence stratigraphy; recent developments and applications. AAPG Memoir,

57. American Association of Petroleum Geologists, Tulsa, 241-266 pp.

Fernandez, J.C. (1981): Geological Map of the Philippines. Bureau of Mines & Geo-Sciences, Manila.

Flügel, E. (1978): Mikrofazielle Untersuchungsmethoden von Kalken. - Springer-Verlag, Berlin - Heidelberg - New York, 454 pp.

Foronda, V.J. (1994): Sequence stratigraphy of a Oligocene-Miocene mixed siliciclastic-carbonate system, Visayan Basin, Central Cebu. - Bonner Geowissenschaftliche Schriften, 11. Rheinische Friedrich-Wilhelms-Universität Bonn, Bonn, 152 pp.

Frakes, L.A., Francis, J.E., and Syktus, J.I. (1992): Climate modes of the Phanerozoic: The history of the earth's climate over ther past 600 million years. - Cambridge University Press, Cambridge, 274 pp.

Frank, D., Carpenter, A.B., and Oglesby, T.W. (1982): cathodoluminescence and composition of calcite cements in the Taum Sauk limestone /Upper Cambrian), Southeast Missouri. - J. Sediment. Petrol., 52: 631-638.

Frykman, P. (1986): Diagenesis in Silurian bioherms in the Klinteberg Formation, Gotland, Sweden. In: J.H. Schroeder and B.H. Purser (eds.), Reef diagenesis. - Springer-Verlag, Berlin - Heidelberg - New York, 399-423 pp.

Fulthorpe, C.S. and Schlanger, S.O. (1989): Paleo-Oceanographic and Tectonic Settings of Early Miocene Reefs and Associated Carbonates of Offshore Southeast Asia. - AAPG Bull., 73(6): 729-756.

Gallagher, J.J. (1987): Philippine microplate tectonics and hyfrocarbon exploration. - Transactions of the 4th Circum Pacific Energy and Mineral Resouces Conference, Singapore, 1987, : 103-119.

Garrison, R.E., Espiritu, E., Horan, L.J., and Mack, L.E. (1979): Petrology, sedimentology, and diaggensis of hemi pelagic limestone and tuffaceous turbidites in the Aksitero Formation, Central Luzon, Philippines. - Unites States Geologiocal Survey, Professional Paper, 1112: 16.

Geel, T. (2000): Recognition of stratigraphic sequences in carbonate platform and slope deposits; empirical models based on microfacies analysis of Palaeogene deposits in southeastern Spain. - Palaeogeogr. Palaeoclimatol. Palaeoecol., 155(3-4): 211-238.

Ghosh, A.K. (2002): Cenozoic coralline algal assemblage from southwestern Kutch and its importance in palaeoenvironment and palaeobathymetry. - Current Science, 83(2): 153-158.

Ginsburg, R.N. (2001): Subsurface geology of a prograding carbonate platform margin, Great Bahama Bank: Results of the Bahamas Drilling Project. - Special Publication, 70. SEPM Society for Sedimentary Geology Special Publication, Tulsa, 271 pp.

Greenlee, S.M., Schroeder, F.W., and Vail, P.R. (1988): Seismic stratigraphic and geohistory analysis of Tertiary strata from the continental shelf off New Jersey; calculation of eustatic fluctuations from stratigraphic data. In: R.E. Sheridan and G.J. A. (eds.), The Atlantic continental margin; U.S. The geology of North America, . Geol. Soc. Am., (Decade of North American Geology), Boulder, 437-444 pp.

Grötsch, J. and Mercadier, C. (1999): Interated 3-D reservair modeling based on 3-D seismic: The Tertiary Malampaya and Camago buildups, offshore Palawan, Philippines. - AAPG Bull., 88(11): 1703-1728.

Grover Jr., G. and Read, J.F. (1983): Paleoaquifer and deep burial related cements defined by regional cathodoluminescence pattern, Middle Ordovician Carbonates, Virginia. - AAPG Bull., 67: 1275-1303.

Habermann, D., Neuser, R.D., and Richter, D.K. (2000): Quantitative high resolution spectral analysis of Mn^{2+} in sedimentary calcite. In: M. Pagel, V. Barbin, P. Blanc, and D. Ohnenstetter (eds.), Cathodoluminescence in Geosciences. Springer-Verlag, Berlin - Heidelberg - New York, 331-358 pp.

Hall, R. (1996): Reconstructing Cenozoic SE Asia. In: R. Hall and D.J. Blundell (eds.), Tectonic evolution of Southeast Asia. Geological Society Special Publications, 106. Geological Society of London, London, 153-184 pp.

Hall, R. (1997): Cenozoic plate tectonic reconstructions of SE Asia. In: A.J. Fraser, S.J. Matthews, and R.W. Murphy (eds.), Petroleum Geology of Southeast Asia. Geological Society Special Publications, 126. Geological Society of London, London, 11-23 pp.

Hall, R. (1998): The plate tectonic of Cenozoic SE Asia and the distribution of land and sea. In: J.D. Holloway and R. Hall (eds.), Biogeography and Geological Evolution of SE Asia. Backbuys Publushers, Leiden, 99-131 pp.

Hall, R. (2002): Cenozoic geological and plate tectonic evolution of SE Asia and the SW Pacific: computer-based reconstructions, model and animations. - J Asian Earth Sci., 20(4): 353-431.

Hall, R., Ali, J.R., and Anderson, C.D. (1995): Cenozoic motion of the Phillipine Sea Plate: palaeomagnetic evidence from eastern Indonesia. - Tectonics, 14(5): 1117-1132.

Hall, R. and Wilson, M.E.J. (2000): Neogene sutures in eastern Indonesia. - J Asian Earth Sci., 18: 781-808.

Hallock, P. and Glenn, E.C. (1986): Large foraminifera; a tool for paleoenvironmental analysis of Cenozoic carbonate depositional facies. - Palaios, 1(1): 55-64.

Hamilton, W. (1979): Tectonics of the Indonesian region. - U.S. Geol. Survey Prof. Pap., 1078: 1-345.

Hanshaw, B.B., Back, W., and Dieke, R.G. (1971): A geochemical hypothesis for dolomitization by groundwater. - Econ. Geol., 66: 710-724.

Hanzawa, S. and Hashimoto, W. (1970): Larger Foraminifera from the Philippines, Part 1; contributions to the Geology and Palaeontology of Southeast Asia, LXXXVI. - Geol. Palaeont. Southeast Asia, 8: 187-230.

Haq, B.U., Hardenbol, J., and Vail, P.R. (1987): Chronology of fluctuating sea levels since the Triassic. - Science, 235: 1156-1167.

Haq, B.U., Hardenbol, J., and Vail, P.R. (1988): Mesozoic and Cenozoic chronostratigraphy and cycles of sea-level change. In: C. Wilgus, B.S.K. Hastings, C.A. Ross, H.W. Posamentier, J. van Wagoner, and C.G.S.C. Kendall (eds.), Sea-level changes; an integrated approach. Special Publication - Society of Economic Paleontologists and

Mineralogists, 42. SEPM Society for Sedimentary Geology Special Publication, Tulsa, 72-108 pp.

Hashimoto, W. (1981): Geologic development on the Philippines. - Geol. Palaeont. Southeast Asia, 22: 83-170.

Hashimoto, W. and Matsumaru, K. (1982): Large foraminifera from the Philippines, part XIV. On some larger foraminifera-bearing rocks from Palawan. - Geol. Palaeont. Southeast Asia (Tokyo), 24: 39-44.

Hashimoto, W. and Matsumaru, K. (1984): Mesozoic and Cenozoic larger foraminifera of the Philippines and references to those found from Borneo by the APRSA's palaeontological reconnaissance. - Geol. Palaeont. Southeast Asia, 25: 147-166.

Hashimoto, W., Matsumaru, K., Kurihara, K., David, P.P., and Balce, G.R. (1977): Larger foraminiferal assemblages useful for the correlation of the Cenozoic marine sediments in the mobile belt of the Philippines. - Geol. Palaeont. Southeast Asia, 18: 103-123.

Henderson, B. and Imbusch, G.F. (1989): Optical spectroscopy of inorganic solids. - Clarendon Press, Oxford, 645 pp.

Hine, A.C. and Steinmetz, J.C. (1984): Cay Sal Bank, Bahamas; a partially drowned carbonate platform. - Mar. Geol., 59(1-4): 135-164.

Hinz, K., Roeser, H.A., Icay, W., Kudrass, H.R., and Wiedicke, M. (1983): Abschlußbericht über die Arbeiten am Projekt Geowissenschaftliche Untersuchungen mit MS SONNE (Fahrt SO-23) in der Sulu See und dem Südchinesischen Meer. Abschlussbericht, BGR, Hannover, Germany.

Hinz, K. and Schlüter, H.U. (1985): Geology of the Dangerous Grounds, South China Sea, and the continental margin off Southwest Palawan; results of Sonne cruises SO-23 and SO-27. - Energy (Oxford), 10(3-4): 297-315.

Holloway, N.H. (1982): North Palawan Block, Philippines; its relation to Asian mainland and role in evolution of South China Sea. - AAPG Bulletin, 66(9): 1355-1383.

Hughes, G.W. and Varol, O. (1982): The biostratigraphy of the Phillips Philippines Anepahan A-1X well, and sidetrack, drilles offshore west Palawan, Philippines. unpubl. report No. 1106, Robertson Research (Singapore).

Hutchison, C.S. (1986): Tertiary basins of S.E. Asia - their diseparate tectonic origins and eustatic stratigraphic similarities. - Geological Society of Malaysia Bulletin, 19: 109-122.

Isern, A.R., Anselmetti, F.S., Blum, P., and Party, L.S. (2001): ODP Leg 194: Sea level Magnitudes recorded by continental margin sequences on the Marion Plateau, Northeast Australia. - Joides Journal, 27(2): 7-11.

Isern, A.R., McKenzie, J.A., and Feary, D.A. (1996): The role of sea-surface temperature as a control on carbonate platform development in the western Coral Sea. - Palaeogeogr. Palaeoclimatol. Palaeoecol., 124(3-4): 247-272.

James, J.P. and Bone, Y. (1991): Origin of cool-water, Oligo-Miocene deep shelf limestone, Eucla Platform, southern Australia. - Sedimentology, 38: 323-341.

James, N.P. and Ginsburg, R.N. (1979): The seaward margin of Belize barrier and atoll reefs. - Special Publications, Int. Ass. Sediment., 3, 191 pp.

Joachimski, M.M. (1991): Stabile Isotope (C, O) und Geochemie der Purbeck-Mikrite in Abhängigkeit von Fazies und Diagenese (Berriasian/Schweizer und Französischer Jura, Südengland). - Erlanger geologische Abhandlungen, 119: 1-114.

Johnson, C.C., Barron, E.J., Kauffman, E.G., Arthur, M.A., Fawcett, P.J., and Yasuda, M.K. (1996): Middle Cretaceous reef collapse linked to ocean heat transport. - Geology, 24: 376-380.

Jordan Jr., C.F. (1990): An overview of Miocene Reefs. - AAPG Bull., 74: 688.

Jurgan, H. (1980): Geology and hydrocarbon prospects of the Visayan Basin. Appendix III: Younger Teriary carbonate rocks. unpubl. report, , Rep. Bur. of Energy Development, Manila.

Jurgan, H. and Domingo, R.M.A. (1989): Younger Tertiary limestone formations in the Visayan Basin, Philippines. In: H. Porth and C.H. von Daniels (eds.), On the geology and hydrocarbon prospects of the Visayan Basin, Philippines, 70. BGR, Hannover, 207-275 pp.

Katz, B.J. and Kelley, P.A. (1987): Central Sumatra and East African Rift lake sediments: An organic geochemical comparison. - Proceeding of the 16th Annual Convention of the Indonesian Petroleum Association, 16: 259-274.

Kidwell, S.M. and Holland, S.M. (1991): Field description of coarse bioclastic fabrics. - Palaios, 6: 426-434.

Kiessling, W. (2001): Paleoclimatic significance of Phanerozoic reefs. - Geology, 29(8): 751-754.

Kiessling, W. and Flügel, E. (2000): Late Paleozoic and Late Triassic limestones North Palawan Block (Philippines): Microfacies and paleogeographical implications. - Facies, 43: .

Kudrass, H.R., Wiedicke, M., Cepek, P., Kreuzer, H., and Müller, P. (1986): Mesocoic and Cenozoic rocks dredged from South China Sea (Reed Bank area) and Sulu Sea and their significance for plate-tectonic reconstructions. - Marine Petrol. Geol., 3: 19-30.

Land, L.S. and Goreau, T.F. (1970): Submarine lithification of Jamaican reef. - J. Sediment. Petrol., 40: 457-462.

Lee, T.-Y. and Lawver, L.A. (1994): Cenozoic plate reconstruction of South China Sea region. - Tectonophysics, 235: 149-180.

Levitus, S. and Boyer, T.P. (1994): World Ocean Atlas 1994 Volume 4: Temperature. - NOAA Atlas NESDIS, 4. U.S. Department of Commerce, Washington, D.C..

Longley, I.M. (1997): The tectonostratigraphic evolution of SE Asia. In: A.J. Fraser, S.J. Matthews, and R.W. Murphy (eds.), Petroleum Geology of Southeast Asia, 126. Geological Society Special Publication, 311-339 pp.

Longman, M.W. (1985): Fracture porosity in reef talus of a Miocene pinnacle-reef reservoir, Nido B Field, the Philippines. In: P.O. Roehl and P.W. Choquette (eds.), Carbonate Petroleum Reservoirs. Springer, New York, 547-560 pp.

Longman, M.W. and Brownlee, D.N. (1980): Characteristics of karst topography, Palawan, Philippines. - Zeitschrift für Geomorphologie, 24(3): 299-317.

Masaferro, J.L. and Eberli, G.P. (1994): Structural control on the evolution of a carbonate

platform along a compressional plate boundary, southern Great Bahama Bank. - Geological Society of America, Annual meeting, 1994, 26(7): 364-365.

Matthews, S.J., Fraser, A.J., Lowe, S., Todd, S.P., and Peel, F.J. (1997): Structure, stratigraphy and petroleum geology of the southeast Nam Con Son Basin, offshore Vietnam. In: A.J. Fraser, S.J. Matthews, and R.W. Murphy (eds.), Petroleum Geology of SE Asia. Special Publication, 126. Geological Society of London, London, 89-106 pp.

May, J.A. and Eyles, D.R. (1985): Well log and seismic character of Tertiary Terumbu carbonate, South China Sea, Indonesia. - AAPG Bull., 60(9): 1339-1358.

Mayall, M.J., Bent, A., and Roberts, D.M. (1997): Miocene carbonate buildups offshore Socialist Republic of Vietnam. In: A.J. Fraser, S.J. Matthews, and R.W. Murphy (eds.), Petroleum Geology of SE Asia. Special Publication, 126. Geological Society of London, London, 117-120 pp.

McArthur, J.M. (1994): Recent trends in strontium isotope stratigraphy.- Terra Nova, 6: 331-358.

McArthur, J.M., Howarth, R.J., and Bailey, T.R. (2001): Strontium isotope stratigraphy: LOWESS version 3: Best fit to the marine Sr-isotope curve for 0-509 Ma and accompanying Look-up table for deriving numerical age. - J. Geol., 109: 155-170.

McKenzie, J.A. and Davies, P.J. (1993): Cenozoic evolution of carbonate platforms on the northeastern Australian margin; synthesis of Leg 133 drilling results. - Proc. Ocean Drill. Progr., Sci. Results, 133: 763-770.

Melim, L.A. and Masaferro, J.L. (1997): Geology of the Bahamas: Subsurface geology of the Bahamas Banks. In: H.L. Vacher and T.M. Quinn (eds.), Geology and hydrogeology of carbonate islands. Elsevier Scientific Publishing Co., Amsterdam, 161-182 pp.

Miall, A.D. (1992): Exxon global cycle chart: An event for every occasion? - Geology, 20(9): 787–790.

Miller, K.G., Mountain, G.S., Browning, J.V., Kominz, M., Sugarman, P.J., Christie-Blinck, N., Katz, M.E., and Wright, J.D. (1998): Cenozoic global sea level sequences and the New Jersey Transect: Results from coastal plain and slope drilling. - Reviews of Geophysics, 36: 569-601.

Milliman, J.D. (1974): Marine Carbonate. - Springer, Berlin - Heidelberg - New York, 375 pp.

Mitchell, A.H.G., Estacio, R., Flores, R., Lazo, E., Manuel, E., Salvado, H., and Santiago, A. (1985): Geology of cental Palawan. - The Phillipine Geologist, 39(5): 1-43.

Mitchell, A.H.G., Hernandez, F., and Dela Cruz, A.P. (1986): Cenozoic evolution of the Philippine Archipelago. - Journal of Southeast Asian Earth Sciences, 1: 3– 22.

Morley, R.J. (1998): Palynological evidence for Tertiary plant dispersals in the SE Asian region in relation to plate tectonics and climate. In: R. Hall and J.D. Holloway (eds.), Biogeography and Geological Evolution of SE Asia. Backhuys Publishers, Leiden, 211-234 pp.

Mountain, G.S., Miller, K.G., and Blum, P. (1994): New Jersey continental slope and rise. - JOIDES Journal, 20(1): 9-13.

Mozetic, A., Bausa, G.J.G., and Ocampo, I.U. (2000): The Malampaya deep water gas to power project. - Annual Meeting American Association of Petroleum Geologists, New Orleans, 2000, Program & Abstracts: 102-103.

Müller, C. and von Daniels, C.H. (1981): Stratigraphical and paleoenvironmental studies (Oligocene - Quarternary) in the Visayan Basin, Phillipines. - Newsl. Stratigr., 10(1): 52-64.

Müller, C., von Daniels, C.H., Cepek, P., Gramann, F., Bausa, G.J.G., and Leon, M.M.d. (1989a): Biostratigraphy and paleoenvironment studies in the Tertiary of the Visayan Basin, Philippines. In: H. Porth and C.H. von Daniels (eds.), On the geology and hydrocarbon prospects of the Visayan Basin, Philippines, 70. BGR, Hannover, 89-145 pp.

Müller, C., Jurgan, H., and Porth, H. (1989b): Paleogeographic outlines of the Visayan Basin. In: H. Porth and C.H. von Daniels (eds.), On the geology and hydrocarbon prospects of the Visayan Basin, Philippines, 70. BGR, Hannover, 303-315 pp.

Nation, L. (1994): Ideas shared at K.L. Meeting. - AAPG Explorer Magazine, 10: 28-29.

Neumann, A.C. and Macintyre, I. (1985): Reef response to sea level rise: Keep-up, Catch-up or Give-up. - Proceeding of the Fifth International Coral Reef Congress, Tahiti, 1985, 3: 105-110.

Noad, J. (2001): The Gomantong Limestone of eastern Borneo: a sedimentological comparison with the near-contemporaneous Luconia Province. - Palaeogeogr. Palaeoclimatol. Palaeoecol., 175: 273-302.

Olson, C.C. and Dorobek, S.L. (2000): Styles and significance of structural inversion across the Nam Con Son Basin, offshore SE Vietnam. - Annual Meeting Expanded Abstracts - American Association of Petroleum Geologists, 2000: 109.

Park, R.K. and Peterson, R.M. (1979): Sedimentary history, basin development, and petroleum potentential of the Miocene, Palawna, Philippines. unpublished repor, Exploration Projects Section, Natural Resources Group, Oklahoma.

Pekar, S. and Miller, K.G. (1996): New Jersey Oligocene "Icehouse" sequence (ODP Leg 150X) correlated with global ∂18O and Exxon eustatic record. - Geology, 24(6): 567-570.

Pekar, S.F., Christie-Blick, N., Kominz, M.A., and Miller, K.G. (2002): Calibration between eustatic estimates from backstripping and oxygen isotopic records for the Oligocene. - Geology, 30(10): 903-906.

Petschick, R. (2001): MacDiff - freeware, http://servermac.geologie-uni-frankfurt.de/Rainer.html, Frankfurt.

Pomar, L. (1991): Reef geometries, erosion surfaces and high-frequency sea-level changes, upper Miocene Reef Complex, Mallorca, Spain. - Sedimentology, 38: 243-269.

Pomar, L. (1993): High-resolution sequence stratigraphy in prograding Miocene carbonates: Application to seismic interpretation. In: R.G. Loucks and J.F. Sarg (eds.), Carbonate Sequence Stratigraphy: Recent Developments and Applications. AAPG Memoir 57, 389-407 pp.

Pomar, L. (2001a): Types of carbonate platforms: a genetic approach. - Basin Research, 13(3): 313-334.

Pomar, L. (2001b): Ecological control of sedimentary accommodation: evolution from a carbonate ramp to rimmed shelf, Upper Miocene, Balearic Islands. - Palaeogeogr. Palaeoclimatol. Palaeoecol., 175: 249-272.

Pomar, L. and Ward, W.C. (1995): Sea-level changes, carbonate production and platform architecture: The Llucmajor platform, Mallorca, Spain. In: B.U. Haq (ed.), Sequence stratigraphy and depositional response to eustatic, tectonic and climatic forcing. Kluwer Academic Press, Dordrecht, 87-112 pp.

Porth, H. (1984): On the stratigraphy and hydrocarbon prospects of Palawan. unpublished report, , BGR/ BED, Hannover.

Porth, H., Müller, C., and von Daniels, C.H. (1989): The sedimentary formations of the Visayan Basin, Philippines. In: H. Porth and C.H. von Daniels (eds.), On the geology and hydrocarbon prospects of the Visayan Basin, Philippines, 70. BGR, Hannover, 29-87 pp.

Porth, H. and von Daniels, C.H. (1989): On the geology and hydrocarbon prospects of the Visayan Basin, Philippines, Geologisches Jahrbuch Reihe B, 70. BGR, Hannover, 428 pp.

Purdy, E.G. and Waltham, D.A. (1999): Reservoir implications of modern karst topography. - AAPG Bull., 83(11): 1774-1794.

Ramos-Guerrero, E., Rodriguez-Perea, A., Sabat, F., and Serra-Kiel, J. (1989): Cenozoic tectosedimentary evolution of Mallorca Island. - Geodinamica Acta, 3(1): 53-72.

Rangin, C., Müller, C., and Porth, H. (1989): Neogene geodynamic evolution of the Visayan region. In: H. Porth and C.H. von Daniels (eds.), On the geology and hydrocarbon prospects of the Visayan Basin, Philippines, 70. BGR, Hannover, 7-27 pp.

Rasser, M. and Piller, W.E. (1997): Depth distribution of calcareous encrusting associations in the norhtern Red Sea (Safaga, Egypt) and their geological implication. - 8th Int. Coral Reef Sym., Panama, 1997, Proc. 8th Int. Coral Reef Sym., 1.

Read, J.F. (1982): Carbonate platforms of passive (extensional) continental margins: Types, characteristics and evolution. - Tectonophysics, 81: 195-212.

Read, J.F. (1985): Carbonate platform facies models. - AAPG Bull., 69: 1-21.

Renema, W. and Troelstra, S.R. (2001): Larger foraminifera distribution on a mesotrophic carbonate shelf in SW Sulawesi (Indonesia). - Palaeogeogr. Palaeoclimatol. Palaeoecol., 175: 125-146.

Reyes, C.A. (1971): Geological investigation of Palawan Island. unpubl. report, Oriental Petrol and Mineral Corporation, Manila.

Rillera, F.G. (1983): Generalized stratigraphic table for the SW Palawan-Balabac area. unpubl. BED report, Bureau of Energy Development, Manila/ Philippines.

Robertson, A.H.F. (1998): Late Miocene paleoenvironments and tectonic setting of the southern margin of cyprus and the Eratosthenes Seamount. - Proc. Ocean Drill. Progr., Sci. Results, 160: 453-463.

Rossi, C. and Canaveras Juan, C. (1999): Pseudospherulitic fibrous calcite in paleo-groundwater, unconformity-related diagenetic carbonates (Paleocene of the Ager Basin and Miocene of the Madrid Basin, Spain). - J. Sediment. Res., 69(1): 224-238.

Ru, K. and Pigott, J.D. (1986): Episodic rifting and subsidence in the South China Sea. -

AAPG Bull., 70(9): 1136-1155.

Rudolph, K.W. and Lehmann, P.J. (1989): Platform Evolution and sequence stratigraphy of the Natuna platform, South China Sea. - Soc. Econ. Paleontol. Mineral., 44: 353-361.

Sager, W.W., Winterer, E.L., Firth, J.V., and et al. (1993): Northwest pacific atolls and guyots, Proc. Ocean Drill. Progr., Init. Repts., 143. ODP, 6-29 pp.

Saller, A.H. (1984): Petrologic and geochemical constraints on the origin of subsurface dolomitization by normal seawater. - Geology, 12: 217-220.

Saller, A.H., Armin, R., Ichram, L.O., and Glenn-Sullivan, C. (1993): Sequence stratigraphy of aggrading and backstepping carbonate shelves, Central Kalimatan, Indonesia. In: R.G. Loucks and J.F. Sarg (eds.), Carbonate sequence stratigraphy, recent developments and applications. Memoir, 57. AAPG, Tulsa, 267-290 pp.

Salm, R.V. and Halim, M.I. (1984): Marine Conservation Atlas. - IUCN/ WWF Project 3108, Marine Conservation.

Sarewitz, D.R. and Karig, D.E. (1986): Processes of allochthonous terrane evolution, Mindoro island, Philippines. - Tectonics, 5: 525-552.

Savin, S.M., Abel, L., Barrera, E., Hodell, D.A., Kennett, J.P., Murphy, M., Keller, G., Killingley, J., and Vincent, E. (1985): The evolution of Miocene surface and near-surface marine temperature - oxygene isotope evidence. - GSA Memoir, 163, 49-82 pp.

Schlager, W. (1981): The paradox of drowned reefs and carbonate platforms. - Geol. Soc. Am. Bull., 92(1): 197-211.

Schlager, W. (1989): Drowning Unconformities on Carbonate Platforms. - SEPM Special Publication, 44: 15-25.

Schlager, W. (1998): Exposure, drowning and sequence boundaries on carbonate platforms. - Spec. Publs int. Ass. Sediment., 25: 3-21.

Schlager, W. and Ginsburg, R.N. (1981): Bahama carbonate platforms; the deep and the past. - Mar. Geol., 44(1-2): 1-24.

Schlager, W., Reijmer, J.J.G., and Droxler, A. (1994): Highstand shedding of carbonate platforms. - Journal of Sedimentary Research, Section B: Stratigraphy and Global Studies, 64(3): 270-281.

Schlanger, S.O. (1964): Petrology of the limestones of Guam. - U.S. Geol. Survey Prof. Pap., 403(D): 1-52.

Schlüter, H.U., Hinz, K., and Block, M. (1996): Tectono-stratigraphic terranes and detachment faulting of the South China Sea and Sulu Sea. - Mar. Geol., 130(1-2): 39-78.

Schmidt, W. (1925): Gefügestatistik. - Tschermaks miner. petrogr. Mitt., 30: 392-423.

Shaw, R.D. (1999): Frontier basins of SE Asia: A review of their hydrocarbon potential. - Proceeding Southeast Asia Petroleum Exploration Society (Seapex), 1999, IX: 69-80.

Smith, W.D. (1907): The asbestos and manganese deposits of Ilocos Norte with notes on the geology of the region. - Philippine Journal of Sciences, A 2(3).

Tamesis, E.V., Manalac, E.V., Reyes, C.A., and Ote, L.M. (1973): Late Tertiary geologic history of the continental shelf off Northwestern Palawan, Philippines. - Bull. Geol. Soc. Malaysia, 6: 165-176.

Tapponnier, P., Peltzer, G., Le Dain, A.Y., Armijo, R. and Cobbold, P. (1982): Propagating extrusion tectonics in Asia: nea insights from simple experiments with plasticine. - Geology, 10: 611-616.

Taylor, B. and Hayes, D.E. (1980): The tectonic evolution of the South China Basin. In: D.E. Hayes (ed.), The tectonic and geologic evolution of Southeast Asian Seas and islands, Part 1. Geophys. Monogr., 22. Am. Geophys. Union, 89-104 pp.

Taylor, B. and Hayes, D.E. (1983): Origin and history of the South China Basin. In: D.E. Hayes (ed.), The tectonic and geologic evolution of Southeast Asian Seas and islands, Part 2, 27. Am. Geophys. Union, 23-56 pp.

Ten Have, T. and Heijnen, W. (1985): Cathodoluminescence activation and zonation in carbonate rocks: An experimental approach. - Geologie en Mijnbouw, 64: 297-310.

Teven, J.S. (1956): Philippines, Asia. - Lexique Stratigraphic International, 3(5): 167 pp.

Tidey, G.L., Troelstra, S.R., Attewell, R.A.K., Haseldonckx, A., and Denison, C. (1975): The micropalaeontology and stratigraphy of the interval 9000' - 14000' from the Champlin Philippines Incorporated Penascosa No. 1 well drilled offshore Palawan island, Philippines. unpubl. report No. 351, Robertson Research (Singapore), Singapore.

Tomascik, T., Mah, A.J., Nontji, A., and Moosa, M.K. (1997): The ecology of the Indonesian Seas. - Periplus Editions Ltd, Singapore, 1388 pp.

Troelstra, S.R. (1981): The biostratigraphy of the Phillips Petroleum Company Philippines Santiago A-1X well, drilled offshore Palawan island, the Philippines. unpubl. report No. 944, Robertson Research (Singapore), Singapore.

Tucker, M.E. and Wright, V.P. (1990): Carboante sedimentology. - Blackwell Scientific Publications, Oxford - London, 482 pp.

Vahrenkamp, V.C. (1998): Sr-isotope stratigraphy of Miocene carbonates, Luconia. - Annual Meeting - American Association of Petroleum Geologists, 1998, Abstracts & Program.

Vahrenkamp, V.C. (2000): Sr-Isotope stratigraphy of Miocene carbonates, Luconia Provinve, Sarawak, Malaysia: Implication for platform growth and demise and regional reservoir behaviour. In: P.D. Crevello, V.C. Vahrenkamp, and U. Singh (eds.), Carbonate depositional systems and high-resolution reservoir stratigraphy: methods and applications for building integrated reservoir simulation models. American Association of Petroleum Geologists Short Course, American Association of Petroleum Geologists, Tulsa, 8.2-1 - 8.2-4 pp.

Vahrenkamp, V.C., Ross, R., Crevello, P., and Sams, M.S. (2000): Assessing the impact of reservoir architecture, faulting and. - AAPG Bulletin, 84(9): 1509.

Vail, P.R., Mitchum, R.M.J., Todd, R.G., Widmier, J.M., Thompson, S.I., Sangree, J.B., Bubb, J.N., and Hatlelid, W.G. (1977): Seismic stratigraphy and global changes of sea level. In: C.E. Payton (ed.), Seismic stratigraphy - Applications to hydrocarbon exploration. AAPG Memoir, 26. American Association of Petroleum Geologists, Tulsa, 49-212 pp.

van der Vlerk, I.M. and Umbgrove, J.H.F. (1927): Tertiaere gidsforaminiferen van Nederlandsch Oost India. - Wetensch. Meded., 6: 1-35.

Wiedicke, M. (1987): Biostratigraphie, Mikrofazies und Diagenese tertiärer Karbonate aus dem Südchinesischen Meer (Dangerous Grounds - Palawan, Philippinen). - Facies, 16: 195-302.

Williams, H.H. (1992): Geochemistry of Palawan oils Philippines: Source implications. - Proceedings of the 9th Offshore Southeast Asia Conference, Singapore, 1992.

Wilson, M.E.J. (2002): Cenozoic carbonates in Southeast Asia: implications for equatorial carbonate development. - Sedimentary Geology, 147(3-4): 295-428.

Wilson, M.E.J. and Bosence, D.W.J. (1997): Platform top and ramp deposits of the Tonasa carbonate platform, Sulawesi, Indonesia. In: A.J. Fraser, S.J. Matthews, and R.W. Murphy (eds.), Petroleum geology of SE Asia. Special Publication, 126. Geological Society of London, London, 247-279 pp.

Wilson, M.E.J., Bosence, D.W.J., and Limbong, A. (2000): Tertiary syntectonic carbonate platfom development in Indonesia. - Sedimentology, 47: 395-419.

Wilson, M.E.J. and Moss, S.J. (1999): Cenozoic palaeogeographic evolution of Sulawesi and Borneo. - Palaeogeogr. Palaeoclimatol. Palaeoecol., 145: 303-337.

Wolfart, R., Cepek, P., Gramann, F., Kemper, E., and Porth, H. (1986): Stratigraphy of Palawan Island, Philippines. - Newsletters on Stratigraphy, 16(1): 19-48.

Yang, C., Homman, N.P.-O., Johansson, L., Halden, N.M., and Barbin, V. (1995): Ionoluminescence - A new tool for the nuclear microprobe in geology. - Scann. Microsc., 9(1): 43-62.

Zachos, J., Pagani, M., Sloan, L., Thomas, E., and Billups, K. (2001): Trends, rhythms, and aberrations in global climate 65 Ma to present. - Science, 292: 686-693.

Ziegler, B. (1983): Spezielle Paläontologie; Protisten, Spongien und Coelenteraten, Mollusken. - Einführung in die Paläobiologie Teil 2. E. Schweizerbart'sche Verlagsbuchhandlung, Stuttgart, 409 pp.

Plates

Plate 1

Field photographs

Fig. 1-1: Foundation Area - shale to fine sandstone layers 0.5 to 3 cm thick below Taglupa Profile, i.e. representing base of the SW Palawan carbonates in the onshore area.

Fig. 1-2: Salty Creek 2 Profile - lower part made up of massive pack- to floatstones with dm-sized coral heads, upper part of well-bedded foraminifera grain- to packstones; lower- and upper part are separated by a significant horizon with erosive base and top, 0.8 to 1.5-m thick and made up of well-bedded packstones containing large biogenous component and gravel up to dm-size. Profile shows the transition from a lagoonal- to a ramp-like setting throughout the 12.5-m high outcrop.

Fig. 1-3: Tumarabong River Section - part of the 150-m long and 20-m high jungle cliff at the Tumarabong River; lower part made up of floatstones with some coral accumulations, upper part of well-bedded foraminifera grain- to packstones. Profile covers the similar transition from a lagoonal- to a ramp-like setting as in Salty Creek 2 Profile and indicates the lateral extension of the paleoenvironmental change.

Fig. 1-4: Slope Profile - part of the Slope Profile showing sedimentary structures within the shoal; well-bedded packstone beds of underlying set toplap to the erosive overlying set made up of well-bedded packstones as well.

Fig. 1-5: Theo's Place - outcrop of mud- to wackestone layers during low tide as the youngest lateral extended carbonates in the onshore study area.

Fig. 1-6: Devel Peak - siliciclastic base of deep marine shales below Devel Peak on the southern side of the build-up.

Fig. 1-7: Devel Peak - NE cliff side of Devel Peak showing two levels of coral horizons in the top area.

Fig. 1-8: Devel Peak - view from the sea to the SE on Devel Peak showing the characteristic vertical cliff on the NE side and a steep flank on the SW side of the build-up.

Fig. 1-9: Albion Head - view from the sea to the W on the NE flank of Albion Head showing two lines of reefal structures.

Fig. 1-10: Albion Head - north-westwards view across the Malanut Bay to the carbonate complex of the peninsula of Albion Head.


5


10


4


9


3


8


2


7

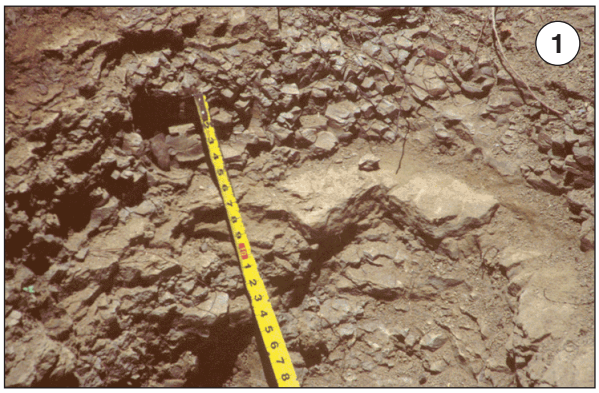
1


6

Plate 2

Thin section photographs of onshore samples: Microfacies Analysis

Scale bar: 2 mm

Fig. 2-1: Internal bedded siltstones with some plant debris collected in the Foundation Area closely below the carbonates of the Taglupa Profile (FA2).

Fig. 2-2: Poorly sorted rudstone containing echinoderm, corals, bryozoans, red algae and oyster fragments as well as a high content of quartz grains, gravels and some plant debris from the Taglupa Profile (TA17).

Fig. 2-3: Rud- to floatstone made up of bryozoans, larger foraminifera, bivalves, red algae and echinoderms in a micritic to shaly matrix collected at the Taglupa Profile (TA14).

Fig. 2-4: Moderate sorted bryozoan-larger foraminifera rudstone from the Taglupa Profile (TA12).

Fig. 2-5: Intercalation of marine shales with some plant debris from a protected shallow-water area in the lower part of the Salty Creek Section (SC0).

Fig. 2-6: Wackestone with Soritidae, Alveolinidae, green algae fragment, gastropods and small benthic foraminifera in a muddy matrix collected in the lower part of the Salty Creek Section (SC2)

Fig. 2-7: Coral-floatstones here with an oyster fragment in a micritic matrix with some small and fragile molluscs shells and echinoderms discovered in the lower part of the Salty Creek Section (SC8)

Fig. 2-8: Coral-Floatstone with some content of smaller skeletal debris in the micritic matrix made up of Alveolinidae, small benthic foraminifera, red algae and molluscs found in the lower part of the Salty Creek Section (SC10).

Fig. 2-9: Wackestone from the lower part of the Salty Creek Section containing larger foraminifera, molluscs beside undefined biogenous debris (SC12).

Fig. 2-10: Massive Poritidae coral with partly sediment-filled, partly cement-filled hole resulting in a geopetal structure. Bivalve with both shells is preserved as ghost structure (SC12B).

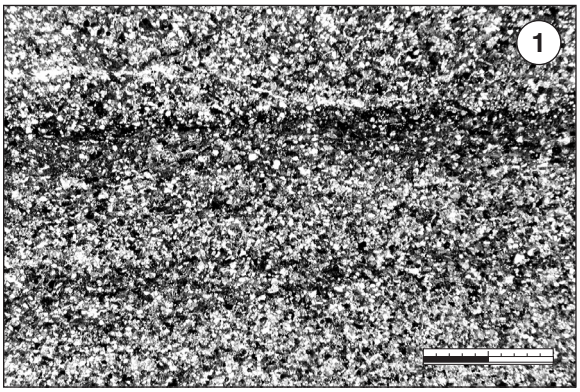
1

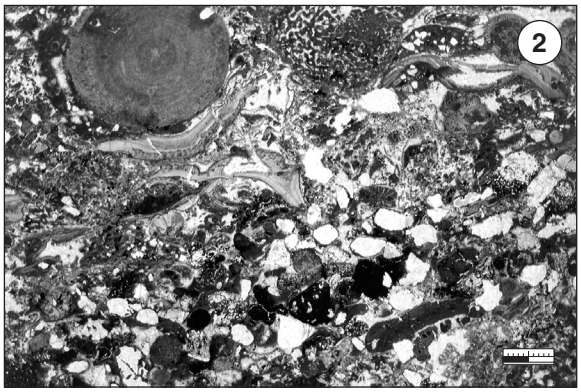
2


3

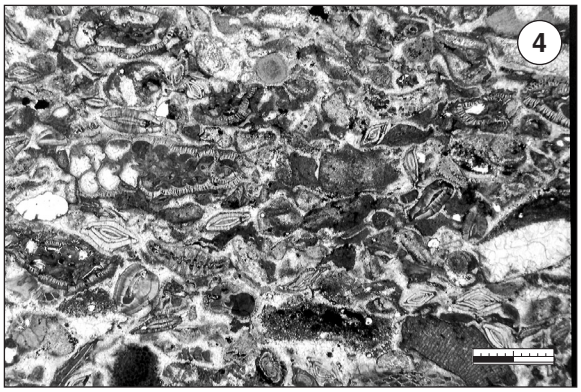
4

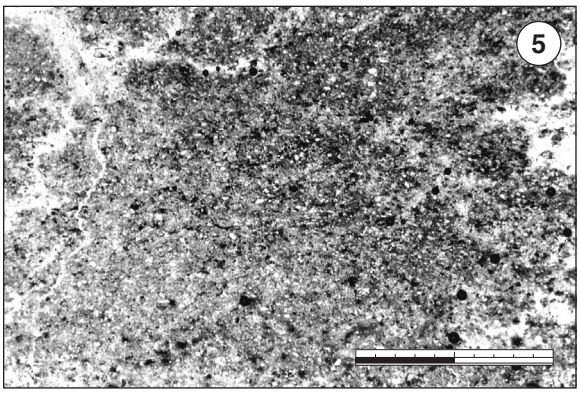
5

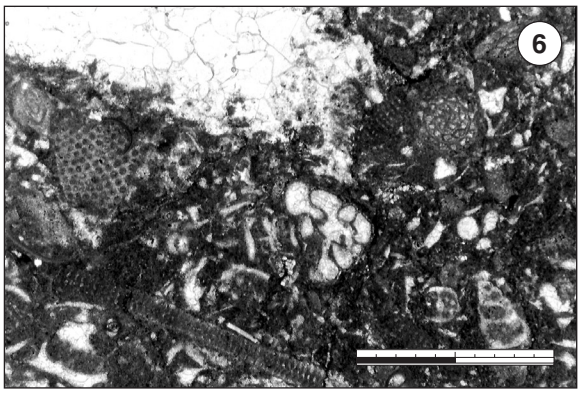
6

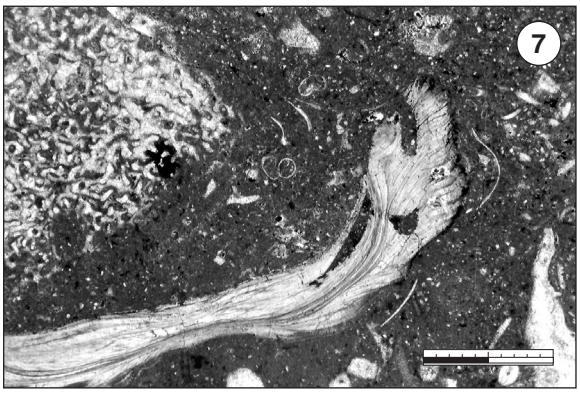
7

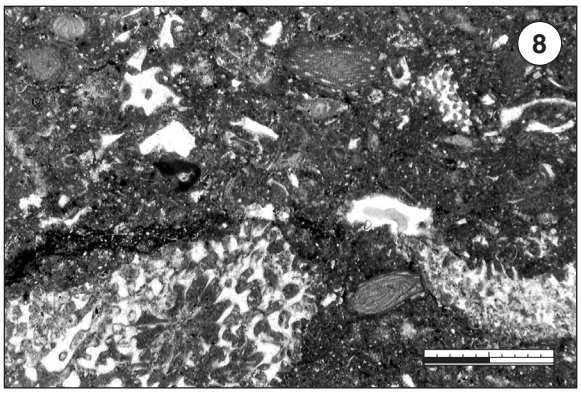
8

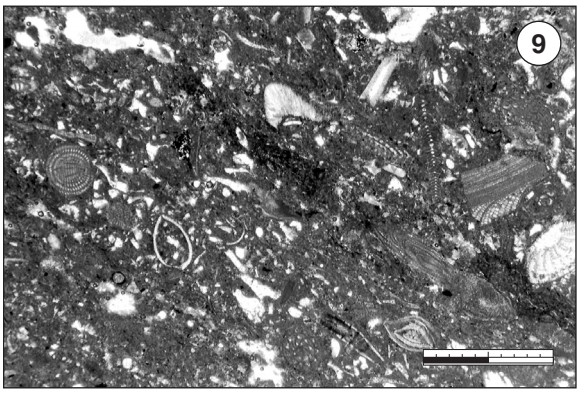
9

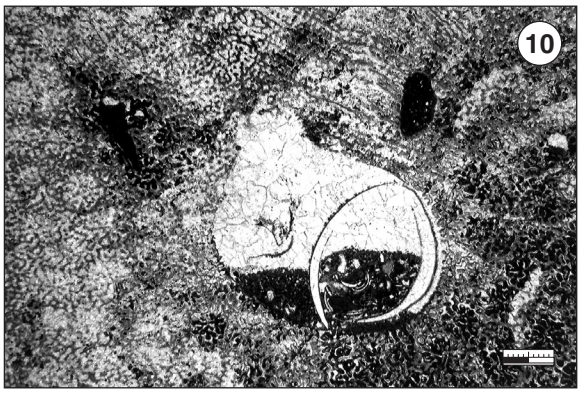
10

Plate 3

Thin section photographs of onshore samples: Microfacies Analysis

Scale bar: 2 mm

Fig. 3-1: Field photography of the Salty Creek 2 Profile indicating the sample level of the thin section SC22 and SC33. The horizon, where SC22 was taken from, represents the change from a lagoonal- to a ramp-like setting with well-bedded packstones containing poorly sorted large biogenous components and gravel of cm- to dm-size.

Fig. 3-2: Biogenous packstone with large gastropod and high content of quartz grains from the significant horizon made up to well-bedded packstones containing large biogenous components and gravel of dm-size (SC20).

Fig. 3-3: Moderate sorted larger foraminifera-grainstone containing echinoderms and bryozoans from the Salty Creek 2 profile representing slope deposits (SC33).

Fig. 3-4: Well bedded larger foraminifera grainstone from the Salty Creek 2 Profile showing orientated Lepidocyclinidae (SC35).

Fig. 3-5: Relative well-sorted grainstone with larger foraminifera, bivalves, bryozoans, small benthic foraminifera and brachiopods from the upper Salty Creek Section (SC41).

Fig. 3-6: Well-sorted grainstone with high content of quartz and some cm-sized gravel as intercalation in the slope deposits of the Salty Creek Section (SC47).

Fig. 3-7: Larger foraminifera-grainstone with Nummulitidae, Lepidocyclinidae, Amphisteginidae and Homotrematidae beside echinoderms, bachiopods and a few planktonic foraminifera characterise slope deposits of the Salty Creek Section (SC51).

Fig. 3-8: Larger foraminifera-grainstone with Amphisteginidae, Nummulitidae, Lepidocyclinidaem bryozoans, echinoderms, mollucs and a few planktonic foraminifera show slight changes in the composition compared to the previous thin section 5 m below in the succession of the Salty Creek Section (SC52).

Fig. 3-9: Fine and moderate-sorted bioclastic packstone on the deeper slope of the Salty Creek Section containing small bivalves, small benthic foraminifera, planktonic foraminifera beside some small larger foraminifera (TD-E1).

Fig. 3-10: Fine well-sorted bioclastic packstone with planktonic foraminifera beside a high amount of very small undefined skeletal grains (SC57).

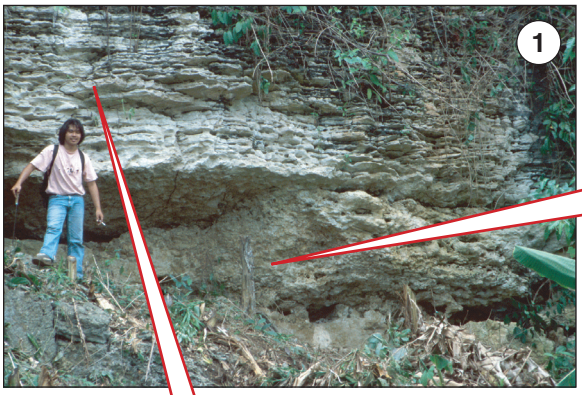
1

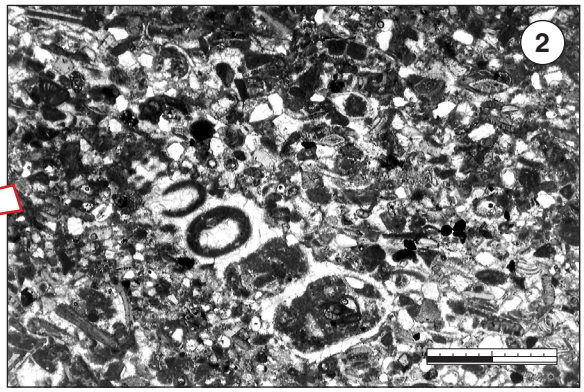
2

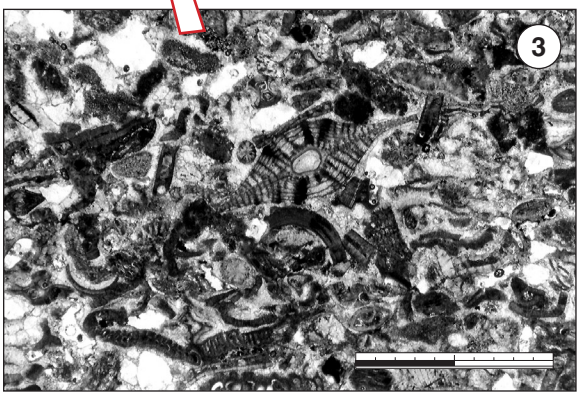
3

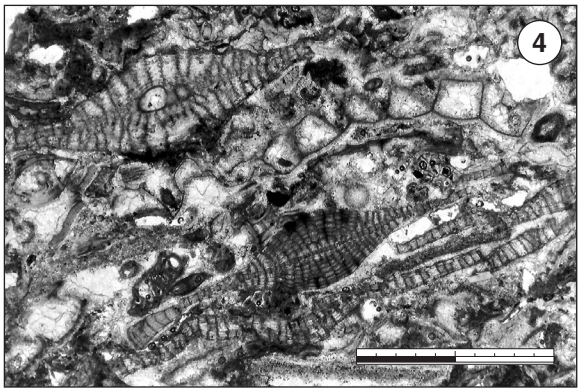
4

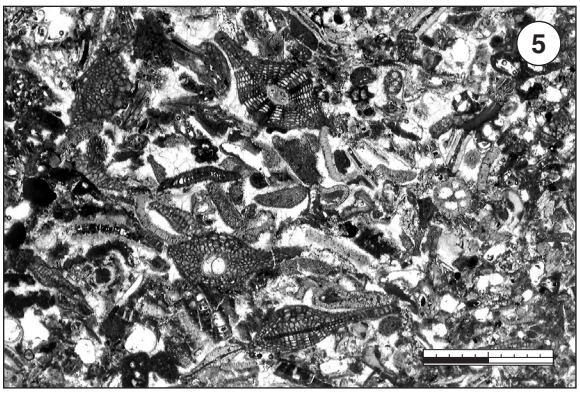
5

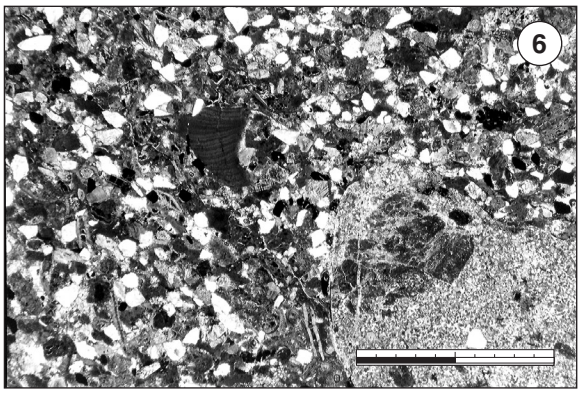
6

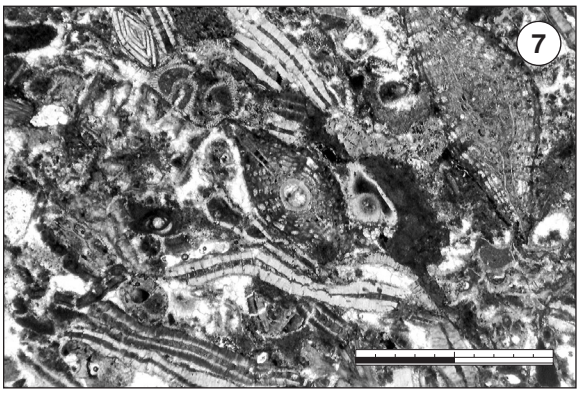
7

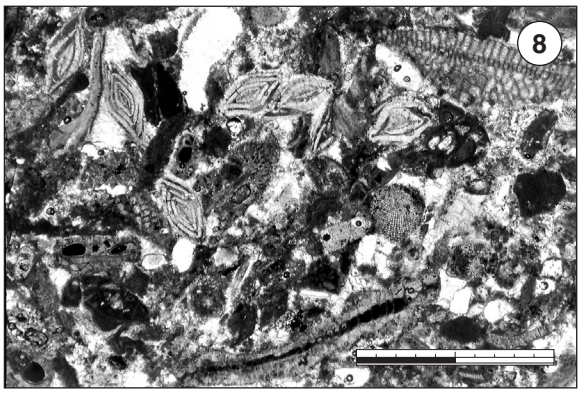
8

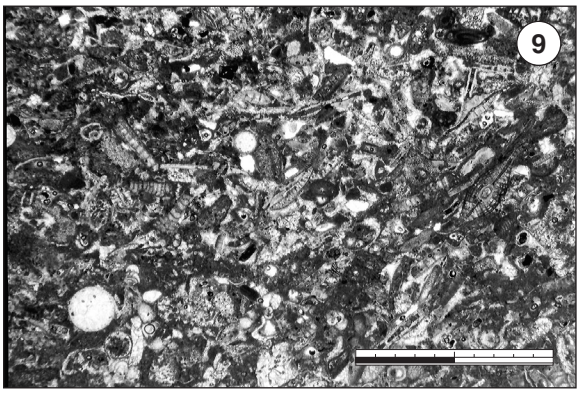
9

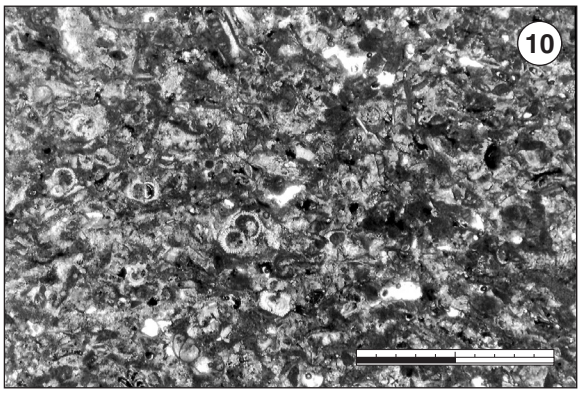
10

Plate 4

Thin section photographs of onshore samples: Microfacies Analysis

Scale bar: 2 mm

Fig. 4-1: Very fine packstone with mostly undefined skeletal grains beside some planktonic foraminifera and pellets from the upper part of the Salty Creek Section (SC64).

Fig. 4-2: Very fine packstone or wackestone with planktonic foraminifera in a partly shaly matrix found in the uppermost part of the Salty Creek Section (SC72).

Fig. 4-3: Planktonic foraminifera-wackestone from the Maasion Profile (MA0).

Fig. 4-4: Mudstone with a few planktonic foraminifera such as *Orbulina* (Ma1).

Fig. 4-5: Sample of floatstone from the base of Devel Peak. Corals, larger foraminifera, molluscs, brachiopods and echinoderms are poorly sorted in a micritic matrix.

Fig. 4-6: Sample of the coral-boundstones from the coral horizon 100-m above the base of Devel Peak; platy Porites encrusted by larger foraminifera trap very fine grained to micritic sediment.

Fig. 4-7: Poorly sorted rudstone of reef debris including red algae, larger foraminifera, small benthic foraminifera, echinoderms and molluscs form the middle part of Devel Peak collected on the NE flank.

Fig. 4-8: Poorly sorted floatstone dominated by recrystallised molluscs from the SW side of Devel Peak.

Fig. 4-9: Poorly sorted rudstone with large fragment of mollusc, coralline red algae, echinoderms, larger foraminifera (Soritidae) and small benthic foraminifera from the upper part of Devel Peak.

Fig. 4-10: Poorly sorted rudstone made up of corals, red algae, green algae, larger foraminifera, plenty of planktonic foraminifera, echinoderm and molluscs from the offshore well Santiago A-1X. With the exception of the high amount of planktonic foraminifera equivalent skeletal grains are observed as in the samples from the onshore build-up Devel Peak (S5).

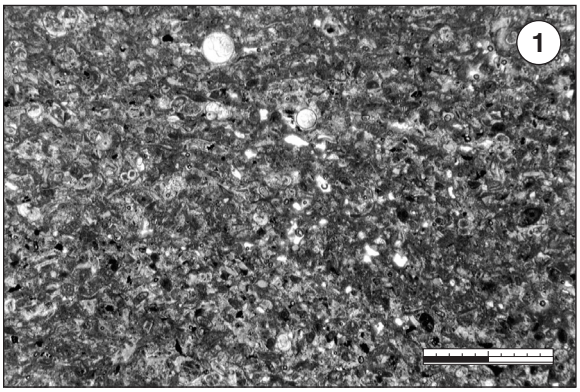
1

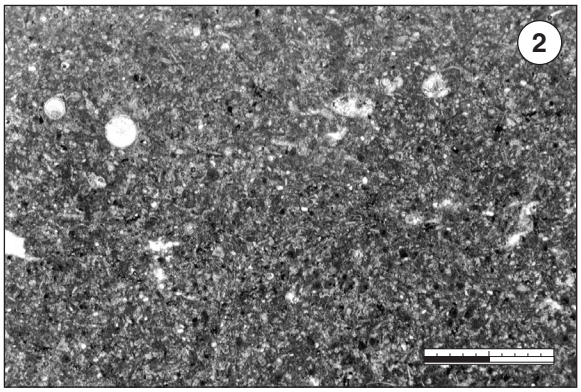
2

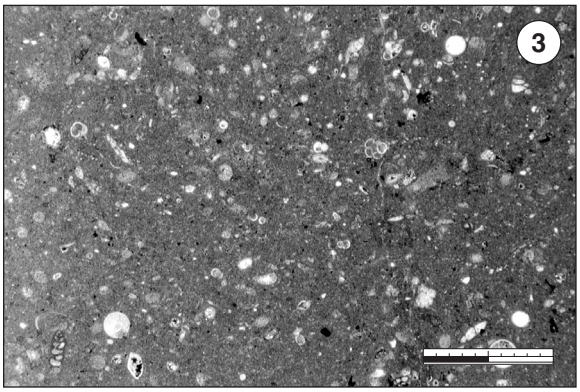
3

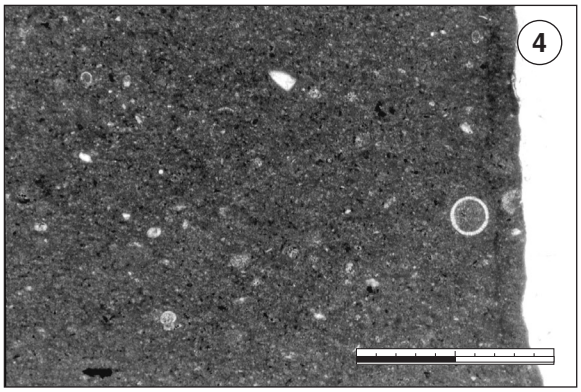
4


5

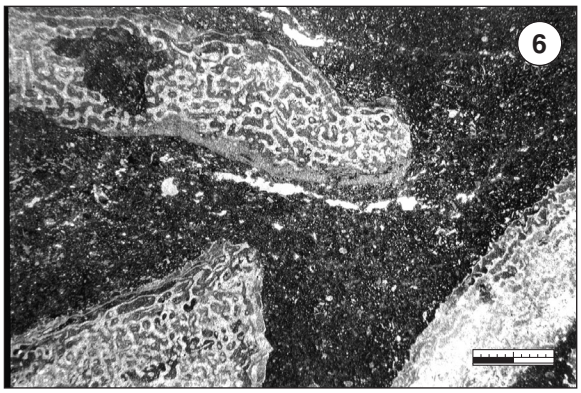
6

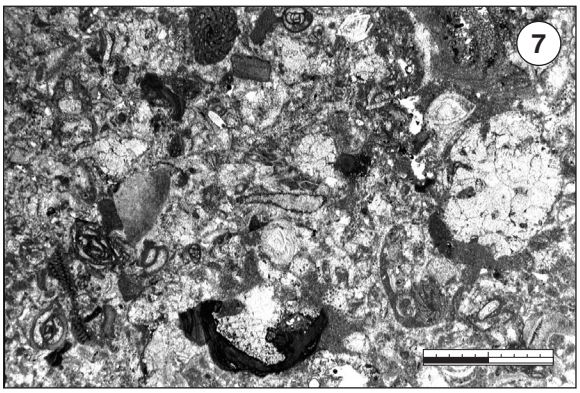
7


8

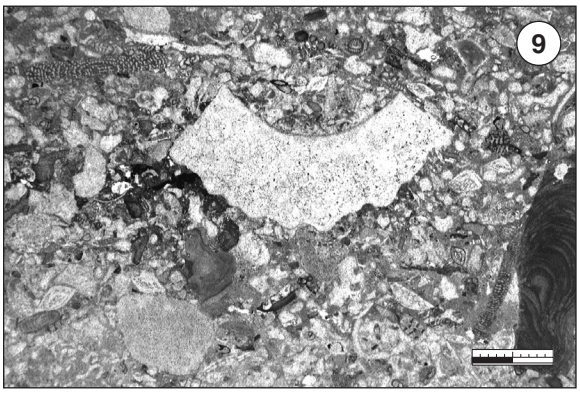
9

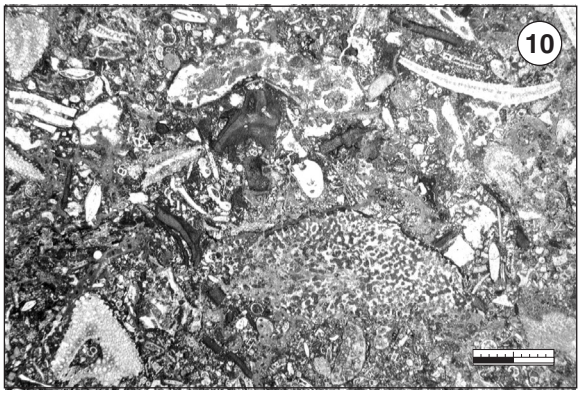
10

Plate 5

Red algae photographs of the SW Palawan Carbonates

Scale bar: 0.5 mm

Fig. 5-1: *Lithoporella* from the well Santiago A-1X (S12).

Fig. 5-2: *Aethesolithon problematicum* as abundant coralline red algae from the lower part of the Salty Creek Section (SC3).

Fig. 5-3: *Amphiroa*, very small fragment in the pack- to grainstones of the slop deposits, here collected at the Tumarabong River Section (T-VP1A).

Fig. 5-4: *Corallina* common as fragments in the grain- to packstones of the slope deposits, here an example from the Tumarabong River Section (T11)

Fig. 5-5: *Neogoniolithon* sp. encrusted mostly coral branches and coexists often with encrusting larger foraminifera in the upper part of the water column; examples are found in the lagoonal- and reefal deposits, whereas this sample was collected at the Tumarabong River Section (T-E2).

Fig. 5-6: *Mesophyllum* sp. is beside *Neogoniolithon* sp. another common encrusting red algae, forming thick red algae crusts, but predominately in slightly deeper parts of the water column such as at the base of Devel Peak or in the deeper slop, like the shown example (SP59).

Fig. 5-7: *Peyssonelia*, a not very frequent encrusting red algae observed at Devel Peak (SEP11).

Fig. 5-8: *Hydrolithon* as additional variety of a encrusting red algae is related to more quite water conditions of the shallow water, here from the lower Salty Creek Section (SC7).

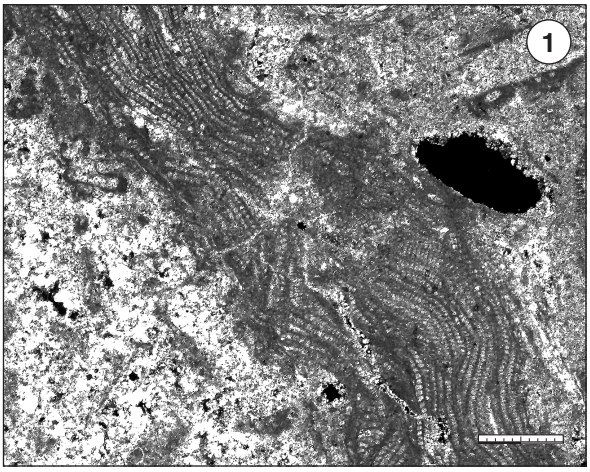
1

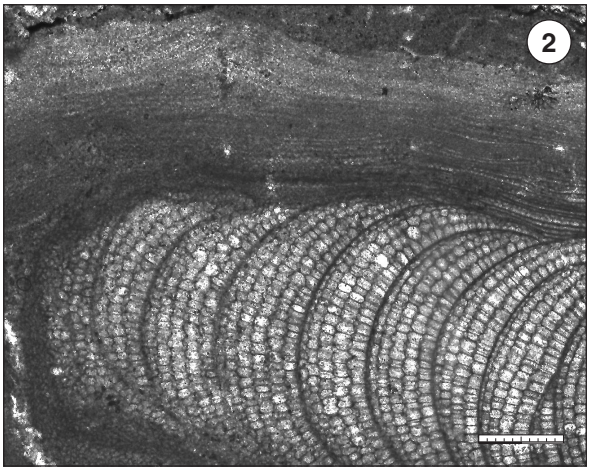
2

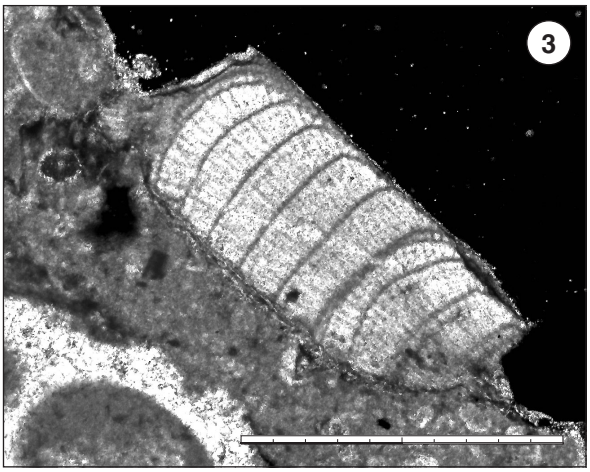
3

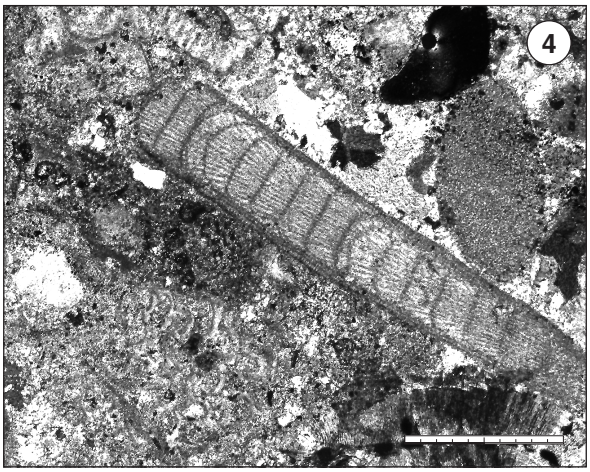
4

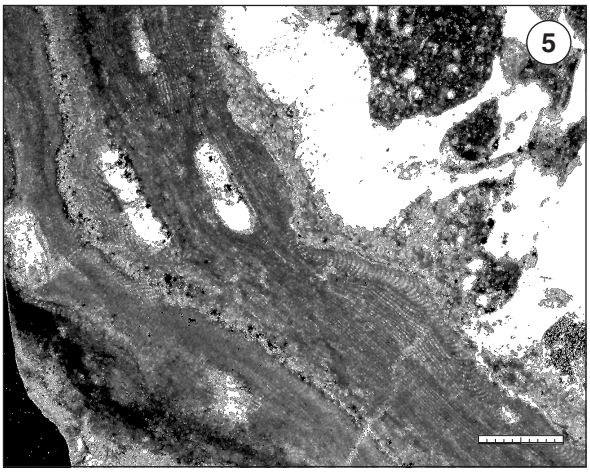
5

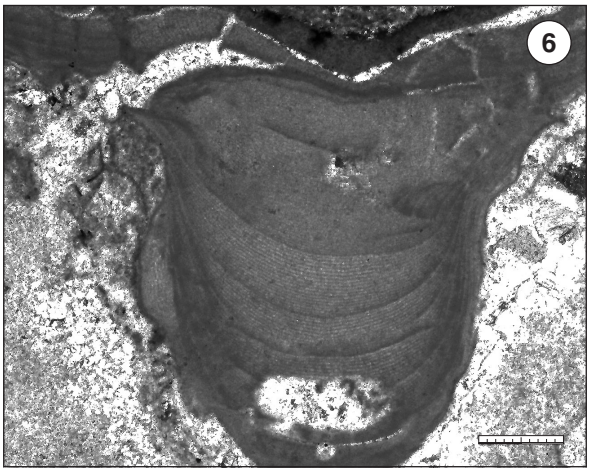
6

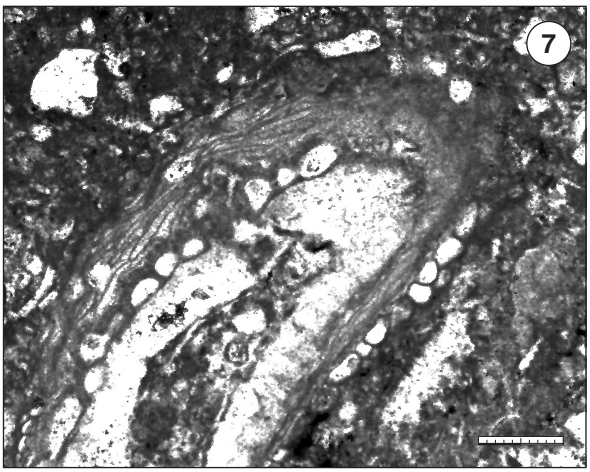
7

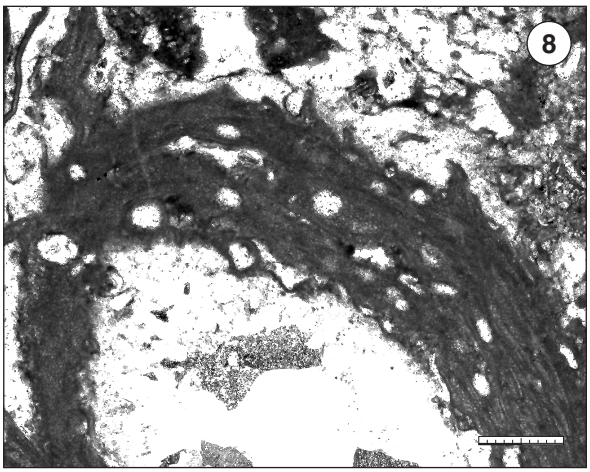
8

Plate 6

Diagenesis, onshore

Scale bar: 0.5 mm; Fig. 6-5 = 2 mm

Fig. 6-1: Neomorphic spars: local granular to drusy calcite displaces matrix and components; relicts of micritic matrix and some skeletal grains still exist (SC20).

Fig. 6-2: Example of very rare bladed-prismatic calcite on a micritic rim refers an early stage of cementation; bladed cement was formed after dissolution of the coral (SC8).

Fig. 6-3: Two generations of granular cements in a coral; (a) recrystallisation of primary aragonitic Porites, (b) calcitic filling of pore space with large blocky calcite (SC8).

Fig. 6-4: Large open pore in recrystallised coral indicates the limited cementation by granular to drusy calcite probably due to restricted pore fluid circulation (low permeability) (SC8).

Fig. 6-5: Broken larger foraminifera reflect compaction of grainstone (SC28).

Fig. 6-6: Shelter porosity below large biogenous component (SC3).

Fig. 6-7: Early fibrous cement needles around skeletal grains of bioclastic grain- to packstone (SC38).

Fig. 6-8: Syntaxial cements around echinoderms in bioclastic grain- to packstone (SC38).

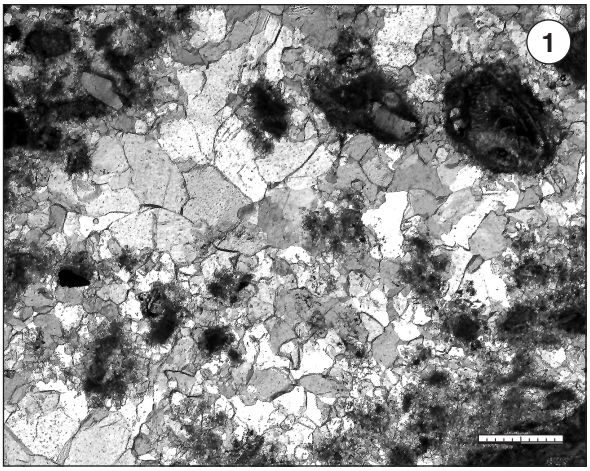
1

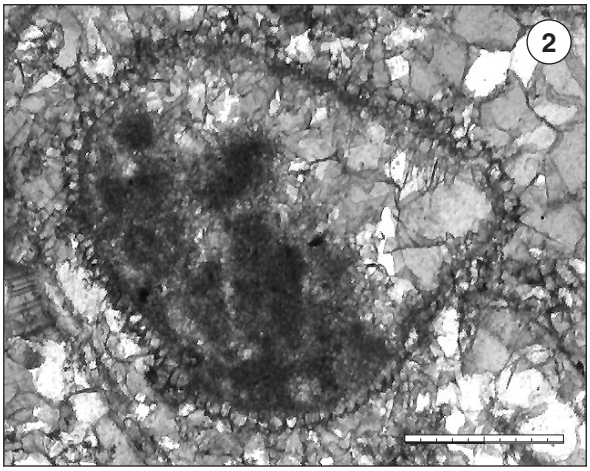
2

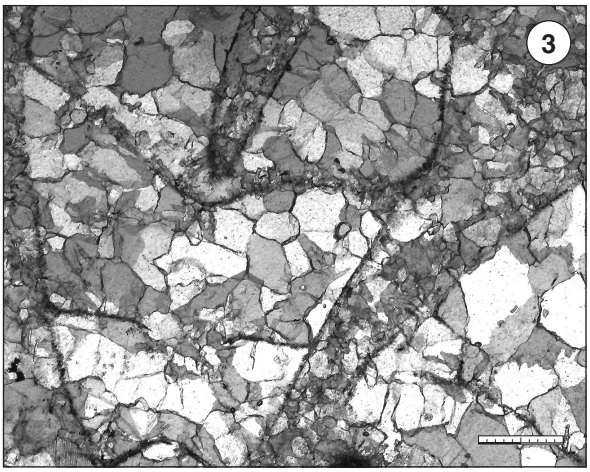
3

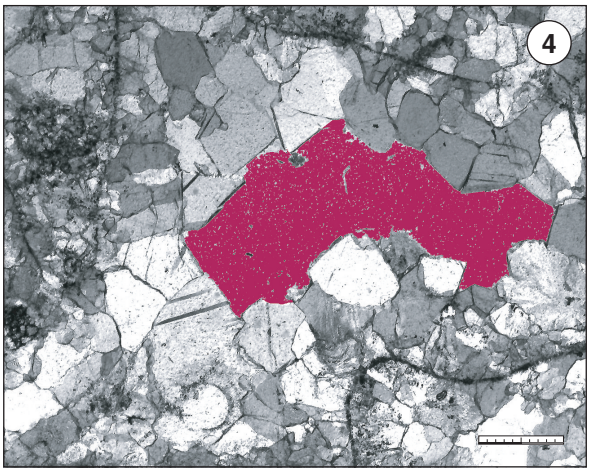
4

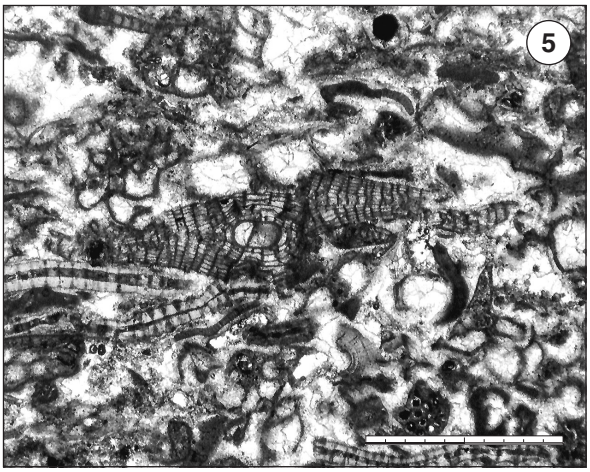
5

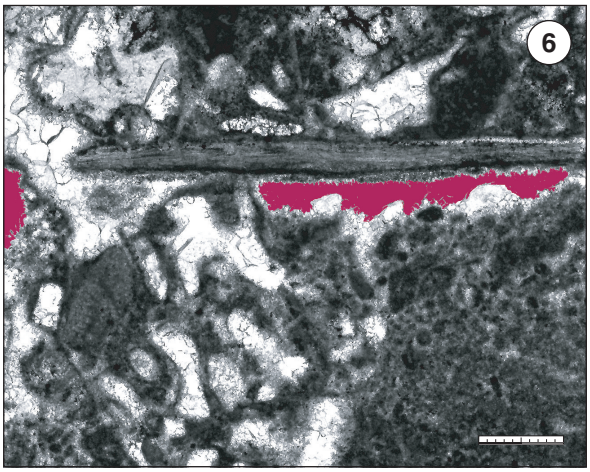
6


7

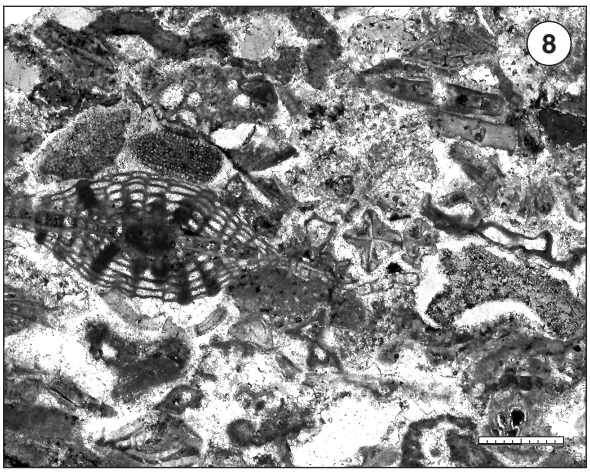
8

Plate 7

Diagenesis, offshore (Anepahan A-1X)

Scale bar: 2 mm; Fig. 7-4 = 0.5 mm

Fig. 7-1: Subaerial speleothem crust covering wall of vug porosity and larger foraminifera (AN4).

Fig. 7-2: Subaerial speleothem crust covering wall of larger vug; the left open porosity was closed with later drusy cements of burial diagenesis (AN4).

Fig. 7-3: *Microcodium* affecting non-fabric selective the carbonate (AN5).

Fig. 7-4: Detail of *Microcodium*, cutting into a larger foraminifera (AN5).

Fig. 7-5: Scatted, dominantly small dolomite crystals in the micritic matrix (AN 2).

Fig. 7-6: Fine granular dolomite follows fractures in the carbonate (AN6).

Fig. 7-7: Early pore with rim of primary aragonitic botryoidal cement, filled with some internal sediment, before a meteoric influence produced vadose silt; finally, the open pore was closed with late drusy cement (AN9)

Fig. 7-8: Part of a partly ghost of a gastropod: (a) encrusting of gastropod by larger foraminifera, (b) bioerosion by boring activities, (c) dissolution, (d) early fibrous cement followed by (e) drusy cement; open poro still exist (AN6).

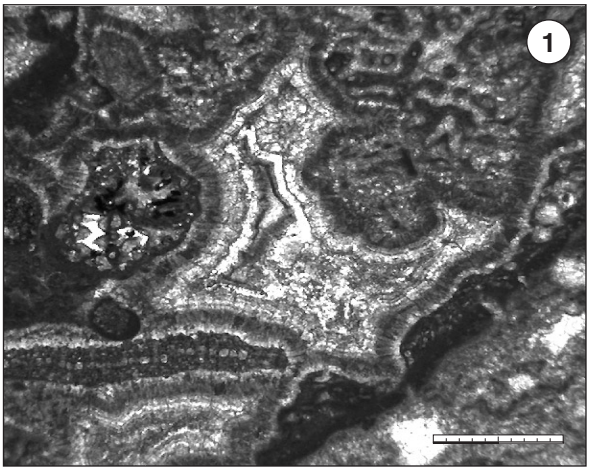
1

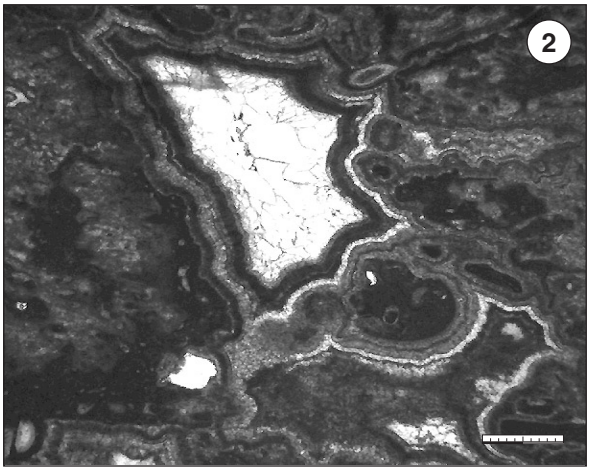
2

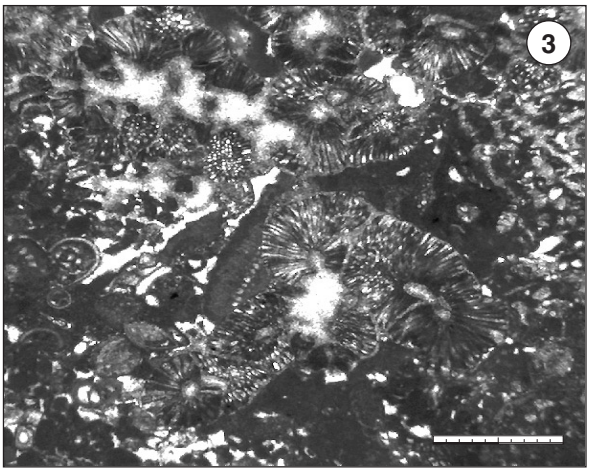
3

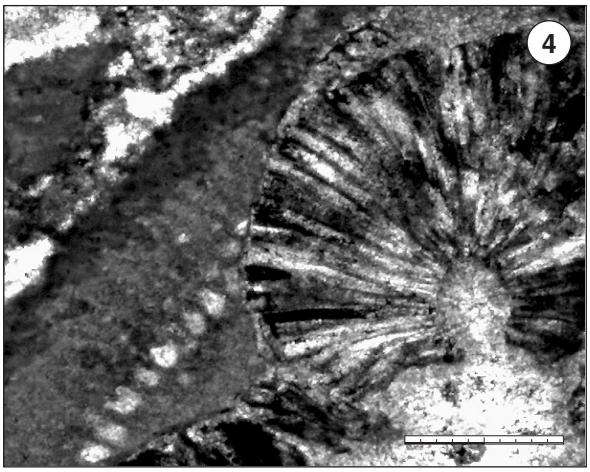
4

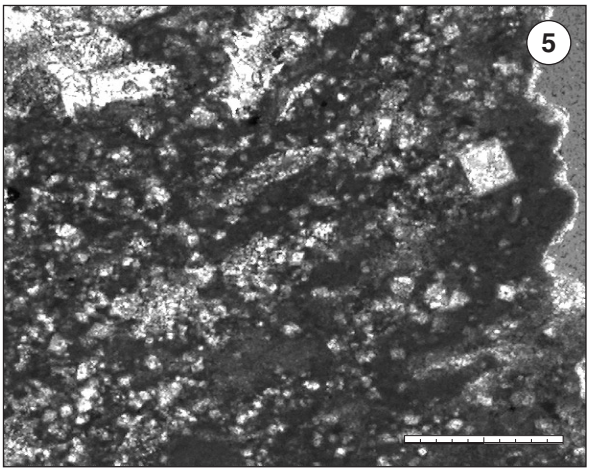
5


6

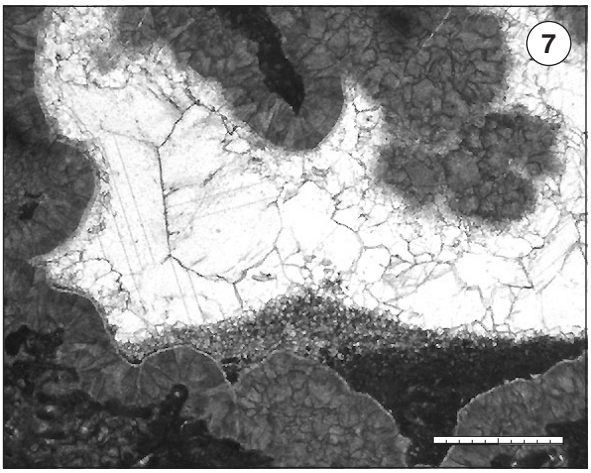
7

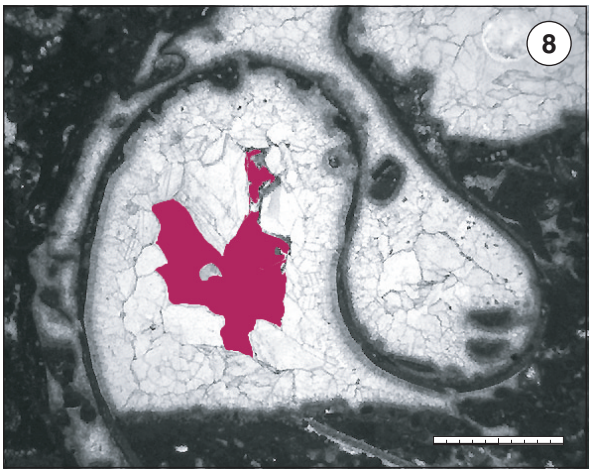
8

Appendix

Content

Location	No. (Stratigraphy)		131	130	129	128	127	126	125	123	122	121	120	119	118	117	116	115	114	113	1	2	3	4	5	6	7	8	9	10	11	12	13	14	15	16	17
	Sample Code		1	2	3	4	5	6	7	9	10	11	12	13	14	15	16	17	18	19	1	2	3	4	5	6.1	6.2	7	8	9	10	11	12	12B	13	14	15
			TA	TA	TA	TA	TA	TA	TA	TA	TA	TA	TA	TA	TA	TA	TA	TA	TA	TA	SC	SC	SC	SC	SC	SC	SC	SC	SC	SC	SC	SC	SC	SC	SC	SC	SC
Composition	Matrix	**Micrite** : Sparite	5	9	5	9	9	1	9	1	1	1	1	5	9	1	5	5	9	5	9	9	5	9	9	9	9	9	9	9	9	9	9	9	9	9	9
	Composition (mineral.)	Micrite [%]	50	90	45	75	80	10	90	10	10	10	10	20	75	10	35	40	70	30	60	50	45	80	50	75	75	75	40	75	70	60	70	10	10	70	60
		Sparite [%]	50	10	40	20	20	90	10	85	90	85	90	80	10	80	50	40	10	50	40	50	55	20	50	20	25	25	60	25	30	35	25	90	90	10	30
		Internsed. [%]	0	0	0	1	0	0	1	1	0	0	0	0	5	0	0	0	0	0	0	0	0	0	0	0	0	0	0	5	0	0	0	0	0	15	5
		Sand [%]	1	5	0	5	1	0	1	0	0	0	0	0	5	0	0	0	0	0	0	0	0	0	0	0	0	0	0	0	0	0	0	0	0	0	0
		Open posrosity	0	0	0	1	0	0	0	0	1	0	0	0	0	1	1	5	5	5	1	1	1	0	0	5	1	1	1	1	1	5	0	0	5	5	1
		Shale [%]	1	1	5	5	1	1	1	5	1	5	1	1	5	10	15	15	15	15	10	5	1	10	10	10	10	10	10	10	5	5	10	5	5	10	10
	Components : Matrix		9	5	9	5	9	9	9	9	9	9	9	9	5	9	9	9	9	9	5	5	9	1	9	5	5	5	9	5	5	5	5	9	9	1	5
Components	**Bioclasts** : Biomorpha		5	9	9	9	5	9	9	9	9	9	9	9	5	9	9	9	9	9	9	9	9	9	1	9	5	9	1	5	9	1	9	1	1	9	9
	foraminifera, larger	SORITIDAE	0	1	1	0	0	0	0	0	0	0	0	0	0	0	0	0	0	0	5	10	10	0	0	10	0	0	1	10	1	0	5	0	0	0	10
		ALVEOLINIDAE	1	5	0	0	1	0	1	0	1	0	0	0	1	1	0	0	0	0	5	10	5	1	0	5	0	1	0	10	5	1	10	1	1	1	5
		ROTALIIDAE	0	0	0	0	0	0	0	0	0	0	0	0	0	1	0	0	0	0	0	0	0	0	0	0	0	0	0	0	0	0	0	0	0	0	0
		NUMMULITIDAE	1	1	1	0	1	5	1	10	20	25	20	20	10	10	1	1	0	0	0	0	0	0	0	0	0	0	0	0	1	10	0	0	0	1	0
		MIOGYPSINIDAE	1	1	1	0	0	0	0	1	0	0	0	0	0	1	0	0	0	0	0	0	0	0	0	0	0	0	0	0	0	0	0	0	0	0	0
		AMPHISTEGINIDAE	5	5	5	5	10	10	10	0	0	0	0	0	0	0	0	0	0	0	0	1	0	0	0	0	0	0	0	0	0	0	1	0	0	1	0
		ACERVULINIDAE	1	0	1	1	1	1	1	1	1	1	1	0	0	0	0	0	1	0	0	0	0	0	0	0	0	0	0	0	0	0	1	0	0	0	5
		HOMOTREMATIDAE	1	1	5	0	0	0	0	0	1	0	0	0	1	0	0	0	0	0	0	0	0	0	0	0	0	0	0	0	0	0	1	0	0	0	0
		LEPIDOCYCLINIDAE	0	0	0	0	0	1	1	0	0	0	0	0	0	0	0	0	0	0	0	0	0	0	0	0	0	0	0	0	0	0	0	0	0	0	0
		other	0	0	0	0	0	0	0	0	0	0	0	0	0	0	0	0	0	0	0	0	0	0	0	0	0	0	0	0	0	0	0	0	0	0	0
		SUM	10	14	14	6	13	17	14	12	23	25	21	20	12	13	1	1	1	0	10	21	15	1	0	15	0	1	1	20	6	3	27	1	1	2	21
	- small benthic		0	0	0	0	0	0	0	0	0	0	0	0	0	0	0	0	0	0	0	5	5	0	0	1	0	5	0	5	5	1	1	0	1	0	1
	- planktonic		0	0	0	0	0	0	0	0	0	0	0	0	0	0	0	0	0	0	0	0	0	0	0	0	0	0	0	0	0	0	0	0	0	0	0
	algae	red -	1	1	1	1	1	1	1	1	1	1	1	10	5	10	1	1	5	5	10	5	1	1	0	20	20	10	1	5	5	1	0	0	0	1	10
		green -	0	0	0	1	0	0	0	0	0	0	0	0	0	0	0	0	0	0	0	1	1	0	0	0	1	0	0	0	1	0	0	0	0	0	0
	bryozoans		1	5	1	1	1	1	1	5	5	5	10	1	20	5	10	10	1	5	0	0	0	0	0	0	0	0	0	1	0	0	0	0	0	0	1
	corals	branches	1	1	1	0	0	1	0	1	0	0	0	0	0	0	1	1	0	0	20	10	0	10	0	10	20	0	5	1	10	1	1	0	0	1	10
		heads	0	0	0	1	0	0	0	0	0	0	0	0	0	0	0	0	10	5	0	0	0	0	90	0	0	0	70	0	0	40	0	90	95	0	0
		SUM	1	1	1	1	0	1	0	1	0	0	0	0	0	0	1	1	10	5	20	10	0	10	90	10	20	0	75	1	10	41	1	90	95	1	10
	echinoderms		1	1	1	1	5	5	1	5	5	1	5	1	1	1	1	1	0	10	0	1	0	0	0	0	0	0	0	0	0	0	1	0	0	0	1
	molluscs	bivales/ oysters	1	1	1	1	1	1	5	10	5	5	1	1	5	1	10	10	1	10	5	10	10	1	0	5	10	10	10	5	5	1	5	1	0	5	5
		gastropods	1	1	0	0	0	0	0	0	0	0	0	0	1	0	0	0	0	0	5	5	10	1	0	0	0	0	5	1	1	5	5	0	0	0	1
	brachiopodes		0	0	1	0	0	0	0	0	0	1	0	0	0	1	0	0	1	1	0	0	0	0	0	0	0	0	0	0	0	0	0	0	0	0	0
	ostracods		0	0	0	0	0	0	0	0	0	0	0	0	0	0	0	0	0	0	1	0	0	0	0	0	0	0	0	1	0	0	0	0	0	0	0
	serpulids		0	0	0	0	0	0	0	0	0	0	0	0	0	0	0	0	0	0	0	0	0	0	0	0	0	0	0	0	0	0	0	0	0	0	0
	indetermined		25	25	25	25	25	25	25	25	25	25	25	25	25	25	25	25	10	25	10	25	25	10	0	10	5	25	10	10	10	5	10	0	0	10	10
	Terrigenous comp.	plantes, terr.	0	0	0	0	0	0	1	1	1	0	1	0	1	1	1	1	1	5	0	0	0	0	0	0	0	0	1	1	1	0	1	0	0	0	0
		Detritus/Quarz	0	0	0	0	0	0	0	0	0	0	0	1	0	5	30	40	30	30	0	0	0	0	0	0	0	0	0	0	0	0	0	0	0	0	0
	Authigeneous min.		0	0	0	0	0	0	0	0	0	0	0	0	0	0	0	0	0	0	0	0	0	0	0	0	0	0	0	0	0	0	0	0	0	0	0
	Lithoclasts	Intra-	0	1	1	0	1	0	0	0	0	0	0	0	1	1	10	5	10	10	0	0	0	0	0	0	0	0	0	0	0	0	0	0	0	0	0
		Extra-	0	0	0	0	0	0	0	0	0	0	0	1	0	5	30	30	25	20	0	0	0	0	0	0	0	0	0	0	0	0	0	0	0	0	0
		SUM clasts	0	1	1	0	1	0	0	0	0	0	0	1	0	6	31	40	30	30	0	0	0	0	0	0	0	0	0	0	0	0	0	0	0	0	0
	Pellets		0	1	5	0	1	0	1	0	1	1	0	0	0	0	0	0	0	0	0	0	0	0	0	0	0	0	0	0	0	1	0	1	1	10	10
	Grapestones/ Lumps		0	0	0	0	0	0	0	0	0	0	0	0	0	0	0	0	0	0	0	0	0	0	0	0	0	0	0	0	0	0	0	0	0	0	0
	Onkoides		0	0	0	0	0	0	0	0	1	0	0	0	0	0	0	0	0	0	0	0	0	0	0	0	0	0	0	0	0	0	0	0	0	0	0
	Ooids		0	0	0	0	0	0	0	0	1	0	0	0	0	0	0	0	0	0	0	0	0	0	0	0	0	0	0	0	0	0	0	0	0	0	0

Location	No. (Stratigraphy)		18	19	20	21	22	23																											
	Sample Code		18	9.1	9.2	20																													
			SC	SC	SC	SC	SC	SC																											
Composition	Matrix	**Micrite** : Sparite	9	9	9	5																													
	Composition (mineral.)	Micrite [%]	80	50	80	55																													
		Sparite [%]	10	40	0	25																													
		Internsed. [%]	0	1	10	1																													
		Sand [%]	0	0	0	10																													
		Open posrosity	1	10	10	10																													
		Shale [%]	10	5	5	1																													
	Components : Matrix		9	9	9	9																													
Components	**Bioclasts** : Biomorpha		1	9	5	9																													
	foraminifera, larger	SORITIDAE	0	0	0	0																													
		ALVEOLINIDAE	0	1	0	0																													
		ROTALIIDAE	0	0	0	1																													
		NUMMULITIDAE	0	1	1	10																													
		MIOGYPSINIDAE	0	0	0	0																													
		AMPHISTEGINIDAE	0	1	0	5																													
		ACERVULINIDAE	0	1	1	5																													
		HOMOTREMATIDAE	0	0	1	10																													
		LEPIDOCYCLINIDAE	0	0	0	1																													
		other	0	0	0	0																													
		SUM	0	21	3	32																													
	- small benthic		0	1	1	5																													
	- planktonic		0	0	0	1																													
	algae	red -	5	10	1	1																													
		green -	0	0	0	0																													
	bryozoans		0	0	0	5																													
	corals	branches	0	50	10	20																													
		heads	80	0	40	0	0	0																											
		SUM	80	50	40	10	20	0																											
	echinoderms		0	5	0	5	1	0																											
	molluscs	bivales/ oysters	1	1	1	1	1	5																											
		gastropods	0	0	0	0	0	10																											
	brachiopodes		1	1	0	1	1																												
	ostracods		0	1	0	0	1																												
	serpulids		0	1	0	0	0																												
	indetermined		10	10	10	25	25	25																											
	Terrigenous comp.	plantes, terr.	0	0	0	0	0	5																											
		Detritus/Quarz	0	0	0	0	1	10																											
	Authigeneous min.		0	0	0	0	0	0																											
	Lithoclasts	Intra-	0	0	0	0	0	1																											
		Extra-	0	0	0	0	0	0																											
		SUM clasts	0	0	0	0	0	0																											
	Pellets		10	1	1	0	0	1																											
	Grapestones/ Lumps		0	0	0	0	0	0																											
	Onkoides		0	0	0	0	0	0																											
	Ooids		0	0	0	0	0	0																											

	No. (Stratigraphy)		24	25	26	27	28	29	30	31	32	33	34	35	36	37	38	39	40	41	42	43	44	45	46	47	48	49	50	51	52	53	54	55	56	57	58	59	60	61	62	63	64	65	66
Location	Sample Code		21	22	23	24	25	26	28	29	30A	30C	31	32	33	34	35	36	37	38	39	40	41	42	43	44	45	46	47	48	49	50	51	52	53	54	55	56	57	58	59	60	61	62	64
			SC	SC	SC	SC	SC	SC	SC	SC	SC	SC	SC	SC	SC	SC	SC	SC	SC	SC	SC	SC	SC	SC	SC	SC	SC	SC	SC	SC	SC	SC	SC	SC	SC	SC	SC	SC	SC	SC	SC	SC	SC	SC	SC
Composition	Matrix	**Micrite** : Sparite	9	5	1	1	9	5	5	5	5	5	5	5	5	5	5	5	5	5	5	5	5	5	5	5	5	5	5	5	5	5	5	5	5	5	9	5	5	5	9	5	5	5	9
	Composition (mineral.)	Micrite [%]	70	40	20	20	50	45	45	40	30	60	50	60	50	50	50	45	50	55	50	50	50	50	55	35	60	40	50	35	30	60	25	30	40	60	90	60	70	45	90	70	70	75	90
		Sparite [%]	25	50	70	65	50	40	40	40	55	30	40	20	40	40	40	40	40	40	40	40	40	45	35	60	30	40	30	60	60	30	70	60	50	30	10	40	25	45	10	25	25	20	10
		Internsed. [%]	1	1	1	1	1	0	0	0	0	0	0	0	0	0	0	0	1	0	0	0	0	0	1	0	0	1	0	0	0	0	1	1	1	0	0	0	0	1	0	0	0	0	0
		Sand [%]	0	10	5	10	0	10	5	10	10	5	5	10	5	5	5	5	5	1	5	5	1	1	1	1	1	10	20	1	5	5	1	5	5	5	1	1	1	1	0	0	0	0	0
		Open posrosity	5	1	5	5	0	5	10	10	5	5	5	10	5	5	5	10	5	5	5	5	10	5	10	5	10	10	1	5	5	5	5	5	5	5	1	1	5	10	1	5	5	5	1
		Shale [%]	5	1	0	0	0	0	0	0	0	0	0	0	0	0	0	0	0	0	0	0	0	0	0	0	0	1	0	0	0	0	0	0	0	0	0	0	1	0	1	0	0	1	1
	Components : Matrix		9	9	9	9	5	9	9	9	9	9	9	9	9	9	9	9	9	9	9	9	9	9	9	9	9	9	9	9	9	9	9	9	9	9	9	9	9	9	9	9	9	9	9
Components	**Bioclasts** : Biomorpha		5	9	9	9	9	9	9	9	9	9	9	9	9	9	9	9	9	9	9	9	9	9	9	9	9	9	9	9	9	9	9	9	9	9	9	9	9	9	9	9	9	9	5
	foraminifera, larger	SORITIDAE	0	0	0	0	0	0	0	0	0	0	0	0	0	0	0	0	0	0	0	0	0	0	0	0	0	0	0	0	0	0	0	0	0	0	0	0	0	0	0	0	0	0	0
		ALVEOLINIDAE	0	0	0	0	0	0	0	0	0	0	0	0	0	0	0	0	0	0	0	0	0	0	0	0	0	0	0	0	0	0	0	0	0	0	0	0	0	0	0	0	0	0	0
		ROTALIIDAE	1	0	0	1	1	0	0	0	1	1	0	1	1	0	0	0	0	0	0	1	0	0	5	1	0	1	1	1	1	1	0	1	0	0	0	0	0	0	0	1	0	0	0
		NUMMULITIDAE	0	20	20	10	5	10	5	5	10	5	5	5	10	5	5	5	5	5	10	10	20	25	10	10	10	5	1	5	5	10	10	1	5	5	1	1	5	10	1	1	1	1	1
		MIOGYPSINIDAE	0	0	1	5	0	1	1	5	5	5	1	1	1	5	1	1	1	1	1	1	1	1	1	1	1	0	1	1	0	0	1	0	0	0	0	0	1	0	1	0	0	0	0
		AMPHISTEGINIDAE	1	0	5	5	0	1	5	1	5	1	1	1	1	5	1	1	5	5	1	5	1	5	5	5	5	1	0	5	1	1	1	1	1	5	1	1	1	5	1	1	1	1	0
		ACERVULINIDAE	5	5	1	0	1	0	1	1	0	0	1	0	1	1	1	1	1	1	1	1	1	1	1	1	0	0	0	1	1	1	0	1	1	1	0	0	1	1	1	1	1	1	0
		HOMOTREMATIDAE	5	5	5	1	1	5	1	1	5	10	5	1	5	5	5	5	1	1	5	1	10	5	5	10	10	5	1	5	5	10	10	5	5	10	1	1	1	5	1	0	1	0	0
		LEPIDOCYCLINIDAE	0	1	1	1	0	1	5	5	10	5	5	5	10	5	1	1	1	1	1	10	5	1	1	1	5	1	0	0	0	1	5	0	1	1	0	0	5	10	1	1	1	1	0
		other	0	0	0	0	0	0	0	0	0	0	0	0	0	0	0	0	0	0	0	0	0	0	0	0	0	0	0	0	0	0	0	0	0	0	0	0	0	0	0	0	0	0	0
		SUM	12	31	33	23	8	18	18	18	36	27	18	14	29	26	14	14	14	14	19	29	38	38	28	29	31	13	4	18	13	24	27	9	13	22	3	3	14	31	6	5	5	4	1
	- small benthic		1	1	1	1	0	1	1	1	0	0	0	1	0	0	0	0	0	0	1	1	1	0	1	1	1	5	1	1	1	1	1	5	5	5	10	5	5	5	5	5	5	5	20
	- planktonic		0	1	0	0	0	0	0	0	0	0	0	0	0	0	0	0	0	0	0	1	0	0	0	0	0	5	5	1	0	1	1	1	1	1	5	1	5	1	1	1	5	5	1
	algae	red -	1	1	5	5	5	0	1	1	1	1	1	1	1	1	1	1	1	1	1	1	1	1	5	1	0	1	1	1	1	5	1	1	1	1	0	1	1	10	1	1	1	1	1
		green -	0	0	0	0	0	0	0	0	0	0	0	0	0	0	0	0	0	0	0	0	0	0	0	0	0	0	0	0	0	0	0	0	0	0	0	0	1	0	0	0	0	0	0
	bryozoans		5	1	10	1	0	5	5	5	10	20	10	1	5	10	10	5	5	5	5	1	5	10	1	1	5	1	5	5	5	5	1	5	5	5	0	1	1	10	1	1	1	1	1
	corals	branches	0	5	0	0	0	0	0	0	0	0	0	0	0	0	0	0	0	0	0	0	0	0	0	0	0	0	0	0	0	0	0	0	0	0	0	0	0	0	0	0	0	0	0
		heads	60	0	0	0	0	0	0	0	0	0	0	0	0	0	0	0	0	0	0	0	0	0	0	0	0	0	0	0	0	0	0	0	0	0	0	0	0	0	0	0	0	0	0
		SUM	60	5	0	0	0	0	0	0	0	0	0	0	0	0	0	0	0	0	0	0	0	0	0	0	0	0	0	0	0	0	0	0	0	0	0	0	0	0	0	0	0	0	0
	echinoderms		1	5	5	1	1	1	5	5	10	20	20	25	20	10	10	5	10	5	5	10	5	10	5	10	5	5	5	10	5	1	10	10	10	10	5	5	1	10	5	5	5	10	1
	molluscs	bivales/ oysters	1	1	1	5	10	0	1	1	1	1	1	5	1	5	1	1	5	5	5	5	5	5	5	1	1	1	5	5	1	1	1	5	5	5	10	5	5	10	5	5	5	5	10
		gastropods	0	1	1	0	1	0	0	0	0	0	0	0	0	0	0	0	0	0	0	0	0	0	0	0	0	1	0	1	1	1	0	1	1	0	5	1	1	1	0	0	1	1	1
	brachiopodes		0	1	1	1	5	1	1	0	1	0	0	1	0	0	1	1	1	1	1	1	1	1	0	0	0	1	1	1	1	1	1	1	1	1	0	1	0	0	0	0	0	1	1
	ostracods		0	1	0	1	0	0	0	1	0	0	0	0	0	1	0	0	0	0	0	0	0	0	0	0	0	0	0	0	0	0	0	0	0	0	0	1	1	0	1	1	1	1	0
	serpulids		0	0	0	0	0	0	1	0	0	0	0	0	0	0	1	0	1	1	0	0	0	0	1	0	0	0	0	0	0	1	0	0	1	0	0	0	0	0	0	0	1	0	0
	indetermined		10	10	10	10	25	25	25	25	25	25	25	25	25	25	25	25	25	25	25	25	25	25	25	25	25	25	25	25	25	25	25	25	25	25	50	25	25	25	50	50	50	50	50
	Terrigenous comp.	plantes, terr.	1	5	1	1	0	1	1	5	1	1	1	1	1	1	0	1	0	1	1	1	5	1	1	1	1	1	5	1	1	1	1	10	5	1	1	1	1	1	0	1	1	1	1
		Detritus/Quarz	1	10	5	10	0	10	5	10	10	5	5	10	5	5	5	5	5	1	5	5	1	1	1	1	1	10	20	1	5	5	1	5	5	5	1	1	1	1	1	1	1	1	1
	Authigeneous min.		0	0	0	0	0	0	0	0	0	0	0	0	0	0	0	0	0	0	0	0	0	0	0	0	0	0	0	0	0	0	0	0	0	0	0	0	0	0	0	0	0	0	0
	Lithoclasts	Intra-	0	0	0	0	0	0	0	0	0	0	0	0	0	0	0	0	0	0	0	0	0	0	0	0	0	0	0	0	0	0	0	0	0	0	0	1	0	0	0	0	0	0	0
		Extra-	0	0	0	0	0	0	0	0	0	0	0	0	0	0	0	0	0	0	0	0	0	0	0	0	0	5	5	0	0	0	0	0	0	0	0	0	0	1	0	0	0	0	0
		SUM clasts	0	0	0	0	0	0	0	0	0	0	0	0	0	0	0	0	0	0	0	0	0	0	0	0	0	0	0	0	0	0	0	0	0	0	0	0	0	0	0	0	0	0	0
	Pellets		1	0	0	1	0	0	0	0	0	0	0	0	0	0	0	0	0	0	0	0	0	0	0	0	0	0	0	0	0	0	0	0	0	0	0	0	0	0	0	0	0	0	10
	Grapestones/ Lumps		0	0	0	0	0	0	0	0	0	0	0	0	0	0	0	0	0	0	0	0	0	0	0	0	0	0	0	0	0	0	0	0	0	0	0	0	0	0	0	0	0	0	0
	Onkoides		0	0	0	0	0	0	0	0	0	0	0	0	0	0	0	0	0	0	0	0	0	0	0	0	0	0	0	0	0	0	0	0	0	0	0	0	0	0	0	0	0	0	0
	Ooids		0	0	0	0	0	0	0	0	0	0	0	0	0	0	0	0	0	0	0	0	0	0	0	0	0	0	0	0	0	0	0	0	0	0	0	0	0	0	0	0	0	0	0

Location	No. (Stratigraphy)		67	68	69	70	71	72	73	74	75	76	77	78	79	80	81	82	83	84	85	86	87
	Sample Code		65	66	67	68	69	70	71	72	73	74	75	0	1	2	3	5	6	8	10	11	13
			SC	SC	SC	SC	SC	SC	SC	SC	SC	SC	SC	MA	MA	MA	MA	MA	MA	MA	MA	MA	MA
Composition	Matrix	**Micrite** : Sparite	5	9	9	9	9	9	9	9	9	9	9	9	9	9	9	9	9	9	9	9	9
	Composition (mineral.)	Micrite [%]	55	90	80	80	85	80	90	90	90	90	90	90	100	100	100	100	100	100	100	100	100
		Sparite [%]	40	5	20	5	1	10	5	5	5	5	5	10	1	1	1	1	1	1	1	1	1
		Internsed. [%]	0	0	0	0	0	0	0	0	0	0	0	1	0	0	0	0	0	0	0	0	0
		Sand [%]	0	0	0	0	0	0	0	0	0	0	0	0	0	0	0	0	0	0	0	0	0
		Open posrosity	5	5	1	10	10	10	5	5	5	5	5	1	0	0	0	0	0	1	0	1	0
		Shale [%]	0	10	1	5	5	5	5	5	10	10	10	10	20	10	20	10	10	5	10	5	5
	Components : Matrix		9	9	9	9	5	5	5	5	5	5	5	1	1	1	1	1	1	1	1	1	1
Components	**Bioclasts** : Biomorpha		5	5	5	5	5	5	5	5	5	9	5	5	1	1	1	1	1	1	1	1	1
	foraminifera, larger	SORITIDAE	0	0	0	0	0	0	0	0	0	0	0	0	0	0	0	0	0	0	0	0	0
		ALVEOLINIDAE	0	0	0	0	0	0	0	0	0	0	0	0	0	0	0	0	0	0	0	0	0
		ROTALIIDAE	0	0	1	1	0	0	0	0	0	0	0	5	0	0	0	1	1	1	0	1	0
		NUMMULITIDAE	1	1	1	1	0	0	1	1	0	0	0	0	0	0	0	0	0	0	0	0	0
		MIOGYPSINIDAE	0	0	0	0	0	0	0	0	0	0	0	0	0	0	0	0	0	0	0	0	0
		AMPHISTEGINIDAE	1	1	0	0	0	0	0	0	0	0	0	0	0	0	0	0	0	0	0	0	0
		ACERVULINIDAE	1	0	0	0	0	0	0	0	0	0	0	0	0	0	0	0	0	0	0	0	0
		HOMOTREMATIDAE	1	0	0	0	0	0	0	1	0	0	0	0	0	0	0	0	0	0	0	0	0
		LEPIDOCYCLINIDAE	1	0	0	0	0	0	0	0	0	0	0	0	0	0	0	0	0	0	0	0	0
		other	0	0	0	0	0	0	0	0	0	0	0	0	0	0	0	0	0	0	0	0	0
		SUM	5	2	2	2	0	0	1	2	0	0	0	5	0	0	0	1	1	1	0	1	0
	- small benthic		20	20	20	20	10	20	10	5	5	5	5	1	0	1	0	0	0	1	0	1	0
	- planktonic		1	1	5	5	1	1	5	5	5	5	5	20	5	1	1	1	1	1	1	1	1
	algae	red -	1	0	0	0	0	0	0	0	0	0	0	0	0	0	0	0	0	0	0	0	0
		green -	0	0	0	0	0	0	0	0	0	0	0	0	0	0	0	0	0	0	0	0	0
	bryozoans		5	1	1	1	0	1	1	1	0	1	5	0	0	0	0	0	0	0	0	0	0
	corals	branches	0	0	0	0	0	0	0	0	0	0	0	0	0	0	0	0	0	0	0	0	0
		heads	0	0	0	0	0	0	0	0	0	0	0	0	0	0	0	0	0	0	0	0	0
		SUM	0	0	0	0	0	0	0	0	0	0	0	0	0	0	0	0	0	0	0	0	0
	echinoderms		1	1	0	1	1	1	0	1	1	0	1	1	0	0	1	0	0	0	0	0	0
	molluscs	bivales/ oysters	1	10	10	20	10	10	10	10	10	10	10	5	1	1	1	1	0	0	1	1	1
		gastropods	1	5	1	1	1	1	0	0	0	0	0	0	0	0	0	0	0	0	0	0	0
	brachiopodes		0	0	0	0	0	0	0	1	0	0	1	0	0	0	0	0	0	0	0	0	0
	ostracods		0	0	0	0	0	0	1	1	1	1	1	0	0	0	0	0	0	0	0	0	0
	serpulids		0	0	0	0	0	0	0	0	0	0	0	0	0	0	0	0	0	0	0	0	0
	indetermined		50	75	75	75	50	50	50	50	50	50	50	25	1	5	5	1	1	1	5	5	5
	Terrigenous comp.	plantes, terr.	1	1	0	0	0	0	1	1	1	1	1	0	1	1	1	0	0	0	0	1	0
		Detritus/Quarz	1	0	0	0	0	0	0	1	1	1	1	1	1	1	1	1	1	1	1	1	1
	Authigeneous min.		0	0	0	0	0	0	0	0	0	0	0	0	0	0	0	0	0	0	0	0	0
	Lithoclasts	Intra-	0	0	0	0	0	0	0	0	0	0	0	0	0	0	0	0	0	0	0	0	0
		Extra-	0	0	0	0	0	0	0	0	0	0	0	0	0	0	0	0	0	0	0	0	0
		SUM clasts	0	0	0	0	0	0	0	0	0	0	0	0	0	0	0	0	0	0	0	0	0
	Pellets		0	10	10	10	5	5	10	10	5	5	5	1	0	0	0	0	5	5	5	10	5
	Grapestones/ Lumps		0	0	0	0	0	0	0	0	0	0	0	0	0	0	0	0	0	0	0	0	0
	Onkoides		0	0	0	0	0	0	0	0	0	0	0	0	0	0	0	0	0	0	0	0	0
	Ooids		0	0	0	0	0	0	0	0	0	0	0	0	0	0	0	0	0	0	0	0	0

Location	No. (Stratigraphy)		1	2	3	4	5	6	7	8	9	10	11	12	13	14	15	16	17	18	19	20
	Sample Code		E4-01	31.2	31.1	29	28A	27	E1B-01	E1A-01	26	E2-01	25B	24	23.2	21.1	20B	18	17	16	13	E3-01
			T	T	T	T	T	T	T	T	T	T	T	T	T	T	T	T	T	T	T	T
Composition	Matrix	**Micrite** : Sparite	9	9	5	9	9	9	9	9	9	9	9	9	9	9	9	9	9	9	9	9
	Composition (mineral.)	Micrite [%]	60	50	45	80	50	75	75	75	40	75	70	60	70	10	10	70	60	25	75	80
		Sparite [%]	40	50	55	20	50	20	25	25	60	25	30	35	25	90	90	10	30	75	20	10
		Internsed. [%]	0	0	0	0	0	0	0	0	0	5	0	0	0	0	0	15	5	0	0	0
		Sand [%]	0	0	0	0	0	0	0	0	0	0	0	0	0	0	0	0	0	0	0	0
		Open posrosity	1	1	1	0	0	5	1	1	1	1	1	1	5	0	0	5	5	1	5	10
		Shale [%]	10	5	1	5	5	5	1	1	5	1	1	1	1	5	5	1	1	5	5	1
	Components : Matrix		5	5	9	1	9	5	5	5	9	5	5	5	5	9	9	1	5	1	9	5
Components	**Bioclasts** : Biomorpha		9	9	9	9	1	9	5	9	1	5	9	1	9	1	1	9	9	1	9	5
	foraminifera, larger	SORITIDAE	1	5	5	0	1	10	5	5	5	5	10	5	5	10	5	5	5	0	1	5
		ALVEOLINIDAE	1	5	5	1	1	10	5	10	10	10	20	5	5	5	5	1	1	0	1	5
		ROTALIIDAE	0	0	0	0	0	0	0	0	0	0	0	0	0	0	1	0	0	0	0	0
		NUMMULITIDAE	1	0	0	0	0	0	0	0	1	0	0	0	0	0	1	0	1	0	0	1
		MIOGYPSINIDAE	0	0	0	0	0	0	0	0	0	0	0	0	0	0	0	0	0	0	0	0
		AMPHISTEGINIDAE	1	0	0	0	0	1	0	0	0	0	1	1	0	0	0	0	0	0	0	0
		ACERVULINIDAE	1	1	1	0	10	5	5	1	5	1	0	0	0	0	1	1	1	0	0	0
		HOMOTREMATIDAE	0	0	0	0	0	1	1	0	0	0	0	0	0	0	0	0	0	0	0	0
		LEPIDOCYCLINIDAE	0	0	0	0	0	0	0	0	0	0	0	0	0	0	0	0	0	0	0	0
		other	0	0	0	0	0	0	0	0	0	0	0	0	0	0	0	0	0	0	0	0
		SUM	5	11	11	1	12	27	16	16	21	16	31	11	10	15	13	7	8	0	2	11
	- small benthic		1	1	5	1	0	1	1	1	1	5	5	5	5	1	1	1	5	1	1	10
	- planktonic		0	0	0	0	0	0	0	0	0	0	0	0	0	0	0	0	0	0	0	5
	algae	red -	5	5	5	0	1	10	1	1	5	10	1	1	1	0	5	10	10	1	1	5
		green -	0	0	0	0	0	0	0	0	0	0	0	0	0	0	0	0	0	0	0	1
	bryozoans		0	0	0	0	0	1	0	0	0	0	0	1	0	0	0	0	0	0	0	10
	corals	branches	5	0	0	0	50	5	20	5	10	10	10	5	10	25	40	50	15	0	10	10
		heads	0	10	10	95	40	0	0	0	0	0	0	0	0	25	10	0	0	95	0	0
		SUM	5	10	10	95	90	5	20	5	10	10	10	5	10	50	50	50	15	95	10	10
	echinoderms		5	5	5	0	1	5	1	5	10	1	10	10	10	5	1	1	1	0	5	10
	molluscs	bivales/ oysters	5	10	5	1	1	10	5	10	5	5	10	5	5	5	5	1	1	10	5	5
		gastropods	5	0	0	0	1	1	5	5	1	10	10	10	10	5	5	1	1	0	0	5
	brachiopodes		0	0	0	0	0	0	0	0	0	0	0	0	1	1	1	1	1	0	0	0
	ostracods		1	0	0	0	0	0	0	0	5	0	1	5	5	1	1	0	0	0	1	1
	serpulids		0	0	0	0	0	0	0	1	0	0	0	0	1	0	0	0	0	0	0	0
	indetermined		25	25	25	25	25	25	25	25	25	25	25	25	25	25	25	25	25	25	25	25
	Terrigenous comp.	plantes, terr.	0	0	0	0	0	0	0	0	0	0	0	0	0	0	0	0	0	0	0	0
		Detritus/Quarz	0	0	0	0	0	0	0	0	0	0	0	0	0	0	0	0	0	0	0	0
	Authigeneous min.		0	0	0	0	0	0	0	0	0	0	0	0	0	0	0	0	0	0	0	0
	Lithoclasts	Intra-	0	0	0	0	0	0	0	0	0	0	0	0	0	0	0	0	0	0	0	0
		Extra-	0	0	0	0	0	0	0	0	0	0	0	0	0	0	0	0	0	0	0	0
		SUM clasts	0	0	0	0	0	0	0	0	0	0	0	0	0	0	0	0	0	0	0	0
	Pellets		0	0	0	0	0	0	0	0	0	0	0	0	0	0	0	0	0	0	0	0
	Grapestones/ Lumps		0	0	0	0	0	0	0	0	0	0	0	0	0	0	0	0	0	0	0	0
	Onkoides		0	0	0	0	0	0	0	0	0	0	0	0	0	0	0	0	0	0	0	0
	Ooids		0	0	0	0	0	0	0	0	0	0	0	0	0	0	0	0	0	0	0	0

Location	No. (Stratigraphy)		21	22	23	24	25	26	27	28	29	30	31	32	33	34	35
	Sample Code		12A T	12B T	VP1A T	VP1B T	11 T	10 T	9 T	8 T	7 T	6 T	5 T	4 T	2 T	1 T	0 T
Composition	Matrix	**Micrite** : Sparite	9	9	5	9	5	5	5	5	5	5	5	5	5	5	5
	Composition (mineral.)	Micrite [%]	50	80	55	70	45	40	30	60	50	45	40	30	60	50	60
		Sparite [%]	40	0	25	25	40	40	55	30	40	40	40	55	30	40	20
		Internsed. [%]	1	10	1	1	0	0	0	0	0	0	0	0	0	0	0
		Sand [%]	0	0	10	0	5	10	10	5	5	5	10	10	5	5	10
		Open posrosity	10	10	10	5	10	10	5	5	5	10	10	5	5	5	10
		Shale [%]	5	5	1	5	0	0	0	0	0	0	0	0	0	0	0
	Components : Matrix		5	5	9	9	9	9	9	9	9	9	9	9	9	9	9
Components	**Bioclasts** : Biomorpha		9	9	9	5	9	9	9	9	9	9	9	9	9	9	9
	foraminifera, larger	SORITIDAE	5	5	0	1	0	0	0	0	0	0	0	0	0	0	0
		ALVEOLINIDAE	1	1	0	0	0	0	0	0	0	0	0	0	0	0	0
		ROTALIIDAE	0	0	0	0	0	1	0	5	5	1	0	5	1	5	0
		NUMMULITIDAE	0	1	1	5	5	10	10	20	10	5	1	10	5	5	5
		MIOGYPSINIDAE	0	0	0	0	1	0	1	0	1	0	0	0	1	0	0
		AMPHISTEGINIDAE	0	10	10	5	10	20	20	20	20	10	20	20	10	10	20
		ACERVULINIDAE	0	5	1	1	5	0	1	5	5	10	5	0	1	0	1
		HOMOTREMATIDAE	0	1	5	5	0	0	0	1	0	0	0	0	1	1	0
		LEPIDOCYCLINIDAE	0	0	1	10	5	5	10	5	10	20	20	20	20	10	10
		other	0	0	0	1	1	0	1	1	0	5	1	5	10	5	5
		SUM	6	23	18	28	27	36	43	57	51	51	47	60	49	36	41
	- small benthic		1	1	10	10	10	1	10	1	5	0	5	1	5	1	0
	- planktonic		1	0	1	5	1	1	0	5	1	0	0	0	5	1	1
	algae	red -	10	5	10	5	10	1	20	1	10	1	1	5	5	5	0
		green -	0	0	0	1	0	0	0	0	0	0	0	0	0	0	0
	bryozoans		1	1	10	20	10	20	20	10	10	20	10	20	10	10	5
	corals	branches	20	20	10	0	0	0	0	0	1	0	0	0	0	0	0
		heads	0	0	0	0	0	0	0	0	0	0	0	0	0	0	0
		SUM	20	20	10	0	0	0	0	0	1	0	0	0	0	0	0
	echinoderms		5	5	10	10	10	5	10	10	10	20	20	10	10	10	5
	molluscs	bivales/ oysters	5	5	5	10	5	5	5	5	5	0	0	1	5	1	1
		gastropods	1	0	5	5	1	0	0	0	0	0	0	0	0	0	0
	brachiopodes		0	0	0	1	0	0	0	0	0	0	0	0	0	0	0
	ostracods		1	0	1	1	0	0	0	0	0	0	0	0	0	0	0
	serpulids		0	0	0	0	0	0	0	0	0	0	5	0	5	0	0
	indetermined		25	25	25	25	25	10	10	10	10	10	10	10	10	10	10
	Terrigenous comp.	plantes, terr.	0	0	0	0	0	0	0	0	0	0	0	0	0	0	0
		Detritus/Quarz	0	0	0	0	0	1	0	1	0	1	0	1	0	1	0
	Authigeneous min.		0	0	0	0	0	0	0	0	0	0	0	0	0	0	0
	Lithoclasts	Intra-	0	0	0	0	0	0	0	0	0	0	0	0	0	0	0
		Extra-	0	0	0	0	0	0	0	0	0	0	0	0	0	0	0
		SUM clasts	0	0	0	0	0	0	0	0	0	0	0	0	0	0	0
	Pellets		0	0	0	0	0	0	0	0	0	0	0	0	0	0	0
	Grapestones/ Lumps		0	0	0	0	0	0	0	0	0	0	0	0	0	0	0
	Onkoides		0	0	0	0	0	0	0	0	0	0	0	0	0	0	0
	Ooids		0	0	0	0	0	0	0	0	0	0	0	0	0	0	0

Location	No. (Stratigraphy)		1	2	3	4	5	6	7	8	11	12	14	15	16	17	18	19	20	22	23	24	25	26	27	28	29	32	34	35	37	38	39	40	41	42	43	44	45	46	48	49	50	51	52	53
	Sample Code		B 37	B 36	B 35	B 34	B 33	B 32	B 31	B 30	B 27	B 26	B 24	B 23	B 22	B 21	B E1	B 20	B 19	B 17	B 16	B 15	B 14	B 13	B 12	B 11	B 10	B 7	B 5	B 4	B 1	SEP 45	SEP 44	SEP 43	SEP 41	SEP 40	SEP 39	SEP 38	SEP 37	SEP 36	SEP 33	SEP 32	SEP 31	SEP 30	SEP 29	SEP 28
Composition	Matrix	**Micrite** : Sparite	9	9	9	5	5	9	9	9	9	9	9	9	9	5	5	5	9	5	5	9	9	9	9	5	5	9	9	9	9	5	5	5	5	9	9	9	9	9	5	9	5	9	9	5
	Composition (mineral.)	Micrite [%]	20	15	20	30	50	70	70	65	70	75	60	80	75	70	45	60	80	60	80	80	65	75	80	45	65	60	60	50	50	65	75	80	70	65	65	60	75	75	50	60	60	65	60	65
		Sparite [%]	0	0	1	30	25	30	30	30	20	25	30	20	20	30	40	40	20	40	20	20	30	20	15	40	30	30	30	40	50	30	20	20	30	30	30	30	20	20	40	35	35	30	20	50
		Internsed. [%]	0	0	0	0	1	0	0	0	0	0	0	0	0	1	0	0	0	0	0	0	0	0	0	1	0	0	5	1	0	0	0	0	0	1	0	5	0	0	5	0	0	10	5	0
		Shale [%]	5	5	5	1	1	1	1	1	5	1	0	0	0	0	0	0	1	0	1	1	1	1	1	0	0	0	0	0	0	0	0	0	0	0	0	5	0	0	0	0	0	5	5	0
		Sand [%]	75	80	70	20	20	0	0	0	0	0	1	1	1	1	1	1	0	0	0	0	0	0	0	0	0	0	0	0	0	0	0	0	0	0	0	0	0	0	0	0	0	0	0	0
		Open posrosity	1	1	5	1	5	1	1	5	5	1	10	1	5	1	5	1	1	1	1	1	5	5	5	5	5	10	5	10	1	5	5	1	1	5	5	1	5	5	5	5	3	1	10	5
	Components : Matrix		9	9	9	9	9	9	9	9	9	9	9	9	9	9	9	9	9	9	9	9	9	9	9	9	9	9	9	9	9	9	9	9	9	9	9	9	9	9	9	9	9	9	9	9
Components	**Bioclasts** : Biomorpha		0	0	9	9	9	9	9	9	9	9	9	9	9	9	8	9	9	9	9	9	9	9	9	9	9	9	9	9	9	9	9	9	8	8	9	5	9	9	9	9	9	9	9	9
	foraminifera, larger	SORITIDAE	0	0	1	0	0	0	0	0	0	0	0	0	0	0	0	0	0	0	0	0	0	0	0	0	0	1	1	0	1	0	0	0	0	0	0	0	0	0	0	0	0	0	0	0
		ALVEOLINIDAE	0	0	0	0	0	0	0	0	1	0	1	1	1	0	1	1	0	0	0	0	0	0	0	0	0	1	1	5	0	0	0	0	0	0	0	0	0	0	0	1	1	0	0	1
		ROTALIIDAE	0	0	0	0	1	1	0	1	0	1	1	1	1	1	1	5	1	1	1	1	1	1	0	1	1	1	1	1	1	1	0	0	0	0	0	0	1	0	0	0	0	0	0	0
		NUMMULITIDAE	1	1	1	5	5	5	1	5	1	1	10	5	5	1	5	10	1	1	1	1	5	1	5	1	5	10	5	10	5	5	5	5	1	5	1	1	1	5	1	1	5	1	1	5
		MIOGYPSINIDAE	0	0	0	0	0	0	1	0	0	0	1	0	0	0	0	0	1	0	0	0	0	0	0	0	0	0	1	0	0	0	0	0	0	0	0	0	0	0	0	1	0	0	0	0
		AMPHISTEGINIDAE	1	0	0	10	10	5	1	1	1	1	5	5	5	1	5	5	1	1	1	1	1	1	1	1	1	5	1	1	1	5	1	1	1	5	0	0	0	0	1	0	0	0	1	5
		ACERVULINIDAE	0	0	0	0	0	0	1	10	1	1	0	0	0	5	1	0	0	1	0	0	1	0	0	10	1	5	1	10	5	5	10	1	5	10	1	0	1	1	1	1	1	5	1	5
		HOMOTREMATIDAE	0	0	0	0	0	0	0	0	0	0	0	0	0	0	0	0	0	0	0	0	0	0	0	0	0	0	0	0	5	0	0	0	0	0	0	0	0	0	0	0	0	0	0	0
		LEPIDOCYCLINIDAE	0	0	0	0	0	0	0	0	0	0	0	0	0	0	0	0	0	0	0	0	0	0	0	0	0	0	0	0	0	0	0	0	0	0	0	0	0	0	0	0	0	0	0	0
		other	0	0	0	0	0	0	0	0	0	0	0	0	0	0	0	0	0	0	0	0	0	0	0	0	0	0	0	0	0	1	1	0	1	0	0	1	0	1	0	1	1	0	0	0
		SUM	2	1	2	15	16	11	4	17	4	4	18	12	12	8	13	21	4	4	3	3	8	3	6	13	8	23	11	27	18	17	17	7	8	20	2	2	3	7	3	5	8	6	3	16
	- small benthic		0	1	1	5	1	5	1	1	1	5	5	5	1	1	1	1	5	5	5	1	5	5	5	5	10	5	1	5	1	5	5	1	5	5	1	0	5	5	1	1	5	1	1	5
	- planktonic		0	0	1	0	1	0	0	0	0	5	5	5	1	1	1	5	5	5	1	1	1	0	1	1	1	0	0	1	1	1	1	1	1	0	0	0	1	0	1	1	1	0	0	0
	algae	red -	1	0	1	1	5	1	1	1	1	1	5	1	5	5	10	5	1	1	1	5	5	1	1	5	10	10	5	10	1	10	1	1	5	5	5	5	5	1	0	1	1	5	1	1
		green -	0	0	0	0	0	1	0	0	0	1	0	5	1	0	1	1	0	1	0	0	0	0	0	0	0	1	0	1	10	0	0	0	0	0	1	0	0	0	0	0	10	0	0	0
	bryozoans		0	0	1	5	1	1	1	0	0	1	0	1	1	1	1	1	1	1	1	1	1	1	1	1	5	1	5	1	5	1	0	0	0	0	0	0	1	5	0	0	1	0	0	0
	corals	branches	0	0	0	0	1	5	0	0	20	0	10	0	0	0	0	0	0	0	1	0	0	0	0	0	0	0	0	5	10	5	0	0	1	5	20	50	10	0	0	0	1	10	1	0
		heads	0	0	0	0	0	5	10	5	0	0	0	0	1	0	0	1	0	0	0	0	0	0	0	20	0	0	20	5	1	0	0	0	0	0	0	0	0	0	20	60	0	0	0	10
		SUM	0	0	0	0	1	10	10	5	20	0	10	0	1	0	0	1	0	0	1	0	0	0	0	20	0	0	20	10	11	5	0	0	1	5	20	50	10	0	20	60	1	10	1	10
	echinoderms		0	0	1	5	1	5	1	5	1	5	5	1	1	1	5	1	1	1	1	5	5	1	1	5	5	5	10	1	1	1	1	1	1	1	1	0	1	1	1	5	1	1	5	5
	molluscs	bivales/ oysters	0	0	1	5	5	5	5	5	5	5	5	5	5	5	5	5	5	5	5	5	5	5	5	5	5	5	10	1	10	5	5	5	5	5	5	5	5	5	5	5	5	5	5	5
		gastropods	0	0	1	0	1	1	1	5	0	0	5	1	1	1	1	0	1	0	0	0	0	0	0	0	0	1	0	0	5	0	0	0	0	0	0	1	0	0	0	0	0	0	0	0
	brachiopodes		0	0	0	0	0	0	0	0	0	0	0	0	0	0	0	0	0	0	0	0	5	5	1	1	1	1	0	1	0	0	0	1	0	0	0	0	1	0	0	1	0	0	0	0
	ostracods		0	0	0	0	0	0	0	0	0	0	0	0	0	0	0	0	1	1	1	0	0	0	0	1	0	0	0	0	0	1	0	0	0	0	0	0	0	0	0	1	0	0	0	1
	serpulids		0	0	0	0	0	0	0	0	0	0	0	0	0	0	0	0	0	0	0	0	0	0	0	0	0	0	0	0	0	0	0	0	0	1	1	0	0	1	0	1	0	0	0	1
	indetermined		0	0	5	10	10	10	10	25	10	10	10	10	10	10	10	10	10	10	25	25	25	25	25	25	25	25	25	25	25	25	25	25	25	25	25	10	25	25	25	25	25	25	40	25
	Terrigenous comp.	plantes, terr.	5	1	5	5	5	1	1	1	0	0	1	1	1	1	1	1	1	1	0	0	0	0	0	0	0	0	0	0	0	1	1	0	0	0	0	0	0	0	0	0	0	0	0	0
		Detritus/Quarz	90	95	85	90	25	0	1	1	0	0	5	1	1	1	1	5	1	0	0	0	1	1	1	1	0	0	1	1	1	0	0	0	0	0	0	0	0	0	0	0	0	0	0	0
	Authigeneous min.		0	0	0	0	0	0	0	0	0	0	0	0	0	0	0	0	0	0	1	0	0	0	0	0	0	0	0	0	0	0	0	0	0	0	0	0	0	0	0	0	0	0	0	0
	Lithoclasts	Intra-	0	0	0	10	10	0	0	0	0	0	0	0	0	0	0	0	0	0	0	0	0	0	0	0	0	0	0	1	0	0	0	0	0	0	0	0	0	0	0	0	0	0	0	0
		Extra-	1	1	1	10	5	0	0	0	0	0	10	1	5	1	1	1	0	0	0	0	0	0	0	0	0	0	0	0	1	0	0	0	0	0	0	0	0	0	0	0	0	0	0	0
		Sum	1	1	1	20	15	0	0	0	0	0	10	1	5	1	1	1	0	0	0	0	0	0	0	0	0	0	0	1	1	0	0	0	0	0	0	0	0	0	0	0	0	0	0	0
		SUM detritus	91	96	86	110	40	0	1	1	0	0	15	2	6	2	2	6	1	0	1	0	1	1	1	1	0	0	1	2	2	0	0	0	0	0	0	0	0	0	0	0	0	0	0	0
	Pellets		0	0	0	0	0	0	0	0	1	0	0	0	0	0	0	0	0	0	0	0	0	0	0	1	0	0	0	0	0	0	0	0	0	0	0	0	0	0	0	5	0	5	1	0
	Grapestones/ Lumps		0	0	0	0	0	0	0	0	0	0	0	0	0	0	0	0	0	0	0	0	0	0	0	0	0	0	0	0	0	0	0	0	0	0	0	0	0	0	0	0	0	0	0	0
	Onkoides		0	0	0	0	0	0	0	0	0	0	0	0	0	0	0	0	0	0	0	0	0	0	0	0	0	0	0	0	0	0	0	0	0	0	0	0	0	0	0	0	0	0	0	0
	Ooids		0	0	0	0	0	0	0	0	0	0	0	0	0	0	0	0	0	0	0	0	0	0	0	0	0	0	0	0	0	0	0	0	0	0	0	0	0	0	0	0	0	0	0	0

Location	No. (Stratigraphy)		54	55	56	57	58	59	60	61	62	63	64	66	67	69	70	71	72	73	74	75	76	77	80	81	84	85	86	87	88	89	90	91	92	93	94	95	97	99	100	101	102	103	104	105
	Sample Code		SEP	SEP	SEP	SEP	SEP	SEP	SEP	SEP	SEP	SEP	SEP	SEP	SEP	SEP	SEP	SEP	SEP	SEP	SEP	SEP	SEP	SP	SP	SP	SP	SP	SP	SP	SP	SP	SP	SP	SP	SP	SP	SP	SP	SP	SP	SP	SP	SP	SP	SP
			26	25	24	22	21	20	19	18	17	16	15	13	12	10	9	7	6	5	4	3	1	96	92	91	88	87	86	84	83	82	81	80	79	78	77	76	74	71	69	68	67	66	64	63
Composition	Matrix	**Micrite** : Sparite	9	5	9	5	9	9	9	9	5	9	9	9	9	9	9	9	9	9	9	9	5	9	9	9	9	9	5	5	5	5	9	9	5	9	9	5	5	5	5	9	9	9	5	5
	Composition (mineral.)	Micrite [%]	55	60	50	55	80	65	90	90	80	75	50	70	70	60	80	65	85	75	75	85	75	60	50	80	70	60	90	85	90	95	85	55	60	55	60	60	50	30	40	60	60	65	60	50
		Sparite [%]	30	30	40	40	10	30	1	5	20	20	50	30	30	40	20	30	10	20	20	10	20	40	35	30	30	40	5	5	10	5	5	40	40	20	35	40	45	70	60	40	40	30	40	35
		Internsed. [%]	10	5	1	1	0	0	0	0	0	0	0	0	0	0	0	0	0	0	0	0	0	1	10	0	0	0	0	0	0	0	0	5	1	5	5	0	5	0	0	0	0	0	0	0
		Shale [%]	0	0	0	0	0	0	10	0	0	5	1	0	0	1	0	0	0	0	0	0	0	0	5	1	1	1	0	0	0	0	0	0	0	5	0	0	0	0	0	0	0	0	0	10
		Sand [%]	0	0	0	0	0	0	0	0	0	0	0	0	0	0	0	0	0	0	0	0	0	0	0	0	0	0	0	0	0	0	0	0	0	0	0	0	0	0	0	0	0	0	0	0
		Open posrosity	5	5	10	5	10	5	1	5	1	5	0	1	1	0	1	5	5	5	5	5	5	0	1	1	1	1	5	10	1	1	10	1	1	5	1	1	1	1	1	1	5	5	1	5
	Components : Matrix		9	9	9	9	5	9	5	9	9	9	9	9	9	9	9	9	5	5	5	5	5	9	9	9	9	9	9	9	9	9	9	9	9	9	9	9	9	9	9	9	9	9	9	9
Components	**Bioclasts** : Biomorpha		9	9	9	9	9	9	5	9	9	9	1	9	9	5	9	9	9	8	9	9	9	9	5	9	9	5	8	9	9	9	9	9	9	9	9	9	9	9	9	9	9	9	9	9
	foraminifera, larger	SORITIDAE	0	0	0	1	0	1	0	0	0	1	0	5	0	0	0	0	1	0	1	0	0	0	0	0	1	1	0	0	1	0	0	1	0	1	1	0	1	1	1	1	1	1	0	0
		ALVEOLINIDAE	0	1	5	5	5	0	0	1	5	1	0	5	5	1	1	0	0	1	0	0	0	1	1	1	5	1	0	0	1	1	1	1	1	0	0	0	0	1	5	0	1	0	1	0
		ROTALIIDAE	0	0	0	0	0	0	1	1	1	0	0	0	0	0	0	0	0	0	0	0	0	0	0	0	0	0	0	0	0	0	0	0	0	0	0	0	1	1	1	0	1	0	0	0
		NUMMULITIDAE	1	5	5	10	5	1	5	10	10	1	1	5	1	0	1	1	0	1	0	1	5	10	5	1	1	1	1	1	1	5	5	5	5	1	1	1	1	5	1	0	1	1	5	5
		MIOGYPSINIDAE	0	0	0	0	0	0	0	1	1	0	0	0	0	0	0	0	0	0	0	0	0	0	0	0	0	0	0	0	1	0	0	0	0	0	0	1	0	1	0	0	0	0	0	0
		AMPHISTEGINIDAE	1	1	1	1	0	1	1	5	1	0	0	1	1	0	0	0	0	0	0	0	0	1	1	0	0	1	1	0	0	1	0	1	1	1	0	1	1	5	1	0	1	1	1	1
		ACERVULINIDAE	1	1	1	1	5	5	1	1	1	0	0	10	5	1	5	1	5	1	1	1	0	5	10	5	5	0	1	1	0	1	1	1	1	1	5	1	1	1	1	1	1	5	1	1
		HOMOTREMATIDAE	0	0	0	0	0	0	0	0	0	0	0	0	0	0	0	0	0	0	0	0	0	0	0	0	0	0	0	0	0	0	0	0	0	0	0	0	0	0	0	0	0	0	0	0
		LEPIDOCYCLINIDAE	0	0	0	0	0	0	0	0	0	0	0	0	0	0	0	0	0	0	0	0	0	0	0	0	0	0	0	0	0	0	0	0	0	0	0	0	0	0	0	0	0	0	0	0
		other	0	0	0	0	0	0	0	0	0	0	0	0	0	0	0	0	1	0	0	0	0	0	0	0	0	0	0	0	0	0	0	0	0	0	0	0	0	0	0	0	1	1	1	1
		SUM	3	8	12	18	15	8	8	19	19	3	1	26	12	2	7	2	7	3	2	2	5	17	17	7	12	4	3	2	4	8	7	9	8	4	7	4	5	15	10	2	7	9	9	8
	- small benthic		1	1	1	1	1	1	1	1	1	1	0	5	1	1	1	1	1	1	1	1	1	1	1	1	5	1	1	1	1	1	1	1	1	1	1	1	1	5	5	5	1	1	5	1
	- planktonic		0	0	0	1	0	0	0	1	0	0	0	1	0	0	1	0	0	0	0	0	0	1	0	1	0	0	0	0	0	0	0	0	1	1	0	0	0	0	0	0	0	0	0	0
	algae	red -	1	1	10	10	1	1	1	5	5	5	10	1	5	5	10	10	5	5	5	0	1	5	5	5	5	5	5	5	5	1	1	1	1	5	10	1	5	1	5	1	1	5	5	10
		green -	0	0	0	0	0	5	0	0	0	0	1	1	0	1	1	1	0	0	1	0	0	1	40	1	1	0	0	0	0	0	0	0	0	0	0	0	1	0	1	0	0	1	0	0
	bryozoans		0	0	0	1	0	0	1	1	1	0	0	0	0	0	5	0	0	1	0	0	0	1	0	1	0	0	0	0	0	0	0	0	1	1	1	1	0	0	1	0	1	0	1	0
	corals	branches	0	0	0	0	0	0	0	0	0	5	0	10	10	0	10	20	10	10	10	5	0	20	0	5	0	0	0	1	0	0	10	0	5	0	0	0	30	0	0	0	1	5	0	50
		heads	60	60	20	10	0	5	0	0	0	0	80	0	0	30	0	0	0	0	0	0	0	0	0	50	20	60	0	0	0	0	0	60	0	20	40	0	0	0	60	60	20	0	0	0
		SUM	60	60	20	10	0	5	0	0	0	5	80	10	10	30	10	20	10	10	10	5	0	20	0	55	20	60	0	1	0	0	10	60	5	20	40	0	30	0	60	60	21	5	0	50
	echinoderms		1	1	1	1	1	1	1	5	1	1	1	5	1	1	1	1	1	1	1	1	5	5	1	1	1	1	1	1	1	1	1	1	5	1	1	5	1	1	1	1	1	1	1	1
	molluscs	bivales/ oysters	1	1	1	1	1	1	1	1	1	1	1	5	5	5	1	1	1	1	1	5	1	10	1	1	1	5	1	1	1	1	1	1	1	1	1	1	5	1	1	1	1	1	1	1
		gastropods	0	0	0	0	0	0	0	0	1	1	1	1	1	1	1	1	1	5	1	1	1	1	1	5	0	0	0	0	1	0	0	0	1	1	0	0	1	5	5	1	1	1	0	0
	brachiopodes		0	0	0	0	0	0	0	1	0	1	0	1	0	0	0	0	0	0	0	0	1	1	0	1	0	0	0	0	0	0	0	1	0	1	1	0	0	1	0	0	0	0	1	0
	ostracods		0	0	0	0	0	0	1	0	0	0	0	0	0	0	0	0	0	1	0	0	0	0	1	1	1	0	0	0	0	0	1	0	0	0	1	1	0	0	0	1	0	0	0	0
	serpulids		0	0	0	0	0	0	0	0	0	0	0	0	0	0	0	0	0	0	0	0	0	0	0	0	0	0	0	0	0	0	0	0	0	0	0	0	0	0	0	0	0	0	0	0
	indetermined		25	25	25	25	25	25	25	25	25	25	10	25	25	25	25	10	10	25	25	25	25	10	10	10	20	20	25	40	40	25	25	25	25	25	25	25	25	25	25	25	25	25	30	40
	Terrigenous comp.	plantes, terr.	0	0	0	0	0	0	0	0	0	0	0	0	0	0	0	0	0	0	0	0	0	0	0	0	0	0	0	0	0	0	0	0	0	0	0	0	0	0	0	0	0	0	0	0
		Detritus/Quarz	0	0	0	0	0	0	0	0	0	0	0	0	0	0	0	0	0	0	0	0	0	1	1	1	1	0	0	0	0	0	0	0	1	1	0	0	0	0	0	0	0	0	0	0
	Authigeneous min.		0	0	0	0	0	0	0	0	0	0	0	0	0	0	0	0	0	0	0	0	0	0	0	0	0	0	0	0	0	0	0	0	0	0	0	0	0	0	0	0	0	0	0	0
	Lithoclasts	Intra-	0	0	0	0	0	0	0	0	0	0	0	0	0	0	0	0	0	0	0	0	0	0	0	0	0	0	0	0	0	0	0	0	0	0	0	0	0	0	0	0	0	0	0	0
		Extra-	0	0	0	0	0	0	0	0	0	0	0	0	0	0	0	0	0	0	0	0	0	0	0	0	0	0	0	0	0	0	0	0	0	0	0	0	0	0	0	0	0	0	0	0
		Sum	0	0	0	0	0	0	0	0	0	0	0	0	0	0	0	0	0	0	0	0	0	0	0	0	0	0	0	0	0	0	0	0	0	0	0	0	0	0	0	0	0	0	0	0
		SUM detritus	0	0	0	0	0	0	0	0	0	0	0	0	0	0	0	0	0	0	0	0	0	1	1	1	1	0	0	0	0	0	0	0	1	1	0	0	0	0	0	0	0	0	0	0
	Pellets		0	0	0	0	0	0	0	0	0	0	0	0	0	0	0	0	0	0	0	5	0	0	1	10	5	20	5	1	5	5	1	1	0	5	1	5	0	0	1	10	5	5	0	0
	Grapestones/ Lumps		0	0	0	0	0	0	0	0	0	0	0	0	0	0	0	0	0	0	0	0	0	0	0	0	0	0	0	0	0	0	0	0	0	0	0	0	0	0	0	0	0	0	0	0
	Onkoides		0	0	0	0	0	0	0	0	0	0	0	0	0	0	0	0	0	0	0	0	0	0	0	0	0	0	0	0	0	0	0	0	0	0	0	0	0	0	0	0	0	0	0	0
	Ooids		0	0	0	0	0	0	0	0	0	0	0	0	0	0	0	0	0	0	0	0	0	0	0	0	0	0	0	0	0	0	0	0	0	0	0	0	0	0	0	0	0	0	0	0

Location	No. (Stratigraphy)		106	107	108	110	111	112	113	114	116	117	118	119	120	121	122	123	124	125	126	127	128	129	132	133	134	135	137	139	141	143	146	148	149	151	152	153	154	157	158	159	160	161	162	163	165	166
	Sample Code		SP 62	SP 61	SP 60	SP 57	SP 56	SP 55	SP 54	SP 53	SP 51	SP 50	SP 48	SP 46	SP 45	SP 44	SP 43	SP 42	SP 41	SP 40	SP 39	SP 38	SP 37	SP 36	SP 32	SP 31	SP 30l	SP 30u	SP 28	SP 26	SP 24	SP 22	SP 19	SP 17	SP 16	SP 14	SP 13	SP 11	SP 10.2	SP 9	SP 8	SP 7	SP 6	SP 5	SP 4	SP 3	SP 1.2	SP 1
Composition	Matrix	**Micrite** : Sparite	5	9	9	9	9	9	9	9	5	5	5	5	5	5	5	5	5	5	5	5	9	5	5	5	1	5	1	1	5	5	5	5	5	5	5	5	5	5	5	5	5	5	9	5	9	9
	Composition (mineral.)	Micrite [%]	80	60	50	70	55	70	75	90	65	75	75	40	50	70	60	60	60	80	80	60	75	70	55	65	30	50	30	40	60	50	55	55	55	60	60	60	50	70	60	30	50	50	50	30	50	70
		Sparite [%]	20	30	40	30	30	20	10	5	25	60	20	50	40	30	40	40	40	20	20	30	10	25	40	30	65	40	65	60	40	50	40	45	40	35	30	30	40	20	40	60	40	40	40	65	40	30
		Internsed. [%]	0	0	0	0	10	5	1	0	0	0	0	0	1	1	0	0	0	0	0	5	5	1	0	0	5	0	5	0	0	0	5	0	0	0	0	0	1	0	0	0	5	0	10	1	5	1
		Shale [%]	1	10	10	1	0	0	10	1	0	0	0	0	0	0	0	0	0	0	0	0	0	0	0	0	0	0	0	0	0	0	0	0	0	0	0	0	0	0	0	0	0	0	0	0	0	0
		Sand [%]	0	0	0	0	0	0	0	0	0	0	0	0	0	0	0	0	0	0	0	0	0	0	0	0	0	0	0	0	0	0	0	0	0	0	0	0	0	0	0	0	0	0	0	0	0	0
		Open posrosity	1	1	0	0	5	5	5	5	10	5	5	10	10	1	1	1	1	1	5	5	10	5	1	5	1	10	1	1	1	0	1	1	5	5	10	10	10	10	10	10	5	10	1	5	5	1
	Components : Matrix		9	9	9	9	9	9	9	9	9	9	9	9	9	9	9	9	9	9	9	9	9	9	9	9	9	9	9	9	9	9	9	9	9	9	9	9	9	9	9	9	9	9	9	9	9	9
Components	**Bioclasts** : Biomorpha		9	5	9	9	9	9	9	9	9	9	9	9	9	9	9	9	9	9	9	9	9	9	9	9	9	5	9	9	9	9	9	9	9	9	9	9	9	9	9	9	9	9	5	9	5	9
	foraminifera, larger	SORITIDAE	0	0	0	0	1	1	5	1	0	0	0	0	0	0	0	0	1	1	1	0	1	0	1	0	1	1	0	0	1	1	1	1	5	0	0	0	0	0	1	1	1	1	0	1	0	1
		ALVEOLINIDAE	1	0	0	0	1	1	0	1	1	1	1	0	1	0	1	1	1	1	1	0	1	0	1	1	0	0	0	1	0	1	1	1	0	0	0	0	0	0	5	5	1	0	0	0	0	1
		ROTALIIDAE	0	0	0	0	0	1	0	0	1	1	1	5	1	1	1	1	1	1	1	1	1	1	5	1	1	10	1	1	1	1	1	0	1	0	0	0	0	0	0	0	1	0	1	0	0	0
		NUMMULITIDAE	5	1	1	1	1	1	1	1	1	1	1	1	1	0	1	1	1	1	1	1	1	1	1	1	1	5	10	5	5	1	1	1	1	1	1	1	1	1	5	1	1	0	1	1	0	0
		MIOGYPSINIDAE	0	0	0	0	0	0	0	0	0	0	0	0	0	0	0	1	0	0	0	0	0	0	0	0	0	0	0	0	0	0	0	0	1	0	0	0	0	0	1	0	0	0	0	0	0	0
		AMPHISTEGINIDAE	1	1	1	1	1	1	1	1	1	1	1	1	1	1	1	0	0	1	1	1	1	0	1	0	0	1	5	1	1	1	1	1	1	1	1	1	1	1	1	1	1	1	0	0	0	1
		ACERVULINIDAE	10	10	5	1	1	1	1	1	1	1	5	1	1	1	5	5	5	1	1	0	1	5	1	1	5	0	5	1	1	1	5	1	1	1	5	1	5	10	1	0	0	1	5	5	1	1
		HOMOTREMATIDAE	0	0	0	0	0	0	0	0	0	0	0	0	0	0	0	0	0	0	0	0	0	0	0	0	0	0	0	0	0	0	0	0	0	0	0	0	0	0	0	0	0	0	0	0	0	0
		LEPIDOCYCLINIDAE	0	0	0	0	0	0	0	0	0	0	0	0	0	0	0	0	0	0	0	0	0	0	0	0	0	0	0	0	0	0	0	0	0	0	0	0	0	0	0	0	0	0	0	0	0	0
		other	0	0	0	0	0	0	0	0	1	0	0	0	0	1	0	0	1	1	1	1	1	1	0	0	0	0	0	0	0	0	1	1	1	0	0	0	0	0	0	0	1	0	0	0	0	0
		SUM	17	12	7	3	5	6	8	5	6	5	9	8	5	4	9	9	10	7	7	4	7	8	10	4	8	17	21	9	9	6	11	6	11	3	7	3	7	12	14	8	6	3	7	7	1	4
	- small benthic		1	1	1	1	1	1	1	1	5	5	1	5	1	1	1	1	1	5	1	1	1	1	1	1	1	0	1	1	1	1	1	5	1	5	1	5	1	1	1	1	1	1	1	1	1	5
	- planktonic		0	0	0	0	0	0	0	0	0	0	0	0	0	0	0	0	0	0	0	0	0	0	0	0	0	0	0	0	0	0	0	0	0	0	1	1	0	0	0	0	0	0	0	0	1	0
	algae	red -	10	10	5	5	1	1	5	5	1	5	1	1	1	1	10	5	5	1	1	5	5	1	5	30	5	1	10	1	5	5	10	5	1	1	5	5	5	10	5	5	1	1	5	5	5	1
		green -	1	0	1	1	1	0	0	1	0	0	1	0	0	0	0	0	1	1	0	0	0	0	0	0	1	0	0	0	0	1	0	0	0	0	0	0	0	0	1	0	0	0	0	0	1	0
	bryozoans		0	0	1	0	0	0	0	0	1	1	0	1	5	1	0	0	1	1	0	0	1	1	5	1	1	1	1	1	0	1	1	1	0	0	0	0	1	1	0	1	0	0	1	1	0	0
	corals	branches	10	30	0	20	20	10	10	10	0	0	0	0	0	0	5	60	5	0	20	0	10	20	0	0	10	0	20	0	0	0	0	1	0	1	1	0	20	1	0	0	20	0	0	0	0	20
		heads	0	0	70	0	0	0	0	0	0	0	0	0	0	50	0	0	0	0	0	40	0	0	0	0	0	0	0	0	0	5	20	0	0	0	0	0	0	0	0	0	10	0	70	0	40	0
		SUM	10	30	70	20	20	10	10	10	0	0	0	0	0	50	5	60	5	0	20	40	10	20	0	0	10	0	20	0	0	5	20	1	0	1	1	0	20	1	0	0	30	0	70	0	40	20
	echinoderms		1	0	0	0	0	0	0	0	1	1	1	5	1	1	5	1	1	1	1	5	5	1	5	5	5	1	1	5	1	1	1	1	1	1	1	1	1	1	5	5	5	10	10	20	1	1
	molluscs	bivales/ oysters	1	1	1	1	1	1	1	1	1	1	1	1	1	1	1	1	1	1	1	1	1	1	1	1	1	1	5	1	1	1	5	1	1	1	5	5	5	1	1	1	1	1	1	5	5	1
		gastropods	0	1	0	1	1	1	0	1	0	0	0	0	0	1	1	0	1	1	0	5	0	1	0	5	1	0	1	1	1	1	1	1	1	1	1	5	1	1	1	0	5	5	1	0	5	1
	brachiopodes		1	1	0	0	0	1	0	0	0	1	1	1	5	5	1	1	1	1	5	1	1	1	1	1	1	1	1	1	1	1	0	1	1	1	1	1	1	0	0	0	1	1	5	1	0	0
	ostracods		0	0	0	0	0	0	0	0	0	0	1	0	0	1	0	0	0	0	0	0	0	0	0	0	0	0	0	1	1	0	1	0	0	0	0	0	0	0	0	0	0	0	1	1	5	0
	serpulids		0	1	0	0	0	0	0	0	0	0	0	0	0	0	0	0	0	0	0	0	0	0	0	0	0	0	1	0	0	0	0	0	0	0	0	0	0	0	1	0	0	0	0	0	0	0
	indetermined		25	25	25	25	25	25	25	25	40	25	25	30	25	25	25	25	25	30	30	25	40	30	30	25	25	25	25	25	30	25	10	25	25	30	25	25	25	30	25	25	25	25	25	25	30	30
	Terrigenous comp.	plantes, terr.	0	0	0	0	0	0	0	0	0	0	0	0	0	0	0	0	0	0	0	0	0	0	0	0	0	0	0	0	0	0	0	0	0	0	0	0	0	0	0	0	0	0	0	0	0	0
		Detritus/Quarz	0	0	0	0	0	0	0	0	0	0	0	0	0	0	0	0	0	0	0	0	0	0	0	0	0	0	1	0	0	0	0	0	0	0	0	0	0	0	0	0	0	0	0	0	0	0
	Authigeneous min.		0	0	0	0	0	0	0	0	0	0	0	0	0	0	0	0	0	0	0	0	0	0	0	0	0	0	0	0	0	0	0	0	0	0	0	0	0	0	0	0	0	0	0	0	0	0
	Lithoclasts	Intra-	0	0	0	0	0	0	0	0	0	0	0	0	0	0	0	0	0	0	0	0	0	0	0	0	0	0	0	0	0	0	0	0	0	0	0	0	0	0	0	0	0	0	0	0	0	0
		Extra-	0	0	0	0	0	0	0	0	0	0	0	0	0	0	0	0	0	0	0	0	0	0	0	0	0	0	0	0	0	0	0	0	0	0	0	0	0	0	0	0	0	0	0	0	0	0
		Sum	0	0	0	0	0	0	0	0	0	0	0	0	0	0	0	0	0	0	0	0	0	0	0	0	0	0	0	0	0	0	0	0	0	0	0	0	0	0	0	0	0	0	0	0	0	0
		SUM detritus	0	0	0	0	0	0	0	0	0	0	0	0	0	0	0	0	0	0	0	0	0	0	0	0	0	0	1	0	0	0	0	0	0	0	0	0	0	0	0	0	0	0	0	0	0	0
	Pellets		0	5	5	10	1	1	5	1	0	1	1	0	0	0	0	0	0	0	1	5	0	0	10	5	0	0	1	0	0	1	10	0	1	25	0	0	10	10	5	0	5	1	1	10	5	1
	Grapestones/ Lumps		0	0	0	0	0	0	0	0	0	0	0	0	0	0	0	0	0	0	0	0	0	0	0	0	0	0	0	0	0	0	0	0	0	0	0	0	0	0	0	0	0	0	0	0	0	0
	Onkoides		0	0	0	0	0	0	0	0	0	0	0	0	0	0	0	0	0	0	0	0	0	0	0	0	0	0	0	0	0	0	0	0	0	0	0	0	0	0	0	0	0	0	0	0	0	0
	Ooids		0	0	0	0	0	0	0	0	0	0	0	0	0	0	0	0	0	0	0	0	0	0	0	0	0	0	0	0	0	0	0	0	0	0	0	0	0	0	0	0	0	0	0	0	0	0

Location	No. (Stratigraphy)		131	130	129	128	127	126	125	123	122	121	120	119	118	117	116	115	114	113
	Sample Code		1	2	3	4	5	6	7	9	10	11	12	13	14	15	16	17	18	19
			TA	TA	TA	TA	TA	TA	TA	TA	TA	TA	TA	TA	TA	TA	TA	TA	TA	TA
Structure	Grainsize	Mikrit	10	60	50	60	40	10	30	10	10	15	10	10	40	10	20	20	20	20
		Calciarenit (63µm -)	80	30	40	30	50	85	60	60	85	80	85	85	40	80	60	50	20	30
		Calcirudit (> 2 mm)	10	10	10	10	10	5	10	30	5	5	5	5	20	10	20	30	60	50
	Particle contacts	no contact	0	40	0	20	10	0	30	0	0	10	0	0	10	0	0	0	0	0
		pointe	60	50	65	70	60	70	50	60	60	60	60	50	65	50	60	45	20	30
		tangential	40	10	30	10	30	30	20	40	40	30	40	50	20	35	25	30	45	30
		concavo-convex	0	0	1	0	1	1	1	1	1	1	1	1	5	10	10	20	30	20
		sutured	0	1	5	0	1	1	1	1	1	1	1	1	0	5	5	5	5	20
	Compaction (0-3)	Index (nil-well)	1	1	2	1	1	2	2	2	2	1	2	2	1	3	2	2	1	1
	Roundness (0-3)	Index (nil-well)	0	0	0	0	0	0	0	0	0	0	0	0	0	1	1	2	2	2
	Sorting (0-3)	Index (nil-well)	1	2	1	1	1	0	1	0	1	1	1	1	0	2	2	2	1	1
	Gradation/ Bedding		0	0	0	0	2	0	0	0	0	0	0	0	0	0	1	2	1	0
	Orientation		0	0	2	0	1	0	0	0	0	1	1	1	0	1	0	1	0	1
Diagenesis	Sparite	Neomorphism	0	0	0	0	0	0	0	0	0	0	0	0	5	0	0	0	0	10
		Cements	100	100	100	100	100	100	100	100	100	100	100	100	95	100	100	100	100	90
	Types of cements	Fibrous	0	0	0	0	0	1	0	0	1	1	1	1	0	2	2	3	0	3
		Granular	1	2	3	3	3	3	3	3	3	3	3	3	3	3	3	3	3	3
		Drusy	0	0	1	2	3	2	2	0	0	1	1	0	1	0	0	1	0	1
		Radiaxial fibrous	3	0	0	0	0	0	0	0	0	0	0	0	0	0	0	0	0	0
		Micrite	1	0	0	0	1	0	0	0	0	1	1	1	2	0	0	0	0	0
		Syntaxial rim	0	0	1	0	0	0	0	1	0	0	0	0	0	0	0	0	0	0
		Meniscus	0	0	0	0	0	0	0	0	0	0	0	0	0	0	0	0	0	0
		Dripstone	0	0	0	0	0	0	0	0	0	0	0	0	0	0	0	0	0	0
		Dog-tooth	0	1	1	3	2	2	1	0	0	1	1	1	0	0	1	0	0	0
	Total porosity		10	10	20	15	15	25	10	25	15	20	15	15	10	25	20	25	20	20
	Typ of Pores	Interparticle	1	0	3	0	1	3	0	3	3	3	3	3	1	3	3	3	2	3
		Intraparticle	0	1	1	0	1	0	1	1	1	1	0	1	1	1	1	1	0	3
		Intercrystal	0	0	0	0	0	0	0	0	0	0	0	0	0	0	0	0	0	0
		Moldic	2	2	0	2	3	3	1	0	0	0	1	0	3	1	1	0	0	2
		Fenestral	0	0	0	0	0	0	0	0	0	0	0	0	0	1	1	0	1	1
		Shelter	0	0	1	0	1	1	2	1	1	1	0	0	1	1	1	0	0	1
		Growth-framework	0	0	0	0	0	0	0	0	0	0	0	0	0	0	0	0	0	0
		Fracture	1	0	1	1	0	0	1	1	0	0	0	1	0	2	1	1	1	1
		Channel	0	0	2	3	0	1	2	0	0	0	0	1	0	0	0	0	1	0
		Vug	1	2	3	3	2	3	3	3	3	3	3	3	2	3	3	3	3	3
		Biogenous	0	0	1	0	1	0	0	1	0	1	0	0	0	1	1	1	1	2
	Dissolution		1	2	3	3	2	3	2	3	3	2	2	2	2	3	3	3	3	3
	Dolomitization		0	0	0	0	0	0	0	0	0	0	0	0	0	0	0	0	0	0
	Dedolomitization		0	0	0	0	0	0	0	0	0	0	0	0	0	0	0	0	0	0
NOTE			y	y	y	y	y	y	y	y	y	y	y	y	y	y	y	y	y	y

Location	No. (Stratigraphy)		1	2	3	4	5	6	7	8	9	10	11	12	13	14	15	16	17	18	19	20	21	22	23
	Sample Code		1	2	3	4	5	6.1	6.2	7	8	9	10	11	12	12B	13	14	15	16	17	18	9.1	9.2	20
			SC	SC	SC	SC	SC	SC	SC	SC	SC	SC	SC	SC	SC	SC	SC	SC	SC	SC	SC	SC	SC	SC	SC
Structure	Grainsize	Mikrit	50	50	20	80	10	50	60	60	20	60	60	60	50	10	10	75	40	20	30	50	40	40	25
		Calciarenit (63µm -)	25	40	75	10	1	25	10	40	10	40	30	10	40	5	1	20	40	10	20	10	50	20	75
		Calcirudit (> 2 mm)	25	10	5	10	90	25	30	1	70	1	10	30	10	85	90	5	20	70	50	40	10	40	1
	Particle contacts	no contact	50	10	0	100	100	50	100	75	100	50	75	100	25	50	100	90	25	80	20	95	30	25	0
		pointe	50	80	70	0	0	50	0	25	0	50	25	0	50	50	0	10	50	20	25	5	60	75	75
		tangential	1	10	25	0	0	0	0	0	0	0	0	0	0	0	0	0	5	0	10	0	0	1	25
		concavo-convex	1	1	1	0	0	0	0	0	0	0	0	0	0	0	0	0	10	0	20	0	10	0	0
		sutured	0	1	5	0	0	0	0	0	0	0	0	0	0	0	0	0	10	0	25	0	0	0	0
	Compaction (0-3)	Index (nil-well)	0	1	2	0	0	1	0	0	0	0	1	1	2	0	0	0	2	0	2	0	1	1	1
	Roundness (0-3)	Index (nil-well)	0	0	0	0	0	0	0	0	0	0	0	0	0	0	0	0	0	0	0	0	0	0	0
	Sorting (0-3)	Index (nil-well)	0	0	1	2	3	0	3	2	2	2	1	2	2	2	3	2	0	2	0	1	0	1	3
	Gradation/ Bedding		0	0	0	0	0	0	0	0	0	0	0	0	1	0	0	0	0	0	0	0	0	0	2
	Orientation		0	0	0	0	0	1	1	0	0	0	1	0	1	0	0	0	0	0	1	1	0	1	2
Diagenesis	Sparite	Neomorphism	50	25	5	5	75	10	75	5	60	5	10	50	5	25	75	5	5	75	75	75	5	0	5
		Cements	50	75	95	95	25	90	25	95	40	95	90	50	95	75	25	95	95	25	25	25	95	0	95
	Types of cements	Fibrous	0	0	0	0	0	0	0	0	0	0	0	0	0	0	0	0	0	0	0	0	0	0	0
		Granular	3	3	3	3	3	3	3	3	3	3	3	3	3	3	3	3	3	3	3	3	3	0	3
		Drusy	2	1	0	1	0	1	0	1	2	2	1	0	0	2	0	0	0	2	0	0	1	0	3
		Radiaxial fibrous	0	0	0	0	0	0	0	0	0	0	0	0	0	0	0	0	0	0	0	0	0	0	0
		Micrite	0	0	0	0	0	0	0	0	0	0	0	0	0	1	1	1	1	1	2	0	0	3	0
		Syntaxial rim	0	0	0	0	0	0	0	0	0	0	0	0	0	0	0	0	0	0	0	0	0	0	0
		Meniscus	0	0	0	0	0	0	0	0	0	0	0	0	0	0	0	0	0	0	0	0	0	0	0
		Dripstone	0	0	0	0	0	0	0	0	0	0	0	0	0	0	0	0	0	0	0	0	0	0	0
		Dog-tooth	0	0	0	0	0	0	0	0	1	0	0	0	0	0	0	0	0	0	0	0	0	0	1
	Total porosity		25	25	40	10	10	10	10	10	25	10	10	10	15	30	5	5	20	10	10	10	20	10	20
	Typ of Pores	Interparticle	0	2	2	0	0	0	0	0	0	0	0	0	0	0	0	0	1	0	0	0	0	0	3
		Intraparticle	1	2	2	0	0	0	1	2	0	2	1	0	1	0	0	2	1	0	2	2	1	1	3
		Intercrystal	0	0	0	0	0	0	0	0	0	0	0	0	0	0	0	0	0	0	0	0	0	0	0
		Moldic	2	2	0	3	0	2	2	2	0	0	1	1	2	2	0	0	1	0	1	1	2	2	2
		Fenestral	0	0	1	0	0	0	0	1	0	1	1	0	0	0	0	0	2	0	0	0	0	2	0
		Shelter	0	0	1	0	0	0	0	0	0	0	0	0	1	0	0	0	0	0	0	0	0	0	0
		Growth-framework	0	0	0	0	0	0	0	0	3	0	0	0	0	3	1	0	0	1	0	0	0	0	0
		Fracture	1	1	2	1	0	0	0	0	0	0	0	0	0	0	0	0	0	0	0	0	0	1	2
		Channel	2	2	0	2	2	3	1	0	0	1	2	2	1	0	0	2	3	0	0	1	1	0	1
		Vug	3	3	3	1	3	3	3	2	0	2	3	3	3	2	2	2	3	3	3	3	3	3	2
		Biogenous	0	0	0	0	2	0	0	0	0	0	0	0	0	2	3	3	3	1	1	0	0	1	0
	Dissolution		1	2	2	1	1	2	1	1	1	1	1	1	2	1	1	1	2	1	2	2	2	2	2
	Dolomitization		0	0	0	0	0	0	0	0	0	0	0	0	0	0	0	0	0	0	0	0	0	0	1
	Dedolomitization		0	0	0	0	0	0	0	0	0	0	0	0	0	0	0	0	0	0	0	0	0	0	0
NOTE			y	y	y	y	y	y	y	y	y	y	y	y	y	y	y	y	y	y	y	y	y	y	y

Location	No. (Stratigraphy)		24	25	26	27	28	29	30	31	32	33	34	35	36	37	38	39	40	41	42	43	44	45	46	47	48	49	50	51	52	53	54	55	56	57	58	59	60	61	62	63	64	65	66
	Sample Code		21	22	23	24	25	26	28	29	30A	30C	31	32	33	34	35	36	37	38	39	40	41	42	43	44	45	46	47	48	49	50	51	52	53	54	55	56	57	58	59	60	61	62	64
			SC	SC	SC	SC	SC	SC	SC	SC	SC	SC	SC	SC	SC	SC	SC	SC	SC	SC	SC	SC	SC	SC	SC	SC	SC	SC	SC	SC	SC	SC	SC	SC	SC	SC	SC	SC	SC	SC	SC	SC	SC	SC	SC
Structure	Grainsize	Mikrit	20	20	10	20	50	20	20	20	20	40	30	50	40	40	30	20	20	20	20	20	20	20	20	5	20	20	10	10	10	25	20	10	20	20	40	20	30	20	30	30	30	30	20
		Calciarenit (63µm -)	30	70	90	70	30	80	80	80	80	60	70	50	55	60	70	80	80	80	80	70	75	80	80	95	80	70	80	90	90	70	75	90	70	70	60	80	70	60	70	70	70	70	80
		Calcirudit (> 2 mm)	50	10	1	10	20	1	1	1	1	1	1	1	5	1	1	0	0	0	0	10	5	1	0	0	1	10	10	0	0	5	5	0	10	10	0	0	0	20	0	0	0	0	0
	Particle contacts	no contact	30	0	0	0	25	0	0	0	0	0	0	0	0	0	0	1	0	0	0	0	0	0	0	1	0	0	0	0	0	0	0	0	0	0	0	0	0	0	0	0	0	0	0
		pointe	50	60	90	80	65	70	60	40	20	10	10	10	30	40	20	60	40	30	20	30	70	60	40	60	20	70	80	50	60	40	45	80	70	70	##	80	80	50	##	95	95	90	100
		tangential	20	30	10	20	10	20	20	30	60	60	75	65	60	55	60	40	60	60	60	65	30	40	60	40	60	30	20	50	40	50	45	20	30	25	0	20	20	30	0	5	5	10	0
		concavo-convex	0	10	0	0	0	5	10	5	10	10	5	5	5	5	10	1	1	5	10	5	1	1	1	1	10	1	0	0	0	5	5	0	0	0	0	0	0	5	0	5	0	0	0
		sutured	0	0	0	0	0	5	10	5	10	20	10	20	5	1	10	1	1	5	10	1	1	1	1	1	10	0	0	0	0	5	5	0	1	5	0	0	1	15	1	0	1	1	0
	Compaction (0-3)	Index (nil-well)	1	1	1	1	1	2	2	2	2	2	2	2	1	1	2	2	2	3	3	2	1	2	2	1	3	1	1	1	1	2	2	0	1	2	1	1	1	3	1	1	1	1	1
	Roundness (0-3)	Index (nil-well)	0	1	1	0	0	1	0	1	1	1	1	1	1	1	2	1	1	1	1	1	1	2	2	1	1	1	1	1	1	1	1	1	1	1	2	1	1	0	0	0	0	0	0
	Sorting (0-3)	Index (nil-well)	1	2	3	2	0	2	2	2	2	2	2	2	2	1	2	2	2	2	2	1	1	2	2	3	2	1	3	3	3	2	1	3	1	1	3	3	2	0	3	3	2	2	3
	Gradation/ Bedding		0	2	1	1	1	1	2	2	3	2	2	2	1	1	2	1	1	2	2	2	0	0	0	0	1	1	0	1	1	3	1	2	2	2	1	1	1	0	0	0	1	1	0
	Orientation		0	2	1	2	0	1	2	2	2	2	1	2	1	1	2	0	0	2	1	1	0	1	1	2	2	1	1	2	2	1	1	2	1	2	0	1	1	2	1	1	1	1	0
Diagenesis	Sparite	Neomorphism	5	5	0	0	5	0	0	0	0	0	0	0	0	0	0	0	0	0	0	0	0	0	0	0	0	0	0	0	0	0	0	0	0	0	0	0	0	0	0	0	0	0	0
		Cements	95	95	100	100	95	100	100	100	100	100	100	100	100	100	100	100	100	100	100	100	100	100	100	100	100	100	100	100	100	100	100	100	100	100	100	100	100	100	100	100	100	100	100
	Types of cements	Fibrous	0	0	1	1	2	0	0	0	1	0	1	1	0	2	1	1	1	1	0	0	1	1	0	1	1	0	0	1	1	0	1	1	1	0	0	0	0	0	0	0	0	0	0
		Granular	3	3	3	2	3	3	3	2	2	2	2	1	3	3	2	2	3	3	3	3	3	3	3	3	3	3	3	3	3	3	3	3	3	3	1	3	3	3	1	2	2	2	2
		Drusy	1	1	0	0	0	0	0	0	0	0	0	0	0	0	0	0	0	0	0	0	0	0	0	0	0	0	0	0	0	0	0	1	0	0	0	0	1	0	0	0	1	0	0
		Radiaxial fibrous	0	0	0	0	0	0	0	0	0	0	0	0	0	0	0	0	0	0	0	0	0	0	0	0	0	0	0	0	0	0	0	0	0	0	0	0	0	0	0	0	0	0	0
		Micrite	0	1	0	0	0	0	0	0	0	0	0	1	1	0	0	0	0	0	0	0	0	0	0	0	0	0	0	0	0	0	0	0	0	0	0	0	0	0	0	0	0	0	0
		Syntaxial rim	0	0	0	1	0	1	1	2	2	2	2	2	1	1	2	2	1	1	1	1	0	1	1	2	1	0	0	1	1	1	1	1	1	0	0	0	0	0	0	0	0	0	0
		Meniscus	0	0	1	0	0	0	0	0	0	0	0	0	0	0	0	0	0	0	0	0	0	0	0	0	0	0	0	0	0	0	0	0	0	0	0	0	0	0	0	0	0	0	0
		Dripstone	0	0	0	0	0	0	0	0	0	0	0	0	0	0	0	0	0	0	0	0	0	0	0	0	0	0	0	0	0	0	0	0	0	0	0	0	0	0	0	0	0	0	0
		Dog-tooth	0	0	1	1	0	0	0	0	0	0	0	0	0	0	0	0	0	0	0	0	0	0	0	0	0	0	0	0	0	0	0	0	0	0	0	0	0	0	0	0	0	0	0
	Total porosity		20	10	30	25	30	10	25	20	25	15	20	15	10	10	20	20	10	10	10	20	25	20	20	25	15	15	5	15	15	15	25	15	15	15	5	10	10	25	5	10	10	10	5
	Typ of Pores	Interparticle	3	1	3	3	0	3	3	3	3	2	2	2	2	2	2	3	3	3	3	3	3	3	3	3	3	2	3	3	3	3	3	3	3	3	1	3	3	3	1	2	2	2	1
		Intraparticle	1	2	2	3	1	1	2	2	2	2	3	1	1	2	2	2	2	2	2	0	2	2	1	2	1	1	0	1	1	1	2	2	2	1	1	1	2	3	2	2	2	2	2
		Intercrystal	0	0	0	0	0	0	0	0	0	0	0	0	0	0	0	0	0	0	0	0	0	0	0	0	0	0	0	0	0	0	0	0	0	0	0	0	0	0	0	0	0	0	0
		Moldic	3	1	1	1	3	0	1	0	0	0	0	0	0	0	0	0	0	0	0	0	0	0	0	0	0	0	0	0	0	0	0	0	0	0	0	0	1	1	0	0	0	0	0
		Fenestral	0	0	0	0	0	0	0	0	0	0	0	0	0	0	0	0	0	0	0	0	0	0	0	0	0	0	0	0	0	0	0	0	0	0	0	0	0	1	0	0	0	0	0
		Shelter	0	1	0	0	0	0	0	0	0	0	0	0	1	1	1	1	1	1	1	1	0	1	0	1	0	0	0	0	0	0	1	0	2	0	0	0	0	1	0	1	0	1	0
		Growth-framework	0	0	0	0	0	0	0	0	0	0	0	0	0	0	0	0	0	0	0	0	0	0	0	0	0	0	0	0	0	0	0	0	0	0	0	0	0	0	0	0	0	0	0
		Fracture	2	0	0	0	0	0	0	0	0	0	0	0	0	0	0	0	0	0	0	0	0	1	1	0	0	0	0	0	0	0	0	0	0	0	0	0	0	0	0	1	0	0	0
		Channel	2	0	1	0	0	0	1	0	0	0	0	1	0	0	0	0	0	0	0	0	1	0	0	1	0	2	0	0	0	0	0	0	0	1	2	0	1	1	1	0	0	0	0
		Vug	2	1	1	1	0	3	2	2	1	1	1	3	3	3	3	2	2	2	2	2	3	2	3	2	3	2	0	2	2	2	2	1	2	2	1	1	1	3	2	2	2	3	1
		Biogenous	1	1	0	0	0	0	0	0	0	0	0	0	0	0	0	0	0	0	0	0	0	1	0	1	0	1	0	0	0	0	0	0	0	0	0	0	0	1	0	0	0	0	3
	Dissolution		2	1	1	1	1	1	2	2	1	1	2	2	1	1	2	2	1	1	1	1	2	1	2	1	2	1	1	1	2	1	2	1	2	2	1	1	1	2	1	1	1	2	1
	Dolomitization		1	0	0	0	0	0	0	0	0	0	0	0	0	0	0	0	0	0	0	0	0	0	0	0	0	0	0	0	0	0	0	0	0	0	0	0	0	0	0	0	0	0	0
	Dedolomitization		0	0	0	0	0	0	0	0	0	0	0	0	0	0	0	0	0	0	0	0	0	0	0	0	0	0	0	0	0	0	0	0	0	0	0	0	0	0	0	0	0	0	0
NOTE			y	y	y	y	y	y	y	y	y	y	y	y	y	y	y	y	y	y	y	y	y	y	y	y	y	y	y	y	y	y	y	y	y	y	y	y	y	y	y	y	y	y	y

Location	No. (Stratigraphy)		67	68	69	70	71	72	73	74	75	76	77	78	79	80	81	82	83	84	85	86	87
	Sample Code		65	66	67	68	69	70	71	72	73	74	75	0	1	2	3	5	6	8	10	11	13
			SC	SC	SC	SC	SC	SC	SC	SC	SC	SC	SC	MA	MA	MA	MA	MA	MA	MA	MA	MA	MA
Structure	Grainsize	Mikrit	20	50	20	50	50	50	40	40	40	40	40	80	95	95	95	95	95	95	95	95	95
		Calciarenit (63µm -)	80	50	80	50	50	50	60	60	60	60	60	20	5	5	5	5	5	5	5	5	5
		Calcirudit (> 2 mm)	0	1	0	0	0	0	0	0	0	0	0	0	0	0	0	0	0	0	0	1	0
	Particle contacts	no contact	0	50	0	50	75	50	50	40	40	40	40	20	100	100	100	100	100	100	100	100	100
		pointe	100	50	100	50	25	50	50	60	60	60	60	80	0	0	0	0	0	0	0	0	0
		tangential	0	0	0	0	0	0	0	0	0	0	0	0	0	0	0	0	0	0	0	0	0
		concavo-convex	0	0	0	0	0	0	0	0	0	0	0	0	0	0	0	0	0	0	0	0	0
		sutured	0	0	0	0	0	0	0	0	0	0	0	0	0	0	0	0	0	0	0	0	0
	Compaction (0-3)	Index (nil-well)	1	0	0	0	0	0	0	0	0	1	0	0	0	0	0	0	1	0	0	0	0
	Roundness (0-3)	Index (nil-well)	0	0	0	0	0	0	0	0	0	0	0	0	0	0	0	0	0	0	0	0	0
	Sorting (0-3)	Index (nil-well)	3	3	3	3	3	3	3	3	3	3	3	2	3	3	3	3	3	3	3	3	3
	Gradation/ Bedding		0	0	1	0	0	0	1	0	1	0	0	0	1	1	1	0	0	0	0	0	0
	Orientation		0	0	0	0	0	0	0	0	1	0	0	0	0	0	0	0	0	0	0	0	0
Diagenesis	Sparite	Neomorphism	0	0	0	0	0	0	0	0	0	0	0	10	0	0	0	1	1	1	0	1	0
		Cements	100	100	100	100	100	100	100	100	100	100	100	90	100	100	100	100	100	100	100	100	100
	Types of cements	Fibrous	0	0	0	0	0	0	0	0	0	0	0	0	0	0	0	0	0	0	0	0	0
		Granular	2	2	2	1	1	2	2	2	2	2	2	2	1	1	1	1	1	1	1	1	1
		Drusy	0	1	0	0	0	2	0	0	0	0	0	0	0	0	0	0	0	0	0	0	1
		Radiaxial fibrous	0	0	0	0	0	0	0	0	0	0	0	0	0	0	0	0	0	0	0	0	0
		Micrite	0	0	0	0	0	0	0	0	0	0	0	0	0	0	0	0	0	0	0	0	0
		Syntaxial rim	0	0	0	0	0	1	0	0	0	0	0	0	0	0	0	0	0	0	0	0	0
		Meniscus	0	0	0	0	0	0	0	0	0	0	0	0	0	0	0	0	0	0	0	0	0
		Dripstone	0	0	0	0	0	0	0	0	0	0	0	0	0	0	0	0	0	0	0	0	0
		Dog-tooth	0	0	0	0	1	2	0	0	0	0	0	0	0	0	0	0	0	0	0	0	0
	Total porosity		10	5	10	5	10	15	5	5	5	10	5	5	1	1	5	1	1	1	1	5	1
	Typ of Pores	Interparticle	2	0	0	0	0	0	1	1	1	2	1	0	0	0	0	0	0	0	0	0	0
		Intraparticle	2	2	1	1	0	1	2	2	2	1	2	1	1	1	1	1	1	1	1	1	1
		Intercrystal	0	0	0	0	0	0	0	0	0	0	0	0	0	0	0	0	0	0	0	0	0
		Moldic	0	0	0	0	0	0	0	0	0	0	0	1	0	0	0	0	0	0	0	0	1
		Fenestral	0	0	0	0	0	0	0	0	0	0	0	0	0	0	0	0	0	0	0	0	0
		Shelter	0	0	0	0	0	0	0	0	0	0	0	0	0	0	0	0	0	0	0	0	0
		Growth-framework	0	0	0	0	0	0	0	0	0	0	0	0	0	0	0	0	0	0	0	0	0
		Fracture	0	0	0	0	0	0	0	0	0	0	0	1	0	0	0	1	0	1	0	1	0
		Channel	0	0	0	0	1	1	0	0	1	0	0	0	0	0	0	0	0	0	0	1	0
		Vug	2	2	2	2	2	2	2	2	2	3	2	2	1	0	1	0	0	0	1	1	0
		Biogenous	3	1	3	3	2	3	3	2	2	2	2	0	0	0	0	0	1	1	0	1	0
	Dissolution		2	2	2	2	2	3	1	1	1	2	1	1	1	0	1	0	0	0	1	1	0
	Dolomitization		0	0	0	0	0	0	0	0	0	0	0	0	0	0	0	0	0	0	0	0	0
	Dedolomitization		0	0	0	0	0	0	0	0	0	0	0	0	0	0	0	0	0	0	0	0	0
NOTE			y	y	y	y	y	y	y	y	y	y	y	y	y	y	y	n	y	y	y	y	n

Location	No. (Stratigraphy)		1	2	3	4	5	6	7	8	11	12	14	15	16	17	18	19	20	22	23	24	25	26	27	28	29	32	34	35	37	38	39	40	41	42	43	44	45	46	48	49	50	51	52	53	54
	Sample Code		B 37	B 36	B 35	B 34	B 33	B 32	B 31	B 30	B 27	B 26	B 24	B 23	B 22	B 21	B E1	B 20	B 19	B 17	B 16	B 15	B 14	B 13	B 12	B 11	B 10	B 7	B 5	B 4	B 1	SEP 45	SEP 44	SEP 43	SEP 41	SEP 40	SEP 39	SEP 38	SEP 37	SEP 36	SEP 33	SEP 32	SEP 31	SEP 30	SEP 29	SEP 28	SEP 26
Structure	Grainsize	Mikrit	10	5	10	20	20	40	40	45	45	30	30	50	50	50	35	55	70	50	70	75	50	40	60	40	45	40	50	40	40	40	40	50	50	40	40	40	40	45	40	30	40	50	50	40	30
		Calciarenit (63µm -)	90	95	85	50	40	40	30	35	25	70	40	50	40	45	45	40	30	50	30	25	50	50	40	30	50	40	30	40	30	40	50	50	45	40	30	20	50	50	40	30	40	20	30	50	20
		Calcirudit (> 2 mm)	1	0	5	30	40	20	30	20	30	1	30	0	10	5	20	5	1	0	0	0	1	10	0	30	5	20	20	20	30	20	10	1	5	20	30	40	10	5	20	40	20	30	20	10	50
	Particle contacts	no contact	0	0	0	0	0	0	0	0	0	0	0	0	0	0	0	0	0	0	0	0	0	0	0	0	0	0	0	0	0	0	0	0	0	0	0	0	0	0	0	0	0	10	20	0	0
		pointe	100	100	100	80	60	90	75	80	90	95	85	95	95	95	85	95	95	95	35	95	95	95	95	70	70	80	75	80	70	90	90	95	90	85	90	95	95	95	95	95	95	90	75	95	95
		tangential	0	0	0	20	30	10	20	20	10	5	10	5	5	5	10	5	5	5	5	5	5	5	5	20	20	20	20	20	20	10	10	5	10	10	10	5	5	5	10	5	5	5	5	5	5
		concavo-convex	0	0	0	0	10	0	5	1	1	0	5	0	0	0	5	0	0	0	0	1	0	0	0	5	5	1	5	1	5	1	0	0	0	0	0	0	0	0	1	0	0	10	0	0	0
		sutured	0	0	0	0	0	0	0	1	0	0	1	0	0	0	0	0	0	0	0	1	0	0	0	5	5	1	1	1	5	1	1	1	0	5	0	0	0	0	5	0	0	5	0	0	0
	Compaction (0-3)	Index (nil-well)	0	0	0	1	2	1	1	2	1	1	2	1	1	1	1	1	1	1	1	1	1	1	1	2	2	1	2	1	1	1	1	1	1	2	1	1	1	1	2	1	1	2	1	1	1
	Roundness (0-3)	Index (nil-well)	1	1	1	1	2	1	1	1	1	1	1	1	1	1	1	1	0	0	1	1	0	0	0	1	1	1	1	1	1	0	0	0	0	0	0	0	0	0	0	0	0	0	0	0	0
	Sorting (0-3)	Index (nil-well)	3	2	2	1	1	1	1	1	1	2	0	1	1	1	1	1	2	3	2	2	2	1	2	1	1	0	0	0	0	1	2	2	1	1	1	1	2	2	1	1	1	1	1	2	2
	Gradation/ Bedding		0	0	0	0	0	0	0	0	0	2	0	0	0	0	0	0	1	0	0	0	1	0	0	0	2	0	0	0	0	0	0	1	1	2	2	2	1	1	0	0	1	1	0	0	0
	Orientation		0	0	0	0	0	0	0	0	0	0	0	0	0	0	0	0	0	0	1	0	0	0	0	0	0	0	0	0	0	0	1	0	1	2	3	2	1	1	0	0	0	2	1	0	0
Diagenesis	Sparite	Neomorphism	0	0	0	20	20	60	50	60	50	20	60	40	30	30	30	30	30	50	30	20	20	20	10	30	20	20	40	40	40	20	10	5	10	20	20	50	10	5	40	60	50	20	10	20	40
		Cements	0	0	##	80	80	40	50	40	50	80	40	60	70	70	20	70	70	50	70	80	80	80	90	70	80	80	60	60	60	80	90	95	90	80	80	50	90	95	60	40	50	80	90	80	60
	Types of cements	Fibrous	0	0	0	0	0	0	0	0	0	0	0	0	0	0	0	0	0	0	1	0	0	0	0	0	0	0	0	0	0	0	0	0	0	0	0	0	0	0	0	0	0	0	0	0	0
		Granular	0	0	0	3	3	3	3	3	3	3	3	3	3	3	3	1	1	3	2	1	1	1	1	3	2	3	2	1	3	3	2	2	3	3	3	3	2	2	3	3	3	3	2	2	2
		Drusy	0	0	1	0	0	0	0	0	0	0	1	0	1	0	0	0	0	0	0	0	0	0	0	0	0	0	0	0	2	1	0	0	0	0	1	2	0	0	1	1	0	0	0	0	0
		Radiaxial fibrous	0	0	0	1	0	0	0	0	0	0	0	0	0	0	0	0	0	0	0	0	0	0	0	0	0	0	0	0	0	0	0	0	0	0	0	0	0	0	0	0	0	0	0	0	0
		Micrite	0	0	0	1	1	0	1	1	1	0	3	1	0	0	0	0	0	0	0	0	0	0	1	0	0	0	0	0	1	0	0	0	0	0	0	0	0	0	0	0	0	0	1	0	0
		Syntaxial rim	0	0	0	0	0	0	0	0	0	0	0	0	0	0	0	0	0	0	0	0	0	0	0	0	0	0	0	0	0	0	0	0	0	0	0	0	0	0	0	0	0	0	0	0	0
		Meniscus	0	0	0	0	0	0	0	0	0	0	0	0	0	0	0	0	0	0	0	0	0	0	0	0	0	0	0	0	0	0	0	0	0	0	0	0	0	0	0	0	0	0	0	0	0
		Dripstone	0	0	0	0	0	0	0	0	0	0	0	0	0	0	0	0	0	0	0	0	0	0	0	0	0	0	0	0	0	0	0	0	0	0	0	0	0	0	0	0	0	0	0	0	0
		Dog-tooth	0	0	0	0	0	0	0	0	0	0	0	0	0	0	0	0	0	0	0	0	0	0	0	0	0	0	0	0	0	0	0	0	0	0	0	0	0	0	0	1	0	0	0	0	0
	Total porosity		5	1	5	5	5	10	10	10	15	5	20	5	10	10	20	5	5	10	5	5	10	5	5	15	10	20	10	10	20	10	10	5	10	10	10	10	5	5	15	10	10	10	10	5	5
	Typ of Pores	Interparticle	2	1	2	2	2	1	1	1	1	1	1	0	1	1	3	1	1	1	1	1	1	1	1	2	2	1	1	1	2	2	1	1	1	1	1	0	1	1	2	0	1	0	0	1	0
		Intraparticle	0	0	0	1	1	1	1	1	1	1	1	1	1	1	1	0	0	0	0	0	1	0	0	1	1	1	1	1	1	1	1	1	1	1	0	0	0	1	1	1	0	1	0	1	0
		Intercrystal	0	0	0	0	0	0	0	0	0	0	0	0	0	0	0	0	0	0	0	0	0	0	0	0	0	0	0	0	0	0	0	0	0	0	0	0	0	0	0	0	0	0	0	0	0
		Moldic	0	0	1	1	1	1	1	2	1	1	1	1	1	1	1	0	1	2	1	0	1	0	1	1	1	1	1	1	2	1	0	0	1	1	1	2	1	0	2	2	1	1	1	0	1
		Fenestral	0	0	0	0	1	0	0	0	0	0	0	0	1	1	1	0	0	0	0	0	0	0	0	0	0	1	0	0	1	1	1	0	0	0	0	0	0	0	0	0	0	0	0	0	0
		Shelter	0	0	0	1	1	0	0	0	0	0	0	0	0	0	0	0	0	0	0	0	0	0	0	0	0	1	0	0	0	0	2	0	0	0	0	0	0	0	0	0	0	0	0	0	0
		Growth-framework	0	0	0	0	0	0	0	0	0	0	0	0	0	0	0	0	0	0	0	0	0	0	0	0	0	0	0	0	0	0	0	0	0	0	0	0	0	0	0	0	0	0	0	0	0
		Fracture	0	0	0	1	1	0	0	1	0	0	1	0	0	0	0	1	0	0	0	0	0	0	0	1	1	1	1	1	0	1	1	0	1	1	0	0	0	0	2	0	1	0	0	0	0
		Channel	0	0	0	0	0	0	0	0	1	0	3	0	2	0	0	0	0	0	1	0	2	0	0	1	0	0	0	0	0	0	2	0	1	0	0	0	0	0	0	2	0	0	0	0	0
		Vug	0	0	0	0	1	0	0	1	3	1	3	1	1	1	0	1	1	2	1	1	1	1	1	2	2	3	2	3	2	1	1	1	2	2	2	3	2	2	3	2	3	2	3	2	2
		Biogenous	0	0	0	0	0	0	0	0	0	0	0	0	0	0	0	0	0	0	0	0	0	0	0	1	0	1	0	0	0	0	0	0	0	0	0	1	0	0	0	2	0	0	0	0	0
	Dissolution		1	1	1	1	1	1	2	2	2	1	0	1	1	1	1	1	1	2	1	1	1	1	1	2	1	2	2	2	2	2	2	1	1	1	1	1	1	1	2	2	2	1	2	1	1
	Dolomitization		0	0	0	0	0	0	0	0	0	0	0	0	0	0	0	0	0	0	0	0	0	0	0	0	0	0	0	0	0	0	0	0	0	0	0	0	0	0	0	0	0	0	0	0	0
	Dedolomitization		0	0	0	0	0	0	0	0	0	0	0	0	0	0	0	0	0	0	0	0	0	0	0	0	0	0	0	0	0	0	0	0	0	0	0	0	0	0	0	0	0	0	0	0	0
NOTE			y	y	y	y	y	y	y	y	y	y	0	y	y	y	y	y	y	y	y	y	y	y	y	y	y	y	y	y	y	y	y	y	y	y	y	y	y	y	y	y	y	y	y	y	y

Location	No. (Stratigraphy)		55	56	57	58	59	60	61	62	63	64	66	67	69	70	71	72	73	74	75	76	77	80	81	84	85	86	87	88	89	90	91	92	93	94	95	97	99	100	101	102	103	104	105	106	107
	Sample Code		SEP	SEP	SEP	SEP	SEP	SEP	SEP	SEP	SEP	SEP	SEP	SEP	SEP	SEP	SEP	SEP	SEP	SEP	SEP	SEP	SP	SP	SP	SP	SP	SP	SP	SP	SP	SP	SP	SP	SP	SP	SP	SP	SP	SP	SP	SP	SP	SP	SP	SP
			25	24	22	21	20	19	18	17	16	15	13	12	10	9	7	6	5	4	3	1	96	92	91	88	87	86	84	83	82	81	80	79	78	77	76	74	71	69	68	67	66	64	63	62	61
Structure	Grainsize	Mikrit	20	30	30	50	50	70	55	40	50	20	40	40	40	40	40	50	40	50	70	50	40	40	30	30	20	50	40	50	50	40	20	45	40	30	40	30	30	20	30	40	40	40	20	40	40
		Calciarenit (63µm -)	30	40	40	30	30	30	40	60	40	10	40	30	20	30	30	30	30	20	20	50	40	20	20	30	20	45	50	50	50	50	30	50	40	30	60	40	65	20	20	30	40	60	20	30	20
		Calcirudit (> 2 mm)	50	30	30	20	20	1	5	1	10	70	20	30	40	30	30	20	30	30	10	1	20	40	50	40	60	5	10	1	1	10	50	5	20	40	1	30	5	60	50	30	20	1	60	30	40
	Particle contacts	no contact	0	0	0	30	20	70	5	0	10	0	0	0	40	20	20	40	40	60	70	0	0	20	0	0	5	0	0	0	0	0	0	0	0	0	0	0	0	0	20	5	0	0	0	0	40
		pointe	95	90	85	70	80	30	95	90	90	90	90	90	60	50	75	60	60	40	30	95	80	75	90	90	85	90	95	95	95	90	80	75	80	70	80	70	65	80	75	90	90	80	80	70	50
		tangential	5	10	10	0	0	0	0	10	1	10	10	10	1	1	5	0	0	0	0	5	10	5	10	10	10	10	5	5	5	10	20	20	20	30	20	30	30	20	5	5	10	20	20	25	10
		concavo-convex	0	1	1	0	0	0	0	1	0	1	1	1	1	0	0	0	0	0	0	0	5	1	1	1	0	0	0	0	0	1	1	1	1	5	0	0	5	1	0	0	0	1	1	1	0
		sutured	0	1	5	0	0	0	0	1	1	1	1	1	1	0	0	0	0	0	0	0	5	1	1	1	0	0	0	0	0	1	1	5	1	5	1	0	1	1	0	0	0	1	1	5	0
	Compaction (0-3)	Index (nil-well)	1	1	1	1	1	0	1	1	1	1	1	1	1	1	1	1	1	1	1	1	1	2	1	1	1	1	1	1	1	1	2	1	2	1	1	1	1	1	1	1	1	1	2	1
	Roundness (0-3)	Index (nil-well)	0	0	0	0	0	0	0	0	0	0	0	0	0	0	0	0	0	0	0	0	1	0	0	0	0	0	0	0	0	0	0	0	0	0	1	1	0	0	0	0	0	0	0	0	0
	Sorting (0-3)	Index (nil-well)	2	1	1	1	1	2	1	1	1	2	1	1	2	1	1	1	1	1	1	2	1	2	2	1	1	2	1	2	2	2	2	1	1	1	2	0	2	2	2	2	1	2	1	1	2
	Gradation/ Bedding		0	0	0	2	1	0	2	0	1	0	0	0	0	0	0	0	0	0	0	1	0	2	0	0	0	1	0	0	0	0	0	1	2	0	1	0	1	0	0	0	0	0	0	0	0
	Orientation		0	0	1	2	1	0	1	0	0	0	0	0	0	0	0	1	0	0	0	0	0	2	0	0	0	1	0	0	0	0	0	0	1	0	0	0	0	0	0	0	0	0	0	0	0
Diagenesis	Sparite	Neomorphism	60	20	20	10	20	0	0	0	20	60	40	40	30	40	70	70	70	90	100	10	50	70	70	60	80	90	95	95	95	95	70	50	80	70	50	50	50	60	40	40	30	10	80	70	50
		Cements	40	80	80	90	80	100	100	100	80	40	60	60	70	60	30	30	30	10	0	90	50	30	30	40	20	10	5	10	5	5	30	50	20	30	50	30	50	40	60	60	70	90	20	30	50
	Types of cements	Fibrous	0	0	0	0	0	0	0	0	0	0	0	1	0	0	0	0	0	0	0	0	0	0	0	0	1	0	0	0	0	0	0	0	0	0	0	0	0	0	0	0	1	0	0	0	1
		Granular	2	3	2	2	2	0	0	1	2	3	3	3	2	3	3	2	3	2	2	2	3	3	2	3	3	1	1	1	1	3	3	3	1	3	3	3	3	3	3	3	3	3	3	3	3
		Drusy	0	0	0	0	0	0	0	0	1	2	1	1	3	0	1	0	0	0	0	0	1	2	1	1	1	0	0	0	0	0	2	1	1	1	1	2	2	2	3	3	0	3	1	1	2
		Radiaxial fibrous	0	0	0	0	0	0	0	0	0	0	0	0	0	0	0	0	0	0	0	0	0	0	0	0	0	0	0	0	0	0	0	0	0	0	0	0	0	0	0	0	0	0	0	0	0
		Micrite	0	0	0	0	0	0	0	0	0	0	0	0	0	0	0	0	0	0	0	0	0	1	1	1	1	0	0	0	0	0	0	0	0	0	0	0	0	1	1	1	1	1	1	1	1
		Syntaxial rim	0	0	0	0	0	0	0	0	0	0	0	0	0	0	0	0	0	0	0	0	0	0	0	0	0	0	0	0	0	0	0	0	0	0	0	0	0	0	0	0	0	0	0	0	0
		Meniscus	0	0	0	0	0	0	0	0	0	0	0	0	0	0	0	0	0	0	0	0	0	0	0	0	0	0	0	0	0	0	0	0	0	0	0	0	0	0	0	0	0	0	0	0	0
		Dripstone	0	0	0	0	0	0	0	0	0	0	0	0	0	0	0	0	0	0	0	0	0	0	0	0	0	0	0	0	0	0	0	0	0	0	0	0	0	0	0	0	0	0	0	0	0
		Dog-tooth	0	0	0	0	0	0	0	0	0	0	0	0	0	2	0	2	0	0	0	0	0	0	0	0	0	0	0	0	0	0	0	0	1	0	0	0	0	2	0	0	0	0	0	0	0
	Total porosity		10	15	10	10	15	5	5	5	10	5	5	5	5	5	10	10	10	10	5	10	5	5	10	5	5	10	15	10	5	10	5	10	5	10	10	10	20	20	20	10	10	10	10	5	10
	Typ of Pores	Interparticle	2	2	2	0	1	0	0	1	0	0	1	1	0	0	0	0	0	0	0	1	1	0	0	0	0	1	1	1	0	0	0	1	0	0	1	0	2	1	0	0	0	2	1	1	0
		Intraparticle	1	1	1	1	1	0	1	1	1	1	1	1	0	1	0	1	1	0	1	0	1	0	2	1	1	1	0	0	1	0	0	1	1	1	0	0	1	1	1	1	1	1	0	1	0
		Intercrystal	0	0	0	0	0	0	0	0	0	0	0	0	0	0	0	0	0	0	0	0	0	0	0	0	0	0	0	0	0	0	0	0	0	0	0	0	0	0	0	0	0	0	0	0	0
		Moldic	1	1	1	0	1	0	0	0	0	1	1	1	1	0	1	0	1	1	0	0	1	1	2	1	1	1	1	1	1	1	1	2	0	1	1	2	3	3	3	3	2	3	1	1	2
		Fenestral	0	0	0	0	0	0	0	0	1	1	0	1	2	1	1	0	0	0	0	0	0	0	2	0	0	0	0	0	0	0	0	0	0	1	0	0	0	0	0	0	0	0	0	1	2
		Shelter	0	0	0	0	0	0	0	0	0	0	0	0	0	1	0	0	0	0	0	0	0	0	0	0	0	0	0	1	0	0	0	0	0	0	0	0	0	0	0	0	1	0	0	1	1
		Growth-framework	0	0	0	0	0	0	0	0	0	0	0	0	0	0	0	0	0	0	0	0	0	0	0	0	0	0	0	0	0	0	0	0	0	0	0	0	0	0	0	0	0	0	0	0	0
		Fracture	0	0	0	0	0	0	0	0	1	0	0	1	1	0	1	0	0	0	0	0	0	1	1	1	0	1	1	1	0	1	0	0	1	0	1	1	0	1	1	1	1	0	0	0	0
		Channel	0	0	0	0	1	0	0	0	0	0	0	0	0	0	0	3	0	0	0	0	0	0	0	0	0	1	1	1	2	0	1	0	2	1	0	0	0	0	3	2	1	1	0	2	3
		Vug	3	3	3	3	3	2	2	1	1	0	2	1	2	1	1	2	3	3	2	2	1	1	1	2	2	3	3	3	2	3	3	2	2	1	1	2	2	1	2	2	3	3	3	3	2
		Biogenous	0	0	0	0	0	0	0	0	0	1	0	0	0	0	0	0	0	0	0	0	0	3	0	3	1	0	0	0	0	0	1	1	0	2	0	1	0	0	0	0	0	0	0	0	0
	Dissolution		2	2	1	2	2	1	1	1	1	1	1	1	1	1	1	2	2	2	2	2	1	1	1	1	1	2	3	2	1	2	1	1	2	1	1	1	2	1	2	2	2	2	2	1	1
	Dolomitization		0	0	0	0	0	0	0	0	0	0	0	0	0	0	0	0	0	0	0	0	0	0	0	0	0	0	0	0	0	0	0	0	0	0	0	0	0	0	0	0	0	0	0	0	0
	Dedolomitization		0	0	0	0	0	0	0	0	0	0	0	0	0	0	0	0	0	0	0	0	0	0	0	0	0	0	0	0	0	0	0	0	0	0	0	0	0	0	0	0	0	0	0	0	0
NOTE			y	y	y	y	y	y	y	y	y	y	y	y	y	y	y	y	y	y	y	y	y	y	y	y	y	y	y	y	y	y	y	y	y	y	y	y	y	y	y	y	y	y	y	y	y

Location	No. (Stratigraphy)		108	110	111	112	113	114	116	117	118	119	120	121	122	123	124	125	126	127	128	129	132	133	134	135	137	139	141	143	146	148	149	151	152	153	154	157	158	159	160	161	162	163	165	166
	Sample Code		SP 60	SP 57	SP 56	SP 55	SP 54	SP 53	SP 51	SP 50	SP 48	SP 46	SP 45	SP 44	SP 43	SP 42	SP 41	SP 40	SP 39	SP 38	SP 37	SP 36	SP 32	SP 31	SP 30l	SP 30u	SP 28	SP 26	SP 24	SP 22	SP 19	SP 17	SP 16	SP 14	SP 13	SP 11	SP 10.2	SP 9	SP 8	SP 7	SP 6	SP 5	SP 4	SP 3	SP 1.2	SP 1
Structure	Grainsize	Mikrit	20	40	40	50	45	50	40	40	40	30	40	30	30	20	40	45	30	30	30	30	30	30	20	35	30	30	35	30	40	40	45	50	50	50	40	30	40	30	30	40	20	20	30	40
		Calciarenit (63µm -)	20	30	40	40	35	40	40	50	50	70	50	40	40	30	50	50	40	40	50	50	50	40	60	60	40	65	60	60	30	50	50	40	40	40	30	40	50	50	30	60	20	40	30	30
		Calcirudit (> 2 mm)	60	30	20	10	20	10	20	10	10	1	10	30	30	50	10	5	30	30	20	20	20	30	20	5	30	5	5	10	30	10	5	10	10	10	30	30	10	20	40	1	60	40	40	30
	Particle contacts	no contact	0	0	0	0	0	0	0	0	0	0	0	0	0	0	0	0	0	0	0	0	0	0	0	0	0	0	0	0	0	0	0	0	0	0	0	0	0	0	0	0	0	0	0	0
		pointe	90	95	95	95	95	85	95	95	95	90	90	80	90	90	90	95	95	90	90	95	80	65	95	90	40	80	70	90	60	90	95	95	95	95	90	95	95	85	90	95	70	60	95	95
		tangential	10	5	5	5	5	10	5	5	5	10	10	20	10	10	10	5	5	10	10	5	10	25	5	10	30	20	30	10	20	10	5	5	5	5	10	5	5	10	10	5	30	30	5	5
		concavo-convex	1	0	0	0	0	1	0	0	1	0	1	1	0	0	0	0	0	1	0	1	5	5	0	1	10	1	1	0	10	0	0	0	0	0	1	0	0	5	1	1	0	5	0	0
		sutured	1	0	0	0	0	5	1	0	1	0	1	1	0	0	0	5	1	0	0	1	5	15	0	1	20	1	1	0	10	0	0	0	0	0	0	0	0	1	1	1	0	5	0	0
	Compaction (0-3)	Index (nil-well)	2	1	1	1	1	1	1	1	1	1	1	1	1	1	1	2	1	1	1	1	2	2	0	1	3	1	1	2	2	1	1	1	1	1	2	1	1	2	1	1	1	2	1	1
	Roundness (0-3)	Index (nil-well)	0	0	0	0	0	0	0	0	0	0	0	0	0	0	0	0	0	0	0	0	0	0	0	0	1	0	0	0	0	0	0	0	0	0	0	0	0	0	0	0	0	0	0	0
	Sorting (0-3)	Index (nil-well)	1	2	2	1	1	1	1	2	1	3	1	1	0	0	1	2	2	1	1	1	1	1	3	14	0	2	2	2	1	2	2	1	1	1	0	1	2	1	2	2	1	0	2	1
	Gradation/ Bedding		0	0	0	0	1	2	0	0	1	0	1	1	0	0	0	3	0	0	0	0	0	0	1	3	0	0	0	3	3	0	0	0	1	0	0	1	1	0	2	0	0	0	0	0
	Orientation		0	0	0	0	1	0	0	1	0	0	0	0	0	0	0	1	0	0	0	0	0	0	0	1	0	0	0	1	1	0	0	0	0	0	0	0	0	0	0	0	0	0	0	0
Diagenesis	Sparite	Neomorphism	40	30	70	30	50	50	90	90	90	80	90	90	50	60	20	40	90	80	90	80	40	30	20	10	40	20	20	20	40	20	10	10	10	10	40	20	10	10	50	10	50	10	50	40
		Cements	60	70	30	70	50	50	10	10	10	20	10	10	50	40	80	60	10	20	10	20	60	70	80	90	60	80	80	80	60	80	90	90	90	90	60	80	90	90	50	90	50	90	50	60
	Types of cements	Fibrous	0	0	0	0	0	0	0	0	0	0	0	0	0	0	0	0	0	0	0	0	0	0	0	0	0	0	0	0	0	0	0	0	0	0	0	0	0	0	0	0	0	0	0	0
		Granular	3	1	2	3	1	1	0	1	1	3	2	2	3	3	3	1	1	2	1	1	3	3	3	3	3	3	3	3	3	3	3	2	2	2	2	2	3	3	3	3	3	3	3	2
		Drusy	1	1	1	0	0	0	0	0	0	0	0	1	2	1	2	0	0	0	0	1	0	0	2	1	2	3	1	2	3	0	0	0	0	1	2	0	0	0	3	1	1	2	3	0
		Radiaxial fibrous	0	0	0	0	0	0	0	0	0	0	0	0	0	0	0	0	0	0	0	0	0	0	0	0	0	0	0	0	0	0	0	0	0	0	1	0	0	0	0	0	0	1	0	0
		Micrite	1	1	1	1	1	0	0	0	0	0	0	0	0	0	0	0	0	1	0	0	0	0	3	0	1	1	1	2	0	0	0	0	0	0	0	0	1	0	1	1	1	1	1	0
		Syntaxial rim	0	0	0	0	0	0	0	0	0	1	1	0	0	0	0	0	0	0	0	0	0	0	0	0	0	0	0	0	0	0	0	0	0	0	0	0	0	0	0	0	0	0	0	0
		Meniscus	0	0	0	0	0	0	0	0	0	0	0	0	0	0	0	0	0	0	0	0	0	0	0	0	0	0	0	0	0	0	0	0	0	0	0	0	0	0	0	0	0	0	0	0
		Dripstone	0	0	0	0	0	0	0	0	0	0	0	0	0	0	0	0	0	0	0	0	0	0	0	0	0	0	0	0	0	0	0	0	0	0	0	1	0	0	0	0	0	0	0	0
		Dog-tooth	0	0	0	0	1	0	0	0	0	0	0	0	0	0	0	0	0	0	0	0	0	0	0	3	1	0	0	0	0	0	0	0	0	0	0	0	0	0	0	0	0	0	0	0
	Total porosity		10	5	5	5	5	5	10	5	5	15	10	5	15	40	10	4	5	10	10	10	10	15	30	15	20	20	15	20	15	15	5	10	10	10	15	10	15	15	15	20	5	20	25	10
	Typ of Pores	Interparticle	0	0	0	0	0	0	0	0	0	2	2	1	2	0	1	0	1	1	0	1	2	2	3	2	3	3	1	3	1	1	2	2	1	1	1	1	2	3	2	3	1	3	1	1
		Intraparticle	0	1	1	1	0	0	0	0	0	0	1	1	2	1	1	1	0	1	1	1	1	1	1	2	2	2	1	2	1	0	1	0	0	1	1	1	0	1	1	2	1	2	1	0
		Intercrystal	0	0	0	0	0	0	0	0	0	0	0	0	0	0	0	0	0	0	0	0	0	0	0	0	0	0	0	0	0	0	0	0	0	0	0	0	0	0	0	0	0	0	0	0
		Moldic	2	2	3	3	1	0	0	0	1	1	0	0	0	1	2	1	1	1	0	0	0	1	3	1	3	3	3	3	3	3	1	0	1	1	1	1	3	2	2	3	1	1	3	2
		Fenestral	1	2	0	0	0	0	0	1	0	0	0	0	1	1	1	0	0	1	1	1	0	3	1	0	1	0	0	1	1	1	0	0	0	0	0	1	0	1	0	0	0	1	0	0
		Shelter	0	1	0	1	0	0	0	0	0	0	0	0	1	0	1	0	0	0	0	0	1	1	0	0	0	0	0	0	1	0	0	1	0	0	0	0	0	0	0	0	0	3	0	0
		Growth-framework	0	0	0	0	0	0	0	0	0	0	0	0	0	0	0	0	0	0	0	0	0	0	0	0	0	0	0	0	0	0	0	0	0	0	0	0	0	0	0	0	0	0	0	0
		Fracture	1	1	0	0	0	0	0	0	0	0	0	0	0	0	0	0	0	0	0	0	2	1	0	0	0	0	0	0	2	0	0	0	0	0	2	1	0	1	0	1	0	1	0	1
		Channel	1	1	1	0	1	1	0	0	0	0	1	1	1	1	0	1	0	0	0	0	0	1	1	0	0	0	0	2	2	0	0	0	0	0	0	0	0	0	0	1	0	0	3	0
		Vug	1	1	3	3	3	2	3	3	3	3	3	2	2	2	2	2	3	2	3	3	1	3	1	2	1	1	2	2	2	2	2	3	3	3	3	3	3	3	2	2	1	3	2	2
		Biogenous	0	2	2	1	0	0	0	0	0	0	0	2	0	0	0	0	0	1	0	0	0	0	0	0	0	0	0	0	1	0	0	3	0	0	2	2	2	0	0	1	0	0	0	0
	Dissolution		1	1	2	1	2	1	2	1	1	2	2	1	1	1	1	1	1	1	2	1	1	2	2	2	2	1	1	2	2	1	1	2	2	2	2	3	2	2	1	2	1	2	2	1
	Dolomitization		0	0	0	0	0	0	0	0	0	0	0	0	0	0	0	0	0	0	0	0	0	0	0	0	0	0	0	0	0	0	0	0	0	0	0	0	0	0	0	0	0	0	0	0
	Dedolomitization		0	0	0	0	0	0	0	0	0	0	0	0	0	0	0	0	0	0	0	0	0	0	0	0	0	0	0	0	0	0	0	0	0	0	0	0	0	0	0	0	0	0	0	0
NOTE			y	y	y	y	y	y	y	y	y	y	y	y	y	y	y	y	y	y	y	y	y	y	y	y	y	y	y	y	y	y	y	y	y	y	y	y	y	y	y	y	y	y	y	y

Location	No. (Stratigraphy)		XV	XI	XVI	XII	VII	VIII	XIII	XIX	XX	XIV	XXI	XXII	XIII	XIV	XV	XVI	VIII
	Sample Code		1	1b	2	2b	3	4	3b	5	6	4b	7	8	9	10	11	12	13
			SA	SA	SA	SA	SA	SA	SA	SA	SA	SA	SA	SA	SA	SA	SA	SA	SA
Composition	Matrix	**Micrite** : Sparite	9	9	9	9	9	9	9	9	9	9	9	9	9	9	9	9	9
	Composition (mineral.)	Micrite [%]	90	90	60	70	60	75	80	70	20	70	75	85	70	50	75	65	90
		Sparite [%]	10	10	30	30	20	20	10	20	70	10	5	10	30	40	20	30	10
		Internsed. [%]	1	0	1	0	20	5	0	5	0	10	0	5	1	5	1	5	0
		Shale [%]	0	0	0	0	0	0	2	0	0	0	0	0	0	0	0	0	0
		Sand [%]	0	0	0	0	0	0	0	0	0	0	0	0	0	0	0	0	0
		Open posrosity	0	1	0	0	5	1	10	5	10	10	20	5	1	5	5	1	0
		Components	5	9	9	9	9	9	9	9	9	9	9	9	9	9	9	9	9
Components		**Bioclasts** : Bio	9	9	9	9	5	9	9	9	9	9	9	9	9	9	9	9	9
	foraminifera, larger	SORITIDAE	0	0	0	0	0	0	0	0	0	1	0	0	0	0	0	0	0
		ALVEOLINIDAE	0	0	0	0	0	0	0	0	0	0	0	0	0	1	0	1	0
		ROTALIIDAE	1	1	0	0	0	0	0	0	0	0	0	1	0	1	0	1	1
		NUMMULITIDAE	5	10	5	1	5	5	5	10	5	5	5	5	5	5	10	10	5
		MIOGYPSINIDAE	0	0	1	1	0	0	0	0	0	0	0	0	0	0	0	0	0
		AMPHISTEGINIDAE	1	5	1	1	1	1	5	1	1	5	1	1	1	1	1	1	5
		ACERVULINIDAE	1	1	5	5	5	5	5	5	5	5	10	5	5	5	5	5	1
		HOMOTREMATIDAE	1	1	1	1	5	1	1	1	10	0	5	1	5	5	1	0	1
		LEPIDOCYCLINIDAE	1	1	5	1	1	1	5	1	1	1	1	0	1	0	0	5	1
		other	0	0	0	0	0	0	0	0	0	0	0	0	0	0	0	0	0
		SUM	10	19	18	10	17	13	21	18	22	17	22	13	17	18	17	23	14
		- small benthic	0	0	1	1	0	1	5	0	5	1	1	0	0	5	0	1	0
		- planktonic	10	5	20	1	40	20	1	20	0	1	1	1	1	5	1	5	20
	algae	red -	1	1	5	5	5	5	5	10	10	5	10	5	5	5	5	5	1
		green -	1	1	5	10	1	5	0	1	1	0	0	1	5	1	0	1	0
		bryozoans	1	1	1	5	5	5	5	5	5	1	1	1	1	1	1	1	1
	corals	branches	1	1	50	0	5	5	0	5	0	10	0	0	10	10	0	10	0
		heads	0	0	0	50	0	0	0	0	0	0	0	50	0	0	40	0	0
		SUM	1	1	50	50	5	5	0	5	0	10	0	50	10	10	40	10	0
		echinoderms	5	5	5	1	1	1	10	1	1	5	5	5	5	1	1	5	5
	molluscs	bivales/ oysters	1	1	1	1	1	1	1	5	1	1	1	1	1	1	1	1	1
		gastropods	0	1	1	1	1	1	1	1	0	0	0	0	0	1	0	0	0
		brachiopodes	0	0	0	1	0	0	5	0	1	1	0	1	1	1	1	1	1
		ostracods	0	0	0	0	0	0	0	0	0	0	0	0	1	0	0	0	0
		serpulids	0	0	0	0	0	0	0	0	0	0	0	0	0	0	0	0	0
	Lithoclasts	Intraclasts	1	5	0	0	0	0	0	0	0	0	1	1	1	1	0	0	0
		Pellets	0	0	0	1	0	0	1	0	0	1	0	0	0	0	0	0	0
Structure	Grainsize	Mikrit	60	50	20	30	30	30	30	30	20	30	30	30	30	30	40	30	40
		Calciarenit (63µm -)	30	40	50	30	50	30	60	50	60	50	40	30	40	40	20	50	55
		Calcirudit (> 2 mm)	10	10	30	40	20	40	10	20	20	20	30	40	30	30	40	20	5
	Particle contacts	no contact	80	40	0	0	0	0	0	0	0	0	0	0	0	0	20	0	10
		pointe	20	50	65	90	95	80	65	80	50	65	65	80	70	75	70	80	80
		tangential	1	10	20	10	2	20	30	20	30	30	30	20	20	30	10	20	20
		concavo-convex	0	0	10	1	0	1	5	0	10	10	5	1	5	5	0	0	0
		sutured	0	0	5	0	0	1	1	0	10	5	1	1	5	1	0	0	0
	Compaction (0-3)	Index (nil-well)	0	1	2	2	0	1	2	1	3	1	1	1	1	2	1	0	0
	Roundness (0-3)	Index (nil-well)	0	0	0	0	0	0	0	0	0	0	0	0	0	0	0	0	0
	Sorting (0-3)	Index (nil-well)	0	1	1	0	1	0	1	1	1	1	1	1	1	0	1	1	2
	Gradation/ Bedding		0	2	0	0	2	0	2	0	2	0	2	0	0	0	0	0	1
	Orientation		0	0	0	0	0	0	2	0	2	2	0	0	0	0	0	0	0
Diagenesis	Sparite	Neomorphism	30	30	80	80	70	70	10	70	90	40	90	60	30	20	50	50	10
		Cements	70	70	20	20	30	30	90	30	10	60	10	10	70	80	50	50	90
	Types of cements	Fibrous	0	0	0	0	0	0	0	0	0	0	0	0	0	0	0	0	0
		Granular	3	3	3	3	3	3	2	3	3	3	1	1	3	3	1	3	2
		Drusy	0	0	0	0	0	0	0	0	0	0	0	0	0	1	0	0	0
		Radiaxial fibrou	0	0	0	0	0	0	0	0	0	0	0	0	0	0	0	0	0
		Micrite	0	0	0	0	0	0	0	0	0	0	0	0	0	1	0	0	0
		Syntaxial rim	0	0	0	0	0	0	0	0	0	0	0	0	0	0	0	0	0
		Meniscus	0	0	0	0	0	0	0	0	0	0	0	0	0	0	0	0	0
		Dripstone	0	0	0	0	0	0	0	0	0	0	0	0	0	0	0	0	0
		Dog-tooth	0	0	0	0	0	0	0	0	0	0	0	0	0	1	0	0	0
	Total porosity		5	5	5	10	5	5	10	5	20	10	20	10	5	15	5	10	5
	Typ of Pores	Interparticle	0	0	0	0	0	0	2	0	3	0	0	0	0	1	0	3	0
		Intraparticle	0	0	0	0	1	1	1	1	1	0	0	1	1	1	0	0	1
		Intercrystal	0	0	0	0	0	0	0	0	0	0	0	0	0	0	0	0	0
		Moldic	2	2	3	3	3	3	2	2	1	3	1	1	2	1	1	1	1
		Fenestral	0	0	1	0	1	1	0	1	0	0	0	0	0	1	0	0	0
		Shelter	0	0	0	0	0	0	0	0	0	0	0	0	0	1	0	0	0
		Growth-framew	0	0	0	0	0	0	0	0	0	0	0	0	0	0	0	0	0
		Fracture	0	1	0	0	0	1	0	1	3	0	0	0	0	2	3	1	0
		Channel	0	1	0	0	1	1	0	1	1	0	2	0	3	3	2	2	0
		Vug	1	1	1	1	1	1	3	2	3	3	3	3	1	1	3	2	0
		Biogenous	0	0	0	0	0	0	0	0	0	0	0	0	0	0	0	0	0
	Dissolution		1	1	2	1	1	1	2	2	3	2	3	3	2	3	2	2	1
	Dolomitization		0	0	0	0	0	0	0	0	0	0	0	0	0	0	0	0	0
	Dedolomitization		0	0	0	0	0	0	0	0	0	0	0	0	0	0	0	0	0
	Speleothems		0	0	0	0	0	0	0	0	0	0	0	0	0	0	0	0	0
	vadose silt		0	0	0	0	0	0	0	0	0	0	0	0	0	0	0	0	0
	Microcodium		0	0	0	0	0	0	0	0	0	0	0	0	0	0	0	0	0
Notes			y	y	y	y	y	y	y	y	y	y	y	y	y	y	y	y	y

Location	No. (Stratigraphy)		I	II	III	IV	V	VI	VII	VIII	IX	X
	Sample Code		1	2	3	4	5	6	7	8	9	10
			AN	AN	AN	AN	AN	AN	AN	AN	AN	AN
Composition	Matrix	**Micrite** : Sparite	5	5	1	9	9	9	5	9	5	9
	Composition (mineral.)	Micrite [%]	65	40	25	70	75	70	20	80	65	70
		Sparite [%]	30	50	75	30	20	20	80	20	30	30
		Internsed. [%]	6	1	1	1	0	0	0	1	5	1
		Shale [%]	0	0	0	0	0	0	0	0	0	0
		Sand [%]	0	0	0	0	0	0	0	0	0	0
		Open posrosity	0	0	1	0	5	10	0	0	0	1
		Components	9	9	9	9	5	5	9	9	9	5
Components		**Bioclasts** : Bio	5	5	5	5	5	9	9	9	9	5
	foraminifera, larger	SORITIDAE	5	5	5	5	5	5	5	1	1	0
		ALVEOLINIDAE	0	0	0	0	0	1	1	0	0	0
		ROTALIIDAE	0	0	0	0	0	0	0	0	0	0
		NUMMULITIDAE	1	0	0	0	0	0	0	0	0	0
		MIOGYPSINIDAE	1	5	5	5	1	1	5	5	0	0
		AMPHISTEGINIDAE	1	1	1	0	1	1	1	1	1	5
		ACERVULINIDAE	5	1	1	1	1	10	5	10	5	1
		HOMOTREMATIDAE	0	0	0	0	0	0	0	0	0	0
		LEPIDOCYCLINIDAE	0	0	1	0	0	0	0	1	1	0
		other	0	0	0	0	0	0	0	0	0	0
		SUM	13	12	13	11	8	18	17	18	8	6
		- small benthic	5	5	5	5	1	1	5	5	1	5
		- planktonic	0	0	0	0	1	1	0	0	0	0
	algae	red -	5	5	10	5	5	10	5	1	5	5
		green -	0	1	1	0	1	5	1	0	0	1
		bryozoans	1	0	0	1	0	5	5	5	10	5
	corals	branches	0	1	0	0	0	0	0	0	0	0
		heads	20	0	0	60	20	20	0	0	0	0
		SUM	20	1	0	60	20	20	0	0	0	0
		echinoderms	1	1	5	1	1	1	5	5	1	1
	molluscs	bivales/ oysters	1	1	1	1	1	1	1	1	1	1
		gastropods	0	1	1	1	5	5	1	5	1	1
		brachiopodes	1	1	1	0	0	0	0	0	0	0
		ostracods	1	5	1	0	1	0	0	0	1	0
		serpulids	0	0	0	0	0	0	0	0	0	0
	Lithoclasts	Intraclasts	0	0	0	0	0	0	0	0	0	0
		Pellets	5	5	5	1	0	1	1	0	5	5
Structure	Grainsize	Mikrit	30	30	15	25	50	40	30	40	40	60
		Calciarenit (63µm -)	30	65	80	25	30	30	50	40	50	35
		Calcirudit (> 2 mm)	40	5	5	50	20	30	10	20	10	5
	Particle contacts	no contact	10	50	0	10	50	10	0	10	0	40
		pointe	70	40	70	70	40	70	80	65	90	55
		tangential	20	10	30	20	10	20	20	10	10	5
		concavo-convex	1	0	1	0	0	0	0	10	1	0
		sutured	1	0	0	0	0	0	0	5	0	0
	Compaction (0-3)	Index (nil-well)	1	0	1	0	0	0	0	2	1	1
	Roundness (0-3)	Index (nil-well)	0	0	1	0	0	0	1	0	0	0
	Sorting (0-3)	Index (nil-well)	1	2	2	0	1	0	1	0	1	1
	Gradation/ Bedding		0	2	1	0	0	0	2	0	0	0
	Orientation		0	1	1	0	0	0	1	0	0	0
Diagenesis	Sparite	Neomorphism	10	10	5	30	50	30	5	5	5	5
		Cements	90	90	95	70	50	70	95	95	95	95
	Types of cements	Fibrous	3	0	1	3	0	1	1	1	0	1
		Granular	3	3	3	2	2	3	3	3	3	3
		Drusy	3	3	2	3	1	2	1	1	2	1
		Radiaxial fibrou	3	0	0	0	0	0	0	0	0	0
		Micrite	2	1	0	1	1	1	1	0	1	0
		Syntaxial rim	0	0	0	0	0	0	0	0	0	0
		Meniscus	0	0	0	0	0	0	0	0	0	0
		Dripstone	0	0	0	0	0	0	0	0	0	0
		Dog-tooth	1	1	1	2	2	1	1	1	1	1
	Total porosity		25	25	20	10	10	15	20	20	20	20
	Typ of Pores	Interparticle	3	3	3	1	0	0	3	0	3	1
		Intraparticle	3	2	1	1	1	3	2	1	1	1
		Intercrystal	0	0	0	0	0	0	0	0	0	0
		Moldic	1	0	0	0	1	3	0	1	3	1
		Fenestral	2	2	0	1	0	1	1	2	2	1
		Shelter	0	1	1	1	0	0	1	0	0	0
		Growth-framew	0	0	0	0	0	0	0	0	0	0
		Fracture	1	1	1	0	0	2	0	2	2	2
		Channel	1	2	0	3	0	0	3	3	3	2
		Vug	3	3	1	3	3	3	3	3	3	3
		Biogenous	1	0	0	2	1	1	0	0	0	0
	Dissolution		3	2	1	3	2	3	2	3	2	2
	Dolomitization		2	1	0	1	1	3	2	1	0	2
	Dedolomitization		0	0	0	0	0	0	0	0	0	0
	Speleothems		0	1	1	3	1	1	2	3	3	3
	vadose silt		1	0	0	0	0	0	0	2	2	0
	Microcodium		0	0	0	0	2	0	0	0	0	0
Notes			y	y	y	y	y	y	y	y	y	y

No.		‰PDB				Code				Setting	
	µg	d13C.c	±s13	d18O.c	±s18	Gruppe					Strata
1	35,8	-8,00	0,02	-8,58	0,03	cements	1	TA18	Taglupa	platform	a
2	77,3	-0,70	0,02	-7,96	0,03	C	2	TA17	Taglupa	platform	a
3	33,4	0,26	0,01	-8,06	0,02	C	3	TA16	Taglupa	platform	a
4	28,6	-4,78	0,01	-6,72	0,02	C	4	TA11	Taglupa	platform	a
5	32,2	-8,19	0,03	-6,58	0,03	C	5	TA9	Taglupa	platform	a
6	29,8	-12,95	0,01	-6,41	0,03	C	6	TA6	Taglupa	platform	a
7	50,0	-9,51	0,01	-6,89	0,04	C	7	TA4	Taglupa	platform	a
8	45,5	-5,76	0,01	-6,85	0,03	C	8	TA1	Taglupa	platform	a
9	8,4	-2,13	0,01	-5,84	0,05	C	9	TA1	Taglupa	platform	a
10	47,7	-5,08	0,01	-6,58	0,01	C	10	TA1	Taglupa	platform	a
11	13,1	-2,57	0,04	-6,36	0,04	C	11	TA1	Taglupa	platform	a
12	10,7	0,54	0,01	-8,46	0,05	C	12	SC3	SCreek	platform	b
13	13,1	0,50	0,01	-9,13	0,04	C	13	SC3	SCreek	platform	b
14	37,0	0,42	0,01	-7,39	0,02	C	14	SC9	SCreek	platform	b
15	113,6	0,84	0,02	-6,74	0,02	C	15	SC12	SCreek	platform	b
16	90,9	0,55	0,01	-6,98	0,03	C	16	SC16	SCreek	platform	b
17	15,5	0,18	0,03	-6,29	0,03	C	17	SC19	SCreek	platform	b
18	47,7	-0,86	0,01	-7,37	0,02	C	18	SC20	SCreek	platform	b
19	45,5	-0,72	0,02	-7,59	0,04	C	19	SC20	SCreek	platform	b
20	26,3	-0,01	0,02	-10,29	0,03	C	20	SC58	SCreek	platform	b
21	44,1	-2,25	0,01	-8,91	0,02	C	21	SP1	DPeak	buildup	f
22	90,9	-3,25	0,02	-9,01	0,03	C	22	SP19	DPeak	buildup	f
23	33,4	-6,05	0,02	-7,27	0,01	C	23	SP20	DPeak	buildup	f
24	151,9	-0,80	0,02	-9,84	0,01	C	24	SP29	DPeak	buildup	f
25	29,8	-6,75	0,02	-7,27	0,02	C	25	SP73	DPeak	buildup	f
26	63,6	-3,33	0,08	-8,54	0,05	C	26	SP75	DPeak	buildup	f
27	21,5	-4,27	0,01	-6,85	0,03	C	27	SP84	DPeak	buildup	f
28	100,0	-11,75	0,01	-6,62	0,03	C	28	SEP10	DPeak	buildup	f
29	22,7	-6,48	0,01	-6,83	0,02	C	29	SEP14	DPeak	buildup	f
30	27,4	-7,02	0,01	-7,49	0,02	C	30	SEP31	DPeak	buildup	f
31	59,1	-1,00	0,02	-9,94	0,03	C	31	SEP38	DPeak	buildup	f
32	41,8	-5,81	0,01	-7,72	0,01	C	32	B9	DPeak	buildup	f
33	25,1	-0,10	0,01	-6,90	0,02	C	33	B25	DPeak	buildup	f
34	16,7	-6,54	0,01	-6,17	0,02	C	34	B29	DPeak	buildup	f
35	11,9	-11,57	0,02	-6,93	0,03	C	35	B31	DPeak	buildup	f
36	22,7	0,36	0,02	-7,31	0,02	sparite	1	SC4	SCreek	platform	b
37	25,1	-4,90	0,01	-7,26	0,02	S	2	SC7	SCreek	platform	b
38	54,5	0,54	0,14	-3,95	0,11	S	3	SC8	SCreek	platform	b
39	54,5	0,78	0,03	-2,81	0,05	S	4	SC8	SCreek	platform	b
40	34,6	0,97	0,02	-3,78	0,02	S	5	SC12	SCreek	platform	b
41	22,7	0,10	0,03	-6,04	0,02	S	6	SC34	SCreek	platform	b
42	20,3	0,00	0,01	-2,86	0,02	S	7	SC46	SCreek	platform	b
43	118,2	-3,53	0,02	-8,62	0,01	S	8	SP1	DPeak	buildup	f
44	26,3	-4,16	0,01	-7,62	0,02	S	9	SP2	DPeak	buildup	f
45	20,3	-3,62	0,01	-9,12	0,02	S	10	SP10	DPeak	buildup	f
46	50,0	-3,09	0,02	-7,23	0,03	S	11	SP20	DPeak	buildup	f
47	72,7	-3,26	0,02	-7,25	0,04	S	12	SP29	DPeak	buildup	f
48	39,4	-3,01	0,02	-7,91	0,02	S	13	SP38	DPeak	buildup	f
49	14,3	-1,31	0,01	-9,68	0,03	S	14	SP43	DPeak	buildup	f
50	16,7	-4,00	0,02	-8,12	0,02	S	15	SP56	DPeak	buildup	f
51	27,4	-6,48	0,01	-8,04	0,01	S	16	SP59	DPeak	buildup	f

No.		‰PDB				Code				Setting	
	µg	d13C.c	±s13	d18O.c	±s18	Gruppe					Strata
52	19,1	-5,09	0,01	-6,95	0,02	S	17	SP71	DPeak	buildup	f
53	17,9	-0,16	0,02	-4,42	0,01	S	18	SP75	DPeak	buildup	f
54	35,8	-3,27	0,04	-8,13	0,04	S	19	SP80	DPeak	buildup	f
55	45,5	-2,22	0,01	-7,55	0,05	S	20	SEP2	DPeak	buildup	f
56	104,5	-3,95	0,01	-7,66	0,02	S	21	SEP8	DPeak	buildup	f
57	34,6	-8,03	0,01	-6,98	0,02	S	22	SEP10	DPeak	buildup	f
58	20,3	-1,08	0,05	-8,50	0,05	S	23	SEP38	DPeak	buildup	f
59	77,3	-4,79	0,02	-6,64	0,04	S	24	SEP45	DPeak	buildup	f
60	20,3	-0,16	0,02	-5,85	0,02	S	25	B6	DPeak	buildup	f
61	50,0	-4,45	0,02	-6,48	0,03	S	26	B9	DPeak	buildup	f
62	33,4	0,31	0,02	-3,94	0,02	micrite	1	TA17	Taglupa	platform	a
63	11,9	0,13	0,02	-3,97	0,05	M	2	SC4	SCreek	platform	b
64	35,8	0,69	0,01	-5,40	0,02	M	3	SC12	SCreek	platform	b
65	15,5	0,87	0,02	-4,24	0,02	M	4	MA2	Maasin	platform	c
66	15,5	0,37	0,03	-4,13	0,04	M	5	MA7	Maasin	platform	c
67	14,3	1,09	0,02	-4,09	0,02	M	6	MA12	Maasin	platform	c
68	28,6	0,73	0,01	-6,00	0,01	M	7	QS9	Quezon	platform	d
69	54,5	0,29	0,03	-5,38	0,04	M	8	QS3	Quezon	platform	d
70	15,5	1,57	0,03	-5,87	0,04	M	9	QS28	Quezon	platform	d
71	17,9	1,84	0,02	-4,86	0,05	M	10	QS22	Quezon	platform	d
72	72,7	1,52	0,02	-5,42	0,03	M	11	QS48	Quezon	platform	d
73	15,5	1,93	0,02	-5,07	0,02	M	12	QS41	Quezon	platform	d
74	113,6	-4,15	0,01	-6,19	0,03	bulk	1	TA17	Taglupa	platform	a
75	566,1	-5,96	0,01	-6,43	0,01	Bu	2	TA11	Taglupa	platform	a
76	140,9	-3,98	0,04	-6,33	0,04	Bu	3	TA1	Taglupa	platform	a
77	179,5	0,57	0,02	-4,89	0,02	Bu	4	SC20	SCreek	platform	b
78	136,4	0,03	0,01	-4,95	0,03	Bu	5	SC15	SCreek	platform	b
79	220,9	-0,25	0,01	-4,69	0,01	Bu	6	SC37	SCreek	platform	b
80	372,8	-0,22	0,02	-4,30	0,03	Bu	7	SC50	SCreek	platform	b
81	220,9	0,47	0,01	-4,33	0,02	Bu	8	SC54	SCreek	platform	b
82	220,9	-0,06	0,01	-4,42	0,03	Bu	9	SC61	SCreek	platform	b
83	510,9	-0,50	0,01	-4,17	0,01	Bu	10	SC75	SCreek	platform	b
84	262,3	0,18	0,02	-4,45	0,01	Bu	11	MA7	Maasin	platform	c
85	207,1	1,03	0,02	-5,46	0,02	Bu	12	QS31	Quezon	platform	d
86	179,5	1,21	0,02	-5,46	0,03	Bu	13	TP7	TPlace	platform	e
87	151,9	-8,11	0,02	-6,13	0,05	Bu	14	B30	DPeak	buildup	f
88	145,5	-2,98	0,01	-7,37	0,02	Bu	15	SEP45	DPeak	buildup	f
89	151,9	-4,96	0,02	-7,10	0,02	Bu	16	SEP2	DPeak	buildup	f
90	248,5	-2,97	0,01	-6,93	0,02	Bu	17	SP88	DPeak	buildup	f
91	262,3	-5,62	0,02	-7,53	0,01	Bu	18	SP55	DPeak	buildup	f
92	386,6	-4,94	0,04	-7,49	0,03	Bu	19	SP3	DPeak	buildup	f

	sites	number of data	average azimuth	average dip
25	Foundation area (Foundation area)	4	124	14
24	Foundation area; N side	4	65	19
23	Taglupa	14	234	17
22	Devel Peak, corr_69	69	280	19
21	Eastern Ridge, selected	7	266	18
20	Maasin Center	2	281	14
19	IR	4	304	19
18	Salty Creek Road-5	15	307	18
17	Salty Creek 2-3	21	298	19
16	HP	10	301	22
15	Maasin School	8	306	18
14	Between Tum R & Iwahig R	1	322	13
13	Waterfalls	3	305	19
12	Tumarabong River Section	25	322	18
11	Slope	46	326	13
10	Trail to the SE	3	318	14
9	surface of bed at the road	1	324	12
8	Theos Place	5	305	14
7	Quezon Town	10	114	09
6	QS3	5	076	18
5	QS2	5	101	21
4	QS1	5	099	19
3	Albion Head, Tar	9	110	23
2	Albion Head, NE shoreline	4	074	25
1	Albion Head, NE	16	023	50
	SUM	296		

	sites	average azimuth	average dip
1	Devel Peak	280	22
2		285	13
3		269	10
4		270	12
5		276	12
6		284	10
7		291	16
8		282	18
9		303	19
10		312	16
11		291	25
12		243	17
13		271	22
14		266	24
15		259	24
16		263	15
17		237	21
18		333	16
19		324	9
20		324	11
21		255	18
22		239	22
23		309	18
24		285	13
25		261	11
26		268	17
27		254	19
28		346	16
29		312	23
30		279	16
31		281	15
32		276	15
33		297	22
34		284	26
35		305	16
36		269	21
37		270	20
38		241	24
39		301	16
40		302	16
41		302	20
42		291	22
43		272	23
44		282	10
45		271	13
46		266	17
47		257	25
48		270	22
49		259	19
50		254	17
51		277	23
52		263	15
53		289	24
54		262	23
55		270	17
56		313	24
57		292	23
58		274	15
59		301	16
60		289	21
61		262	22
62		256	24
63		277	20
64		288	20
65		229	15
66		294	22
67		299	20
68		289	24
69		302	15

	sites	average azimuth	average dip
1	Albion Head N &NE	62	29
2		76	23
3		82	23
4		76	25
5		*53*	*57*
6		*25*	*47*
7		*21*	*57*
8		*28*	*64*
9		*27*	*59*
10		*25*	*51*
11		*10*	*42*
12		*12*	*56*
13		14	24
14		0	17
15		*32*	*50*
16		*32*	*45*

1	Albion Head Tarung Profile	89	36
2		98	34
3		88	23
4		21	15
5		148	24
6		130	23
7		86	25
8		108	14
9		154	12
10		90	18

1	Tamlangon Island	168	22
2		178	20
3		180	16
4		159	27
5		179	20
6		159	17
7		178	37
8		176	31
9		176	34
10		172	28
11		163	29
12		170	25

1	Nakoda Island	204	38
2		194	42
3		195	42
4		196	37

1	Eastern Ridge	*128*	*18*
2		*185*	*17*
3		*158*	*10*
4		256	15
5		*152*	*21*
6		348	21
7		232	13
8		272	16
9		252	15
10		240	22
11		278	20
12		266	21
13		281	16
14		274	19
15		*198*	*14*
16		202	18

	sites	average azimuth	average dip
1	Salty Creek Section +	10	10
2	Maasin Profile	350	9
3		6	18
4		310	19
5		281	21
6		323	18
7		293	21
8		299	25
9		308	20
10		291	19
11		292	15
12		299	25
13		301	16
14		277	20
15		299	18
16		310	18
17		282	24
18		286	26
19		310	15
20		310	14
21		296	14
22		287	13
23		296	26
24		308	17
25		304	22
26		306	19
27		306	15
28		304	22
29		303	14
30		305	22
31		322	17
32		317	16
33		295	18
34		316	17
35		309	20
36		296	22
37		306	15
38		312	18
39		304	16
40		324	16
41		302	15
42		282	24
43		308	21
44		307	14
45		302	15
46		305	13
47		311	28
48		308	22
49		299	27
50		309	13

1	Higher Platform	308	17
2		307	19
3		306	17
4		278	30
5		276	25
6		286	29
7		320	23
8		300	14
9		318	20
10		310	26

1	Tumarabong Waterfalls	310	16
2		308	21
3		298	20

	sites	average azimuth	average dip
1	Tumarabong River Section	325	14
2		316	20
3		325	13
4		311	21
5		329	15
6		321	22
7		326	19
8		338	19
9		327	12
10		335	24
11		316	15
12		328	24
13		314	23
14		307	18
15		297	15
16		312	12
17		324	14
18		348	26
19		304	13
20		296	19
21		10	12
22		13	18
23		310	16
24		308	21
25		298	20

1	Theo's Place	307	16
2		300	16
3		300	15
4		312	12
5		308	13

1	Quezon Section	62	20
2		82	17
3		83	17
4		75	25
5		78	10
6		102	25
7		108	18
8		104	16
9		98	21
10		92	24
11		95	16
12		62	9
13		110	24
14		91	18
15		112	18
16		87	21
17		95	18
18		85	18
19		83	15

1	Maasin Center	282	11
2		278	12
3		282	19

	sites	average azimuth	average dip
1	Slope Profile	341	14
2		334	13
3		324	15
4		322	17
5		324	16
6		322	17
7		340	14
8		338	16
9		340	15
10		342	15
11		330	16
12		348	3
13		357	12
14		323	13
15		358	12
16		8	12
17		348	14
18		347	16
19		8	11
20		2	10
21		1	11
22		344	15
23		347	15
24		323	15
25		319	17
26		347	17
27		355	17
28		326	11
29		335	14
30		350	15
31		353	14
32		*198*	*11*
33		*199*	*11*
34		*168*	*13*
35		216	5
36		343	17
37		340	15
38		352	4
39		295	4
40		321	10
41		354	10
42		286	11
43		294	9
44		298	9
45		6	13
46		8	14

	sites	average azimuth	average dip
1	Taglupa Profile	230	24
2		235	21
3		221	21
4		234	13
5		243	20
6		229	24
7		250	16
8		233	14
9		233	19
10		237	12
11		248	15
12		223	15
13		240	12
14		218	16

1	Foundation Area, in trail	120	15
2	beside the road	123	14
3		123	14
4		129	12
5	norhter side of ridge	55	22
6		75	18
7		79	19
8		52	16
9	Taglupa Base	109	14
10		105	14

	number
Rose diagram W	35
Rose diagram center/E	219
Rose diagram N (offshore)	16
SUM of all data	312

Probe	Einwaage	Counts	cor. Coun.	µg C	% TC	% CaCO3
TA1	5,166	3706989	3698766	586,454	11,352	94,60
TA2	5,623	4142001	4133778	655,427	11,656	97,13
TA3	3,950	2941741	2933518	465,121	11,775	98,12
TA4	5,651	4160498	4152275	658,360	11,650	97,08
TA5	4,298	3204799	3196576	506,830	11,792	98,26
TA6	4,422	3133998	3122845	513,541	11,613	96,77
TA7	4,530	3194898	3183745	523,556	11,558	96,31
TA 8	4,002	2880223	2869070	471,809	11,789	98,24
TA 9	4,296	3081269	3070116	504,870	11,752	97,93
TA 10	5,308	3764953	3753800	617,300	11,630	96,91
TA 11	4,063	2865487	2854334	469,386	11,553	96,27
TA 12	4,849	3451542	3440389	565,760	11,668	97,23
TA 13	5,379	3829829	3818676	627,968	11,674	97,28
TA 14	4,477	3159561	3148408	517,745	11,565	96,37
TA 15	4,251	2924514	2913361	479,092	11,270	93,91
TA 16	4,583	2382738	2371585	389,999	8,510	70,91
TA 17	5,903	3547481	3536328	581,537	9,852	82,09
TA 18	5,148	3093144	3081991	506,823	9,845	82,04
TA 19	4,840	1705906	1694753	278,696	5,758	47,98
TA 20	5,249	228094	214273	29,553	0,563	4,69
FA 12	4,344	115214	101393	13,984	0,322	2,68
FA 5	5,348	80604	66783	9,211	0,172	1,44
FA 4	5,071	145011	131190	18,094	0,357	2,97
FA 3	4,336	132065	118244	16,309	0,376	3,13
FA 2	5,586	110231	96410	13,297	0,238	1,98
FA 1	5,406	190796	176975	24,409	0,452	3,76

Probe	Einwaage	Counts	cor. Coun.	µg C	% TC	% CaCO3
MA13	5,643	3819427	3808274	626,258	11,098	92,48
MA12	4,671	3157234	3146081	517,362	11,076	92,30
MA11	4,591	3079515	3068362	504,582	10,991	91,59
MA10	4,620	3068253	3057100	502,730	10,882	90,68
MA9	4,965	3258235	3247082	533,972	10,755	89,62
MA8	5,212	3510311	3499158	575,425	11,040	92,00
MA7	4,949	3198330	3187177	524,121	10,590	88,25
MA5	4,840	3031667	3020514	496,713	10,263	85,52
MA4	5,580	3614310	3603157	592,527	10,619	88,49
MA3	5,266	3317299	3306146	543,685	10,324	86,03
MA2	5,089	3385535	3374382	554,906	10,904	90,86
MA0	4,574	2947666	2936513	482,900	10,557	87,98
SC75	5,507	3943488	3935265	623,952	11,330	94,41
SC74	4,730	3272933	3264710	517,633	10,944	91,19
SC73	5,335	3733466	3725243	590,652	11,071	92,26
SC72	3,963	2825474	2817251	446,686	11,271	93,92
SC71	4,782	3182194	3173971	503,246	10,524	87,69
SC70	4,965	3467439	3459216	548,472	11,047	92,05
SC69	4,400	3024380	3016157	478,224	10,869	90,57
SC68	5,161	3472363	3464140	549,253	10,642	88,68
SC67	3,940	2583173	2574950	408,269	10,362	86,35
SC66	4,962	3425928	3417705	541,891	10,921	91,00
SC65	5,855	4250816	4242593	672,680	11,489	95,74
SC64	4,666	3353940	3345717	530,477	11,369	94,74
SC63	4,953	3491807	3483584	552,336	11,152	92,93
SC62	3,835	2745745	2737522	434,045	11,318	94,31

Probe	Einwaage	Counts	cor. Coun.	µg C	% TC	% CaCO3
SC61	5,686	4122473	4114250	652,331	11,473	95,60
SC 60	5,941	4325501	4314559	682,899	11,495	95,79
SC 59	4,239	3026964	3016022	477,370	11,261	93,84
SC 58	4,504	3157768	3146826	498,073	11,058	92,15
SC 57	4,473	3224927	3213985	508,703	11,373	94,77
SC 56	4,197	2822168	2811226	444,955	10,602	88,34
SC 55	4,518	2864582	2853640	451,668	9,997	83,31
SC 54	4,965	3295099	3284157	519,810	10,469	87,24
SC 53	4,733	3223327	3212385	508,450	10,743	89,52
SC 52	4,537	2946389	2935447	464,616	10,241	85,33
SC 51	3,842	2694360	2683418	424,726	11,055	92,12
SC 50	3,953	2638544	2627602	415,891	10,521	87,67
SC 49	4,502	2855819	2844877	450,281	10,002	83,35
SC 48	5,318	2775150	2764208	437,513	8,227	68,56
SC 47	4,557	2297525	2286583	361,916	7,942	66,18
SC 46	4,335	2321583	2310641	365,723	8,437	70,30
SC 45	5,238	3711484	3700542	585,714	11,182	93,18
SC 44	4,231	2746673	2735731	433,006	10,234	85,28
SC 43	4,365	2726019	2715077	429,737	9,845	82,04
SC 42	5,424	3631883	3620941	573,115	10,566	88,05
SC 41	4,821	3114321	3103379	491,196	10,189	84,90
SC 40	3,887	2578983	2568041	406,464	10,457	87,14
SC 39	4,097	2734728	2723786	431,115	10,523	87,69
SC 38	5,279	3548734	3537792	559,954	10,607	88,39
SC 37	3,938	2683820	2672878	423,058	10,743	89,52
SC 36	4,371	2939250	2928308	463,486	10,604	88,36
SC 35	5,261	3645562	3634620	575,280	10,935	91,12
SC 34	4,666	3176147	3165205	500,982	10,737	89,47
SC 33	4,305	2921171	2910229	460,625	10,700	89,16
SC 32	4,548	2967225	2956283	467,914	10,288	85,73
SC 31	5,248	3566293	3555351	562,734	10,723	89,35
SC 30	3,965	2427604	2416662	382,504	9,647	80,39
SC 29	4,209	2688838	2677896	423,852	10,070	83,91
SC 28	4,824	3440025	3429083	542,748	11,251	93,75
SC 27	4,692	2980313	2969371	469,986	10,017	83,47
SC 26	4,321	2788337	2777395	439,600	10,174	84,78
SC 25	4,812	3330923	3319981	525,480	10,920	91,00
SC 24	5,058	3045961	3035019	480,376	9,497	79,14
SC 23	4,121	2723428	2712486	429,327	10,418	86,81
SC 22	4,166	2593169	2582227	408,710	9,811	81,75
SC21	4,040	2527978	2517036	398,391	9,861	82,17
SC20	4,825	3029343	3015854	522,978	10,843	90,36
SC19	4,654	3114538	3101049	537,751	11,551	96,26
SC18	4,587	3040975	3027486	524,994	11,445	95,37
SC17	4,316	2788755	2775266	481,257	11,151	92,92
SC16	4,739	3305344	3291855	570,839	12,047	100,39
SC15	5,310	3604533	3591044	622,721	11,728	97,73
SC14	4,363	2865594	2852105	494,582	11,334	94,45
SC13	5,347	3621201	3607712	625,611	11,704	97,53
SC12	5,504	3786979	3773490	654,359	11,891	99,09
SC11	4,221	2818723	2805234	486,454	11,526	96,04
SC10	5,683	3323434	3309945	573,976	10,103	84,19
SC9	5,501	3626578	3613089	626,544	11,380	94,83
SC8	4,433	2553260	2539771	440,420	9,936	82,80
SC7	5,899	3760973	3747484	649,849	11,016	91,80

Probe	Einwaage	Counts	cor. Coun.	µg C	% TC	% CaCO3
SC6	5,258	3253310	3239821	561,816	10,685	89,04
SC5	4,240	2879381	2865892	496,973	11,721	97,67
SC4	4,620	2538367	2524878	437,838	9,478	78,98
SC3	4,224	2861466	2847977	493,866	11,692	97,43
SC2	5,744	3752507	3739018	648,381	11,287	94,05
SC 1	5,254	3332929	3319440	575,622	10,956	91,30
SC0	5,004	54172	45949	7,285	0,146	1,21
IR 8	5,746	3454920	3443767	566,316	9,856	82,13
IR 7	4,964	3227904	3216751	528,984	10,656	88,80
IR6	3,967	2878412	2870189	455,080	11,472	95,59
IR5	5,844	4208626	4200403	665,991	11,396	94,96
IR4	4,301	3041233	3033010	480,896	11,181	93,17
IR3	4,402	3078405	3070182	486,790	11,058	92,15
IR2	3,945	2823199	2814976	446,326	11,314	94,28
IR1	5,655	4122129	4113906	652,276	11,535	96,12

Probe	Einwaage	Counts	cor. Coun.	µg C	% TC	% CaCO3
T 0	3,789	2786184	2780480	440,019	11,613	96,77
T 1	6,374	4559722	4554018	720,687	11,307	94,22
T 2	6,458	4709244	4703540	744,349	11,526	96,05
T 3	4,656	3318449	3312745	524,251	11,260	93,83
T 4	5,426	3899466	3893762	616,199	11,356	94,63
T 5	5,008	3513417	3507713	555,106	11,084	92,37
T 6	5,107	3573550	3567846	564,622	11,056	92,13
T 7	4,695	3372043	3366339	532,733	11,347	94,55
T 8	6,247	4089218	4083514	646,228	10,345	86,20
T 9	6,347	4560651	4554947	720,834	11,357	94,64
T 11	4,304	2888422	2882718	456,198	10,599	88,32
T E3	3,647	2606038	2600334	411,510	11,284	94,03
T 12A	4,180	2882285	2876581	455,227	10,891	90,75
T 12B	4,881	3576645	3570941	565,112	11,578	96,48
T 13	3,735	2635891	2630207	418,490	11,205	93,37
T 16	3,769	2767261	2761577	439,392	11,658	97,15
T 17	5,199	3861366	3855682	613,474	11,800	98,33
T 18	5,308	3831013	3825329	608,644	11,467	95,55
T 20B	4,240	3014869	3009185	478,788	11,292	94,10
T 21.1	5,066	3375772	3370088	536,211	10,585	88,20
T 23.2	4,437	3023178	3017494	480,110	10,821	90,17
T 24	3,782	2540415	2534731	403,298	10,664	88,86
T 25	4,605	3291474	3285790	522,799	11,353	94,60
T E2	4,489	3099224	3093520	489,558	10,906	90,88
T 26	5,334	3782751	3777067	600,965	11,267	93,89
T E1	3,805	2714724	2709020	428,710	11,267	93,89
T 27	4,645	3328104	3322420	528,627	11,381	94,83
T 28A	4,658	3485403	3479719	553,655	11,886	99,05
T 29	4,800	3570155	3564471	567,139	11,815	98,46
T 31.1	3,812	2729347	2723663	433,359	11,368	94,73
T 31.2	4,754	3359839	3354155	533,676	11,226	93,54
T E4	5,980	4225198	4219494	667,747	11,166	93,05

	Einwaage	Counts	cor. Coun.	µg C	% TC	% CaCO3
TP8	5,243	3327253	3316100	545,321	10,401	86,67
TP7	4,552	2776588	2765435	454,766	9,990	83,25
TP6	5,603	3371116	3359963	552,535	9,861	82,18

Probe	Einwaage	Counts	cor. Coun.	µg C	% TC	% CaCO3
TP3	4,485	2793902	2782749	457,614	10,203	85,02
TP2	4,765	2986465	2975312	489,280	10,268	85,56
TP1	5,555	3322031	3310878	544,463	9,801	81,67

Probe	Einwaage	Counts	cor. Coun.	µg C	% TC	% CaCO3
QS41	4,062	2988463	2972934,7	445,998	10,980	91,49
QS43	4,933	3565292	3549763,7	532,534	10,795	89,96
QS46	4,346	3058063	3042534,7	456,440	10,503	87,52
QS50	5,291	3841891	3826362,7	574,029	10,849	90,41
QS22	4,057	3058544	3043015,7	456,512	11,252	93,77
QS27	5,097	3536316	3520787,7	528,187	10,363	86,35
QS29	5,717	4195758	4180229,7	627,116	10,969	91,41
QS31	4,770	3368235	3352706,7	502,971	10,544	87,87
QS33	4,561	3315884	3300355,7	495,118	10,855	90,46
QS1	5,326	3716437	3700908,7	555,208	10,424	86,87
QS3	4,250	3065530	3050001,7	457,560	10,766	89,71
QS5	5,233	3650740	3635211,7	545,353	10,421	86,84
QS7	4,212	2777589	2762060,7	414,363	9,838	81,98
QS9	4,296	2941138	2925609,7	438,899	10,216	85,13

Probe	Einwaage	Counts	cor. Coun.	µg C	% TC	% CaCO3
SP1	4,579	3807145	3791144	542,103	11,839	98,65
SP2	5,208	4380449	4364448	624,081	11,983	99,86
SP3	4,647	3859151	3843150	549,540	11,826	98,54
SP4	4,691	3820236	3804235	543,975	11,596	96,63
SP5	4,967	4102514	4086513	584,339	11,764	98,03
SP6	4,235	3527912	3511911	502,175	11,858	98,81
SP7	5,514	4572309	4556308	651,515	11,816	98,46
SP8	4,018	3341677	3325676	475,545	11,835	98,62
SP9	4,337	3629985	3613984	516,771	11,915	99,29
SP10	5,753	4598995	4582994	655,331	11,391	94,92
SP11	5,692	4710731	4694730	671,309	11,794	98,28
SP12	5,535	4633200	4617199	660,222	11,928	99,40
SP13	4,696	3820920	3804919	544,073	11,586	96,55
SP14	4,512	3745952	3729951	533,353	11,821	98,50
SP15	5,711	4785730	4769729	682,033	11,942	99,52
SP16	5,687	4743598	4727597	676,008	11,887	99,05
SP17	5,455	4535919	4519918	646,312	11,848	98,73
SP18	4,934	4026707	4010706	573,499	11,623	96,86
SP19	5,438	4520464	4504463	644,102	11,844	98,70
SP20	5,878	4874273	4858272	694,694	11,819	98,48
SP21	4,354	3582191	3566190	509,937	11,712	97,60
SP22	4,090	3362189	3346188	478,478	11,699	97,49
SP23	5,485	4464749	4448748	636,135	11,598	96,64
SP24	4,592	3759145	3743144	535,240	11,656	97,13
SP25	4,353	3604591	3588590	513,140	11,788	98,23
SP26	5,631	4681497	4665496	667,128	11,847	98,72
SP27	5,895	4872579	4856578	694,452	11,780	98,17
SP28	4,186	3459141	3443140	492,341	11,762	98,01
SP29	5,709	4757693	4741692	678,024	11,876	98,97
SP30	5,477	4579359	4563358	652,524	11,914	99,28
SP31	4,451	3686684	3670683	524,878	11,792	98,27
SP32	4,449	3674055	3658054	523,072	11,757	97,97
SP33	5,704	4724410	4708409	673,265	11,803	98,36
SP34	5,756	4715497	4699496	671,990	11,675	97,28

Probe	Einwaage	Counts	cor. Coun.	µg C	% TC	% CaCO3
SP35	4,020	3299123	3283122	469,460	11,678	97,31
SP36	5,471	4567550	4551549	650,835	11,896	99,13
SP37	4,273	3502207	3486206	498,499	11,666	97,21
SP38	4,579	3742653	3726652	532,881	11,638	96,98
SP39	5,036	3586768	3570767	510,591	10,139	84,49
SP40	4,063	3380045	3364044	481,031	11,839	98,66
SP 41	5,720	4493783	4481335	675,612	11,811	98,42
SP 42	4,355	3393964	3381516	509,802	11,706	97,55
SP43	5,400	4203821	4191373	631,897	11,702	97,51
SP44	4,114	3209633	3197185	482,012	11,716	97,63
SP45	4,720	3728347	3715899	560,214	11,869	98,90
SP46	4,745	3793851	3781403	570,089	12,015	100,00
SP47	4,548	3618478	3606030	543,650	11,954	99,61
SP48	4,321	3414553	3402105	512,906	11,870	98,91
SP49	4,129	3294269	3281821	494,772	11,983	99,85
SP50	4,049	3221329	3208881	483,775	11,948	99,56
SP51	4,440	3541603	3529155	532,060	11,983	99,86
SP52	5,859	4561084	4548636	685,759	11,704	97,53
SP53	4,176	3277936	3265488	492,309	11,789	98,24
SP54	4,462	3528849	3516401	530,137	11,881	99,01
SP55	4,849	3843239	3830791	577,535	11,910	99,25
SP56	4,347	3443361	3430913	517,249	11,899	99,15
SP57	4,647	3765625	3753177	565,834	12,176	100,00
SP58	4,086	3156312	3143864	473,973	11,600	96,66
SP59	4,700	3785084	3772636	568,768	12,101	100,00
SP60	5,302	4145305	4132857	623,075	11,752	97,93
SP61	5,138	4042759	4030311	607,615	11,826	98,55
SP62	4,060	3136481	3124033	470,983	11,601	96,67
SP63	5,614	4445515	4433067	668,335	11,905	99,20
SP64	5,391	4257419	4244971	639,978	11,871	98,92
SP65	5,114	3949591	3937143	593,569	11,607	96,72
SP66	4,912	3866023	3853575	580,970	11,828	98,56
SP67	4,494	3530774	3518326	530,428	11,803	98,35
SP68	5,244	4161985	4149537	625,590	11,930	99,41
SP69	5,219	4817087	4804639	724,354	13,879	100,00
SP70	5,351	4194533	4182085	630,497	11,783	98,19
SP71	5,684	4430557	4418109	666,080	11,719	97,65
SP72	4,793	3718629	3706181	558,749	11,658	97,14
SP73	4,059	3089635	3077187	463,921	11,429	95,24
SP74	4,255	3337243	3324795	501,251	11,780	98,17
SP75	4,862	3790470	3778022	569,580	11,715	97,62
SP76	4,954	3897693	3885245	585,745	11,824	98,53
SP77	4,249	3307592	3295144	496,780	11,692	97,43
SP78	4,737	3627593	3615145	545,024	11,506	95,88
SP79	4,533	3425014	3412566	514,483	11,350	94,58
SP80	4,541	3465738	3453290	520,623	11,465	95,54
SP 81	5,022	3848901	3833373	575,081	11,451	95,42
SP 82	5,609	4328781	4313253	647,072	11,536	96,13
SP 83	5,587	4327244	4311716	646,841	11,578	96,48
SP 84	4,047	3193440	3177912	476,749	11,780	98,17
SP 85	4,780	3787655	3772127	565,893	11,839	98,65
SP 86	4,825	3858108	3842580	576,462	11,947	99,56
SP 87	4,293	3323971	3308443	496,331	11,561	96,34
SP 88	4,438	3454493	3438965	515,912	11,625	96,87
SP 89	4,309	3326323	3310795	496,684	11,527	96,05

Probe	Einwaage	Counts	cor. Coun.	µg C	% TC	% CaCO3
SP 90	4,198	3249611	3234083	485,175	11,557	96,31
SP 91	4,208	3295436	3279908	492,050	11,693	97,44
SP 92	5,947	4553948	4538420	680,851	11,449	95,40
SP 93	4,449	3331281	3315753	497,428	11,181	93,17
SP 94	4,415	3212125	3196597	479,552	10,862	90,51
SP 95	4,215	3184985	3169457	475,480	11,281	94,00
SP 96	4,561	3379614	3364086	504,678	11,065	92,21
SEP 1	6,035	5200682	5188443	717,369	11,887	99,05
SEP 2	4,478	3822702	3810463	526,845	11,765	98,04
SEP 3	5,729	4896341	4884102	675,290	11,787	98,22
SEP 4	4,353	3711387	3699148	511,455	11,749	97,91
SEP 5	5,290	4507836	4495597	621,574	11,750	97,91
SEP 6	5,412	4428459	4416220	610,599	11,282	94,02
SEP 7	4,181	3562340	3550101	490,847	11,740	97,83
SEP 8	4,531	3900661	3888422	537,624	11,865	98,87
SEP 9	4,080	3432426	3420187	472,885	11,590	96,58
SEP 10	4,285	3698643	3686404	509,693	11,895	99,12
SEP 11	4,998	4175013	4162774	575,557	11,516	95,96
SEP 12	4,075	3423356	3411117	471,631	11,574	96,44
SEP 13	4,409	3712147	3699908	511,560	11,603	96,68
SEP 14	4,158	3452791	3440552	475,701	11,441	95,33
SEP 15	5,049	4329241	4317002	596,881	11,822	98,51
SEP 16	4,771	4083125	4070886	562,852	11,797	98,31
SEP 17	4,592	3975911	3963672	548,029	11,934	99,45
SEP 18	4,286	3694376	3682137	509,103	11,878	98,98
SEP 19	5,055	4361969	4349730	601,406	11,897	99,14
SEP 20	5,983	5183458	5171219	714,988	11,950	99,58
SEP 21	4,480	3794010	3781771	522,878	11,671	97,26
SEP 22	4,868	4196952	4184713	578,590	11,886	99,04
SEP 23	4,200	3527337	3515098	486,007	11,572	96,43
SEP 24	4,250	3282922	3273563	490,627	11,544	96,20
SEP 25	4,137	3259442	3250083	487,108	11,774	98,12
SEP 26	4,719	3744919	3735560	559,869	11,864	98,86
SEP 27	4,581	3584743	3575384	535,863	11,698	97,48
SEP 28	5,015	3951492	3942133	590,830	11,781	98,17
SEP 29	4,578	3594776	3585417	537,366	11,738	97,81
SEP 30	4,231	3235155	3225796	483,468	11,427	95,22
SEP 31	4,355	3448215	3438856	515,401	11,835	98,62
SEP 32	4,621	3645595	3636236	544,983	11,794	98,28
SEP 33	4,046	3176091	3166732	474,616	11,730	97,75
SEP 34	4,785	3789556	3780197	566,559	11,840	98,67
SEP 35	4,262	3349137	3339778	500,551	11,745	97,87
SEP 36	4,196	3255315	3239787	486,031	11,583	96,52
SEP 37	4,220	3326672	3311144	496,736	11,771	98,09
SEP 38	4,674	3463510	3447982	517,264	11,067	92,22
SEP 39	4,364	3376238	3360710	504,172	11,553	96,27
SEP 40	4,231	3261237	3245709	486,920	11,508	95,90
SEP 41	4,004	3176061	3160533	474,142	11,842	98,68
SEP 42	4,169	3314746	3299218	494,947	11,872	98,93
SEP 43	5,704	4444799	4429271	664,477	11,649	97,07
SEP 44	4,530	3502308	3486780	523,085	11,547	96,22
SEP 45	5,176	4060238	4044710	606,785	11,723	97,69
B1	5,130	4254048	4240227	584,827	11,400	95,00
B2	4,475	3778484	3764663	519,235	11,603	96,69
B3	5,041	4243583	4229762	583,383	11,573	96,44

Probe	Einwaage	Counts	cor. Coun.	µg C	% TC	% CaCO3
B4	5,423	4610364	4596543	633,971	11,690	97,42
B5	5,204	4416311	4402490	607,206	11,668	97,23
B6	4,250	3618979	3605158	497,236	11,700	97,49
B7	4,111	3517274	3503453	483,208	11,754	97,95
B8	4,740	4006480	3992659	550,681	11,618	96,81
B9	5,073	4329897	4316076	595,288	11,734	97,78
B10	4,231	3597059	3583238	494,212	11,681	97,34
B11	5,149	4354219	4340398	598,643	11,626	96,88
B12	4,169	3537996	3524175	486,066	11,659	97,15
B13	4,453	3746700	3732879	514,851	11,562	96,35
B14	4,470	3779675	3765854	519,399	11,620	96,83
B15	4,299	3612439	3598618	496,334	11,545	96,21
B16	4,130	3229347	3215526	443,496	10,738	89,48
B17	4,654	3801226	3787405	522,372	11,224	93,53
B18	4,158	3233768	3219947	444,106	10,681	89,00
B19	4,949	3601761	3587940	494,861	9,999	83,32
B20	4,663	3948342	3934521	542,663	11,638	96,98
B21	4,665	3266980	3253159	448,687	9,618	80,15
B22	4,163	3167027	3153206	434,901	10,447	87,05
B23	4,051	3146966	3133145	432,134	10,667	88,89
B24	5,192	3467619	3453798	476,360	9,175	76,45
B25	4,821	2791511	2777690	383,109	7,947	66,22
B26	4,487	3781495	3767674	519,651	11,581	96,51
B27	4,076	3459111	3445290	475,186	11,658	97,15
B28	4,061	3426336	3414097	472,043	11,624	96,86
B29	4,364	3490485	3478246	480,912	11,020	91,83
B30	5,228	4434901	4422662	611,490	11,696	97,47
B31	4,488	3735911	3723672	514,846	11,472	95,59
B32	4,722	3698518	3686279	509,675	10,794	89,94
B33	5,458	3971072	3958833	547,360	10,029	83,57
B34	4,965	3262990	3250751	449,458	9,053	75,43
B35	4,341	1246601	1234362	170,666	3,931	32,76
B36	4,883	2155024	2142785	296,268	6,067	50,56
B37	4,383	1671858	1659619	229,464	5,235	43,63
BDP 1	5,028	44018	31779	4,394	0,087	1,00
BDP 2	5,757	46713	34474	4,766	0,083	1,00
BDP 3	5,452	50833	38594	5,336	0,098	1,00
BDP 4	5,006	82393	70154	9,700	0,194	1,61
BDP 5	4,028	636160	623921	86,265	2,142	17,85
BDP 6	5,968	1156344	1144105	158,187	2,651	22,09
BDP 7	4,530	298388	286149	39,564	0,873	7,28

Probe	Einwaage	Counts	cor. Coun.	µg C	% TC	% CaCO3
HEL 1	3,468	2619101	2613397	413,578	11,926	99,38
HEL 2	5,736	4386862	4381158	693,331	12,087	100,00
HEL 3	3,213	2392881	2387177	377,778	11,758	97,98
HEL 4	4,060	3052411	3046707	482,150	11,876	98,96
HEL 6	5,206	3944037	3938333	623,253	11,972	99,76
HEL 7	5,567	4221275	4215571	667,126	11,984	99,86
HEL 8	4,126	3045396	3039692	481,040	11,659	97,15
HEL 9	4,307	3126124	3120420	493,815	11,465	95,54
HEL 10	5,727	4317051	4311347	682,283	11,913	99,27
HEL 11	4,560	3298029	3292325	521,020	11,426	95,21
HEL 12	3,784	2784242	2778538	439,712	11,620	96,83
HEL 13.1	6,546	4860966	4855262	768,359	11,738	97,81

Probe	Einwaage	Counts	cor. Coun.	µg C	% TC	% CaCO3
HEL 14	3,915	2960273	2954569	467,569	11,943	99,52
HEL 15	5,014	3789215	3783511	598,752	11,942	99,51
HEL 19	5,310	3904846	3899142	617,050	11,621	96,83
HEL 20	3,590	2677819	2672115	422,870	11,779	98,16
HEL 21	4,798	3618834	3613130	571,788	11,917	99,31
HEL 24	5,610	4248846	4243142	671,489	11,970	99,74
TAR 1	4,072	3019584	3010963	482,217	11,842	98,68
TAR 2	3,957	2902099	2893478	463,401	11,711	97,59
TAR 3	4,522	3376157	3367536	539,324	11,927	99,38
TAR 5	4,221	3178303	3169682	507,636	12,026	100,00
TAR 6	4,195	2931938	2923317	468,180	11,160	93,00
TAR 7	4,621	3337163	3328542	533,078	11,536	96,13
TAR 8	4,698	3532651	3524030	564,387	12,013	100,00
TAR 10	5,672	4275136	4266515	683,298	12,047	100,00
TAR 11	5,144	3886209	3877588	621,010	12,073	100,00
TAR 12	4,923	3667562	3658941	585,993	11,903	99,19
TAR 13	4,294	3198232	3189611	510,828	11,896	99,13
TAR 14	4,619	3370201	3361580	538,370	11,656	97,13
TAR 15	4,144	3014712	3006091	481,437	11,618	96,81
TAR 16	5,368	3951235	3942614	631,424	11,763	98,02
TAR 18	5,541	4006931	3998310	640,344	11,556	96,30
TAR 19	6,023	4498657	4490036	719,096	11,939	99,49
TAR 21	4,879	3622481	3613860	578,773	11,863	98,85
TAR 22	4,858	3341908	3333287	533,838	10,989	91,57
TAR 23.2	5,045	3642505	3633884	581,980	11,536	96,13
TAR 24	4,781	3502649	3494028	559,582	11,704	97,53
TAR 25	4,968	3583066	3574445	572,461	11,523	96,02
TAR 26	5,663	4259933	4251312	680,864	12,023	100,00
TAR 28	3,954	2789294	2780673	445,335	11,263	93,85
TAR 30	5,047	3501577	3492956	559,410	11,084	92,36
TAR 31	5,408	3949705	3941084	631,179	11,671	97,26
TAR 32.1	4,341	3299163	3290542	526,993	12,140	100,00
TAR 33	6,234	4077459	4068838	651,640	10,453	87,10
TAR 34	3,778	2777697	2769076	443,478	11,738	97,82
TAR 35A	6,056	4359389	4350768	696,792	11,506	95,88
TAR 36	6,097	4586957	4578336	733,238	12,026	100,00
TAR 38	4,075	2946029	2937408	470,437	11,544	96,20
TAR 40.2	6,023	4373315	4364694	699,022	11,606	96,71
TAR 41	3,639	2666802	2658181	425,718	11,699	97,49
TAR 42	5,168	3837069	3828448	613,140	11,864	98,86
TAR 43	5,668	4181609	4175905	660,849	11,659	97,16
TAR 46	3,677	2705808	2700104	427,299	11,621	96,84
TAR 48	5,510	3964411	3958707	626,477	11,370	94,74
TAR 49.1	5,316	4069927	4064223	643,175	12,099	100,00
TAR 50	7,227	5028557	5022853	794,881	10,999	91,65
IN 1	4,909	3682812	3674191	588,435	11,987	99,89
IN 3	4,477	3265451	3256830	521,594	11,651	97,08
IN 5	3,975	3006522	2997901	480,125	12,079	100,00
MT1	4,278	3112271	3103650	497,061	11,619	96,82
MT 2	6,329	5073597	5064976	811,175	12,817	100,00
MT 3	5,274	4204006	4195385	671,907	12,740	100,00

Probe	Einwaage	Counts	cor. Coun.	µg C	% TC	% CaCO3
TI 1	4,719	52890	39069	5,389	0,114	0,95
TI 4	4,419	26366	12545	1,730	0,039	0,33

Probe	Einwaage	Counts	cor. Coun.	µg C	% TC	% CaCO3
TI 6	4,024	50406	36585	5,046	0,125	1,04
TI 7	4,773	122018	108197	14,923	0,313	2,61
TI 9	5,236	22453	8632	1,191	0,023	0,19